Transport Process Chemical Engineering

Kataoka, Kunio

(Citation)
Transport Process Chemical Engineering:vi, [1]-246

(Issue Date)
2020-09

(Resource Type)
learning object

(Version)
Version of Record

(JaLCDOI)
https://doi.org/10.24546/90008260

(URL)
https://hdl.handle.net/20.500.14094/90008260

TRANSPORT PROCESS CHEMICAL ENGINEERING

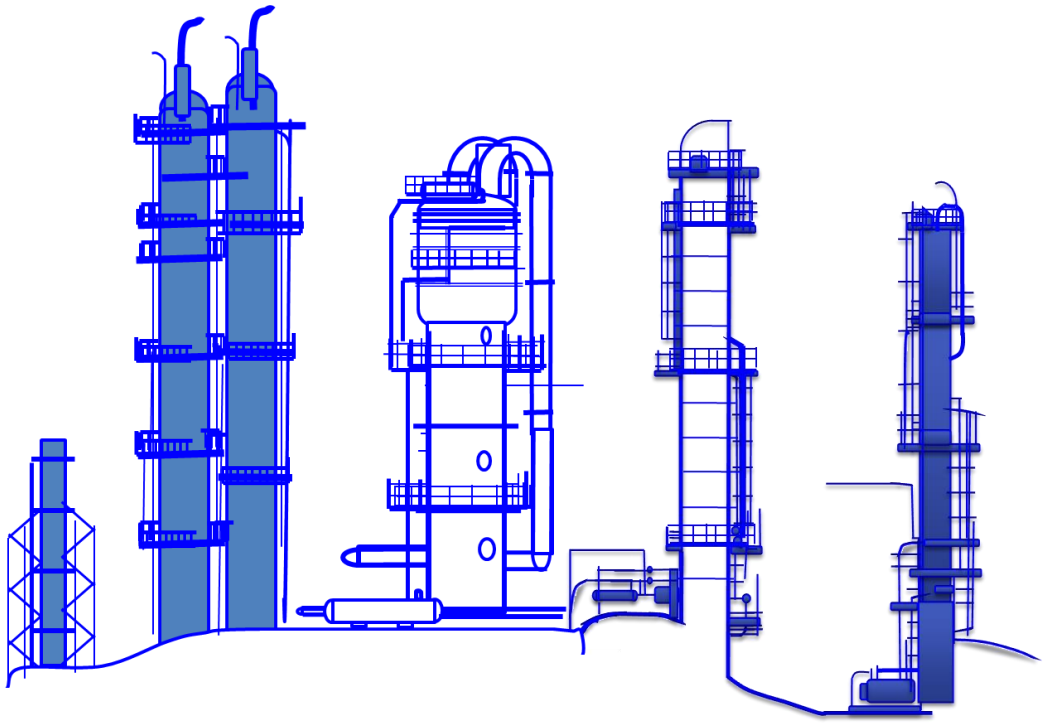

Kunio KATAOKA

Transport Process Chemical Engineering

Transport Process Chemical Engineering (TPCE) is a significant contribution to chemical engineering education. The author Emeritus Professor Kunio Kataoka of Kobe University, Kobe, Japan is eminently qualified having taught this subject for 35 years to both undergraduate and graduate students. TPCE should serve as a supplemental text for both undergraduate and graduate students. While undergraduate students may have been exposed to vector and tensor analysis in a mathematics course, the study of transport processes is likely their first exposure to practical situations where these concepts are required. This exposure can be quite daunting. Graduate students may benefit by reviewing the more practical aspects and as a second source for the more advanced topics.

The text considers microscopic and macroscopic balances of heat, mass, and momentum transfer both separately and simultaneously. The chapters typically begin with a generalized mathematical treatment which is subsequently simplified for special cases. The limits of the simplifying assumptions are clearly specified. Each chapter contains examples with detailed solutions, problems including an answer so that the students may know if their approach is correct, and problems without an answer leaving the students on their own.

It is my experience based on 40 years of teaching that students react to complex materials in different ways. Some respond quite well to one author's presentation while others find that same presentation virtually incomprehensible. The latter group may, however, respond quite well to the same material presented in a somewhat different manner by another author. On another topic the response of the same groups may be totally reversed. To emphasize this point, a respected faculty colleague recently told me that he always tries to have two sources whenever he is preparing a new lecture.

The text is in English and should, therefore, be useful to chemical engineering students worldwide. It is particularly significant that Professor Kataoka has chosen to make the text available to all interested parties free-of-charge on the following web sites

Kobe University (https://doi.org/10.24546/90008260)
Kansai Chemical Engineering Company (https://www.kce.co.jp/en/library).

Emeritus Professor Dr. Douglas P. Harrison
Department of Chemical Engineering
Louisiana State University
Baton Rouge, LA
The United States of America

PREFACE

This book has been organized as a textbook of the three-year sequential course for students of chemical engineering from the junior up to the first-year graduate level.

It is well known that in 1960, Professor R. B. Bird, Professor W. E. Stewart, and Professor E. N. Lightfoot of the University of Wisconsin united fluid flow, heat transfer, and mass transfer into a single concept with the publication of "Transport Phenomena."

I believe that their concept remains unaltered and still alive.

I have 35 years' teaching experience as a faculty member of the Chemical Engineering Department of Kobe University, Kobe, Japan. Since 1968, in particular, I have had the privilege of lecturing for this three-year course from the junior introductory to the first-year graduate advanced course.

Besides I have a fortunate experience of teaching as an invited professor the fundamentals of chemical engineering by using their book "Transport Phenomena" at Louisiana State University for the short term from 1978 to 1979. Some thoughtful comment and advice received from Professor R. B. Bird during that term were invaluable and still remain as a concept of the author's educational standard for this book.

This is intended to serve as a textbook for an integrated understanding of fluid mechanics, thermodynamics, heat transfer, and mass transfer from a viewpoint of process engineers. Radiation is not included because the author thought that a brief summary of radiation transfer consistent with the rest of the text was too difficult. I hope that this book will be useful not only as a reference but also as a textbook to be used either by a class or for self-study.

The objective of the book is to present all the subjects of transport processes rearranged in the developing sequence from the fundamentals to practical application.

Where this book is used for college instruction in chemical engineering, the whole PART I and Chapter 20 of PART II are suitable for undergraduate courses; Chapters 11 through 16 of PART II for graduate studies. The remaining part Chapters 17 through 19 are intended, in particular, for those who expect to do a lot of academic research in those areas.

Chapter 2 of the book presenting basic definitions of physical transport properties is followed by Chapter 3 simply and qualitatively explaining the fundamentals of fluid flow such as the generation of turbulent motion. Chapter 4 introduces a control volume approach for macroscopic balances of momentum, energy and mass, which give us very important fundamental equations practically applicable to various chemical equipment designs. These three chapters are essential for undergraduate courses.

Chapter 5 introduces the microscopic shell balance of momentum, energy and mass, where undergraduate and/or graduate students study how to construct the respective basic differential equations such as the Navier-Stokes equation of motion. They must first learn a little vector and tensor analysis for mathematical generalization.

Chapter 6 provides several applications of those fundamental differential equations. The first two examples deal with simple momentum equations for Newtonian fluids to be followed by two non-Newtonian examples which may be appropriate for graduate course. The remaining parts giving four examples on heat and mass transfer may also be useful for both course students. In every examples, starting by the very difficult partial differential equations, we will study how to simplify them into very simple ordinary differential equations.

Chapters 7 through 10 deal with interphase transfer of momentum, heat and mass, where they will study learn "the film theory" and should learn how practically important it is to define interphase transfer coefficients. Therefore these chapters are the most importance as the primary theme for the undergraduate course because most of chemical engineering processes can be modeled by the control volume approach using the interphase transport concepts. Students will

study how to design various chemical apparatuses from the concept of interphase transfer coefficients. At the end of Chapter 9, the measuring principle of fluid velocities based on the convective heat transfer around a circular cylinder is arranged for graduate-level researchers.

In Part II, Chapters 11 through 13 deal with distillation and humidification processes, both of which proceed with simultaneous heat and mass transfer accompanied by phase transformation. In Chapter 11, undergraduate students will study very simple and useful basic ideas of distillation from a viewpoint of equilibrium stage model. Chapter 12 provides graduate students with the advanced concept of simultaneous heat and mass transfer, where the heat and mass transfer analysis of packed column distillation can be challenged by means of a unique control volume approach. In Chapter 13, undergraduate and/or graduate students will study how to practically design chemical equipment using air-water system such as air-conditioner, cooling tower, and evaporative cooler and condenser from a viewpoint of simultaneous heat and mass transfer. Chapter 14 on ionic mass transfer is arranged especially for graduate students, which will be useful for experimental research on liquid-phase mass transfer. Chapter 15 deals with condensation and boiling heat transfer. Chapter 16 provides the advanced analysis of diffusion processes accompanied with chemical reactions. Because of the very difficult analytical analysis, a computer-aided numerical analysis may be utilized at present. Chapter 17 provides the fundamental aspect of turbulent transport phenomena for graduate students as well as researchers. This will be able to provide various fundamental knowledges as the background useful for the advanced academic research on transport processes. The following Chapters 18 and 19 will give the advanced transport aspects of fluid flow to graduate students. Finally Chapter 20 provides practical consideration of agitating equipment for undergraduate course. Because of the very complicated mixing phenomenon, the useful practical design concept should be studied using a dimensional analysis from a viewpoint of transport processes.

I would like to emphasize that it is getting more and more important to investigate various chemical engineering process and equipment from a viewpoint of transport phenomena. I believe that it must effectively lead to process development, intensification, and technological innovation.

If the various mathematical approaches introduced in this book based on differential equations are difficult to solve analytically, the computer-aided numerical analysis may be utilized as an appropriate tool at the present time.

My friend, Emeritus Professor Dr. D. P. Harrison of Louisiana State University who was the chairman of Department of Chemical Engineering during my stay at LSU read the whole manuscript from his stand of reaction engineering and gave me many helpful suggestions.

In closing, I would like to express my gratitude to all the faculty members and students of Department of Chemical Science and Engineering, Kobe University and to The Society of Chemical Engineers, Japan. In addition, Dr. H. Noda, the President of Kansai Chemical Engineering Co., Ltd., gave me a lot of support and advice from a viewpoint of practical engineering. I would like to appreciate his kind encouragement and valuable comments

I would be very happy if many chemical engineering students will be encouraged by taking an interest in this book.

KUNIO KATAOKA
*Emeritus Professor
Dept. of Chemical Science & Engineering
Kobe University
*Top Supervisor
Engineering Dept.
Kansai Chemical Engineering Co., Ltd.

Kobe
September 2020

CONTENTS

PART I

PART Ⅱ

PART I

CHAPTER 1

INTRODUCTION

1.1 What Do We Study in TRANSPORT PROCESS CHEMICAL ENGINEERING?

In order to understand what and how we will study, let us consider a process producing methane from heavy oil (higher hydrocarbons) as an example of chemical plants.

Figure 1 shows the flow sheet diagram. The heavy oil is usually withdrawn as one of the bottom products from a distillation plant 1 of crude oil. The process consists of gasification, purification, and methanation.

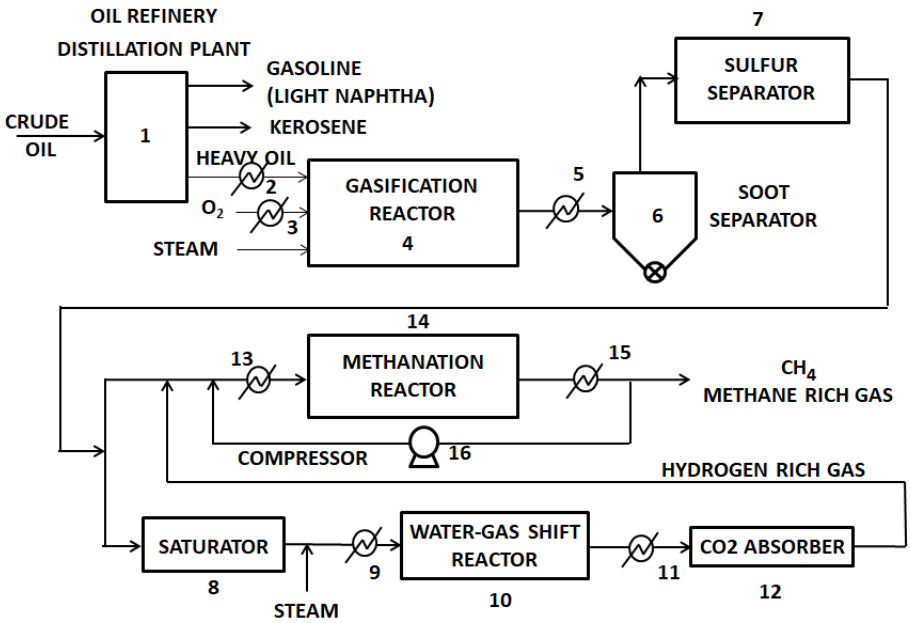

Fig.1.1-1. Example of process flow diagram of a chemical plant

Heavy oil, oxygen, and steam are fed through heat exchangers 2 and 3 to the gasification reactor 4 where the higher hydrocarbons undergo complete reaction to produce CO and H_2 without solid catalyst. The outlet gas from the reactor 4 is cooled, passes through a soot separator 6, and enters a sulfur removing equipment 7. The gas from the separator 7 consists of CO, H_2, and small amount of CO_2. The gas is divided and fed into two sections: purification and methanation sections. In the purification section, the gas is fed through a saturator 8 to a water-gas shift reactor 10. The reactor consists of a fixed bed of solid catalyst particles through which the gas undergoes the reaction $CO + H_2O \rightarrow CO_2 + H_2$ in the presence of nickel based catalyst. The reaction is

reversible and exothermic. The shifted gas is cooled by a contact cooler and heat exchanger 11, and led to a CO_2 absorber 12, where CO_2 is removed from the shifted gas by water or some sort of alkaline solution. The absorber is a column filled with some sort of device or packed with small solids of varying shapes to increase the interfacial area between the trickling liquid and the flowing-up gas. The gas leaving the absorber is hydrogen rich gas. On the other hand, the rest of the gas produced in the gasification process is mixed with the hydrogen rich gas from the purification process, and fed to a series of methanation reactors 14. The reactors are a fixed bed of nickel catalyst particles through which the reaction $CO + 3\ H_2 \rightarrow CH_4 + H_2O$ takes place. The methane rich gas leaving the methanation reactors contains steam. The product of methane rich gas is obtained after removing steam by condenser 15. A certain fraction of the product gas is fed back to the methanation reactors 14 by a compressor 16.

As a prerequisite to the design of industrial equipment, an understanding of the fundamental properties and characteristics of individual operations is required. This plant offers examples of various momentum, energy, and mass transfer processes which will be studied in this course.

In the design of pipelines, we need to know

1) mechanical energy losses of the flowing fluids (or pressure drops)
2) power of pumps, compressors, and blowers and optimal pipe diameters required to attain the desired flow rates

The mechanical energy balance (the modified Bernoulli equation) for calculation of the power requirement and the concept of friction factor, equivalent length, and friction loss factor for calculation of the pressure drops at the individual sections will be studied in this course.

In the design of heat exchangers, we need to know

1) pressure drops of shell- and tube-side streams
2) heat transfer area (i.e. the size of exchangers) required to attain the desired rate of heat transfer.

The energy balance for calculation of the discharge fluid temperatures and the concept of heat transfer coefficient will be studied to size the heat exchangers in this course.

In the design of gas absorbers, we need to know

1) operating conditions (liquid-gas flow ratio, temperature, pressure, *etc*.)
2) height of absorption columns required to attain the desired separation efficiency
3) diameter of absorption columns to attain the desired gas-liquid contact condition

Phase equilibrium should be studied in thermodynamic course. The concept of mass transfer coefficient will be studied for determination of mass transfer area i.e. the height of an absorption column in this course.

Although the above example does not have a distillation process, distillation is one of the most popular unit operations. Many distillation columns are encountered in the oil refinery plants. In the design of distillation columns, we need to know

1) operating conditions (feed rate, reflux-ratio, temperature, pressure, liquid-gas flow ratio, *etc*.)
2) column structures (trayed column, packed column) suitable for the feed mixture properties
3) number of trays, height of packing section suitable for the desired separation efficiency
4) column diameter for attaining the desired gas-liquid contact condition

Phase equilibrium is also very important for distillation process engineering since the most popular design procedure is the equilibrium-stage model.

After learning the fundamentals of engineering calculation based on the equilibrium stage model for the practical design of distillation equipment, we try to understand the distillation processes from a viewpoint of heat and mass transfer.

In the design of reactors, we need to know
1) operating conditions (temperature, pressure, feed composition, etc.)
2) size of reactors required to obtain the desired conversion and product yield
3) selection of suitable catalyst

The reaction kinetics (reaction rate, chemical equilibrium, etc.) should be studied in another course. The flow patterns and heat- and mass-transfer characteristics should also be considered because actual rate of reaction depends on mass transfer of reactants as well as temperature and pressure.

In the design of dust separators, we need to know
1) minimum size of collectable particles
2) collection efficiency

The underlying theory on particle mechanics should be studied with the fluid mechanics.

The main problem in the design of such chemical engineering processes is to determine the size of equipment: to calculate how much contacting area is necessary for the required rate of heat or mass transfer.

Most flows in chemical engineering equipment are turbulent. Of particular importance are the mixing effects of turbulence on heat/mass transfer and chemical reaction. The phenomenological understanding of turbulent flows in this course will be helpful to the reader in the design of new equipment and the improvement of equipment efficiency.

Unfortunately, no general approach to the solution of problems on the turbulent transport phenomena is available. Accurate quantitative predictions cannot be made without relying heavily on empirical data. Recently many trials have been made for the computer-aided modeling of the turbulent transport mechanism but those levels are beyond the concept of this course.

The Transport Process Chemical Engineering is one of the most basic and most important scientific areas constituted for the understanding of individual operations from an engineering viewpoint.

1.2 Concepts and Definitions

(I) Two Viewpoints for Transport Science

Lagrangian and Eulerian Viewpoints

There are two different viewpoints for representation of physical fields. In the Lagrangian approach, the physical variation can be described for a particular element of interest as it moves. The coordinates describe the time-dependent position of the moving element. This viewpoint is mainly used in particle and rigid-body dynamics. On the other hand, in the Eulerian viewpoint, the physical variation is described on a given stationary line or plane of interest. In Transport Science, therefore, fluid can be regarded as a continuum medium.

The Eulerian viewpoint is more useful for description of the physical variation in flowing fluids. This approach gives the value of a fluid variable at a given position at a given time such as the fluid velocity distribution on the cross section of a flow passage.

(II) Units

The International Standard system of units (Systeme International), or the so-called “SI units” will be used in this course. The basic units are mass in kilogram, (kg), length in meters, (m), and time in seconds, (s). The unit of force is newton, (N), which is easily defined using the simplest form of Newton’s law of motion: $\boldsymbol{F} = m\,\boldsymbol{a}$. One newton 1 N is the force required to accelerate a mass of 1 kg at a rate of 1 m/s^2. The unit of energy or work is joule, (J), which can

be easily understood as the product of displacement and force component in its direction. Basically, degrees Kelvin, (K), will be used as the unit of absolute temperature, but degrees Cerlsius, (℃), will be also used for convenience.

Another useful consideration in dealing with units is the concept of the molar units. In processes including chemical reactions, kilogram moles, (kmol), may be much more convenient for mass than kilograms.

(III) Three Categories of Physical Quantities

The physical quantities encountered in this course fall into one of three categories: (1) scalars such as time, temperature, density, and energy; (2) vectors such as velocity, acceleration, momentum, heat-flux and mass-flux; and (3) tensors such as shear stress or momentum-flux and rate of strain. Vectors have three components whereas tensors have nine components.

In rectangular coordinates, for example, a velocity vector is expressed as

$$\boldsymbol{v} = (v_x, v_y, v_z) \tag{1.2-1}$$

And a stress tensor is given by

$$\boldsymbol{\tau} = \begin{bmatrix} \tau_{xx} & \tau_{xy} & \tau_{xz} \\ \tau_{yx} & \tau_{yy} & \tau_{yz} \\ \tau_{zx} & \tau_{zy} & \tau_{zz} \end{bmatrix} \tag{1.2-2}$$

[Example 1.1-E1] Force Balance from the Lagranrian Viewpoint

As an example of Lagrangian methods, let us consider a problem for the trajectory of a flying ball of mass m shown below. The position (x, y) of the ball is a function of time t.

The velocity $\boldsymbol{v}$ at time t can be decomposed as

$$\boldsymbol{v} = \frac{dx}{dt}\boldsymbol{i} + \frac{dy}{dt}\boldsymbol{j} \tag{1.2-3}$$

where $\boldsymbol{i}$ and $\boldsymbol{j}$ are unit vectors in the x- and y-directions, respectively.

The external forces acting on the ball are gravitational force $m\,g$ and the resistance force $\boldsymbol{R} = R_x\boldsymbol{i} + R_y\boldsymbol{j}$ exerted by air.

Applying Newton's second law of motion to the ball:

$$m\frac{d^2x}{dt^2} = -R_x \tag{1.2-4}$$

$$m\frac{d^2y}{dt^2} = -R_y - m\,g \tag{1.2-5}$$

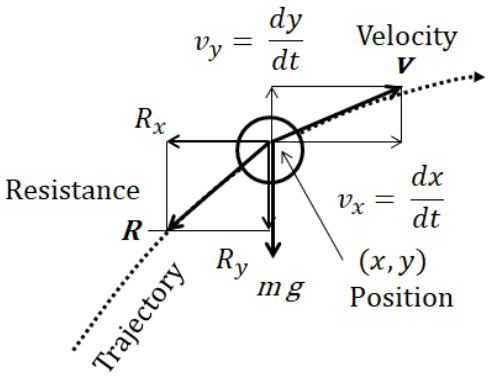

Fig.1.2-1. Equation of motion of a flying ball

If the resistance force is known as a function of velocity, the above set of equations can be solved. The solution will be given by

$$x = x(t) \text{ and } y = y(t) \tag{1.2-6}$$

Eliminating the variable t, the trajectory is expressible as

$$f(x, y) = 0 \tag{1.2-7}$$

This approach is applicable, for example, to calculation of the trajectories of liquid droplets in spray dryers and solid particles in sedimenting centrifuges.

(IV) Transport Intensity

There are two solid plates in which heat is transferred at the same rate. The transport area of one plate is double as much as that of the other plate. For this case, the heat transport intensity (called "heat-flux") of the former plate is half as much as that of the latter plate.

$$\text{flux} = \frac{\text{a quantity of interest transferred}}{(\text{are})(\text{time})} \tag{1.2-8}$$

$$\text{rate} = \frac{\text{a quantity of interest transferred}}{\text{time}} \tag{1.2-9}$$

For example, there are two copper electrodes in an electrolytic solution of copper sulfate, one of the electrodes (anode) has active surface much larger than the other one (cathode). In an electrolytic reaction occurring at some potential difference (emf) between the electrodes, the cathode has a deposition of copper ions while the anode releases copper ions at the same rate. In spite of the same ionic mass transfer rates at the two electrodes, the ionic mass flux due to the copper deposition on the cathode becomes much larger than the mass flux releasing copper ions from the anode. In this case, the resistance to mass transfer near the cathode becomes predominant.

(V) Fluid Forces

(5-1) Body Force and Surface Force

Body force such as gravitational force is proportional to the system's mass. Surface force such as pressure and friction force is proportional to the acting surface area and usually given in terms of orthogonal components, tangent and normal to the surface. They are called tangential and normal forces, respectively.

(5-2) Static Pressure

A fluid deforms continuously when it is subjected to shear stresses. In the case of an element of stationary fluid, stress acts normal to the surface of the fluid element. This normal stress, in the absence of motion, is called static pressure. In fluid flow, a normal stress generally consists of static pressure and additional normal stress due to the fluid motion.

For example, one component of normal stress is expressible as

$$\sigma_{xx} = p + \tau_{xx} \tag{1.2-10}$$

The pressure and stresses have units of N/m^2. Pascal (1 Pa = 1 N/m^2) is often used for the unit of pressure.

(5-3) Hydrostatics

For both compressible and incompressible fluids, static pressure varies with vertical height as

$$\frac{dp}{dy} = \rho\, g \tag{1.2-11}$$

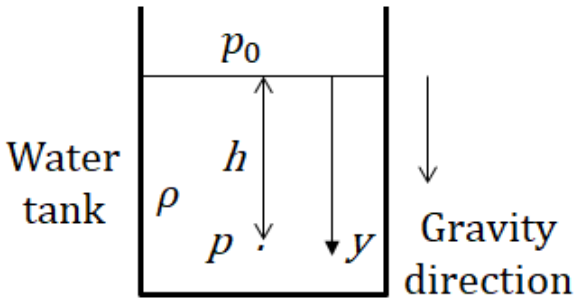

Fig.1.2-2. Hydrostatics of a water tank

Let us consider a tank filled with water. What is the static pressure at a position h below the free surface of water? Water can be considered as an incompressible fluid: ρ = const.

Integrating Eq.(1.2-11) with respect to y gives

$$p - p_0 = \int_{p_0}^{p} dp = \int_0^h \rho\, g\, dy = \rho\, g\, h \qquad (1.2\text{-}12)$$

where p_0 is a pressure at the free surface and usually atmospheric pressure.

[Problem 1.2-P1]

Manometers are a device for measuring pressure difference between two points. A fluid of density ρ is flowing through a circular pipe. The U-tube manometer which has a manometer fluid with density ρ_m has two pressure taps at point A and B, respectively. Determine the pressure difference $p_A - p_B$ by the manometer reading h.

[Problem 1.2-P2]

The cylindrical water tank (diameter D) shown below has a nozzle at the bottom corner. Water is discharged due to the gravity in the following rule:

$$v = c\sqrt{2\, g\, h}$$

where v is (cross-sectional are-averaged) velocity of water issuing the nozzle (nozzle outlet diameter d) and h the water surface height at time t from the nozzle level. The coefficient in front of the square-root is an assumed constant (usually 0.95). At the beginning, the water height is h_0.

How long does it take until the water level arrives at the nozzle height h_N?

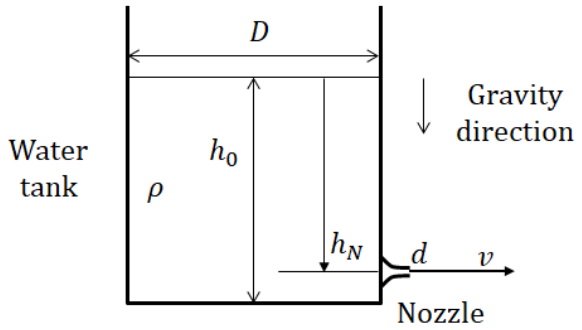

Fig.1.2-P2. Water discharge from a tank

CHAPTER 2

FUNDAMENTAL LAWS OF MOMENTUM, ENERGY AND MASS TRANFER

All materials are generally composed of molecules. However any theory that would predict the individual behaviors of these many molecules would be very difficult, far beyond our abilities at the present level. Most engineering work is usually concerned with the macroscopic behavior considering a fluid as a continuous distribution of matter or a continuum. Therefore we can use the continuum approach in this course. We postulate that velocity, density, pressure, temperature, mass concentration, momentum-flux, energy-flux, mass-flux etc. behave as continuum functions. An exact derivation of these laws of molecular transport can be made by non-equilibrium thermodynamics

2-1 Viscosity (Newton's Law of Viscosity)

The viscosity can be understood with the aid of very simple flow problem. There is a fluid --- either a gas or a liquid --- contained between two large parallel plates a small distance ΔY apart, which extend indefinitely in the x- and z-directions.

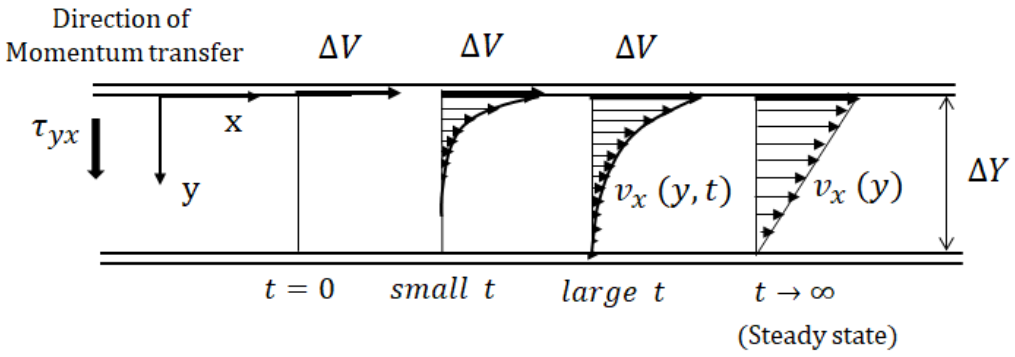

Fig.2.1-1. Momentum transfer across fluid layer between two parallel plates

Initially, the fluid and two plates are at rest, but at time $t = 0$ the upper plate is set in motion in the positive x-direction at a constant velocity ΔV by a force F.

As time proceeds, the fluid distant from the upper plate gains velocity (momentum), and finally the steady-state linear velocity profile is attained. In Transport Science, we interpret that the x-directed momentum $\rho\, v_x$ diffuses in the y-direction. If F is acting on a definite area A of the upper plate, we can get the following empirical relation between F and ΔV:

$$\frac{F}{A} = -\mu \frac{\Delta V}{\Delta Y} \qquad (2.1\text{-}1)$$

The constant of proportionality μ is known as the viscosity of the fluid. Even in steady state the x-momentum $\rho\, v_x$ is steadily transferred in the y-direction to maintain the

linear velocity distribution:

$$\frac{v_x}{\Delta V} = 1 - \frac{y}{\Delta Y} \tag{2.1-2}$$

In a differential form, Eq.(2.1-1) is expressible as

$$\tau_{yx} = -\mu \frac{d\, v_x}{dy} \tag{2.1-3}$$

This is a form of Newton's law of viscosity for one-dimensional flow. This law states that local shear stress τ_{yx} at y is proportional to local velocity gradient $d\, v_x/dy$ at y. The subscript yx indicates that the shear stress is in a plane perpendicular to y and parallel to x or that that the x-momentum diffuses in the y-direction. Since the dimensions of the shear stress is the same as those of momentum flux, it can be considered that local momentum-flux is proportional to local gradient of momentum per unit volume:

$$\tau_{yx} = -\nu \frac{d\, \varrho\, v_x}{dy} \tag{2.1-4}$$

Here $\nu = \mu/\varrho$ is called "kinematic viscosity," which has the same units as diffusivity, i.e. m²/s in SI units. The kinematic viscosity can be considered as molecular diffusivity for momentum.

Fluids are classified as Newtonian or non-Newtonian, depending on the relation of the shear stress with the rate of strain. The fluids which do not obey the Newton's law of viscosity are called "non-Newtonian fluid". All kinds of gases and simple liquids belong to Newtonian fluid. Polymer solutions and their melts, emulsions, slurries, and pastes often behave as non-Newtonian fluids. Some models for non-Newtonian fluids will be described in Section 2.5.

The units of viscosity can be obtained as follows:

$$\tau_{yx}\,(=)\,\frac{M\,L\,T^{-2}}{L^2}\,(=)\,\frac{M\,L\,T^{-1}}{L^2\,T}\,(=)\frac{N}{m^2} \tag{2.1-5}$$

The units of shear stress become the same as that of pressure.

$$\mu\,(=)\,\frac{\tau_{yx}}{(dv_x/dy)}\,(=)\,\frac{M\,L^{-1}\,T^{-2}}{(L/T)\,L^{-1}}\,(=)\,\frac{M}{L\,T}\,(=)\,\frac{kg}{m\,s} \tag{2.1-6}$$

$$\nu\,(=)\,\mu/\varrho\,\,(=)\,\frac{L^2}{T}\,(=)\,\frac{m^2}{s} \tag{2.1-7}$$

where $M,\ L,\ T$ are characteristic dimensions of mass, length and time, respectively.

1 kg/m s (= Pa s) = 10 poise (= g/cm sec) = 1,000 centipoise (= cP).

General form of Newton's law of viscosity is listed given in terms of rectangular, and cylindrical coordinates in Table 2.1-1.

Table 2.1-1 Newton's law of viscosity

[Rectangular coordinates(x, y, z)]

$$\tau_{xx} = -\mu\left[2\,\frac{\partial\, v_x}{\partial x} - \frac{2}{3}\,(\nabla\cdot\boldsymbol{v})\right] \quad \tau_{yy} = -\mu\left[2\,\frac{\partial\, v_y}{\partial y} - \frac{2}{3}\,(\nabla\cdot\boldsymbol{v})\right]$$

$$\tau_{zz} = -\mu\left[2\,\frac{\partial\, v_z}{\partial z} - \frac{2}{3}\,(\nabla\cdot\boldsymbol{v})\right] \quad \tau_{xy} = \tau_{yx} = -\mu\left[\frac{\partial\, v_x}{\partial y} + \frac{\partial\, v_y}{\partial x}\right]$$

$$\tau_{yz} = \tau_{zy} = -\mu\left[\frac{\partial\, v_y}{\partial z} + \frac{\partial\, v_z}{\partial y}\right] \quad \tau_{zx} = \tau_{xz} = -\mu\left[\frac{\partial\, v_z}{\partial x} + \frac{\partial\, v_x}{\partial z}\right]$$

$$(\nabla\cdot\boldsymbol{v}) = \frac{\partial v_x}{\partial x} + \frac{\partial v_y}{\partial y} + \frac{\partial v_z}{\partial z}$$

[Cylindrical coordinates (r, θ, z)]

$$\tau_{rr} = -\mu\left[2\,\frac{\partial v_r}{\partial r} - \frac{2}{3}\,(\nabla\cdot\boldsymbol{v})\right] \quad \tau_{\theta\theta} = -\mu\left[2\left(\frac{1}{r}\,\frac{\partial v_\theta}{\partial \theta} + \frac{v_r}{r}\right) - \frac{2}{3}\,(\nabla\cdot\boldsymbol{v})\right]$$

$$\tau_{zz} = -\mu\left[2\,\frac{\partial v_z}{\partial z} - \frac{2}{3}\,(\nabla\cdot\boldsymbol{v})\right] \quad \tau_{r\theta} = \tau_{\theta r} = -\mu\left[r\,\frac{\partial}{\partial r}\left(\frac{v_\theta}{r}\right) + \frac{1}{r}\,\frac{\partial v_r}{\partial \theta}\right]$$

$$\tau_{\theta z} = \tau_{z\theta} = -\mu\left[\frac{\partial v_\theta}{\partial z} + \frac{1}{r}\,\frac{\partial v_z}{\partial \theta}\right] \quad \tau_{zr} = \tau_{rz} = -\mu\left[\frac{\partial v_z}{\partial r} + \frac{\partial v_r}{\partial z}\right]$$

$$(\nabla\cdot\boldsymbol{v}) = \frac{1}{r}\,\frac{\partial}{\partial r}\,(r\,v_r) + \frac{1}{r}\,\frac{\partial v_\theta}{\partial \theta} + \frac{\partial v_z}{\partial z}$$

[Problem 2.1-P1] There are a pair of concentric cylinders, the outer one of which is rotated at a speed of 20 RPS (rotation per second) and the inner one is at rest. The annular space is filled with 50% aqueous solution of glycerin which has viscosity of 5 cP or 0.0005 Pa s. Both cylinders are 500 mm long and the annular gap width is 2.5 mm.

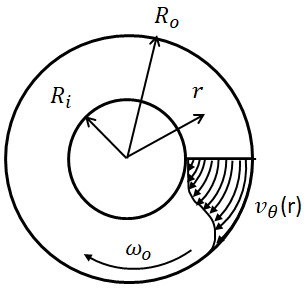

Fig.2.1-P1. Velocity distribution in an annular gap between coaxial cylinders

The radii of the cylinders are $R_i = 25$ mm and $R_o = 27.5$ mm, respectively. The radial distribution of circumferential velocity can be expressed as

$$v_\theta = \frac{R_i R_o}{{R_o}^2 - {R_i}^2} R_o \omega_o \left(\frac{r}{R_i} - \frac{R_i}{r}\right) \qquad (2.1\text{-P1})$$

What is the torque required to maintain the steady rotation?

[Problem 2.1-P2] There are two concentric cylinders, the outer one of which is rotated at a rate of 10 RPS. The radii of the cylinders are 0.04 m and 0.05 m, respectively. The lengths of the cylinders are about 0.75 m. The annulus between the cylinders is filled with a liquid whose viscosity is unknown. The torque $T_q = 5.53 \times 10^{-3}$ N-m is necessary to keep the inner cylinder at rest. What is the viscosity of the fluid?

[Problem 2.1-P3] The velocity distribution in laminar flow through a circular annulus is expressed as

$$\frac{v_z}{V} = \frac{2}{A}\left[1 - \left(\frac{r}{R_o}\right)^2 + B \ln \frac{r}{R_o}\right] \qquad (2.1\text{-P2})$$

where $V =$ average velocity (constant)

$B = (r*^2 - 1)/\ln r*$

$r* = R_i/R_o$

Calculate the shear stresses on the inside surface of the outer tube and the outside surface of the inner tube.

2.2 Thermal Conductivity (Fourier's Law of Heat Conduction)

Similarly to the definition of viscosity, we can define thermal conductivity. There are two very large parallel plates a small distance ΔY apart, which contain a slab of either solid or fluid between them. Initially the slab has a uniform temperature T_0. At time $t = 0$, the upper surface has a step change in temperature from T_0 to a higher constant temperature T_1. As time proceeds, thermal energy diffuses in the y-direction and ultimately a linear temperature profile is attained in steady state. The slab material is stationary. The slab is so thin that we can neglect the effect of natural convection due to density change. We can also neglect the effect of radiative transport.

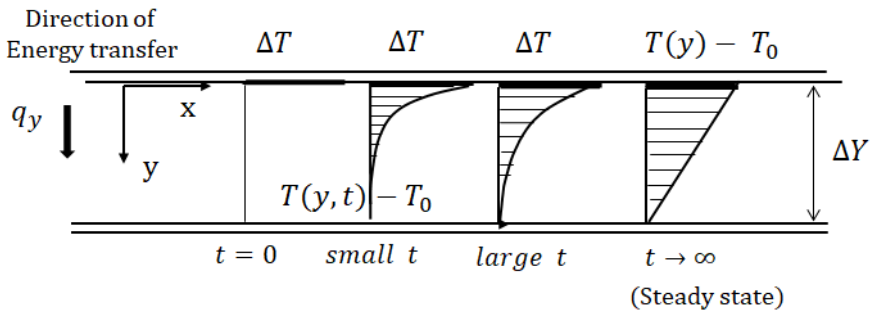

Fig.2.2-1. Energy transfer in a slab put between two large parallel plates

We get the following relation between the rate of heat flow Q through the slab and the temperature difference $\Delta T = T_1 - T_0$:

$$\frac{Q}{A} = -\kappa \frac{\Delta T}{\Delta Y} \tag{2.2-1}$$

The constant of proportionality κ is known as the thermal conductivity of the material. In a differential form, the above equation can be written as

$$q_y = -\kappa \frac{dT}{dy} \tag{2.2-2}$$

This is Fourier's law of heat conduction for one-dimensional heat flow. This law states that local heat-flux q_y is proportional to local gradient of temperature dT/dy. The subscript y indicates the direction of heat flow.

For the case of constant density and heat capacity, the above equation can be rewritten as

$$q_y = -\alpha \frac{d(\rho C_p T)}{dy} \tag{2.2-3}$$

This states that local heat-flux (or local enthalpy-flux) is proportional to local gradient of enthalpy per unit volume. Here $\alpha = \kappa/\varrho C_p$ is called "thermal diffusivity", which has the same units as those of mass diffusivity.

The units of thermal conductivity and diffusivity can be obtained as follows:

$$q_y\ (=)\ \frac{M\,L\,T^{-2}L}{L^2T}\ (=) J/m^2 s\ (=) W/m^2 \tag{2. 2-4}$$

$$\kappa\ (=)\ \frac{q_y}{(-\,dT/dy)}\ (=)\ \frac{M\,L\frac{T^{-2}L}{L^2T}}{t/L}\ (=)\ \frac{M\,L^2T^{-2}}{L\,T\,t}\ (=)\ J/m\,s\,K\ (=)\ W/m\,K \tag{2.2-5}$$

$$\alpha\ (=)\ \kappa/\rho C_p\ (=)\ \frac{M\,L\,T^{-2}L/LTt}{(M/L^3)(M\,L^2T^{-2}/M\,t)}\ (=)\ \frac{L^2}{T}\ (=)\ m^2/s \tag{2.2-6}$$

where t is the characteristic dimension of temperature. General forms of Fourier's law of heat conduction are listed in Table 2.2-1.

Table 2.2-1 Fourier's law of heat conduction

[Rectangular coordinates (x,y,z)]

$$q_x = -\kappa \frac{\partial T}{\partial x},\quad q_y = -\kappa \frac{\partial T}{\partial y},\quad q_z = -\kappa \frac{\partial T}{\partial z}$$

[Cylindrical coordinates (r,θ,z)]

$$q_r = -\kappa \frac{\partial T}{\partial r},\quad q_\theta = -\kappa \frac{1}{r}\frac{\partial T}{\partial \theta},\quad q_z = -\kappa \frac{\partial T}{\partial z}$$

[Problem 2.2-P1] There are a pair of very large steel plates which are parallel placed 2 mm apart and contain mercury between them. The upper plate is kept at 303 K and the lower plate at 285 K. Mercury has a thermal conductivity of 8.4 W/m K. What is the steady-state heat-flux ? Assume that mercury is stationary.

[Problem 2.2-P2] A window has a glass plate (area $A =$ 1 m^2, thickness $\delta = 3$ mm, thermal conductivity $\kappa = 0.814$vW/m K). The inside surface is kept at 15 C and the outside surface at 5 C. What is the heat loss through the glass plate ?

[Problem 2.2-P3] Consider a hollow cylinder, then outside surface of which is kept at T_o and the inside surface of which at T_i $(T_i > T_o)$. The steady temperature distribution is given by

$$T = T_o + \frac{T_i - T_o}{\ln(R_i/R_o)} \ln(r/R_o) \qquad R_i < r < R_o \tag{2.2-P1}$$

The hollow cylinder has thermal conductivity κ. Calculate the heat-flux on the outside surface.

2.3 Diffusivity (Fick's Law of Diffusion)

Diffusion is similar to, but more complicated than the molecular transport of momentum and thermal energy because we have to deal with mixtures in which the velocities of the individual species are different. The mass center may move as the diffusion process proceeds. The mixture velocity must be evaluated by averaging the velocities of all of the species present.

Let us first consider two definitions of concentration for n-component mixture: the mass concentration of species *i* (the mass of species *i* per unit volume of mixture) ρ_i; the molecular concentration of species *i* (the number of moles of species *i* per unit volume of mixture) $C_i = \rho_i/M_i$.

Here M_i is the molecular weight of species *i*.

The mass and molar densities of the mixture are respectively given by

$$\rho = \sum_{i=1}^{n} \rho_i \quad \text{and} \quad c = \sum_{i=1}^{n} C_i \tag{2.3-1}$$

Therefore the mass and mole fractions are given by

$$\omega_i = \rho_i/\rho \quad \text{and} \quad x_i = C_i/c$$

Now consider the averaging of the velocities of species. The absolute velocity of species i is denoted by v_i with respect to stationary coordinate axes.

The mass-average velocity

$$\underline{v} = \sum_{i=1}^{n} \rho_i \underline{v_i} \,/ \sum_{i=1}^{n} \rho_i \tag{2.3-2}$$

This implies the velocity of mass center which corresponds to $\underline{v}$ for pure fluid.

The molar-average velocity $\underline{v^*}$ is defined as

$$\underline{v^*} = \sum_{i=1}^{n} C_i \underline{v_i} \,/ \sum_{i=1}^{n} C_i \tag{2.3-3}$$

This is the velocity of the mixture averaged with respect to the number of molecules.

Then two different diffusion velocities can be defined relative to these average velocities, that is, relative to the local motion of the fluid stream: $\underline{v_i} - \underline{v}$ and $\underline{v_i} - \underline{v^*}$.

The diffusion flux of a given species is a vector quantity denoting the amount of the species that passes through a unit cross section normal to the average velocities.

For simplicity, we restrict our discussion to a binary system of species A and B.

The mass flux relative to the mass average velocity is defined as

$$\underline{j_A} = \rho_A (\underline{v_A} - \underline{v}) \tag{2.3-4}$$

Similarly the molar flux relative to the molar-average velocity is

$$\underline{J_A} = C_A \left(\underline{v_A} - \underline{v^*}\right) \tag{2.3-5}$$

Figure 2.3-1 shows time-dependent composition profiles spreading due to molecular diffusion from a line source.

From a viewpoint of thermodynamics, the driving force of the molecular diffusion is the chemical potential. For a homogeneous ideal solution at constant temperature and pressure, the chemical potential is defined by

$$\mu_c = \mu^0 + R\,T \ln C_A \tag{2.3-6}$$

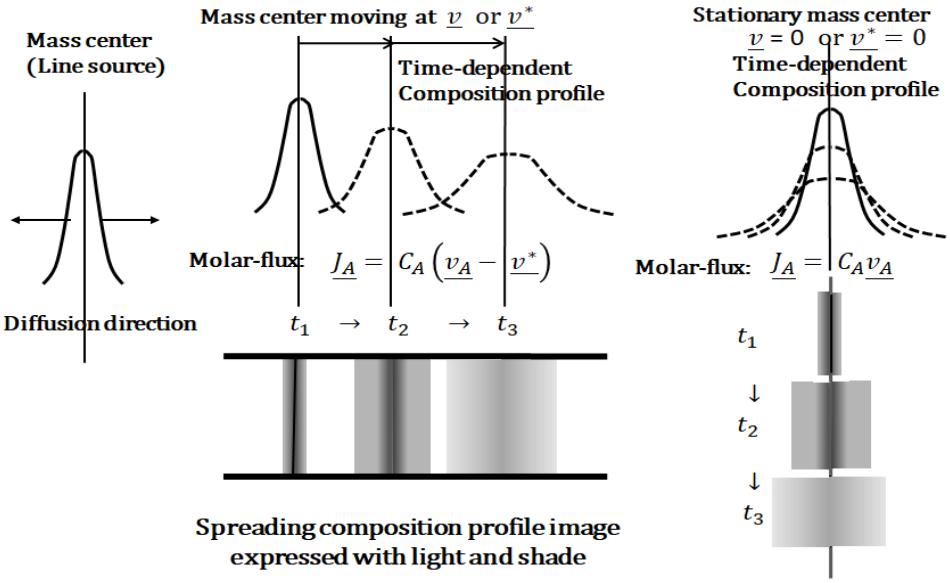

Fig.2.3-1. Composition profiles expressed with light and shade, spreading with molecular diffusion from a line source

The molar diffusion in y-direction occurs owing to the gradient of chemical potential:

$$v_{Ay} - v^*{}_y = -u_A \frac{d\,\mu_c}{dy} \tag{2.3-7}$$

where u_A is the "mobility" of component A, or the resulting velocity of the molecule A under the influence of a unit driving force. From the above equation

$$\frac{d\,\mu_c}{dy} = \frac{R\,T}{C_A}\frac{dC_A}{dy} \tag{2.3-8}$$

Then the y-component of molar flux is given by

$$J_{Ay} = C_A\left(v_{Ay} - v^*{}_y\right) = -u_A\,R\,T\,\frac{d\,C_A}{dy} = -D_{AB}\,\frac{d\,C_A}{dy} \tag{2.3-9}$$

This is Fick's law in a binary mixture for one-dimensional diffusion relative to the molar-average velocity. Here the constant of proportionality D_{AB} is called the "diffusivity" of component A diffusing through component B.

(In addition to concentration gradients, there are many other physical conditions which will produce a chemical potential gradient: temperature gradients, pressure gradients, etc. Our discussion will be restricted to the ordinary diffusion resulting from the concentration gradients.)

Under isothermal, isobaric conditions, the molar density c is constant.

Then

$$J_{Ay} = -\,c\,D_{AB}\,\frac{d\,x_A}{dy} \tag{2.3-10}$$

$$C_A\left(v_{Ay} - v^*{}_y\right) = -\,c\,D_{AB}\,\frac{d\,x_A}{dy} \tag{2.3-11}$$

For the binary system,

$$v^*{}_y = (C_A\,v_{Ay} + C_B\,v_{By})/c \tag{2.3-12}$$

Therefore

$$C_A v^*{}_y = x_A(C_A\,v_{Ay} + C_B\,v_{By}) \tag{2.3-13}$$

Substituting this relation

$$C_A\,v_{Ay} = C_A\,v^*{}_y - -D_{AB}\,\frac{d\,C_A}{dy} = x_A\left(C_A\,v_{Ay} + C_B\,v_{By}\right) - D_{AB}\,\frac{d\,C_A}{dy} \tag{2.3-14}$$

The terms $C_A\,v_{Ay}$ and $C_B\,v_{By}$ imply the y-component molar fluxes of component A and B relative to stationary coordinates. They are denoted by N_{Ay} and N_{By}.

Finally we obtain

$$N_{Ay} = x_A\left(C_A\,v_{Ay} + C_B\,v_{By}\right) - c\,D_{AB}\,\frac{d\,x_A}{dy} \tag{2.3-15}$$

This equation states that local molar flux at a plane fixed in the stationary coordinates consists of the bulk motion of the binary mixture (first term) and the molecular diffusion (second term) being proportional to local gradient of concentration or mass of component A per unit volume.

In an analogous fashion, the Fick's law can be expressed in terms of mass flux:

$$j_{Ay} = -D_{AB}\frac{d\rho_A}{dy} = -\rho D_{AB}\frac{d\omega_A}{dy} \tag{2.3-16}$$

$$n_{Ay} = \omega_A(n_{Ay} + n_{By}) - \rho D_{AB}\frac{d\omega_A}{dy} \tag{2.3-17}$$

The subscript y indicates the direction of diffusion.

General forms of Fick's law relative to the average velocity v^* are listed in Table 2.3-1 .

Table 2.3-1 Fick's law of molecular diffusion based on average velocity

[Rectangular coordinates (x, y, z)]

$$j_x = -D_{AB}\frac{\partial C_A}{\partial x},\quad j_y = -D_{AB}\frac{\partial C_A}{\partial y},\quad j_z = -D_{AB}\frac{\partial C_A}{\partial z}$$

[Cylindrical coordinates (r, θ, z)]

$$j_r = -D_{AB}\frac{\partial C_A}{\partial r},\quad j_\theta = -D_{AB}\frac{1}{r}\frac{\partial C_{AB}}{\partial \theta},\quad j_z = -D_{AB}\frac{\partial C_{AB}}{\partial z}$$

It is noted that the Fick's law has the same functional form as the Fourier's law.

The units of mass flux, concentration, and diffusivity are

$$J_{Ay}, N_{Ay}\ (=)\frac{M}{L^2T}\ (=)\ \frac{kmol\ of\ A}{m^2 s} \tag{2.3-18}$$

$$C_A\ (=)\frac{M}{L^3}\ (=)\ \frac{kmol\ of\ A}{m^3} \qquad x_A\ (=)\ \frac{kmol\ of\ A}{kmol\ of\ mixture} \qquad \rho_A\ (=)\ \frac{kg\ of\ A}{kg\ of\ mixture}$$

$$j_{Ay}, n_{Ay}\ (=)\ \frac{kg\ of\ A}{m^2 s} \qquad \omega_A\ (=)\ \frac{kg\ of\ A}{kg\ of\ mixture} \qquad D_{AB}\ (=)\ \frac{J_{Ay}}{(dC_A/dy)}\ (=)\ \frac{(M/L^2T)}{(M/L^3/L)}\ (=)\ \frac{L^2}{T}\ (=)\ m^2/s$$

Diffusion is confusion? The phenomenon of diffusion is so difficult that we will understand its fundamental aspect with simplified models in this course.

2.4 Similarity among Molecular Transports of Momentum, Energy, and Mass (Prandtl number and Schmidt number)

For constant physical property fluid (ρ, C_p: constant), one-dimensional transports of momentum, energy, and mass can be rewritten as

$$\tau_{yx} = -\nu\frac{d(\varrho v_x)}{dy} \tag{2.4-1}$$

$$q_y = -\alpha\frac{d(\varrho C_p T)}{dy} \tag{2.4-2}$$

$$J_{Ay} = -D_{AB}\frac{dC_A}{dy} \tag{2.4-3}$$

All these equations state the following common rule:

(Flux of a quantity of interest) = (Diffusivity)(Gradient of the quantity per unit volume)

The ratio of the momentum to the energy diffusivity is called "Prandtl number": $Pr = \nu/\alpha$.

If this dimensionless parameter is 1.0, heat and momentum diffuse through the fluid at the same rate.

The ratio of the momentum to the mass diffusivity is called "Schmidt number": $Sc = \nu/D_{AB}$.

If $Sc = 1.0$, mass and momentum also diffuse at the same rate. The ratio of the Prandtl to the Schmidt number, called "Lewis number", is also sometimes used: $Le = Pr/Sc = D_{AB}/\alpha$.

[Problem 2.4-P1] Compare Prandtl number of liquid mercury at 373 K with Prandtl number of low pressure hydrogen gas at 10 mmHg and 10 K. Discuss heat transfer in fluid at very low Prandtl numbers. The hydrogen gas has very low viscosity whereas the mercury has very large thermal conductivity.

[Problem 2.4-P2] Compare Schmidt number of very viscous polymer fluid with Schmidt number of an electrolytic solution. The polymer solution (density $\rho = 1{,}200\ kg/m^3$) has viscosity of 10 Pa s and diffusivity of 10^{-4} m^2/s whereas the electrolytic solution (density $\rho = 1{,}100\ kg/m^3$) has viscosity of 10^{-3} Pa s and diffusivity of 10^{-9} m^2/s. Discuss mass diffusion at very high Schmidt numbers taking into account the difference in flow condition.

2.5 Non-Newtonian Fluids

As studied in Section 2.1, Newton's law of viscosity states that the momentum flux (shear stress) in a usual fluid flow is proportional to velocity gradient (rate of strain). However Newton's law of viscosity does not always predict the shear stress in all fluids. In general, the relation between shear stress and the rate of shearing strain can be expressed by

$$\tau_{yx} = -\eta \frac{dv_x}{dy} \tag{2.5-1}$$

In the case of usual Newtonian fluids, η can be regarded as a proportional constant, i.e. viscosity $\eta = \mu$. As shown in Fig.2.5-1, however, there are various industrial materials having η as a function of either dv_x/dy or τ_{yx} and they are referred to as non-Newtonian fluids.

There are numerous empirical models proposed but the subject of non-Newtonian flow is beyond the objective of this course.

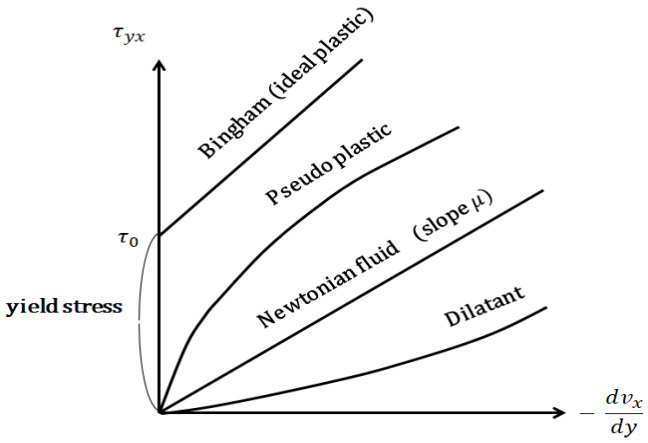

Fig.2.5-1. Schematic picture of momentum-flux against velocity gradient for non-Newtonian fluids

As slightly simpler representative example, the following two-parameter models are available:

(1) The Bingham model

$$\tau_{yx} = -\mu_0 \frac{dv_x}{dy} + \tau_0 \quad \text{if } \tau_{yx} > \tau_0 \tag{2.5-2}$$

$$\frac{dv_x}{dy} = 0 \quad \text{if } \tau_{yx} < \tau_0 \tag{2.5-3}$$

This model states that when the shear stress τ_{yx} is smaller than the yield stress τ_0, the fluid behaves like a rigid body but it flows like a Newtonian fluid when $\tau_{yx} > \tau_0$.

(2) The Power law model

$$\tau_{yx} = -m \left|\frac{dv_x}{dy}\right|^{n-1} \frac{dv_x}{dy} \quad (2.5\text{-}4)$$

This equation reduces to Newton's law of viscosity with $m = \mu$ when $n = 1$. The behavior of fluid is pseudo-plastic when $n < 1$ and dilatant when $n > 1$.

The laminar flow of a Bingham plastic (ideal plastic) fluid in a circular pipe will be studied in the later section.

Nomenclature

A	surface area of two parallel plates, [m^2]
C_A	concentration of component A, [kmol/m^3]
Cp	heat capacity, [J/kg K]
c	total molar density, [kmol/m^3]
D_{AB}	diffusivity, [m^2/s]
F	shear force, [N]
$j_A,\ J_A$	molar flux relative to mass-average and molar-average velocity, [kg/m^2s] or [kmol/m^2s]
n_A, N_A	mass flux, molar flux in stationary coordinates, [kg/m^2s] or [kmol/m^2s]
Pr	Prandtl number, [-]
Q	heat transfer rate, [W]
q_r, q_θ, q_z	heat flux in cylindrical coordinates
q_x, q_y, q_z	heat flux in rectangular coordinates
r, θ, z	cylindrical coordinates, [m, - , m]
Sc	Schmidt number, [-]
t	time, [s]
v_i	mass velocity, [m/s]
v^*	molar velocity, [m/s]
v_r, v_θ, v_z	velocity component in cylindrical coordinates
v_x, v_y, v_z	velocity component in rectangular coordinates, [m/s]
$x, y, z,$	rectangular coordinates, [m]
x_i	mole fraction, [-]
ΔT	constant temperature difference given to the upper plate, [K]
ΔV	constant velocity given to the upper plate, [m/s]
ΔY	distance between two parallel plates, [m]
α	thermal diffusivity, [m^2/s]
κ	thermal conductivity, [W/m K]
μ	viscosity, [kg/m s]
μ_c	chemical potential, [J/mol]
ν	kinematic viscosity or momentum diffusivity, [m^2/s]
ρ	density, [kg/m^3]
$\tau_{xx}, \tau_{yx}, \tau_{zx}, --$	momentum flux or shear stress, [N/m^2] or [kg/s^2m]
τ_0	yield stress, [N/m^2]
ω	mass fraction, [-]

Subcripts

A	component A
w	wall

CHAPTER 3

VISCOUS FLOW
(LAMINAR AND TURBULENT FLOWS)

3.1 Laminar and Turbulent Flows in a Circular Pipe

When a fluid moves through a system, either one of two different types of fluid flow may occur. As shown in Fig.3.1-1, suppose that water flows steadily through a transparent pipe, and a threadlike stream of dye is injected into it. If the velocity of water is small enough, the dye will flow in parallel, straight lines. When the velocity exceeds a certain critical value, it is noted that the dye introduced is instantly mixed across the entire cross section of the pipe and the entire mass of water becomes colored.

The first type of flow is called laminar; the fluid particles move along streamlines in a laminated form. In laminar flow, momentum, energy, and mass are transferred in the transverse direction due to molecular effect only.

The second type is called turbulent; the fluid particles move irregularly with violent eddy motion. Therefore momentum, energy, and mass can be radially transferred much more rapidly for turbulent flow than for laminar flow.

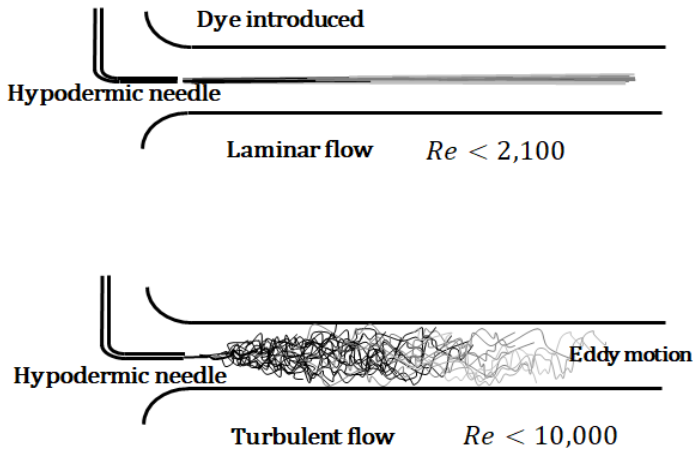

Fig.3.1.1. Characteristics of laminar and turbulent flow (Reynolds' experiment)

In 1883, this systematic experiment was first conducted by Osborne Reynolds[1)], who suggested the dimensionless parameter $Re = V\,D\,\rho/\mu$ as the criterion for predicting the type of flow. Here V is the average velocity in the pipe, D the pipe diameter, ρ the density, and μ the viscosity of the fluid. This parameter called the Reynolds number, is a basic parameter in the study of fluid motion. In pipe flow, the transition from laminar to turbulent flow may occur at about $Re = 2{,}100$ for commercial pipes.

For laminar pipe flow the velocity profile is parabolic. The theoretical curve is expressible as

$$v_z = v_{max}[1 - (r/R)^2] \qquad (3.1\text{-}1)$$

This analytical approach will be studied in Chapter 6.

[Problem 3.1-P1] A viscous liquid ($\mu = 0.05$ kg/m s, $\rho = 1050$ kg/m^3) is flowing in a 50 mm ID circular tube. The distribution of axial velocity is described as $v_z = v_{zmax}[1 - (r/R)^2]$ where the maximum velocity $v_{zmax} = 0.5$ m/s and the pipe radius $R = 0.025$ m. Calculate the friction force acting over 5 m of the inside surface of the tube, the flow rate, and the Reynolds number.

1. Reynolds, O., Trans. Roy. Soc. (London), **174A**, 935 (1883)

3.2 Generation of Turbulent Motion (Transition to Turbulent Flow)

As shown in Fig.3.2-1, when the fluid flow rate is increased, the parabolic velocity profile for laminar flow has an increase in maximum velocity accompanied with an increase in velocity gradient near the pipe wall.

Let us consider a fluid particle moving along the streamlines near the pipe wall. As shown in Fig. 3.2-2, the fluid velocity near the pipe wall becomes larger on the upper side than on the lower side of the fluid particle. The friction force for acceleration is exerted on the upper side whereas the friction force for deceleration is exerted on the lower side. As a result, these forces cause angular acceleration for the rotating motion.

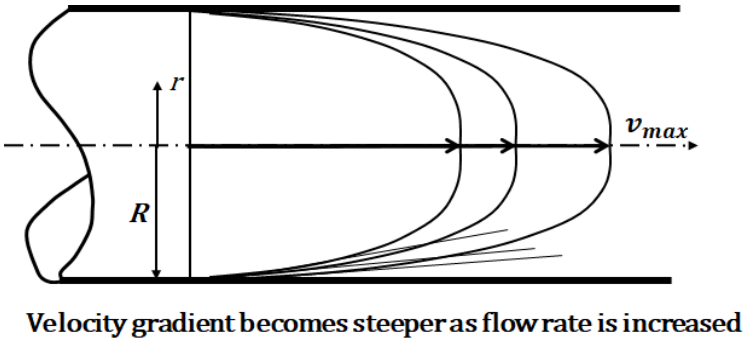

Fig.3.2-1. Instability of laminar flow in a circular pipe

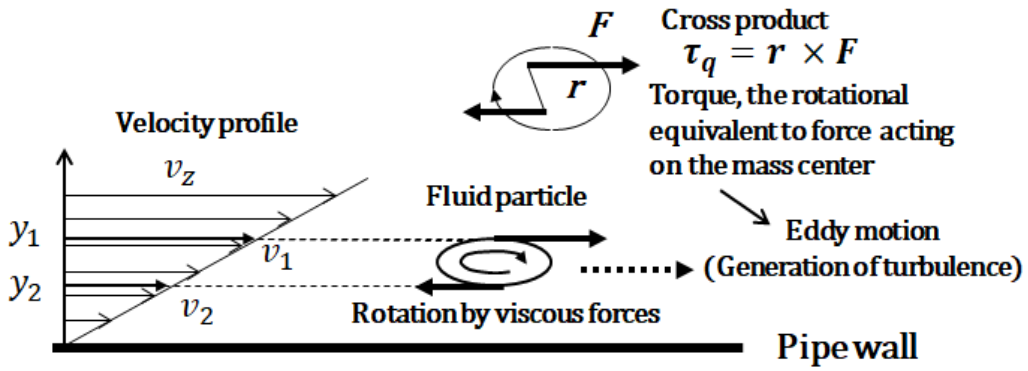

Fig.3.2-2. Generation of turbulent motion in a viscous parallel flow

Therefore, when the flow rate or the velocity gradient near the wall exceeds some critical value, the fluid particle undergoes a strong rotating angular acceleration due to the steep velocity gradient, so that eddy motion is generated by rotation of the fluid particle. This rotating condition is realized when the velocity difference $v_1 - v_2$ between two vertical positions becomes large. This is a qualitative understanding of an origin of turbulence or a transition to turbulent flow.

In turbulent flow, the velocity at a fixed position in the fluid fluctuates randomly about its time-averaged value. This unsteady fluctuating motion comes from such a complicated eddy motion, which gives a very large effect of mixing due to the transverse-directed interchange of fluid particles.

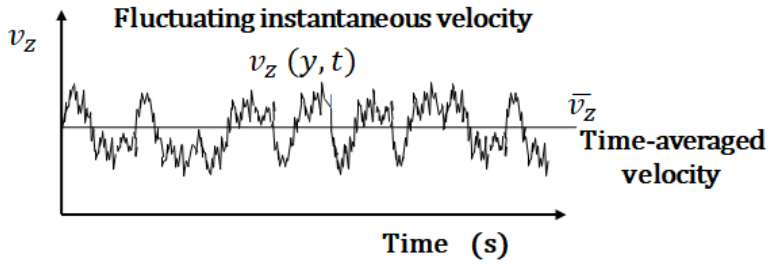

Fig.3.2-3. Velocity fluctuations in turbulent flow

When the flow rate goes beyond a certain critical value, the laminar shear flow near the wall becomes unstable due to the rotational moment causing eddy motion, and then the transition to turbulent flow occurs.

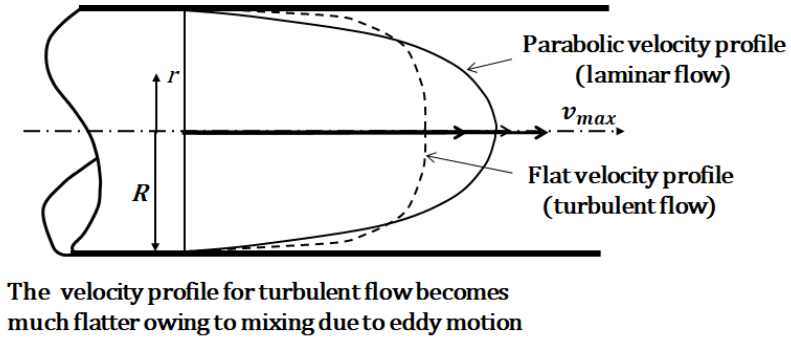

Fig.3.2-4. Characteristics of turbulent flow in a circular pipe

For turbulent pipe flow, therefore, the distribution of time-averaged velocity is much flatter in the main flow region and very steep near the pipe wall.
A semi-empirical equation of the time-averaged velocity distribution is given by

$$\bar{v}_z = v_{max}\,[1 - (r/R)]^{1/7} \qquad (3.2\text{-}1)$$

This expression known as the "1/7th power law gives a good approximation for the Reynolds number range 10^4 to 10^5. It should be kept in mind that this law cannot describe precisely the turbulent structure of the flow field.

The Reynolds number is a product of a characteristic velocity, a characteristic length, and the density of the fluid divided by its viscosity. The result is a dimensionless number which represents the ratio of the inertial to the viscous forces in the fluid. The critical Reynolds number depends, in general, upon the surface condition of the inside wall of the pipe.

$$Re = \frac{V\,D\,\rho}{\mu}[-] = \frac{\text{inertial force}}{\text{viscous force}} \qquad (3.2\text{-}2)$$

[Problem 3.2-P1] Obtain a relation between the mean (flow-area-average) velocity v_z and the maximum velocity v_{zmax} for turbulent flow inside a circular pipe using the 1/7th power law.

[Problem 3.2-P2] An aqueous solution of sodium hydroxide is flowing at a volumetric flow rate of 50 m^3/h in a circular pipe of inside diameter of 100 mm. The density and viscosity of the solution

at 50 C (= 323 K)b are 1,510 kg/m^3 and 0.025 kg/m s, respectively. Calculate the Reynolds number.. Is the flow turbulent?

[Problem 3.2-P3] A viscous liquid ($\mu = 50$ cp. = 0.05 kg/m s, $\rho = 1{,}050$ kg/m^3) is flowing in a 50 mm ID circular tube. The velocity distribution is described by the following equation:

$v_z = v_{zmax}\,[1 - (r/R)^2]$

where v_z is the axial velocity in m/s and r the radial coordinate in m. The maximum velocity $v_{zmax} =$ 0.5 m/s and the pipe radius $R = 0.025$ m. Calculate the friction force acting over 5 m of the inside surface of the tube, the flow rate, and the Reynolds number.

Answer: 25.12 N, 4.91 m^3/s, and *Re* = 262.5.

[Problem 3.2-P4] In the above problem, the velocity gradient on the inner wall of the pipe is given for laminar flow in a term of average velocity by

$$\left.\frac{dv_z}{dr}\right|_{r=R} = -\frac{4\,v_{av}}{R}$$

If the critical Reynolds number Re_{cr} is given as 2,100, what is the critical velocity gradient?

Answer: - 320 (1/s)

Nomenclature

D	characteristic length or pipe diameter, [m]
r, θ, z	cylindrical coordinates, [m, - , m]
R	pipe radius, [m]
V	characteristic velocity, [m/s]
v_z	axial velocity component in pipe flow, [m/s]
y	distance from pipe wall
τ_q	torque, [Nm]
Re	Reynolds number, [-]

CHAPTER 4

MACROSCOPIC BALANCES: CONTROL VOLUME APPROACH

4.1 Principles of Momentum, Energy, and Mass Conservation

In this course, the laws of conservation of momentum, conservation of energy, and conservation of mass may be stated for a general control volume as follows:

$$\begin{pmatrix} rate\ of \\ momentum \\ accumulation \end{pmatrix} = \begin{pmatrix} rate\ of \\ momentum \\ IN \end{pmatrix} - \begin{pmatrix} rate\ of \\ momentum \\ OUT \end{pmatrix} + \begin{pmatrix} sum\ of\ exyternal \\ forces\ acting \\ on\ system \end{pmatrix} \tag{4.1-1}$$

$$\begin{pmatrix} rate\ of \\ energy \\ accumulation \end{pmatrix} = \begin{pmatrix} rate\ of \\ energy \\ IN \end{pmatrix} - \begin{pmatrix} rate\ of \\ energy \\ OUT \end{pmatrix} + \begin{pmatrix} rate\ of\ work \\ done\ by\ the \\ surroundings \end{pmatrix} \tag{4.1-2}$$

$$\begin{pmatrix} rate\ of \\ mass \\ accumulation \end{pmatrix} = \begin{pmatrix} rate\ of \\ mass \\ IN \end{pmatrix} - \begin{pmatrix} rate\ of \\ mass \\ OUT \end{pmatrix} \tag{4.1-3}$$

$$\begin{pmatrix} rate\ of \\ mass\ of\ A \\ accumulation \end{pmatrix} = \begin{pmatrix} rate\ of \\ mass\ of\ A \\ IN \end{pmatrix} - \begin{pmatrix} rate\ of \\ mass\ of\ A \\ OUT \end{pmatrix} + \begin{pmatrix} rate\ of\ production \\ of\ mass\ of\ A\ by \\ homogeneous \\ chemical\ reactions \end{pmatrix} \tag{4.1-4}$$

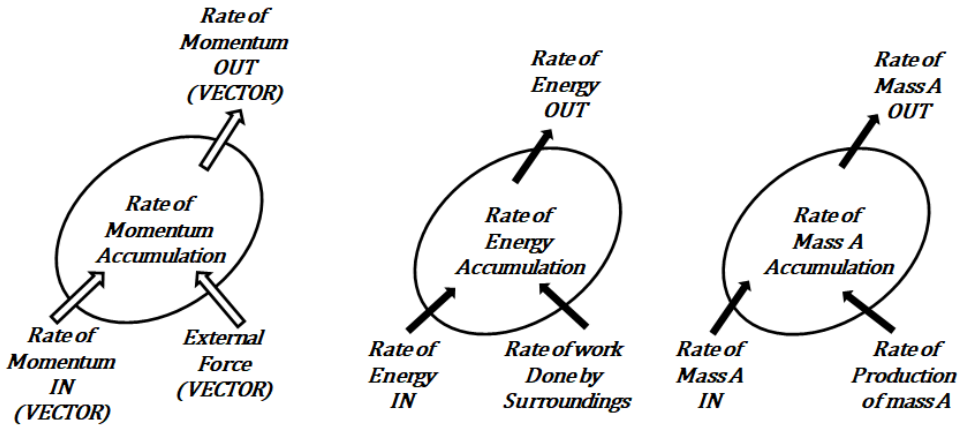

Fig. 4.1-1. Shell balances of momentum, energy, and mass of component A over a control volume

4.2 Macroscopic Mass Balance

The mass balance should be set up over a control volume shown in Fig.4.2-1.

The mass present at t in some arbitrary small volume within the control volume is $\rho\Delta V$. Therefore the mass of the control volume at t is

$$m = \int_V \varrho\, dV \tag{4.2-1}$$

where density $\rho = \rho(x, y, z, t)$.

Accumulation of mass in time Δt is the difference between the mass in the control volume at t and that at $t + \Delta t$:

$$\int_V \varrho \, dV\Big|_{t+\Delta t} - \int_V \varrho \, dV\Big|_t = \frac{d}{dt} \int_V \varrho \, dV \cdot \Delta t \qquad (4.2\text{-}2)$$

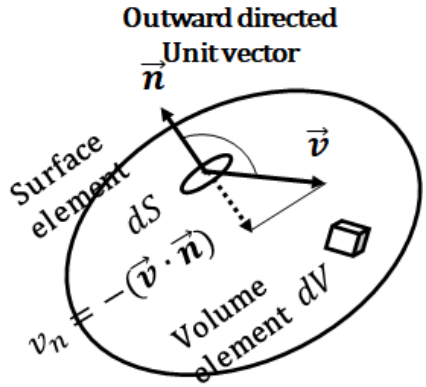

Fig.4.2-1. Macroscopic mass balance

The mass can be transferred by velocity component normal to the surface, so the velocity component v_n into the control volume can be expressed as

$$v_n = -(\vec{v} \cdot \vec{n}) = -v \cos \alpha \qquad (4.2\text{-}3)$$

where $\vec{n}$ is the outward directed unit vector normal to the surface at that point and α is the angle between $\vec{v}$ and $\vec{n}$.

The rate of mass transferred = (mass)/(unit time) = (mass/unit volume)(length/unit time)(area)

This is the net rate of mass in over the whole surface of the control volume $= \int_S \rho \, v_n dS$

Then application of the principle of mass conservation yields

$$\frac{d}{dt} \int_V \rho \, dV = -\int_S \rho \, (\vec{v} \cdot \vec{n}) \, dS \qquad (4.2\text{-}4)$$

This is the macroscopic mass balance.

For a simpler flow system shown below

$$\frac{dm}{dt} = \rho_1 \langle \boldsymbol{v_1} \rangle S_1 - \rho_2 \langle \boldsymbol{v_2} \rangle S_2 \qquad (4.2\text{-}5)$$

Introducing the symbol of mass flow rate

$$w = \rho \langle v \rangle S = -\int_S \rho \, (\vec{v} \cdot \vec{n}) \, dS \qquad (4.2\text{-}6)$$

to get the unsteady-state macroscopic mass balance:

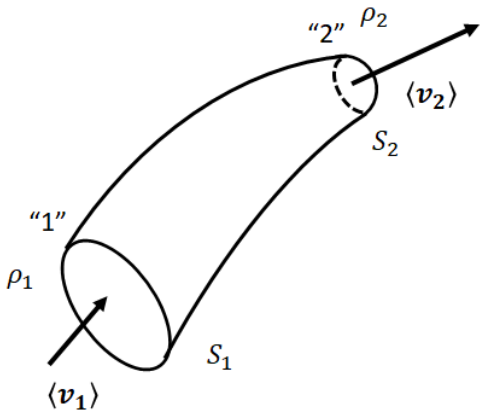

Fig.4.2-2. Simpler pipe system with a single inlet and a single exit

$$\frac{dm}{dt} = -\Delta w \tag{4.2-7}$$

For steady state

$$\Delta w = 0 \quad \text{or} \quad w_2 = w_1 \tag{4.2-8}$$

[Problem 4.2-P1] A pipe system shown is carrying water through section 1 at an average velocity of 0.3 m/s in steady state. The diameter at section l is 0.3 m. The same flow passes through section 2 where the diameter is 0.1 m. Find the average velocity at section 2.

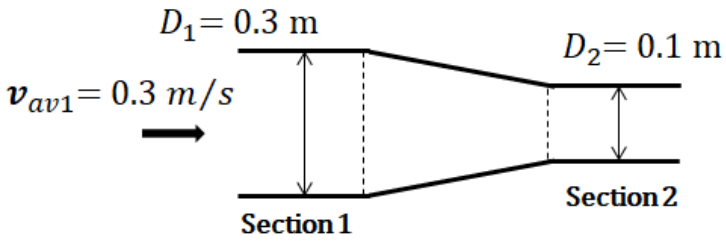

Fig.4.2-P1. Mass balance in a horizontal pipe accompanied with contraction of cross section

4.3 Macroscopic Momentum Balance

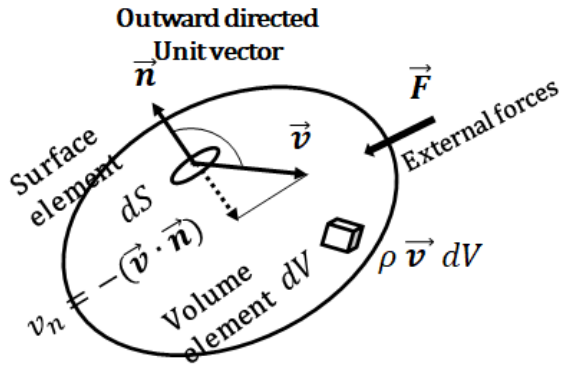

Fig.4.3-1 Control volume for macroscopic momentum balance

Consider a small surface element of area ΔS of a control volume, through which momentum $\rho\,\vec{v}$ is entering or leaving. The rate of momentum entering or leaving through ΔS may be written as

$$(\rho\,\vec{v})\ v_n\,dS = (\rho\ \vec{v})[-(\vec{v}\cdot\vec{n})dS] \tag{4.3-1}$$

Here the minus sign is necessary since the unit vector $\vec{n}$ is outward directed. Therefore the net rate of momentum in over the whole surface of the control volume is

$$-\int_S \rho\,\vec{v}\ (\vec{v}\cdot\vec{n})dS \tag{4.3-2}$$

Since the momentum in a small volume element ΔV is $\rho\,\vec{v}\,\Delta V$, the rate of momentum accumulation in the control volume is

$$\frac{d}{dt}\int_V \rho\,\vec{v}\,dV \tag{4.3-3}$$

The sum of external forces acting on the system is $\sum\vec{F}$.

Applying the principle of momentum conservation,

$$\frac{d}{dt}\int_V \rho\,\vec{v}\,dV = -\int_S \rho\,\vec{v}\ (\vec{v}\cdot\vec{n})dS + \sum\vec{F} \tag{4.3-4}$$

This is the macroscopic momentum balance corresponding to Newton's second law of motion. Note

that the force term $\sum \vec{F}$ comprises viscous forces $\sum \vec{F_f}$, pressure force $-\int_S p\,\vec{n}\,dS$, and gravitational force $m\,\vec{g}$ acting on the fluid.
For steady state the left side of the above equation is zero

$$-\int_S \rho\,\vec{v}\,(\vec{v}\cdot\vec{n})dS + \sum \vec{F} = 0 \qquad (4.3\text{-}5)$$

For turbulent pipe flow the following approximation may be employed for cross-sectional averaging.

$$\langle v\rangle \cong \langle v^2\rangle/\langle v\rangle \qquad (4.3\text{-}6)$$

For turbulent pipe flow, therefore, the force acting on the pipe wall is given by

$$\vec{F'} = -\vec{F_f} = w_1\langle\vec{v_1}\rangle - w_2\langle\vec{v_2}\rangle - p_1S_1\vec{n_1} - p_2S_2\vec{n_2} + m\,\vec{g} \qquad (4.3\text{-}7)$$

Note that the unit vectors are outward directed.

For an incompressible flow in a straight pipe (inside diameter D, length L) inclined by θ, the friction force acting on the inside surface of the pipe is given by the following familiar equation of force balance:

$$F' = (p_0 - p_L)\frac{\pi}{4}D^2 + \frac{\pi}{4}D^2L\,\rho g\,\cos\theta = \tau_w\,\pi DL \qquad (4.3\text{-}8)$$

This result indicates that the net force acting downstream on the cylindrical fluid column by virtue of the pressure difference and gravitational acceleration is balanced by the friction force the pipe wall exerts. The above equation is valid whether the flow is laminar or turbulent.

[Example 4.3-E1] Consider the problem of finding the force exerted on a horizontal 90 degree pipe bend. Water at 20°C is flowing at a rate of 700 kg/s for cooling in an oil refinery. The pipeline is 300 mm ID steel pipe. A diagram of the pipe bend and the quantities relating to the analysis are shown in Figure 4.3-E1.

[Solution] Actually there will be a small pressure drop caused by viscous force acting on the piped bend wall. At this point, however, we assume negligibly small pressure drop between sections "1" and "2". The first step is to choose as the control volume the region bounded by two planes "1" and "2" normal to the streamliners and the inner wall of the bend. Assuming turbulent flow (almost flat velocity distribution), the overall momentum balance may be written, term by term, as

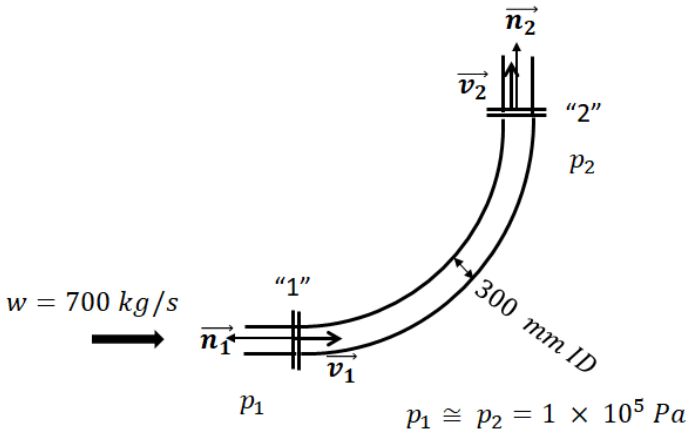

Fig.4.3-E1 Force acting on 90 degree bend

$$-\int_S \rho\vec{v}\,(\vec{v}\cdot\vec{n})dS = -\int_{S_1} \rho\vec{v}\,(\vec{v}\cdot\vec{n})dS - \int_{S_2} \rho\vec{v}\,(\vec{v}\cdot\vec{n})dS = w_1\vec{v_1} - w_2\vec{v_2} \qquad (4.3\text{-}E1)$$

There is a sign difference because α (the angle between $\vec{v}$ and $\vec{n}$ **)** is 180 degree at the inlet "1" and 0 degree at the outlet 2".
For the macroscopic mass balance

$$w_1 = w_2 = w = const$$

And volumetric flow rate $Q_1 = Q_2 = Q = const$

Therefore for steady state, Eq.(4.3-4) becomes

$$w\,(\overrightarrow{v_2} - \overrightarrow{v_1}) = \sum \overrightarrow{F} \qquad \text{(4.3-E2)}$$

where $\overrightarrow{v_1} = Q(-\overrightarrow{n_1})/S$ and $\overrightarrow{v_2} = Q\,\overrightarrow{n_2}/S$

Then

$$\sum \overrightarrow{F} = \left(\frac{Q}{S}\right)(\overrightarrow{n_2} + \overrightarrow{n_1})w \qquad \text{(4.3-E3)}$$

Since the pipeline is horizontal, we do not have to consider the gravitational effect. The total force on the fluid is made up of the pressure force $\overrightarrow{F_p}$ and the force exerted by the bend $\overrightarrow{F_b}$.

$$\overrightarrow{F_p} = -p\,S\,(\overrightarrow{n_1} + \overrightarrow{n_2}) \qquad \text{(4.3-E4)}$$

Here we used the assumption of equal pressure at sections "1" and "2". Recall that the force sought is the reaction to $\boldsymbol{F_b}$ and has components equal in magnitude and opposite in sense to $\boldsymbol{F_b}$.

$$\overrightarrow{F_b} = \left(\frac{Q}{S}\right)w(\overrightarrow{n_1} + \overrightarrow{n_2}) + p\,S\,(\overrightarrow{n_1} + \overrightarrow{n_2}) = \left(\frac{wQ}{S} + p\,S\right)(\overrightarrow{n_1} + \overrightarrow{n_2}) \qquad \text{(4.3-E5)}$$

It remains to insert the numerical values:

$$\overrightarrow{F_b} = \left[\frac{\left(700\frac{kg}{s}\right)^2}{\left(1000\frac{kg}{m^3}\right)(0.0707\,m^2)} + (1 \times \frac{10^5\,N}{m^2})(0.0707\,m^2)\right] \times (\overrightarrow{n_1} + \overrightarrow{n_2}) = 1.4 \times 10^4(\overrightarrow{n_1} + \overrightarrow{n_2})\ \text{N}$$

The force acting on the bend $\overrightarrow{F'_b} = -\overrightarrow{F_b}$.

[Problem 4.3-P1] Water 20℃ is flowing at a rate of $Q = 5 \times 10^{-2}\ m^3/s$ through a horizontal convergent pipe shown below. The upstream pressure is $p_1 = 2 \times 10^5$ Pa. Calculate the pressure p_2 at the end of the converging section and the force acting on the convergent section. Assume the friction loss negligibly small in the converging section.

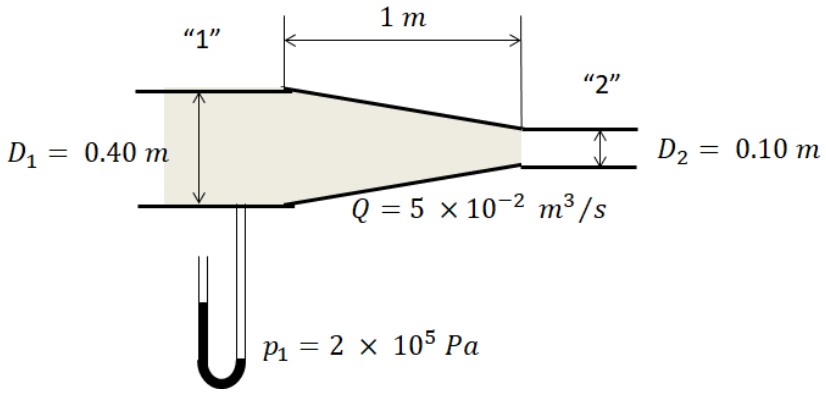

Fig.4.3-P1 Fluid force acting on the wall of a horizontal convergent pipe

4.4 Macroscopic Energy Balance

In this section, we shall deduce a macroscopic balance of energy in general form from the beginning to get the first law of thermodynamics. This deductive part may be skipped in case of time limitation.

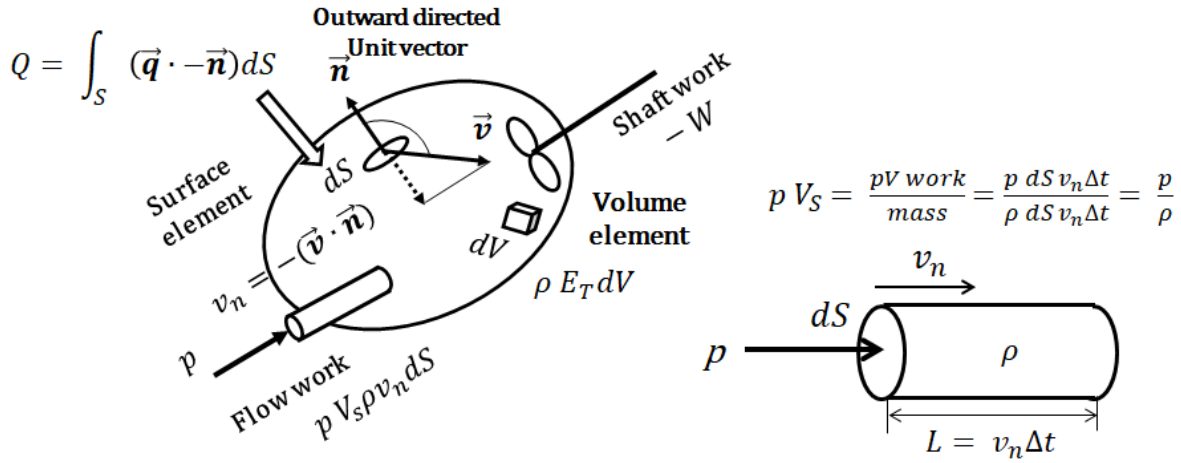

Fig.4.4-1 Control volume for macroscopic energy balance

Energy associated with mass can be classified: potential energy E_p, kinetic energy E_k, and internal energy E_u.

Strictly speaking, the rate of the total energy $E_T = E_p + E_k + E_u$ accumulation in the control volume is given by

$$\frac{d}{dt} \int_V \rho E_T \, dV \qquad (4.4\text{-}1)$$

The net rate of energy in over the whole surface of the control volume is

$$\int_S E_T \rho v_n dS = -\int_S E_T \rho(\vec{v} \cdot \vec{n}) \, dS \qquad (4.4\text{-}2)$$

To get the mass of fluid inside the control volume, some of the fluid should be compressed into the control volume. To do work on the surroundings, the boundary of the control volume should be expanded. This is called "flow work". The flow work required to add a unit mass to the control volume can be written as (pressure) (specific volume) $p V_s$ like piston work. Therefore the flow work is

$$W_f = -\int_S p V_s \rho(\vec{v} \cdot \vec{n}) \, dS \qquad (4.4\text{-}3)$$

According to thermodynamics, enthalpy is expressed as $H_e = E_u + p V_s$. Hence the net rate of energy transferred across the boundary with mass becomes

$$-\left[\int_S E_T \rho(\vec{v} \cdot \vec{n}) \, dS + \int_S p V_s \rho(\vec{v} \cdot \vec{n}) \, dS\right] = -\int_S \left(H_e + E_k + E_p\right)\rho(\vec{v} \cdot \vec{n}) \, dS \qquad (4.4\text{-}4)$$

The thermal energy not associated with mass crossing the boundary per unit volume is Q (thermal energy into the system is regarded positive). Finally applying the principle of energy conservation we get

$$\frac{d}{dt} \int_V \rho E_T \, dV = -\int_S \left(H_e + E_k + E_p\right)\rho(\vec{v} \cdot \vec{n}) \, dS + Q - W \qquad (4.4\text{-}4)$$

This is a general form of macroscopic energy balance.

<Simplification of the macroscopic energy balance>

For a flow system having a single fluid entrance (at plane "1" with cross-sectional area S_1) and a single exit (at plane "2" with cross-sectional area S_2), the macroscopic energy balance reduces to

$$\begin{aligned}\frac{d}{dt} \int_V \rho E_T \, dV &= -\int_{S_1} \left(H_{e1} + E_{k1} + E_{p1}\right)\rho_1(\overrightarrow{v_1} \cdot \overrightarrow{n_1}) dS_1 \\ &\quad - \int_{S_2} \left(H_{e2} + E_{k2} + E_{p2}\right)\rho_2(\overrightarrow{v_2} \cdot \overrightarrow{n_2}) dS_2 + Q - W \\ &= (H_{e1} + E_{k1} + E_{p1})\rho_1\langle v_1\rangle S_1 - \left(H_{e2} + E_{k2} + E_{p2}\right)\rho_2\langle v_2\rangle S_2 + Q - W \\ &= -\Delta\left[\left(H_e + E_k + E_p\right)w\right] + \mathrm{Q} - \mathrm{W} \qquad (4.4\text{-}5)\end{aligned}$$

Here $\langle \ \rangle$ means cross-sectional area-averaged value and $w = \rho\langle v\rangle S$ is mass flow rate.

Strictly speaking, the above simplification is valid only when the density and other quantities

H_e, E_k, E_p, E_T do not vary very much across the cross section at planes "1" and "2". Especially for the kinetic energy term, the flow should be turbulent, which has nearly flat velocity profiles. Usually the kinetic energy and potential energy in the constant gravitational field can be written as $(1/2)\,\rho v^2 + \rho\, g\, h$.

Finally the above equation becomes

$$\frac{dE_{Tot}}{dt} = -\Delta\left[\left(H_e + \frac{1}{2}\langle v\rangle^2 + g\,h\right)w\right] + Q - W \tag{4.4-6}$$

Here $E_{Tot} = \int_V \rho\, E_T\, dV = \int_V \rho\left(E_u + E_k + E_p\right)dV$

This is a form of the first law of thermodynamics applied to a flow system, which may be regarded as the starting equation for dealing with energy-related chemical engineering applications.

Dividing through by constant mass flow rate w at steady state:

$$-\Delta\left(H_e + \frac{1}{2}\langle v\rangle^2 + g\,h\right) + Q_m - W_m = 0 \tag{4.4-7}$$

Here Q_m is the heat added per unit mass of the fluid into the system and W_m is the amount of work done per unit mass of the fluid on the surroundings.

This equation can be further simplified into a convenient form.

For ideal gases ($p\,V = (1/M)\,R\,T$)

$$\int_{T_1}^{T_2} C_p\, dT + \Delta\frac{1}{2}\langle v\rangle^2 + g\,\Delta h = Q_m - W_m \tag{4.4-8}$$

For incompressible fluids ($\rho = const,\ C_v = C_p$)

The enthalpy change is given as

$$\Delta H_e = \Delta E_u + \Delta(p\,V_s) = \Delta E_u + V_s\Delta p = \Delta E_u + (1/\rho)\,\Delta p \tag{4.4-9}$$

Then

$$\int_{T_1}^{T_2} C_p\, dT + \frac{p_2 - p_1}{\rho} + \Delta\frac{1}{2}\langle v\rangle^2 + g\,\Delta h = Q_m - W_m \tag{4.4-10}$$

The above equation is usually applied for a flow system accompanied with heat input or output.

4.5 Mechanical Energy Balance

The equation of mechanical energy balance called "Bernoulli equation" is very important and useful for practical applications to various piping designs.

For a flow system without heat exchange ($Q_m = 0$)

$$\Delta H_e = \Delta E_h + \Delta(pV_s) = T\,\Delta S + V_s\Delta p \tag{4.5-1}$$

The presence of friction renders the process irreversible owing to the frictional heating. That is,

$$T\,\Delta S = Q_m + Fr_m \quad \text{Therefore} \quad \Delta H_e = Q_m + Fr_m + V_s\Delta p. \tag{4.5-2}$$

where Fr_mindicates the thermal energy generation transformed from mechanical energy.

Substituting this into the steady-state energy balance equation

$$\int_{p_1}^{p_2} V_s\, dp + \Delta\frac{1}{2}\langle v\rangle^2 + g\,\Delta h = -Fr_m - W_m \tag{4.5-3}$$

This is a generalized form of "Bernoulli equation" which is applicable to both ideal gases and incompressible fluids. Here Fr_m is the rate of mechanical energy loss per unit mass due to the frictional effect. This indicates that a part of mechanical energy is irreversibly converted to thermal energy due to viscous dissipation. The mechanical energy loss Fr_m is often called "friction loss". For steady-state isothermal case with no additional heat input, the rate of thermal energy produced by viscous dissipation becomes equal to the rate of heat removed from the control volume.

For ideal gases ($V_s = (R\,T/M)(1/p)$

$$\frac{R\,T}{M}\ln\frac{p_2}{p_1} + \Delta\frac{1}{2}\langle v\rangle^2 + g\,\Delta h = -Fr_m - W_m \tag{4.5-4}$$

For incompressible fluids ($V_s = 1/\rho = const$)

$$\frac{p_2 - p_1}{\rho} + \Delta\frac{1}{2}\langle v\rangle^2 + g\,\Delta h = -Fr_m - W_m \tag{4.5-5}$$

For laminar flow the kinetic energy term $\Delta(1/2)\langle v\rangle^2$ should be replaced by $\Delta\langle v\rangle^2$ because the parabolic velocity distribution gives the relation: $\langle v^3\rangle/\langle v\rangle = 2\,\langle v\rangle^2$.

[PROBLEM 4.5-P1] Ideal gas (molecular weight $M = 29$) is in isothermal turbulent flow at temperature $T = 298$ K (= 25℃) through a straight horizontal pipe with cross section $S = 3.14 \times 10^{-2}\ m^2$. The absolute pressures at reference planes "1" and "2" are $p_1 = 1.013 \times 10^5\ Pa$ (= $1\ atm$) and $p_2 = 0.87 \times 10^5\ Pa$, respectively. The mass flow rate measured is $w = 0.15\ kg/s$. Evaluate $Fr_{21} = w\,Fr_{m21}$ in $kg\ m^2/s^3$ from the length $L = 20\ m$ of pipe between "1" and "2". The gas constant is given by $R = 8.314 \times 10^3\ (kg\ m^2/s^2)/kmol\ K$.

[PROBLEM 4.5-P2] Water flows through a turbine at an average velocity of 10 m/s at the entrance of flow cross section 0.1 m^2. The static pressures are 1 MPa at the entrance and 2 MPa at the outlet of flow cross section 0.3 m^2. The elevation difference between the entrance and outlet is 10 m. Calculate the theoretical power assuming negligibly small viscous dissipation.

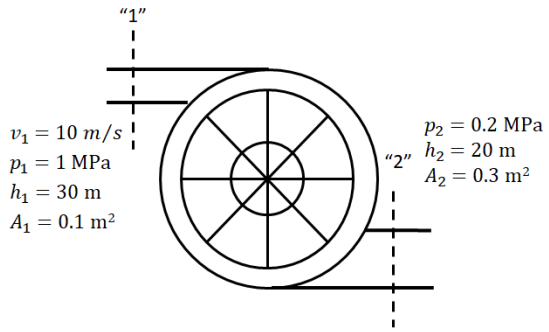

Fig.4.4-P2. Calculation of power obtained by water turbine

[EXAMPLE 4.5-E1] A fireboat has a circular convergent nozzle shown below. A jet of water ($\rho = 1{,}000\ kg/m^3$) issues from the nozzle at an average velocity of $100\ m/s$. Assuming negligible friction loss and gravitational effect, determine the static pressure p_1 at plane "1" and the horizontal component of the force required to keep the nozzle stationary. This nozzle is placed on an angle of 30 degree with the horizontal. The nozzle exit diameter is 80 mm and the diameter of the upstream pipe is 150 mm.

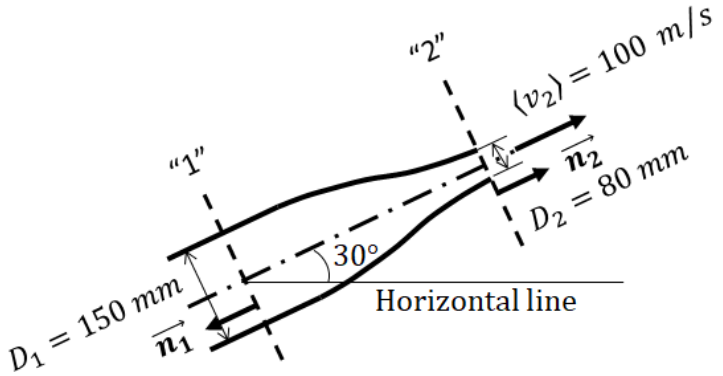

Fig.4.5-E2. Circular convergent nozzle

Solution: Assuming turbulent flow with incompressible fluid, the mechanical energy balance can be applied to this system as

$$\frac{1}{2}\langle v_2\rangle^2 - \frac{1}{2}\langle v_1\rangle^2 + \frac{p_2 - p_1}{\rho} = 0 \qquad (4.5\text{-E1})$$

where $g\,\Delta h = 0$, $Fr_{m21} = 0$ and $W_m = 0$ are assumed.

Then for steady-state flow of incompressible fluid, the upstream pressure is given by

$$p_1 = \frac{1}{2}\rho\,(\langle v_2\rangle^2 - \langle v_1\rangle^2) + p_2 \quad \text{(4.5-E2)}$$

$$w = \rho\langle v_2\rangle S_2 = \rho\langle v_1\rangle S_1 = const \quad \text{(4.5-E3)}$$

At the nozzle exit the pressure p_2 becomes atmospheric pressure.
Therefore

$$\langle v_1\rangle = (S_2/S_1)\langle v_2\rangle = (80/150)^2\,(100\ m/s) = 28.4\ m/s \quad \text{(4.5-E4)}$$

Then

$$p_1 = (1/2)(1000\ kg/m^3)[(100\ m/s)^2 - (28.4\ m/s)^2] + 1.013 \times 10^5\ Pa$$
$$= 4.70 \times 10^6\ Pa = 4.70\ MPa \quad \text{(4.5-E5)}$$

At the nozzle exit the pressure becomes atmospheric pressure.
The mass flow rate is calculated as

$$w = \rho\langle v\rangle S = (1000\ kg/m^3)(100\ m/s)(\pi/4)(0.08\,m)^2 = 502.7\ kg/s \quad \text{(4.5-E6)}$$

Applying the momentum balance to this system with $m_{tot}g = 0$ assumed,

$$\vec{\boldsymbol{F}} = -(\overrightarrow{\boldsymbol{v_2}}w - \overrightarrow{\boldsymbol{v_1}}w) - (p_2S_2\boldsymbol{n_2} + p_1S_1\boldsymbol{n_1}) \quad \text{(4.5-E7)}$$

The force acting on the nozzle in the direction of nozzle axis is given by

$$F = -(502.7\ kg/s)(100\ m/s - 28.4\ m/s) - (1.013 \times 10^5\ kg/m\,s^2)$$
$$\times (\pi/4)(0.08\,m)^2 + (4.70 \times 10^6\ kg/m\,s^2)(\pi/4)(0.15\,m)^2$$
$$= 4.66 \times 10^4\ kg\,m/s^2 = 4.66 \times 10^4\ N \quad \text{(4.5-E8)}$$

The horizontal force required to keep the nozzle stationary is

$$F_x = F\cos 30° = (4.66 \times 10^4)\sqrt{3}/2 = 4.04 \times 10^4\ N \quad \text{(4.5-E9)}$$

[EXAMPLE 4.5-E2] To measure the friction loss of a glove valve, we use a horizontal pipeline with a constant cross section shown. We use water (density ρ_w) as the flowing fluid and mercury (density ρ_m) as the manometer fluid. Determine the friction loss when the manometer reading is h. Assume that the friction losses in the sections l_1 and l_2 are small compared with that of the valve.
Solution: Use the macroscopic mechanical energy balance for incompressible, isothermal flow between the pressure taps

$$\frac{p_2 - p_1}{\rho_w} + \Delta\frac{1}{2}\langle v\rangle^2 + g\,\Delta h = -Fr_m - W_m \quad \text{(4.5-E10)}$$

Since $\langle v_1\rangle = \langle v_2\rangle$, $\Delta\frac{1}{2}\langle v\rangle^2 = 0$ for a pipe with constant cross section.
$\Delta h = 0$ for a horizontal pipeline. There is no power equipment in the system $W_m = 0$

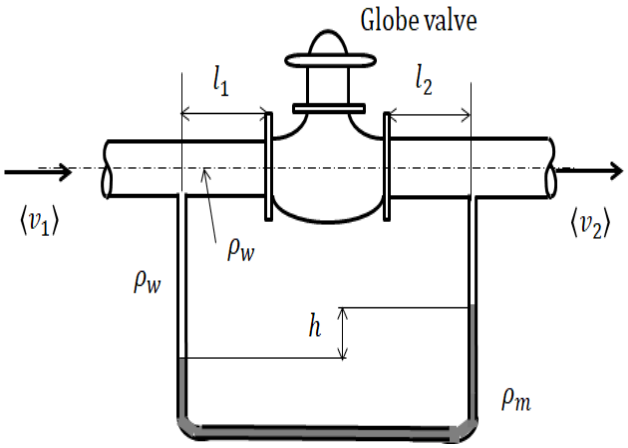

Fig.4.5-E2. Determination of friction loss for a globe valve

From the force balance of the stationary fluids in the manometer

$$p_1 - p_2 = (\rho_m - \rho_w)g\,h \quad \text{(4.5-E11)}$$

Then we get the friction loss

$$Fr_m = \frac{\rho_m - \rho_w}{\rho_w}\,g\,h \quad \text{(4.5-E12)}$$

[EXAMPLE 4.5-E3] Pitot tube for velocity measurement

One of the most common, traditional devices for measuring velocity distributions in a flowing stream is the pitot tube. As shown in Fig.4.5-E3, it consists of two concentric tubes, the inner one of which is open at the end and the outer one is sealed at the same end of the inner tube. The side wall of the outer tube near the front tip has several small drilled holes.

Both tubes are filled with the flowing fluid and connected to the opposite ends of a manometer. The pitot tube is placed to confront the opening of the inner tube (impact-tube opening) with the velocity to be measured. As the fluid impinges on the impact-tube opening, its kinetic energy is converted to pressure energy (sometimes called dynamic pressure).

Along a streamline the mechanical energy balance with an assumption of incompressible fluid is applicable over the short distance of the approaching flow from 1 to 2:

$$\frac{1}{2}\,v^2 - 0 + \frac{p_s - p_t}{\rho} = 0 \quad \text{or}$$

$$v = \sqrt{\frac{2\,(p_t - p_s)}{\rho}} \tag{4.5-E13}$$

where the impact pressure $(1/2)\,\rho\,v^2$ is the difference between the static pressure p_t at the impact-tube opening and the static pressure p_s of the stream. The pressure acting on the side holes of the outer tube is approximately equal to p_s because the streamlines near the side wall are almost parallel to the side wall.

The relation of manometer reading h with the velocity v is

$$v = \sqrt{\frac{2\,(\rho_m - \rho)g\,h}{\rho}} \tag{4.5-E14}$$

where ρ_m is the density of manometer fluid. The pitot tube responds slowly to changing velocities owing to inertia effect, so it can measure only the time-averaged velocity in the turbulent flow.

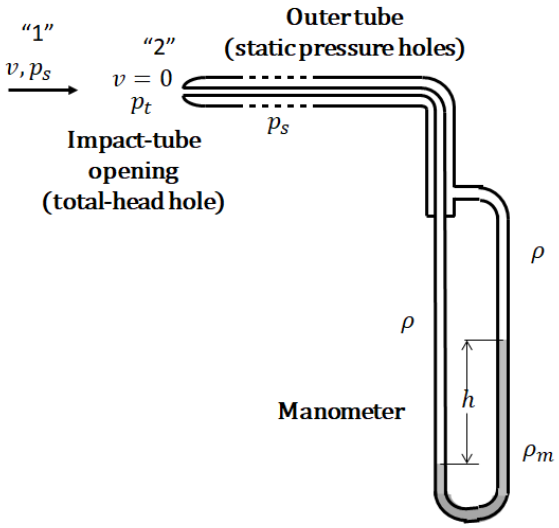

Fig.4.5-E3. Pitot tube

[PROBLEM 4.5-P3] The following table is some experimental data for a Pitot tube traverse for the flow of water (temperature 20℃) inside a circular tube of 60 mm ID. The manometer fluid is carbon tetra chloride (density $\rho_m = 1{,}600$ kg/m^3).

Calculate the local velocities and plot those data to obtain the power-law expression for the velocity distribution. What is the Reynolds number?

Position of Pitot tube Radial distance from the pipe axis (mm)	Manometer readings (mm)
0.0	375
2.0	364
5.0	357
10.0	330
15.0	300
20.0	268
25.0	225
27.0	202
28.0	168
29.0	140
29.5	119
29.8	93

[EXAMPLE 4.5-E4] As shown in Fig.4.5-P1, let us consider an orifice-flowmeter installed in the straight section of a horizontal circular tube (inside diameter D_1).

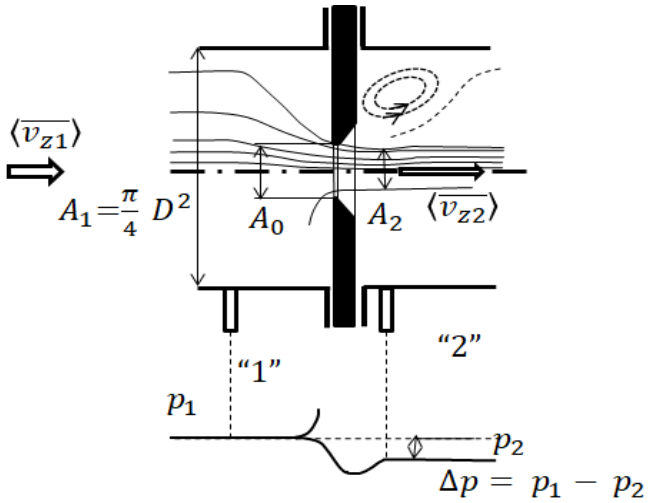

Fig.4.5-E4. Orifice flowmeter

The orifice circular plate has a hole in the middle, the sharp edge of which has a very short straight section of diameter D_0. The following mechanical energy balance of a constant density fluid flow is set up over the region between planes "1" and "2" located at the two pressure taps under a condition of no work effect and no potential energy change:

$$\frac{\langle \overline{v_{z2}} \rangle^2}{2} - \frac{\langle \overline{v_{z1}} \rangle^2}{2} + \frac{p_2 - p_1}{\rho} + \varsigma \frac{1}{2} \langle \overline{v_{z2}} \rangle^2 = 0 \qquad (4.5\text{-E15})$$

where ς is called "friction loss factor" (dimensionless). The last term gives the friction loss caused by an abrupt change in the cross-sectional flow area $A_1 \rightarrow A_2$. Usually for highly turbulent flow, the flow cross-sectional area is changed from A_0 to A_2. Here the A_2 indicates the flow cross-sectional area at the most-contracted position.

The minimum flow area is called "Vena-contracta." Owing to a complicated flow pattern, only for simplicity, the so-called contraction coefficients α_1 are assumed to be unity in front of the first term. The contraction coefficient is defined as

$\alpha = A_2/A_0$

, which is varied with $m = A_0/A_1$. Therefore $\langle \overline{v_{z2}} \rangle = \langle \overline{v_{z1}} \rangle A_1/A_2$

According to the continuity condition,

$A_1 \langle \overline{v_{z1}} \rangle = A_2 \langle \overline{v_{z2}} \rangle$. For engineering convenience, the discharge coefficient C_d is introduced

instead of making α_2 to be unity, and then $\langle\overline{v_{z1}}\rangle = C_d m \langle\overline{v_{z2}}\rangle$. The discharge coefficient of a given installation varies mainly with the Reynolds number. After all, the average velocity at the most-contracted position can be obtained as

$$\langle\overline{v_{z2}}\rangle = \frac{1}{\sqrt{1-{C_d}^2 m^2}} \sqrt{\frac{2(p_1-p_2)}{\rho}} \tag{4.5-E16}$$

Then the velocity at the hole of the orifice is given by

$$\langle\overline{v_z}\rangle_0 = \left(\xi C_d / \sqrt{1-{C_d}^2 m^2} \right) \sqrt{2(p_1 - p_2)/\rho} \tag{4.5-E17}$$

As a result, the volumetric flow rate is given by the following equation:

$$V = \langle\overline{v_z}\rangle_0 A_0 = C_c A_0 \sqrt{2(p_1 - p_2)/\rho} \tag{4.5-E18}$$

Here C_c is the correction coefficient taking into account the effect of $\xi C_d / \sqrt{1-{C_d}^2 m^2}$.

Even for liquid flows, the calibration of flowmeters is necessary.

For compressible fluids, deviation from isentropic conditions is significant, and the calibration of orifice flowmeters to be used with gases must be carried out by means of the gasometer system.

4.6 Thermal Energy Balance for non-Isothermal System

For non-isothermal flow system, kinetic and potential energy effects are negligibly small compared with thermal energy term. For many practical problems of heat transfer, therefore, the energy balance reduces to

$$\Delta H_e = Q_m - W_m \tag{4.6-1}$$

Hence the friction loss term can be neglected except when the mechanical energy loss should be determined. If the system does not have a pump or other work-producing device (e.g. turbine and mixing stirrer), the enthalpy balance equation reduces to the following simple form:

$$\Delta H_m = Q_m \tag{4.6-2}$$

[EXAMPLE 4.6-E1] Consider an incompressible fluid like water flowing through the pipeline shown below, which comprises a pump and a heat exchanger connected by a circular pipe with constant cross-sectional area.

(I) pump: Consider the subsystem including the pump and the short horizontal pipe length between planes "1" and "2". The energy balance becomes

$$-\Delta\left(H_m + \frac{1}{2}\langle v\rangle^2 + g\,h\right) + Q_m - W_m = 0 \tag{4.6-E1}$$

The mechanical energy balance is

$$\int_{p_1}^{p_2} V_s\, dp + \Delta\frac{1}{2}\langle v\rangle^2 = -Fr_m - W_m \tag{4.6-E2}$$

Since we do not have a heat exchanger in this subsystem, the term Q_m is generally small compared with the work done on the pump W_m. The term ΔH_e in Eq.(4.4-9) is the enthalpy change of the fluid as it passes through the pump. Pumps for liquids and gases are usually designed so that entering and leaving velocities are equal, i.e. $\Delta(1/2)\langle v\rangle^2 = 0$

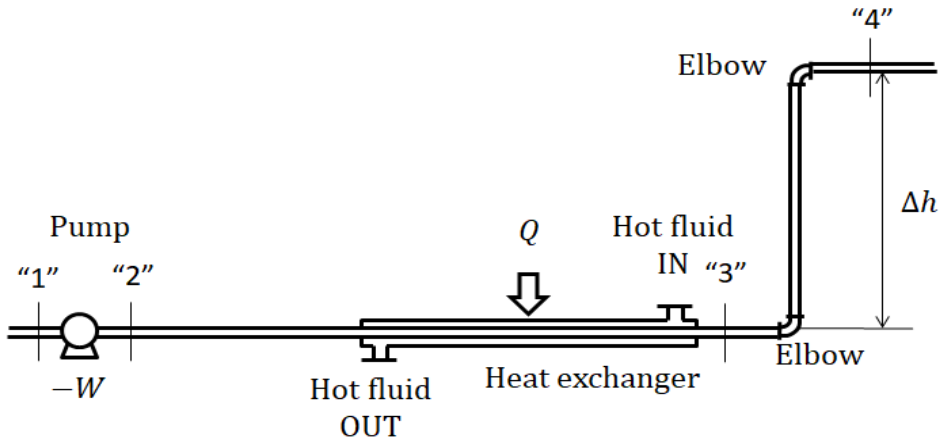

Fig.4.6-E1. Macroscopic energy balance for a simple pipeline system

For incompressible fluid

$$\Delta H_m = \int_{p_1}^{p_2} V_s\, dp + Fr_m = \frac{p_2 - p_1}{\rho} + Fr_{m21} \qquad (4.6\text{-E3})$$

The power required for the pump is given by

$$-W_m = \frac{p_2 - p_1}{\rho} + Fr_{m21} \qquad (4.6\text{-E4})$$

The pipe section is so short that the friction loss Fr_{m21} can often be neglected.

(Ⅱ) heat exchanger: Typical heat exchangers are so designed that there is no shaft work and negligibly small difference in elevation between the entrance and exit. Then

$W_m = 0$ and $\Delta h = 0$

For incompressible fluid, kinetic energy balance is also negligibly small. The friction loss term Fr_m becomes important only when the power requirement is calculated by using the mechanical energy balance. Then

$$\int_{p_1}^{p_2} V_s\, dp = -Fr_m \quad \text{or} \quad \frac{p_3 - p_2}{\rho} = -Fr_{m32} \qquad (4.6\text{-E5})$$

Regarding the total energy balance

$$\int_{T_2}^{T_3} C_p\, dT + \frac{p_3 - p_2}{\rho} = Q_m \qquad (4.6\text{-E6})$$

The pressure change term is small compared with the enthalpy change due to the heat transfer. For constant heat capacity

$$Q_m = C_p\,(T_3 - T_2) \quad \text{i.e.} \quad Q = w\,C_p\,(T_3 - T_2) \qquad (4.6\text{-E7})$$

This equation indicates that the incompressible fluid gets an increase in enthalpy equal to the rate of heat input. For example, in the case when another hot fluid is supplied into an annular space of double-tube exchanger at flow rate w'

$$Q = w' C_p' (T'_3 - T'_2) = w\,C_p\,(T_3 - T_2) \qquad (4.6\text{-E8})$$

where T'_3 and T'_2 are the inlet and outlet temperatures of the hot fluid. This is the fundamental heat balance equation for the design of heat exchangers.

(Ⅲ) pipe: Since this subsystem having a change in elevation is adiabatic, the term Q_m is zero. There is no shaft work: $W_m = 0$. The incompressible fluid does not have any velocity change through the pipe with constant cross-sectional area, i.e. $\langle v \rangle_4 = \langle v \rangle_3$.

The mechanical energy balance becomes

$$\frac{p_4 - p_3}{\rho} + g\,(h_4 - h_3) = -Fr_{m43} \qquad (4.6\text{-E9})$$

Summing up those three equations, the overall mechanical energy balance becomes

$$\frac{p_2 - p_1}{\rho} + \frac{p_3 - p_2}{\rho} + \frac{p_4 - p_3}{\rho} + g(h_4 - h_3) = -(Fr_{m21} + Fr_{m32} + Fr_{m43}) - W_m \qquad (4.6\text{-E10})$$

Finally we get

$$\frac{p_4 - p_1}{\rho} + g(h_4 - h_3) + \sum Fr_m = -W_m \qquad (4.6\text{-E11})$$

This can be considered as a mechanical energy balance equation applied between planes "1" and "4" and implies that the work done on the fluid $-W_m$ required to keep a given constant flow rate should be equal to the sum of differences in flow work and potential energy and the total friction loss (mechanical energy loss) due to viscous dissipation over the whole length of the pipeline.
This is the design equation of piping. The required power of pump is given by

$$Pw = -w\,W_m \qquad \text{(4.6-E12)}$$

[EXAMPLE 4.6-E2] We want to cool dry oxygen gas of W_o kg/s from T_i to $T_o\,K$ by means of horizontal double-pipe heat exchanger shown. The cross sectional area of the inner pipe is $S\ m^2$. If we supply coarse liquid nitrogen as the cooling medium into the annular space at its saturation temperature, nucleate boiling occurs on the outer surface of the inner pipe. Its latent heat of vaporization is $\lambda_N\ J/kg$. The pressures at the inlet and outlet of the inner pipe are p_i and $p_o\,Pa$, respectively. Calculate the rate of energy removed by the coarse liquid nitrogen across the pipe wall. Assume turbulent flow of ideal gas with constant heat capacity of oxygen $Cp_O\ J/kmol\,K$.

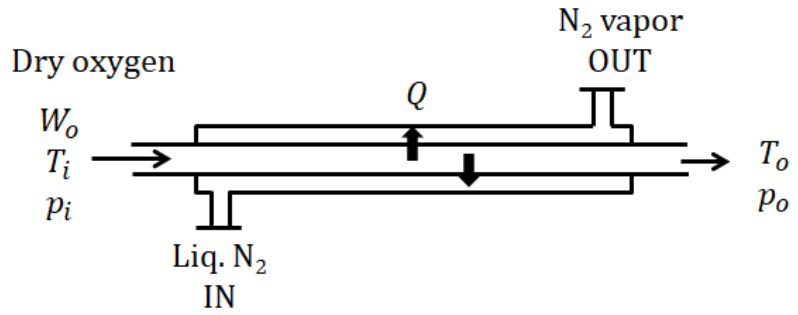

Fig.4.6-E1. Energy balance for cooling dry oxygen by liquid nitrogen

Solution: The macroscopic energy balance between the inlet and exit of the inner pipe is

$$-\Delta\left(H_m + \frac{1}{2}\langle v\rangle^2 + g\,h\right) + Q_m - W_m = 0 \qquad \text{(4.6-E13)}$$

For an ideal gas with constant capacity

$$\Delta H_m = \int_{T_i}^{T_o} Cp_m\,dT = \frac{1}{M}\int_{T_i}^{T_o} Cp_O\,dT = \frac{Cp_O}{M}(T_o - T_i) \qquad J/kg \qquad \text{(4.6-E14)}$$

From the mass balance $\rho_i\langle v_i\rangle S_i = \rho_o\langle v_o\rangle S_o = W_o$.
The perfect gas law is

$$\frac{1}{\rho} = \frac{1}{M}\frac{R\,T}{p} \qquad \text{(4.6-E15)}$$

Then

$$\Delta\frac{1}{2}\langle v\rangle^2 = \frac{1}{2}(W_o/S)^2[(RT_o/M\,p_o)^2 - (RT_i/M\,p_i)^2] \qquad J/kg \qquad \text{(4.6-E16)}$$

$W_m = 0$ and $\Delta h = 0$
Therefore

$$Q\ \ kJ/s = W_o\,Q_m = (W_o Cp_O/M)(T_o - T_i) + \frac{1}{2}W_o(W_o/S)^2\,[(RT_o/M\,p_o)^2 - (RT_i/M\,p_i)^2] \qquad \text{(4.6-E17)}$$

On the other hand, the coarse liquid nitrogen should be fed at a rate of $Q/\lambda_N\ \ kg/s$.

[PROBLEM 4.6-P1] Mineral oil ($\rho = 850\ \ kg/m^3$, $Cp = 2.3\ kJ/kg\,K$, $\mu = 0.03\,Pa\,s$ and $\kappa = 0.143\ \ W/m\,K$) is flowing at an average velocity $\langle v\rangle = 0.4\ m/s$ in a 25 mm ID circular steel pipe. The pipe wall is heated from outside at constant heat flux $q_w = 80\ W/m^2$ (based on the inside wall area). Calculate the Reynolds number. How many degrees does the average temperature rise per unit pipe length?

[PROBLEM 4.6-P2] A basic solution is to be fed to an absorption column operating at pressure of 0.4 MPa at a rate of 0.001 m^3/s from a storage tank. The physical properties of the basic solution can be assumed to be approximately equal to those of water. As a result of calculation, the total friction loss of this system is given by $Fr_m = 18\ J/kg$. Calculate the power of pump required for the given feed rate when 30 mm ID pipe is used for the pipe line. Assume turbulent flow.

[PROBLEM 4.6-P3] Mineral oil ($\rho = 800\ \ kg/m^3,\ Cp = 2.1\ kJ/kg\ K$) is transferred at a rate of 10 ton/h from a tank to a hydrogen plant. On the pipeline there is a heat exchanger to heat the oil from 308 K to 321 K. The pressure drop between the entrance and exit of the exchanger is 5 kPa. Determine the friction loss in m^2/s^2 and the heat transfer rate in J/h of the exchanger. The pressures at the inlet (suction side) and outlet (discharge side) of the pump are 0.08 MPa and 1.8 MPa, respectively. Determine the power of pump in kW.

4.7 Macroscopic Mass Balance of Individual Components

Even when the total mass is conserved, an individual species is not, in general, conserved under processes including chemical reaction. By applying the principle of mass conservation to the control volume having a homogeneous chemical reaction, the mass balance of component A can be written as

$$\frac{d}{dt}\int_V C_A\, dV = -\int_S C_A\,(\vec{\boldsymbol{v}}\cdot\vec{\boldsymbol{n}})\, dS + \int_V r_A\, dV \qquad (4.7\text{-}1)$$

where C_A is the mass concentration of component A and r_A is the reaction rate indicating the rate of mass generation per unit volume of component A.

[EXAMPLE 4.7-E1] A typical distillation plant shown below (Fig. 4.7-E1) comprises a distillation column, a total overhead condenser, and a partial bottom reboiler. The feed of mixture F of A and B, which is to be separated into fractions, is introduced to the column. Some of the less volatile component B is condensed from the vapor going up the column, and at the same time, some of the more volatile component A is vaporized from the liquid going down the column. These phase transformations take place due to the giving and receiving of latent heat between A and B components.

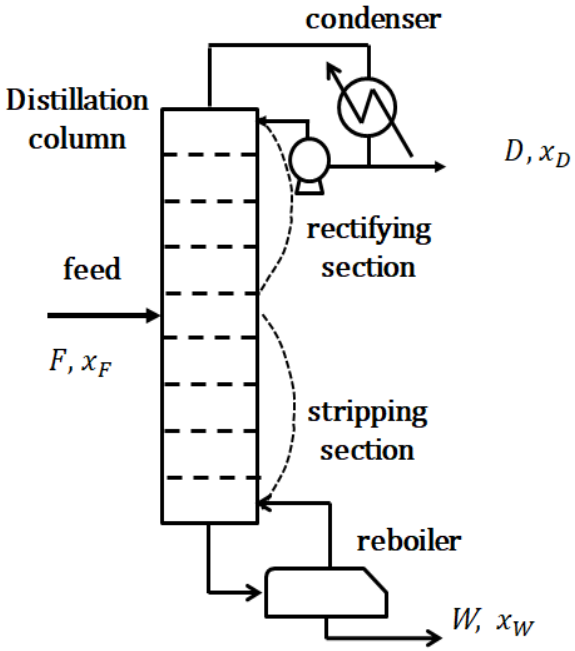

Fig.4.7-E1. Distillation plant

The liquid reaching the bottom is partially vaporized in a reboiler heated by steam. The vapor is sent back to the bottom of the column to provide the upflowing vapor in the stripping section (section below the feed stage). The remainder of the bottom liquid, which has high concentration of the less volatile component B, is withdrawn as the bottom product. On the other hand, the vapor reaching the top is completely condensed by an overhead condenser cooled by water. Some fraction of the condensate is returned by a reflux pump to provide the downflowing liquid (internal reflux liquid) in the rectifying section (section above the feed stage). The distillation process cannot proceed without the intimate contact of vapor with the internal reflux liquid.

The remainder of the condensate , which has high concentration of the more volatile component A, is withdrawn as the overhead product. The column fed with F kmol/h of mole fraction x_F of component A produces D kmol/h of overhead product of mole fraction x_D and W kmol/h of bottom product of mole fraction x_W.

For steady-state operation, the overall mass balances can be written as

Total mass balance: $F = D + W$ (4.7-E1)

Mass balance of component A: $F\,x_F = D\,x_D + W\,x_W$

The reflux liquid: $L_R = V_t - D$

where V_t is the vapor rate from the column top to the overhead condenser. (4.7-E2)

[EXAMPLE 4.7-E2] Consider a flow system (gas absorption column) in which a gas stream is in contact with a liquid stream. The system, as shown in Fig.4.7-E2, has a single entrance and a single exit. The cross-sectional area S is constant. The gas stream contains component A soluble into the liquid.

The macroscopic mass balance of component A in gas phase is

$$\frac{d}{dt}\int_V C_A\,dV = C_{A1}\langle v_1\rangle S - C_{A2}\langle v_2\rangle S - W_{Ai} + \int_V r_A\,dV \quad \text{(4.7-E3)}$$

Here $\langle v_1\rangle$ and $\langle v_2\rangle$ are the "superficial velocities" at the entrance and exit (the average velocities the gas would have in the column if the column were occupied with the gas only) and W_{Ai} is the rate of mass transfer of component A across the gas-liquid contacting interface to the liquid.

At steady state with no chemical reaction

$$(C_{A1}\langle v_1\rangle - C_{A2}\langle v_2\rangle)S = W_{Ai} \quad \text{(4.7-E4)}$$

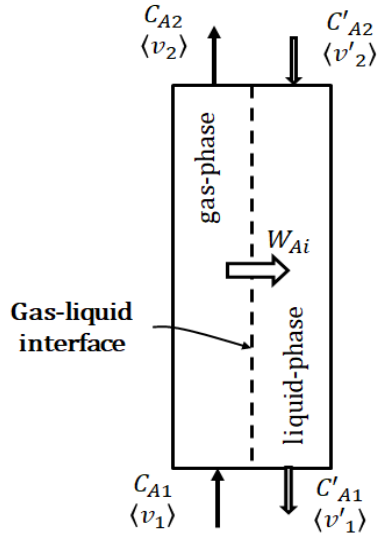

Fig.4.7-E2. Gas absorption column

Similarly the macroscopic mass balance in the liquid phase at steady state with no chemical reaction

$$(C'_{A1}\langle v'_1\rangle - C'_{A2}\langle v'_2\rangle)S = W_{Ai} \quad \text{(4.7-E5)}$$

Where the prime denotes the liquid phase. Here $\langle v'_1\rangle$ and $\langle v'_2\rangle$ are the superficial velocities

(the average velocities the liquid would have in the column if the column were occupied with the liquid only.).

[PROBLEM 4.7-P1] Nitrogen gas is flowing in a pipe of porous wall, through which hydrogen gas is injected from outside into the pipe at a rate of m_H kg/m^2 s. At the entrance ($L = 0$) to the porous pipe, the flow rate of nitrogen is w_N kg/s. he molecular weights of N_2 and H_2 are M_N and M_H, respectively. Obtain the expressions for the total mass flow rater as a function of pipe length L and the gas composition in mole fraction at a position L downstream of the porous pipe.

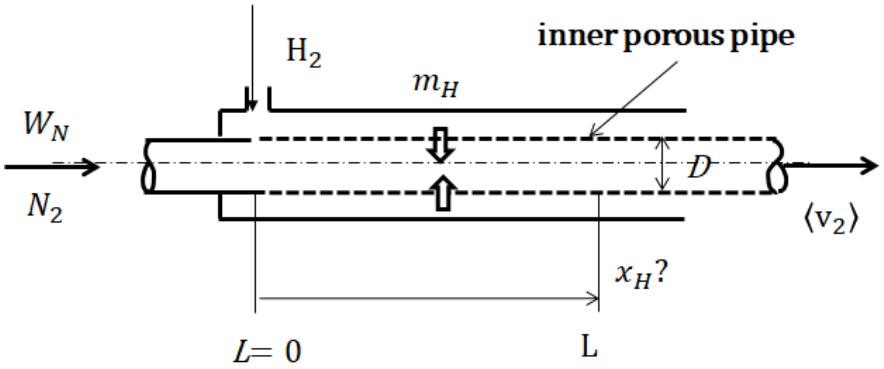

Fig.4.7-P1. Nirogen gas stream with hydrogen gas injected through porous pipe wall

Nomenclature

C_A	molar concentration of component A, [kmol/m^3]
Cp	heat capacity, [J/kg K]
D	pipe inside diameter, [m] or overhead product in distillation column, [kmol/s]
E_k, E_p, E_u	kinetic, potential, internal energy, [J/kg]
$\vec{\boldsymbol{F}}$	external force vector,
F	feed rate in distillation column, [kmol/s]
Fr	friction loss or mechanical energy loss, [J/kg]
g	gravitational acceleration, [m/s^2]
H_e	enthalpy, [J/kg]
h	height, [m]
L	pipe length, [m]
L_R	reflux liquid rate in distillation column, [kmol/s]
m	mass of control volume, [kg]
$\vec{\boldsymbol{n}}$	unit vector
p	pressure, [Pa]
Q	volumetric flow rate, [m^3/s] or heat input from surroundings, [J/s]
r_A	reaction rate, [kmol/m^{3}s]
S	surface area, [m^2] or entropy, [J/kg K]
t	time, [s]
$\vec{\boldsymbol{v}}$	velocity vector
V	volume, [m^3]
V_s	specific volume, [m^3/kg]
V_t	vapor flow rate at top of distillation column, [kmol/s]
v	velocity, [m/s]
W	work done by fluid on surroundings, [W] or bottom product in distillation column, [kmol/s]
w	mass flow rate, [kg/s]
x_F, x_D, x_W	mole fraction of more-volatile component of feed, overhead product, and bottom product, [-]
ρ	density, [kg/m^3]
τ_w	wall shear stress, [N/m^2]

CHAPTER 5

MICROSCOPIC DIFFERENTIAL BALANCES

5.1 Differential Balances of Mass and Momentum (Equations of Continuity and Motion)

In this section, we shall set up the equations of conservation of mass and momentum in general form (Bird et al., 1960). Once we have developed these general equations, we can start with them and simplify them to fit the problem at hand.

---

1. Bird, R.B., Stewart, W.E., and Lightfoot, E.N., Transport Phenomena, Wiley, New York, Chapt.3 (1960)

5.1-1 Differential mass balance (Equation of continuity)[1)]

Let us consider a differential mass balance over a stationary differential control volume $\Delta x \Delta y \Delta z$ shown in Fig.5.1-1.

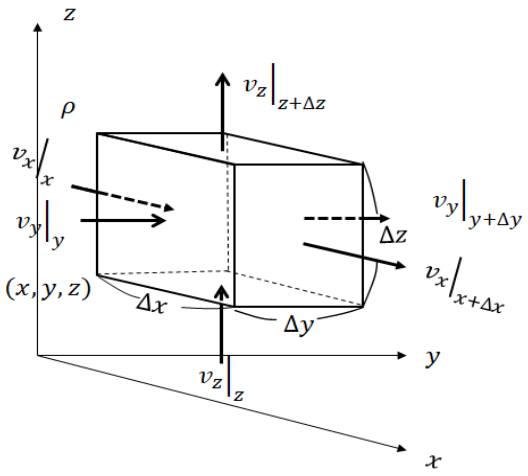

Fig.5.1-1. Differential control volume in rectangular coordinate system

Generally the fluid is flowing through all six faces of the control volume. The fluid is homogeneous, but the density changes with temperature and pressure.
The rate of mass transfer) can be written as

(rate of mass in) = (mass transferred)/(unit time)
= (mass/unit volume)(length/unit time)(area)

Therefore, as shown in Fig.5.1-2, mass is transferred across the pair of $\Delta y \Delta z$ faces perpendicular to the x-axis by v_x only. Hence the rate of mass in through the face at x is $\rho|_x v_x|_x \Delta y \Delta z$ and the rate of mass out through the face at $\rho|_{x+\Delta x} v_x|_{x+\Delta x} \Delta y \Delta z$. Similar expressions can be obtained for the remaining two pairs of faces.

The masses of the control volume at time t and $t + \Delta t$ are $\rho|_t \Delta x \Delta y \Delta z$ and $\rho|_{t+\Delta t} \Delta x \Delta y \Delta z$, repectively. Therefore the mass accumulation per unit time is given by

$$\left(\frac{\rho|_{t+\Delta t} - \rho|_t}{\Delta t} \right) \Delta x \Delta y \Delta z$$

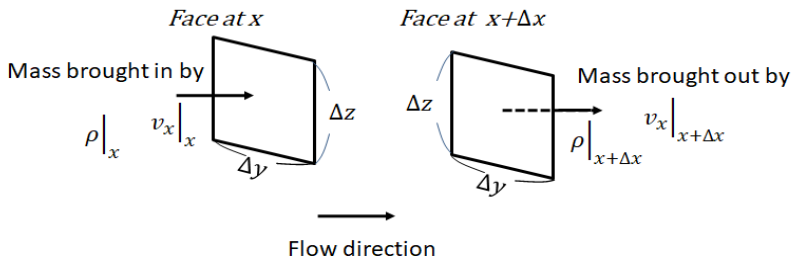

$$\left(\frac{mass}{unit\ volume}\right)\left(\frac{length}{time}\right)(area)$$

$$(\rho)\big|_x\, v_x\big|_x\, \Delta y \Delta z$$

Fig. 5.1-2 Mass flow rate transferred across planes x and $x+\Delta x$ of control volume

Then applying the principle of mass conservation, the following equation yields

$$\left(\frac{\rho|_{t+\Delta t}-\rho|_t}{\Delta t}\right)\Delta x\Delta y\Delta z = [\rho|_x v_x|_x - \rho|_{x+\Delta x} v_x|_{x+\Delta x}]\Delta y\Delta z + \left[\rho|_y v_y\big|_y - \rho|_{y+\Delta y} v_y\big|_{y+\Delta y}\right]\Delta z\Delta x - [\rho|_z v_z|_z - \rho|_{z+\Delta z} v_z|_{z+\Delta z}]\Delta x\Delta y \quad (5.1\text{-}1)$$

Dividing through by the volume $\Delta x\Delta y\Delta z$ and taking the limit as $\Delta t, \Delta x, \Delta y, \Delta z$ go to zero, we get

$$\frac{\partial \rho}{\partial t} = -\left(\frac{\partial\, \rho v_x}{\partial x} + \frac{\partial\, \rho v_y}{\partial y} + \frac{\partial\, \rho v_z}{\partial z}\right) \quad (5.1\text{-}2)$$

This is the equation of continuity in general form.

This equation can be written in vector notation:

$$\frac{\partial \rho}{\partial t} = -\nabla \cdot \rho\vec{\boldsymbol{v}} \quad (5.1\text{-}3)$$

This equation describes the rate of change in density at a fixed position from the Eulerian view point. That is, if the right side of the equation is expanded, we get

$$\frac{\partial \rho}{\partial t} + v_x\frac{\partial \rho}{\partial x} + v_y\frac{\partial \rho}{\partial y} + v_z\frac{\partial \rho}{\partial z} = -\rho\left(\frac{\partial\, v_x}{\partial x} + \frac{\partial\, v_y}{\partial y} + \frac{\partial\, v_z}{\partial z}\right) \quad (5.1\text{-}4)$$

The left side describes the rate of change in density observed by following the fluid motion from the Lagrangian viewpoint. Therefore if the fluid is at rest, all terms vanish. The derivative of the left-hand side is called the substantial derivative.

In engineering problems, we very frequently assume the fluid density to be constant as incompressible fluid. For constant density fluids, all the left-side terms vanish, and then the right side becomes zero:

$$\frac{\partial\, v_x}{\partial x} + \frac{\partial\, v_y}{\partial y} + \frac{\partial\, v_z}{\partial z} = 0 \quad (5.1\text{-}5)$$

This is a very important form of the equation of continuity. In vector form it can be written as

$$\nabla \cdot \vec{\boldsymbol{v}} = 0 \quad (5.1\text{-}6)$$

General forms of the equation of continuity are listed in Table 5.1-1.

Table 5.1-1 Equation of continuity for fluid with constant density

(1) rectangular coordinates

$$\frac{\partial\, v_x}{\partial x} + \frac{\partial\, v_y}{\partial y} + \frac{\partial\, v_z}{\partial z} = 0$$

(2) cylindrical coordinates

$$\frac{1}{r}\frac{\partial\, r v_r}{\partial r} + \frac{1}{r}\frac{\partial\, v_\theta}{\partial \theta} + \frac{\partial\, v_z}{\partial z} = 0$$

5.1-2 Differential momentum balance (Navier-Stokes equation)[1)]

Following the procedure established in the differential equation of continuity, let us apply the principle of momentum conservation to the same differential control volume. (see Fig.5.1-1).

1. Bird, R.B., Stewart, W.E., and Lightfoot, E.N., Transport Phenomena, Wiley, New York, Chapt.3 (1960)

Since momentum is a vector, the conservation equation can be resolved into its three orthogonal scalar momentum equations.

Consider the x momentum of each term. The x-momentums of the control volume at time t and $t+\Delta t$ are $(\rho v_x)|_t \Delta x\Delta y\Delta z$ and $(\rho v_x)|_{t+\Delta t}\Delta x\Delta y\Delta z$, respectively. Then the accumulation of x-momentum per unit time (i.e. the rate of x-momentum accumulation) becomes

$$\left(\frac{(\rho v_x)|_{t+\Delta t}-(\rho v_x)|_t}{\Delta t}\right)\Delta x\Delta y\Delta z \qquad (5.1\text{-}7)$$

In general, momentum may be transferred into and out of the control volume by two mechanisms: by convection (i.e. by virtue of fluid motion) and by diffusion (i.e. by virtue of molecular motion).

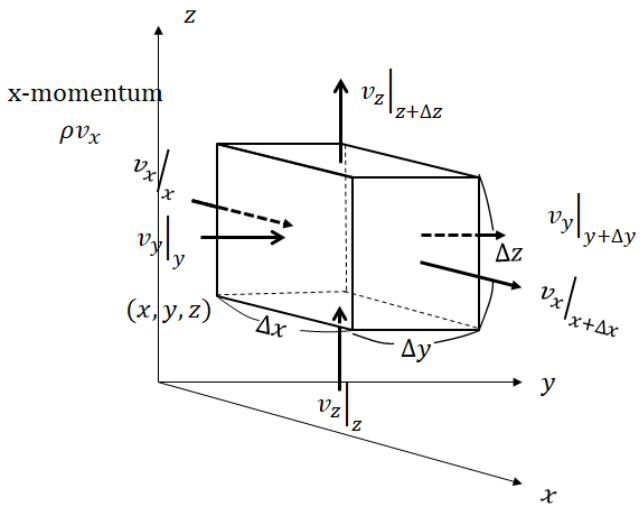

Fig.5.1-3 Control volume for differential momentum balance

First let us consider the convective transport of the x-momentum. Assuming the momentum flux to be uniform on each face, the rate of the x-momentum entering the face at x by $v_x|_x$ is $(\rho v_x v_x)|_x \Delta y\Delta z$, and similarly the rate of the x-momentum leaving the face at $x+\Delta x$ by $v_x|_{x+\Delta x}$ is $(\rho v_x v_x)|_{x+\Delta x}\Delta y\Delta z$. The ρv_x has dimensions of momentum per unit volume, the $v_x\Delta y\Delta z$ has dimensions of volume per unit time, and then the $\rho v_x v_x|_x \Delta y\Delta z$ has dimensions of momentum transferred per unit time (that is, the rate of momentum transferred).

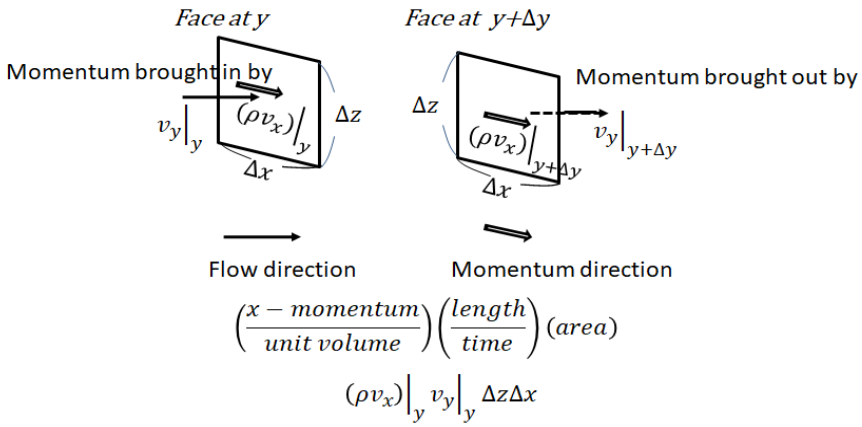

Fig.5.1-4 Convective transport of x-momentum across faces at y and $y+\Delta y$

Across the face of area $\Delta z\Delta x$ at y, as shown in Fig.5.1-4, the x-momentum $(\rho v_x)|_y$ can be transferred by the velocity component $v_y|_y$ perpendicular to the face. The rate of the x-momentum entering the face at y by $v_y|_y$ is $(\rho v_x v_y)|_y \Delta z\Delta x$ and the rate of the x-momentum leaving the face $y+\Delta y$ by $v_y|_{y+\Delta y}$ is $(\rho v_x v_y)|_{y+\Delta y}\Delta z\Delta x$. Therefore the net rate of the x-momentum

transferred across all six faces by convection becomes

$$[(\rho v_x v_x)|_x - (\rho v_x v_x)|_{x+\Delta x}]\Delta y\Delta z + \left[(\rho v_x v_y)\big|_y - (\rho v_x v_y)\big|_{y+\Delta y}\right]\Delta z\Delta x + [(\rho v_x v_z)|_z - (\rho v_x v_z)|_{z+\Delta z}]\Delta x\Delta y \quad (5.1\text{-}8)$$

Next let us consider the diffusion (molecular transport) of x-momentum assuming the momentum flux to be uniform on each face. The rate of x-momentum entering the face at x by diffusion is $\tau_{xx}|_x \Delta y\Delta z$, and the rate of x-momentum leaving the face at $x+\Delta x$ is also $\tau_{xx}|_{x+\Delta x}\Delta y\Delta z$. Note that τ_{xx} is the normal stress in the x direction on the face perpendicular to the x axis. Similarly the rate of x-momentum entering the face at y by diffusion is $\tau_{yx}\big|_y \Delta z\Delta x$, and the rate of x-momentum leaving the face at $y+\Delta y$ is $\tau_{yx}\big|_{y+\Delta y}\Delta z\Delta x$.

Recall that τ_{yx} is the flux of x-momentum through a face perpendicular to the y axis. In other word, τ_{yx} is the shear stress on the face normal to the y axis and acting in the x direction. Therefore the net rate of x-momentum transferred across all six faces by diffusion becomes

$$(\tau_{xx}|_x - \tau_{xx}|_{x+\Delta x})\Delta y\Delta z + \left(\tau_{yx}\big|_y - \tau_{yx}\big|_{y+\Delta y}\right)\Delta z\Delta x + (\tau_{zx}|_z - \tau_{zx}|_{z+\Delta z})\Delta x\Delta y \quad (5.1\text{-}9)$$

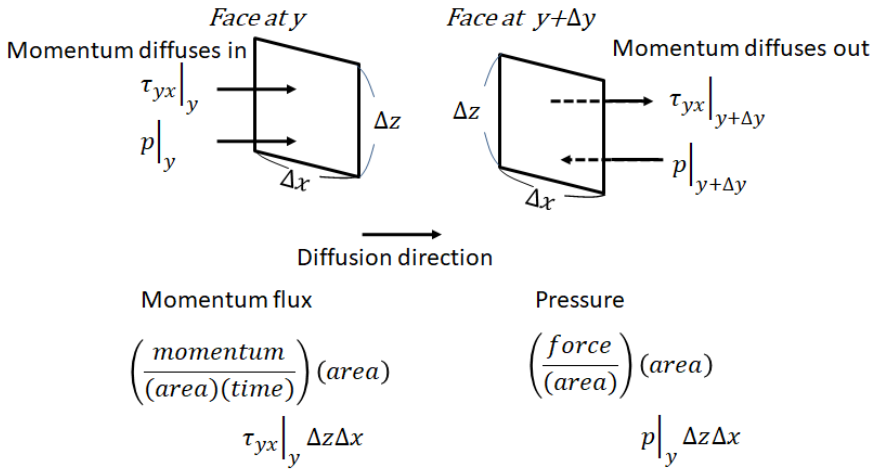

Fig.5.1-5 Molecular transport of x-momentum by diffusion in y direction and pressure force

Pressure is a scalar, but the pressure force is a vector perpendicular to the acting face. The net effect of the x-directed pressure forces is

$$(p|_x - p|_{x+\Delta x})\Delta y\Delta z \quad (5.1\text{-}10)$$

The gravitational force acts on the mass center of the control volume as body force. The x-component of the gravitational force is $\rho g_x \Delta x\Delta y\Delta z$.

Substituting all the foregoing contributions into the equation of momentum conservation law, and dividing the resulting equation by $\Delta x\Delta y\Delta z$, we get

$$\frac{(\rho v_x)|_{t+\Delta t} - (\rho v_x)|_t}{\Delta t} = -\left[\frac{(\rho v_x v_x)|_{x+\Delta x} - (\rho v_x v_x)|_x}{\Delta x} + \frac{(\rho v_x v_y)\big|_{y+\Delta y} - (\rho v_x v_y)\big|_y}{\Delta y} + \frac{(\rho v_x v_z)|_{z+\Delta z} - (\rho v_x v_z)|_z}{\Delta z}\right] - \left[\frac{\tau_{xx}|_{x+\Delta x} - \tau_{xx}|_x}{\Delta x} + \frac{\tau_{yx}\big|_{y+\Delta y} - \tau_{yx}\big|_y}{\Delta y} + \frac{\tau_{zx}|_{z+\Delta z} - \tau_{zx}|_z}{\Delta z}\right] - \frac{p|_{x+\Delta x} - p|_x}{\Delta x} + \rho g_x \quad (5.1\text{-}11)$$

Taking the limit as $\Delta t, \Delta x, \Delta y, \Delta z$ go to zero, we obtain the x-component of the equation of motion in general form:

$$\frac{\partial}{\partial t}(\rho v_x) = -\left(\frac{\partial \rho v_x v_x}{\partial x} + \frac{\partial \rho v_x v_y}{\partial y} + \frac{\partial \rho v_x v_z}{\partial z}\right) - \left(\frac{\partial \tau_{xx}}{\partial x} + \frac{\partial \tau_{yx}}{\partial y} + \frac{\partial \tau_{zx}}{\partial z}\right) - \frac{\partial p}{\partial x} + \rho g_x \quad (5.1\text{-}12)$$

The remaining two can be written by analogy.

In vector symbolism, these equations can be combined into one vector equation:

$$\frac{\partial \rho \vec{v}}{\partial t} = -\nabla \cdot \rho \vec{v}\vec{v} - \nabla \cdot \vec{\vec{\tau}} - \nabla p + \rho \vec{g} \qquad (5.1\text{-}13)$$

One of the most advantageous points of vector equation is that vector equation is valid for any orthogonal coordinate system. The above vector equation is also valid for cylindrical and spherical coordinates. The tedious transformation from rectangular to curvilinear coordinates is not discussed here. Keep in mind that these equations are valid for both Newtonian and non-Newtonian fluids.

In order to determine velocity distributions, the relation between stresses and velocity gradients should be plugged into the τ- term of the equation of motion.

For simplicity, we assume Newtonian fluid with constant density and viscosity, and rewrite the equation of motion with the aid of the equation of continuity as follows:

$$\frac{\partial}{\partial t}(\rho v_x) + \left(\frac{\partial \rho v_x v_x}{\partial x} + \frac{\partial \rho v_x v_y}{\partial y} + \frac{\partial \rho v_x v_z}{\partial z}\right) = \rho\left(\frac{\partial v_x}{\partial t} + v_x\frac{\partial v_x}{\partial x} + v_y\frac{\partial v_x}{\partial y} + v_z\frac{\partial v_x}{\partial z}\right)$$

$$\frac{\partial \tau_{xx}}{\partial x} + \frac{\partial \tau_{yx}}{\partial y} + \frac{\partial \tau_{zx}}{\partial z} = -\mu\left(\frac{\partial^2 v_x}{\partial x^2} + \frac{\partial^2 v_x}{\partial y^2} + \frac{\partial^2 v_x}{\partial z^2}\right)$$

Then the x-component of the equation of motion becomes

$$\rho\left(\frac{\partial v_x}{\partial t} + v_x\frac{\partial v_x}{\partial x} + v_y\frac{\partial v_x}{\partial y} + v_z\frac{\partial v_x}{\partial z}\right) = -\frac{\partial p}{\partial x} + \mu\left(\frac{\partial^2 v_x}{\partial x^2} + \frac{\partial^2 v_x}{\partial y^2} + \frac{\partial^2 v_x}{\partial z^2}\right) + \rho g_x \qquad (5.1\text{-}14)$$

The remaining two can be written by analogy.

These equations for constant physical properties can be combined by the following vector equation:

$$\rho\left[\frac{\partial \vec{v}}{\partial t} + (\vec{v}\cdot\nabla)\vec{v}\right] = -\nabla p + \mu\nabla^2\vec{v} + \rho\vec{g} \qquad (5.1\text{-}15)$$

This is well known as the Navier-Stokes equation. The differential operator ∇^2 is called the Laplacian operator.

These equations derived in this section are tabulated in rectangular and cylindrical coordinates in Table 5.1-1.

Only for simplification and convenience, the equation of change for spherical coordinate system is omitted from the table. If we wish to rewrite these equations in spherical coordinates, we should obtain the relations between $(x, y, z)$and (r, θ, ϕ) with the relations between (v_x, v_y, v_z) and (v_r, v_θ, v_ϕ). However wen will not have to wade through the details of this tedious process.

Table 5.1-2 Equation of motion (Navier-Stokes equation) for a Newtonian fluid with constant density and viscosity

(1) rectangular coordinates

x: $\rho\left(\frac{\partial v_x}{\partial t} + v_x\frac{\partial v_x}{\partial x} + v_y\frac{\partial v_x}{\partial y} + v_z\frac{\partial v_x}{\partial z}\right) = -\frac{\partial p}{\partial x} + \mu\left(\frac{\partial^2 v_x}{\partial x^2} + \frac{\partial^2 v_x}{\partial y^2} + \frac{\partial^2 v_x}{\partial z^2}\right) + \rho g_x$

y: $\rho\left(\frac{\partial v_y}{\partial t} + v_x\frac{\partial v_y}{\partial x} + v_y\frac{\partial v_y}{\partial y} + v_z\frac{\partial v_y}{\partial z}\right) = -\frac{\partial p}{\partial y} + \mu\left(\frac{\partial^2 v_y}{\partial x^2} + \frac{\partial^2 v_y}{\partial y^2} + \frac{\partial^2 v_y}{\partial z^2}\right) + \rho g_y$

z: $\rho\left(\frac{\partial v_z}{\partial t} + v_x\frac{\partial v_z}{\partial x} + v_y\frac{\partial v_z}{\partial y} + v_z\frac{\partial v_z}{\partial z}\right) = -\frac{\partial p}{\partial z} + \mu\left(\frac{\partial^2 v_z}{\partial x^2} + \frac{\partial^2 v_z}{\partial y^2} + \frac{\partial^2 v_z}{\partial z^2}\right) + \rho g_z$

(2) cylindrical coordinates

r: $\rho\left(\frac{\partial v_r}{\partial t} + v_r\frac{\partial v_r}{\partial r} + \frac{v_\theta}{r}\frac{\partial v_r}{\partial \theta} - \frac{{v_\theta}^2}{r} + v_z\frac{\partial v_r}{\partial z}\right) = -\frac{\partial p}{\partial r} + \mu\left[\frac{\partial}{\partial r}\left(\frac{1}{r}\frac{\partial}{\partial r}(r v_r)\right) + \frac{1}{r^2}\frac{\partial^2 v_r}{\partial \theta^2} - \frac{2}{r^2}\frac{\partial v_\theta}{\partial \theta} + \frac{\partial^2 v_r}{\partial z^2}\right] + \rho g_r$

θ: $\rho\left(\frac{\partial v_\theta}{\partial t} + v_r\frac{\partial v_\theta}{\partial r} + \frac{v_\theta}{r}\frac{\partial v_\theta}{\partial \theta} + \frac{v_r v_\theta}{r} + v_z\frac{\partial v_\theta}{\partial z}\right) = -\frac{1}{r}\frac{\partial p}{\partial \theta} + \mu\left[\frac{\partial}{\partial r}\left(\frac{1}{r}\frac{\partial}{\partial r}(r v_\theta)\right) + \frac{1}{r^2}\frac{\partial^2 v_\theta}{\partial \theta^2} + \frac{2}{r^2}\frac{\partial v_r}{\partial \theta} + \frac{\partial^2 v_\theta}{\partial z^2}\right] + \rho g_\theta$

z: $\rho\left(\frac{\partial v_z}{\partial t} + v_r\frac{\partial v_z}{\partial r} + \frac{v_\theta}{r}\frac{\partial v_z}{\partial \theta} + v_z\frac{\partial v_z}{\partial z}\right) = -\frac{\partial p}{\partial z} + \mu\left[\frac{1}{r}\frac{\partial}{\partial r}\left(r\frac{\partial v_z}{\partial r}\right) + \frac{1}{r^2}\frac{\partial^2 v_z}{\partial \theta^2} + \frac{\partial^2 v_z}{\partial z^2}\right] + \rho g_z$

5.2 Differential Balance of Energy (Equation of energy)[1)]

As aforementioned in macroscopic energy balance, the energy associated with mass consists of potential, kinetic and internal energies. In general, non-isothermal processes accompanied with fluid motion take place undergoing various work effects such as viscous dissipation, pressure work and gravitational work. At this stage, it is too difficult to derive a general form of energy equation. In this section, therefore, we shall develop the differential equation of thermal energy transfer written for incompressible fluid with constant physical properties. This equation is widely used in non-isothermal system with moderate change in temperature and velocity.

The following assumptions are made:

(1) incompressible fluid with constant heat capacity and thermal conductivity
(2) negligible kinetic- and potential-energy effects
(3) negligible work done by static pressure force
(4) negligible work done by viscous normal and shear forces
(5) negligible work done by gravitational force
(6) negligible radiative heat transfer

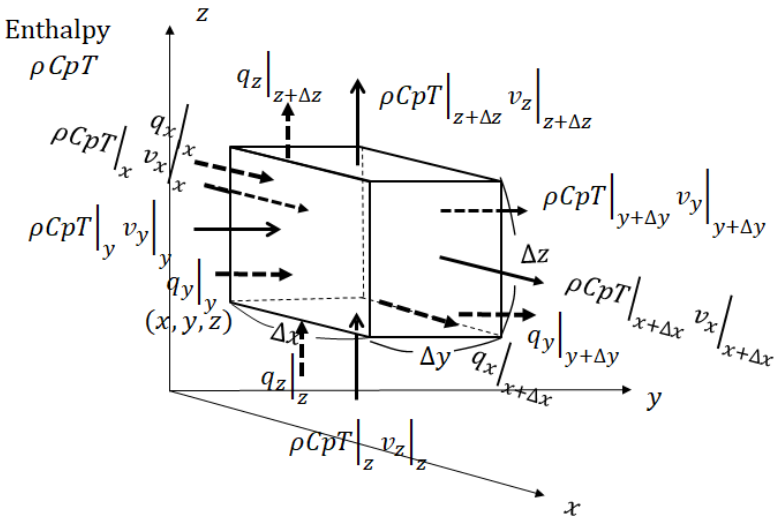

Fig.5.2-1 Enthalpy balance for convective and conductive transport

1. Bird, R.B., Stewart, W.E., and Lightfoot, E.N., Transport Phenomena, Wiley, New York, Chapt.10 (1960)

Let us apply the principle of energy conservation to the differential control volume $\Delta x\Delta y\Delta z$ shown in Fig.5.2-1. The thermal energy can be written in a form of enthalpy ρCpT for fluids having constant properties.

The accumulation rate of thermal energy is

$$\frac{(\rho CpT)|_{t+\Delta t} - (\rho CpT)|_t}{\Delta t}\ \Delta x\Delta y\Delta z \qquad (5.2\text{-}1)$$

In general, thermal energy may be transferred into the control volume by convection and conduction (diffusion).

(1) Convective transport:

First let us consider the convective effect. The x-component of velocity v_x brings in thermal energy ρCpT across the face $\Delta y\Delta z$ at a rate of $(\rho CpT)|_x v_x|_x \Delta y\Delta z$. Similarly the rate of thermal energy brought out is $(\rho CpT)|_{x+\Delta x} v_x|_{x+\Delta x} \Delta y\Delta z$. Therefore the net rate of thermal energy transferred across all six faces by convection becomes

$$[(\rho CpTv_x)|_x - (\rho CpTv_x)|_{x+\Delta x}]\Delta y\Delta z + \left[(\rho CpTv_y)\big|_y - (\rho CpTv_y)\big|_{y+\Delta y}\right]\Delta z\Delta x + [(\rho CpTv_z)|_z - (\rho CpTv_z)|_{z+\Delta z}]\Delta x\Delta y \quad (5.2\text{-}2)$$

(2) Conductive transport:

Next let us consider the conductive effect. The rate of thermal energy entering the face $\Delta y\Delta z$ at x by conduction is $q_x|_x\Delta y\Delta z$, and the rate of thermal energy leaving the face $\Delta y\Delta z$ at $x + \Delta x$ is $q_x|_{x+\Delta x}\Delta y\Delta z$. Note that q_x is the heat flux through a face perpendicular to the x-axis.

Therefore the net rate of thermal energy transferred across all six faces by conduction becomes

$$[q_x|_x - q_x|_{x+\Delta x}]\Delta y\Delta z + \left[q_y\big|_y - q_y\big|_{y+\Delta y}\right]\Delta z\Delta x + [q_z|_z - q_z|_{z+\Delta z}]\Delta x\Delta y \quad (5.2\text{-}3)$$

After substituting all the foregoing contributions into the equation of energy conservation law, and dividing through the resulting equation by $\Delta x\Delta y\Delta z$, if the limit is taken as $\Delta t, \Delta x, \Delta y, \Delta z \rightarrow 0$, we get

$$\frac{\partial(\rho CpT)}{\partial t} = -\left[\frac{\partial(\rho CpTv_x)}{\partial x} + \frac{\partial(\rho CpTv_y)}{\partial y} + \frac{\partial(\rho CpTv_z)}{\partial z}\right] - \left(\frac{\partial q_x}{\partial x} + \frac{\partial q_y}{\partial y} + \frac{\partial q_z}{\partial z}\right) \quad (5.2\text{-}4)$$

In vector symbolism

$$\frac{\partial(\rho CpT)}{\partial t} + \left(\vec{\nabla}\cdot\rho CpT\,\vec{\boldsymbol{v}}\right) + \left(\vec{\nabla}\cdot\vec{\boldsymbol{q}}\right) = \mathbf{0} \quad (5.2\text{-}5)$$

The vector equation is also valid for cylindrical coordinates.

The above equation is rewritten for incompressible fluid with the aid of the equation of continuity and the Fourier's law of conduction as

$$\rho Cp\left(\frac{\partial T}{\partial t} + v_x\frac{\partial T}{\partial x} + v_y\frac{\partial T}{\partial y} + v_z\frac{\partial T}{\partial z}\right) = \kappa\left(\frac{\partial^2 T}{\partial x^2} + \frac{\partial^2 T}{\partial y^2} + \frac{\partial^2 T}{\partial z^2}\right) \quad (5.2\text{-}6)$$

In vector symbolism

$$\rho Cp\left[\frac{\partial T}{\partial t} + \left(\vec{\boldsymbol{v}}\cdot\vec{\boldsymbol{\nabla}}\right)\boldsymbol{T}\right] = \kappa\,\nabla^2 T \quad (5.2\text{-}7)$$

The vector equation is valid for all kinds of orthogonal coordinate systems. These equations are listed in Table 5.2-1, except for spherical coordinates. Note that since the rate of energy transfer depends on the fluid velocity, it is necessary to solve the hydrodynamic problem before the temperature distribution is calculated.

Table 5.2-1 Equation of energy for a Newtonian fluid of constant ρ and κ

(1) rectangular coordinates

$$\rho Cp\left(\frac{\partial T}{\partial t} + v_x\frac{\partial T}{\partial x} + v_y\frac{\partial T}{\partial y} + v_z\frac{\partial T}{\partial z}\right) = \kappa\left(\frac{\partial^2 T}{\partial x^2} + \frac{\partial^2 T}{\partial y^2} + \frac{\partial^2 T}{\partial z^2}\right)$$

(2) cylindrical coordinates

$$\rho Cp\left(\frac{\partial T}{\partial t} + v_r\frac{\partial T}{\partial r} + \frac{v_\theta}{r}\frac{\partial T}{\partial \theta} + v_z\frac{\partial T}{\partial z}\right) = \kappa\left(\frac{1}{r}\frac{\partial}{\partial r}\left(r\frac{\partial T}{\partial r}\right) + \frac{1}{r^2}\frac{\partial^2 T}{\partial \theta^2} + \frac{\partial^2 T}{\partial z^2}\right)$$

5.3 Differential Balances of Mass (Equations of mass transport)[1)]

In this section, we shall develop the equation of mass A in a binary mixture A and B setting up the mass balance over the same differential control volume. For convenience, we use the following form of Fick's law written in terms of mass concentration in place of molar concentration:

$$n_{Ax} = \omega_A(n_{Ax} + n_{Bx}) - \rho\,D_{AB}\frac{\partial \omega_A}{\partial x} \quad (5.3\text{-}1)$$

where $\omega_A = \rho_A/\rho$ = mass fraction, ρ_A = mass density of component A in kg of A/m^3, ρ = total mass density in kg of (A+B)/m^3, and n_{Ax} = x-component of mass flux of species A in kg of A/m^2/s.

This equation indicates that the mass flux in a stationary coordinate system consists of both convection (first term) and diffusion (second term).

The accumulation rate of species A is

$$\frac{\rho_A|_{t+\Delta t} - \rho_A|_t}{\Delta t}\,\Delta x\Delta y\Delta z$$

The net rate of species A input due to both convection and diffusion is

$$-\left[\frac{n_{Ax}|_{x+\Delta x} - n_{Ax}|_x}{\Delta x} + \frac{n_{Ay}|_{y+\Delta y} - n_{Ay}|_y}{\Delta y} + \frac{n_{Az}|_{z+\Delta z} - n_{Az}|_z}{\Delta z}\right]\Delta x\Delta y\Delta z$$

The rate of generation of mass A by chemical reaction is

$$r_A\,\Delta x\Delta y\Delta z$$

Summing up all the contributions divided by $\Delta x\Delta y\Delta z$ and taking the limit as $\Delta t, \Delta x, \Delta y, \Delta z \rightarrow 0$, we get

$$\frac{\partial \rho_A}{\partial t} = -\left(\frac{\partial n_{Ax}}{\partial x} + \frac{\partial n_{Ay}}{\partial y} + \frac{\partial n_{Az}}{\partial z}\right) + r_A \tag{5.3-2}$$

This is a general form of the equation of continuity for species A. In vector symbolism

$$\frac{\partial \rho_A}{\partial t} = -\nabla \cdot \overrightarrow{\boldsymbol{n_A}} + r_A \tag{5.3-3}$$

The mass flux vector for a binary mixture can be related with fluid velocity:

$$\vec{n}_A + \vec{n}_B = \rho\,\vec{\boldsymbol{v}} \tag{5.3-4}$$

We shall get more convenient form of the equation using the following form of Fick's law.

$$\overrightarrow{n_A} = \omega_A(\vec{n}_A + \vec{n}_B) - \rho\, D_{AB}\,\nabla\omega_A = \rho_A\vec{\boldsymbol{v}} - \rho D_{AB}\nabla\omega_A \tag{5.3-5}$$

Substituting this expression into Eq.(5.3-3), we get

$$\frac{\partial \rho_A}{\partial t} = -\rho_A(\nabla\cdot\vec{\boldsymbol{v}}) - (\vec{\boldsymbol{v}}\cdot\nabla)\rho_A + \rho D_{AB}\nabla^2\omega_A + r_A$$

That is, in rectangular coordinates

$$\frac{\partial \rho_A}{\partial t} = -\left[\frac{\partial \rho_A v_x}{\partial x} + \frac{\partial \rho_A v_y}{\partial y} + \frac{\partial \rho_A v_z}{\partial z}\right]$$
$$+ \left[\frac{\partial}{\partial x}\left(\rho D_{AB}\frac{\partial \omega_A}{\partial x}\right) + \frac{\partial}{\partial y}\left(\rho D_{AB}\frac{\partial \omega_A}{\partial y}\right) + \frac{\partial}{\partial z}\left(\rho D_{AB}\frac{\partial \omega_A}{\partial z}\right)\right] + r_A$$

For a fluid with constant ρ and D_{AB} this equation can be simplified as follows.

$$\frac{\partial \rho_A}{\partial t} + \rho_A(\nabla\cdot\vec{\boldsymbol{v}}) + (\vec{\boldsymbol{v}}\cdot\nabla)\rho_A = D_{AB}\nabla^2\rho_A + r_A$$

According to the equation of continuity for constant ρ, $(\nabla\cdot\vec{\boldsymbol{v}}) = 0$. Therefore

$$\frac{\partial \rho_A}{\partial t} + (\vec{\boldsymbol{v}}\cdot\nabla)\rho_A = D_{AB}\nabla^2\rho_A + r_A \tag{5.3-6}$$

Dividing through by molecular weight M_A, we get

$$\frac{\partial C_A}{\partial t} + (\vec{\boldsymbol{v}}\cdot\nabla)C_A = D_{AB}\nabla^2 C_A + R_A \tag{5.3-7}$$

where $C_A = \rho_A/M_A$ in kmol of A/m^3 and $R_A = r_A/M_A$ in kmol of A/m^3/s.

This is the diffusion equation for dilute solution at constant temperature and pressure where we can assume constant density and diffusivity. The equation of continuity for species A written in terms of molar fluxes can be obtained dividing Eq.(5.3-2) by molecular weight M_A,:

$$\frac{\partial C_A}{\partial t} = -\left(\frac{\partial N_{Ax}}{\partial x} + \frac{\partial N_{Ay}}{\partial y} + \frac{\partial N_{Az}}{\partial z}\right) + R_A \tag{5.3-8}$$

or

$$\frac{\partial C_A}{\partial t} + \left(\nabla\cdot\vec{N}_A\right) = R_A$$

The following tables give the diffusion equations in orthogonal coordinate systems.

Table 5.3 – 1 The equation of continuity of component A[1)]

(1) rectangular coordinates (x, y, z)

$$\frac{\partial C_A}{\partial t} + \left(\frac{\partial N_{Ax}}{\partial x} + \frac{\partial N_{Ay}}{\partial y} + \frac{\partial N_{Az}}{\partial z}\right) = R_A$$

(2) cylindrical coordinates (r, θ, z)

$$\frac{\partial C_A}{\partial t} + \left[\frac{1}{r}\frac{\partial}{\partial r}(r\,N_{Ar}) + \frac{1}{r}\frac{\partial N_{A\theta}}{\partial \theta} + \frac{\partial^2 N_{Az}}{\partial z^2}\right] = R_A$$

Table 5.3 – 2 The equation of diffusion for constant ρ and D_{AB}[1)]

(1) rectangular coordinates (x, y, z)

$$\frac{\partial C_A}{\partial t} + v_x \frac{\partial C_A}{\partial x} + v_y \frac{\partial C_A}{\partial y} + v_z \frac{\partial C_A}{\partial z} = D_{AB} \left(\frac{\partial^2 C_A}{\partial x^2} + \frac{\partial^2 C_A}{\partial y^2} + \frac{\partial^2 C_A}{\partial z^2} \right) + R_A$$

(2) cylindrical coordinates (r, θ, z)

$$\frac{\partial C_A}{\partial t} + v_r \frac{\partial T}{\partial r} + \frac{v_\theta}{r} \frac{\partial C_A}{\partial \theta} + v_z \frac{\partial C_A}{\partial z} = D_{AB} \left(\frac{1}{r} \frac{\partial}{\partial r} \left(r \frac{\partial C_A}{\partial r} \right) + \frac{1}{r^2} \frac{\partial^2 C_A}{\partial \theta^2} + \frac{\partial^2 C_A}{\partial z^2} \right) + R_A$$

1. Bird, R.B., Stewart, W.E., and Lightfoot, E.N., Transport Phenomena, Wiley, New York, Chapt.18 (1960)

Nomenclature

Cp	heat capacity, [J/kg K]
g	gravitational acceleration, [m/s^2]
N_{Ax}, N_{Ay}, Nn_{Az}	molar flux in rectangular coordinates, [kmol/m^{2}s]
n_{Ax}, n_{Ay}, n_{Az}	mass flux in rectangular coordinates, [kg/m^{2}s]
p	pressure, [Pa]
q_r, q_θ, q_z	heat flux in cylindrical coordinates, [J/m^{2}s]
q_x, q_y, q_z	heat flux in rectangular coordinates, [J/m^{2}s]
r_A, R_A	reaction rate, [kg/m^{3}s], [kmol/m^{3}s]
r, θ, z	cylindrical coordinates, [m, - , m]
T	temperature, [K]
t	time, [s]
v_r, v_θ, v_z	velocity component in cylindrical coordinates
v_x, v_y, v_z	velocity component in rectangular coordinates, [m/s]
$x, y, z,$	rectangular coordinates, [m]
μ	viscosity, [kg/m s]
ρ	density, [kg/m^3]
τ_w	wall shear stress, [N/m^2]
$\tau_{xx}, \tau_{yx}, \tau_{zx}, - -$	momentum flux or shear stress, [N/m^2] or [kg/s^{2}m]

CHAPTER 6

APPLICATION OF DIFFERENTIAL TRANSPORT EQUATIONS

6.1 Application of the Equation of Motion (Ⅰ)

In this section, we shall study how to use the differential equation of fluid motion. One of the most useful velocity profiles is for flow in a circular pipe.

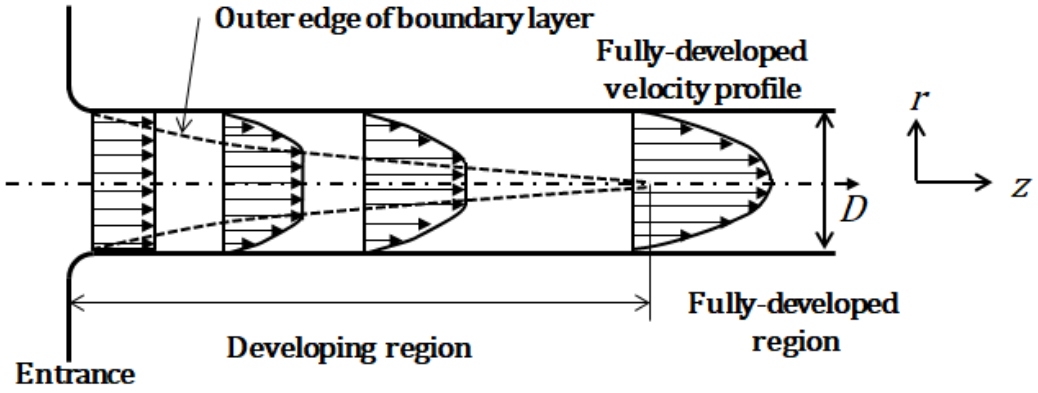

Fig.6.1-1 Flow development in the entrance region of a circular pipe

Generally speaking, it takes a certain length L_{ent} from the entrance until the velocity profile becomes fully developed. At the entrance to the pipe as shown in Fig.6.1-1, the velocity profile is almost uniform like a plug owing to the sudden contraction of flow area. As the fluid moves down the pipe, a boundary layer of low-velocity fluid grows by deceleration due to the viscous force on the wall surface. After the edge of the boundary layer coincides with the pipe axis, the downstream velocity profile no longer varies with axial length z. We shall speak of the fully developed velocity profile as the fixed velocity distribution in the fully developed region. When the Reynolds number Re is less than 2,100, the flow remains laminar and the fully-developed velocity profile is parabolic.

Let us consider the laminar incompressible flow inside an inclined pipe of length L and radius R. The pressure drop over the length L is given by $(p_0 - p_L)$.

What coordinate system is the most appropriate for this flow system? The cylindrical coordinates are the most convenient to describe positions in a pipe.

(1) What component of momentum (or the equation of motion) should be considered? We can assume only z-momentum to be important in laminar flow.

Therefore z-component of the equation of motion for constant ρ and μ may be written

$$\rho\left(\frac{\partial v_z}{\partial t} + v_r\frac{\partial v_z}{\partial r} + \frac{v_\theta}{r}\frac{\partial v_z}{\partial \theta} + v_z\frac{\partial v_z}{\partial z}\right) = -\frac{\partial p}{\partial z} + \mu\left[\frac{1}{r}\frac{\partial}{\partial r}\left(r\frac{\partial v_z}{\partial r}\right) + \frac{1}{r^2}\frac{\partial^2 v_z}{\partial \theta^2} + \frac{\partial^2 v_z}{\partial z^2}\right] + \rho g_z \tag{6.1-1}$$

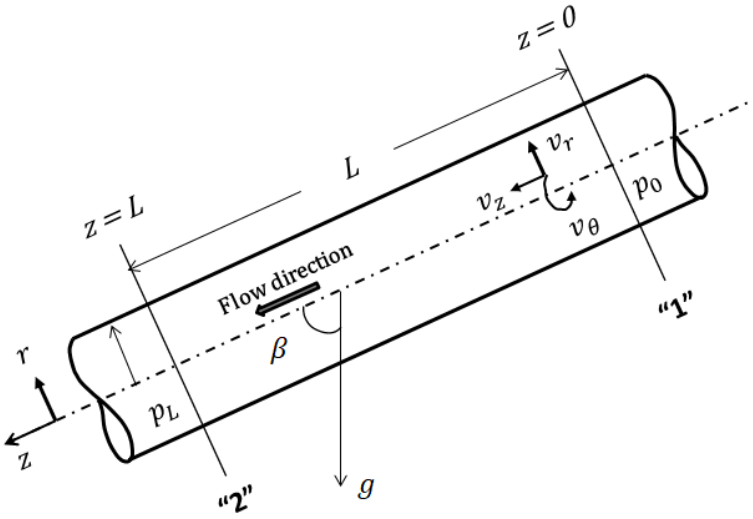

Fig.6.1-2 Laminar flow in a fully-developed region of circular pipe

(2) The next step is simplification of the above equation to fit the problem at hand. We can easily imagine that in steady state laminar flow the fluid particles move along straight streamlines parallel to the pipe axis. Therefore $\frac{\partial v_z}{\partial t} = 0$ and $v_\theta = v_r = 0$.

The flow can be assumed axisymmetric, i.e. $\frac{\partial v_z}{\partial \theta} = \frac{\partial^2 v_z}{\partial \theta^2} = 0$

The flow is fully developed: $\frac{\partial v_z}{\partial z} = \frac{\partial^2 v_z}{\partial z^2} = 0$

Therefore we can expect v_z to be a function of r only: $\frac{\partial}{\partial r}\left(r\,\frac{\partial v_z}{\partial r}\right) = \frac{d}{dr}\left(r\,\frac{dv_z}{dr}\right)$

This type of internal flow is caused by the combined effect of pressure and gravitational forces. We assume the static pressure to be uniform over the pipe cross section: $p = p(z)$.

The z-component of the gravitational acceleration is given by $g_z = g\cos\beta$.

Then the equation of motion becomes

$$0 = -\frac{dp}{dz} + \mu\,\frac{1}{r}\,\frac{d}{dr}\left(r\,\frac{dv_z}{dr}\right) + \rho\, g\cos\beta \qquad (6.1\text{-}2)$$

Differentiate with respect to z, we get $\frac{d^2p}{dz^2} = 0$.

If we integrate with respect to z, we can find $\frac{dp}{dz} = const.$ Thus $\frac{dp}{dz} = \frac{p_L - p_0}{L}$

We get the second-order ordinary differential equation for v_z:

$$\mu\,\frac{1}{r}\,\frac{d}{dr}\left(r\,\frac{dv_z}{dr}\right) = -\frac{p_0 - p_L}{L} - \rho\, g\cos\beta = -\frac{\boldsymbol{P_0 - P_L}}{L} \qquad (6.1\text{-}3)$$

Here the effective pressure $\boldsymbol{P}$ is defined as $\boldsymbol{P} = p - \rho\, g\, z\, cos\,\beta$. If the reference plane at $z = 0$ is chosen at the position 1: $\boldsymbol{P_0} = p_0$ and $\boldsymbol{P}_L = p_L - \rho\, g\, L\, cos\,\beta$.

(3) Integration of the above differential equation gives

$$\frac{dv_z}{dr} = -\frac{\boldsymbol{P_0 - P_L}}{2\mu L}\, r + \frac{C_1}{r} \qquad (6.1\text{-}4)$$

We can use the boundary condition at the pipe axis to evaluate the integration constant C_1:

B.C.1 at $r = 0$ $\quad \frac{dv_z}{dr} = 0$ (6.1-5)

(This boundary condition states that the velocity profile becomes flat at the center of the pipe.)

Then C_1 must be zero. Integration gives

$$v_z = -\frac{\boldsymbol{P_0 - P_L}}{4\mu L} r^2 + C_2 \tag{6.1-6}$$

The other boundary condition is

B.C.2 at $r = R$ $\quad v_z = 0$ (6.1-7)

(This boundary condition states that the fluid does not slip on the wall surface.)

Then C_2 must be

$$C_2 = \frac{\boldsymbol{P_0 - P_L}}{4\mu L} R^2 \tag{6.1-8}$$

Substituting this expression into E.(6.1-6), we get the following equation of parabolic velocity distribution:

$$v_z = \frac{\boldsymbol{P_0 - P_L}}{4\mu L} R^2 \left[1 - \left(\frac{r}{R}\right)^2\right] \tag{6.1-9}$$

This equation indicates that the maximum velocity occurs at the center of the pipe:

$$v_{z,max} = \frac{\boldsymbol{P_0 - P_L}}{4\mu L} R^2 \tag{6.1-10}$$

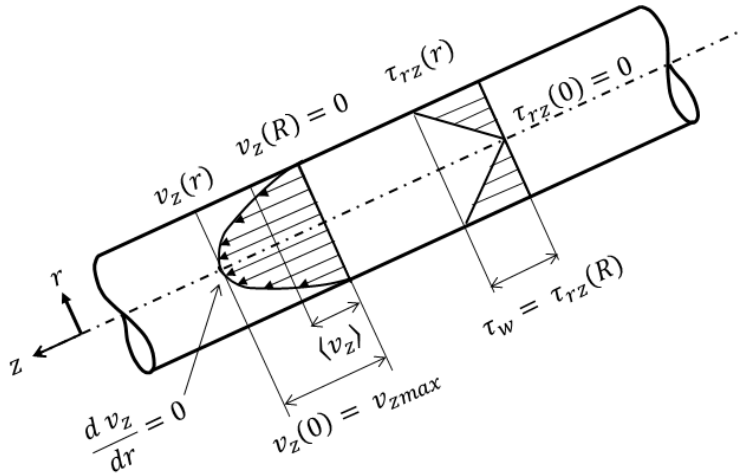

Fig. 6.1-3. Parabolic distribution of velocity and linear distribution of shear stress in a laminar pipe flow

(4) In general, the average velocity taken over the flow cross section is defined as the area-averaged value: $\langle v \rangle = \frac{\int_A v\, dA}{\int_A dA}$. For axisymmetric flow in a circular pipe, substituting the velocity distribution function into the integration, we get

$$\langle v_z \rangle = \frac{\int_0^R v_z\, 2\pi r\, dr}{\int_0^R 2\pi r\, dr} = \frac{\boldsymbol{P_0 - P_L}}{8\mu L} R^2 \tag{6.1-11}$$

Note that the average velocity for laminar flow is just half of the maximum velocity.

(5) The volumetric flow rate can be calculated

$$Q = \int_0^R v_z\, 2\pi r\, dr = \frac{\pi(\boldsymbol{P_0 - P_L})}{8\mu L} R^4 \tag{6.1-12}$$

This equation is known as the Hagen-Poiseuille equation which gives the relation between the volumetric flow rate and the effective pressure drop. If we express the equation in terms of the average velocity or the Reynolds number

$$\boldsymbol{P_0} - \boldsymbol{P_L} = 8\mu L\ \langle v_z\rangle/R^2 \ \text{ or } \ \boldsymbol{P_0} - \boldsymbol{P_L} = 4\ \frac{16}{Re}\ \frac{L}{D}\ \frac{1}{2}\ \rho\langle v_z\rangle^2 \qquad (6.1\text{-}13)$$

This result gives a very important designing formula predicting the pressure drop in a laminar pipe flow.

(6) The shear stress distribution τ_{rz} may now be obtained with the aid of Newton's law of viscosity:

$$\tau_{rz} = -\mu\left(\frac{\partial v_z}{\partial r} + \frac{\partial v_r}{\partial z}\right)$$

In this case $v_r = 0$ and $v_z = v_z(r)$. Therefore

$$\tau_{rz} = -\mu\ \frac{dv_z}{dr}$$

Substitute the velocity distribution into the differentiation and get

$$\tau_{rz} = \frac{\boldsymbol{P_0 - P_L}}{2L}\ r \qquad (6.1\text{-}14)$$

Notice that the shear stress (the momentum flux) has the linear distribution and the maximum value occurs at the wall of the pipe.

$$\tau_{rz,max} = \tau_w = \frac{\boldsymbol{P_0 - P_L}}{2L} R \qquad (6.1\text{-}15)$$

(7) For circular pipe flow, we very frequently use the following definition of friction factor called the Fanning friction factor:

$$P_0 - P_L = 4\ f\ \frac{L}{D}\ \frac{1}{2}\ \rho\langle v_z\rangle^2 \qquad (6.1\text{-}16)$$

The left side term is usually considered to be static pressure drop without the gravitational effect.

Eq.(6.1-13) indicates that for laminar flow inside a circular pipe the friction factor is given by

$$f = \frac{16}{Re} \qquad (6.1\text{-}17)$$

[PROBLEM 6.1-P1] A viscous Newtonian fluid (density $\rho = 1{,}050\ kg/m^3$, viscosity$\mu = 1.0\ poise = 0.10\ kg/m\,s$) is transported through a horizontal 30-mm-ID circular pipe from a storage tank to an agitated tank reactor shown below. The volumetric flow rate is $2 \times 10^{-4}\ m^3/s$. The effective length of the pipeline including the contribution from both ends and a valve is 50 m. Determine the pressure drop between both ends of the pipeline. Calculate the power of the pump.

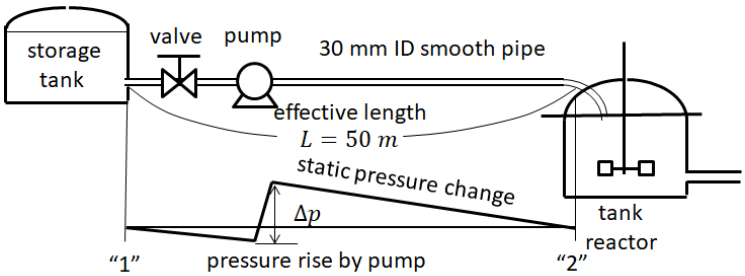

Fig.6.1-P1 Design of feed-supplying pipeline for an agitated tank reactor

6.2 Application of the Equation of Motion (Ⅱ)

In this section, using the equation of motion in cylindrical coordinate system, we shall consider shear flow of an incompressible Newtonian fluid in an annulus between two coaxial vertical long

cylinders, the outer one of which is rotating with a constant angular velocity ω. In steady state there exists stable rotating flow.

Let us determine the velocity distribution neglecting end effects.

The θ-component equation of motion is the most appropriate for this problem:

$$\rho\left(\frac{\partial v_\theta}{\partial t}+ v_r\frac{\partial v_\theta}{\partial r}+ \frac{v_\theta}{r}\frac{\partial v_\theta}{\partial \theta}+ \frac{v_r v_\theta}{r}+ v_z\frac{\partial v_\theta}{\partial z}\right)= -\frac{1}{r}\frac{\partial p}{\partial \theta}$$
$$+\mu\left[\frac{\partial}{\partial r}\left(\frac{1}{r}\frac{\partial}{\partial r}(r v_\theta)\right)+ \frac{1}{r^2}\frac{\partial^2 v_\theta}{\partial \theta^2}+ \frac{2}{r^2}\frac{\partial v_r}{\partial \theta}+\frac{\partial^2 v_\theta}{\partial z^2}\right]+ \rho\, g_\theta \qquad (6.2\text{-}1)$$

All streamlines will form circles coaxial about the axis of rotation. Then the velocity components v_r and v_z are zero and the peripheral velocity v_θ is a function of r alone because of axi-symmetry. Since these cylinders are placed vertically, $g_\theta = 0$.

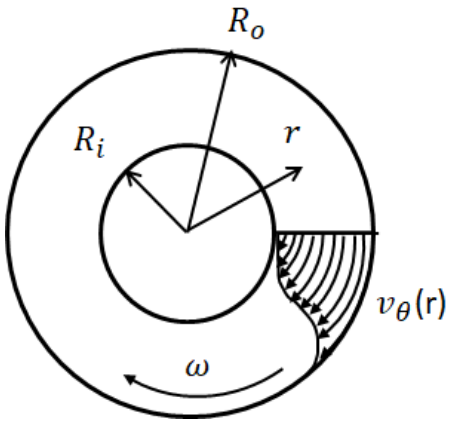

Fig.6.2-1 Laminar shear flow in an annular space between two concentric cylinders when the outer cylinder is rotating.

The θ-component equation of motion then reduces to a second-order ordinary differential equation for v_θ:

$$0 = \frac{d}{dr}\left(\frac{1}{r}\frac{d}{dr}(r\, v_\theta)\right) \qquad (6.2\text{-}2)$$

Integration with respect to r twice gives

$$v_\theta = \frac{C_1}{2}\, r + \frac{C_2}{r} \qquad (6.2\text{-}3)$$

We now have two integration constants to be evaluated by two boundary conditions:

B.C.1 at $r = R_i$ $\qquad v_\theta = 0$

B.C.2 at $r = R_o$ $\qquad v_\theta = R_o\omega$

We obtain

$$\frac{C_1}{2} = \frac{R_i\omega}{R_o-(R_i{}^2/R_o)} = \frac{R_o{}^2}{R_o{}^2- R_i{}^2}\,\omega$$

$$C_2 = -\frac{R_i\omega}{(1/R_i)-(R_i/R_o{}^2)} = -\frac{R_i{}^2 R_o{}^2}{R_o{}^2- R_i{}^2}\,\omega$$

Then we get the hyperbolic velocity distribution:

$$v_\theta = \frac{R_i R_o}{R_o{}^2- R_i{}^2}\, R_o\omega\left[\frac{r}{R_i}- \frac{R_i}{r}\right] \qquad (6.2\text{-}4)$$

According to Newton's law of viscosity, the shear stress $\tau_{r\theta}$ can be written as

$$\tau_{r\theta} = -\mu\left[r\,\frac{\partial}{\partial r}\left(\frac{v_\theta}{r}\right)+ \frac{1}{r}\frac{\partial v_r}{\partial \theta}\right] \qquad (6.2\text{-}5)$$

In this flow system

$$\tau_{r\theta} = -\mu\, r\frac{d}{dr}\left(\frac{v_\theta}{r}\right) \qquad (6.2\text{-}6)$$

Substituting the velocity distribution we get

$$\tau_{r\theta} = -2\mu\omega\,\frac{R_i{}^2 R_o{}^2}{R_o{}^2- R_i{}^2}\,\frac{1}{r^2} \qquad (6.2\text{-}7)$$

This equation indicates that $\tau_{r\theta}$ is always negative, and that the θ-component of momentum transfers in the negative r-direction (inwards).

We may need information about the torque required to turn the shaft of the outer cylinder. Recall that a torque $\vec{\mathbf{T}}$ is a moment, that is, a vector product of force $\vec{\mathbf{F}}$ and lever arm $\vec{\mathbf{r}}$ from the center of rotation. In this system, the lever arm is the radius of the outer cylinder and the force is the shear force acting on the inner surface of the outer cylinder:

$$T_q = \left|\vec{\mathbf{T}}\right| = (2\pi R_o L)(-\tau_{r\theta})|_{r=R_o} \cdot R_o = 4\pi\mu L {R_o}^2 \omega^2 \frac{{R_i}^2}{{R_o}^2 - {R_i}^2}$$

$$= 8\pi^2 \mu L {R_o}^2 N_r \frac{{R_i}^2}{{R_o}^2 - {R_i}^2} \qquad (6.2\text{-}8)$$

This result implies that the torque is proportional to the number of rotation N_r (1/s) and the constant of proportionality is the viscosity of the fluid. This is a principle of Couette-Hatschek viscometers.

Laminar flow in this system is strongly stabilized by centrifugal forces. Thus a fluid particle near the outer cylinder opposes being moved inwards since the centrifugal force acting on it is greater than on particle nearer the inner cylinder. As a result, the flow can remain laminar up to very high Reynolds number.

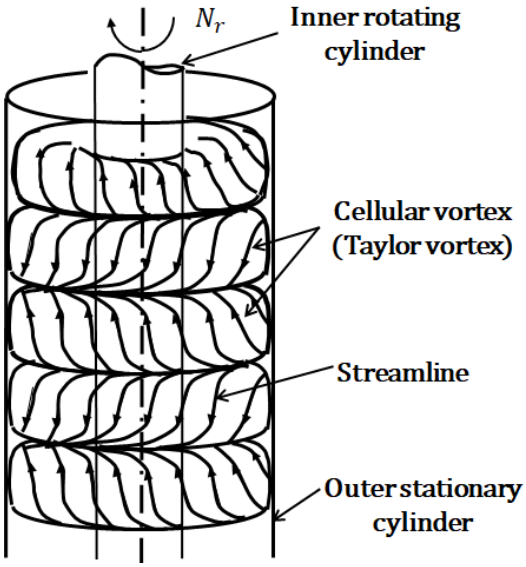

Fig.6.2-2. Pairs of cellular vortices between two concentric cylinders when the inner cylinder is rotating.

On the other hand, it might be very interesting to consider the corresponding flow system in which the inner cylinder is rotating and the outer one is at rest. The fluid velocity increases with decreasing the radial distance. Hence the centrifugal forces tend to introduce instability.

We use a modified Reynolds number for the system:

$$Ta = \frac{\rho R_i \omega_i d}{\mu} \sqrt{\frac{d}{R_i}} \qquad (6.2\text{-}9)$$

This dimensionless parameter is sometimes called Taylor number in honor of the pioneer[1)] in fluid mechanics of this system. The curvature effect (centrifugal effect) can be taken into account introducing $\sqrt{d/R_i}$. When the Taylor number exceeds a certain critical value (i.e. $Ta_{cr} = 41.2$ for very small gap between two coaxial cylinders), there appear ring doughnut-shaped counter-rotating cellular vortices arrayed axially in the annular space due to the centrifugal force. The critical Taylor number for the onset of the cellular vortex flow depends slightly on the geometry d/R_i. For example, $Ta_{cr} = 51.4$ for $d/R_i = 1/3$. This vortex flow is not turbulent, but an elaborate laminar flow with toroidal motion. After successive transitions, the purely turbulent flow can be

attained at a high Taylor number. (e.g. $Ta > about\ 15{,}000$ for relatively large gaps $d/R_i = 0.62$ to 1.14).

This flow system has a very interesting instability scenario[2)] with increasing Taylor number, beginning from the Taylor instability (laminar Taylor vortex flow) via. two sequential wave instabilities (wavy vortex flow, and amplitude-modulated wavy vortex flow) to the final transition to chaotic turbulent flow. Local time-dependent mass transfer controlled by the axial array of cellular vortices was observed on the inner wall of the stationary outer cylinder[2, 3)] by using a diffusion-controlled electrolytic reaction. (see Chapter 14)

1. Taylor, G.I., Phil. Trans., **A223**, 289m (1923), Proc. Roy. Soc. (London), **A151**, 494 (1935)0
2. Kataoka, K., "Taylor vortices and instabilities in circular Couette flows," Encyclopedia of Fluid Mechanics, Gulf Pub., Houston, ed. by N. P. Cheremisinoff, Chap. 9, pp.236 – 274 (1986)
3. Kataoka, K., Doi, H., and Komai, T., *Int. J. Heat Mass Transfer,* **20**, 50 (1977)

6.3 Application of the Equation of Motion (Ⅲ) for non-Newtonian Fluid

We read in section 2.5 that there are some particular fluids which cannot be described by Newton's law of viscosity. For reference, we shall study the Bingham plastic fluid flow in a horizontal circular pipe.

The pressure drop over the length L is given by $(p_0 - p_L)/L$.

In cylindrical coordinates, a simplified equation of the Bingham model is given by

$$\tau_{rz} = -\mu_0 \frac{dv_z}{dr} + \tau_0 \qquad \text{if } \tau_{rz} > \tau_0 \tag{6.3-1a}$$

$$\frac{dv_z}{dr} = 0 \qquad \text{if } \tau_{rz} < \tau_0 \tag{6.3-1b}$$

In general, the z-component equation of motion (for a horizontal pipe flow $g_z = 0$) becomes in cylindrical coordinate system as follows:

$$\rho\left(\frac{\partial v_z}{\partial t} + v_r\frac{\partial v_z}{\partial r} + \frac{v_\theta}{r}\frac{\partial v_z}{\partial \theta} + v_z\frac{\partial v_z}{\partial z}\right) = -\frac{\partial p}{\partial z} - \left(\frac{1}{r}\frac{\partial}{\partial r}(r\,\tau_{rz}) + \frac{1}{r}\frac{\partial \tau_{\theta z}}{\partial \theta} + \frac{\partial \tau_{zz}}{\partial z}\right) \tag{6.3-2}$$

As in section 6.1, assuming incompressible laminar flow with $v_\theta = v_r = 0$, the equation of motion is simplified as

$$\frac{1}{r}\frac{d}{dr}(r\,\tau_{rz}) = \frac{p_0 - p_L}{L} \tag{6.3-3}$$

Integration with respect to r gives

$$\tau_{rz} = \frac{p_0 - p_L}{2L}\,r + \frac{C_1}{r} \tag{6.3-4}$$

The shear stress can be expressed as

$$\tau_{rz} = -\mu_0\frac{dv_z}{dr} + \tau_0 = \frac{p_0 - p_L}{2L}\,r + \frac{C_1}{r}$$

B.C.1 $\tau_{rz} = \tau_0$ at $r = r_0$

Therefore we can evaluate the integration constant as

$$C_1 = r_0\tau_0 - \frac{p_0 - p_L}{2L}{r_0}^2$$

In other words, this implies that the velocity gradient becomes zero at $r = r_0$.

Then the following equation is obtained:

$$\frac{dv_z}{dr} = -\frac{p_0 - p_L}{2\mu_0 L}\,r + \frac{\tau_0}{\mu_0} - \frac{C_1}{\mu_0}\frac{1}{r}$$

Integration gives

$$v_z = -\frac{p_0 - p_L}{2\mu_0 L}\frac{r^2}{2} + \frac{\tau_0}{\mu_0} - \frac{C_1}{\mu_0}\ln r + C_2 \tag{6.3-5}$$

We have to solve the above ordinary differential equation by using the following boundary conditions:

B.C.2 at $r = R$ $v_z = 0$ (no slip condition) (6.3-6)

Therefore

$$C_2 = \frac{p_0 - p_L}{2\mu_0 L}\frac{R^2}{2} + \frac{\tau_0}{\mu_0} - \frac{C_1}{\mu_0}\ln R \quad (6.3\text{-}7)$$

Finally the velocity distribution can be expressed as

$$v_z = -\frac{p_0 - p_L}{2\mu_0 L}\frac{r^2}{2} + \frac{\tau_0}{\mu_0} - \frac{C_1}{\mu_0}\ln r + C_2 \qquad r_0 < r < R \quad (6.3\text{-}8)$$

$$v_z = -\frac{p_0 - p_L}{2\mu_0 L}\frac{{r_0}^2}{2} + \frac{\tau_0}{\mu_0} - \frac{C_1}{\mu_0}\ln r_0 + C_2 = const \qquad 0 < r < r_0 \quad (6.3\text{-}9)$$

where $C_1 = r_0\tau_0 - \frac{p_0 - p_L}{2L}{r_0}^2$ $C_2 = \frac{p_0 - p_L}{2\mu_0 L}\frac{R^2}{2} + \frac{\tau_0}{\mu_0} - \frac{C_1}{\mu_0}\ln R$

The radius r_0 indicates the position where shear stress becomes the threshold value τ_0.

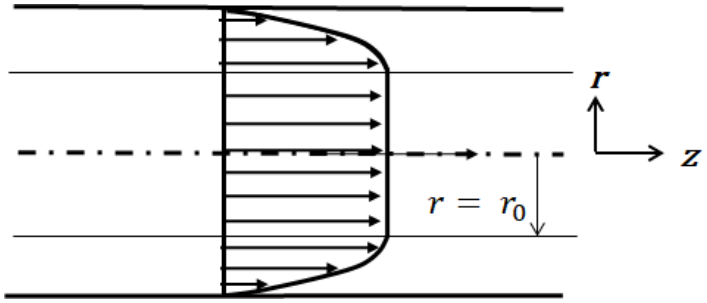

Fig.6.3-1 Flow of a Bingham plastic fluid in a circular pipe

As can be seen in Fig.6.3-1, the fluid flows like a Newtonian fluid in the vicinity of the pipe wall $r_0 < r < R$ but like a plug with uniform velocity in the central region $0 < r < r_0$.

6.4 Application of the Equation of Motion (Ⅳ) for non-Newtonian Fluid

As in Eq.(2.5-3) of section2.5, we should also take an interest in "power law model, which is sometimes called the Ostwald-de Waele Model.

Some expressions of the power law are

$$\tau_{yx} = -m\left|\frac{dv_x}{dy}\right|^{n-1}\frac{dv_x}{dy} \quad (6.4\text{-}1)$$

$$\tau_{rz} = -m\left|\frac{dv_z}{dr}\right|^{n-1}\frac{dv_z}{dr} \quad (6.4\text{-}2)$$

$$\tau_{r\theta} = -m\left|r\frac{d}{dr}\left(\frac{v_\theta}{r}\right)\right|^{n-1} r\frac{d}{dr}\left(\frac{v_\theta}{r}\right) \quad (6.4\text{-}3)$$

The first equation can be used for flow inside rectangular channels, boundary layer flow along a flat plate, film flow along a solid wall, and so on. The second equation can be used for flow inside circular tubes and flow between concentric circular cylinders (the so-called annular flow). The third equation is for rotating flow such as tangential flow in annular space between two concentric rotating cylinders.

For $n = 1$, the power law model reduces to Newton's law of viscosity with m = μ.

[EXAMPLE 6.4-E1] Consider laminar flow of non-Newtonian fluid inside a horizontal circular pipe.

The power law model for this case should be of the form:

$$\tau_{rz} = m\left(-\frac{dv_z}{dr}\right)^n \tag{6.4-E1}$$

The Navier-Stokes equation to be solved is Eq.(6.3-2):

$$\rho\left(\frac{\partial v_z}{\partial t} + v_r\frac{\partial v_z}{\partial r} + \frac{v_\theta}{r}\frac{\partial v_z}{\partial \theta} + v_z\frac{\partial v_z}{\partial z}\right) = -\frac{\partial p}{\partial z} - \left(\frac{1}{r}\frac{\partial}{\partial r}(r\,\tau_{rz}) + \frac{1}{r}\frac{\partial \tau_{\theta z}}{\partial \theta} + \frac{\partial \tau_{zz}}{\partial z}\right)$$

For steady state $\partial v_z/\partial t = 0$, For axisymmetric flow $\partial v_z/\partial\theta = 0$ and $\partial \tau_{\theta z}/\partial\theta = 0$.

In the fully-developed flow region $\partial v_z/\partial z = 0$ and $\partial \tau_{zz}/\partial z = 0$.

Since all streamlines are parallel to the tube wall, $v_r = 0$

Then the equation becomes

$$\frac{1}{r}\frac{\partial}{\partial r}(r\,\tau_{rz}) = -\frac{\partial p}{\partial z} \tag{6.4-E2}$$

For a horizontal tube flow

$$-\frac{\partial p}{\partial z} = \frac{p_0 - p_L}{L} \tag{6.4-E3}$$

Then the equation becomes an ordinary differential equation:

$$\frac{1}{r}\frac{d}{dr}(r\,\tau_{rz}) = \frac{p_0 - p_L}{L} \tag{6.4-E4}$$

Integration with respect to z gives

$$\tau_{rz} = \frac{p_0 - p_L}{2L}\,r + \frac{C_1}{r} \tag{6.4-E5}$$

Since τ_{rz} does not become infinite at the tube axis, C_1 must be zero. Then

$$\tau_{rz} = \frac{p_0 - p_L}{2L}\,r \tag{6.4-E6}$$

Note that the linear distribution of shear stress is the same in form as Eq.(6.1-14) for Newtonian fluid flow.

If the power law model can be used for τ_{rz}, the above equation becomes

$$m\left(-\frac{d\,v_z}{dr}\right)^n = \frac{p_0 - p_L}{2L}\,r \quad \text{or}$$

$$-\frac{d\,v_z}{dr} = \left(\frac{p_0 - p_L}{2\,mL}\right)^{1/n} r^{1/n} \tag{6.4-E7}$$

Integration gives

$$v_z = -\left(\frac{p_0 - p_L}{2\,mL}\right)^{1/n}\frac{n}{1+n}\,r^{1+n/n} + C_2$$

At $r = R$, $v_z = 0$. Therefore

$$C_2 = \left(\frac{p_0 - p_L}{2\,mL}\right)^{1/n}\frac{n}{1+n}\,R^{1+n/n}$$

Then the laminar velocity distribution is

$$v_z = \left(\frac{p_0 - p_L}{2\,mL}\right)^{1/n}\frac{n}{1+n}\,R^{1+n/n}\left[1 - \left(\frac{r}{R}\right)^{1+n/n}\right] \tag{6.4-E8}$$

For $n = 1$, it reduces to the parabolic velocity distribution for Newtonian fluid flow.

[PROBLEM 6.4-P1] An incompressible fluid of density ρ and viscosity μ is in laminar flow in a rectangular horizontal channel of width W and height $2H$, as shown. The static pressure decreases at a rate of $(p_0 - p_L)/L$.

Obtain the expression for the velocity distribution in the fully developed region. What is the ratio of average to maximum velocity $\langle v_z\rangle/v_{max}$? What is the shear stress acting on the upper wall? Obtain the expression of volumetric flow rate.

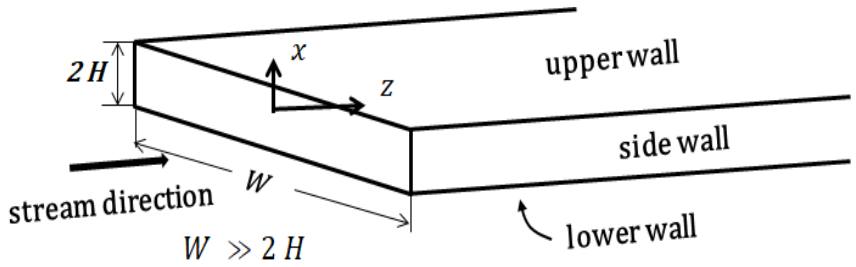

Fig.6.4-P1 Laminar flow in a rectangular channel

[PROBLEM 6.4-P2] A Newtonian fluid with constant ρ and μ is in laminar liquid film flowing downward on the inside wall of a vertical, long circular tube shown below. The radius of the tube is R and the film thickness is δ in the fully-developed region. Obtain the following steady velocity distribution in the fully-developed region:

$$v_z = \frac{\rho g R^2}{4\,\mu}\left[(1-\left(\frac{r}{R}\right)^2 + 2\left(1-\frac{\delta}{R}\right)^2 \ln\left(\frac{r}{R}\right)\right] \qquad (6.4\text{-P1})$$

What is the Reynolds number?

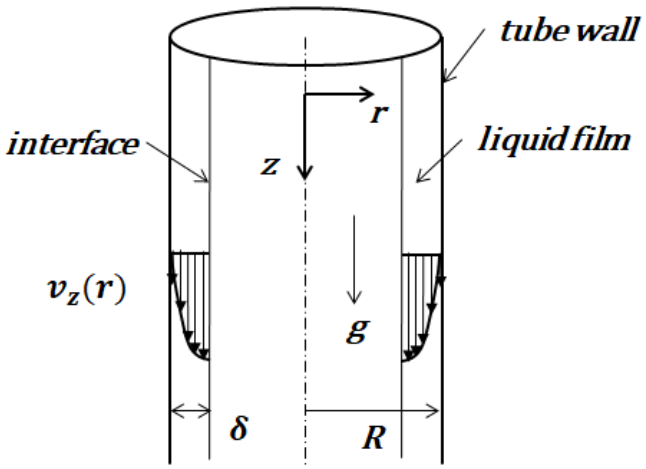

Fig.6.4-P2. Liquid film stream falling along inside a tube wall

[PROBLEM 6.4-P3] We are now in a process to design an oil line shown below. Crude oil at 15℃ is to be pumped through a horizontal 80 mm ID smooth pipe at a volumetric flow rate $1 \times 10^{-2}\, m^3/s$. The viscosity and density of the crude oil at 15℃ are $8 \times 10^{-2}\ kg/m\,s$ and $880\ kg/m^3$, respectively. If pumps with $4 \times 10^5\, Pa$ pressure rise are used, how far apart can they be located?

Calculate the power of pumps, assuming that the pumps operate at an efficiency of 100 percent. Neglect the contribution from fittings and valves to the total pressure drop.

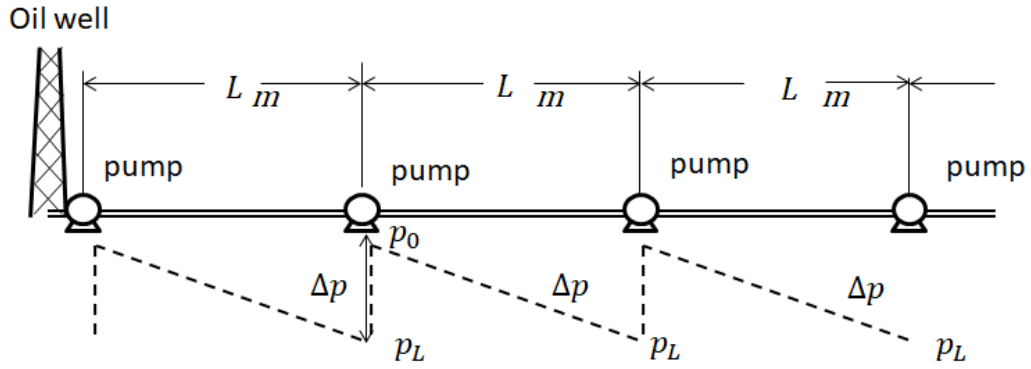

Fig.6.4-P3 Oil line to be designed and its pressure change

6.5 Application of the Equation of Energy (Ⅰ)

Let us consider the heat transfer problem in laminar flow inside a pipe. We assume constant physical properties and negligibly small viscous dissipation. The equation of energy written in the cylindrical coordinate system can be employed:

$$\rho Cp\left(\frac{\partial T}{\partial t}+ v_r\frac{\partial T}{\partial r}+ \frac{v_\theta}{r}\frac{\partial T}{\partial \theta}+ v_z\frac{\partial T}{\partial z}\right) = \kappa\left(\frac{1}{r}\frac{\partial}{\partial r}\left(r\frac{\partial T}{\partial r}\right)+\frac{1}{r^2}\frac{\partial^2 T}{\partial \theta^2}+\frac{\partial^2 T}{\partial z^2}\right) \quad (6.5\text{-}1)$$

(1) In general, this equation cannot independently solved without information of the velocity distribution. Let us restrict the problem to the fully-developed laminar flow at steady state.

Therefore we start by noting that $v_r = v_\theta = 0$ and $\partial T/\partial t = 0$.

We assume axisymmetric heat transfer i.e. $\partial T/\partial\theta = \partial^2 T/\partial\theta^2 = 0$.

Then the above equation becomes

$$\rho Cp\, v_z\frac{\partial T}{\partial z} = \kappa\left[\frac{1}{r}\frac{\partial}{\partial r}\left(r\frac{\partial T}{\partial r}\right)+\frac{\partial^2 T}{\partial z^2}\right] \quad (6.5\text{-}2)$$

Usually the axial conduction (the term containing $\partial^2 T/\partial z^2$ can be neglected relative to radial conduction (the first term on the right side of Eq.(6.5-2)).

We finally obtain

$$\frac{1}{r}\frac{\partial}{\partial r}\left(r\frac{\partial T}{\partial r}\right) = \frac{v_z}{\alpha}\frac{\partial T}{\partial z} \quad (6.5\text{-}3)$$

where $\alpha = \kappa/\rho Cp$.

(2) Let us further restrict the problem to fully-developed temperature field. First we have to visualize that there exists, under certain heating conditions, a dimensionless temperature profile invariant with pipe length.

The volumetric flow rate is given by

$$Q = \int_0^R v_z\, 2\pi r\, dr = \frac{\pi(\boldsymbol{p_0}-\boldsymbol{p_L})}{8\mu L}R^4 \quad (6.1\text{-}12)$$

For convenience the mean fluid temperature T_m is defined as

$$\rho Cp\, Q\, T_m = \int_0^R \rho Cp\, T\, v_z\, 2\pi r\, dr \quad (6.5\text{-}4)$$

For constant physical properties

$$T_m = \frac{2}{\langle v_z\rangle R^2}\int_0^R v_z T\, r dr \quad (6.5\text{-}5)$$

This temperature T_m is sometimes referred to as the bulk fluid temperature or the cup-mixing temperature.

The dimensionless temperature is also defined in terms of T_m as $(T_w - T)/(T_w - T_m)$.

If it is invariant in the axial direction

$$\frac{\partial}{\partial z}\left(\frac{T_w - T}{T_w - T_m}\right) = 0 \qquad (6.5\text{-}6)$$

Differentiate it with respect to r

$$\frac{\partial}{\partial r}\frac{\partial}{\partial z}\left(\frac{T_w - T}{T_w - T_m}\right) = 0$$

Changing the order of differentiation, integrating with respect to z,

$$\frac{\partial}{\partial r}\left(\frac{T_w - T}{T_w - T_m}\right)\Big|_{r=R} = const \qquad (6.5\text{-}7)$$

By noting that T_m and T_w are not a function of r, we get

$$\frac{-\frac{\partial T}{\partial r}\Big|_{r=R}}{T_w - T_m} = const \qquad (6.5\text{-}8)$$

Let us define a heat transfer coefficient in terms of the mean temperature:

$$q_w = h\,(T_w - T_m) = -\kappa\left(\frac{\partial T}{\partial r}\right)\Big|_{r=R} \qquad (6.5\text{-}9)$$

Keep in mind that this is the case whether the flow is laminar or turbulent. Eqs.(6.5-4) to (6.5-9) are valid even for turbulent flow. This definition implies that the heat flux from the pipe wall to the fluid is proportional to the characteristic temperature difference. Since the temperature gradient at the wall $(\partial T/\partial r)|_{r=R}$ is dependent on the flow condition, the heat transfer coefficient is a function of flow condition (e.g. the Reynolds number) as well as physical properties (e.g. the Prandtl number).

Thus

$$\frac{h}{\kappa} = \frac{-\frac{\partial T}{\partial r}\Big|_{r=R}}{T_w - T_m} = const \quad \text{or} \quad h = const \qquad (6.5\text{-}10)$$

This indicates that the fully-developed temperature field can be observed far downstream of the entrance for constant heat transfer coefficient conditions.

In fact, most heat exchangers are designed based on constant heat transfer coefficient assumption.

Getting back to the definition of the fully-developed temperature profile

$$\frac{\partial}{\partial z}\left(\frac{T_w - T}{T_w - T_m}\right) = 0$$

That is

$$\frac{\partial T}{\partial z} = \frac{dT_w}{dz} - \frac{T_w - T}{T_w - T_m}\frac{dT_w}{dz} + \frac{T_w - T}{T_w - T_m}\frac{dT_m}{dz}$$

Substituting into the equation of energy

$$\frac{1}{r}\frac{\partial}{\partial r}\left(r\frac{\partial T}{\partial r}\right) = \frac{v_z}{\alpha}\left[\frac{dT_w}{dz} - \frac{T_w - T}{T_w - T_m}\frac{dT_w}{dz} + \frac{T_w - T}{T_w - T_m}\frac{dT_m}{dz}\right] \qquad (6.5\text{-}11)$$

This equation can be solved by at least two boundary conditions:

Case Ⅰ: constant heat flux $q_w = h\,(T_w - T_m) = -\kappa\left(\frac{\partial T}{\partial r}\right)\Big|_{r=R} = const$ (6.5-12)

Case Ⅱ: constant wall temperature $T_w = const$ (6.5-13)

The first heating condition is often encountered in counter-current heat exchangers when the fluid capacity rates are the same for both fluids. $w\,cp = W\,Cp$, where w, W are the mass flow rates of the hotter and the colder fluids and cp, Cp the corresponding specific heats.

If $h = const$, $T_w - T_m = const$. Therefore

$$\frac{dT_w}{dz} - \frac{dT_m}{dz} = 0 \quad \text{i.e.} \quad \frac{dT_m}{dz} = \frac{dT_w}{dz} = \frac{\partial T}{\partial z} \qquad (6.5\text{-}14)$$

The equation to be solved for constant heat flux is

$$\frac{1}{r}\frac{\partial}{\partial r}\left(r\,\frac{\partial T}{\partial r}\right)=\frac{v_z}{\alpha}\frac{dT_m}{dz} \qquad (6.5\text{-}15)$$

The second heating condition is also encountered in heat exchangers when one of the two fluid streams has phase transformation such as condensation and evaporation. In this case

$$\frac{dT_w}{dz}=0 \qquad (6.5\text{-}16)$$

The equation of energy to be solved for constant wall temperature becomes

$$\frac{1}{r}\frac{\partial}{\partial r}\left(r\,\frac{\partial T}{\partial r}\right)=\frac{v_z}{\alpha}\frac{T_w-T}{T_w-T_m}\frac{dT_m}{dz} \qquad (6.5\text{-}17)$$

We shall solve these differential equations Eq.(6.5-15) and Eq.(6.5-17) in the following example.

The corresponding temperature variations with pipe length for these two cases are shown below.

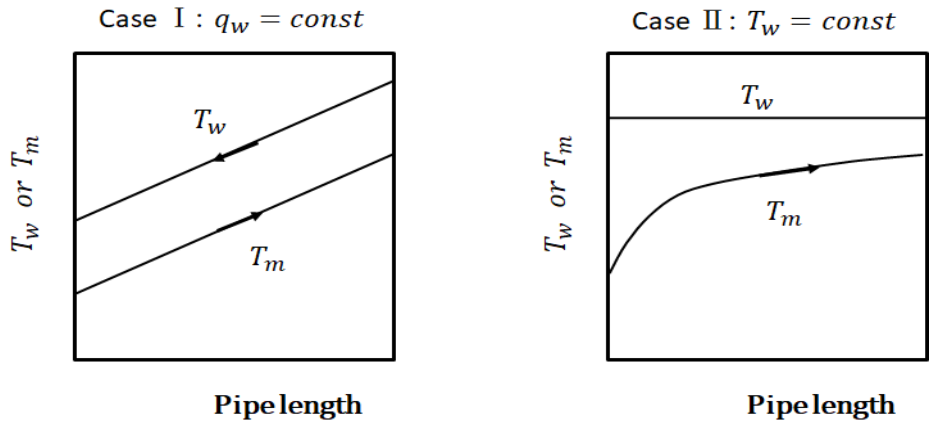

Fig.6.5-1 Temperature variation along pipe axis

[EXAMPLE 6.5-E1]

Let us solve the first case:

Case I : constant heat flux $q_w = h\,(T_w - T_m) = -\kappa\left(\frac{\partial T}{\partial r}\right)\Big|_{r=R} = const$

We assume the fully-developed parabolic velocity distribution and substitute it into the equation to be solved:

$$\frac{1}{r}\frac{\partial}{\partial r}\left(r\,\frac{\partial T}{\partial r}\right)=\frac{2\langle v_z\rangle}{\alpha}\left[1-\left(\frac{r}{R}\right)^2\right]\frac{dT_m}{dz} \qquad (6.5\text{-E1})$$

Integrating with respect to r

$$r\,\frac{\partial T}{\partial r}=\frac{2\langle v_z\rangle}{\alpha}\left[\frac{r^2}{2}-\frac{r^4}{4R^2}\right]\frac{dT_m}{dz}+C_1$$

The following boundary condition is applicable to evaluate the integration constant C_1:

B.C.1 at $r=0$ $\frac{\partial T}{\partial r}=0$. Then C_1: must be zero. $C_1=0$

Integration gives

$$T=\frac{2\langle v_z\rangle}{\alpha}\left[\frac{r^2}{4}-\frac{r^4}{16R^2}\right]\frac{dT_m}{dz}+C_2$$

The integration constant C_2 can be evaluated from the following boundary condition:

B.C.2 at $r = R$ $T = T_w$.

Thus

$$C_2 = T_w - \frac{2\langle v_z\rangle}{\alpha}\frac{3}{16}R^2\frac{dT_m}{dz}$$

Substituting this expression, we finally obtain the following temperature profile:

$$T = T_w + \frac{2\langle v_z\rangle}{\alpha}\left[\frac{r^2}{4} - \frac{r^4}{16R^2} - \frac{3}{16}R^2\right]\frac{dT_m}{dz} \quad (6.5\text{-E2})$$

According to the definition of the mean temperature

$$T_m = \frac{2}{\langle v_z\rangle R^2}\int_0^R v_z T\, r\, dr = T_w - \frac{11}{96}\frac{2\langle v_z\rangle}{\alpha}\frac{dT_m}{dz}R^2 \quad (6.5\text{-E3})$$

Then the driving force is given by

$$\Delta T = T_w - T_m = \frac{11}{96}\frac{2\langle v_z\rangle}{\alpha}\frac{dT_m}{dz}R^2 \quad (6.5\text{-E4})$$

On the other hand, the temperature gradient at the wall is calculated as

$$\left(\frac{\partial T}{\partial r}\right)\Big|_{r=R} = \frac{\langle v_z\rangle}{2\alpha}R\frac{dT_m}{dz} \quad (6.5\text{-E5})$$

Using Eq.(6.5-E4), the heat flux becomes

$$q_w = h(T_w - T_m) = h\frac{11}{96}\frac{2\langle v_z\rangle}{\alpha}R^2\frac{dT_m}{dz}$$

Using Eq.(6.5-E5), the wall heat flux is also given by

$$q_w = \kappa\left(\frac{\partial T}{\partial r}\right)\Big|_{r=R} = \kappa\frac{\langle v_z\rangle}{2\alpha}R\frac{dT_m}{dz}$$

Solving for h from these two equations,

$$h = \frac{24}{11}\frac{\kappa}{R}$$

The dimensionless group called the Nusselt number becomes for laminar pipe flow with constant heat flux :

$$Nu = \frac{hD}{\kappa} = \frac{48}{11} = const \quad (6.5\text{-E6})$$

The Nusselt number implies the ratio of convective to conductive heat transfer rate:

$$Nu = \frac{h\Delta T}{\kappa(\Delta T/D)} \quad (6.5\text{-E7})$$

The Stanton number is defined as

$$St = \frac{h}{\varrho Cp\langle v_z\rangle} = \frac{Nu}{Re\,Pr} \quad (6.5\text{-E8})$$

Then the Stanton number becomes for heat transfer with constant heat flux in laminar pipe flow:

$$St\,Pr = \frac{(48/11)}{Re} \quad (6.5\text{-E9})$$

Note the similarity in form to the corresponding friction factor:

$$f = \frac{16}{Re} \quad (6.5\text{-E10})$$

The above Nusselt number is a limiting value far downstream of the heating section in a pipe.

Eq.(6.5-E6) is applicable to the thermal entry region:

$$\frac{L_{ent}}{D} > 0.05\,Re\,Pr \quad (6.5\text{-E11})$$

Experimental data are correlated by Sieder and Tate by the equation:

$$Nu_m = 1.86\,[Re\,\mathrm{Pr}(D/L)]^{1/3}(\mu/\mu_w)^{0.14} \quad (6.5\text{-E12})$$

[PROBLEM6.5-P1] A Newtonian fluid of constant physical properties (ρ, μ, κ) is in laminar flow inside a rectangular horizontal channel.(see Problem 6.4-P1). Although the heat transfer rate depends on the fluid flow rate, the upper wall is kept at T_{w1} and the lower wall is cooled at T_{w2}. ($T_{w1} > T_{w2}$). Both the side walls are thermally insulated. Therefore it can be assumed that the fluid temperature does not change in the transverse direction y. Obtain the temperature distribution in the vertical direction in the fully developed region. Using the velocity distribution obtained in Problem 6.4-P1, calculate the enthalpy flow rate across the cross-sectional area $2\,W\,H$. What is the heat flux required to keep the wall temperatures T_{w1} and T_{w2}.?

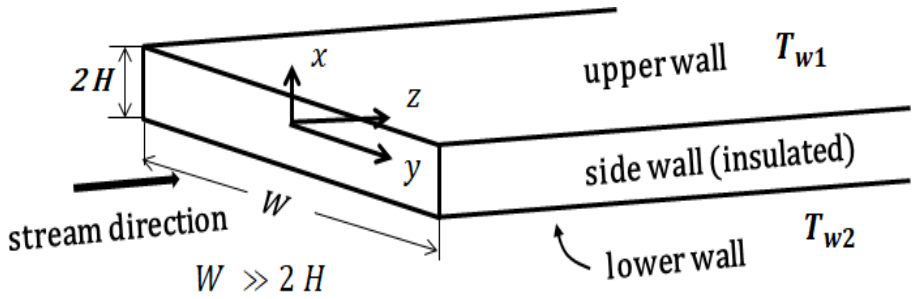

Fig.6.5-P1 Temperature distribution of fully developed laminar flow inside a rectangular horizontal channel.

6.6 Application of the Equation of Energy (Ⅱ)

6.6-1 Steady Heat Conduction

Let us consider the composite wall of blast furnace consisting of three different materials as an example of heat conduction in hollow cylinders.

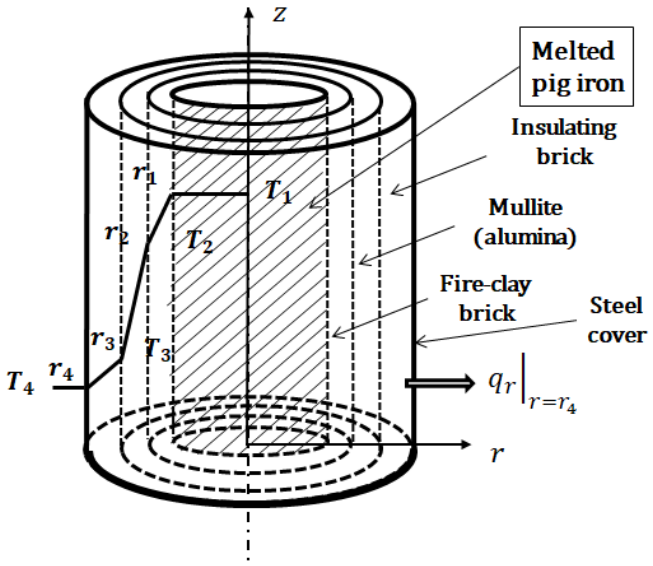

Fig.6.6-1 Temperature profile in insulating brick layers of furnace

For steady-state operation the inside surface of the fire-clay brick and the outside surface of steel cover are held at constant temperature T_1 and T_4, respectively. Since the steel cover has very large thermal conductivity, that is, the heat conduction resistance of the steel cover can be assumed negligibly small, so that the outer surface temperature of the insulating brick can be assumed equal to T_4. $(T_1 > T_4)$ The

thermal conductivities of the fire-clay brick, Mullite (alumina brick), and the insulating brick are κ_1, κ_2, κ_3, respectively. Let us determine the heat loss over the height L from the outer surface of the furnace.

In the equation of energy in cylindrical coordinates, all velocity components vanish. We can also assume the local temperature to be constant with respect to z and θ. Therefore the temperature should be a function of r only.

For this problem, the equation to be solved becomes

$$\frac{d}{dr}\left(r\,\frac{dT}{dr}\right) = 0 \qquad (6.6\text{-}1)$$

Integrating twice with respect to r, the general solution is obtained:

$$T = C_1 \ln r + C_2 \qquad (6.6\text{-}2)$$

These two constants of integration can be evaluated in each brick layer from the following boundary conditions:

B.C.1 at $r = r_1$, $T = T_1$
B.C.2 at $r = r_2$, $T = T_2$
B.C.3 at $r = r_3$, $T = T_3$
B.C.4 at $r = r_4$, $T = T_4$

Here the temperatures corresponding to radii r_2 and r_3, are unknown and temporarily denoted by T_2 and T_3, respectively.

Making use of a pair of terminal temperatures T_1 and T_2, the temperature distribution in the fire-clay brick layer can be written as

$$T = T_2 + \frac{T_1 - T_2}{\ln(r_1/r_2)}\ln(r/r_2) \qquad r_1 \le r \le r_2 \qquad (6.6\text{-}3)$$

Similarly

$$T = T_3 + \frac{T_2 - T_3}{\ln(r_2/r_3)}\ln(r/r_3) \qquad r_2 \le r \le r_3 \qquad (6.6\text{-}4)$$

$$T = T_4 + \frac{T_3 - T_4}{\ln(r_3/r_4)}\ln(r/r_4) \qquad r_3 \le r \le r_4 \qquad (6.6\text{-}5)$$

For this problem, Eq.(6.6-1) implies

$$\frac{d}{dr}(r\,q_r) = 0 \qquad (6.6\text{-}6)$$

By integrating, we find

$$r\,q_r = r_4\,q_r|_{r=r_4} = const \qquad (6.6\text{-}7)$$

We now evaluate dT/dr at the surface $r = r_4$ with the aid of the temperature distribution

$$\left.\frac{dT}{dr}\right|_{r=r_4} = \frac{T_3 - T_4}{r_4\,ln\,(r_3/r_4)}$$

Then we get

$$r_4\,q_r|_{r=r_4} = \kappa_3\,\frac{T_3 - T_4}{\ln(r_4/r_3)} \qquad (6.6\text{-}8)$$

Similarly

$$r_3\,q_r|_{r=r_3} = \kappa_2\,\frac{T_2 - T_3}{\ln(r_3/r_2)} \qquad (6.6\text{-}9)$$

$$r_2\,q_r|_{r=r_2} = \kappa_1\,\frac{T_1 - T_2}{\ln(r_2/r_1)} \qquad (6.6\text{-}10)$$

The above three equations are combined as

$$r_4\,q_r|_{r=r_4} = \frac{T_1 - T_2}{\frac{1}{\kappa_1}\ln\left(\frac{r_2}{r_1}\right)} = \frac{T_2 - T_3}{\frac{1}{\kappa_2}\ln\left(\frac{r_3}{r_2}\right)} = \frac{T_3 - T_4}{\frac{1}{\kappa_3}\ln\left(\frac{r_4}{r_3}\right)} = \frac{T_1 - T_4}{\frac{1}{\kappa_1}\ln\left(\frac{r_2}{r_1}\right) + \frac{1}{\kappa_2}\ln\left(\frac{r_3}{r_2}\right) + \frac{1}{\kappa_3}\ln\left(\frac{r_4}{r_3}\right)} \qquad (6.6\text{-}11)$$

Each denominator can be interpreted as the thermal resistance of a single layer.

The thermal resistance of the steel cover is so small that its term is omitted in the denominator.

The total resistance of three layers in series is given by

$$R_{total} = \frac{1}{\kappa_1}\ln\left(\frac{r_2}{r_1}\right) + \frac{1}{\kappa_2}\ln\left(\frac{r_3}{r_2}\right) + \frac{1}{\kappa_3}\ln\left(\frac{r_4}{r_3}\right) \tag{6.6-12}$$

Finally we obtain the heat loss Q from the outer surface of the furnace:

$$Q = 2\pi r_4 L q_r|_{r=r_4} = \frac{2\pi L\,(T_1 - T_4)}{\frac{1}{\kappa_1}\ln\left(\frac{r_2}{r_1}\right) + \frac{1}{\kappa_2}\ln\left(\frac{r_3}{r_2}\right) + \frac{1}{\kappa_3}\ln\left(\frac{r_4}{r_3}\right)} \tag{6.6-13}$$

The electrical analog for a three-layer cylinder with specified temperature is shown in Fig.6.6-2.

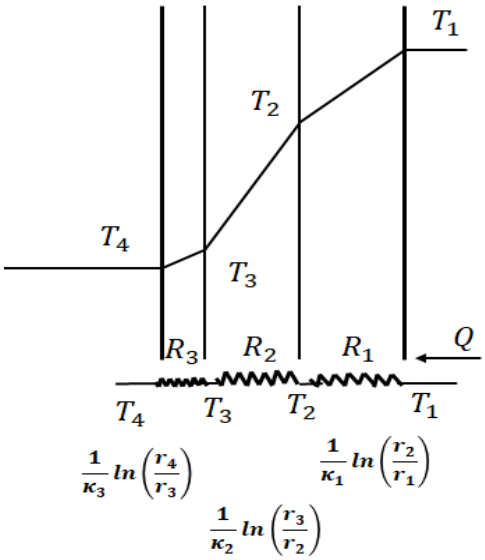

Fig.6.6-2 Heat transfer resistances in series

As the thickness of insulating-brick increases (as r_3/r_2 increases), the heat loss decreases. From an economic viewpoint, the optimum thickness can be calculated by taking into account the energy cost and the cost of insulating material. Obviously this approach can be extended to any number of layers of material. We have tacitly assumed no contact resistance between the layers of different materials. Even thin air gap formed in between the layers results in considerable contact resistance to heat transfer.

[PROBLEM 6.6-P1] A cylindrical rod (radius R m) of thermal conductivity κ W/m K is cooled at steady state by air of temperature T_{air}K in order to keep the rod surface at a safe temperature T_0 K decided by the safety regulation. This rod has a uniform volume production of heat Q_E (W/m^3) inside it.

(a) Derive the equation of heat conduction for obtaining the temperature profile.
(b) Obtain an expression for dimensionless temperature profile.
(c) Confirm that the heat released from the rod surface becomes equal to the heat generation.

6.6-2 Unsteady Heat Conduction[1)]

Let us consider a problem of unsteady cooling a finite slab having a thickness of $2b$ in y-direction. The dimensions in x- and z-direction are infinitely large. The slab is initially kept at T_0. At time $t = 0$, both the surfaces at $y = \pm b$ are instantaneously cooled to T_c and kept at T_c. We shall find the time-dependent profile.

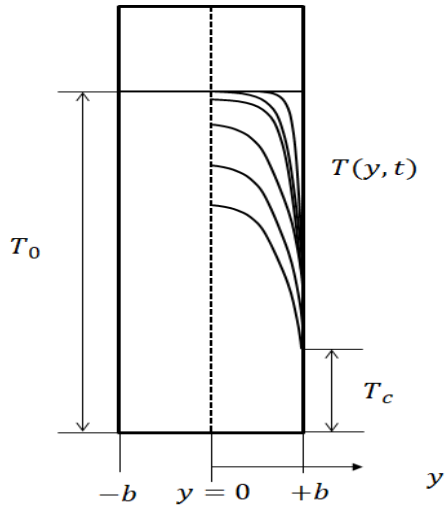

Fig.6.6-3. Cooling a finite slab of solid

The differential equation of energy transport to be applied reduces to

$$\frac{\partial T}{\partial t} = \alpha \frac{\partial^2 T}{\partial y^2} \quad (6.6\text{-}14)$$

We introduce the following dimensionless variables:

Temperature $\Theta = \frac{T - T_c}{T_0 - T_c}$ (6.6-15)

y-directional length $\eta = \frac{y}{b}$ (6.6-16)

Time $\tau = \frac{\alpha t}{b^2}$ (6.6-17)

where $\alpha = \kappa/\rho Cp$ is thermal diffusivity.

Therefore the dimensionless equation and the boundary conditions become simpler as follows:

$$\frac{\partial \Theta}{\partial \tau} = \alpha \frac{\partial^2 \Theta}{\partial \eta^2} \quad (6.6\text{-}18)$$

I.C. at $\tau = 0$ $\Theta = 1$ (6.6-19)

B.C.1 at $\eta = +1$ $\Theta = 0$ (6.6-20)

B.C.2 at $\eta = -1$ $\Theta = 0$ (6.6-21)

Using the method of separation of variables, the following temperature function can be assumed:

$$\Theta(\eta, \tau) = f(\eta) g(\tau) \quad (6.6\text{-}22)$$

Substituting the function into Eq.(6.6-18)

$$\frac{1}{g}\frac{dg}{d\tau} = \frac{1}{f}\frac{d^2 f}{d\eta^2} \quad (6.6\text{-}23)$$

The left side is a function of τ only whereas the right side is a function of η only.

This condition can be valid only if both sides equal a constant $-c^2$. Therefore this problem reduces to the following two ordinary equations:

$$\frac{dg}{d\tau} = -c^2 g \quad (6.6\text{-}24)$$

$$\frac{d^2 f}{d\eta^2} = -c^2 f \quad (6.6\text{-}25)$$

These equations can be integrated as

$$f = K_1 \sin c\ \eta + K_2 \cos c\ \eta \quad (6.6\text{-}26)$$

$$g = K_3 \exp(-c^2 \tau) \quad (6.6\text{-}27)$$

It can be considered that the temperature profile should be symmetric about the centerline of the slab. Therefore K_1 must be zero. From the boundary conditions, $f_{\eta=0} = K_2 \cos c = 0$ This suggests that

$$c = (n + 1/2)\pi \qquad n = 0, \pm 1, \pm 2, - - - - - - \quad (6.6\text{-}28)$$

After all, the following form of the solution can be obtained:

$$\Theta = \sum_{n=0}^{\infty} C_n \exp(-(n+1/2)^2\pi^2\tau)\ \cos(n+1/2)\,\pi\,\eta \quad (6.6\text{-}29)$$

The unknown constant C_n should be determined by using the initial condition.

At $\tau = 0 \quad \Theta = 1 \quad \rightarrow \quad 1 = \sum_{n=0}^{\infty} C_n\ \cos(n+1/2)\,\pi\,\eta$ (6.6-30)

Multiplying by $\cos(m+1/2)\,\pi\,\eta\,d\eta$ and then integrating from $\eta = -1$ to $\eta = +1$

$$\int_{-1}^{+1} \cos(m+1/2)\,\pi\,\eta\,d\eta = \sum_{n=0}^{\infty} C_n \int_{-1}^{+1} \cos(m+1/2)\,\pi\,\eta \cos(n+1/2)\,\pi\,\eta\,d\eta \quad (6.6\text{-}31)$$

The integration on the right becomes zero except for the case $n = m$. Eq. (6.6-32) becomes

$$\frac{\sin(m+1/2)\,\pi\,\eta}{(m+1/2)\,\pi}\Bigg|_{\eta=-1}^{\eta=+1} = C_m \left(\frac{\left(\frac{1}{2}\right)(m+1/2)\pi\,\eta + \left(\frac{1}{4}\right) sin\,(m+1/2)\,2\pi\,\eta}{(m+1/2)\pi} \right)\Bigg|_{\eta=-1}^{\eta=+1}$$

Solving for C_m, we get

$$\frac{2\,(-1)^m}{(m+1/2)\,\pi} = C_m$$

Finally the temperature profile can be expressed as

$$\frac{T-T_c}{T_0-T_c} = 2\sum_{n=0}^{\infty} \frac{(-1)^n}{(n+1/2)\,\pi} \exp\left(-(n+\tfrac{1}{2})^2\pi^2\,\alpha t/b^2\right) \cos(n+1/2)\,\frac{\pi y}{b} \quad (6.6\text{-}32)$$

This solution can be used for many unsteady-state heat conduction problems. It can be kept in mind that for very short times the convergence becomes slow.

---

1. Bird, R.B., Stewart, W.E., and Lightfoot, E.N., Transport Phenomena, Wiley, New York, Chapt.3 (1960)
2. Carslaw, H. S., and Jaeger, J. C., Conduction of Heat in Solid, Oxford Univ. Press, p. 101 (1959)

[PROBLEM 6.6-P2] A rectangular parallelepiped iron ingot with dimensions 0.3 m by 2 m by 10 m is fixed vertically and kept uniformly at a temperature 1,050℃. The hot ingot are rapidly and uniformly cooled by striking water jet (40℃) on the two side surfaces of 2 m by 10 m. Owing to the film boiling taking place on the ingot surface, the surface temperature is assumed to be kept at 180℃ for the cooling term. Find the time required for the center ($z = 0$) temperature of the ingot to reach 300℃. The density and thermal conductivity of the ingot can be assumed to be constant at 730 kg/m^3 and 49 W/m K, respectively.

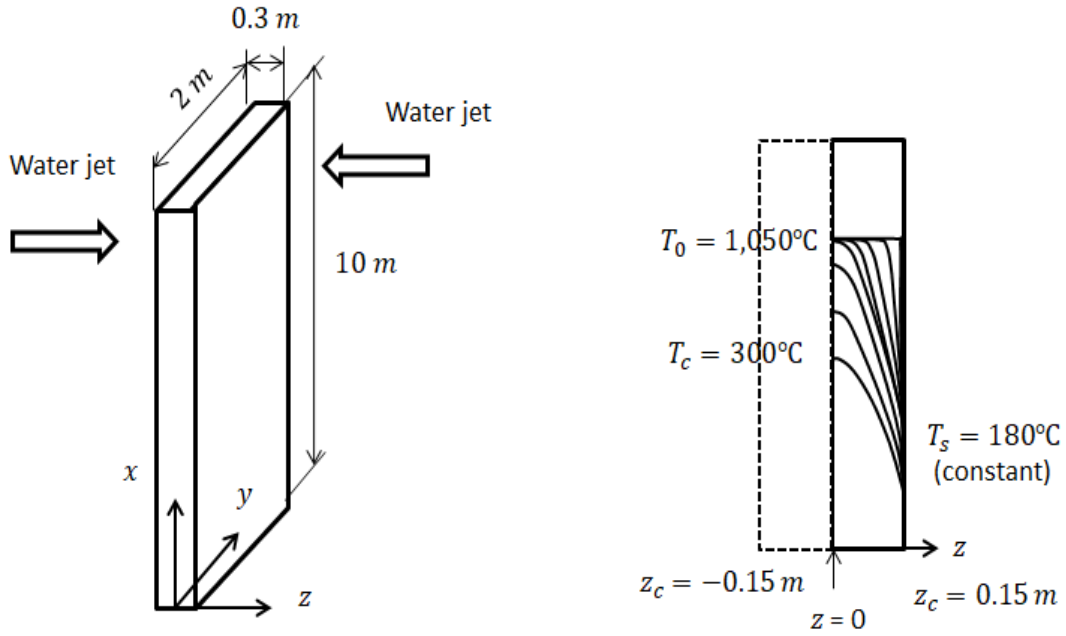

Fig. 6.6-P1. Cooling an iron ingot by striking water jets from two directions

6.7 Application of the Equation of Mass Transport

Let us consider the mass transfer problem on the cylindrical surface of laminar liquid jet flowing downward vertically through a vessel which contains the pure solute gas.

The carbon dioxide gas contained in a large vessel is absorbed by a water jet formed with a sharp-edged convergent nozzle. The jet surface is smooth and free of ripples. The gas phase resistance is negligible since the pure CO_2 gas exists surrounding the liquid jet. A small amount of carbon dioxide is absorbed in the short contact time (order of 10 ms), so the CO_2 penetration depth is very small relative to the jet diameter (order of 1 mm). Therefore the problem may be treated as though the surface were flat. The water jet has uniform velocity distribution across the cross section: $v_z = V = const.$. A well-designed convergent nozzle can discharge such a water jet with uniform velocity

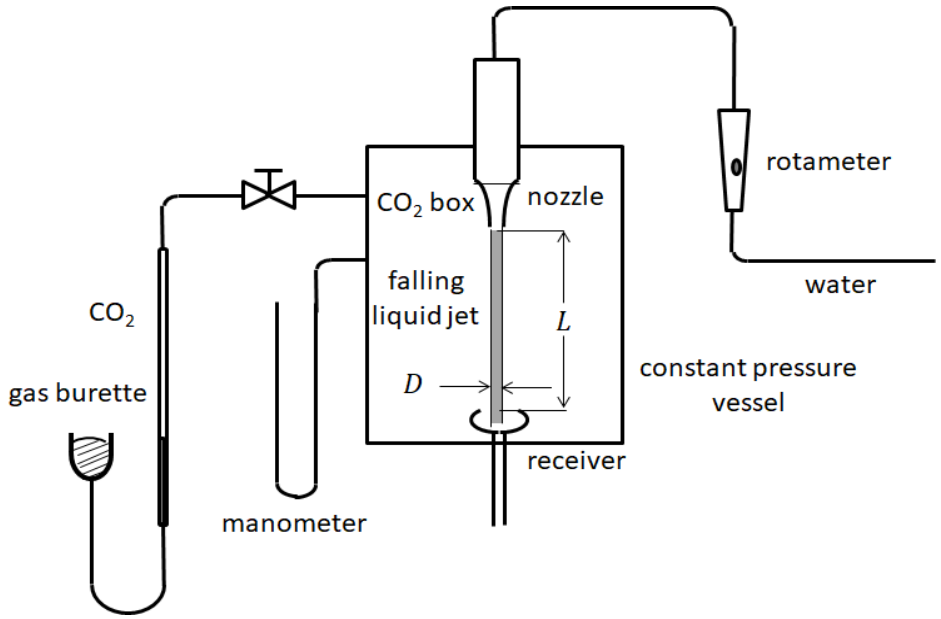

Fig.6.7-1 Experimental apparatus for CO_2 gas absorption

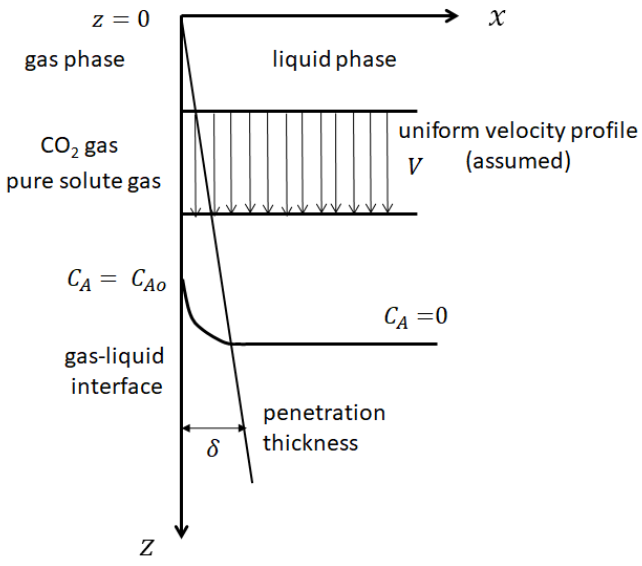

Fig.6.7-2 Situation of CO_2 gas absorbed into a falling liquid jet

The equation written in the rectangular coordinate system is applicable inside the liquid jet:

$$\frac{\partial C_A}{\partial t} + v_x \frac{\partial C_A}{\partial x} + v_y \frac{\partial C_A}{\partial y} + v_z \frac{\partial C_A}{\partial z} = D_{AB} \left(\frac{\partial^2 C_A}{\partial x^2} + \frac{\partial^2 C_A}{\partial y^2} + \frac{\partial^2 C_A}{\partial z^2} \right) + R_A$$

For steady state $\partial C_A/\partial t = 0$. We can ignore the chemical reaction between CO_2 and H_2O: $R_A = 0$.

All streamlines are parallel to the jet axis. Then $v_x = v_y = 0$. We can expect that C_A will be changing both with x and z. However $\partial C_A/\partial y = 0$.

Then the above equation reduces to

$$v_z \frac{\partial C_A}{\partial z} = D_{AB} \left(\frac{\partial^2 C_A}{\partial x^2} + \frac{\partial^2 C_A}{\partial z^2} \right) \qquad (6.7\text{-}1)$$

The carbon dioxide is transferred in the z-direction primarily because of the convective flow of the jet, the diffusive contribution (the term containing $\partial^2 C_A/\partial z^2$) can be neglected.

We get the partial differential equation for C_A

$$V \frac{\partial C_A}{\partial z} = D_{AB} \frac{\partial^2 C_A}{\partial x^2} \qquad (6.7\text{-}2)$$

The applicable boundary conditions are:

B.C.1 at $z = 0$, $C_A = 0$

B.C.2 at $x = 0$, $C_A = C_{A0}$ (solubility of CO_2 into H_2O)

B.C.3 at $x = \infty$, $C_A = 0$

Since the jet length between the nozzle and receiver is short (order of 50 mm), CO_2 does not penetrate very far from the surface. The third boundary condition indicates that the problem can be treated as if the jet were of infinite thickness moving with the constant velocity V.

Let us define dimensionless variables:

$$\phi = \frac{C_A}{C_{Ao}} \qquad \eta = \frac{x}{\sqrt{4 D_{AB} z/V}} \qquad (6.7\text{-}3)$$

By the method of combination of variables the partial differential equation reduces to the following ordinary differential equation:

$$\phi'' + 2\eta\, \phi' = 0 \qquad (6.7\text{-}4)$$

where primes $'$ indicates total differentiation with respect to η.

The boundary conditions become

B.C.2 at $\eta = 0$, $\phi = 1$ (6.7-5)

B.C.1 and 3 at $\eta = \infty$, $\phi = 0$ (6.7-6)

If ϕ' is replaced by ψ, the above equation becomes

$$\psi' + 2\,\eta\,\psi = 0 \qquad (6.7\text{-}7)$$

Integration gives $\psi = \phi' = C_1\, e^{-\eta^2}$

At this stage we do not have an appropriate boundary condition.

A second integration then gives

$$\phi = C_1 \int_0^{\eta} e^{-\eta^2}\, d\eta + C_2 \qquad (6.7\text{-}8)$$

From the first boundary condition, C_2 must be one.

Application of the second boundary condition gives

$$C_1 = -\frac{1}{\int_0^{\infty} e^{-\eta^2}\, d\eta} = -\frac{2}{\sqrt{\pi}}$$

The solution to the equation at hand is given by

$$\phi = 1 - \frac{2}{\sqrt{\pi}} \int_0^{\eta} e^{-\eta^2}\, d\eta = 1 - erf\ \eta \qquad (6.7\text{-}9)$$

or

$$\frac{C_A}{C_{Ao}} = 1 - erf\ \frac{x}{\sqrt{4 D_{AB} z/V}}$$

Here erf X is known as the "error function", whose definition is

$$erf\ X = \frac{2}{\sqrt{\pi}} \int_0^{\xi} e^{-\xi^2}\, d\xi$$

Once the concentration profile is known, the total absorption rate can be calculated. Note that z/V is the time for fluid particle to move from the nozzle to axial distance z. The molecular diffusion in the x-direction can be considered to be much larger than convective transport in the x-direction because of the low solubility of A in B.

Therefore the local mass flux at the surface ($x = 0$) can be expressed as

$$N_{Ax}|_{x=0} = -D_{AB}\left.\frac{\partial C_A}{\partial x}\right|_{x=0} = C_{Ao}\sqrt{\frac{D_{AB}V}{\pi z}} \qquad (6.7\text{-}10)$$

Then the total absorption rate is

$$W = \pi D \int_0^L N_{Ax}|_{x=0}\, dz = \pi DL\sqrt{\frac{4\,D_{AB}V}{\pi L}}\, C_{Ao} \qquad (6.7\text{-}11)$$

Let us define a mass transfer coefficient as the ratio of the mass flux to the driving force (characteristic concentration difference):

$$N_{Ax}|_{x=0} = k_L(C_{Ao} - C_{A\infty}) \qquad (6.7\text{-}12)$$

In this case, k_L is the average mass transfer coefficient on the liquid side of the interface. The CO_2 concentration becomes approximately zero at a certain depth from the surface.

The depth δ is called a thickness of liquid film where the main resistance to mass transfer takes place. Then at $x = \delta$ $C_{A\infty} = 0$

Therefore Eq.(6.7-12) becomes

$$N_{Ax}|_{x=0} = k_L C_{Ao} \qquad (6.7\text{-}13)$$

Comparing this to the equation Eq,(6.7-11) of the total absorption rate

$$k_L = \sqrt{\frac{4\,D_{AB}V}{\pi L}} \qquad (6.7\text{-}14)$$

Note that L/V corresponds to the contact time t_c.

Much industrial gas-liquid contacting equipment operates with short contact time. As in this example, diffusion from interface to bulk fluid proceeds as a transport process. This is an example of Higbie's penetration theory [1)] indicating that the mass transfer coefficient is proportional to the square root of diffusivity divided by contact time. This system is often used to measure molecular diffusivity of CO_2 into H_2O.

1. Higbie, R., *Trans. A.I.Ch.E.*, **31**, 365 (1935)

[EXAMPLE 6.7-E1]

Let us consider how to measure molecular diffusivity by using this system (Fig. 6.7-1).

The absorption rate W can be determined from the feed rate of fresh CO_2 gas to the vessel (absorber) from a constant-pressure source. The jet surface area πDL and contact time $t_c = L/V$ can be calculated directly from measurement of jet length, diameter, and water flow rate.

Then we determine the molecular diffusivity

$$D_{AB} = \frac{\pi L}{4V}\left(\frac{w}{\pi DL\, C_{Ao}}\right)^2 \qquad (6.7\text{-E1})$$

In this case, the gas-phase resistance was negligible.

< Two film theory >

If the ambient gas-phase includes inert gas (e.g. N_2) insoluble to liquid-phase, there generates another resistance to mass transfer on the gas side of the interface. The concentration gradient is formed in the gas-phase, too.

In general, a solute is transferred at constant rate through two resistances in series from gas- to liquid-phase.

We define two individual mass transfer coefficients:

$$N_A = k_G(y_{Ab} - y_{Ai}) = k_L\,(C_{Ai} - C_{Ab}) \qquad (6.7\text{-E2})$$

Here y_A and C_A are mole fraction in gas-phase and molar concentration in liquid-phase of component A, respectively.

Assuming equilibrium at the interface

$$y_{Ai} = H\, C_{Ai} \qquad \text{(6.7-E3)}$$

This is known as the Henry's law.

For practical purposes of process design, it is convenient to express transport rate (mass-flux) in terms of the bulk phase concentrations and an overall mass transfer coefficient. The definition is

$$N_A = K_G(y_{Ab} - HC_{Ab}) = K_L\,(y_{Ab}/H - C_{Ab}) \qquad \text{(6.7-E4)}$$

The overall driving force should be used for definition of the overall mass transfer coefficients. However, note that we cannot use the expression as $N_A = K_G(y_{Ab} - C_{Ab})$ because C_A and y_A use different bases for units of concentration. For unit conversion, Henry's constant can be used. That is, HC_{Ab} is the imaginary concentration y^*_{Ab} of gas-phase in equilibrium to C_{Ab} whereas y_{Ab}/H is the imaginary concentration C^*_{Ab} of liquid-phase in equilibrium to y_{Ab}.

Combining these equations, we get the flux equation analogous to Ohm's law:

$$N_A = \frac{y_{Ab} - HC_{Ab}}{\frac{1}{K_G}} = \frac{y_{Ab} - y_{Ai}}{\frac{1}{k_G}} = \frac{HC_{Ai} - HC_{Ab}}{\frac{H}{k_L}} = \frac{y_{Ai} - y^*_{Ab}}{\frac{H}{k_L}}$$

Therefore the following equation can be obtained by solving for $1/K_G$:

$$N_A = \frac{y_{Ab} - y^*_{Ab}}{\frac{1}{K_G}} = \frac{y_{Ab} - y_{Ai}}{\frac{1}{k_G}} = \frac{y_{Ai} - y^*_{Ab}}{\frac{H}{k_L}} = \frac{y_{Ab} - y^*_{Ab}}{\frac{1}{k_G} + \frac{H}{k_L}} \qquad \text{(6.7-E5)}$$

That is

$$\frac{1}{K_G} = \frac{1}{k_G} + \frac{H}{k_L} \qquad \text{(6.7-E6)}$$

This states that the overall mass transfer resistance is the sum of the resistances in series of gas-phase and liquid-phase.

Similarly

$$\frac{1}{K_L} = \frac{1}{H\,k_G} + \frac{1}{k_L} \qquad \text{(6.7-E7)}$$

Since these two equations indicate the same meaning, either will do.

[PROBLEM6.7-P1] The diffusivity of CO_2 into pure water is measured by using the falling liquid jet method. The vessel containing deaerated water jet surrounded by pure CO_2 gas is kept at $p = 1\ atm\ (1.013 \times 10^5\ Pa)$ and 20℃. The feed rate of pure water measured by a rotameter is $1.5\ ml/s$. The diameter and length of the water jet are $1.2\ mm$ and $40\ mm$, respectively. The CO_2 absorption rate measured by gas burette is $0.038\ ml/s$.

Henry's law for the CO_2-H_2O system is given by $p = H\,C_A$, where the constant $H = 25.5\ (atm\,m^3/kmol)$ at 20℃.

(1) Calculate the diffusivity of CO_2 into H_2O at 20℃.

(2) The penetration thickness δ is defined as that distance x for which C_A has dropped to a value $0.01\,C_{Ao}$:

$$\delta = 4\sqrt{D_{AB}\,z/V}$$

Estimate the penetration thickness just above the receiver, i.e. at the lowest point of the water jet.

[Answer: $D_{AB} = 1.7 \times 10^{-9}$ m²/s, $\delta = 2.86 \times 10^{-2}$ mm]

Nomenclature

C_A	concentration of component A, [kg/m^3]
Cp	heat capacity, [J/kg K]
D	pipe inside diameter, [m]
D_{AB}	diffusivity, [m^2/s]
f	friction factor, [-]
g	gravitational acceleration, [m/s^2]
H	Henry's constant, [m^3/kmol]
h	heat transfer coefficient, [W/m^{2}K]
K_G	overall mass transfer coefficient on vapor-phase concentration basis, [kmol/m^{2}s]
k_G	gas-phase mass transfer coefficient, [kmol/m^{2}s]
K_L	overall mass transfer coefficient on liquid-phase concentration basis, [m/s]
k_L	liquid-phase mass transfer coefficient, [m/s]
L	pipe length, [m] or liquid jet length, [m]
N_A	mass flux of component A, [kg/m^{2}s] or [kmol/m^{2}s]
Nu	Nusselt number, [-]
Pr	Prandtl number, [-]
p	pressure, [Pa]
Q	volumetric flow rate, [m^3/s] or heat loss, [J/s]
q_w	wall heat flux, [W/m^2]
R	pipe radius, [m]
R_i, R_o	cylinder radius, inner and outer cylinders, [m]
Re	Reynolds number, [-]
r, θ, z	cylindrical coordinates, [m, - , m]
St	Stanton number, [-]
T	temperature, [K]
Ta	Taylor number, [-]
T_q	torque, [N m]
V	velocity of falling liquid jet, [m/s]
v_r, v_θ, v_z	velocity component in cylindrical coordinates
W	total absorption rate, [kg/s]
α	thermal diffusivity, [m^2/s]
δ	penetration thickness, [m]
κ	thermal conductivity, [W/m K]
μ	viscosity, [kg/m s]
ρ	density, [kg/m^3]
τ_{rz}	shear stress at r in pipe flow, [N/m^2]
τ_0	yield stress, [N/m^2]
ω	angular velocity, [1/s]

Brackets

$\langle\ \rangle$	averaged over flow cross section

Subscripts

m	bulk or mixed mean
w	wall

CHAPTER 7

INTERPHASE MOMENTUM TRANSPORT

7.1 Turbulent Flow Properties

In laminar flow, all the streamliners have smooth curves or straight lines. Especially in steady laminar flow, the streamlines are at rest. However in turbulent flow all the streamlines oscillate irregularly in all directions. It is true that the equations of continuity and motion apply to turbulent flow. Since the instantaneous velocity and pressure are irregularly oscillating function, any simplest turbulent flow problems have not yet been solved exactly. For the purpose of application in engineering, other approaches have been necessary.

Let us consider a steady turbulent flow in a circular pipe as an example.

Suppose that we could stand at a fixed point in the flow field and observe the velocity and pressure at the position. The instantaneous velocity v_z and pressure p are fluctuating at random about their finite mean values, whereas v_r and v_θ are fluctuating around the zero mean values. The oscillograms are shown in Fig.7.1-1.

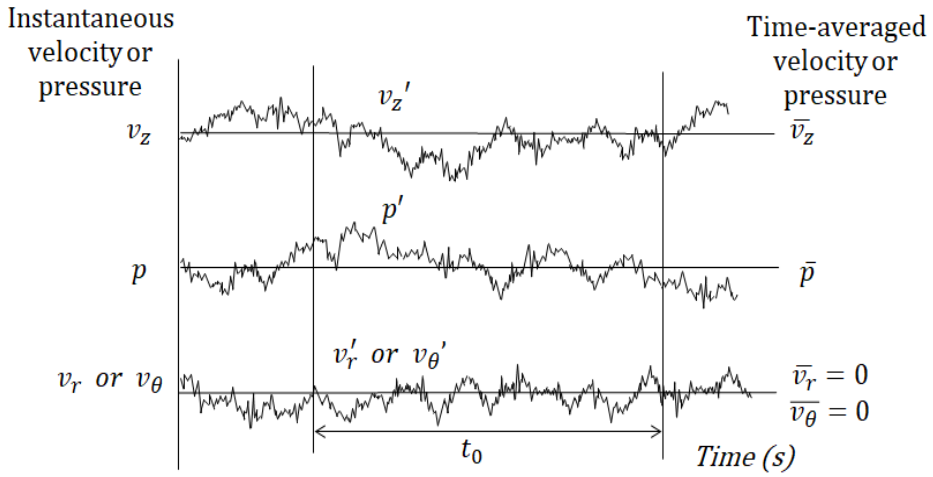

Fig.7.1-1. Oscillograms of fluctuating velocity and pressure for a circular pipe flow

The time-averaged velocity and pressure are defined as

$$\bar{v}_z = \frac{1}{t_0}\int_t^{t+t_0} v_z \, dt \qquad (7.1\text{-}1)$$

$$\bar{p} = \frac{1}{t_0}\int_t^{t+t_0} p \, dt \qquad (7.1\text{-}2)$$

These are time-averages of instantaneous velocity and pressure taken over a time interval t_0 from an arbitrary chosen reference time t. The time interval can be taken to be large compared to the periodic time of fluctuations.

Then we can split up the instantaneous velocity and pressure into the time-averaged values and their fluctuations:

$$v_z(r,\theta,z,t) = \bar{v}_z(r,\theta,z) + v_z'(r,\theta,z,t) \qquad (7.1\text{-}3)$$

$$p(r,\theta,z,t) = \bar{p}(r,\theta,z) + p'(r,\theta,z,t) \qquad (7.1\text{-}4)$$

Note that for steady turbulent flow in a pipe
$\bar{v}_z = \bar{v}_z(r,z)$ and $\bar{p} = \bar{p}(\mathrm{r},\mathrm{z})$
By definition,

$$\overline{v_z'} = \frac{1}{t_0}\int_t^{t+t_0} v_z'\, dt = 0$$

Similarly $\overline{p'} = 0$ $\overline{v_r} = \overline{v_\theta} = 0$ and $\overline{v_r'} = \overline{v_\theta'} = 0$
The instantaneous velocity fluctuations v_r', v_θ', v_z' can become negative very often, but ${v_r'}^2$, ${v_\theta'}^2$, ${v_z'}^2$ cannot be negative. Therefore $\overline{{v_z'}^2}$ will not be zero. As a measure of magnitude of the turbulence the level or intensity of turbulence is defined as $Tu = \frac{\sqrt{\overline{{v_z'}^2}}}{\overline{v_z}}$ (7.1-5)
This turbulence intensity may have values 0.01 to 0.10 in typical turbulent flow conditions.

Of the many methods for the measurement of turbulent velocity, the hot-wire anemometer is the most satisfactory. The detecting element consists of a very fine short metal wire (e.g. $5\,\mu m$ dia. And 5 mm long platinum wire for air stream), which is heated by an electric current to a constant temperature above the stream temperature.
The wire is placed perpendicular to the velocity component to be measured. The rate of heat loss to the ambient stream from the wire is proportional to the square root of the stream velocity $\sqrt{v}$ in the usual stream condition. The wire is of such low heat capacity that the temperature of the wire can follow the rapid velocity fluctuations. The rate of heat loss is equal to the rate of heat generated by the electric current through the wire I^2R, where I is the electric current and R the electric resistance of the wires. In the modern method, the electric resistance is kept constant as far as possible by using an electronic feedback system. Instead, the feedback system changes the current through the wire as soon as a variation in electric resistance occurs. The response time to the change in approach velocity is of the order shorter than 0.1 ms.
Then we have the relation between I^2 and v:

$$I^2R = \alpha + \beta\sqrt{v} \qquad (7.1\text{-}6)$$

Where the constants α and β are usually determined by experiment. If we substitute $I = \bar{I} + I'$ and $v = \bar{v} + v'$ into the above equation, we get the approximate relation between I' and v':

$$(\bar{I} + I')^2R = \alpha + \beta\sqrt{\bar{v} + v'}$$

The mean velocity is given by the equation

$$\bar{I}^2R = \alpha + \beta\sqrt{\bar{v}} \qquad (7,1\text{-}7)$$

The first approximation when $v' \ll \bar{v}$, i.e. $I' \ll \bar{I}$ gives

$$I' = \frac{\beta}{4\bar{I}R}\frac{\sqrt{\bar{v}}}{\bar{v}}\, v' \qquad (7.1\text{-}8)$$

We can measure the fluctuating velocity v' by the use of the above relation.
A simple block diagram of hot-wire anemometer for constant temperature method is shown below.

[PROBLEM 7.1-1] A component of turbulent velocity at a position is assumed to be of the form
$v_z = a + \sum_{n=1}^{\infty} b_n \cos 2\pi n\, t \qquad (a,\ b_1, - - - -,\ b_n, - - -: constant)$ (7.1-P1)
Calculate the time-averaged velocity and the intensity of turbulence.

(Solution) $\bar{v}_z = a, \quad Tu = \frac{\sqrt{\overline{{v_z'}^2}}}{\overline{v_z}} = \frac{1}{\sqrt{2}\,a}\sqrt{\sum_{n=1}^{\infty} {b_n}^2}$

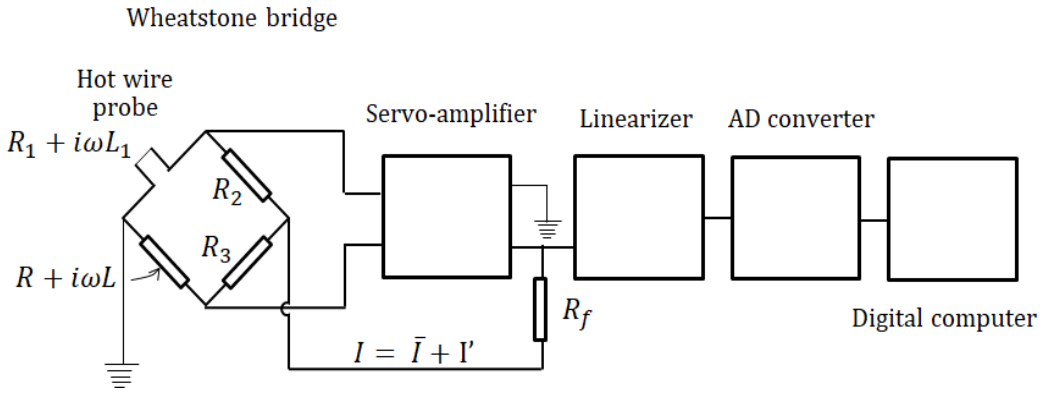

Fig.7.1-2 Block diagram of hot-wire anemometer for constant temperature method

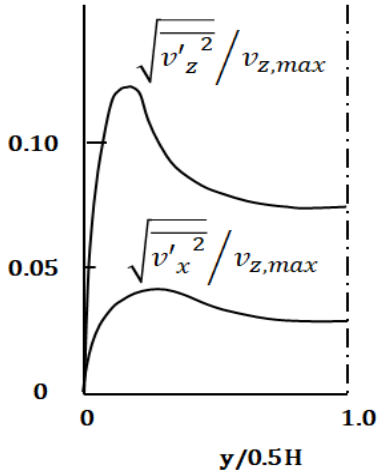

Fig.7.1-3 Distribution of velocity fluctuations in a rectangular channel

As shown in Fig.7.1-3, the turbulence intensity in a rectangular channel becomes maximum near the wall. This suggests that the turbulence is produced due to the instability of velocity gradient in the vicinity of the pipe wall and diffuses both toward the center and the wall. The fluctuations in the streamwise direction, or in the z direction, are greater than the fluctuations in the transverse direction, or in the x direction. In the vicinity of the wall, molecular momentum transport becomes important, but the fluctuations become very small. Turbulent flow in a pipe also has similar tendency.

We usually consider turbulent pipe flow by dividing the flow region into three zones. (three-layer concept)

The first layer very close to the wall is called the viscous sublayer, where Newton's law of viscosity can be applied to describe the flow. Since molecular transport is predominant, this sublayer causes the main resistance to interphase transport. The second is called the buffer zone or transition zone, where the laminar and turbulent effects are comparable and both important. And the third is called the region of fully developed turbulence or the turbulent core, where viscous effects are negligibly important.

[PROBLEM 7.1-2] Show how to measure the intensity of turbulence by use of hot-wire anemometer.

(Solution) $Tu = \dfrac{\sqrt{\overline{v\prime^2}}}{\bar{v}} = \dfrac{4\,\bar{I}\,R\sqrt{\overline{I\prime^2}}}{\bar{I}\,R - \alpha}$

7.2 Friction Factor and Pressure Drop for Channel Flows

Most problems of engineering importance occur in the region of turbulent flow.
Let us consider the momentum transport in turbulent flow inside a circular pipe. Figure 7.2-1 shows the time-averaged velocity distribution in the fully-developed region. The flow region can be subdivided into three regions: the turbulent core, the buffer zone, and the viscous sublayer near the wall.

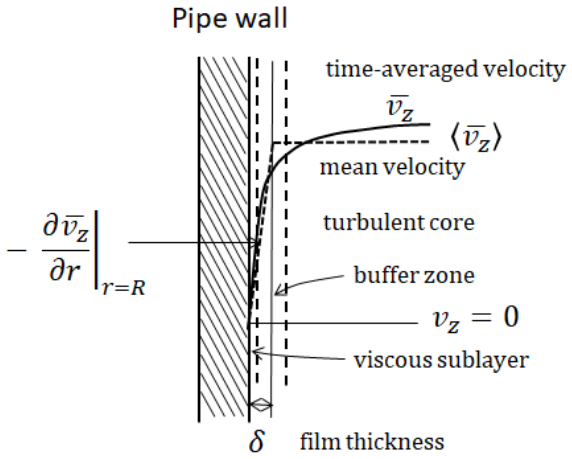

Fig.7.2-1 Time-averaged velocity profile and three subregions of turbulent pipe flow field

In the turbulent core, the velocity gradient is very small but momentum is transferred very rapidly by virtue of eddy motion. However, close to the wall, eddy motion is suppressed by viscous effect. Especially in the viscous sublayer, momentum is transferred by molecular diffusion only. Hence the main resistance to momentum transfer takes place in very thin film of the fluid near the wall, where most of the total velocity change occurs.

Then the momentum flux (i.e. the shear stress) at the pipe wall is given by

$$\tau_w = -\mu \left.\frac{\partial \overline{v_z}}{\partial r}\right|_{r=R} \tag{7.2-1}$$

The velocity distribution near the wall can be approximated by

$$-\left.\frac{\partial \overline{v_z}}{\partial r}\right|_{r=R} = \frac{\langle \overline{v_z} \rangle}{\delta} \tag{7.2-2}$$

Here δ is the thickness of a fictitious viscous film.
The equation can be rewritten as

$$\tau_w = \mu \frac{\langle \overline{v_z} \rangle}{\delta} \tag{7.2-3}$$

The film thickness is a complicated function of the flow condition, the fluid properties, and the geometry of the flow system.

For flow in channels, pressure drop data are usually desired and correlations given in terms of a friction factor. This factor is defined by setting the magnitude of the acting force F proportional to the dynamic head or the characteristic kinetic energy K:

$$F = f\, K\, A \tag{7.2-4}$$

This is a useful definition because f is only a function of Re for a given geometrical shape:

$$f = f(Re) \tag{7.2-5}$$

For flow in a circular pipe, A is taken to be the wetted surface $2\pi R\, L$, K is taken to be the kinetic energy based on the average velocity, i.e. $(1/2)\rho\langle \overline{v_z} \rangle^2$. The force F' acting on the inner wall is $F' = 2\pi R\, L\, \tau_w$. Then

$$\tau_w = f\, \frac{1}{2}\, \rho \langle \overline{v_z} \rangle^2 \tag{7.2-6}$$

This indicates that the wall shear stress for pipe flow is proportional to the kinetic energy.
Combining the equation with the foregoing equation for δ, we get

$$\mu \frac{\langle \bar{v}_z \rangle}{\delta} = f \frac{1}{2} \rho \langle \bar{v}_z \rangle^2 \quad (7.2\text{-}7)$$

From the equation,

$$\frac{\delta}{D} = \frac{2}{Re} \frac{1}{f(Re)} \quad (7.2\text{-}8)$$

This suggests that the dimensionless film thickness is a function of the Reynolds number only.

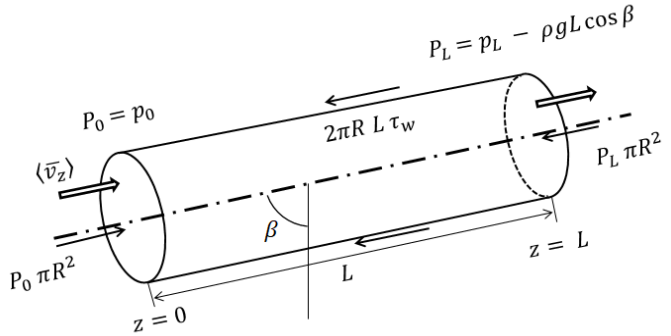

Fig.7.2-2 Force balance of inclined circular pipe flow

According to the force balance on the fluid between $z = 0$ and L in the flow direction for fully developed flow

$$2\pi R\, L\, \tau_w = (P_0 - P_L)\, \pi\, R^2 \quad (7.2\text{-}9)$$

Substituting the relation into the defining equation for f

$$P_0 - P_L = 4\, f\, \frac{L}{D} \frac{1}{2} \rho \langle \bar{v}_z \rangle^2 \quad (7.2\text{-}10)$$

This is known as the Fanning friction factor. If the pipe is horizontal, the equation becomes

$$p_0 - p_L = 4\, f\, \frac{L}{D} \frac{1}{2} \rho \langle \bar{v}_z \rangle^2 \quad (7.2\text{-}11)$$

Once we know as the relation between f and Re, we can calculate the pressure drop.

[EXAMPLE 7.2-1]

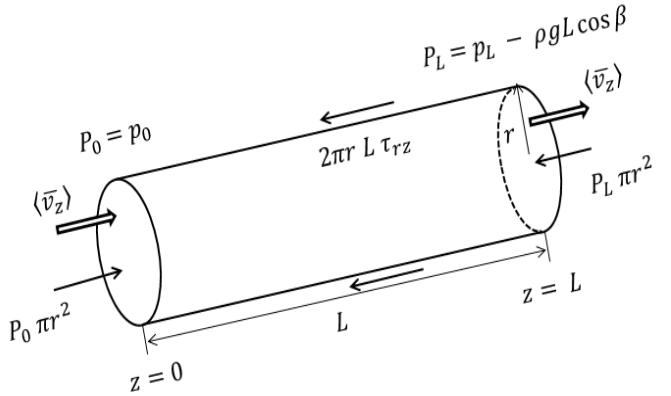

Fig.7.2-E1 Force balance on a cylindrical fluid element of radius *r*

As shown in Fig.7.2-E1, we can set up the force balance on the cylindrical fluid element of length L and radius r in the fully developed turbulent flow:

$$(P_0 - P_L)\, \pi\, r^2 = \tau_{rz}\, 2\pi r\, L \quad (7.2\text{-}E1)$$

Here τ_{rz} is the total apparent shear stress or the sum of molecular and turbulent contributions. Then we divide by the foregoing equation for τ_w

$$\frac{\tau_{rz}}{\tau_w} = \frac{r}{R} \quad (7.2\text{-}E2)$$

Note that in a fully-developed pipe flow, whether laminar or turbulent, the total apparent shear

stress varies linearly from zero at the pipe axis to a maximum at the wall.
The friction factor can be measured experimentally by using the following equation:

$$f = \frac{1}{4}\frac{D}{L}\frac{P_0 - P_L}{\frac{1}{2}\rho\langle\overline{v_z}\rangle^2} \quad (7.2\text{-E3})$$

7.3 Dimensional Analysis of Friction Factor for Channel Flows

Next let us consider the friction factor by applying a dimensional analysis to the equation of motion. The turbulent effect on momentum transfer becomes of negligible importance in the viscous sublayer.
The following equation is valid in the viscous sublayer, whether the flow is laminar or turbulent:

$$\rho\left(\frac{\partial v_z}{\partial t} + v_r\frac{\partial v_z}{\partial r} + \frac{v_\theta}{r}\frac{\partial v_z}{\partial \theta} + v_z\frac{\partial v_z}{\partial z}\right) = -\frac{\partial p}{\partial z} + \mu\left[\frac{1}{r}\frac{\partial}{\partial r}\left(r\frac{\partial v_z}{\partial r}\right) + \frac{1}{r^2}\frac{\partial^2 v_z}{\partial \theta^2} + \frac{\partial^2 v_z}{\partial z^2}\right] + \rho g_z \quad (7.3\text{-}1)$$

The equation could be solved with the following conditions:

$$v_r = v_\theta = v_z = 0 \text{ and } \tau_w = \tau_{rz}|_{r=R} = -\mu\left.\frac{\partial\overline{v_z}}{\partial r}\right|_{r=R} \text{ at } r = R$$

$$-\frac{\partial p}{\partial z} + \rho g_z = \frac{P_0 - P_L}{L} \quad (7.3\text{-}2)$$

Next we introduce the dimensionless quantities

$$r^* = r/D,\ z^* = z/D,\ v_r^* = v_r/\langle\overline{v_z}\rangle,\ v_\theta^* = v_\theta/\langle\overline{v_z}\rangle,\ v_z^* = v_z/\langle\overline{v_z}\rangle,\ p^* = (P_0 - P_L)/\rho\langle\overline{v_z}\rangle^2 \quad (7.3\text{-}3)$$

According to the definition of friction factor

$$\tau_w = f\frac{1}{2}\rho\langle\overline{v_z}\rangle^2 \quad (7.3\text{-}4)$$

Then the friction factor has the following form:

$$f = \frac{\tau_w}{\frac{1}{2}\rho\langle\overline{v_z}\rangle^2} = \frac{-\mu\left.\frac{\partial\overline{v_z}}{\partial r}\right|_{r=R}}{\frac{1}{2}\rho\langle\overline{v_z}\rangle^2} = -\frac{2}{Re}\left.\frac{\partial v_z^*}{\partial r^*}\right|_{r^*=1/2} \quad (7.3\text{-}5)$$

For steady state, the above momentum equation is made dimensionless

$$v_r^*\frac{\partial v_z^*}{\partial r^*} + \frac{v_\theta^*}{r^*}\frac{\partial v_z^*}{\partial \theta} + v_z^*\frac{\partial v_z^*}{\partial z^*} = -\frac{\partial p^*}{\partial z^*} + \frac{1}{Re}\left[\frac{1}{r^*}\frac{\partial}{\partial r^*}\left(r^*\frac{\partial v_z^*}{\partial r}\right) + \frac{1}{r^{*2}}\frac{\partial^2 v_z^*}{\partial \theta^2} + \frac{\partial^2 v_z^*}{\partial z^{*2}}\right] \quad (7.3\text{-}6)$$

where $Re = D\langle\overline{v_z}\rangle\rho/\mu$.
This equation is too difficult to solve analytically. But the solution can be expected to be of the form

$$v_r^* = v_r^*(r^*, \theta, z^*, Re),\ v_\theta^* = v_\theta^*(r^*, \theta, z^*, Re),\ v_z^* = v_z^*(r^*, \theta, z^*, Re) \quad (7.3\text{-}7)$$

We assume the fully-developed, axisymmetric velocity field:

$$\frac{\partial v_z^*}{\partial z^*} = 0 \quad \text{and} \quad \frac{\partial v_z^*}{\partial \theta} = 0$$

Then we get

$$v_z^* = v_z^*(r^*, Re) \quad (7.3\text{-}8)$$

The velocity gradient at the wall $\left.\frac{\partial v_z^*}{\partial r^*}\right|_{r^*=1/2}$ is a function of Re only. Therefore the friction factor is found to be a function of Re alone in the fully-developed velocity field:

$$f = f(Re) \quad (7.3\text{-}9)$$

It is suggested that it is sufficient to plot only a single curve of f against Re rather than determine how f varies for separate values of $D, \langle\overline{v_z}\rangle, \rho, \mu$.
Fig.7.3-1 gives the friction factor chart or empirical correlation of f and Re for circular tube flow.
For laminar flow, the friction factor can be derived theoretically from the Hagen-Poiseuille law:

$$f = \frac{16}{Re} \quad (7.3\text{-}10)$$

The turbulent curve for hydraulically smooth tubes is curve-fitted from $Re = 2.1 \times 10^3$ to 5×10^6 by the equation:

$$\frac{1}{\sqrt{f}} = 4.0\ log_{10}\left(Re\sqrt{f}\right) - 0.40 \quad (7.3\text{-}11)$$

A similar expression exists for $2.1 \times 10^3 < Re < 5 \times 10^5$:

$$f = \frac{0.0791}{Re^{1/4}} \tag{7.3-12}$$

This is known as the Blasius formula.

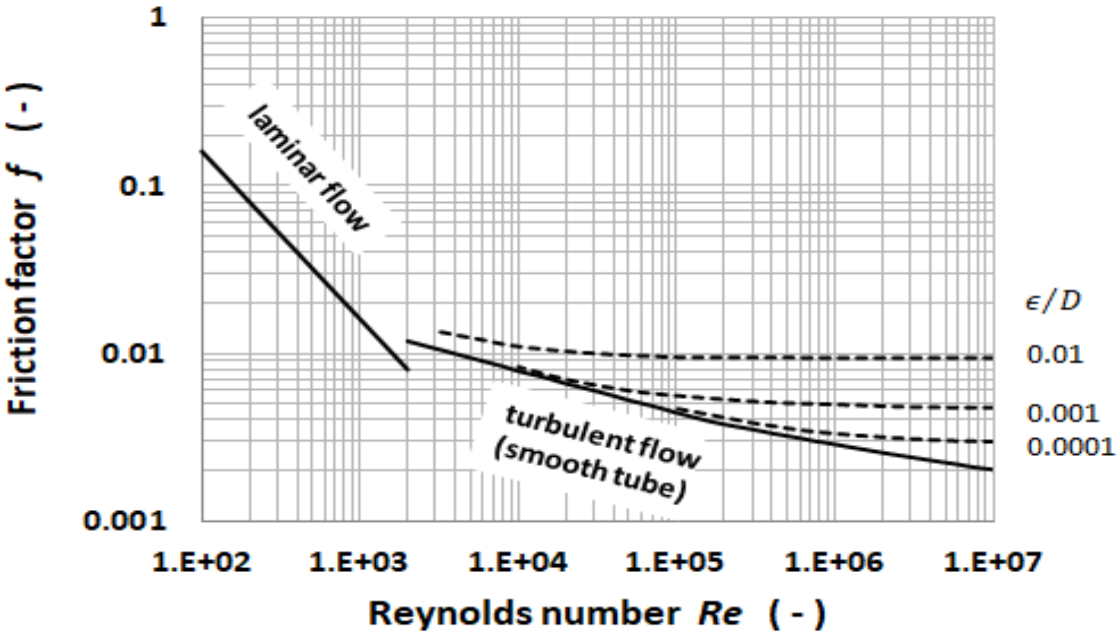

Fig.7.3-1 Friction factor for smooth tubes

If pipes are rough, then in the turbulent flow higher pressure drop is required for a given flow rate than that expected for smooth pipes. The friction factor for rough pipes is a function of not only the Reynolds number but also the relative roughness ϵ/D, where ϵ is the height of a protrusion.
If the roughness-element height ϵ does not extend beyond the viscous sublayer, the roughness has little effect on the turbulent-flow profiles. This condition is called "hydraulically smooth." If the roughness extends partly into the buffer layer, there is an added resistance to flow due to the form drag.

[PROBLEM 7.3-1] Gasoline ($\mu = 0.4\,cP,\ \rho = 710\ kg/m^3$) is to be delivered at $10\ \mathrm{m}^3/\mathrm{min}$ through a smooth straight pipe (400 mmID, length $L = 2\,km$) from a refinery to an airport. Calculate the pump horse power if the pump operates at an efficiency of 70%. For the case of relative roughness $\epsilon/D = 0.001$, what is the power requirement of the pump?
[PROBLEM 7.3-2] Water (at 20°C) flows in a circular tube of 50 mmID at a flow rater of $0.15\ m^3/min$. Calculate the thickness of the viscous film defined by Eq.(7.2-8).

7.4 Mechanical Energy Loss

7.4-1 Mechanical energy losses in pipelines

As shown in Fig.7.4-1, we set up the macroscopic momentum balance over the inclined pipe section between planes 1 and 2.

$$-\vec{F} = w_1\langle\overrightarrow{v_1}\rangle - w_2\langle\overrightarrow{v_2}\rangle - p_1\overrightarrow{n_1}\,\mathrm{S} - p_2\overrightarrow{n_2}\mathrm{S} + \rho\mathrm{V}\vec{g} \tag{7.4-1}$$

$$F = \pi DL\,\tau_w, \quad \langle\overrightarrow{v_1}\rangle = \langle\overrightarrow{v_2}\rangle, \quad (P_1 - P_2)S = (p_1 - p_2)S + \rho Vg\cos\theta$$

Here $P = p - \rho gz\cos\theta$

Then the momentum balance equation reduces to

$$F = \pi DL\,\tau_w = (P_1 - P_2)S \tag{7.4-2}$$

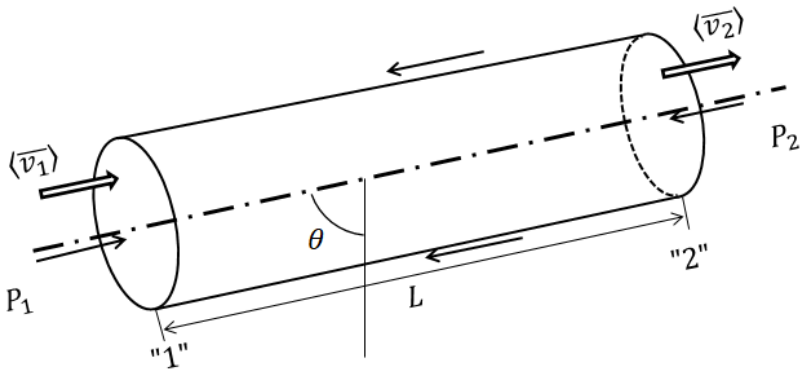

Fig.7.4-1 Macroscopic momentum balance for turbulent flow in an inclined pipe section

Next we set up the macroscopic mechanical energy balance over the same pipe section:

$$\frac{\Delta P}{\rho} + \Delta\frac{1}{2}\langle v\rangle^2 = -Fr_m - W_m \tag{7.4-3}$$

In this case $W_m = 0$, $\langle v_1\rangle = \langle v_2\rangle$

$$\frac{P_1 - P_2}{\rho} = Fr_m \tag{7.4-4}$$

Comparing Eq.(7.2-26) to Eq.(7.2-24), we get

$$F = \rho\, Fr_m S \tag{7.4-5}$$

From the definition of friction factor

$$\mathrm{F} = \mathrm{f}\,\frac{1}{2}\,\rho\langle v\rangle^2\pi DL \tag{7.4-6}$$

Finally we get

$$Fr_m = 4f\,\frac{L}{D}\,\frac{1}{2}\,\langle v\rangle^2 \tag{7.4-7}$$

This is the defining equation of friction factor for turbulent pipe flow.

Once the friction factor is given in terms of the Reynolds number, we can calculate from this equation the mechanical energy loss (friction loss) over the straight pipe section of length L.

In a general flow system the pipeline may not be of a uniform diameter and/or there may be various kinds of valves, elbows, and fittings which will cause mechanical energy losses. For most calculations, losses caused by fittings and valves are treated by the equivalent length model. This model is based on the assumption of high Reynolds number. Equivalent length L_{eq} for fittings and valves is defined as a pipe length that would give the same flow rate. Equivalent lengths for standard-size fittings and valves are given as

$$Fr_m = 4f\,\frac{L_{eq}}{D}\,\frac{1}{2}\,\langle v\rangle^2 \tag{7.4-8}$$

Then we obtain the useful equation of mechanical energy balance for isothermal system of turbulent flows (This is called the modified Bernoulli equation).

$$\Delta\frac{1}{2}\langle v\rangle^2 + g\Delta h + \int_{p_1}^{p_2}\frac{dp}{\rho} + W_m + \sum_i\left(4f\,\frac{L}{D}\,\frac{1}{2}\,\langle v\rangle^2\right)_i + \sum_j\left(4f\,\frac{L_{eq}}{D}\,\frac{1}{2}\,\langle v\rangle^2\right)_j = 0 \tag{7.4-9}$$

7.4-2 Mechanical energy losses due to pipe fittings[1,2)]

We can also use the friction loss factor model for fittings, valves, and enlargements and contractions of the flow cross section:

$$Fr_m = \varsigma\,\frac{1}{2}\,\langle v\rangle^2 \tag{7.4-10}$$

where ς is the friction loss factor, dimensionless. This model is based on the fact that the friction factor of rough pipes becomes almost constant in the range of turbulent flow.

(1) Sudden expansion of the flow cross section

$$Fr_m = \frac{1}{2}\langle v\rangle^2 \left(1 - \left(\frac{D_1}{D_2}\right)^2\right)^2 \quad (7.4\text{-}11)$$

Here $\langle v\rangle$ is the upstream velocity, D_1 the diameter of upstream pipe, and D_2 the diameter of downstream pipe.

(2) Sudden expansion into very large regions, e.g. tanks

$$Fr_m = \frac{1}{2}\langle v\rangle^2 \quad (7.4\text{-}12)$$

This implies $\varsigma = 1$ for the case ($D_2/D_1 \rightarrow \infty$).

Typical values for friction loss factor and/or equivalent length are listed below.

(1) Sudden contraction at a sharp-edged entrance

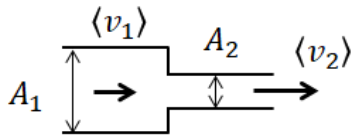

A_2/A_1	0	0.2	0.4	0.6	0.8	1.0
ς	0.5	0.45	0.36	0.21	0.07	0

(2) Contraction at a round entrance with a radius of rounding greater than 15% of the pipe diameter *D*

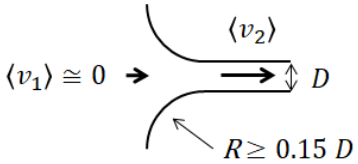

$$Fr_m = \varsigma\,\frac{1}{2}\langle v_2\rangle^2$$

$$\varsigma = 0.04$$

(3) Sudden enlargement at a sharp-edged exit

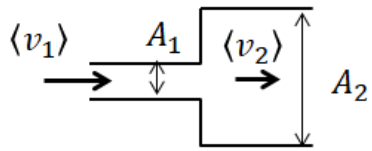

$$Fr_m = \varsigma\,\frac{1}{2}\langle v_1\rangle^2$$

$$\varsigma = \left(1 - \frac{A_1}{A_2}\right)^2$$

(4) Valves we use the equation for ς: $Fr_m = \varsigma\,\frac{1}{2}\langle v_2\rangle^2$

(i) Gate valve

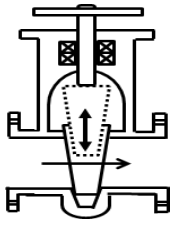

Gate valve	Fully open	3/4 open	1/2 open	1/4 open
ς	0.17	0.9	4.5	24.0
L_{eq}/D	7	40	200	800

(ii) Diaphragm valve

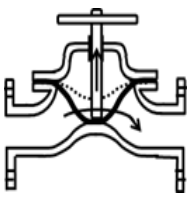

Diaphragm valve	Fully open	3/4 open	1/2 open	1/4 open
ς	2.3	2.6	4.3	21.6
L_{eq}/D	125	140	235	1140

(iii) Globe valve

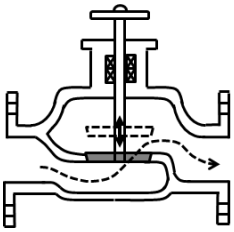

Bevel seat	Fully open	1/2 open
ς	6.0	9.5

Composition seat	Fully open	1/2 open
ς	6.0	8.5
L_{eq}/D	330	470

Plug disk	open	3/4 open	1/2 open	1/4 open
ς	9.0	13.0	36.0	112.0

(iv) Check valve (fully open only)

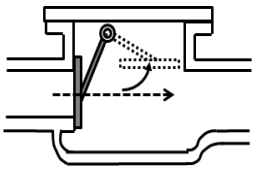

Check valve	swing	disk	ball
ς	2.0	10.0	65
L_{eq}/D	110	500	3500

(5) Pipe fittings[1, 2)]

Standard tee

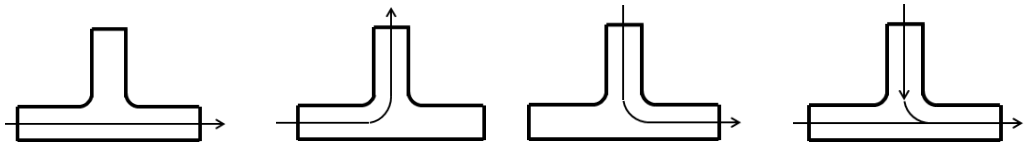

ς	0.4	1.3	1.5	1.0
L_{eq}/D	20	60	70	46

Standard elbow

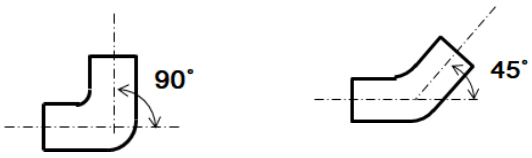

ς	0.74	0.3
L_{eq}/D	32	15

Bend

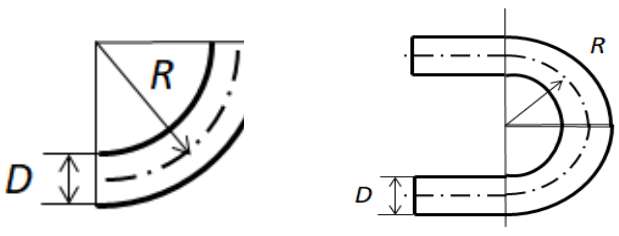

90° bend 180° bend

90° bend

R/D	0.5	1.0	2.0	4.0	8.0
L_{eq}/D	36	16.5	10	10	14.5

180° bend $R \gg D$

$\varsigma = 1.2$ $\frac{L_{eq}}{D} = 50$

1. Perry, R.H. and Chilton, C.H., Chemical Engineers' Handbook, McGraw-Hill, New York, 5th ed. (1973)
2. Lydersen, A. L., Fluid Flow and Heat Transfer, John Wiley, New York, p.9(1979)

[EXAMPLE 7.4-1] An example of local exhaust system is shown in Fig.7.4-E1.
A canopy type of hood draws in the air contaminated with lead fumes at a flow rate of 300 m^3/h. The diameter of the pipeline is 100 mm. In gas flow we do not need to consider the potential energy change. The air has a density of 0.89 kg/m^3 and a viscosity of 0.022 cp or 2.2×10^{-5} kg/m s. The pressure drop at the hood is expressed as

$$\Delta p_{hood} = \varsigma \frac{1}{2} \varrho \langle v \rangle^2 \qquad (7.4\text{-E1})$$

Here $\langle v \rangle$ is the downstream velocity. The friction loss factor for the hood is given by $\varsigma = 0.4$.
The pressure drop at the compact electrostatic precipitator is $\Delta p_{EP} = 30\ mm\ H_2O$ for the given flow rate. The pipeline has five standard elbows and an exhaust stack. The exhaust stack has pressure drop of $7\ mm\ H_2O$. Calculate the power requirement of the turbo-blower assuming 60% efficiency.

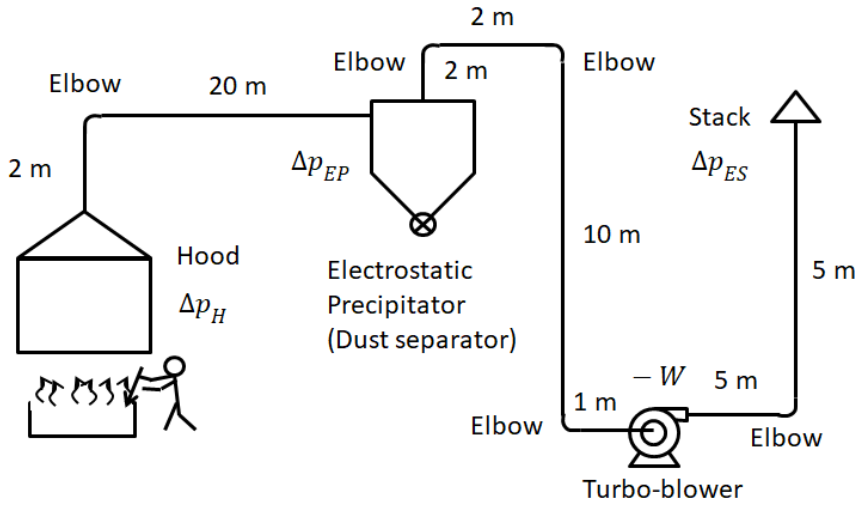

Fig.7.4-E1 Pipeline of local exhaust system

(Solution) The average velocity in the pipe is

$$\langle v \rangle = \frac{Q}{(\pi/4)D^2} = \left(\frac{300\ m^3}{3600\ s}\right)\frac{4}{\pi(0.10\ m)^2} = 10.6\ m/s \qquad (7.4\text{-E2})$$

The Reynolds number shown below indicates that the flow is turbulent.

$$Re = \frac{D\langle v \rangle \varrho}{\mu} = \frac{(0.10\ m)(10.6\ m/s)(0.89\ kg/m^3)}{2.2 \times 1 - 0^{-5}\ kg/m\ s)} = 4.3 \times 10^4 > 2{,}100$$

The reference planes are chosen outside the hood and exhaust stack. If we assume constant density

and viscosity, the modified Bernoulli equation becomes

$$\frac{1}{2}(\langle v_2\rangle^2 - \langle v_1\rangle^2) + g(h_2 - h_1) + (p_2 - p_1)/\rho + W_m + \sum_i \left(4f\ \frac{L}{D}\ \frac{1}{2}\ \langle v\rangle^2\right)_i$$

$$+ \sum_j \left(4f\ \frac{L_{eq}}{D}\ \frac{1}{2}\ \langle v\rangle^2\right)_j + (\Delta p_H + \Delta p_{EP} + \Delta p_{ES})/\rho = 0 \qquad (7.4\text{-E3})$$

From the chart of *f* vs. *Re*, the friction factor $f = 0.0055$ for $Re = 4.3 \times 10^4$

The pipeline has a constant pipe diameter. The total length of straight pipe sections is given as

$$L_{total} = (2 + 20 + 2 + 5 + 10 + 1 + 5 + 5)m = 50\ m$$

The pressure drop at the hood is

$$\Delta p_H = \zeta\ \frac{1}{2}\ \varrho\langle v\rangle^2 = (0.4)(1/2)(0.89)(10.6)^2 = 20.0\ kg/m\ s^2 \qquad (7.4\text{-E4})$$

From the above table, the equivalent length for the standard elbow is given by $L_{eq} = 3.20\ m$ for $= 0.10\ m$.

$$\Delta p_{EP} = 30\ mm\ H_2O = (1000\ kg/m^3)(9.8\ m/s^2)(0.03\ m) = 294\ kg/m\ s^2 \qquad (7.4\text{-E5})$$

$$\Delta p_{ES} = 7\ mm\ H_2O = 68.6\ kg/m\ s^2 \qquad (7.4\text{-E6})$$

At planes 1 and 2 $\langle v_1\rangle = \langle v_2\rangle = 0$ and $p_2 = p_1$

We neglect the potential energy effect: $g(h_2 - h_1) \cong 0$

Then the Bernoulli equation reduces to

$$-W_m = \frac{4f}{D}\ \frac{1}{2}\ \langle v\rangle^2\left(\sum_i L_i + \sum_j L_{eqj}\right) + \frac{\Delta p_H + \Delta p_{EP} + \Delta p_{ES}}{\rho} = \frac{4(0.0055)}{0.10}\ \frac{1}{2}\ 10.6^2\ (50 + 5 \times 3.20) +$$

$$\frac{20+294+68.6}{0.89} = 816 + 430 = 1{,}246\ m^2/s^2 \qquad (7.4\text{-E7})$$

Therefore the power requirement can be calculated as

$$-W = \frac{w(-W_m)}{\eta} = \frac{\rho Q(-W_m)}{\eta} = \frac{(0.89)(300/3600)(1246)}{0.60} = 154\ kg\ m^2/s^3 = 0.154\ kW \qquad (7.4\text{-E8})$$

7.4-3 Non-circular channels (Equivalent diameter)

The friction loss in long straight channels of noncircular cross section can be estimated by using the equations for circular pipes if the equivalent diameter as the characteristic length and the average velocity as the characteristic velocity are used for the Reynolds number.

The equivalent diameter D_{eq} is defined as the ratio of four times the cross-sectional area of the channel to the wetted perimeter of the channel:

$$D_{eq} = \frac{4 \times S_c}{L_{wp}} \qquad (7.4\text{-13})$$

Naturally for the special case of a circular pipe, the equivalent diameter becomes coincident with the pipe diameter. The equivalent diameter is a useful parameter for turbulent flow, but the simple equivalent-diameter rule does not apply to laminar flow without correction factor.

The equivalent diameter concept is based on the following information. For turbulent flow the velocity distribution over most of the flow cross-section is flat and most of the velocity change is in the viscous sublayer near the wall. Therefore, as long as the wall shear stress around the periphery is almost uniform, the wall shear stress should be independent of the flow cross-sectional shape.

The Reynolds number is defined as

$$Re_{eq} = \frac{D_{eq}\ G}{\mu} \qquad (7.4\text{-14})$$

Here $G = \rho\ \langle v\rangle$.

[EXAMPLE 7.4-2]

Water is flowing at an average velocity $\langle v\rangle = 1.5\ m/s$ in a horizontal annular space formed between two coaxial pipes shown below. The inner pipe has an outside diameter of $0.10\ m$ and the outer pipe has an inside diameter of $0.20\ m$. The temperature of water is 20 °C. Assuming the

fully-developed flow and the smooth wetted surfaces, calculate the pressure drop per unit pipe length.

(Solution) The density and viscosity of water are
$\rho = 1{,}000\ kg/m^3$ and $\mu = 1\ cP = 1 \times 10^{-3}\ kg/m\,s$
The equivalent diameter of the annulus is

$$D_{eq} = \frac{4(\pi/4)\left({D_o}^2 - {D_i}^2\right)}{\pi(D_o + D_i)} = D_o - D_i = 0.2 - 0.1 = 0.1\,m$$

The Reynolds number is
$Re_{eq} = \frac{D_{eq}\rho\langle v_z\rangle}{\mu} = \frac{(0.10)(1000)(1.5)}{1\times 10^{-3}} = 1.5 \times 10^5$ (turbulent flow)
From the friction factor chart for circular pipes
$f = 0.0041$ at $Re_{eq} = 1.5 \times 10^5$
From the defining equation of Fanning friction factor for a horizontal pipe

$$\frac{p_0 - p_L}{L} = 4f\,\frac{1}{D_{eq}}\,\frac{1}{2}\,\rho\langle v_z\rangle^2 = \frac{4(0.0041)}{0.1}\,\frac{1}{2}\,(1000)(1.5)^2 = 184.5\ Pa/m$$

7.5 Drag Force on Submerged Objects

Similarly to the defining equation Eq.(7.2-4) for a circular tube flow, the friction factor (called "drag coefficient") for submerged objects can be defined as

$$F_D = C_D\,K\,A \qquad (7.5\text{-}1)$$

where F_D is the drag force, K the kinetic energy of the surrounding fluid flow as $(1/2)\rho{v_\infty}^2$, and A the characteristic area taken as the projected area of the submerged object.
Usually the coefficient C_D is called the drag coefficient instead of the friction factor. As in pipe flows, the drag coefficient is a function of the Reynolds number alone:

$$C_D = C_D(Re) \qquad (7.5\text{-}2)$$

Let us consider a fluid flow past a sphere of diameter D_p. In this case, the kinetic energy is $K = (1/2)\rho{v_\infty}^2$ and characteristic area is $A = (\pi/4){D_p}^2$. The Reynolds number is defined as $Re = D_p v_\infty \rho/\mu$.

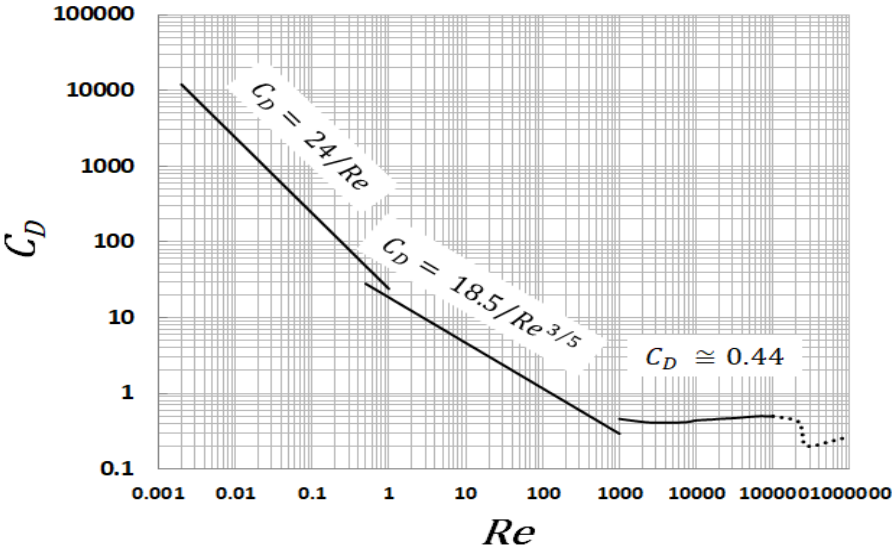

Fig.7.5-1. Variation of drag coefficient with Reynolds number for a single sphere

For a single sphere surrounded by the fluid flow of velocity v_∞, a chart of C_D versus Re shown in Fig.7.5-1 is available. As distinct from a circular tube flow, there is no sharp transition from laminar to turbulent flow. However as the flow rate or v_∞ increases, there is an increase in the amount of vortical motion behind the sphere. The sudden drop in the curve at about $Re = 2 \times 10^5$ results from the shift of the separation position of the boundary layer from the front to the rear side of the sphere. This sphere is subjected to both friction drag and form drag.

The following set of equations is the representative correlations obtained from many experimental data:

(1) $C_D = \frac{24}{Re}$ $Re < 0.1$ (7.5-3)

(2) $C_D = \frac{18.5}{Re^{3/5}}$ $2 < Re < 5 \times 10^2$ (7.5-4)

(3) $C_D \cong 0.44$ $5 \times 10^2 <$ Re $< 2 \times 10^5$ (7.5-5)

The first equation comes from Stokes's law given by

$$F_D = 3\pi\mu D_p v_\infty \quad (7.5\text{-}6)$$

The second equation is an approximate equation in the intermediate region.

The third equation known as the Newton's law gives an approximately constant. This suggests that the drag force is proportional to the kinetic energy of the fluid flow.

Nomenclature

D	pipe inside diameter, [m]
D_{eq}	equivalent diameter, [m]
F	external force, [N]
Fr	friction loss, [m^2/s^2]
f	friction factor, [-]
G	mass velocity, [kg/m^2s]
H	height of rectangular channel, [m]
I	electric current, [A]
L	pipe length, [m]
L_{eq}	equivalent length, [m]
p	pressure, [Pa]
R	electric resistance of hot wire, [Ω] or Wheatstone bridge resistance, [Ω]
Re	Reynolds number, [-]
Tu	turbulence intensity, [-]
t	time, [s]
v_r, v_θ, v_z	velocity component in cylindrical coordinates
W	power requirement, [W]
y	distance from wall, [m]
δ	thickness of fictitious viscous film, [m]
ς	friction loss factor, [-]
μ	viscosity, [kg/m s]
τ_w	wall shear stress, [N/m^2]

Superscripts

´	fluctuation
¯	time-averaged

Brackets

⟨ ⟩	averaged over flow cross section

CHAPTER 8

INTERPHASE ENERGY TRANSPORT

8.1 Turbulent Heat Transfer and Definition of Heat Transfer Coefficient

There are three distinct ways in which heat may transfer from a source to a receiver: conduction, convection, and radiation. Conduction is the transfer of thermal energy due to molecular motion independent of net bulk flow of the material. We already know that the Fourier's law describes heat transfer by conduction. Radiation is the transfer of energy due to the emission and subsequent absorption of electromagnetic radiation.

Convection is the transfer of energy due to fluid motion or bulk flow of the fluid. Let us consider the heat flow from a flowing fluid to a pipe wall.

As shown in Fig.8.1-1, instantaneous fluid temperature is also fluctuating in a turbulent flow field where convective heat transfer takes place. Therefore the following time-averaged temperature is used for analysis of convective heat transfer.

$$\bar{T} = \frac{1}{t_0}\int_t^{t+t_0} T\,dt \tag{8.1-1}$$

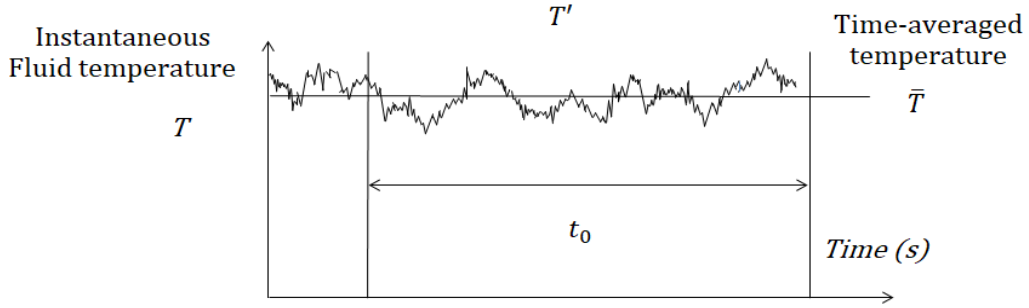

Fig.8.1-1 Instantaneous fluid temperature in a turbulent flow field

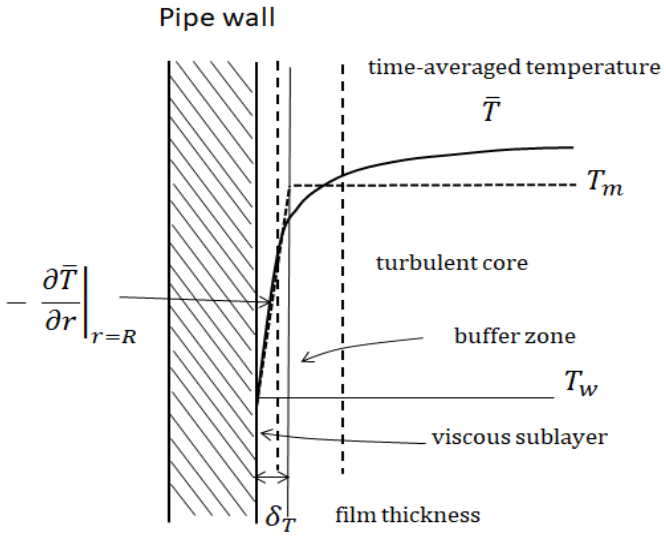

Fig.8.1-2 Time-averaged temperature profile in the neighborhood of a heat transfer solid surface

For the case of forced convective heat transfer in a turbulent pipe flow, the time-averaged temperature profile, as shown in Fig,8.1-2, is formed in the neighborhood of the solid surface for heat transfer. Convective and conductive heat transfers are intimately related because heat transferred by convection ultimately involves conduction.

In the turbulent core, the time-averaged temperature has almost uniform distribution due to mixing by eddy motion. The temperature gradient is very small but energy is transferred very rapidly. However in the viscous sublayer near the pipe wall, such an eddy motion is suppressed to have steep linear temperature distribution by molecular transport effect only. The buffer zone has a transitional temperature profile, where the turbulent effect becomes of comparable order to molecular transport effect.

Hence the main resistance to heat transfer takes place in very thin film of the fluid near the wall. Then the heat-flux through the film toward the pipe wall can be expressed at the heat transfer surface as

$$.q_w = q_r|_{r=R} = -\kappa \left.\frac{\partial T}{\partial r}\right|_{r=R} \tag{8.1-2}$$

Introducing a thermal film thickness δ_T, this temperature gradient can be approximated as

$$q_r|_{r=R} = \kappa \frac{T_m - T_w}{\delta_T} \tag{8.1-3}$$

where T_m is the mixed mean temperature (bulk temperature), T_w the wall temperature, and δ_T the thickness of an fictitious conduction film. The definition of the mixed mean temperature is

$$T_m - T_w = \frac{\int_0^R 2\pi r\, v_z \rho Cp (T - T_w) dr}{\int_0^R 2\pi r\, v_z \rho Cp\, dr} \tag{8.1-4}$$

Then the equation becomes

$$q_w = \frac{\kappa}{\delta_T}(T_m - T_w) = h\,(T_m - T_w) \qquad (T_m > T_w)$$

$$q_w = \frac{\kappa}{\delta_T}(T_w - T_m) = h\,(T_w - T_m) \qquad (T_m < T_w) \tag{8.1-5}$$

This is one of the defining equations for heat transfer coefficient:

$$h = \kappa/\delta_T \tag{8.1-6}$$

The film thickness is a complicated function of the flow condition, the fluid properties, and the geometry of the flow system, that is, a function of Re and Pr. Therefore the heat transfer coefficient can be expressed to be a function of the same parameters. The heat transfer coefficient has units of $J/m^2\, s\, K$ in SI unit system.

8.2 Application of the Equation of Energy for Turbulent Heat Transfer

The turbulent effect on heat transfer becomes of negligible importance in the viscous sublayer. The following equations are valid in the viscous sublayer, whether the flow is laminar or turbulent:

$$\rho\left(\frac{\partial v_z}{\partial t} + v_r\frac{\partial v_z}{\partial r} + \frac{v_\theta}{r}\frac{\partial v_z}{\partial \theta} + v_z\frac{\partial v_z}{\partial z}\right) = -\frac{\partial p}{\partial z} + \mu\left[\frac{1}{r}\frac{\partial}{\partial r}\left(r\frac{\partial v_z}{\partial r}\right) + \frac{1}{r^2}\frac{\partial^2 v_z}{\partial \theta^2} + \frac{\partial^2 v_z}{\partial z^2}\right] \tag{8.2-1}$$

$$\rho Cp\left(\frac{\partial T}{\partial t} + v_r\frac{\partial T}{\partial r} + \frac{v_\theta}{r}\frac{\partial T}{\partial \theta} + v_z\frac{\partial T}{\partial z}\right) = \kappa\left[\frac{1}{r}\frac{\partial}{\partial r}\left(r\frac{\partial T}{\partial r}\right) + \frac{1}{r^2}\frac{\partial^2 T}{\partial \theta^2} + \frac{\partial^2 T}{\partial z^2}\right] \tag{8.2-2}$$

In the last equation the viscous dissipation term and the pressure work term have been neglected.

These equations could be solved with the following boundary conditions

$$v_z = v_r = v_\theta = 0 \quad \text{and} \quad -\mu\frac{\partial v_z}{\partial r} = \tau_w \qquad \text{at } r = R \tag{8.2-3}$$

$$T = T_w \quad \text{and} \quad -\kappa\frac{\partial T}{\partial r} = q_w \qquad \text{at } r = R \tag{8.2-4}$$

According to the definition of heat transfer coefficient

$$q_r|_{r=R} = q_w = h\,(T_w - T_m) \tag{8.2-5}$$

That is

$$h = \frac{1}{T_w - T_m}\left(-\kappa \frac{\partial T}{\partial r}\right)\Big|_{r=R} \tag{8.2-6}$$

Then let us start with dimensional analysis for application of the equation of energy transport.

The following dimensionless quantities should be introduced:

$$r^* = r/D,\ z^* = z/D,\ T^* = (T_w - T)/(T_w - T_m),\ v_r^* = v_r/\langle v_z\rangle,$$
$$v_\theta^* = v_\theta/\langle v_z\rangle,\quad v_z^* = v_z/\langle v_z\rangle,\quad p^* = (p - p_0)/(\rho\,\langle v_z\rangle^2)$$

$\langle v_z\rangle$ is the representative velocity averaged over the cross section.

The above energy equation is made dimensionless

$$v_r^*\frac{\partial T^*}{\partial r^*} + \frac{v_\theta^*}{r^*}\frac{\partial T^*}{\partial \theta} + v_z^*\frac{\partial T^*}{\partial z^*} = \frac{1}{Re\,Pr}\left[\frac{1}{r^*}\frac{\partial}{\partial r^*}\left(r^*\frac{\partial T^*}{\partial r^*}\right) + \frac{1}{r^{*2}}\frac{\partial^2 T^*}{\partial \theta^2} + \frac{\partial^2 T^*}{\partial z^{*2}}\right] \tag{8.2-7}$$

where $Re = \rho\, D\,\langle v_z\rangle/\mu$ and $Pr = C_p\mu/\kappa$

Note that these dimensionless parameters Re and Pr appear automatically in the dimensional analysis.

The equation of motion is also made dimensionless for steady state:

$$v_r^*\frac{\partial v_z^*}{\partial r^*} + \frac{v_\theta^*}{r^*}\frac{\partial v_z^*}{\partial \theta} + v_z^*\frac{\partial v_z^*}{\partial z^*} = -\frac{\partial p^*}{\partial z^*} + \frac{1}{Re}\left[\frac{1}{r^*}\frac{\partial}{\partial r^*}\left(r^*\frac{\partial v_z^*}{\partial r^*}\right) + \frac{1}{r^{*2}}\frac{\partial^2 v_z^*}{\partial \theta^2} + \frac{\partial^2 v_z^*}{\partial z^{*2}}\right] \tag{8.2-8}$$

In general, this equation is too difficult to solve analytically. However the velocity solution can be expected to be of the form:

$$v_r^* = v_r^*(r^*, \theta, z^*, Re)$$
$$v_\theta^* = v_\theta^*(r^*, \theta, z^*, Re) \tag{8.2-9}$$
$$v_z^* = v_z^*(r^*, \theta, z^*, Re)$$

If the above dimensionless energy equation could be solved by substituting the dimensionless velocity solutions. Therefore the temperature solution can also be expected to be of the form:

$$T^* = T^*(r^*, \theta, z^*, Re, Pr) \tag{8.2-10}$$

We assume the fully-developed, axisymmetric temperature field

$\frac{\partial T^*}{\partial z^*} = 0$ and $\frac{\partial T^*}{\partial \theta} = 0$

Then we get $T^* = T^*(r^*, Re, Pr)$

The temperature gradient at the wall $\left.\frac{\partial T^*}{\partial r^*}\right|_{r^*=1/2}$ should be a function of Re and Pr only.

The boundary condition is made dimensionless:

$$Nu = \frac{h\,D}{\kappa} = \frac{\left.\frac{\partial (T_w - T)}{\partial r}\right|_{r=R}}{(T_w - T_m)/D} = -\left.\frac{\partial T^*}{\partial r^*}\right|_{r^*=\frac{1}{2}} \tag{8.2-11}$$

The new dimensionless parameter is known as the Nusselt number. The above equation states that the Nusselt number is the dimensionless temperature gradient at the heat transfer surface. Therefore the Nusselt number is found to be a function of dimensionless parameters Re and Pr in the fully-developed temperature field. Note that the Nusselt number gives a local heat transfer coefficient.

$$Nu = Nu\,(Re, Pr) \tag{8.2-12}$$

Similarly the Nusselt number averaged over the pipe length is also a function of Re and Pr.

It may be convenient to use a new dimensionless group defined as

$$j_H = \frac{h}{C_p G}\left(\frac{C_p\mu}{\kappa}\right)_f^{2/3} = Nu\,Re^{-1}Pr^{-1/3} \tag{8.2-13}$$

where G is mass velocity = (fluid density) x (average fluid velocity) $\rho\langle v\rangle$.

This is called the j-factor for heat transfer. This parameter is often used when the convective transport mechanism is discussed among momentum, energy, and mass transfer.

The subscript f denotes properties evaluated at the film temperature

$$T_f = \frac{T_m + T_w}{2}$$

For large temperature changers, the variation in μ should be taken into account.

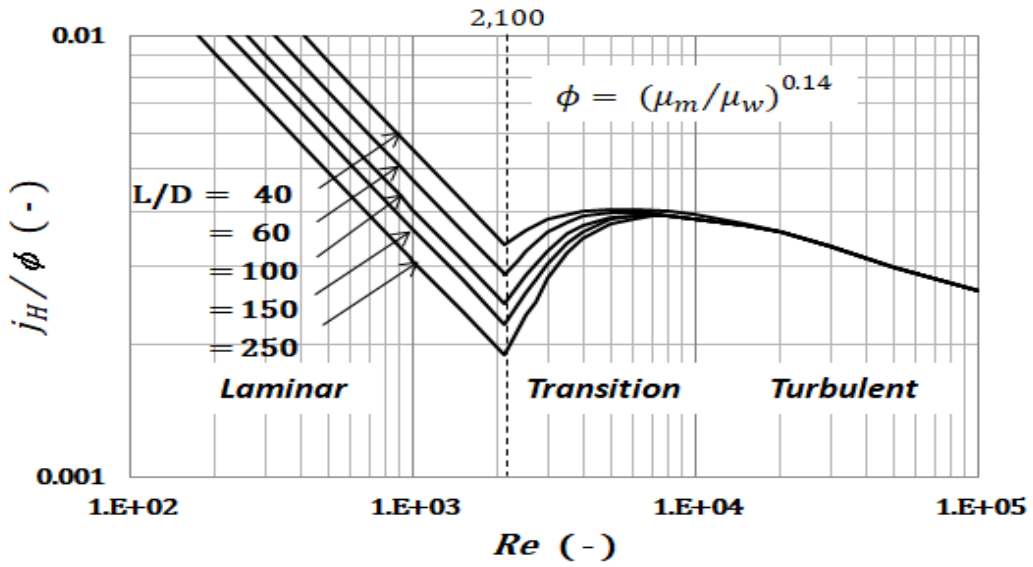

Fig.8.2-1 j-factor correlation for heat transfer of circular pipe flows

Figure 8.2-1 shows the j-factor for heat transfer in circular pipes which includes the correction factor ϕ for viscosity: $\phi = (\mu_b/\mu_w)^{-0.14}$
In the highly turbulent flow range, the following empirical analogy for long smooth pipes is proposed by Colburn:

$$j_H = \frac{f}{2} \qquad (8.2\text{-}14)$$

This analogy relation will be demonstrated for a laminar boundary layer flow over a flat plate in Chapter 17.

The analogy permits one to predict heat transfer coefficients from friction data for the same flow conditions. It should be noted that the laminar Nusselt number or j-factor depends on the ratio L/D. In the range of turbulent heat transfer, the following empirical correlation is available:

$$\frac{h}{C_p G}\left(\frac{C_p \mu}{\kappa}\right)_f^{2/3}\left(\frac{\mu_b}{\mu_w}\right)^{-0.14} = 0.026\left(\frac{D\,G}{\mu}\right)_b^{-0.2} \qquad Re = \frac{D\,G}{\mu} > 10^4 \quad 0.6 < \mathrm{Pr} < 100 \qquad (8.2\text{-}15)$$

Colburn, A.P., Trans. *A.I.Ch.E.*, **29**, 174-210 (1933)
Sieder, E.N. and Tate, G.E., *Ind. Eng. Chem.*, **28**, 1429 (1936)

8.3 Overall Heat Transfer Coefficient and Heat Exchangers

8.3-1 Definition of overall heat transfer coefficient

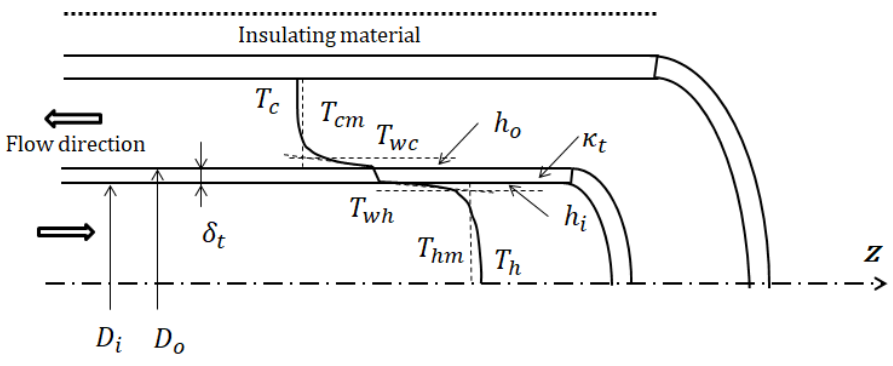

Fig.8.3-1 Double-pipe heat exchanger

As a very simple and comprehensible example of heat exchangers, Figure 8.3-1 shows a double-pipe heat exchanger consisting of two concentric pipes. For definiteness, we assume that the hot fluid is flowing through the inner pipe and the cold fluid in the annular space; heat is transferred rapidly across the wall of the inner pipe. If the two fluids flow in opposite directions, the type of flow is called "counter-current flow." If the two fluids flow in the same direction, the flow is called "parallel flow." Steady-state turbulent flow may be assumed here. Heat losses from the wall of the outer pipe to the surroundings may be neglected. The actual change in temperature with the radial distance is shown schematically by the solid lines T_h, T_{wh}, T_{wc}, T_c. The dotted lines show the temperature change modified by the film theory to define two heat transfer coefficients h_i, h_o. The mixed mean temperature T_{hm} of the hot stream is somewhat lower than the maximum temperature T_h , whereas the mixed mean temperature T_{cm} of the cold stream is somewhat higher than the minimum temperature T_c. The thickness and thermal conductivity of the inner pipe wall are given by δ_t and κ_t, respectively.

It is convenient to utilize an overall resistance concept in calculation of the heat transfer rate across many layers in series: the inside film, the tube wall, and the outside film resistances. The heat flux can be expected to be proportional to the temperature difference $T_{hm} - T_{cm}$ as the driving force.

The rate of heat transfer over a very small pipe length dz can be expressed in terms of the individual temperature drops in three layers:

$$dQ = h_i \pi D_i dz\,(T_{hm} - T_{wh}) = \kappa_t \pi D_{av} dz \frac{T_{wh} - T_{wc}}{\delta_t} = h_o \pi D_o dz\,(T_{wc} - T_{cm}) \qquad (8.3\text{-}1)$$

This equation can be rewritten as

$$dQ = \frac{T_{hm} - T_{wh}}{\frac{1}{h_i \pi D_i dz}} = \frac{T_{wh} - T_{wc}}{\frac{\delta_t}{\kappa_t \pi D_{av} dz}} = \frac{T_{wc} - T_{cm}}{\frac{1}{h_o \pi D_o dz}} \qquad (8.3\text{-}2)$$

where D_{av} is the logarithmic mean of the outer and inner diameters of the inner pipe.

This equation indicates a heat transfer analog to Ohm's law of electrical current. That is, the heat transfer rate dQ corresponds to the electrical current. The individual temperature drops correspond to the voltage drops in the separate resistances operating in series. Each denominator indicates the corresponding thermal resistance.

Adding these numerators and denominators separately, we get

$$dQ = \frac{T_{hm} - T_{cm}}{\frac{1}{h_i \pi D_i dz} + \frac{\delta_t}{\kappa_t \pi D_{av} dz} + \frac{1}{h_o \pi D_o dz}} \qquad (8.3\text{-}3)$$

The denominator indicates the overall thermal resistance. The numerator indicates a local value of the overall temperature difference. Then we can define an overall heat transfer coefficient U_o based on the outside area of the inner pipe by the equation

$$dQ = \frac{T_{hm} - T_{cm}}{\frac{1}{U_o\, \pi D_o dz}} = U_o\, \pi D_o dz\,(T_{hm} - T_{cm}) \qquad (8.3\text{-}4)$$

The denominator can be considered to be an overall resistance. Comparing this equation with Eq.(8.3-3), we get the following relation:

$$U_o = \frac{1}{\frac{1}{h_i}\frac{D_o}{D_i} + \frac{\delta_t}{\kappa_t}\frac{D_o}{D_{av}} + \frac{1}{h_o}} \qquad (8.3\text{-}5)$$

The individual terms of the denominator on the right-hand side represent the individual resistances of the two fluid films and of the tube wall. Note that U_o means a local value of the overall heat-transfer coefficient.

[Fouling]

Usually actual heat exchanger surfaces are subject to deposition of a film of foreign materials. This phenomenon called "Fouling" very often occurs on the heat transfer surfaces on the cooling water side when using natural water such as sea, river or well water. The film growing due to the accumulation of unwanted materials on solid surfaces offers a thermal resistance.

Therefore the heat transfer resistance should be taken into account in the overall heat transfer

coefficient:

$$\frac{1}{U_o} = \frac{1}{h_i}\frac{D_o}{D_i} + \frac{1}{h_{si}}\frac{D_o}{D_i} + \frac{\delta_t}{\kappa_t}\frac{D_o}{D_{av}} + \frac{1}{h_o} + \frac{1}{h_{so}} \quad (8.3\text{-}6)$$

where h_{si} and h_{so} are the reciprocals of the fouling thermal resistances on the inner and outer tube walls, respectively.

8.3-2 Logarithmic mean temperature difference[1)]

Since the overall temperature difference varies from point to point along the pipe, the heat flux also varies with pipe length. The temperature variation for counter-current flow is shown as an example in Figure 8.3-2.

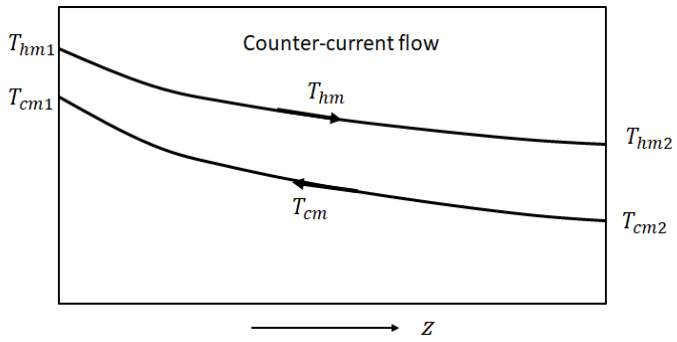

Fig.8.3-2. Temperature variation with pipe length for countercurrent flow in a double tube exchanger

To apply the defining equation for U_o to the entire area of the exchanger, the equation must be integrated with the simplifying assumptions: (1) the overall coefficient is constant and (2) the heat capacities of the two fluids are kept constant.

Figure 8.3-3 shows a double-pipe counter-flow heat exchanger. The outside and inside diameters of the inner pipe are D_o and D_i and the inner pipe length for heat exchange is L.

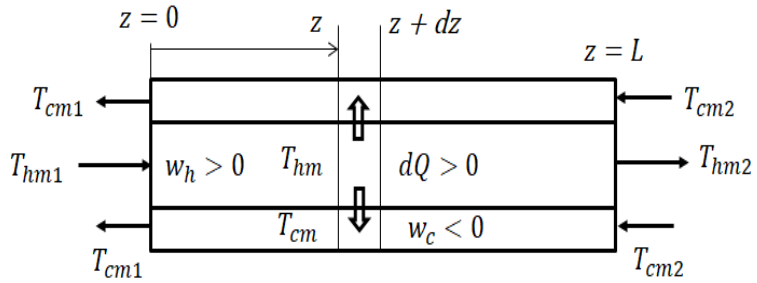

Fig.8.3-3. Interphase heat transfer in a double-pipe countercurrent exchanger

The hot fluid is flowing through the inner pipe and the cold fluid through the annular space.
If we set up the differential energy balance over the volume element between z and z + dz,

$$dQ = -w_h Cp_h\, dT_{hm} = w_c Cp_c\, dT_{cm} \quad (8.3\text{-}7)$$

The flow rate of the cold fluid w_c is negative since the cold fluid flows in opposite direction. The temperature gradients are $dT_{hm}/dz < 0$, $dT_{cm}/dz < 0$. The minus sign in front of w_h comes from the condition of positive dQ.

According to the equation for U_o,

$$dQ = U_o \pi D_o\, dz\, (T_{hm} - T_{cm}) \quad (8.3\text{-}8)$$

From these equations we get the following equations for the hot and cold streams, respectively.

$$-\frac{dT_{hm}}{T_{hm} - T_{cm}} = U_o \frac{\pi D_o dz}{w_h Cp_h} \quad (8.3\text{-}9)$$

$$\frac{dT_{cm}}{T_{hm} - T_{cm}} = U_o \frac{\pi D_o dz}{w_c Cp_c} \quad (8.3\text{-}10)$$

By adding these equations, we obtain

$$-\frac{d(T_{hm}-T_{cm})}{T_{hm}-T_{cm}} = U_o\left(\frac{1}{w_h Cp_h}+\frac{1}{w_c Cp_c}\right)\pi D_o dz \tag{8.3-11}$$

For constant coefficient U_o, we can integrate between both ends of the exchanger:

$$\ln\left(\frac{T_{hm1}-T_{cm1}}{T_{hm2}-T_{cm2}}\right) = U_o\left(\frac{1}{w_h Cp_h}+\frac{1}{w_c Cp_c}\right)\pi D_o L \tag{8.3-12}$$

According to the energy balance between $z = 0$ and L, the total rate of heat exchange is

$$Q = w_h Cp_h(T_{hm1} - T_{hm2}) = -w_c Cp_c(T_{cm1} - T_{cm2})$$
$$= \frac{T_{hm1}-T_{hm2}}{\frac{1}{w_h Cp_h}} = -\frac{(T_{cm1}-T_{cm2})}{\frac{1}{w_c Cp_c}} = \frac{(T_{hm1}-T_{hm2})-(T_{cm1}-T_{cm2})}{\frac{1}{w_h Cp_h}+\frac{1}{w_c Cp_c}} \tag{8.3-13}$$

Then we get

$$\frac{1}{w_h Cp_h}+\frac{1}{w_c Cp_c} = \frac{[(T_{hm1}-T_{cm1})-(T_{hm2}-T_{cm2})]}{Q} \tag{8.3-14}$$

Substituting it into the foregoing equation, Eq,(8.3-12), we get

$$Q = U_o\,\pi D_o L\left\{\frac{(T_{hm1}-T_{cm1})-(T_{hm2}-T_{cm2})}{\ln\left(\frac{T_{hm1}-T_{cm1}}{T_{hm2}-T_{cm2}}\right)}\right\} \tag{8.3-15}$$

or

$$Q = U_o A_o(T_{hm} - T_{cm})_{lm} = U_o A_o(\Delta T_m)_{lm} \tag{8.3-16}$$

where

$$(\Delta T_m)_{lm} = \frac{\Delta T_{m1}-\Delta T_{m2}}{\ln\frac{\Delta T_{m1}}{\Delta T_{m2}}} \tag{8.3-17}$$

This equation, valid for both parallel and counter-current flows, is the basic equation for engineering calculation of heat exchangers. The result indicates that we should use the logarithmic mean of the mixed mean temperature differences at both ends (abbreviated LMTD) to determine the total area for the required heat transfer rate.

We can understand from this analysis for a double-pipe exchanger that the LMTD is appropriate as the characteristic temperature difference for thermal engineering design of various exchangers

---

1. Bird, R.B., Stewart, W.E. and Lightfoot, E.N., *Transport Phenomena*, Wiley, New York, Chapt.15, Example 15.4-2 (1960)

Nomenclature

Cp	heat capacity, [J/kg K]
D	pipe diameter, [m]
f	friction factor, [-]
G	mass velocity, [kg/m^{2}s]
h	heat transfer coefficient, [W/m^{2}K]
j_H	j-factor for heat transfer, [-]
Nu	Nusselt number, [-]
Pr	Prandtl number, [-]
Q	heat transfer rate, [W]
q_r, q_w	heat flux at *r*, wall heat flux, [W/m^2]
R	pipe radius, [m]
Re	Reynolds number, [-]
r, θ, z	cylindrical coordinates, [m, - , m]
T	temperature, [K]
t	time, [s]
U	overall heat transfer coefficient, [W/m^{2}K]
v_r, v_θ, v_z	velocity component in cylindrical coordinates
w_c, w_h	mass flow rate of cold fluid, hot fluid, [kg/s]
z	axial coordinate, [m]
δ_t	tube wall thickness, [m]
δ_T	film thickness for heat transfer, [m]
μ	viscosity, [kg/m s]
κ	thermal conductivity, [W/m K]

ρ	density, [kg/m^3]
ϕ	correction factor for viscosity, [-]

Superscripts

$*$	dimensionless
$\acute{}$	fluctuation
$\bar{}$	time-averaged

Subscripts

c	cold
f	film
h	hot
i	inner tube
l.m.	logarithmic mean
m	bulk or mixed mean
o	outer tube or outside surface
t	tube
w	wall

Brackets

$\langle\ \rangle$	averaged over flow cross section

CHAPTER 9

HEAT TRANSFER EQUIPMENT

9.1 Shell-and-Tube Heat Exchanger

There are various kinds of heat exchangers in industrial processes: double-pipe exchanger, shell-and-tube exchanger, cross-flow plate exchanger, etc.

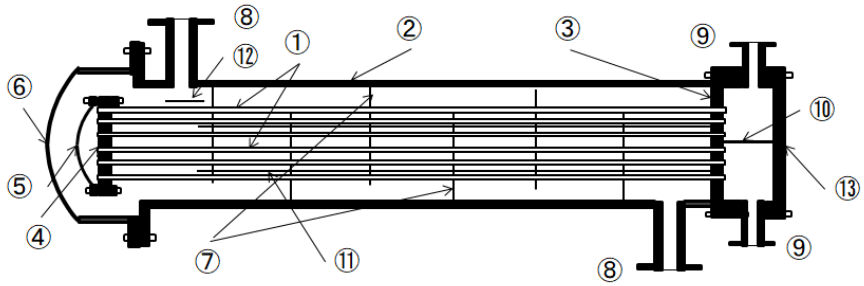

1:tubes, 2:shell, 3:stationary tubesheet, 4:floating tubesheet, 5:floating head cover, 6:shell cover, 7:baffles, 8:shell nozzle, 9:stationary head nozzle, 10:pass partition, 11:tie rods and spacers, 12:impingement baffle, 13:channel cover

Fig.9.1-1. Floating-head 1-2 heat exchanger

Figure 9.1-1 shows a floating-head one-shell-pass, two-tube-pass heat exchanger.

Here we deal with the thermal analysis of shell-and-tube exchangers, which are widely used because they can be constructed with large heat-transfer surfaces in a relatively small volume. The above figure is a sketch of a shell-and-tube heat exchanger with one shell pass and two tube passes. Usually the hot fluid flows through the tubes and the cold fluid through the shell. The shell-side and tube-side heat transfer coefficients are of comparable importance, and both must be large to attain a satisfactorily large overall coefficient. Heat transfer tubes are laid out on either square or triangular patterns.

The tube pitch P_t is the shortest center-to-center distance between adjacent tubes. Usually we use 1.25 times the outside diameter of the tubes for triangular pitch. Since the velocity on the shell side is usually low in comparison with that on the tube side, 25%-cut baffles are installed in the shell to decrease the flow cross-section and to cause the fluid to flow across the tube bank rather than parallel with it. An increase in the shell-side coefficient is obtained by this type of cross flow across the tube bank. Standard length of tubes is usually 5 m. Shells are fabricated from pipe or by rolling plate of steel or stainless steel. It is often difficult to obtain a high velocity when the tube-side fluid flows through all the tubes in a single pass. Multipass construction by means of the pass partitions are used to increase the tube-side velocity with a corresponding increase in the tube-side coefficient. The sizes of tubes which are frequently used are in the range 15 to 30 mm OD.

9.2 Tube-side Heat Transfer Coefficient

In the last chapter, we concluded that the Nusselt number for fully-developed temperature field is

a function of Reynolds number and Prandtl number. The inside heat transfer coefficient h_i for the tube-side fluid can also be correlated in the j-factor form:

$$j_H = \frac{Nu}{Re} Pr^{-1/3} \left(\frac{\mu_m}{\mu_w}\right)^{-0.14} \quad (9.2\text{-}1)$$

where μ_m, μ_w are the viscosities of the tube-side fluid at the mixed-mean temperature T_m and wall temperature T_w. Unless the temperature difference between T_m and T_w is very large, the viscosity correction term $\phi = (\mu_m/\mu_w)^{-0.14}$ may be considered to be unity.

For highly turbulent pipe flow, we can use the empirical equation (Sieder and Tate correlation)[1)]

$$\frac{h_i D}{\kappa} = 0.026 \left(\frac{D\,G}{\mu}\right)^{0.8} \left(\frac{Cp\,\mu}{\kappa}\right)^{1/3} \left(\frac{\mu_m}{\mu_w}\right)^{0.14} \quad (9.2\text{-}2)$$

or in the Colburn j-factor form

$$j_H = 0.026\, Re^{-0.2} \quad (9.2\text{-}3)$$

which gives the heat transfer coefficient within ± 20 % error in the range $Re = 10^4 \sim 10^5$, $\mathrm{Pr} = 0.6 \sim 100$, and $L/D > 10$. In moderate heat transfer conditions $\mu_m/\mu_w \cong 1$.

We can also use

$$\frac{h_i D}{\kappa} = 0.023 \left(\frac{D\,G}{\mu}\right)^{0.8} \left(\frac{Cp\,\mu}{\kappa}\right)^{1/3} \quad (9.2\text{-}4)$$

For laminar flow we have to consider the boundary layer effect of entrance length developing from the pipe entrance. We can use the following equation

$$\frac{h_i D}{\kappa} = 1.86\, (Re\,\mathrm{Pr}\,D/L)^{1/3} \left(\frac{\mu_m}{\mu_w}\right)^{0.14} \quad (9.2\text{-}5)$$

which is good within ± 20 for $Re\,\mathrm{Pr}\,L/D > 10$. Keep in mind that Eq.(9.2-5) gives an average heat transfer coefficient in the developing temperature field.

Note that Figure 8.2-1 gives this laminar flow correlation in the form of parallel straight lines.

1. Sieder, E.N. and Tate, G.E., *Ind. Eng. Chem.*, **28**, 1429 (1936)

9.3 Heat Transfer Coefficient in Annular Space of Double-tube Exchangers[1)]

For evaluating the heat transfer coefficient of the annular side, we have to consider the hydraulic equivalent diameter for noncircular flow passage.

The heat transfer through the inner tube-side wall in turbulent annular flow can be correlated by equations similar to those used for circular tube flow accounting for the annular geometry.

Here the equivalent diameter D_{eq} is used.

One of the correlative equations is

$$\frac{h_o D_{eq}}{\kappa} = 0.023 \left(\frac{D_{eq}\,G}{\mu}\right)^{0.8} \left(\frac{Cp\,\mu}{\kappa}\right)^{0.4} \left(\frac{D_2}{D_1}\right)^{0.45} \quad (9.3\text{-}1)$$

$$D_{eq} = D_2 - D_1, \quad Re > 10^4$$

where D_2 and D_1 are the inside diameter of the outer tube and the outside diameter of the inner tube, respectively.

1. Kern, D. Q., Process Heat Transfer, McGraw-Hill, New York, 137 (1950)

9.4 Shell-side Heat Transfer Coefficient

As shown in Fig.9.4-1, the triangular pitch gives high shell-side heat transfer coefficients because the shell-side fluid flowing between adjacent tubes impinges directly on the succeeding tube row.

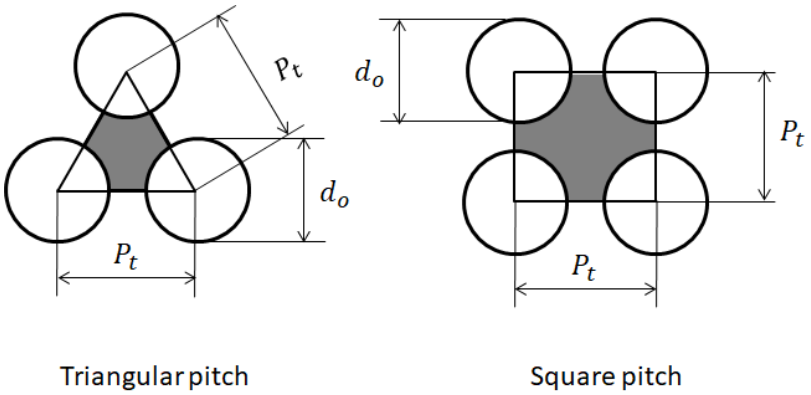

Fig.9.4-1. Two kinds of tube layouts for exchangers and equivalent diameter

Because the fluid flows partly parallel to the tube bank and partly across it, we would use a characteristic mass velocity and an equivalent diameter appropriate for the flow pattern.
The mass velocity G_c for cross flow is the mass flow rate divided by the total flow area S_c for transverse flow between the tubes in the row at or closest to the centerline of the exchanger.

$$G_c = \frac{W_s}{P_b D_s - (D_s/P_t) P_b d_o} \quad \text{for either square or triangular pitch} \qquad (9.4\text{-}1)$$

where P_t is the tube pitch and P_b the baffle pitch.

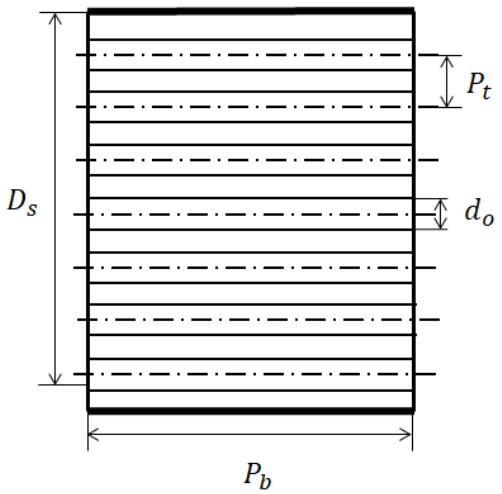

Fig.9.4-2. Shell-side flow passage in tube bundles

We choose the cross-flow mass velocity G_c for the characteristic mass velocity. The equivalent diameter for the shell is taken as the equivalent diameter for the fictitious parallel flow without baffles:

$$D_{eq} = \frac{4\left(\frac{\sqrt{3}}{4} {P_t}^2 - \frac{\pi}{4} {d_o}^2 \frac{1}{2}\right)}{\pi\, d_o \frac{1}{2}} \quad \text{for triangular pitch} \qquad (9.4\text{-}2)$$

$$D_{eq} = \frac{4\left({P_t}^2 - \frac{\pi}{4} {d_o}^2\right)}{\pi\, d_o} \quad \text{for square pitch} \qquad (9.4\text{-}3)$$

If we use G_c and D_e as the mass velocity and equivalent diameter, the Nusselt number is correlated with the Reynolds number in the form

$$\frac{h_o D_{eq}}{\kappa} = 0.36 \left(\frac{D_{eq} G_c}{\mu}\right)^{0.55} \left(\frac{Cp\,\mu}{\kappa}\right)^{1/3} \left(\frac{\mu_m}{\mu_w}\right)^{0.14} \qquad (9.4\text{-}4)$$

$Re = 2{,}000 \sim 1{,}000{,}000.$

9.5 True Temperature Difference for 1-2 Exchangers[1)]

The temperature-length curves for a 1-2 exchanger having the nozzle arrangement indicated are shown in Figure 9.5-1. The curve $T_{hi} \rightarrow T_{ht}$ and $T_{ci} \rightarrow T_{co}$ can be considered as those of a counter-flow exchanger, and the curves $T_{ht} \rightarrow T_{ho}$ and $T_{ci} \rightarrow T_{co}$ correspond to a parallel-flow exchanger.

The LMTD for counter-flow can be formally written as

$$LMTD = (\Delta T)_{lm} = \frac{(T_{hi} - T_{co}) - (T_{ho} - T_{ci})}{\ln \frac{T_{hi} - T_{co}}{T_{ho} - T_{ci}}} \qquad (9.5\text{-}1)$$

This cannot be used without correction to calculate the true mean temperature difference. A correction factor F is so defined that when it is multiplied by the counter-flow LMTD, the product is the correct mean temperature difference. Figure 9.5-2 shows the factor F for 1-2 exchangers as a function of the two dimensionless parameters. This correction factor shown in Fig.9.5-2 can also be used for exchangers with one shell pass and even tube passes.

1. Bowman, R.A., Mueller, A.C. and Nagle, W.M., *Trans. A.S.M.E.*, **62**, 283 (1940)

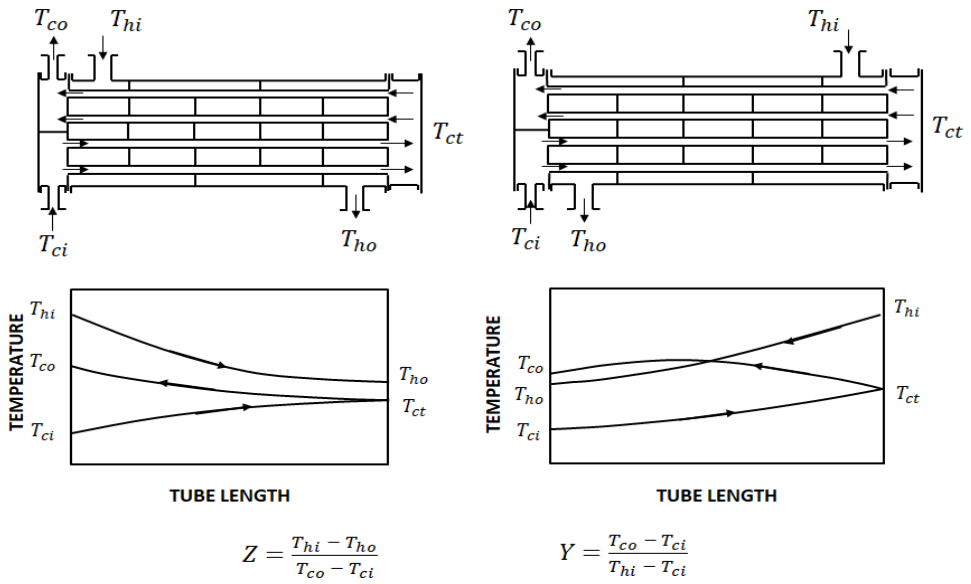

Fig.9.5-1. Temperature—pipe length curve for 1-2 exchanger

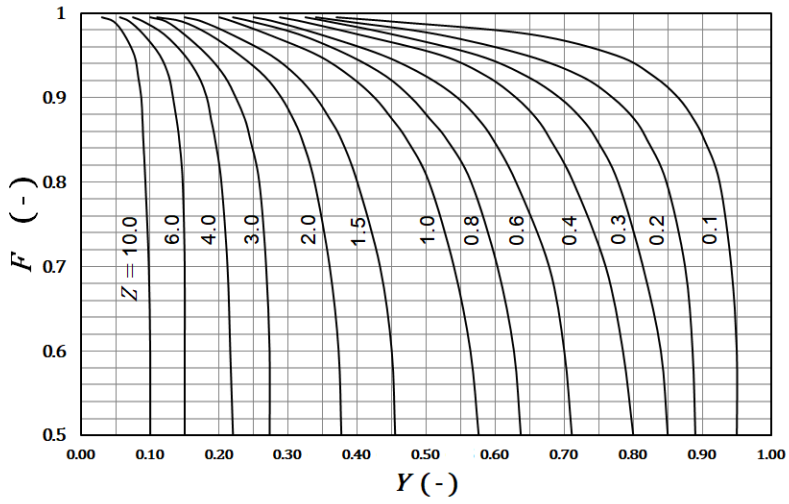

Fig.9.5-2 Correction factor plot for exchangers with one shell pass and two, four, or any multiple passes

Therefore the heat transfer surface area A_o of a shell-and-tube exchanger can be calculated by

$$Q = U_o A_o (\Delta T)_{lm} F \quad (9.5\text{-}2)$$

where the LMTD to be used with this kind of correction factor is for a counter-flow double-pipe heat exchanger with the same fluid inlet and exit temperatures. The correction factors F for various and complex configurations are omitted here. If necessary, you should refer to the handbooks.

9.6 Engineering Design of a Shell-and-Tube Heat Exchanger

Only for simplicity, we will study the fundamental calculation method.

(1) Pressure drop in heat exchanger

(1-A) Tube-side pressure drop

The tube -side pressure drop can be calculated in a manner basically similar to the pressure drop in a single straight pipe. That is, the tube-side pressure drop is the sum of the pressure drop over the straight pipe section and the pressure drop due to the change of flow direction caused in the front and rear heads when entering or leaving the tube-sheets.

The pressure drop over the straight pipe section is given by

$$\Delta p_t = \frac{4 f {G_t}^2 L n}{2 D \rho \phi_t} \quad (9.6\text{-}1)$$

where n is the number of tube passes. Therefore $(1/2){G_t}^2/\rho$ means $(1/2)\rho {v_t}^2$ and $L n$ is the total length of path. The viscosity correction term $\phi = (\mu_m/\mu_w)^{-0.14}$

The pressure drop due to the abrupt change of direction in flowing from one pass into the next pass can be considered as four velocity-heads per pass:

$$\Delta p_r = 4 n \frac{1}{2} \varrho {v_t}^2 \quad (9.6\text{-}2)$$

(1-B) Shell-side pressure drop

It can be considered that the pressure drop is proportional to the number of times and the distance the fluid crosses the tube bundle between baffles. Using a modification of Eq.(7.4-8), an empirical correction available for calculation of the pressure drop through the shell side:

$$\Delta p_s = 4 f_s \frac{{G_c}^2 D_s (N+1)}{(1/2) \rho D_e \phi_s} \quad (9.6\text{-}3)$$

where $(1/2){G_c}^2/\rho$ implies the kinetic energy $(1/2)\rho {v_c}^2$ and $D_s (N+1)$ is a kind of equivalent length the fluid travels. The viscosity correction term is $\phi = (\mu_m/\mu_w)^{-0.14}$. If N is the total number of baffles in the shell, the shell-side fluid crosses (N + 1) times the tube bundle. That is, (N + 1) equals the ratio of tube length L to baffle spacing P_b. The equivalent diameter D_{eq} is the same as for heat transfer. The above equation includes entrance and exit losses.

The friction factor $f_s = 0.43 {Re_s}^{-0.19}$ $\quad 500 < Re_s < 10^5$ (9.6-4)

where $Re_s = \frac{D_{eq} G_c}{\mu}$.

9.6-1 Thermal design procedure of double-tube exchangers

[EXAMPLE 9.6-1] 4,000 kg/h of 98 mol% methanol from an overhead condenser is to be cooled from 62 C (=335 K) to 30 C (=3034 K) by a double-tube exchanger which consists of 50 mm OD, 2 mm thick copper tube and 80 mm ID copper tube. Methanol solution is placed on the tube side and cooling water is supplied into the annulus in counter-current direction. The inlet water temperature is 20 C (=293 K) and the outlet temperature is desired to be 25 C (=298 K). Obtain the necessary total length of double tubes.

[Solution] The physical properties of methanol at mean temperature 46 C (=319 K) are:

$\rho = 780\ kg/m^3,\ Cp = 2.59\ \times\ 10^3\ J/kg\ K,\quad \mu = 0.0004\ kg/m\ s$, and $\kappa = 0.196\ W/m\ K$.

Heat balance: $Q = (4000)(2.59\ \times\ 10^3)(335 - 303) = W\ (4.183\ \times\ 10^3)(298 - 293)$
$= 3.3165\ \times\ 10^9\ J/h = 0.921\ \times\ 10^5\ W$

From this equation, the required water rate is

$W = 1.585\ \times\ 10^4\ kg/h$

Heat transfer coefficient on methanol side:

Mass velocity

$G = \frac{(4000/3600)}{(\pi/4)(0.046)^2} = 668.6\ \ kg/m^2s$

$Re = D\ G/\mu = (0.046)\ (668.6)/0.0004 = 76{,}900$ (turbulent flow)

$Pr = Cp\ \mu/\kappa = (2.59\ \times\ 10^3)\ (0.0004/0.196) = 5.286$

From Eq.(9.2-4)

$h_i = 0.023\ (\kappa/D)\ Re^{0.8}\ Pr^{1/3} = (0.023)(0.196/0.046)(76{,}900)^{0.8}(5.286)^{1/3}$
$= 1{,}380\ \ W/m^2K$

Heat transfer coefficient on water side:

$D_{eq} = D_2 - D_{10} = 0.08 - 0.05 = 0.03\ m$

$G_o = \frac{(1.6585 \times 10^4/3{,}600)}{(\pi/4)((0.08)^2 - (0.05)^2)} = 1{,}440\ \ kg/m^2s$

The physical properties of water at 22.5 C (=295.5 K) are: $\rho = 1{,}000\ kg/m^3$, $Cp = 4.183\ \times\ 10^3\ J/kg\ K,\ \mu = 0.0009\ \ kg/m\ s$, and $\kappa = 0.616\ \ W/m\ K$.

$Re_{eq} = D_{eq}\ G_o/\mu = (0.03)(1440/0.0009) = 48{,}000$

$Pr = Cp\ \mu/\kappa = (4.183\ \times\ 10^3)\ (0.0009/0.616) = 6.11$

From Eq.(876)

$h_o = 0.023\ (\kappa_b/D_{eq})(D_{eq}G_o/\mu)^{0.8}(Cp\ \mu/\kappa)^{0.4}(D_2/D_1)^{0.45}$
$= 0.023\ (0.616/0.03)(48000)^{0.8}(6.11)^{0.4}(80/50)^{0.45} = 6690\ \ W/m^2K$

Neglecting the thermal resistance of copper tube wall and assuming the overall fouling resistance of $1/h_s = 4.4\ \times\ 10^{-4}\ (W/m^2K)^{-1}$, the overall coefficient is

$$U_o = \frac{1}{\frac{1}{1380}\ \frac{0.050}{0.046} + 4.4\ \times\ 10^{-4} + \frac{1}{6690}} = 726.1\ \ W/m^2K$$

Temperature difference:

$LMTD = (\Delta T)_{lm} = \frac{(335-298)-(303-293)}{\ln\frac{335-298}{303-293}} = 20.6\ K$

Then the area required for the heat transfer rate is

$A_o = Q/U_o(\Delta T)_{lm} = (0.921\ \times\ 10^5)/(726.1)(20.6) = 6.16\ m^2$

The necessary total tube length is

$L = A_o/\pi D = 6.16/\pi(0.05) = 39.2\ m$

9.6-2 Thermal design procedure of shell-and-tube exchangers

[EXAMPLE 9.6-2] 30,000 kg/h of liquid mixture of organic compounds is to be heated from 30℃(= 303 K) to 70℃ (= 343 K) by a shell-and-tube exchanger before feeding into a distillation column.

The liquid mixture is placed on the shell side and as the heating medium, 42,000 kg/h of toluene from the reboiler of another column is supplied at 105℃ (= 378 K) into the tube side. Plant practice uses 25 mm OD, 22 mm ID smooth steel pipes 5 m long on 35 mm square pitch and baffles 250 mm apart. A $1\ \times\ 10^5$ Pa pressure drop is permissible on both streams. Assume the overall fouling resistance factor $1/h_{st}$ to be $3.8\ \times\ 10^{-4}$ $(W/m^2K)^{-1}$. Obtain the necessary size of shell-and-tube exchanger for the requirement.

Table 9.6 Physical properties

Organic liquid mixture

T ℃	ρ kg/m^3	μ kg/m s	κ W/m K	Cp J/kg K
30	890	0.0017	0.150	1.85 x 10^3
50	870	0.0012	0.147	1.91 x 10^3
70	855	0.00094	0.145	1.98 x 10^3
90	845	0.00076	0.142	2.04 x 10^3

Toluene

T ℃	ρ kg/m^3	μ kg/m s	κ W/m K	Cp J/kg K
50	850	0.00040	0.128	1.80 x 10^3
70	820	0.00034	0.124	1.88 x 10^3
90	800	0.00028	0.117	1.97 x 10^3
110	770	0.00021	0.114	2.05 x 10^3

[Solution]

Average heat capacities are

Liquid mixture $Cp_o = 1.91 \times 10^3$ J/kg K at $T_{co} = \frac{30+70}{2} = 50\ ℃$

Toluene $Cp_i = 1.97 \times 10^3$ J/kg K at $T_{co} = \frac{105+77.4}{2} = 91.2\ ℃$

（Because the toluene side exit temperature is unknown, the above toluene heat capacity is determined by trial-and-error method applied to the following total heat balance）

(i) Heat Balance:

$$Q = (30{,}000)(1.91 \times 10^3)(70-30) = 2.292 \times 10^9 \frac{J}{h} = 6.367 \times 10^5\ W$$
$$= (42{,}000)\ Cp_i\ (105 - T_{i2})$$

From the equation, the outlet temperature of the tube-side stream is $T_{i2} = 77.4\ ℃$.

(ii) True temperature difference:

$$LMTD = (\Delta T)_{lm} = \frac{(105-70)-(77.4-30)}{\ln\frac{105-70}{77.4-30}} = 40.9\ \text{K}$$

For 1 – 4 exchanger $Z = \frac{105-77.4}{70-30} = 0.69$ $Y = \frac{70-30}{105-30} = 0.533$

From Fig.9.5-2, F = 0.88

Therefore the true temperature difference $\Delta T = (\Delta T)_{lm} F = (40.9)(0.88) = 36.0\ K$

(iii) Trial:

Assume $U_o = 300\ W/m^2K$

Then the total heat-transfer area $A_o = Q/U_o\Delta T = 6.367 \times 10^5/(300)(36.0) = 58.95\ m^2$

Outside surface area per tube $a_o = \pi D_o L = \pi(0.025)(5) = 0.393\ m^2$

Total number of tubes $n_t = A_o/a_o = 58.95/0.393 = 150 < 152$

Each tube pass can accommodate 38 tubes.

Then a new overall heat transfer coefficient is re-assumed.

$$U_o = Q/n_t a_o \Delta T = 6.367 \times 10^5/(152)(0.393)(36.0) = 296.1\ W/m^2K$$

Tube-side

Flow area per tube $a_t = (\pi/4)\ {D_i}^2 = (\pi/4)(0.022)^2 = 3.80 \times 10^{-4}\ m^2$

Flow area per pass: $A_t = (152/4)(3.80 \times 10^{-4}) = 0.0144\ m^2$

Mass velocity $G_{i0} = W_i/A_t = (42{,}000/3600)/(0.0144) = 810.2\ kg/m^2\ s$

Toluene viscosity at $T_{ci} = 91.2\ ℃$: $\mu_i = 0.000276\ kg/m\ s$

Reynolds number on the tube side: $Re_i = (0.022)\ (810.2)/0.000276 = 64{,}600$

$L/D_i = 5/0.022 = 227,$

Then from the turbulent flow curve of Fig.8.2-1, $j_{Hi} = 0.0028$ at $Re_i = 64{,}6000.$

At $T_{ci} = 91.2\ ℃$, $Cp_i = 1.97 \times 10^3$ J/kg K, $\kappa_i = 0.117\ W/m\ K$

Prandtl number $Pr_i = Cp_i\mu_i/\kappa_i = 4.65.$
Then the inside heat-transfer coefficient is

$$h_i/\phi_i = (j_{Hi}/\phi_i)(\kappa_i/D_i)Re_i\ Pr_i^{1/3} = (0.0028)(0.117/0.022)(64{,}600)(4.65)^{1/3}$$
$$= 1{,}606\ W/m^2K$$

Shell side

The inside diameter of shell accommodating 152 heat-transfer tubes of 25 mm OD can be estimated from the tube layout on 35 mm square pitch. Since one square which has area of $(0.035)^2 = 0.00123\ m^2$ can accommodate one tube. From the following equation,

$(\pi/4)\ D_s^{\ 2} = (0.00123)(152) = 0.187\ m^2$

we get $D_s = 0.488\ m$ as the first approximate value.

We need to avoid a collision between the inside wall of the shell and the outer-most tubes. A space for $D_o/2$ is still necessary at both ends of the shell diameter:

$D_s = 0.488 + (0.0125\ \times 2) = 0.513\ m$

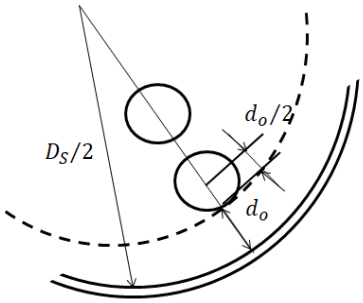

Further about a tube diameter space for tie-rods is necessary between the outer edge of the tube bundle and the inside wall of the shell:

$D_s = 0.513 + (0.025\ \times 2) = 0.563\ m$

Equivalent diameter for square pitch is

$$D_{eq} = \frac{4\ (P_t^{\ 2} - (\pi/4)\ D_o^{\ 2})}{\pi D_o} = \frac{4\ ((0.035)^2 - (\pi/4)\ (0.025)^2)}{\pi(0.025)} = 0.0374\ m$$

Mass velocity for crossflow position

$$G_c = \frac{W_o}{P_b\ D_s - (D_s/P_t)P_bD_o} = \frac{(30{,}000/3{,}600)}{(0.25)(0.563) - (0.563/0.035)(0.25)(0.25)}$$
$$= 207.2\ kg/m^2s$$

At $T_{co} = 50\ ℃,\ Cp_o = 1.91\ \times\ 10^3\ J/kg\ K,\ \mu_o = 0.0012\ kg/m\ s,$
$\kappa_o = 0.147\ W/m\ K,$
Prandtl number: $Pr_o = 15.6.$
Reynolds number: $Re_o = D_{eq}\ G_c/\mu_o = (0.0374)\ (207.2)/0.0012 = 6{,}460$
From Eq.9.4-4, we obtain

$$h_o/\phi_o = 0.36\ (\kappa_o/D_{eq})\ Re_o^{\ 0.55}\ Pr_o^{\ 1/3}$$
$$= (0.36)(0.147/0.0374)(6460)^{0.55}\ (15.6)^{1/3} = 440.6\ W/m^2s\ K$$

Tube-wall temperature

From heat balance neglecting the fouling resistance

$$\frac{h_i}{\phi_i}\ (T_w - T_{ci}) = \frac{1}{\frac{\phi_i}{h_i} + \frac{\phi_o}{h_o}}\ (T_{co} - T_{ci})$$

That is

$$T_w = T_{ci} + \frac{h_o/\phi_o}{(h_i/\phi_i) + (h_o/\phi_o)}\ (T_{co} - T_{ci})$$

= 91.2 + (440.6)(50 – 91.2)/(1606 + 440.6) = 82.3 C (= 355.3 K)
At $T_w = 82.3\ C \quad \mu_{wo} = 0.000829\ kg/m\ s, \quad \mu_{wi} = 0.000303\ kg/m\ s$

$$\phi_o = (\mu/\mu_w)^{0.14} = (0.0012/0.000829)^{0.14} = 1.05$$
$$\phi_i = (\mu/\mu_w)^{0.14} = (0.000276/0.000 - 303)^{0.14} = 0.99$$

Corrected heat –transfer coefficients

$h_o = (h_o/\phi_o)\ \phi_o = (440.6)(1.05) = 462.6\ \text{W/m}^2\text{K}$

$h_i = (h_i/\phi_i)\,\phi_i$ = (1606)(0.99) = 1590 W/m²K
The thermal conductivity of steel tube: $\kappa_t = 45.0\ W/m\ K$
Average tube-diameter (logarithmic mean)

$$D_{av} = \frac{(D_o - D_i)}{\ln \frac{D_o}{D_i}} = \frac{0.025 - 0.022}{\ln \frac{0.025}{0.022}} = 0.0235\ m$$

Overall heat-transfer coefficient

$$U_o = \frac{1}{\frac{1}{h_i}\frac{D_o}{D_i} + \frac{\delta_t}{\kappa_t}\frac{D_o}{D_{av}} + \frac{1}{h_o} + \frac{1}{h_{st}}}$$

$$= \frac{1}{\frac{1}{1590}\frac{0.025}{0.022} + \frac{0.0015}{45.0}\frac{0.025}{0.0236} + \frac{1}{462.6} + 3.8\times 10^{-4}} = 303.8 \text{ W/m}^2\text{K} \quad (\text{vs. } 296 \text{ assumed})$$

(If the calculated coefficient is greatly different from the assumed value, the foregoing calculation should be repeated with new values assumed.)
The overall coefficient calculated above is only 2.6% larger on the safe side than the assumed value. The exact value of the shell diameter D_s should be determined from drawing of tubes laid on 35 mm square pitch taking into account the spaces for pass partition, tie rods, etc.

SHELL SIDE	TUBE SIDE
1 pass	4 tube passes
D_s = 0.563 m	D_o = 0.0-25 m, D_i = 0.022 m, L = 5 m
T_{o1} = 30 C	T_{i1} T_{i1} = 105 C
T_{o2} = 70 C	T_{i2} = 77.4 C
T_{co} = 50 C	T_{ci} = 91.2 C
Re_o = 6,460	Re_i = 64,600
h_o = 462.6 W/m²K	h_i = 1,590 W/m²K

Q = 6.367 x 10⁵ W
ΔT = 36.0 K, T_w = 82.3 C
n_t = 152
U_o = 303.8 W/m²K

(iv) Pressure drop
(a) Shell side:
From Eq.(9.6-4), $f_s = 0.43\ Re_s^{-0.19} = 0.0812$ at $Re_s = 6{,}460$
In Eq.(9.6-3), $N = 20$, $\phi_s = 1.05$, $G_c = 207.2$ kg/m² s, $D_s = 0.563$ m
$\varrho = 870\ kg/m^3$, $D_{eq} = 0.0374\ m$

$$\Delta p_s = 4\,(0.0812)\,\frac{(207.2)^2(0.563)(21)}{2\,(870)(0.0374)(1.05)} = 2{,}400 < 10^5\ Pa6$$

This value is smaller than the permissible limit.
(b) Tube side:
From Fig.7.3-1, $f = 0.0049$ at $Re_i = 64{,}600$
In Eq.(9.6-1), $G_t = 810.2\ kg/m^2 s$, L = 5 m, $n = 4$, $\phi_t = 0.99$, $\varrho = 798\ kg/m^3$, $D_i = 0.022\ m$

$$\Delta p_t = \frac{4\,(0.0049)(810.2)^2(5)(4)}{2\,(0.022)(798)(0.99)} = 7{,}403\ Pa$$

In Eq.(9.6-4), $v_t = G_i/\rho = 810.2/798 = 1.02\ m/s$

$\Delta p_r = 4\,(4)(1/2)(798)(1.02)^2 = 6{,}642\ Pa$
Then the total pressure drop on the tube side is
$\Delta p = \Delta p_t + \Delta p_r = 7{,}403 + 6{,}642 = 1.04 \times 10^4 < 10^5 Pa$
This value is also smaller than the permissible limit.

[PROBLEM 9.6-1]

A triangular pitched 1-2 shell-and-tube exchanger is operated to cool 4,000 kg/h of oil. At the present time, the oil, which is the tube-side fluid, is being cooled from 90 C (=363 K) to 63 C (= 336 K), while water as the shell-side fluid is being heated from 30 C (= 303 K) to 38 C (= 311 K). The exchanger has the effective heat-transfer area of 10 m^2 on the basis of the outside diameter. The oil has average heat capacity $Cp = 2.2 \times 10^3\ J/kg\ K$ and density $\rho = 880\ kg/m^3$. Determine the present value of the overall heat-transfer coefficient.
(Answer: 162.2 W/m^{2}K)

[PROBLEM 9.6-2]

100,000 kg/h of crude oil is to be heated from 70 C (= 343 K) to 100 C (=373 K) by a shell-and-tube exchanger before feeding into the first distillation column of oil refinery. The crude oil is placed on the tube side and as the heating medium, 65,000 kg/h of kerosene is supplied at 200 C (= 473 K) into the shell side. Plant practice uses 25 mm OD, 22 mm ID smooth steel pipes 5 m long on 35 mm triangular pitch and 25%-cut bafflers 250 mm apart. Permissible pressure drops on the tube-side and the shell-side streams are 3×10^5 and $1 \times 10^5\ Pa$, respectively.
Calculate the heat transfer area required and obtain the size of the shell-and-tube exchanger. Determine the appropriate number of the tube passes.
The following values of the fouling resistance factors can be used.
$1/h_{si} = 3.5 \times 10^{-4}\,(W/m^2K)^{-1}$, $1/h_{so} = 1.8 \times 10^{-4}\,(W/m^2K)^{-1}$

Table 9.6-2 Physical properties of kerosene and crude oil

T ℃	ρ kg/m^3	Cp $kJ/kg\,K$	μ $kg/m\,s$	κ $W/m\,K$	T ℃	ρ kg/m^3	Cp $kJ/kg\,K$	μ $kg/m\,s$	κ $W/m\,K$
120	740	2.39	0.00048	0.135	60	820	2.08	0.0032	0.132
140	720	2.47	0.00039	0.133	80	810	2.16	0.0023	0.131
160	710	2.55	0.00031	0.131	100	790	2.24	0.0017	0.130
180	690	2.63	0.00026	0.130	120	780	2.34	0.0013	0.129
200	680	2.71	0.00021	0.128	140	770	2.43	0.00096	0.128
					160			0.00071	

9.7 Convective Heat Transfer around Submerged Objects

9.7-1 A circular cylinder in cross flow[1,2)]

Let us consider a circular cylinder (diameter D) submerged in the free stream with uniform velocity v_∞ and temperature T_∞. The cylinder surface is kept at a temperature T_S.

The Nusselt number and Reynolds number are defined as

$$Nu_D = \frac{h_{loc}D}{\kappa_f} \qquad Re_D = \frac{v_\infty D \rho_\infty}{\mu_f}$$

where the viscosity μ_f and thermal conductivity κ_f should be evaluated at the film temperature.

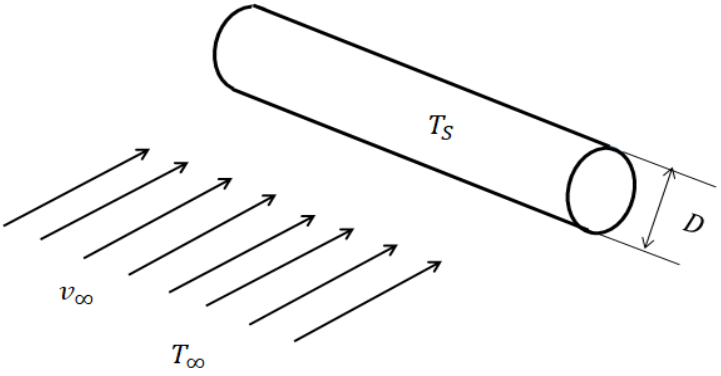

Fig.9.7-1. A circular cylinder in a uniform flow normal to its axis

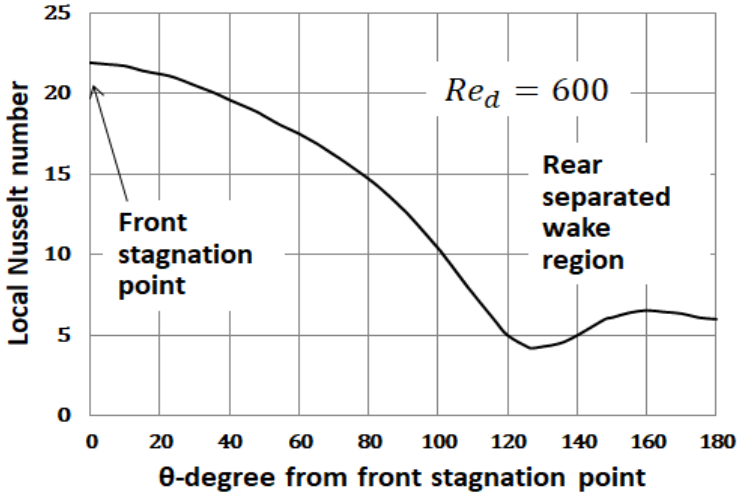

Fig.9.7-2 Local Nusselt numbers around a circular cylinder in a transverse air stream

When the Reynolds number is small enough, the boundary layer developing from the front stagnation point is kept laminar and the flow in the separated region formed on the back side is still laminar.

Fig. 9.7-2 indicates a typical continuously decreasing variation in the Nusselt number at low Reynolds numbers. We can see a slight rise in the separated wake region of the cylinder. When the Reynolds number becomes sufficiently large, the boundary layer undergoes transition from laminar to turbulent flow and the local distribution of heat transfer changes characteristically. The point of separation shifts upstream to a value beyond 90 degree and the heat transfer coefficients become very large in the separated region.

For engineering calculations, the main interest is in the total rate of heat transfer, or in the heat transfer coefficient h_{av} averaged over the circumstance.

The following equations are available as the empirical heat transfer correlations in two Reynolds number ranges:

$$Nu_D = (0.43 + 0.50\, Re_D^{0.5}) Pr^{0.38} \qquad 1 < Re_D < 10^3 \qquad (9.7\text{-}1)$$

$$Nu_D = 0.25\, Re_D^{0.6}\, Pr^{0.38} \qquad 10^3 < Re_D < 2 \times 10^5 \qquad (9.7\text{-}2)$$

Here the ratio of Prandtl number Pr_∞ / Pr_S coming from the temperature difference between the wall and fluid bulk temperatures is assumed to be approximately unity. The Nusselt number is defined as

$$Nu_D = \frac{h_{av} D}{\kappa_f} \qquad (9.7\text{-}3)$$

1. Eckert, E. R. G. and R. M. Drake, Jr.: "Analysis of Heat and Mass Transfer," McGraw-Hill, Chap.9, 406 (1972)
2. Zhukauskas, A. A., V. Makarevicius and A. Shlanciauskas: "Heat Transfer in Banks of Tubes in Crossflow of Fluid," Mintis, Vilnius, Lithuania (12968)

9.7-2 Hot-wire anemometry

Eq. (9.7-1) is very important equation to be utilized for the principle of hot-wire anemometry. Two basic forms; the constant-current type and the constant-temperature type are available. Both utilize the same physical principle but in different ways.

The heat transfer from a fine, long wire (hot wire diameter d, length l, and electric resistance R_w) of tungsten or platinum to a flowing air (velocity v_∞, temperature T_∞) may be described by the follow dimensionless equation:

$$Nu_d = \alpha + \beta\sqrt{Re_d} \tag{9.7-4}$$

This equation is one form of Eq. (9.7-1) applied in the range of very small Reynolds numbers, where the effect of Prandtl number is also assumed to be constant. Only for simplicity, let us study the constant-temperature mode.

The wire attains an equilibrium temperature when the heat I^2R_w generated in it is just balanced by the convective heat loss from its surface.

The wire temperature T_w can be observed in terms of its electric resistance $R_w = R_{w0}(1 + r_0(T_w - T_0))$ which can be measured by the bridge circuit shown in Fig.9.7-2. The constant r_0 is given by the temperature coefficient of the wire resistance.

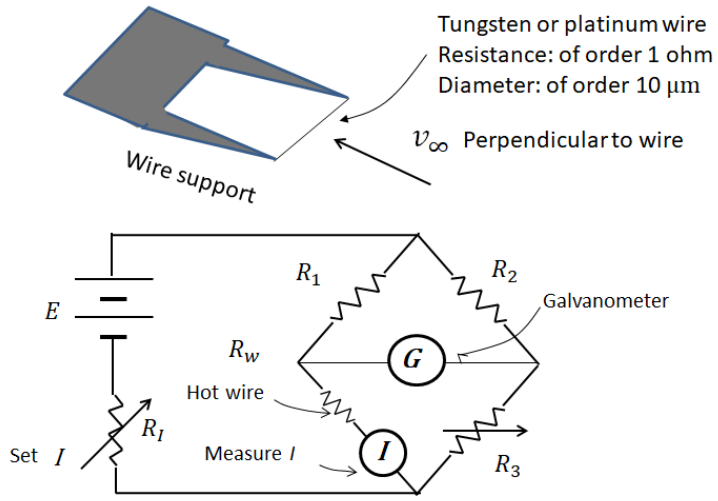

Fig.9.7-3. Hot wire and bridge circuit for hot-wire anemometry

The heat transfer coefficient can be calculated by the following equation:

$$h_{av} = \frac{I^2R_w}{\pi dl(T_w - T_\infty)} \tag{9.7-5}$$

The Reynolds number is given by

$$Re_d = \frac{v_\infty d\rho_\infty}{\mu_\infty} \tag{9.7-6}$$

Because of a very thin hot wire, the Reynolds number is kept very low.

Finally the approach velocity v_∞ can be measured from the electric current I measured by the bridge circuit with a balance-detecting galvanometer by using the following equation:

$$I^2 = \alpha' + \beta'\sqrt{v_\infty} \tag{9.7-7}$$

where the constant α' and β' must be determined by calibration. Once calibrated, the hot-wire

probe can be used to measure an unknown local velocity by adjusting R_I until the bridge balance is achieved.

9.7-3 A circular sphere in cross flow

Let us consider a circular sphere (diameter D) submerged in the free stream with uniform velocity v_∞.

Similarly to the case of circular cylinders, the heat transfer distribution changes depending on the Reynolds number. For engineering purposes, the main interest is in the heat transfer coefficient averaged over the spherical circumference.

The famous heat transfer correlation applicable in a wide range of the Reynolds number is given by Ranz and Marshall[1)]:

$$\frac{h_m D}{\kappa_f} = 2.0 + 0.60 \left(\frac{D\,\rho_f\,v_\infty}{\mu_f}\right)^{1/2} \left(\frac{Cp\,\mu_f}{\kappa_f}\right)^{1/3} \qquad 1 < Re < 7 \times 10^4 \quad 0.6 < \mathrm{Pr} < 400 \qquad (9.7\text{-}8)$$

where the physical properties are evaluated at the film temperature $T_f = (T_\infty + T_S)/2$.

This equation is practically very convenient for estimating the heat transfer coefficients of particles, bubbles and droplets flying in an infinite fluid flow.

1. Ranz, W. E. and W.R. Marshall, Jr.: Chem. Eng. Prog., vol.48, 141, 173 (1962)

Let us consider again the convective heat transfer around a circular cylinder and a circular sphere in a free stream with uniform velocity and temperature. Figure 9.7-4 shows a comparison between those convective heat transfer correlation curves. It is very interesting that both heat transfer correlations are correspondent exactly to each other.

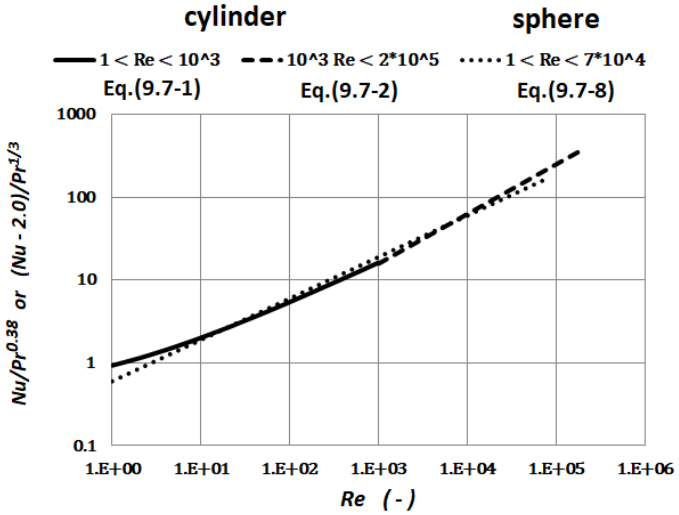

Fig.9.7-4. Comparison of convective heat transfer correlations between two submerged objects.

[PROBLEM 9.7-1] A liquid droplet of toluene is suspended at the hot junction of a very thin wire thermocouple in a superheated toluene vapor (pressure 1 atm, temperature $T_\infty = 125$ ℃) flowing upward at uniform velocity 1 m/s. The droplet can be assumed to be kept as a sphere in shape. The droplet temperature is almost kept at the boiling point $T_S = 110$℃. At the starting time $t = 0$, the droplet diameter $\mathrm{D} = D_0 = 4\ mm$. How long does it take until the droplet disappears?

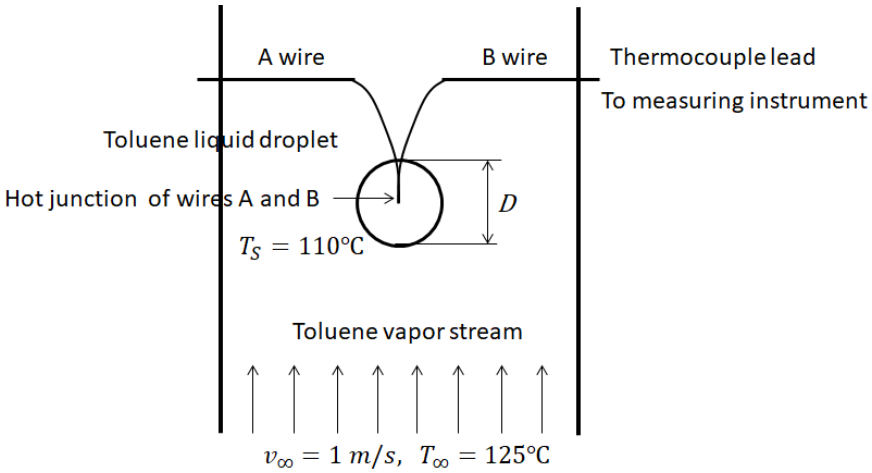

Fig.9.7-P1. A single droplet suspended in a superheated vapor stream

Nomenclature

A	heat transfer area, [m^2]
Cp	heat capacity, [J/kg K]
D	tube inside diameter, [m], cylinder diameter, [m] or sphere diameter, [m]
D_{eq}	equivalent diameter, [m]
D_s	inside diameter of shell, [m]
d	hot-wire diameter, [m]
d_o	outside diameter of heat transfer tube, [m]
F	correction factor for temperature difference, [-]
f	friction factor, [-]
G	mass velocity, [kg/m^{2}s]
G_c	mass velocity in cross flow section, [kg/m^{2}s]
h	heat transfer coefficient, [W/m^{2}K]
I	electric current of hot wire, [A]
j_H	j-factor for heat transfer, [-]
L	tube length, [m]
N	total number of baffles, [-]
Nu	Nusselt number, [-]
n	number of tube passes, [-]
n_t	total number of heat transfer tubes, [-]
Pr	Prandtl number, [-]
P_b	baffle pitch of tube layout, [m]
P_t	pitch of tube layout, [m]
Q	heat transfer rate, [W]
Re	Reynolds number, [-]
T	temperature, [K]
T_s	surface temperature, [K]
U	overall heat transfer coefficient, [W/m^{2}K]
μ	viscosity, [kg/m s]
ϕ	correction factor for viscosity, [-]

Subscripts

c	cold
D	cylinder
f	film
h	hot
i	inner tube, inside surface or inlet
m	bulk or mixed mean
o	outer tube, outside surface or outlet
s	shell side
t	tube side
w	wall
∞	free stream

CHAPTER 10

INTERPHASE MASS TRANSPORT

10.1 Definition of Mass Transfer Coefficient

Mass transfer mechanism also falls into one of the two large categories: molecular and convective transports. The Fick's law describes the ordinary diffusion as

$$N_A - x_A(N_A + N_B) = -c\,D_{AB}\frac{\partial x_A}{\partial y} \qquad (10.1\text{-}1)$$

where x_A is mole fraction of component A and c the total molar density. The second term of the left side represents the contribution of the bulk motion.

Applying the Fick's law to the interface

$$N_{Aw} - x_{Aw}(N_{Aw} + N_{Bw}) = -c\,D_{AB}\left.\frac{\partial x_A}{\partial y}\right|_{y=0} \qquad (10.1\text{-}2)$$

The mass transfer analog of the defining equation of heat transfer coefficient becomes

$$N_{Aw} - x_{Aw}(N_{Aw} + N_{Bw}) = k_x^*(x_{Am} - x_{Aw}) \qquad (10.1\text{-}3)$$

Note that the mass transfer coefficient can be considered to be a function of the mass transfer rate.

Let us consider as an example the mass transfer of component A from a pipe wall to a flowing fluid. Dissolution of benzoic acid (solid) from a pipe wall of cast benzoic acid to a turbulent flow of water is a good example. Fig.10.1-1 shows its concentration profile near the wall.

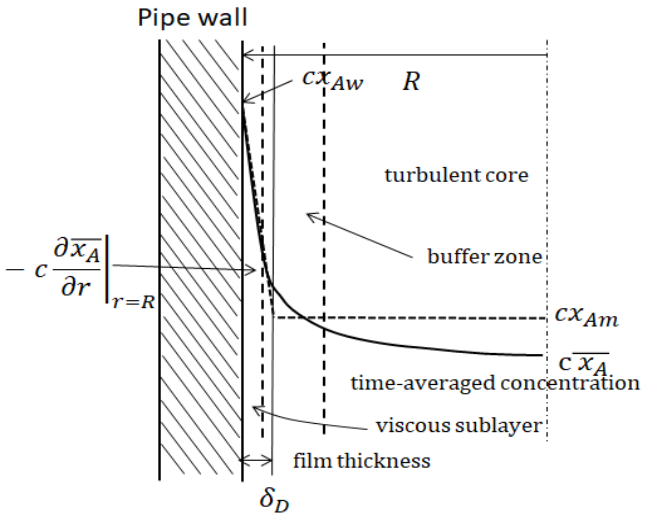

Fig.10.1-1. Time-averaged concentration profile near the wall of benzoic acid cast pipe

Then the mass flux at the pipe wall can be written by Fick's law:

$$N_A|_{r=R} - x_A(N_A + N_B)|_{r=R} = -c\,D_{AB}\left.\frac{\partial x_A}{\partial r}\right|_{r=R} \qquad (10.1\text{-}4)$$

The main resistance to mass transfer takes place in very thin fluid film near the pipe wall, where most of the total concentration drop occurs. Therefore the following approximation can be made defining δ_D the thickness of a fictitious diffusion film:

$$-\left.\frac{\partial x_A}{\partial r}\right|_{r=R} = \frac{x_{Aw} - x_{Am}}{\delta_D} \qquad (10.1\text{-}5)$$

Here x_{Am} is the mixed mean concentration (bulk concentration) of component A, x_{Aw} the wall concentration (solubility of benzoic acid in this case).
The definition of the mixed mean concentration in a circular pipe flow is

$$x_{Aw} - x_{Am} = \frac{\int_0^R 2\pi r\, v_z\, (x_{Aw} - x_A) dr}{\int_0^R 2\pi r\, v_z\, dr} \quad (10.1\text{-}6)$$

The above equation, Eq.(10.1-4) becomes the defining equation of convective mass transfer coefficient:

$$[N_A - x_A(N_A + N_B)]_{r=R} = (c\, D_{AB}/\delta_D)(x_{Aw} - x_{Am}) = k_x^*(x_{Aw} - x_{Am}) \quad (10.1\text{-}7)$$

In this case, k_x^* has unit of kmol/m^{2}s.
The mass transfer analog of the Nusselt number is defined by

$$Sh = \frac{k_x^* D}{c\, D_{AB}} \quad (10.1\text{-}8)$$

This dimensionless group is called the Sherwood number. As in the derivation of heat transfer correlation, the mass transfer correlation for low mass transfer rate can be found to be of the form:

$$Sh = Sh(Re, Sc, L/D) \quad (10.1\text{-}9)$$

Actually, most of the available mass transfer data have been correlated using the following definition:

$$N_{Aw} = k_x(x_{Am} - x_{Aw}) \quad (10.1\text{-}10)$$

For the case of mass transfer in a gas phase, the partial pressure difference can be used as the driving force

$$N_{Aw} = k_G(p_{Am} - p_{Aw}) \quad (10.1\text{-}11)$$

The k_G has units of kmol/m^{2}s atm.

If the molar concentration difference is used as the driving force for liquids

$$N_{Aw} = k_L(C_{Am} - C_{Aw}) \quad (10.1\text{-}12)$$

The k_L has units of m/s.

It should be kept in mind that as distinct from k_x^*, these coefficients include the contribution of the bulk fluid motion.

For the case in which one component is transferred and the other is stagnant i.e. $N_B = 0$,

$$N_{Aw} = \frac{k_x^*}{(1 - x_{Aw})}(x_{Am} - x_{Aw}) = \frac{k_x^*}{x_{Bw}}(x_{Am} - x_{Aw}) = k_x(x_{Am} - x_{Aw}) \quad (10.1\text{-}13)$$

For gases

$$N_{Aw} = \frac{k_x^*}{x_{Bw}}(x_{Am} - x_{Aw}) = k_G(p_{Am} - p_{Aw}) \quad (10.1\text{-}14)$$

Here $x_{Bw} = p_{Bw}/P$ (P : total pressure).

$$k_x^* = k_x x_{Bw},\ k_x^* = k_G p_{Bw},\ k_x^* = k_L C_{Bw} \quad (10.1\text{-}15)$$

Gas absorption belongs to this case.
For liquids

$$N_{Aw} = \frac{k_x^*}{x_{Bw}}(x_{Am} - x_{Aw}) = k_L(C_{Am} - C_{Aw}) \quad (10.1\text{-}16)$$

Here $x_{Bw} = C_{Bw}/c$ (c : total molar density).
For the case of equimolar counter-diffusion i.e. $N_A = -N_B$

$$k_x^* = k_x,\ k_x^* = k_G P,\ k_x^* = k_L c \quad (10.1\text{-}17)$$

Distillation belongs to this case.

10.2 Analogy between Heat and Mass Transfer

By dimensional analysis, we can also obtain the same functional similarity for Nu and Sh:

$$Nu = Nu(Re, Pr)$$
$$Sh = Sh(Re, Sc)$$

A new dimensionless group for mass transfer is defined as

$$j_D = \frac{k_x}{G_M}\left(\frac{\mu}{\rho D_{AB}}\right)_f^{2/3} = Sh\, Re^{-1}\, Sc^{-1/3} \qquad (10.2\text{-}1)$$

The subscript f refers to properties evaluated at the film temperature $T_f = (T_m + T_w)/2$ and the film composition $x_{Af} = (x_{Am} + x_{Aw})/2$.

The Chilton-Colburn analogy[1)] is one of the important empirical analogies:

$$j_D = j_H \quad \text{or} \quad \frac{k_x}{G_M}\left(\frac{\mu}{\rho D_{AB}}\right)_f^{2/3} = \frac{h}{Cp\, G}\left(\frac{Cp\,\mu}{\kappa}\right)_f^{2/3} \qquad (10.2\text{-}2)$$

This analogy permits one to calculate mass-transfer coefficients from heat-transfer data for the equivalent boundary conditions. The analogy between j_D and j_H is also applicable to simultaneous heat and mass transfer.

1. Chilton, T. H. and A. P. Colburn, Ind. Eng. Chem., **26**, 1183 (1934)

10.3 Theory of Interphase Mass Transfer

Most of mass transfer processes in chemical engineering involve mass transfer across the interface between two phases, as in gas absorption and distillation. Interphase transfer occurs owing to the concentration gradients resulting from a deviation from equilibrium.

10.3-1 Fundamentals --- Gas-liquid equilibrium relationship for absorption

In gas absorption, we usually neglect the solubility of the inert gas (e.g., air) and the presence of vapor from the liquid (e.g., water) in the gas. Therefore there are four variables: pressure, temperature, and the concentrations of solute component A in liquid and gas. For simplicity, the temperature and pressure are usually fixed: one concentration may be chosen as the remaining independent variable. The equilibria of interest are those between a nonvolatile absorbing liquid and a solute gas. The equilibrium relationship in absorption can be expressed as the diagram of the concentration of solute x_e in the liquid against the concentration of solute y_e in the gas. One of the important fundamental expression is the Henry's law:

$$y_A = H\, x_A \qquad (10.3\text{-}1)$$

or

$$p_A = H'\, C_A \qquad (10.3\text{-}2)$$

where x_A the mole fraction of solute A, and H the Henry's constant.

In the second equation, p_A is the partial pressure of the gas phase, and C_A the molar concentration of solute A, and the modified Henry's constant.

Fig.10.3-1 is a schematic diagram of the solubility of gases into a solvent such as water.

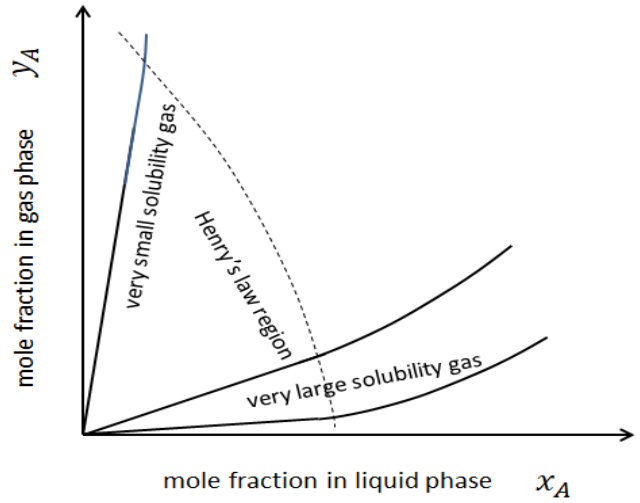

Fig.10.3-1 Schematic picture of gas solubility

10.3-2 Interphase mass transfer for gas absorption

Consider a transferring component A in an inert gas B which is in contact with a nonvolatile liquid C.

A simple example is the removal of sulfur dioxide from stack gases by water using a wetted wall column.

Water is flowing downward by gravity in the form of liquid film falling along the inside surface of a circular cylinder whereas the stack gas is flowing upward in the form of counter-current inside the cylinder.

In general, there exist three resistances in series to the interphase transfer of component A: the gas phase film, the interface, and the liquid phase film. The concentration gradients in the two phases are shown in Fig.10.3-2.

Note that components B and C do not diffuse in spite of the concentration gradients.

Two-film theory, initially suggested by Whitman, is appropriate at this stage to explain this process.

First, three assumptions are made: (1) that there is no resistance to transport of component A across the actual interface, (this is equivalent to assuming that the two phases are approximately in equilibrium just at the actual interface), (2) that the holdup of component A in the boundary layers on both sides of the interface is negligibly small compared to the amount transferred, and (3) that the bulk of each phase is well mixed. For the case of packed columns for gas absorption, the gas flows up and liquid trickles down.

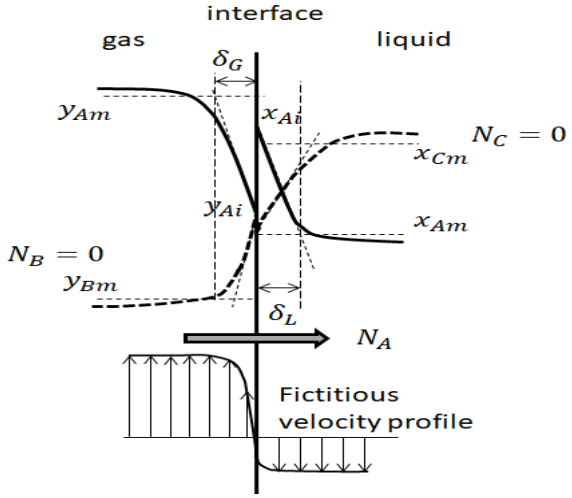

Fig.10.3-2. Concentration profile in the neighborhood of gas-liquid contacting interface

The velocity distribution near the interface is also shown in Fig.10.3-2. Since there is no slip at the interface, gas film is in enough contact with the liquid film to establish the phase equilibrium at the interface.

Using mass transfer coefficients defined by the two-film theory, the steady-state mass flux is expressible as

$$N_A = k_{yA}(y_{Am} - y_{Ai}) = k_{xA}(x_{Ai} - x_{Am}) \quad (10.3\text{-}3)$$

Here y_{Am} and x_{Am} are the mixed mean concentrations (the bulk concentrations) and k_{yA} and k_{xA} are the convective mass transfer coefficients having units of kmol of A/m^2 s in the gas and liquid phases, respectively.

According to the assumption made, the gas and liquid concentrations at the interface lie on the equilibrium curve given by

$$y_{Ai} = f(x_{Ai}) \quad (10.3\text{-}4)$$

where f is the equilibrium function. These equilibrium concentrations would be obtained if the two

phases had been in contact for an infinite period of time. Henry's law is an example of the equilibrium function for dilute solution:

$$y_{Ai} = m\, x_{Ai} \tag{10.3-5}$$

in which *m* is the Henry's constant. For simplicity, the Henry's law is assumed for the remaining development.

It is convenient to define an overall mass transfer coefficient K_{yA} and K_{xA} based on an overall driving force between the bulk concentration y_{Am} or x_{Am} because the interface concentrations are very difficult to measure. This treatment is similar to that in defining the overall heat transfer coefficient. However the bulk concentration y_{Am} and x_{Am} do not have the same units; y_{Am} has units of kmol of A/kmol of A+B whereas x_{Am} has units of kmol of A/kmol of A+C.

The above equation Eq.(10.3-3) can be rewritten as

$$N_A = \frac{y_{Am} - y_{Ai}}{\frac{1}{k_{yA}}} = \frac{x_{Ai} - x_{Am}}{\frac{1}{k_{xA}}} \tag{10.3-6}$$

Multiplying the numerator and denominator of the right-most term by *m*,
a new fraction having the same value is obtained by the law of additivity as

$$N_A = \frac{y_{Am} - y_{Ai}}{\frac{1}{k_{yA}}} = \frac{m(x_{Ai} - x_{Am})}{\frac{m}{k_{xA}}} = \frac{y_{Am} - y^*_{Am}}{\frac{1}{k_{yA}} + \frac{m}{k_{xA}}} = K_{yA}(y_{Am} - y^*_{Am}) \tag{10.3-7}$$

Here $y^*_{Am} = m\, x_{Am}$ is the bulk concentration of the liquid phase expressed with the units of the gas-phase concentration by using the Henry's law. The overall mass transfer coefficient K_{yA} is given by

$$K_{yA} = \frac{1}{\frac{1}{k_{yA}} + \frac{m}{k_{xA}}} \tag{10.3-8}$$

Similarly the following formulae are available.

$$N_A = \frac{(y_{Am}/m) - (y_{Ai}/m)}{\frac{1}{mk_{yA}}} = \frac{x_{Ai} - x_{Am}}{\frac{1}{k_{xA}}} = \frac{x^*_{Am} - x_{Am}}{\frac{1}{mk_{yA}} + \frac{1}{k_{xA}}} = K_{xA}(x^*_{Am} - x_{Am}) \tag{10.3-9}$$

$$K_{xA} = \frac{1}{\frac{1}{mk_{yA}} + \frac{1}{k_{xA}}} \tag{10.3-10}$$

Notice that K_{yA} and K_{xA} represent the basic information in different units of concentration.

10.3-3 Mass transfer model for gas absorption

Gas absorption is the typical mass transfer operation in which one or more soluble gases are absorbed from their mixture with an inert gas into a liquid. The absorption process may be purely physical or involve chemical reactions in the liquid. A typical example is the washing sulfur dioxide from the boiler-exhaust gas by means of water or alkaline solution.

The gas absorption equipment is designed to provide intimate contact of a gas and a liquid. A typical continuous gas-absorber is the packed column which consists of a vertical column filled with a randomly arranged packing of small inert solid or equipped with structured packing. The packing provides a large interfacial area of contact between the two phases. Figure 10.3-3 shows some example of random packings and structured packing.

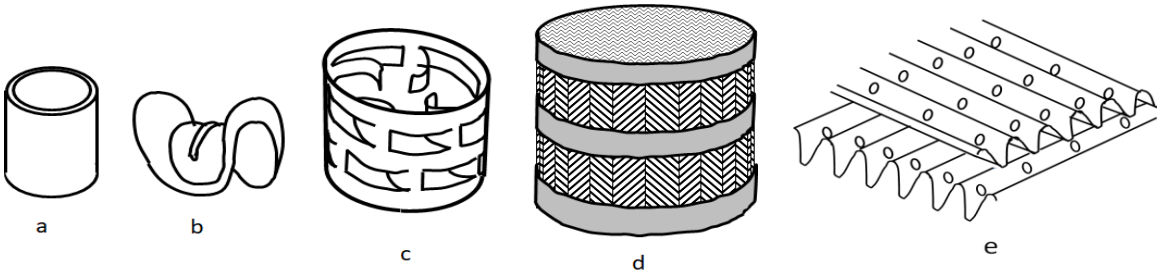

Fig.10.3-3. Random packings and structured packing (a: Raschig ring, b: Berl saddle, c: Pall ring, and d: corrugated structured packing, e: partial structure of structured packing)

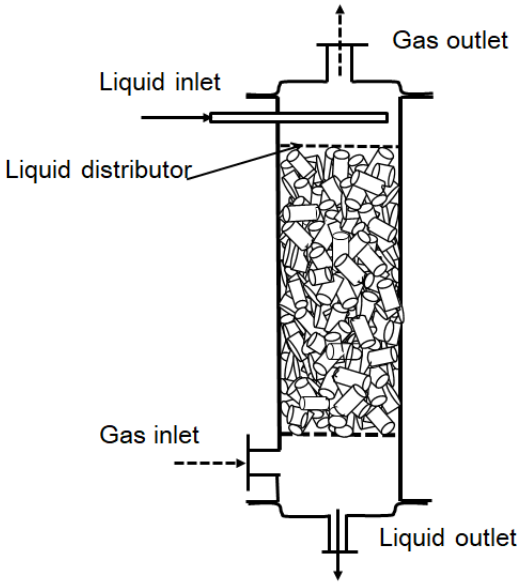

Fig.10.3-4. Packed column absorber equipped with Raschig rings

For simplicity, we will deal with the physical absorption of one soluble component A from a mixture with an inert gas B by non-volatile liquid solvent C.

Fig.10.3-4 shows a conventional packed column equipped with Raschig rings. The liquid is sprayed evenly over the top of the packed bed by the distributor and trickles down over the packing surfaces by gravity. The solute-containing gas is fed into the column from below the packing and flows upward through the interstices due to the pressure drop through the bed of the packing. This countercurrent direct contacting permits the transfer of component A from the gas to the liquid. The liquid is enriched in component A as it flows down the packing, and the concentrated liquid leaves the column through the liquid outlet. The bulk concentration of component A in the gas stream decreases as the gas flows up, and the lean gas leaves the column through the gas outlet.

Let us develop an expression for the column height Z_T required to get the desired degree of recovery of component A. The column height is calculated from a viewpoint of mass-transfer area. Assume that the mass transfer takes place isothermally. In usual absorption operations the liquid and gas flow rates L_M and G_M vary appreciably with the elevation from the bottom of the packed section. It is convenient to use units of flow rate and concentration on a solute-free basis because the molar flow rates of the inert gas B and nonvolatile liquid C are constant over the total height of the packed column. The gas stream enters the column at molar velocity of G'_M on an A-free basis. The mole fraction of A in the entering gas stream is y_{A1}. In usual situation for the design of an absorber, the designer is required to determine the molar liquid velocity L'_M, the concentration x_{A2} of which is usually known. The outlet gas concentration y_{A2} is also given in terms of the specified degree of recovery of component A.

The overall material balance of component A may be written as

$$G'_M \frac{y_{A1}}{1-y_{A1}} + L'_M \frac{x_{A2}}{1-x_{A2}} = G'_M \frac{y_{A2}}{1-y_{A2}} + L'_M \frac{x_{A1}}{1-x_{A1}} \qquad (10.3\text{-}11)$$

Note that each term has units of

$$\frac{\text{kmol of B}}{(\text{m}^2 \text{ of the bed})(\text{s})} \frac{\text{kmol of A}}{\text{kmol of B}} = \frac{\text{kmol of A}}{(\text{m}^2 \text{ of the bed})(\text{s})}$$

These molar velocities G'_M and L'_M are the so-called superficial molar velocities the gas and liquid would have in the column on an A-free basis if no packing were present.

At the present stage, L'_M and x_{A1} are unknown. The above equation indicates that the outlet liquid concentration x_{A1} increases as the liquid flow rate is decreased. Choosing the portion of the column above an arbitrary section as a control volume, as shown by the dotted line in Fig.10.3-5, we get a material balance on component A:

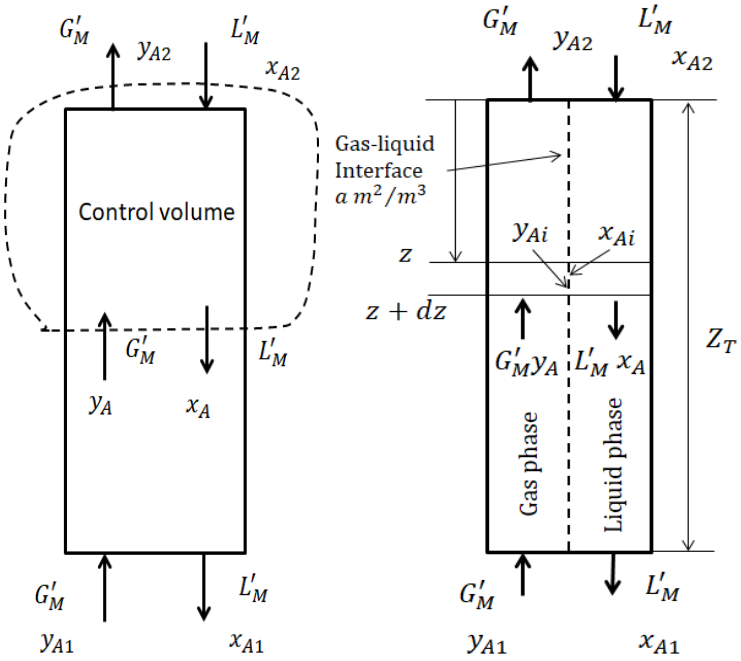

Fig.10.3-5. Control volume for mass balance and differential control volume of interphase mass transfer model for a packed column absorber

$$G'_M\left(\frac{y_A}{1-y_A}-\frac{y_{A2}}{1-y_{A2}}\right)=L'_M\left(\frac{x_A}{1-x_A}-\frac{x_{A2}}{1-x_{A2}}\right) \qquad (10.3\text{-}12)$$

This is the equation for the operating line which gives the relation between the bulk concentrations of the gas and liquid at an arbitrary position. The liquid flow rate L'_M can be determined from the viewpoint of the limiting liquid-gas ratio.

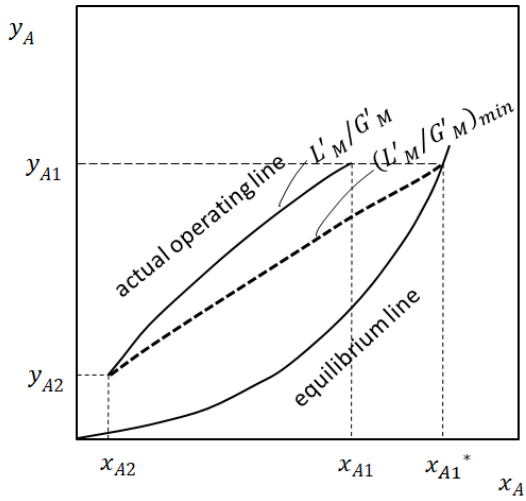

Fig.10.3-6. Concept of limiting liquid-gas ratio.

Figure 10.3-6 shows a graphical relation of the operating line with the equilibrium line for gas absorption. For a given gas flow rate G'_M, a reduction in liquid flow rate L'_M decreases the slope of the operating line. As the liquid flow rate is decreased fixing the terminal concentrations y_{A2}, x_{A2}, and y_{A1}, the upper end of the operating line approaches the equilibrium line. Just when the operating line touches the equilibrium line, the minimum possible liquid flow rate $(L'_M)_{min}$ is obtained.

At this condition, an infinitely long packed section is required owing to very small driving forces in the vicinity of the bottom of the column.

In an actual column, the liquid rate must be greater than the minimum. Replacing y_A and x_A of Eq.(10.3-12) by y_{A1} and x^*_{A1}, we obtain the limiting liquid-gas ratio:

$$\left(\frac{L'_M}{G'_M}\right)_{min} = \frac{y_{A1}/(1-y_{A1}) - y_{A2}/(1-y_{A2})}{x^*_{A1}/(1-x^*_{A1}) - x_{A2}/(1-x_{A2})} \quad (10.3\text{-}13)$$

Here $x^*_{A1} = y_{A1}/m'$ is the liquid-phase concentration that would be in equilibrium with the inlet gas-phase concentration. From the economical viewpoint, the optimum liquid rate is usually found by making the operating line parallel to the equilibrium line:

$$\frac{(L'_M/G'_M)}{m'} = 1 \quad (10.3\text{-}14)$$

The actual liquid rate is usually 25 to 100% greater than the minimum. Once the actual liquid rate is decided in this way, we can calculate the concentration x_{A1} in the exit liquid stream.

The equipment size required for the desired separation cannot be determined without considering the relation between mass transfer rate and mass transfer area. The behavior of an actual packed column is too complicated to be modeled in a straight-forward way. We simplify the actual column to a system consisting of the two streams flowing side-by-side without back mixing and in contact with one another.

The interfacial area "a" per unit packed-bed volume and the mass transfer coefficients k_y, k_x, K_y, K_x are assumed to be constant over the packed section.

First we set up the mass balance within a differential height dZ at an arbitrarily chosen distance Z from the top of the packed bed:

$$N_A\, a\, dZ\, S = G'_M S \left(\frac{y_A}{1-y_A}\Big|_{Z+dZ} - \frac{y_A}{1-y_A}\Big|_{Z}\right) = L'_M S \left(\frac{x_A}{1-x_A}\Big|_{Z+dZ} - \frac{x_A}{1-x_A}\Big|_{Z}\right) \quad (10.3\text{-}15)$$

That is

$$N_A\, a\, dZ = G'_M\, d\left(\frac{y_A}{1-y_A}\right) = L'_M\, d\left(\frac{x_A}{1-x_A}\right) \quad (10.3\text{-}16)$$

or

$$N_A\, a\, dZ = G'_M \frac{dy_A}{(1-y_A)^2} = L'_M \frac{dx_A}{(1-x_A)^2} \quad (10.3\text{-}17)$$

The cross-sectional area S of the packed section is usually determined by ban empirical relation between the pressure drop per unit height of the packing and the gas velocity from a viewpoint of the stable flow regime for intimate gas-liquid contact.

The interphase mass transfer is also expressed as

$$N_A\, a\, dZ = k_y a(y_A - y_{Ai}) dZ = k_x a(x_{Ai} - x_A) dZ \quad (10.3\text{-}18)$$

$$N_A\, a\, dZ = K_y a(y_A - y^*_A) dZ = K_x a(x^*_A - x_A) dZ \quad (10.3\text{-}19)$$

From one of these equations

$$G^*_M \frac{dy_A}{(1-y_A)^2} = K_y a(y_A - y^*_A) dZ \quad (10.3\text{-}20)$$

The coefficients $k_y a, k_x a, K_y a, K_x a$ are called "volumetric mass transfer coefficients."

Integrating the equation gives the column height of packing section required for the desired separation:

$$Z_T = \frac{\overline{G^*_M}}{K_y a} \int_{y_{A2}}^{y_{A1}} \frac{dy_A}{(1-y_A)^2 (y_A - y^*_A)} \quad (10.3\text{-}21)$$

Similar equations can also be obtained from the remaining three equations as follows.

$$\begin{aligned} Z_T &= \frac{\overline{G^*_M}}{k_y a} \int_{y_{A2}}^{y_{A1}} \frac{dy_A}{(1-y_A)^2 (y_A - y_{Ai})} \\ &= \frac{\overline{L^*_M}}{K_x a} \int_{x_{A2}}^{x_{A1}} \frac{dx_A}{(1-x_A)^2 (x^*_A - x_A)} \\ &= \frac{\overline{L^*_M}}{k_x a} \int_{x_{A2}}^{x_{A1}} \frac{dx_A}{(1-x_A)^2 (x_{Ai} - x_A)} \end{aligned} \quad (10.3\text{-}22)$$

The quantities $\overline{G'_M/K_y a}, \overline{G'_M/k_y a}, \overline{L'_M/K_x a}, \overline{L'_M/k_x a}$ are roughly approximated parameters called "Height of a Transfer Unit," averaged between the top and bottom of the packing section. These mass transfer capacity coefficients $K_y a,\ K_x a,\ k_y a,\ k_x a$ depend on the mass velocity of the gas

$G_M = G'_M/(1-y_A)$ and decrease from bottom to top. From this viewpoint the precision may be better if the following expressions are used:

$$Z_T = \frac{\overline{G_M}}{K_y a} \int_{y_{A2}}^{y_{A1}} \frac{dy_A}{(1-y_A)(y_A - y_A^*)} \quad (10.3\text{-}23)$$

[PROBLEM 10.3-1]

30 kmol/h of air contaminated by chlorine gas (mole fraction of Cl_2: $y_A = 0.06$) is contacted with water in a packed column to get the exit concentration $y_A = 0.005$. The column operates at 1 atm and 20°C(=293 K).

Determine the minimum liquid flow rate assuming physical absorption. The solubility of Cl_2 into water (at 1 atm and 20°C) is approximately expressed as $p = 1.92 \times 10^9 x^{2.16}$

where x = mole fraction of Cl_2 in water and p = partial pressure (mmHg) of Cl2 in air.

10.3-4 Mass transfer coefficients in a packed column absorber

Usually the mass transfer data for packed-tower absorption are correlated in the form

$$H_{OG} = \frac{\overline{G_M}}{K_y a} \quad , \quad H_G = \frac{\overline{G_M}}{k_y a} \quad , \quad H_{OL} = \frac{\overline{L_M}}{K_x a} \quad , \quad H_L = \frac{\overline{L_M}}{k_x a} \quad (10.3\text{-}24)$$

These parameters are called the height of a transfer unit (HTU). The concept is based on the idea of dividing the packed section into a number of contact units called transfer units.

The following integrals are designated as the number of transfer units (NTU):

$$N_{OG} = \int_{y_{A2}}^{y_{A1}} \frac{dy_A}{(1-y_A)(y_A - y_A^*)} \quad (10.3\text{-}25)$$

$$N_G = \int_{y_{A2}}^{y_{A1}} \frac{dy_A}{(1-y_A)(y_A - y_{Ai})}$$

$$N_{OL} = \int_{x_{A2}}^{x_{A1}} \frac{dx_A}{(1-x_A)(x_A^* - x_A)}$$

$$N_L = \int_{x_{A2}}^{x_{A1}} \frac{dx_A}{(1-x_A)(x_{Ai} - x_A)}$$

Therefore the tower height may be calculated as the product of the number of transfer units and the height of a transfer unit (HTU):

$$Z_T = H_{OG} N_{OG} = H_G N_G = H_{OL} N_{OL} = H_L N_L \quad (10.3\text{-}26)$$

Using the two-film theory, the overall heights of transfer unit can be related to the single-phase transfer units as

$$H_{OG} = H_G + \frac{m G_M}{L_M} H_L \quad \text{and} \quad H_{OL} = H_L + \frac{L_M}{m G_M} H_G \quad (10.3\text{-}27)$$

These equations indicate that the overall resistance of interphase mass transfer consists of the gas-phase and liquid-phase resistances in series.

10.4 Mass Transfer Correlations for Packed Columns

As in Eq.(10.3-25), the overall resistance to the interphase mass transfer comprises the gas-phase film resistance H_G and the liquid-phase film resistance $(mG_M/L_M)H_L$.

10.4-1 Height of a liquid-phase transfer unit

Sherwood and Holloway[1] measured the desorption of oxygen, hydrogen, and carbon dioxide from water in the range of gas flow rate up to the loading point and obtained the following correlation:

$$H_L = \frac{1}{\alpha} \left(\frac{L}{\mu_L}\right)^n \left(\frac{\mu_L}{\rho_L D_L}\right)^{0.5} \quad (10.4\text{-}1)$$

Temperature $278 < T < 313K$ and liquid flow rate $0.556 < L < 20.8\ kg/m^2 s$, where μ_L is liquid viscosity (kg/m s), D_L diffusivity for liquid (m^2/s) and ρ_L liquid density (kg/m^3).

1. Sherwood, T.K. and Holloway, F.A.L.: Trans. Am. Inst. Chem. Engrs., vol.36, 39 (1940)

Table 10.4-1 HTU_L correlation parameters

Packing	size in.(I= 25.4 mm)	α	n
Raschig rings	3/8	3,100	0.46
	1/2	1,400	0.35
	1	430	0.22
	1 1/2	380	0.22
	2	340	0.22
Berl saddles	1/2	600	0.28
	1	780	0.28
	1 1/2	730	0.28

Note that the transfer unit H_L up to the loading point is independent of the gas flow rate.

Onda *et al*.[1] obtained a dimensionless correlation:

$$k_L \left(\frac{\rho_L}{\mu_L g}\right)^{1/3} = 0.0051 \left(\frac{L}{a_w \mu_L}\right)^{2/3} \left(\frac{\mu_L}{\rho_L D_L}\right)^{-0.5} (a_t D_p)^{0.4} \qquad (10.4\text{-}2)$$

where the wetted surface area a_w is given taking into account the liquid surface tension by

$$a_w/a_t = 1 - \exp\{-1.45\,(\sigma_c/\sigma)^{0.75}\,(L/a_t\mu_L)^{0.1}\,(L^2 a_t/{\rho_L}^2 g)^{-0.05}(L^2/\rho_L \sigma a_t)^{0.2}\} \qquad (10.4\text{-}3)$$

1. Onda, K., Takeuchi, H., and Okumoto, Y., J. Chem. Eng. Japan, **1**(1), 56 (1968)

The total surface area a_t, the size D_p of the packing are obtainable in relation with the void fraction ε on the dry basis in Table 10.4-2.

Table 10.4-2 Geometrical data of Packings[1]

Packing	Size in. (= 25.54 mm)	a_t m^2/m^3	ε m^3/m^3
Steel Raschig rings	3/4	364	0.73
	1	184	0.86
	1 1/2	128	0.90
	2	95.1	0.92
Steel Pall rings	5/8	341	0.93
	1	207	0.94
	1 1/2	128	0.95
	2	102	0.96
Ceramic Raschig rings	1/4	712	0.62
	1/2	367	0.64
	3/4	243	0.72
	1	190	0.74
	1 1/2	121	0.73
	2	91.9	0.74
Ceramic Berl saddles	1/4	899	0.60
	1/2	466	0.62
	3/4	285	0.66
	1	249	0.68
	1 1/2	151	0.71
	2	105	0.72

1. Perry, R. H., and Chilton, C. H., Chemical Engineers' Handbook, McGraw-Hill, New York, 5th ed.,Table 18-6 (1973)

Hikita[1] obtained the following Sherwood number correlation:

$$\frac{k_L D_p}{D_L} = c \left(\frac{4\,L}{a_w \mu_L}\right)^{0.45} \left(\frac{\mu_L}{\rho_L D_L}\right)^{0.5} \left(\frac{{\rho_L}^2 g\, {D_p}^3}{{\mu_L}^2}\right)^{1/6} \qquad (10.4\text{-}4)$$

Liquid Reynolds number $\frac{4\,L}{a_w \mu_L} = 50 \sim 1{,}000$

Here $c = 0.31$ for Raschig rings, $c = 0.37$ for Berl saddles.

L (kg/m^{2}h): liquid flow rate, D_p (cm): packing size, and σ (dyne/cm): surface tension.

The empirical relations between the wetted surface and the total surface area proposed by Hikita are given as follows:

$a_w/a_t = 0.0406\ L^{0.455}\ \sigma^{(-0.83\ {D_p}^{-0.48})}$ for Raschig rings

$a_w/a_t = 0.0078\ L^{0.455}\ \sigma^{(-0.495\ {D_p}^{-0.98})}$ for Berl saddles (10.4-5)

1. Hikita, H.: Kagakukogaku (Chem. Eng. Japan), vol.26, 725 (1962)

10.4-2 Height of a gas-phase transfer unit

Fellinger's ammonia-air-water absorption data up to the loading point are correlated in the form[1] :

$$H_G = c\ G^p\ L^q\ \left(\frac{\mu_G}{\rho_G D_G}\right)^{2/3} \quad (10.4\text{-}6)$$

where H_G = height of a gas-phase transfer unit m, G = gas flow rate 1,000 ~ 3,500 kg/m^2 h, L = liquid flow rate 2,500 ~ 7,500 kg/m^2 h

1. Fellinger, L. Sc.D. thesis in Chem. Eng. M.I.T. (1941) from Perry, J.H.: Chemical Engineers' Handbook, 4th ed. Vol.18-42, McGraw-Hill, New York (1963).

The unknown parameters p, q, c calculated by Hikita are given in Table 10.4-3.

Table 10.4-3 Parameters for correlation Eq.(10.4-6)

Packing	size in.(I= 25.4 mm)	p	q	c
Raschig rings	3/8	0.45	- 0.47	0.85
	1/2	0.43	- 0.60	4.2
	1	0.32	- 0.51	3.07
	1 1/2	0.38	- 0.66	9.59
	2	0.41	- 0.45	1.44
Berl saddles	1/2	0.30	- 0.24	0.262
	1	0.36	- 0.40	0.745
	1 1/2	0.32	- 0.45	2.20

Hikita, H.: Kagakukogaku (Chem. Eng. Japan), vol.26, 725 (1962)

The gas-phase mass transfer correlation is experimentally obtained by Onda *et al.*[1]:

$$\frac{k_G}{a_p D_G} = 5.23\ \left(\frac{G}{a_p \mu_G}\right)^{0.7} \left(\frac{\mu_G}{\rho_G D_G}\right)^{1/3} \left(a_p D_p\right)^{-2} \quad (10.4\text{-}7)$$

The H_G can be calculated by using the following defining equation with the superficial gas velocity u_{sf}

$$H_G = \frac{u_{sf}}{k_G a_e} \quad (10.4\text{-}8)$$

Here a_e is the effective interfacial area for gas-liquid contact per unit volume.

1. Onda, K., Takeuchi, H., amnd Okamoto, Y., *J. Chem. Eng. Japan*, **1**, No.1, 56 (1982)

10.5 Column Diameter and Pressure Drop of Packed Columns

The power of blower required to feed gas mixture at the specified rate is mainly related to the pressure drop in the packing section. The pressure drop per unit height of the packing section $\Delta p/Z_T$ is characterized graphically in Figure 11.4-1. As can be seen, for the case of countercurrent gas absorber, the pressure drop is increased due to reduction in free volume by the liquid.

When gas mass-velocity G is increased at a constant liquid mass-velocity L, three flow conditions may occur successively. At very low gas velocities, the pressure drop is proportional

approximately to square of the gas velocity, as for dry packing. When G is further raised, $\Delta p/Z_T$ ceases to increase with G^2. It is attributable to the fact that a portion of the kinetic energy of the gas stream is used to support the liquid in the interstices of packing. This is called the "loading point." The transition from preloading to loading is usually gradual. When G exceeds a certain critical value, the liquid cannot flow downward over the packing, and then the column floods. This is called the "flooding point."

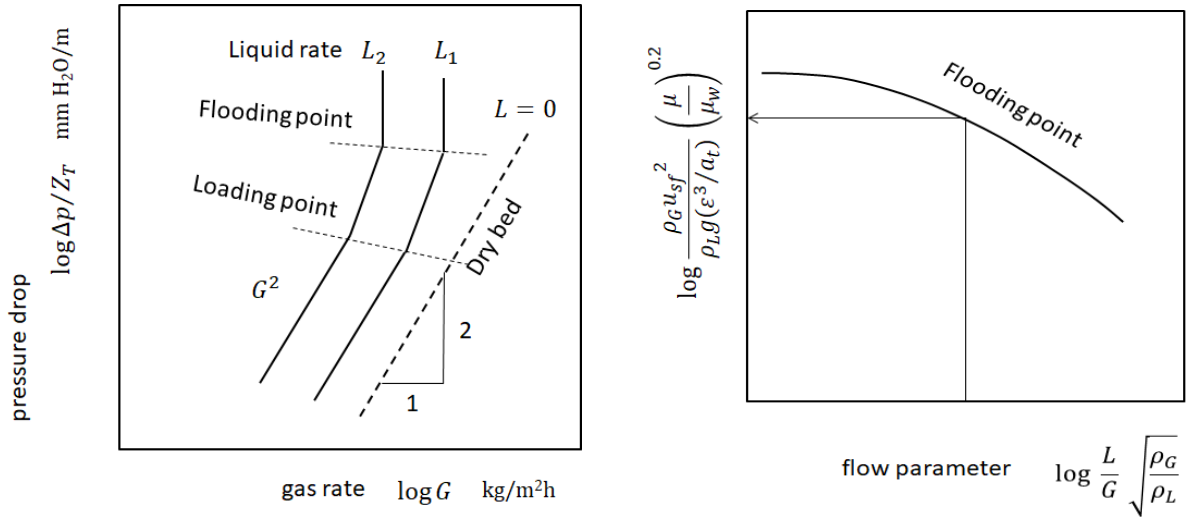

Fig.10.5-1. Pressure drop characteristics and flooding gas velocity of a packed column absorber

One of the earliest correlations of the flooding data, which has been modified later by Eckert, is in the form:

$$\frac{\rho_G {u_{sf}}^2}{\rho_L g(\varepsilon^3/a_t)}\left(\frac{\mu_L}{\mu_w}\right)^{0.2} \quad vs. \quad \frac{L}{G}\sqrt{\frac{\rho_G}{\rho_L}}$$

where u_{sf} = superficial gas-velocity at the flooding point (m/s), ρ_G and ρ_L = gas and liquid densities (kg/m^3), μ_L and μ_w = liquid and water viscosities (kg/m s), a_t= total surface area (m^2/m^3) and ε = void fraction (m^3 interstices/m^3 packed bed). Note that the left-side fraction implies the ratio of the kinetic energy of the gas stream to the potential energy of the liquid stream. For several kinds of packings, a_t and ε are tabulated with respect to their sizes in the last section. The pressure drop in packed columns can be expressed as the function of

$$\frac{G^2 F_p \psi\,(\mu_L/\mu_w)^{0.2}}{\rho_G \rho_L g} \quad vs. \quad \frac{L}{G}\sqrt{\frac{\rho_G}{\rho_L}}$$

Here $\psi = \rho_w/\varrho_L$ is the ratio of water density to liquid density and F_p the packing factor in 1/m, which should usually be given as the characteristics of various random packings. For example, 25-mm (1 in.) steel Pall rings give $F_p = 157$ 1/m.

It should be noted that as long as $(\mu_L/\mu_w)^{0.2}$ is regarded as a kind of correction factor, the remaining left-side term is a characteristic dimensionless kinetic energy ${u_s}^2$ group.

Fig.11.3-1 shows generalized correlations of pressure drop for various random packing towers recalculated after Eckert correlation[1].

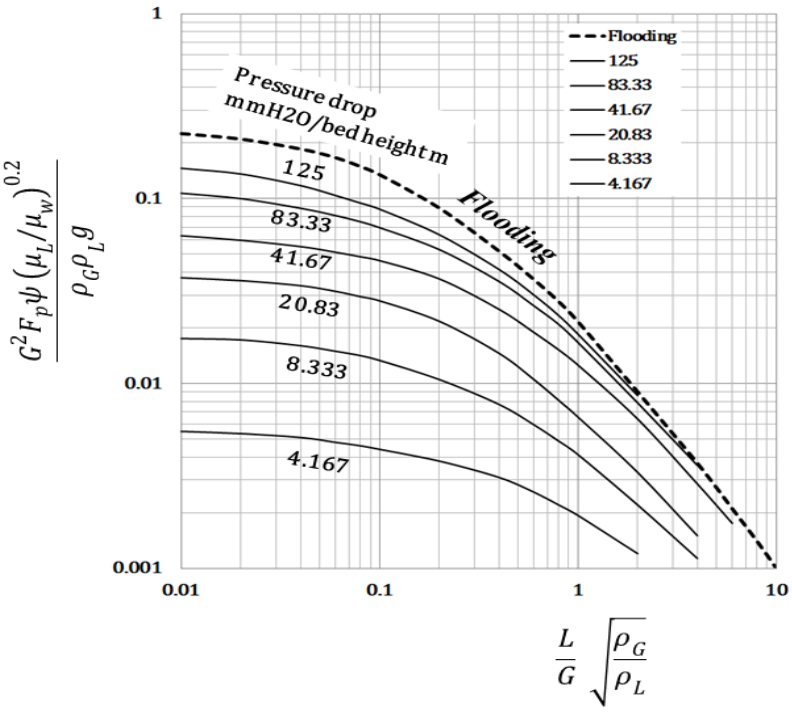

Figure 10.5-2. Generalized correlation for flooding and pressure drop in packed towers. (After Eckert)

---

1. Eckert, E. R. G., *Chem. Eng. Progr.*, **66**(3), 39 (1970)

[PROBLEM 10.5-1] A gas absorber packed with 25-mm Pall rings ($\boldsymbol{F_p = 157\ 1/m}$) deals with 500 m^3 of entering gas per hour.
The SO_2 content of the entering gas is 2 mol% and the remaining can be considered as air. Water is used as SO_2-free absorbent. The temperature is 25°C and pressure 1 atm. Ehen the ratio of gas flow to liquid flow is 1 kg gas/1 kg water, the gas velocity is one-half of the flooding velocity.
(a) Calculate the tower diameter.
(b) What is the pressure drop when the packing section is 7 m high?

10.6 Pressure Drop of Dry Packed Columns

The pressure drop studied in the last section is for the gas-liquid countercurrent flow in a packed column. Regarding the single phase fluid flow in a packed bed, the following empirical equation is available.[1, 2)]

$$\frac{P_0 - P_L}{L} = \frac{150\,\mu u_s}{{D_p}^2}\frac{(1-\epsilon)^2}{\epsilon^3} + \frac{1.75\,\rho {u_s}^2}{D_p}\frac{(1-\epsilon)}{\epsilon^3} \qquad (10.6\text{-}1)$$

This equation gives the pressure drop $P_0 - P_L$ through the length L of a packed bed. The first term is the Blake-Kozeny equation for laminar flow and the second term is the Burke-Plummer equation for turbulent flow. As distinct from packed column gas absorbers, the packing material may be spheres, cylinders, or various kinds of commercial packing. Here u_s is the superficial velocity, ϵ the void fraction, and D_p is the mean packing particle diameter (e.g. sphere diameter). The mean diameter is defined by

$$D_p = 6/a_v \qquad (10.6\text{-}2)$$

where a_v is the specific surface area of a nonspherical packing particle (particle surface/particle volume).
We define the friction factor for the packed bed by the following equation:

$$\frac{P_0 - P_L}{\frac{1}{2}\rho {u_s}^2} = \frac{L}{D_p} f \quad (10.6\text{-}3)$$

Analogously to the friction factor for a circular tube flow, the first term can be rewritten as

$$f = \left(\frac{(1-\epsilon)^2}{\epsilon^3}\right) \frac{75}{D_p \rho u_s / \mu} \quad (10.6\text{-}4)$$

This equation corresponds to the following equation for the laminar flow in a circular tube:

$$f = \frac{16}{Re} \quad (6.1\text{-}17)$$

Similarly the second term may give

$$f = 0.875 \frac{1-\epsilon}{\epsilon^3} \quad (10.6\text{-}5)$$

Usually the friction factor becomes constant in the turbulent flow region, except for the turbulent flow along smooth-walls.

For the case of smooth tubes, the Blasius equation for the turbulent tube flow is available as an example.

$$f = \frac{0.0791}{Re^{1/4}} \quad (7.3\text{-}12)$$

The above correlation Eq.(10.6-5) can be understood from the following facts of various flows.

As can be seen in Fig.7.3-1, we note that for highly turbulent flow in rough tubes or pipe fittings the friction factors become constant and a function of the roughness or the fittings structure only. As will be studied in Chapter 20, the power number (a kind of friction factor) for baffled agitated vessel also has the same tendency in the turbulent flow condition.

1. Bird, R. B., Stewart, W. E., and Lightfoot, E. N., "Transport Phenomena," Wiley, New York (1960)
2. Ergun, S., *Chem. Eng. Prog.*, **48**, 89 (1952)

Nomenclature

a, a_e	effective interfacial area per unit volume of packed bed, [m^2/m^3]
a_t	total surface area of packing, [m^2/m^3]
a_v	specific surface area of non-spherical packing particles, [m^2/m^3]
C_A	molar concentration of solute A, kmol/m^3 solution
Cp	heat capacity, [J/kg K]
c	total mole density, [kmol/m^3]
D	pipe diameter, [m]
D_{AB}	diffusivity of component A, [m^2/s]
D_p	size or diameter of packing particle, [m]
F_p	packing factor, [1/m]
f	friction factor, [-]
G, L	mass velocity of gas and liquid, [kg/m^2s] or [kg/m^2h]
G_M, L_M	gas- and liquid-phase molar velocity, [kmol/m^2s]
$H,\ H'$	Henry's constant, mole fraction gas-phase/mole fraction liquid-phase or Pa gas-phase/(kmol A/m^3 liquid)
$H_G,\ H_L$	gas- and liquid-phase HTU (Height of a Transfer Unit), [m]
$H_{oG},\ H_{oL}$	overall HTU, [m]
$j_D,\ j_H$	j-factor for mass transfer, j-factor for heat transfer, [-]
k_G, k_L	gas-phase, and liquid-phase mass transfer coefficient, [kmol/m^2s Pa], [m/s]
K_y, K_x	overall mass transfer coefficient using gas-phase, and liquid-phase concentration, [kmol/m^2s]
k_y, k_x	gas-, and liquid-phase mass transfer coefficient using mole fraction, [kmol/m^2s]
L	pipe length, [m]
m	Henry's constant, [-]
N_A	molar mass-flux of component A, [kmol/m^2s]
Nu	Nusselt number, [-]
$N_G,\ N_L$	gas- and liquid-phase NTU (Number of Transfer Units), [m]
$N_{oG},\ N_{oL}$	overall NTU, [m]
p	pressure, [Pa]
p_A	partial pressure of solute gas A, [Pa]
R	pipe radius, [m]
Re	Reynolds number, [-]
r	radial coordinate, [m]
Sc	Schmidt number, [-]

Sh	Sherwood number, [-]
x_A	mole fraction of component A, [-]
u_s	superficial velocity of gas, [m/s]
u_{sf}	superficial gas velocity at flooding point, [m/s]
Z	height of packed section, [m]
y	distance from pipe wall, [m]
δ_D	film thickness for mass transfer, [m]
ε	void fraction, [-]
μ	viscosity, [kg/m s]
κ	thermal conductivity, [W/m K]
σ	surface tension, [N/m]

Subscripts

f	film
G	gas
i	interface
L	liquid
m	bulk or mixed mean
w	wall nor wetted

PART Ⅱ

CHAPTER 11

MASS TRANSPORT EQUIPMENT

11.1 Distillation Fundamentals

11.1-1 Phase Equilibria for Distillation

The rate of inter-phase mass transport increases with the deviation from the vapor-liquid equilibrium. We should have to some degree the knowledge of gas-liquid equilibrium. The following phase rule is available to establish the number of independent variables or degree of freedom in a specific situation:

$$\boldsymbol{F = C - P + 2} \qquad (11.1\text{-}1)$$

Assume a binary solution having two components to be distilled, so $\boldsymbol{C} = 2$, $\boldsymbol{P} = 2$, and $\boldsymbol{F} = 2$. Both components are found in both phases. It can be considered that there are four variables: pressure, temperature, and the concentrations of component A in the liquid and vapor phases. For example, if the pressure is fixed, only one variable, e.g., liquid-phase concentration, can be changed independently, and temperature and vapor-phase concentration follow. Therefore equilibrium data are expressed in temperature-composition diagram under the condition of constant pressure. Such an equilibrium curve is given by plotting y_e, vapor-phase mole fraction , against x_e, liquid-phase mole fraction. Here only a very simple equilibrium case is introduced.

At equilibrium the activities of component A in the vapor and liquid should be equal.

For ideal solutions, Raoult's law can be applied:

$$p_A = P_A\, x_A \qquad (11.1\text{-}2)$$

where p_A is the partial pressure of component A in the vapor phase, P_A the vapor pressure of pure component A, and x_A the mole fraction of component A in the liquid. For the case of two-component system (binary system), the total pressure is

$P = p_A + p_B$ and $x_A + x_B$. Therefore the vapor concentration can be calculated as

$$y_A = \frac{P_A x_A}{P} \qquad (11.1\text{-}3)$$

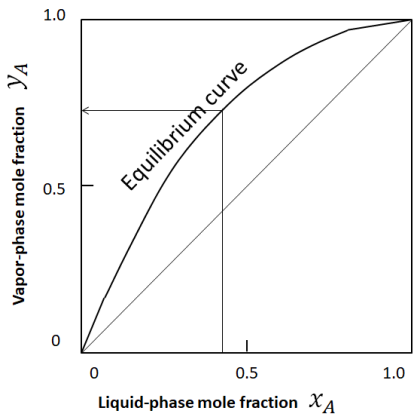

Fig.11.1-1 Equilibrium diagram expressed mole fraction y_A against x_A

The x-y diagram for binary equilibrium relationship is plotted for the more-volatile component A. A more general equilibrium relation is usually expressed as

$$y_A = K_A\, x_A \tag{11.1-4}$$

where K is called the vapor-liquid equilibrium constant.

For arbitrarily-chosen two components A and B, the relative volatility is defined as

$$\alpha_{AB} = \frac{y_A/x_A}{y_B/x_B} = \frac{K_A}{K_B} \tag{11.1-5}$$

For a binary system, the vapor-liquid equilibrium relation can be written by using α_{AB}:

$$y_A = \frac{\alpha_{AB}\, x_{AB}}{1+(\alpha_{AB}-1)\, x_{AB}} \tag{11.1-6}$$

Since the relative volatility does not vary so much in the small range of temperature, the equation can be used with an assumption of constant α_{AB}. Eq.(11.1-6) is useful for analytical process simulation.

11.1-2 Boiling-point diagram

As a simple example of equilibrium relation, a two-phase two-component system can be interpreted in terms of the temperatures and mole fractions by reference to Fig.11.1-2 called "Boiling point diagram."

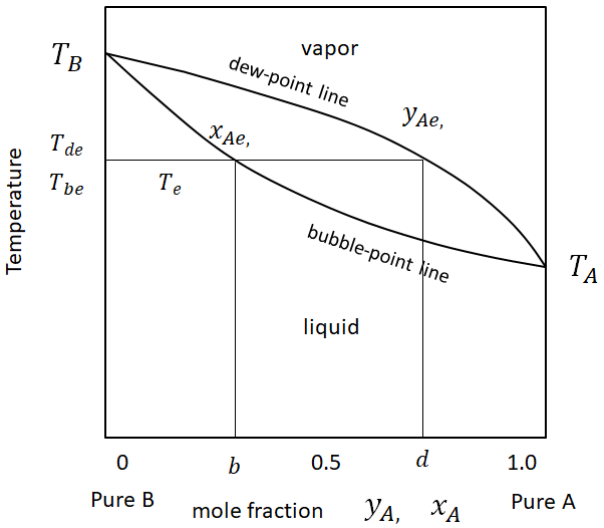

Fig.11.1-2 Boiling-point diagram (constant pressure)

The boiling-point diagram at constant pressure for mixtures of component A (the more-volatile component), boiling at temperature T_A, and component B, boiling at temperature T_B. The diagram consists of two curves, the ends of which coincide at the positions of pure A-component and pure B-component, respectively. The upper line (called the dew-point curve) represents the vapor y_{Ae} that will just begin to condense at temperature T_{de} (dew point). The lower line (called the bubble-point curve) represents the liquid x_{Ae} that will just begin to boil at temperature T_{be} (bubble point). Any two points d and b on the same horizontal line represent concentrations of liquid and vapor in equilibrium.at the temperature T_e. For all points above the dew-point line, the mixture is entirely vapor whereas for all points below the bubble-point line, the mixture is liquid. For points between the two lines, the mixture is partly liquid and partly vapor. As shown in Fig.11.1-2, the horizontal line indicates the vapor-liquid equilibrium relation that the vapor y_{Ae} is in equilibrium with the liquid x_{Ae} at temperature $T_{de} = T_{be}$.

11.2 Distillation Equipment

11.2-1 Continuous distillation plate column

Mass transfer equipment is designed to bring the two phases into intimate contact. Let us study how to design a continuous fractionating plate column. A typical distillation column with the major accessories is shown in Figure 11.2-1. The distillation system consists of the main fractionating column, an overhead condenser, and a bottom reboiler. Assume that the feed to be distilled is supplied into a plate in the central portion of the column as the liquid saturated at its bubble point. All plates above this feed plate constitute the rectifying section, and all plates below the feed plate constitute the stripping section which usually includes the feed plate.

The liquid feed flows down the column by gravity to the bottom reboiler and is subjected to rectification by the vapor rising from the reboiler. The vapor generated in the reboiler passes up the entire column, and is condensed in the overhead condenser. A portion of the condensate is returned to the top plate to provide the downflowing liquid in contact with the upflowing vapor in the rectifying section. This feedback liquid stream is called reflux. The bottom product liquid is withdrawn from the liquid pool in the reboiler. The overhead product is also withdrawn from the condensate collected in the accumulator.

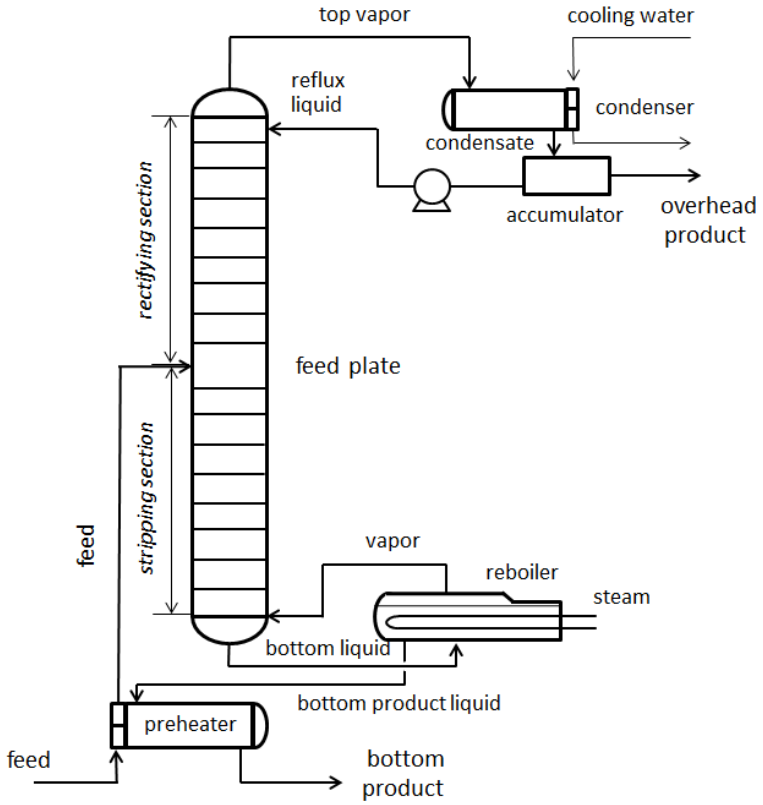

Fig.11.2-1. A typical continuous distillation plate column system.

Various types of crossflow and dual-flow plates are available. As shown in Fig.11.2-2, vapor flows upward through the passage of both types of plates. Liquid flows downward through the side pipe called “downcomer” for crossflow plates. For dual-flow plates, liquid flows directly downward from the perforations or openings of the plater itself.

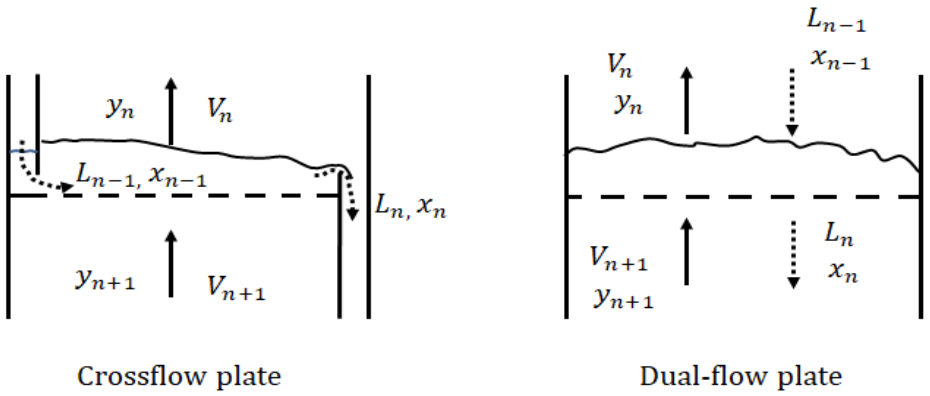

Fig.11.2-2. Vapor and liquid flows for crossflow and dual-flow trays

Bubble-plate and sieve-plate columns are commonly used in industrial distillation. A liquid mixture to be distilled, for example, is fed continuously into the central portion of the column. All plates above the feed plate constitute the rectifying section, and all plates below the feed plate (including the feed plate) constitute the stripping section. The liquid flows down the stripping section by gravity to the bottom of the column. The liquid reaching the bottom is partially vaporized by the reboiler and the vapor is sent back to the bottom of the column to provide the upflowing vapor stream in the stripping section. A definite rate of liquid as the bottom product is withdrawn from the pool of liquid in the reboiler. The vapor rises through the rectifying section after the stripping section toward the top of the column. The vapor arriving at the top of the column is cooled and completely condensed in the overhead condenser. Part of the condensate is returned to the top plate of the column to provide the downflowing liquid stream in the rectifying section. This return liquid is called “reflux.” Without the reflux there is no liquid stream in the rectifying section, and so no rectification would occur. A definite rate of the condensate is withdrawn as the overhead product from the condenser.

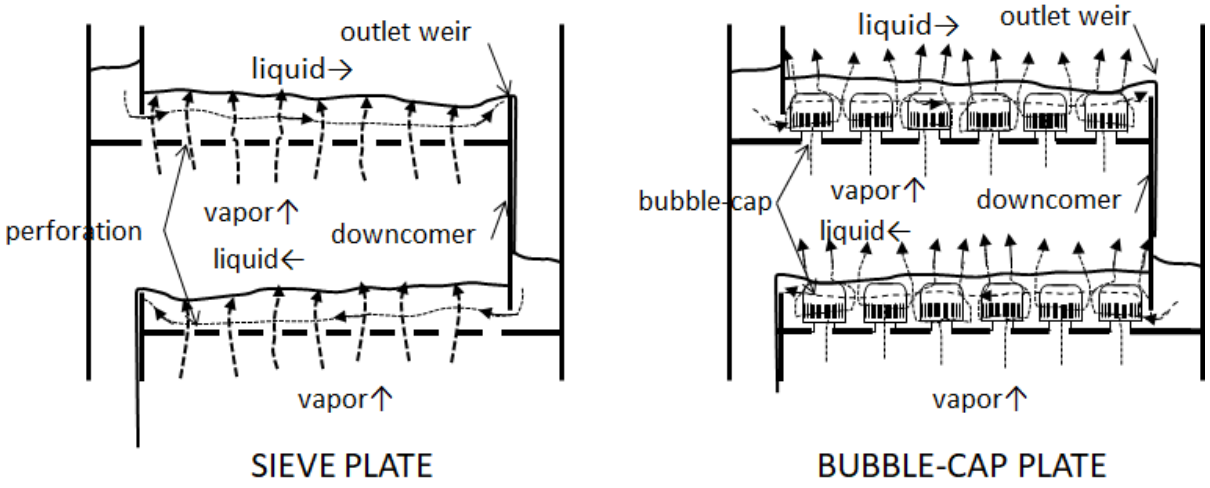

Fig.11.2-3. Typical traditional crossflow plates

Two typical traditional plates are shown in Fig.11.2-3. For cross-flow type plates, there are an outlet weir and a downcomer for liquid overflowing and then downflowing to the downstair tray. At each plate, bubbles of vapor are formed at the bottom of a liquid pool by forcing the vapor through small holes drilled in the plate or under slotted caps immersed in the liquid. Therefore interphase mass transfer occurs across the bubble interface while the bubbles rise up through the liquid pool. Some of the less-volatile component existing within the bubble is condensed while some of the more-volatile component existing in the liquid pool is vaporized. The result is a vapor phase which

becomes richer in the more-volatile component as it passes up the column and a liquid phase which becomes richer in the less-volatile component as it cascades downward.

The mass transfer process in an actual distillation column is too complicated to model in any direct way. For engineering design of actual distillation columns, therefore, the ideal plate concept is introduced to overcome this difficulty, and then the plate efficiency concept is taken into account. We shall firstly study the ideal plate model and engineering design method before considering distillation from a viewpoint of mass transfer.

11.2-2 Plate column fundamentals

11.2-2-1 Definition of ideal stage

Let us consider a single plate (the *n*th plate from the top) in a column. As shown in Fig.11.2-4, two fluid streams enter the *n*th plate, and two leave it. A stream of liquid, L_{n-1} kmol/s, from the plate n-1, and a stream of vapor, V_{n+1} kmol/s, from plate n+1, are brought into intimate contact on the *n*th plate. A stream of vapor, V_n and a stream of liquid, L_n leave the *n*th plate. The definition of ideal stage or plate states that the vapor and liquid leaving the *n*th stage or plate are in equilibrium, so x_{An} and y_{An} represent equilibrium concentrations.

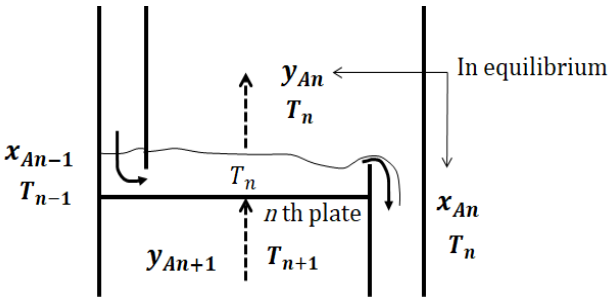

Fig.11.2-4 Definition of ideal plate or stage

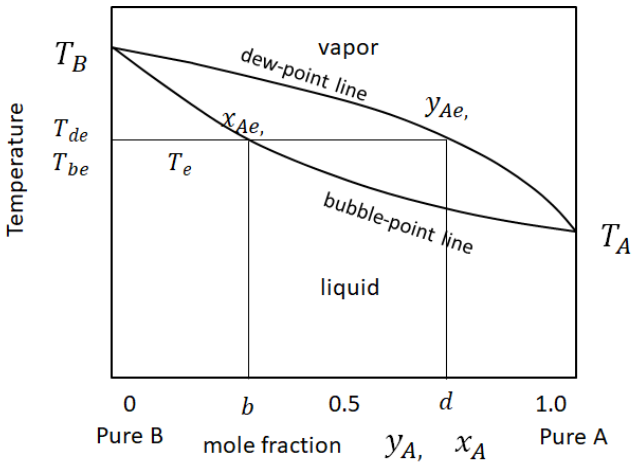

Fig.11.2-5 Boiling-point diagram (constant pressure)

Fig.11.2-5 shows the boiling-point diagram. Usually the concentrations of the volatile component in both phases increase with the height of the column. Although the two streams y_{An} and x_{An} leaving the *n*th plate are in equilibrium, those entering it y_{An+1} and x_{An-1} are not in general. The vapor from plate n+1 and liquid from plate n-1 are brought into *n*th plate, and then some of the more-volatile component A is vaporized from the liquid whereas some of the less-volatile component B is condensed from the vapor. As a result, the liquid concentration decreases from x_{An-1} to x_{An} and the vapor concentration increases from y_{An+1} to y_{An}. For an ideal solution such as the benzene-toluene binary system, the latent heat necessary to vaporize component A can

be supplied by the latent heat released in the condensation of component B. This situation is expressed in Fig.11.2-6.

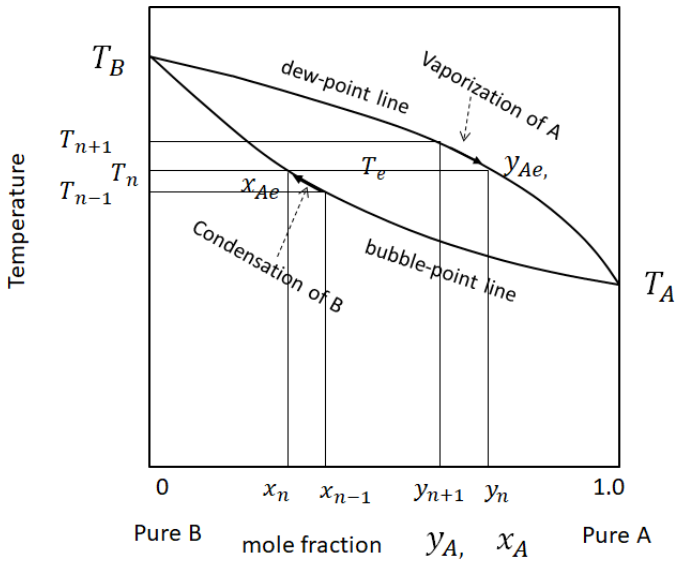

Fig.11.2-6 Concentration change due to rectification on ideal plate in boiling-point diagram

11.2-2-2 Material balance

As shown in Fig.11.2-7, the column is fed with F kmol/h of concentration x_F (mole fraction of more-volatile component A). The D kmol/h of overhead product of concentration x_D and the B kmol/h of bottom product of concentration x_B are withdrawn. The vapor V_t from the column top is condensed. Part of the condensate is returned as the reflux liquid R to the top plate.

The overall material balances can be written:

Total material balance

$$F = D + B \tag{11.2-1}$$

Component A balance

$$Fx_F = Dx_D + Bx_B \tag{11.2-2}$$

A material balance around the overhead condenser is

$$D = V_t - R \tag{11.2-3}$$

The (external) reflux ratio is defined as

$$r = \frac{R}{D} = \frac{V_t - D}{D} \tag{11.2-4}$$

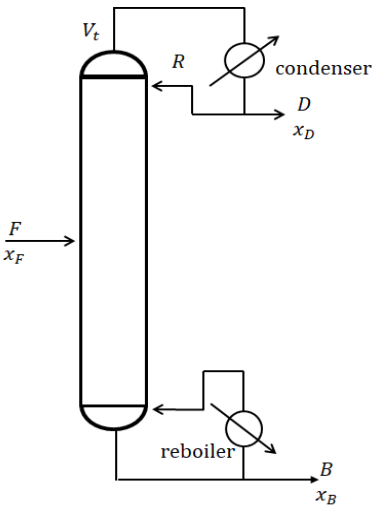

Fig.11-2-7. Distillation column for total material balances

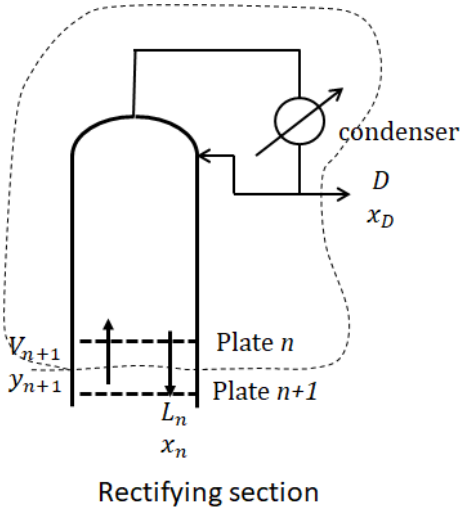

Fig.11.2-8. Material balance in rectifying section

Let us consider the nth plate from the top, where the plates are numbered serially from the top down.

A stream of liquid, L_{n-1} kmol/h of concentration x_{n-1} from the plate $n-1$, and a stream of vapor, V_{n+1} kmol/h of concentration y_{n+1} from the plate $n+1$, are brought into intimate contact on the nth plate. A stream of vapor, V_n kmol/h of concentration y_n, and a stream of liquid, L_n kmol/h of concentration x_n leave the nth plate. At each plate the liquid is at the bubbling point and the vapor is at the dew point. Some of the less volatile component B is condensed from the vapor while some of the more volatile component A is vaporized by the latent heat released in the condensation of component B.

Choosing the rectifying section above plate $n+1$ including the overhead condenser as a control volume, we get material balances:

$$D = V_{n+1} - L_n \qquad (11.2\text{-}5)$$

$$D\,x_D = V_{n+1}y_{n+1} - L_n\,x_n \qquad (11.2\text{-}6)$$

This equation can be written as

$$y_{n+1} = \frac{L_n}{V_{n+1}}x_n + \frac{D}{V_{n+1}}\,x_D \qquad (11.2\text{-}7)$$

This is the equation for the operating line in the rectifying section which gives the relation between the concentrations of the entering vapor V_{n+1} and the leaving liquid L_n.

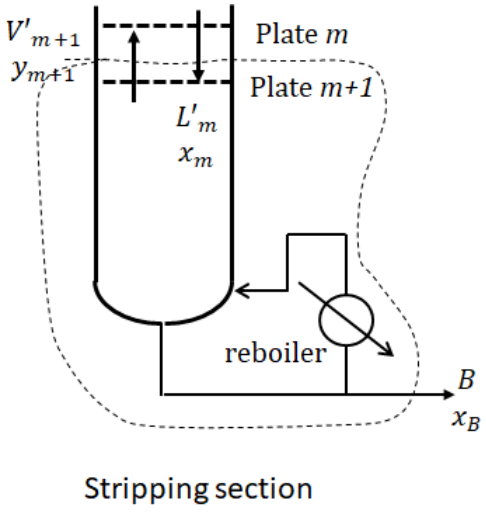

Fig.11-2-9 Material balance in stripping section

Similarly choosing the stripping section below plate m including the reboiler as a control volume, we get material balances:

$B = L'_m - V'_{m+1}$ (11.2-8)

$B\,x_B = L'_m x_m - V'_{m+1} y_{m+1}$ (11.2-9)

The lower equation

$y_{m+1} = \frac{L'_m}{V'_{m+1}} x_m - \frac{B}{V'_{m+1}}\, x_B$ (11.2-10)

This is the equation for the operating line in the stripping section.

11.2-2-3 McCabe-Thiele method

The number of ideal plates required to accomplish a specified separation can be computed by use of the McCabe-Thiele step-by-step construction of ideal plates. The ideal plate definition is that the vapor V_n leaving the *n*th plate is in equilibrium with the liquid L_n leaving the same plate.

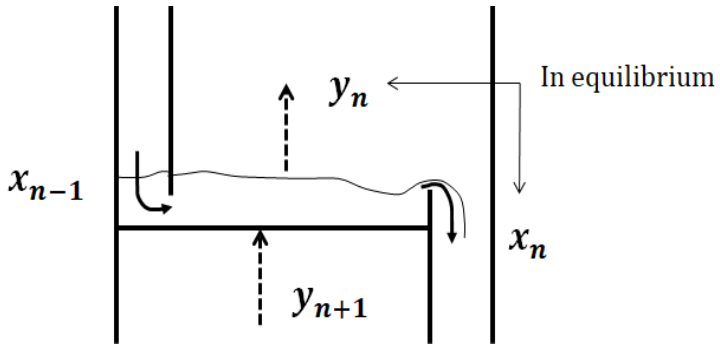

Fig.11.2-10. Definition of ideal plate

Regarding the simplification of vapor-liquid equilibrium, the concept of volatility can be considered. The relative volatility for a binary solution A and B can be defined as

$\alpha = \frac{y_A/x_A}{y_B/x_B}$ (11.2-11)

where $y_B = 1 - y_A,\ x_B = 1 - x_A$.

Assuming constant relative volatility α, the equilibrium can be approximated as

$y = \frac{\alpha\, x}{1+(\alpha-1)x}$ (11.2-12)

The x-y diagram for binary equilibrium relationship is plotted for the more-volatile component.

The McCabe-Thiele method is based on the following two assumptions:

(1) Equimolar heats of vaporization for the two components and

(2) No heat leaks and no heat of mixing.

Then the concept of constant molar overflow is obtained:

(Rectifying section)

$V_n = V_{n-1} = ------ = V_1 = V_t = V$ (11.2-13)

$L_n = L_{n-1} = ------ = L_1 = R = L$ (11.2-14)

(Stripping section)

$V'_m = V'_{m+1} = ------ = V'$ (11.2-15)

$L'_m = L'_{m+1} = ------ = L'$ (11.2-16)

Therefore the equations for the operating lines become

$y_{n+1} = \frac{L}{V}\, x_n + \frac{D}{V}\, x_D$ (11.2-17)

$y_{m+1} = \frac{L'}{V'}\, x_m - \frac{B}{V'}\, x_B$ (11.2-18)

The slope L/V of the operating line is sometimes called the internal reflux ratio:

$$\frac{L}{V} = \frac{R}{V_t} = \frac{r}{1+r} \quad (11.2\text{-}19)$$

A mass balance around the feed plate is

$$L' = L + q\,F \quad (11.2\text{-}20)$$

$$V = V' + (1-q)F \quad (11.2\text{-}21)$$

Here the q is a measure of the thermal condition of the feed:

$$q = \frac{\text{energy to convert 1 mole of feed to saturated vapor}}{\text{molar heat of vaporization}}$$

If a saturated vapor mixture is fed, the q becomes 0.

Then

$$L' = L$$

$$V = V' + F \quad (11.2\text{-}22)$$

If a saturated liquid mixture is fed, the q becomes 1.

Then

$$L' = L + F$$

$$V = V' \quad (11.2\text{-}23)$$

The q-line, as shown in Fig.11.2-11, passes through the intersection point of the two operating lines at the feed plate.

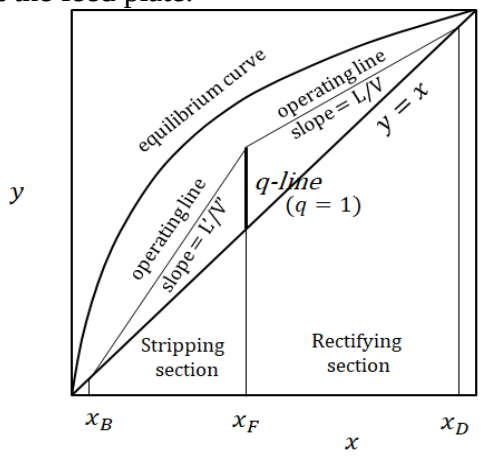

Fig.11.2-11. Interrelation of q-line with two operating lines

The general equation of q-line is given by

$$y = \frac{q}{q-1}\,x - \frac{1}{q-1}\,x_F \quad (11.2\text{-}24)$$

When $q = 0, \quad y = x_F$

When $q = 1, \quad x = x_F \quad (11.2\text{-}25)$

11.2-2-4 McCabe-Thiele step-by-step calculation method[1)]

The operating line for the rectifying section intersects the diagonal ($y = x$) at the overhead product concentration x_D. Similarly, the operating line for the stripping section intersects the diagonal at the bottom product concentration x_B.

1. McCabe, W. L., and Thiele, E. W., Ind. Eng. Chem., 17, 605 (1925)

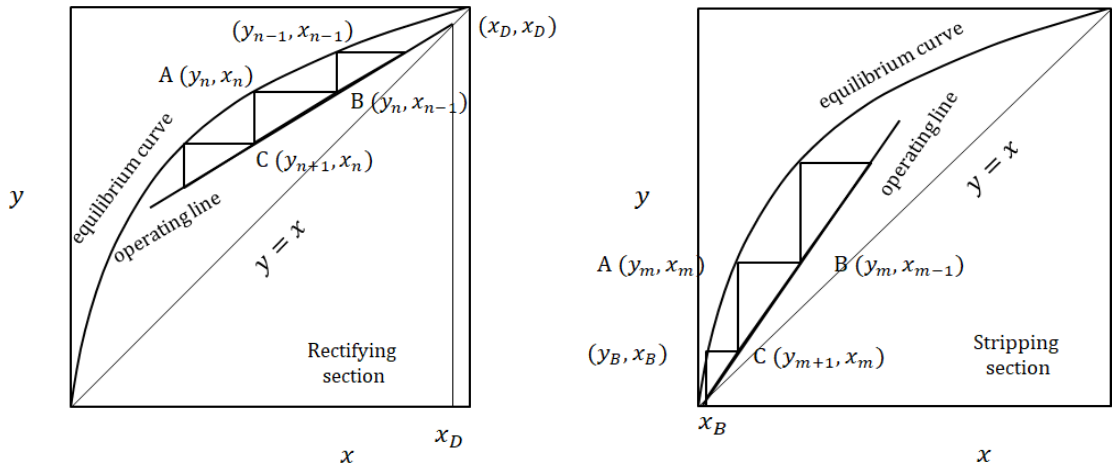

Fig.11.2-12. McCabe-Thiele step-by-step construction of ideal plates

Since, by definition of an ideal plate, y_n and x_n are the concentrations of the equilibrium vapor and liquid leaving the *n*th plate, point A(y_n, x_n) on the equilibrium curve represents the equilibrium plate *n*. The operating line represents the concentrations of all possible pairs of passing streams within the section. A horizontal line AB at y_n passing through the point B (y_n, x_{n-1}) on the operating line gives the concentrations of vapor leaving and liquid entering plate *n*. A vertical line AC at x_n intersecting the point C((y_{n+1}, x_n) on the operating line gives the concentrations of vapor entering and liquid leaving plate $n+1$. Likewise, we can count the ideal plates downward (or upward) from the starting point (x_D, x_D) through the rectifying section (or stripping section) by alternating use of the equilibrium curve and the operating lines…

The number of ideal plates (hypothetical equilibrium stages) must be converted to the number of actual plates by means of Murphree plate efficiency for practical column design, which will be studied later..

11.2-2-5 Reflux ratio

As the reflux ratio is decreased, the intersection point of the two operating lines approaches the equilibrium curve. When the intersection point touches the equilibrium curve, an infinite number of ideal plates would be required to accomplish a specified separation. The reflux ratio corresponding to this situation is the minimum reflux ratio. The economical (optimum) reflux ratio of actual columns usually falls around 1.5 times the minimum reflux ratio.

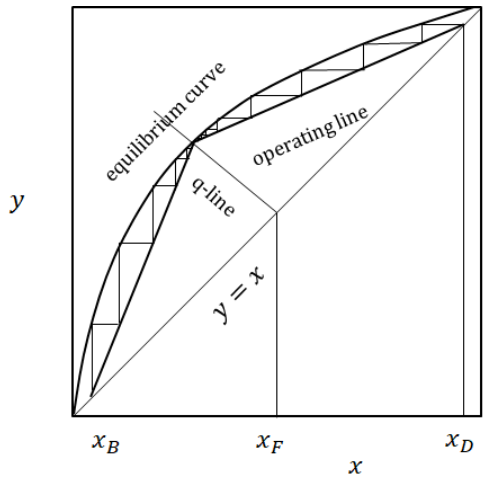

Fig.11.2-13. McCabe-Thiele diagram for minimum reflux ratio

11.2-2-6 Enthalpy-composition method (Ponchon-Savarit step-by-step method)[1,2)]

Analysis of fractionating columns can be done by using an enthalpy balance in conjunction with material balances and phase equilibria. This method is based on the graphical analysis of an enthalpy-composition diagram. Fig.11.2.14 is its schematic picture. The abscissa indicates the composition of a binary solution and the ordinate gives the enthalpy of the mixture of component A and B. Similarly to the boiling-point diagram, the curve KL is a dew point line and the curve MN indicates a bubble point line. The enthalpy of the ordinate includes latent heat, heats of mixing, and sensible heats and all these effects are built into the diagram, so that none of them need be considered separately. The balances of mass and enthalpy are set up over a control volume shown in Fig.11.2-8.

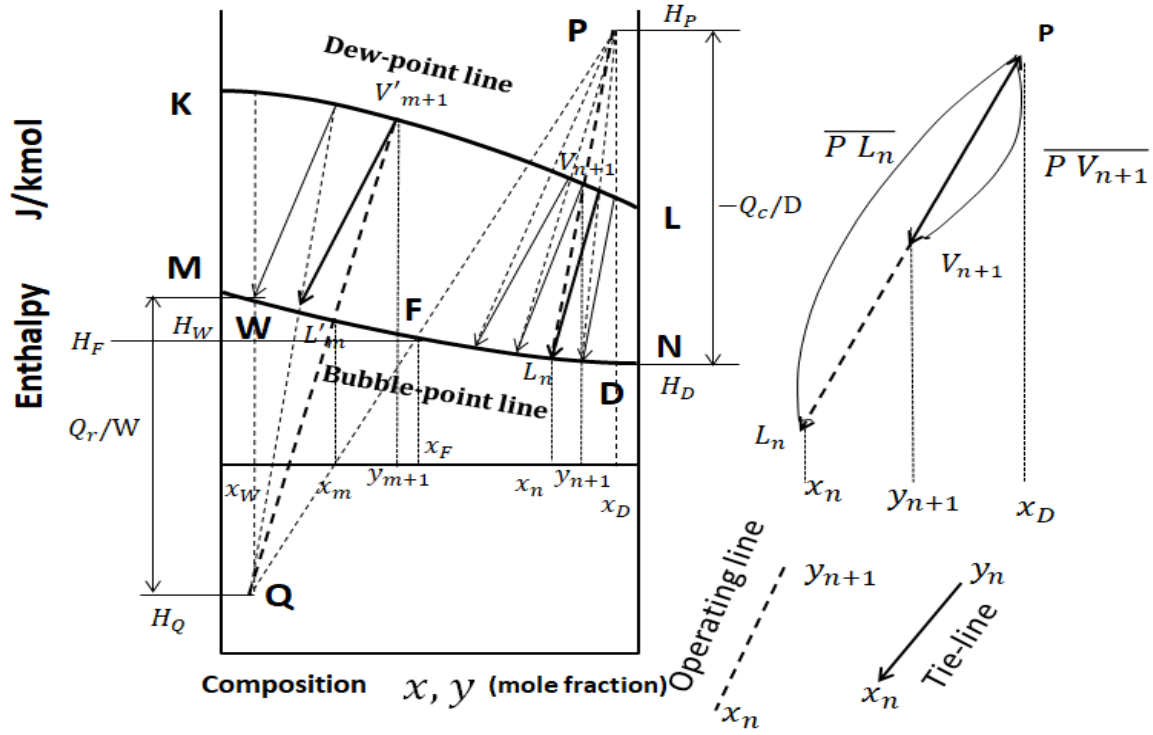

Fig.11.2-14. Enthalpy-composition diagram for Ponchon-Savarit method.

Regarding the rectifying section shown in Fig.11.2-14, the enthalpy of the vapor stream (flow rate V_{n+1}) rising from plate n+1 is given by H_{Vn+1} and the enthalpy of the liquid stream (flow rate L_n) leaving plate n is given by H_{Ln}. If the column is assumed adiabatic, points P, V_{n+1}, L_n are collinear. This line is called "enthalpy operating line." Point P represents a common operating point for all values of V_{n+1} and L_n. According to the center-of gravity principle,

$$\frac{V_{n+1}}{L_n} = \frac{\overline{PL_n}}{\overline{PV_{n+1}}} = \frac{x_D - x_n}{x_D - y_{n+1}} \qquad (11.2\text{-}26)$$

Similarly for the stripping section

$$\frac{V'_{m+1}}{L'_m} = \frac{x_m - x_w}{y_{m+1} - x_w} \qquad (11.2\text{-}27)$$

In this rectifying section for adiabatic operation, the difference between the enthalpy carried upward by the vapor stream and that carried downward by the liquid stream is constant. In this control volume, enthalpy is removed by the overhead condenser in an amount Q_c (usually fixed)

Setting up the enthalpy balance over the control volume

$$L_n H_{Ln} + D H_D + Q_c = V_{n+1} H_{Vn+1} \qquad (11.2\text{-}28)$$

$$H_P = H_D + Q_c/D \qquad (11.2\text{-}29)$$

Then

$$D H_P = V_{n+1} H_{Vn+1} - L_n H_{Ln} \qquad (11.2\text{-}30)$$

For adiabatic operation, DH_P (the difference between the enthalpy carried by the vapor and liquid streams) becomes the same everywhere in the rectifying section.

Similarly in the stripping section we get

$$WH_W = L'_m H_{Lm} - V'_{m+1} H_{Vm+1} + Q_r \quad (11.2\text{-}31)$$

$$H_Q = H_W - Q_r \quad (11.2\text{-}32)$$

$$WH_Q = L'_m H_{Lm} - V'_{m+1} H_{Vm+1} \quad (11.2\text{-}33)$$

Since D and W are constant, H_P and H_Q are also constant.

WH_Q becomes the same everywhere in the stripping section.

In a manner similar to McCabe-Thiele method, the enthalpy operating lines are used alternately with the tie-lines to give a step-by-step determination of the number of ideal plates necessary to accomplish a specified separation. This is called the "Ponchon-Savarit method."

Regarding the reflux ratio, the center-of-gravity principle gives

$$R = \frac{H_P - H_{V1}}{H_{V1} - H_D} \quad (11.2\text{-}34)$$

This equation indicates that Point P is specified by the reflux ratio.

---

1) Randall, M. and Longtin, B., *Ind. Eng. Chem.*, 30, 1063, 1188 (1938)
2) McCabe, W. L. and Smith, J. C., "Unit Operations of Chemical Engineering," McGraw-Hill, 3rd ed., 571 – 585(1976)

[EXAMPLE 12.2-1] A 2 kmol/h mixture of 0.4 mole fraction of methanol and 0.6 mole fraction of water is to be separated into overhead and bottom products of 0.85 and 0.2, respectively, by a column operated with a reflux ratio of 3 at 1 atm. The feed is supplied as a saturated liquid.
(Attention: The specified concentrations of the overhead and bottom products are made intentionally moderate for easy explanation on the enthalpy-composition diagram, especially the bottom product concentration is specified larger than usual.)

(1) Per kmol of overhead product, how much heat must be withdrawn at the overhead condenser and how much heat per kmol of bottom product must be added at the reboiler?
(2) Explain the step-by-step method for obtaining the number of ideal plates on the diagram.

Solution:

(1) From the overall material balance, $D = 0.615$ and $W = 1.385$ kmol/h, respectively.
Point F is placed on the bubble-point line at $x_F = 0.4$. Points D and W are also located on the bubble-point line at $x_D = 0.85$ and $x_W = 0.2$, respectively. The point P can be determined from the specified reflux ratio $R = 3$ as follows:
From Fig.11.2-E1, we obtain $H_{V1} = 42{,}610$, and $H_D = 5{,}645$ kJ/kmol . Then
$H_P = R(H_{V1} - H_D) + H_{V1} = 3 \times (42{,}610 - 5{,}645) + 42{,}610 = 79{,}575$ kJ/kmol
The point P is decided as $H_P = 79{,}575$ kJ/kmol and $x_D = 0.85$. Then
$-Q_c/D = 79{,}575 - 5{,}645 = 73{,}930$ kJ/kmol. The cooling duty becomes
$-Q_c = 73{,}930$ kJ/kmol $\times 0.615$ kmol/h $= 45{,}470$ kJ/h
The point W is obtained at the intersection of the overall-enthalpy line PF with the line $x_W = 0.2$, where $H_W = 6{,}245$ kJ/kmol. Therefore
$Q_r/W = H_W - H_Q = 6{,}245 - (-27{,}000) = 33{,}240$ kJ/kmol. The heat duty is

$$Q_r = 33{,}240 \text{ kJ/kmol} \times 1.385 \text{ kmol/h} = 46{,}040 \text{ kJ/h}$$

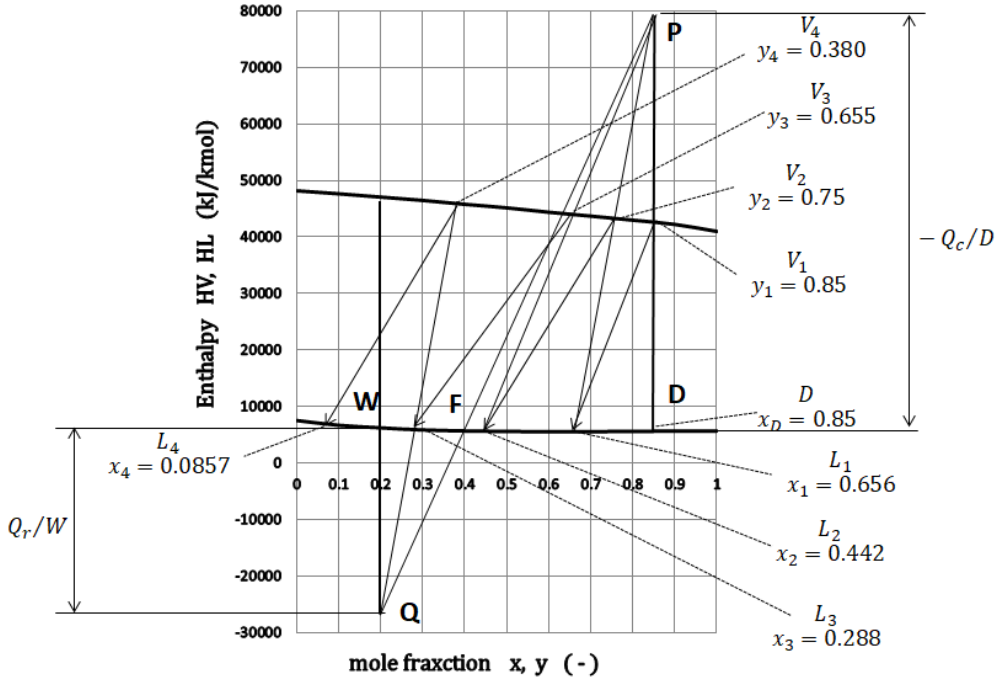

Fig.11.2-E1. Ponchon-Savarit step-by-step method for a fractionating column

(2) Since $x_D = y_1 = 0.85$, the point V_1 is on the dew-point line at $x_D = 0.85$. According to the vapor-liquid equilibrium relation, when $y_1 = 0.85$ is in equilibrium with $x_1 = 0.656$. This indicates that point L_1 should lie on the bubble-point line at $x_1 = 0.656$. Therefore the arrow $V_1 \rightarrow L_1$ shown in the figure is the tie-line. The next operating line through P and L_1 intersects the dew-point line at point V_2 ($y_2 = 0.75$). Using the VL equilibrium relation, the next tie-line gives point L_2 on the bubble-point line at $x_2 = 0.442$. Similarly point V_3 is obtained at $y_3 = 0.655$. The next tie-line $V_3 \rightarrow L_3$ crosses the overall-enthalpy line. It can be considered that the rectifying operating lines should be placed on the right of the overall-enthalpy line and the stripping lines to the left. The best location of the feed plate is on the first plate where the liquid concentration is less than the abscissa of the intersection of the bubble-point line and the overall-enthalpy line. Therefore the feed plate should be on the No.4 plate. Since L_3 is at the left of line PFQ, the next operating line should be drawn from point Q. This operating line intersects the dew-point line at V_4 (at $y_4 = 0.380$). Since $x_4 = 0.0857$ is less than x_w, four steps can be considered to be sufficient. A reboiler plus three ideal plates should be specified with feed plate located at No.3 plate. (Attention: Because of the concentration of the bottom product specified larger than the usual value in this example, the feed plate is located at No.3 plate above the reboiler.)

11.3 Mass Transfer in Distillation Column (Plate Column)

In general, an actual column does not work well in the same manner as the ideal plate column above mentioned. Let us consider the distillation efficiency of plate columns from a viewpoint of mass transport phenomena. The plate efficiency calculation is based on the two-film theory. Assuming equal molar heat of vaporization for a binary mixture of A and B, the basic equations can be derived from the interphase mass transfer equations.

Three assumptions have been made:

(1) the rate of mass transfer of a component within a phase is proportional to the difference in its concentration in the bulk of the phase and at the vapor-liquid contacting interface,

(2) the vapor and liquid at the interface are in equilibrium , and

(3) the holdup of the transferring component in the boundary layers on both sides of the interface is negligibly small compared to the amount transferred in the process.

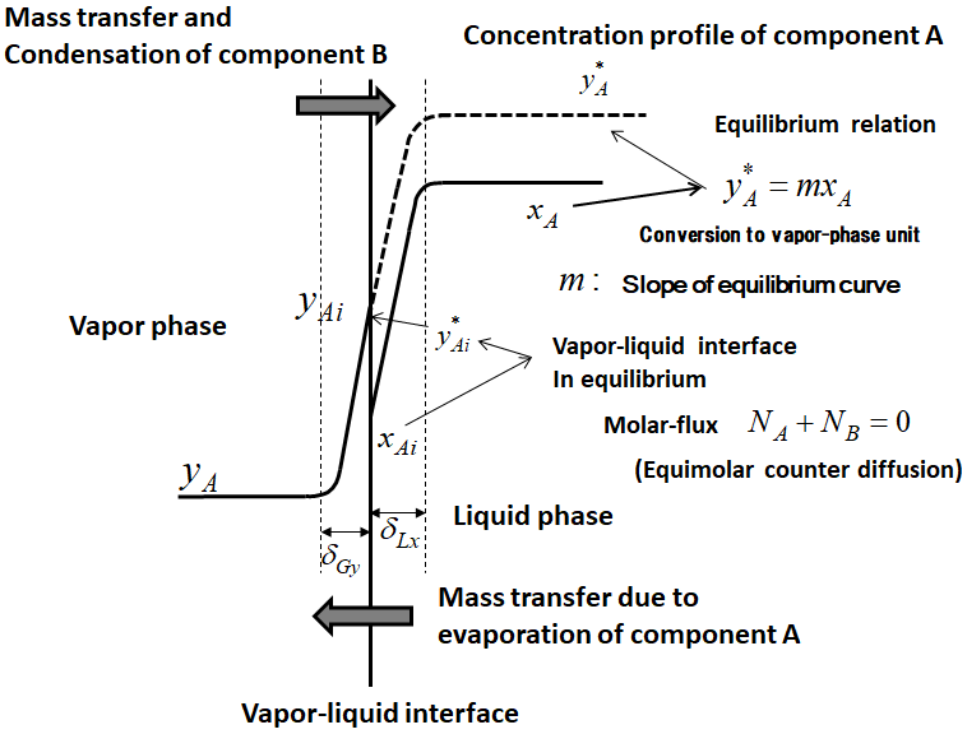

Fig.11.3-1. Composition profile in the neighborhood of vapor-liquid interface

The rate of mass transfer per unit area or the mass flux may be expressed by

$$N_A = K_{yA}(y_A^* - y_A) = k_{yA}(y_{Ai} - y_A) = k_{xA}(x_A - x_{Ai}) \quad (11.3\text{-}1)$$

where x_A and y_A are mole fractions of the more volatile component A.

The film coefficients of mass transfer k_y, k_x are defined as

$$k_{yA} = D_G/\delta_{Gy}, \quad k_{xA} = D_L/\delta_{Lx} \quad (11.3\text{-}2)$$

According to the two-film theory, two resistances in series to interphase mass transfer can be expressed as

$$\frac{1}{K_{yA}} = \frac{1}{k_{yA}} + \frac{m}{k_{xA}}, \qquad \frac{1}{K_{xA}} = \frac{1}{m\,k_{yA}} + \frac{1}{k_{xA}} \quad (11.3\text{-}3)$$

Consider the vapor bubbling up through a pool of liquid on plate *n*.

At the differential control volume $dz \times 1 \times 1$, the mass balance of more volatile component A is

$$G_M\, dy_A = K_{yA}\,(y_A^* - y_A) a\, dz \quad (11.3\text{-}4)$$

Here a is the interfacial area per unit volume of gas and liquid holdup in m^2/m^3.

Integrating with assumption that $K_{yA}a/G_M$ is constant, we get

$$N_{OG} = \int_{y_{n+1}}^{y'_n} \frac{dy}{y_A^* - y_A} = \frac{K_{yA} a\, Z_p}{G_M} \quad (11.3\text{-}5)$$

This equation is the equation defining a local value of the number of transfer unit on plates of distillation column. Here Z_p is the bubbling pool height on plate *n*.

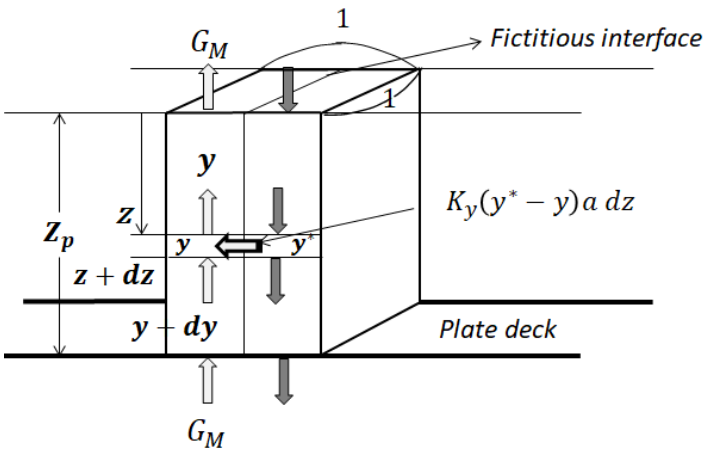

$$G_M(1 \times 1)dy = K_y(y^* - y)a\,(dz \times 1 \times 1)$$

Fig.11.3-2. Material balance of component A over a differential control volume *dz* of bubbling foam layer (height Z_p) on a plate

The inlet vapor is assumed to be well mixed, so that y_{An+1} can be regarded as a constant. The concentration of the outlet vapor y'_{An} is generally a function of the length from the outlet weir along plate *n* for this kind of crossflow plate. The right-hand side term $HTU = \frac{K_{yA}a\,Z_p}{G_M}$ is called "Height of Transfer Unit." Similar equations are obtained with the other transfer units:

$$N_G = \int_{y_{n+1}}^{y'_n} \frac{dy}{y_{Ai} - y_A} = \frac{k_{yA}a\,Z_p}{G_M} \quad (11.3\text{-}6)$$

$$N_{OL} = \int_{x'_n}^{x''_n} \frac{dx}{x_A - x_A^*} = \frac{K_{xA}a\,Z_p}{L^*_M} \quad (11.3\text{-}7)$$

$$N_L = \int_{x'_n}^{x''_n} \frac{dx}{x_A - x_{Ai}} = \frac{k_{xA}a\,Z_p}{L^*_M} \quad (11.3\text{-}8)$$

Note that the above definition of local liquid-phase transfer units assuming the counter-current flow does not describe actual mass transfer situations, since the actual liquid stream flows horizontally on the plates.

We should interpret that x'_n and x''_n are hypothetical liquid concentrations at the top and bottom of the liquid pool and that L^*_M is hypothetical molar flow rate divided by the effective plate area. In the later section, the average values of the transfer units will be defined.

The relation between hypothetical and actual molar flow rates is given by

$$L_M Z_p = L^*_M L_t \quad (11.3\text{-}9)$$

where L_t is the effective length of liquid travel on plate *n*.

The overall mass transfer resistance is expressed in terms of the individual gas-phase and liquid-phase resistances:

$$\frac{G_M}{K_{yA}\,a} = \frac{G_M}{k_{yA}a} + \frac{m\,G_M}{k_{xA}a} \quad (11.3\text{-}10)$$

where the vapor-liquid equilibrium curve is assumed to be locally a straight line.

$$y^* = m\,x + b \quad (11.3\text{-}11)$$

Since $Z_p = \frac{G_M}{K_{yA}\,a} N_{OG} = \frac{G_M}{k_{ya}\,a} N_G = \frac{L^*_M}{k_{xa}a} N_L$,

$$\frac{G_M}{K_{yA}a} = \frac{Z_p}{N_{OG}}, \quad \frac{G_M}{k_{yA}a} = \frac{Z_p}{N_G}, \quad \frac{m\,G_M}{k_{xA}a} = \left(m\,\frac{G_M}{L^*_M}\right)\frac{L^*_M}{k_{Ax}a} = \left(m\,\frac{G_M}{L^*_M}\right)\frac{Z_p}{N_L},$$

Thus Eq.(11.2-10) can be rewritten as

$$\frac{1}{N_{OG}} = \frac{1}{N_G} + \frac{\lambda}{N_L} \quad (11.3\text{-}12)$$

where $\lambda = m/(L^*_M/G_M)$ is the slope ratio of the equilibrium and operating liners called "the stripping factor." The transfer units averaged over the effective plate area may be applied to Eq.(11.2-10) for commercial-scale columns except for extremely large columns.

11.4 Tray Model (Plate Efficiency)

11.4-1 Murphree Plate Efficiency

The following assumptions are made: (1) that the inlet and outlet vapors are well mixed with concentrations of y_{n+1} and y_n respectively, and (2) that the inlet and outlet liquids are also well mixed, but the liquid concentration will vary between x_{n-1} and x_n.

The Murphree plate efficiency is defined as

$$E_{MG} = \frac{y_n - y_{n+1}}{y^*_n - y_{n+1}} \qquad (11.4\text{-}1)$$

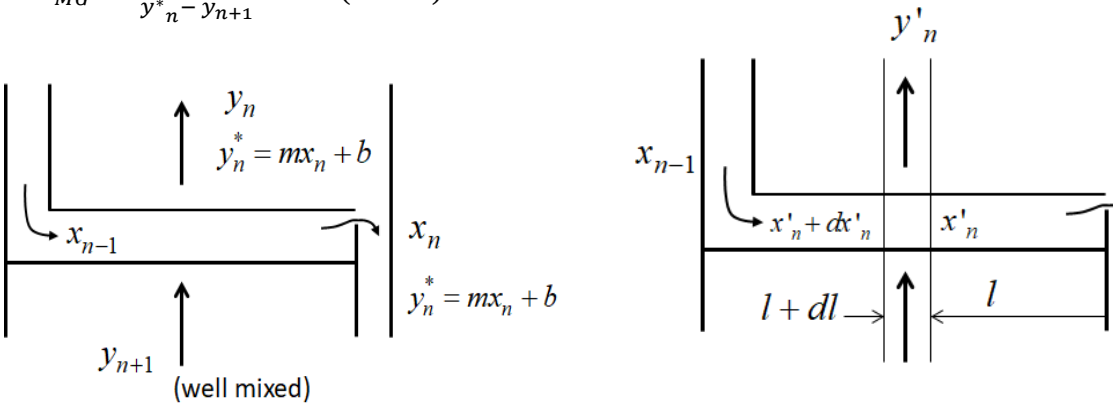

Fig. 11.3-1. Murphree plate efficiency and point efficiency

Here y^*_n is the concentration of the vapor that would be in equilibrium with the liquid of concentration x_n leaving the plate, i.e. $y^*_n = m\,x_n + b$. The y_{n+1} can be considered as a constant concentration since the inlet vapor is well mixed. As mentioned in the section of McCabe-Thiele method, for an ideal plate the vapor rising from the plate n is in equilibrium with the liquid of concentration x_n leaving the plate. Therefore $E_{MG} = 1$.

Similarly the plate efficiency for the liquid phase is also defined as

$$E_{ML} = \frac{x_{n-1} - x_n}{x_{n-1} - x^*_n} \qquad (11.4\text{-}2)$$

A point efficiency for the vapor phase can be defined as

$$E_{PG} = \frac{y'_n - y_{n+1}}{y'^*_n - y_{n+1}} \qquad (11.4\text{-}3)$$

Similarly

$$E_{PL} = \frac{x_{n-1} - x'_n}{x_{n-1} - x'^*_n} \qquad (11.4\text{-}4)$$

Here y'_n and x'_n are local concentrations of the leaving vapor and the crossing liquid at distance l from the outlet weir.

The point efficiency is related with the local value of the number of transfer unit on plates of distillation column Eq. (11.3-5).[1)]

Assume that over the liquid-flow cross section the liquid is well mixed i.e. $y'^*_n = constant$. Combining the definition of N_{OG} with the definition of E_{PG}

$$N_{OG} = \int_{y_{n+1}}^{y'_n} \frac{dy}{y^* - y} = -\ln \frac{y'^*_n - y'_n}{y'^*_n - y_{n+1}}$$

$$\exp(-N_{OG}) = \frac{y'^*_n - y'_n}{y'^*_n - y_{n+1}} = 1 - E_{PG} \qquad (11.4\text{-}5)$$

This is the equation for calculating the point efficiency from the number of transfer units.

The transfer units averaged over the whole effective plate area can be expressed as

$$\overline{N_{OG}} = \int_{y_{n+1}}^{y_n} \frac{dy}{y^* - y} = \frac{K_y a\, Z_p}{G_M}, \quad \overline{N_G} = \int_{y_{n+1}}^{y_n} \frac{dy}{y_i - y} = \frac{k_y a\, Z_p}{G_M}$$

$$\overline{N_{OL}} = \int_{x_n}^{x_{n-1}} \frac{dx}{x - x^*} = \frac{K_x a\, Z_p}{L^*_M}, \quad \overline{N_{OL}} = \int_{x_n}^{x_{n-1}} \frac{dx}{x - x_i} = \frac{k_x a\, Z_p}{L^*_M} \qquad (11.4\text{-}6)$$

In the above definition of liquid-phase transfer units, the inlet and outlet concentrations x_{n-1}, x_n are adopted in place of the concentrations at the top and bottom of the liquid pool. These averaged transfer units are more useful than the local transfer units because they are measurable by experiment.

In the case when the liquid on the plate is also completely mixed, the point and plate efficiencies become identical :

$$E_{PG} = E_{MG} = 1 - \exp(-\overline{N_{OG}}) \qquad (11.4\text{-}7)$$

---

1. Kister, H. Z., Distillation Design, McGraw-Hill, Newb York, P.367 (1992)

11.4-2 Mass Transfer Experiment[1)]

In order to understand the mass transfer in plate column distillation processes, vapor-phase and liquid-phase mass transfer coefficients should be discussed separately. The numbers of transfer units are a function of mass transfer coefficient and interfacial area. The transfer units can be considered of the form

$$\overline{N_G} = \overline{N_G}\left(Sc_G, We, Re_G, h_w/L_t,\ \ d/L_t,\ \ L_M/V_M,\ \ n\,L_t^{\,2}\right)$$
$$\overline{N_L} = \overline{N_L}\left(Sc_L, We, Re_L, h_w/L_t,\ \ d/L_t,\ \ L_M/V_M,\ \ n\,L_t^{\,2}\right) \qquad (11.4\text{-}8)$$

Here We is known as the Weber number which represents the ratio of inertia to surface tension force:

$$We = \frac{{u_{G0}}^2 \rho_G d}{\sigma} \qquad (11.4\text{-}9)$$

The Reynolds numbers are

$$Re_G = \frac{u_{G0}\varrho_G d}{\mu_G}$$
$$Re_L = \frac{u_{L0}\varrho_L d_{eq}}{\mu_L} \qquad (11.4\text{-}10)$$

The n , d and h_w are the number of holes per unit area of plate, the hole diameter, and the height of the outlet weir, respectively. The u_{G0} is the vapor velocity in a hole and u_L is the liquid velocity along the plate deck. The d_{eq} is the equivalent hydraulic diameter on plate.

As an example, regarding the distillation column efficiency, the experimental data on bubble cap tray reported very many years ago by AIChE Research Committee[1)] is still available.

Fig.11.4-1 shows the geometry of a crossflow tray and bubbling foam layer.

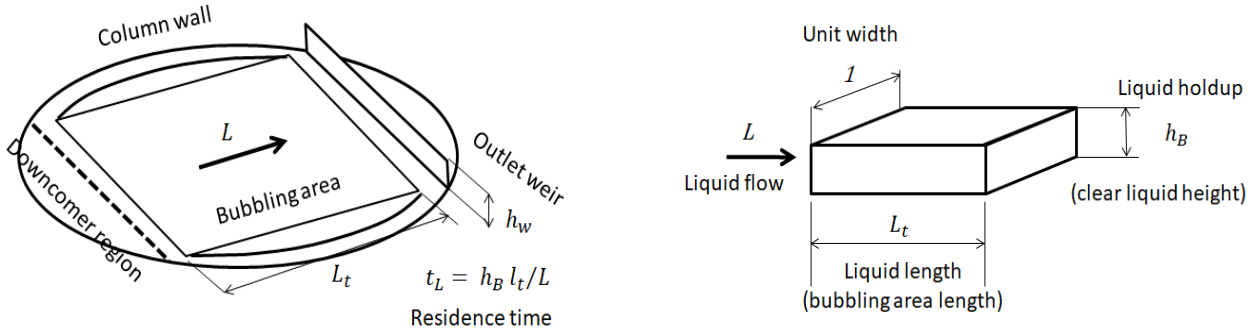

Fig. 11.4-1 Geometry of a crossflow tray and bubbling foam or froth layer

The superficial vapor velocity u_G (m/s) is based on the effective area of plate (bubbling area). The correlation equation[1,2)] developed on the basis of the gas-phase efficiency was obtained from the ammonia-air-water system and acetone-benzene system:

$$N_G = \frac{1}{\sqrt{Sc_G}}\,(0.776 + 4.57\,h_w - 0.238\,F + 105\,L) \qquad (11.4\text{-}11)$$

where h_w is the outlet weir height, F the F-factor given by $u_G\sqrt{\rho_G}$ in (m/s)(kg/m^3)$^{1/2}$, and

L the liquid volume flow-rate per unit width of plate in m^3/m s.
The liquid holdup per unit bubbling area length h_B is also given by

$$h_B = 4.2 \times 10^{-2} + 0.19\, h_w - 1.36 \times 10^{-2} F + 2.49\, L \quad (11.4\text{-}12)$$

The number of transfer unit on the liquid-phase is given by the following correlation:

$$N_L = 2.08 \times 10^4 \sqrt{D_L}\,(0.213\, F + 0.15) t_L \quad (11.4\text{-}13)$$

Here D_L is the diffusivity in the liquid in m^2/s. The residence time t_L (s) is the time of liquid crossing the liquid length L_t on the bubbling area shown in Fig.11.4-1.

1. AIChE Research Committee, Bubble Tray Design Manual, New York (1958)
2. AIChE Research Committee, Tray Efficiencies in Distillation Columns, Final Report from the Univ. Delaware (1958)

Let us learn how to predict the plate efficiency from these mass transfer correlations expressed as the number of transfer units.

[EXAMPLE 11.4-1] A liquid mixture of benzene and toluene is to be distilled by a bubble tray column which is 2 m in diameter and which contains eighteen trays on 0.50 m tray-to-tray spacing. The feed containing 54 mol% benzene is supplied as the liquid at the bubbling point. The operating conditions and tray geometry are listed in Table 11.3-1. Obtain the plate efficiency of the rectifying section assuming that the liquid is completely mixed.

Table 11.4-1 Operating conditions

Feed rate	0.139 kmol/s
Feed composition	54 mol% benzene
Overhead rate	0.075 kmol/s
Overhead composition	99 mol% benzene
Reflux ratio	1.67

Rectifying section

Vapor flowrate	0.20 kmol/s (Rectifying section)
Liquid flowrate	0.125 kmol/s (Rectifying section)
Average temperature	98℃
Average pressure	0.15 MPa
Average liquid composition	90 mol% benzene
Average vapor composition	94 mol% benzene

Tray geometry

Tray diameter	2 m
Cap size	0.0762
Cap layout	triangular
Bubbling area	1.7 m (average width)
	1.2 m (average length)
Outlet weir height	0.08 m
Outlet weir length	1.5 m

Solution:

(Step Ⅰ) Calculation of N_G: The physical properties of the vapor at 98℃ and 0.15 MPa are $\rho_G = 4.0$ kg/m^3, $\mu_G = 8.5 \times 10^{-6}$ kg/m s, and $D_G = 2.94 \times 10^{-6}\, m^2/s$, respectively. Then the Schmidt number is $Sc_G = 0.72$. The average molecular weight of the vapor $M_G = 78.8$ kg/kmol. Then the volumetric vapor flow rate is

$$G' = G_M M_G/\rho_G = (0.20)(78.8)/4 = 3.94 \text{ m}^3/\text{s}$$

The superficial velocity based on the bubbling area is

$$u_G = G'/A = 3.94/(1.2 \times 1.7) = 1.93 \text{ m/s}$$

Then the F-factor is obtained

$F = u_G\sqrt{\rho_G} = (1.93)\sqrt{4} = 3.86\ (\mathrm{m/s})(\mathrm{kg/m^3})^{1/2}$
The average density of the liquid is $\rho_L = 800\ \mathrm{kg/m^3}$. The average molecular weight is $M_L = 79.4\ \mathrm{kg/kmol}$
The volumetric liquid flow rate is
$L' = L_M M_L/\rho_L = (0.125)(79.4)/800 = 0.0124\ \mathrm{m^3/s}$
Then the liquid rate per unit width of the outlet weir is obtained
$L = 0.0124/1.5 = 0.00827\ \mathrm{m^3/s\ m}$
Then Eq.(11.4-11) gives
$N_G = (0.72)^{-1/2}(0.776 + 4.57\ (0.08) - 0.238\ (3.86) + 105b\ (0.00827)) = 1.286$
(Step II) Calculation of N_L: From Eq.(11.4-12), the liquid holdup on the trays is calculated:
$h_B = 4.2 \times 10^{-2} + 0.19\ (0.08) - 1.36 \times 10^{-2}\ (3.86) + 2.49\ (0.00827) = 0.0253\ \mathrm{m}$
The contact time of liquid should be calculated based on the bubbling area
$t_L = h_B L_t/L = (0.0253)(1.2)/0.00827 = 3.67\ s$
The liquid-phase diffusivity is given by
$D_L = 6 \times 10^{-9}\ \mathrm{m^2/s}$
Then Eq.(11.4-13) gives
$N_L = (2.028 \times 10^4)\ (6 \times 10^{-9})^{1/2}\ (0.213 \times 3.86 + 0.15)(3.67) = 5.605$
(Step III) Calculation of N_{OG}:
The slope of the equilibrium curve gives $m = 0.5$ at $x = 0.90$. Then
$\lambda = m\ G_M/L_M = (0.50)\ (0.20)/0.125 = 0.80$
Eq.(11.3-12) gives
$\frac{1}{N_{OG}} = \frac{1}{N_G} + \frac{\lambda}{N_L} = \frac{1}{1.286} + \frac{0.80}{5.605} = 0.920$ or $N_{OG} = 1.087$
(Step IV) Calculation of point efficiency:
Eq.(11.4-7) gives
$E_{PG} = 1 - \exp(-N_{OG}) = 1b - \exp(-1.087) = 0.663$
For the case of completely mixed liquid flow the point and plate efficiencies become identical.
The plate efficiency is given by

$$E_{MG} = E_{PG} = 0.663 \text{ or } 66.3\%$$

11.5 Design Calculation Procedure of Distillation Columns

The design calculation for the total number of actual plates required to accomplish a specified separation should be done in the following order:

(i) Number of ideal plates
The step-by-step calculation needs the following information:
Vapor-liquid equilibrium relationship, material balances, optimum reflux ratio, operating lines, and McCabe-Thiele stage-by-stage method based on stage equilibrium model for ideal plate construction.

(ii) Plate efficiency
The plate efficiency should be considered from mass transfer information:
Vapor-phase transfer unit, liquid-phase transfer unit, total number of transfer units, point efficiency, and plate efficiency taking into account the mixing effect.

(iii) Overall efficiency
The overall efficiency is defined as the ratio of the number of ideal plates to the number of actual plates. If the equilibrium and operating lines are straight, the overall efficiency

$$E_{OV} = \frac{\ln[1 + E_{MG}(\lambda - 1)]}{\ln \lambda} \quad (11.5\text{-}1)$$

As an alternative method, the modified McCabe-Thiele method can be used. The number of

actual plates can be computed replacing the true equilibrium curve y_e by an effective curve y_e' with the aid of known Murphree plate efficiencies in the McCabe-Thiele step-by-step method:

$$y_e' = y + E_{MG}(y_e - y) \qquad (11.5\text{-}2)$$

Figure 11.5-2 shows the modified McCabe-Thiele method.

11.6 Heat Balance of Distillation Column System

A continuous distillation column shown below is designed to separate F (kmol/h) of a binary mixture of x_F (mole fraction) of the more volatile component X and $(1 - x_F)$ of the less volatile component Y into an overhead product containing x_D of component X and a bottom product containing $(1 - x_B)$ of component Y.

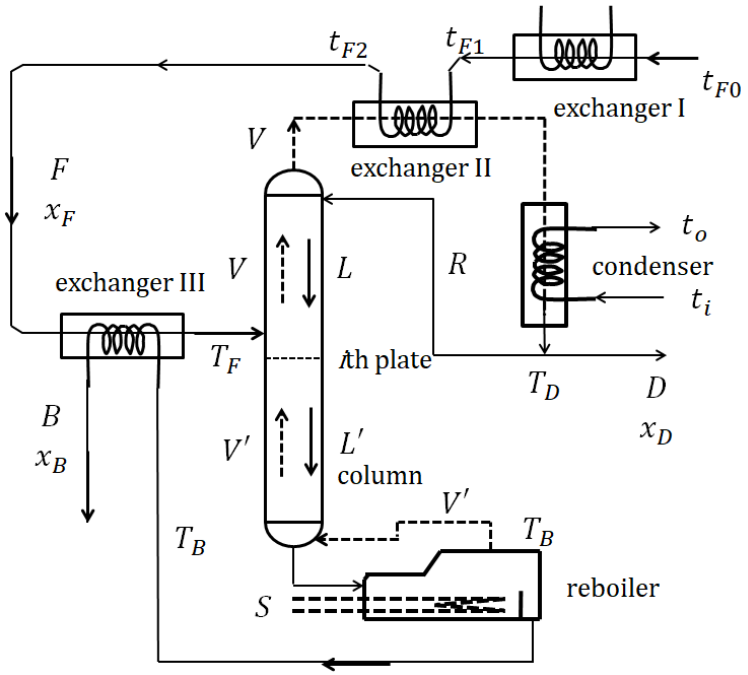

Fig.11.6-1. Flow sheet of distillation column system

(i) Calculate the overhead and bottom products.
A reflux ratio $r = R/D$ is to be used and the reflux is at its bubbling point. The feed is to be heated from t_{F0} to t_{F1} (K) by exchanger I, from t_{F1} to t_{F2} (K) by exchanger II, and from t_{F2} to T_F (K) by exchanger III, so that it can be introduced into the column as saturated liquid at its bubbling point.

(ii) Obtain the equations of operating line and q-line.
The molar latent heat and heat capacity of the mixture can be approximated as
$\Delta H_M = x\,\Delta H_X + (1-x)\Delta H_Y$ (J/kmol)
$Cp_M = x\,Cp_X + (1-x)Cp_Y$ (J/kmol K)
The vapor leaving the top of the column is to be completely condensed at its dew point T_D (K) by exchanger II and the overhead condenser,

(iii) If cooling water enters the overhead condenser at t_i (K) and leaves at t_o (K), how much water is required?

(iv) The bottom product leaves the reboiler at its bubbling point T_B (K). If the heat released by steam at pressure P_S (Pa) in the reboiler is assumed equal to the heat of

vaporization H_S (J/kg), how much steam is required?

(v) What is the temperature of the bottom product at the outlet of exchanger III?

(vi) If a constant Murphree vapor-phase plate-efficiency E_{MG} (-) is given to each stage excluding the reboiler, how many actual plates are needed? Where should the feed be introduced?

Solution:

(i) Overall mass balances:

$$F = D + B \tag{11.6-1}$$

$$F\,x_F = D\,x_D + B\,x_B \tag{11.6-2}$$

From these equations, the overhead and bottom products D and B (kmol/h) are found:

$$D = \frac{x_F - x_B}{x_D - x_B}\,F, \qquad B = \frac{x_D - x_F}{x_D - x_B}\,F$$

(ii) Since the feed is introduced as saturated liquid, $q = 1$ and the q-line equation becomes $x = x_F$. For $q = 1$, the liquid and vapor flow rates are

$L' = L + F$ and $V' = V$

These quantities can be expressed in terms of the reflux ratio:

$$L' - F = L = R = r\,D \tag{11.6-3}$$

$$V' = V = R + D = (r+1)D \tag{11.6-4}$$

Then the equations for the operating lines are found:

(Rectifying section)

$$y = \frac{L}{V}\,x + \frac{D}{V}\,x_D = \frac{r}{r+1}\,x + \frac{1}{r+1}\,x_D \tag{11.6-5}$$

(Stripping section)

$$y = \frac{L'}{V'}\,x - \frac{B}{V'}\,x_B = \frac{f+r}{r+1}\,x - \frac{b}{r+1}\,x_B \tag{11.6-6}$$

where $f = F/D$ and $b = B/D$.

(iii) The vapor flow rate in the rectifying section is

$V = (r+1)D$

The total rate of heat released in condensation of the vapor is

$$(r+1)D\,[x_D\Delta H_X + (1 - x_D)\Delta H_Y]$$

Assuming the average heat capacity not to be a function of temperature, the rate of heat transfer at exchanger II is given by

$$F\,[x_F Cp_X + (1 - x_F)Cp_Y](t_{F2} - t_{F1})$$

By heat balance set up at the condenser, the water flow rate W (kg/h) can be calculated as

$$(r+1)D\,[x_D\Delta H_X + (1 - x_D)\Delta H_Y] - F\,[x_F Cp_X + (1 - x_F)Cp_Y](t_{F2} - t_{F1}) = W\,Cp_w(t_o - t_i) \tag{11.6-7}$$

Here Cp_w is heat capacity of water in (J/kg K).

(iv) The heat required for vaporizing V' (kmol/h) of liquid is

$$V'[x_B\Delta H_X + (1 - x_B)\Delta H_Y] = S\,\Delta H'_S \tag{11.6-8}$$

From this equation, the steam needed, S (kg/h) can be calculated.

(v) By heat balance set up at exchanger III the outlet temperature t_B (K) can be calculated.

$$F\,[x_F Cp_X + (1 - x_F)Cp_Y](T_F - T_{F2}) = B[x_B Cp_X + (1 - x_B)Cp_Y](T_B - t_B) \tag{11.6-9}$$

(vi) As shown in Fig.12.1-2, the effective equilibrium curve y'_e vs. x can be obtained from the true equilibrium curve y_e vs. x by using the following equation:

$$y'_e = y + E_{MG}\,(y_e - y) \tag{11.6-10}$$

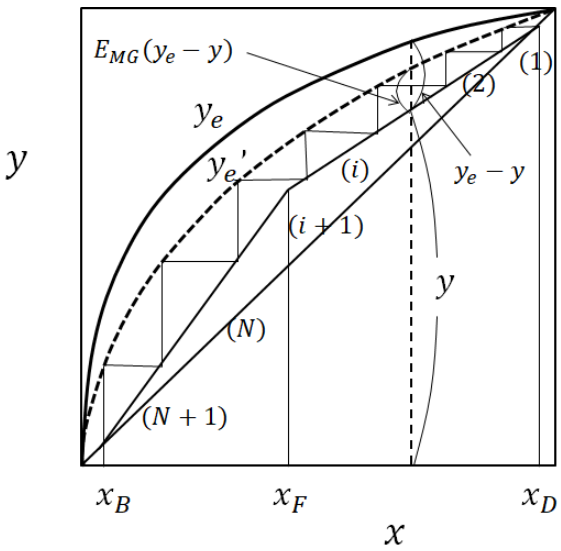

Fig.11.6-2. Modified McCabe-Thiele step-by-step method

As shown in Fig.11.6-2, the McCabe-Thiele step-by-step construction can be made between the effective equilibrium curve and the operating lines to determine the number of actual plates. The true equilibrium curve is used for the last step which corresponds to the reboiler. It is found that a reboiler and *N* actual plates are needed and the feed should be introduced on the *i* th plate from the top.

Nomenclature

a	effective interfacial area per unit packed volume, [m^2/m^3]
Cp	heat capacity, [J/kmol K]
D	overhead product, [kmol/s]
D_G, D_L	diffusivity in gas- and liquid-phase, [m^2/s]
E_{MG}	Murphree plate efficiency, [-]
E_{PG}, E_{PL}	point efficiency for vapor- and liquid-phase, [-]
F	feed rate, [kmol/s] or F-factor [(m/s)$(kg/m^3)^{0.5}$]
G_M	superficial molar gas-mass velocity, [$kmol/m^2s$]
H_X, H_Y	latent heat (enthalpy) of x- and y- component, [J/kmol]
h_{ETP}	HETP (Height Equivalent to a Theoretical Plate), [m]
h_w	outlet weir height, [m]
K	vapor-liquid equilibrium constant, [-]
K_x, K_y	overall mass transfer coefficients defined by vapor-phase and liquid-phase concentrations [$kmol/m^2s$]
k_x, k_y	mass transfer coefficients of vapor-phase and liquid-phase film [$kmol/m^2s$]
m	slope of equilibrium curve, dy/dx,
N_{OG}, N_G, N_L	number of transfer unit, OG:overall, G:gas phase, L:liquid phase, [-]
n	theoretical plate/stage number, [-]
Re	Reynolds number, [-]
Sc	Schmidt number, [-]
T, t	temperature, [K]
x_A, y_A	mole fraction of component A, liquid- and vapor-phase, [-]
z	height of packing section, [m]
α_{AB}	relative volatility, [-]
δ_G, δ_L	thicknesses of gas-phase and liquid-phase film, [m]
λ	stripping factor, [-]
μ	viscosity, [kg/m s]

Subscripts

A, B	component A, B
G, L	gas-phase, liquid-phase
i	interface

CHAPTER 12

SIMULTANEOUS HEAT AND MASS TRANSFER - I

12.1 Theory of Simultaneous Heat and Mass Transfer - I

As distinct from gas absorption, a distillation process takes place in the form of non-isothermal counter-diffusion accompanied with the enthalpy releasing due to condensation of less-volatile component B and the enthalpy receiving vaporization of more-volatile component A in the neighborhood of vapor-liquid contacting interface. Even at present, however, it is still very difficult to confirm whether or not the enthalpy released by the component B is totally consumed for the vaporization of component A. This is an important theme for the investigators of non-equilibrium thermodynamics.

In this chapter, we consider the distillation process by the simultaneous heat and mass transfer based on the assumption that the total molar enthalpy $N_B \Delta H_B$ released by condensation of component B is consumed for the vaporization of component A. The following enthalpy balance should exist:

$$N_B \Delta H_B = N_A \Delta H_A \qquad (12.1\text{-}1)$$

If $\Delta H_B = \Delta H_A$, $N_B = N_A$.

That is, this condition indicates the equimolar counter-diffusion.

For example, benzene and toluene have approximately equal molar enthalpy for condensation and vaporization.

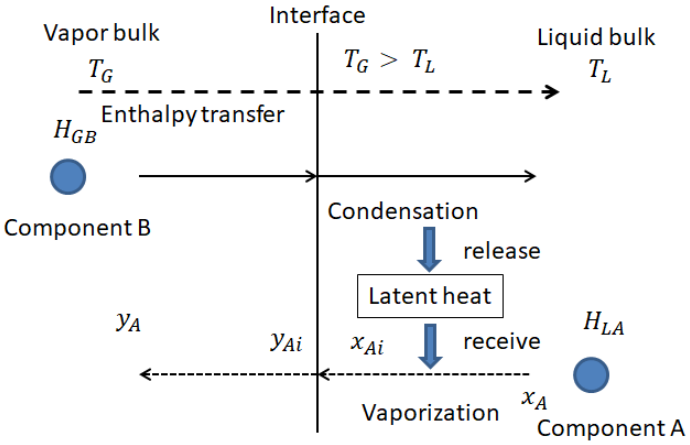

Fig.12.1-1. Heat and mass transfer in a distillation process

As shown in Fig.12.1-1, in the counter-current condition of vapor and liquid streams, less-volatile component B having enthalpy H_{GB}in the vapor bulk arrives by convective mass transfer at the interface and then the latent heat $N_B \Delta H_B$ released due to condensation of component B is absorbed for vaporization by more-volatile component A which arrives at the interface by convective mass transfer in the opposite direction from the liquid bulk. At the same time, thermal energy is transported by convective heat transfer accompanied with the counter-diffusion from the vapor bulk to the liquid bulk across the interface. Only for simplicity, it can be considered by the

above-mentioned assumption that there is no temperature jump in the neighborhood of the interface.

We will pay attention to the mass transfer of component A from liquid to vapor phase in a packed column (cross-section area S).

If their molar latent heats are equal: $\Delta H_A = \Delta H_B$ (J/kmol), equimolar counter-diffusion takes place. The interphase mass transfer of component A can be expressed by the following mass-flux equation based on Fick's law and the two film theory:

$$N_A = -\rho_G D_{ABG} \left.\frac{dy_A}{dz}\right|_{z=0} = -\rho_L D_{ABL} \left.\frac{dx_A}{dz}\right|_{z=0} \quad (12.1\text{-}2)$$

where ρ_G and ρ_L (kmol/m^3) are molar densities of vapor and liquid, and D_{ABG} and D_{ABL} (m^2/s) are vapor-phase and liquid-phase diffusivities of component A in B, respectively.

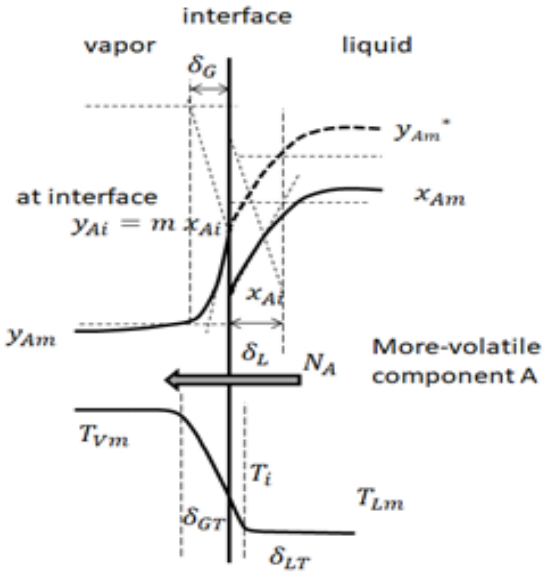

Fig.12.1-2. Composition and temperature profiles in the neighborhood of vapor-liquid contacting interface

Therefore the convective heat and mass transfer coefficients can be defined as

$$N_A = -\rho_G D_{ABG} \left.\frac{dy_A}{dz}\right|_{z=0} = \rho_G (D_{ABG}/\delta_G)(y_{Ai} - y_A) = k_{yA}(y_{Ai} - y_A) \quad (12.1\text{-}3)$$

$$N_A = -\rho_L D_{ABL} \left.\frac{dx_A}{dz}\right|_{z=0} = \rho_L (D_{ABL}/\delta_L)(x_A - x_{Ai}) = k_{xA}(x_A - x_{Ai}) \quad (12.1\text{-}4)$$

$$Q = -\kappa_G \left.\frac{dT_G}{dz}\right|_{z=0} = (\kappa_G/\delta_G)(T_G - T_i) = h_G(T_G - T_i) \quad (12.1\text{-}5)$$

$$Q = -\kappa_L \left.\frac{dT_L}{dz}\right|_{z=0} = (\kappa_L/\delta_L)(T_i - T_L) = h_L\big((T_i - T_L)\big) \quad (12.1\text{-}6)$$

It should be noticed that as distinct from gas absorption, the mass transfer coefficients in distillation do not include the effect of bulk transfer owing to equimolar counter-diffusion.

As shown in Fig.12.1-2, the overall driving force can be considered to be the liquid bulk concentration x_{Am} minus the vapor bulk concentration y_{Am}. However it is necessary to use a concentration unit on the common basis.

If we use vapor-phase concentration unit in mole fraction, the overall driving force is given by $y_A^* - y_A$, where y_A^* is fictitious concentration in equilibrium with the liquid bulk concentration x_A. Usually the liquid-bulk concentration x_A is converted into y_A^* by using a vapor-liquid equilibrium relation such as $y_A = m\, x_A$.

12.2 Transport Phenomena in a Packed Column Distillation Process

12.2-1 Simultaneous mass and energy transfer model

Unless a process fluid mixture to be distilled has any problem in thermal processes such as fouling, polymerization, and/or thermal decomposition, a packed bed column is very often employed for distillation operation.

Let us consider a packed column distillation. It is very instructive to reconsider a distillation process from a standpoint of simultaneous heat and mass transfer. It should be kept in mind that as distinct from gas absorption, a usual distillation process takes place under the condition of equimolar counter-diffusion. That is, there is no stagnant incondensable component near the vapor-liquid interface.

Figure 12.2-1 shows a usual packed column, in which random packings or structured packings are equipped in the three packing sections. The upper packing section above the feed stage is called rectifying section and the lower one below the feed stage is called stripping section. In each empty space above the respective packing beds, a liquid collector and a liquid distributor are installed in order to avoid maldistribution of liquid stream in the packing section.

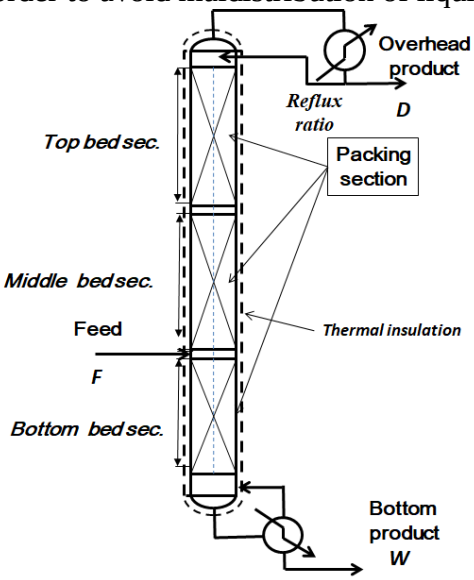

Fig.12.2-1. Packed distillation column

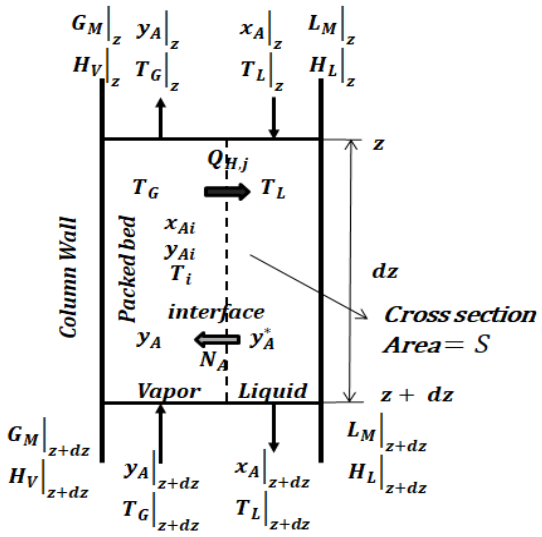

Fig.12.2-2. Shell balance of mass and enthalpy set up over a differential control volume of packed distillation columns

Fig.12.2-2 shows a schematic picture of control volume having differential height dz for setting up heat and mass balances.

For distillation processes, molar rates of vapor and liquid G_M and L_M can be assumed to be kept constant due to equimolar counter-diffusion.

Therefore, referring to Eqs.(12.1-3~6), the differential heat and mass balance equations can be written as

$$N_A S\,dz = G_M\,dy_A S = k_{yA}a\,(y_{Ai} - y_A)S\,dz = k_{xA}a\,(x_A - x_{Ai})S\,dz \quad (12.2\text{-}1)$$

$$Q\,S\,dz = G_M\,dH_G\,S = h_G a\,(T_G - T_i)S\,dz = h_L a\,(T_i - T_L)S\,dz \quad (12.2\text{-}2)$$

where G_M and L_M $(kmol/m^2\,s)$ are superficial molar velocities of vapor and liquid streams. The molar mass-flux N_A and enthalpy-flux Q have units of $(kmol/m^2 s)$ and (W/m^2), respectively.

Using the overall volumetric coefficients $K_{yA}a$ and Ua

$$G_M dy_A = K_{yA}a\,(y_A^* - y_A)dz \quad (12.2\text{-}3)$$

$$G_M\,dH_G = U\,a\,(T_G - T_L)dz \quad (12.2\text{-}4)$$

In these equations, the effective interfacial area per unit packed-bed volume a (m^2/m^3) is introduced.

Usually it is not so easy to measure vapor-liquid-contacting interfacial area a (m^2/m^3), so the overall volumetric coefficients $K_{yA}a$ and $K_{xA}a$ are employed for the packed bed mass transfer.

Similarly it is possible to define the following overall coefficient K_{xA} based on liquid-phase concentration:

$$N_A a\,Sdz = K_{xA}a(x_A - x_A^*)Sdz \quad (12.2\text{-}5)$$

where x_A^* is fictitious concentration in equilibrium with the vapor bulk concentration y_A.

According to Eq.(11.2-3),

$$dz = \frac{G_M}{K_{yA}a}\frac{dy_A}{y_A^* - y_A} \quad (12.2\text{-}6)$$

Assuming the coefficient $\frac{G_M}{K_{yA}a}$ to be constant, integration from column top to bottom gives

$$Z_T = \int_0^{Z_T} dz = \overline{\frac{G_M}{K_{yA}a}} \int_{y_{A1}}^{y_{A2}} \frac{dy_A}{y_A^* - y_A} \quad (12.2\text{-}7)$$

Here the quantity $H_{OG} = \overline{\frac{G_M}{K_{yA}a}}$ averaged over the column height is called "Height of a Transfer Unit." Strictly speaking, HTU actually increases in the vertical direction from the bottom toward the top of the packed bed. In order to calculate the total packed bed height Z_T required for a separation specification, however, the overall volumetric coefficient $K_{yA}a$ should be evaluated by considering the vapor-phase and the liquid-phase mass transfer, separately.

The interphase mass transfer resistance based on two film theory is expressed by

$$\frac{1}{K_{yA}} = \frac{1}{k_{yA}} + \frac{m}{k_{xA}} \quad (12.2\text{-}8)$$

where the slope of equilibrium curve m is used for conversion of liquid-phase to vapor-phase concentration unit.

If the vapor-phase and liquid-phase volumetric coefficients k_{yA} and k_{xA} are given, the total height of the packed column can be calculated with the aid of Eq.(12.2-8).

Concerning the mass transfer resistance, the following parameters are defined: Height of Overall Transfer Unit and Height of gas-phase and liquid-phase transfer units

$$H_{OG} = \frac{G_M}{K_{yA}a}, \quad H_{OL} = \frac{L_M}{K_{xA}a} \quad (12.2\text{-}9)$$

$$H_G = \frac{G_M}{k_{yA}a}, \quad H_L = \frac{L_M}{k_{xA}a} \quad (12.2\text{-}10)$$

Therefore multiplying Eq.(11.2-8) by molar vapor velocity G_M, the following equation is obtained indicating the two mass transfer resistances in series in the neighborhood of the interface:

$$H_{OG} = H_G + \lambda\,H_L \quad (12.2\text{-}11)$$

where $\lambda = m/(L/V)$ is the slope ratio of the equilibrium curve to the operating line, called "stripping factor.".
This equation is very important to check which phase resistance is predominant over the interphase mass transfer, vapor-phase or liquid-phase.

Although these mass transfer parameters are available in some degree in the correlation databank, we should consider it rather difficult to apply them for engineering column design without experiment for checking.

12.2-2 Efficiency of packed distillation columns

The concept of plate efficiency cannot be applied to packed distillation columns.

In place of the Murphree plate efficiency, the distillation efficiency of a packed column can be evaluated by the HETP (Height Equivalent to Theoretical Plate). This is defined as the total height of the packing section divided by the required number of theoretical stages. Therefore this characteristic value can be determined by comparing the result of distillation experiment conducted in a real packed column with the calculation result using the McCabe-Thiele stage-by-stage process simulation calculation based on the equilibrium-stage model in an ideal column. However if we consider local variation in distillation efficiency in a packed column, we should introduce a control volume approach for definition of the local HETP. Fig. 12.2-3 indicates the significance of HETP defined by using a control volume approach. In this case, the HETP can be defined as the control volume height of a real column required for the condition that the vapor (concentration y_{An}) leaving the control volume from the top should have an equilibrium relation with the liquid (concentration x_{An}) leaving from the bottom.

The mass balance of more volatile component A is set over the *n*th control volume as follows:

$$G_{Mn}y_{An} - G_{Mn+1}y_{An+1} = K_{yA,n}a\,(y^*_{An} - y_{An})_{l.m.}h_{ETP,n} \qquad (12.2\text{-}12)$$

where logarithmic mean of the concentration difference as the mass transfer driving forces is used between the top and bottom of each control volume. The concentration y^*_{An} is the bulk concentration of the liquid phase x_{An} converted with the units of the gas-phase concentration. This equation is similar to Eq. 12.2-3.

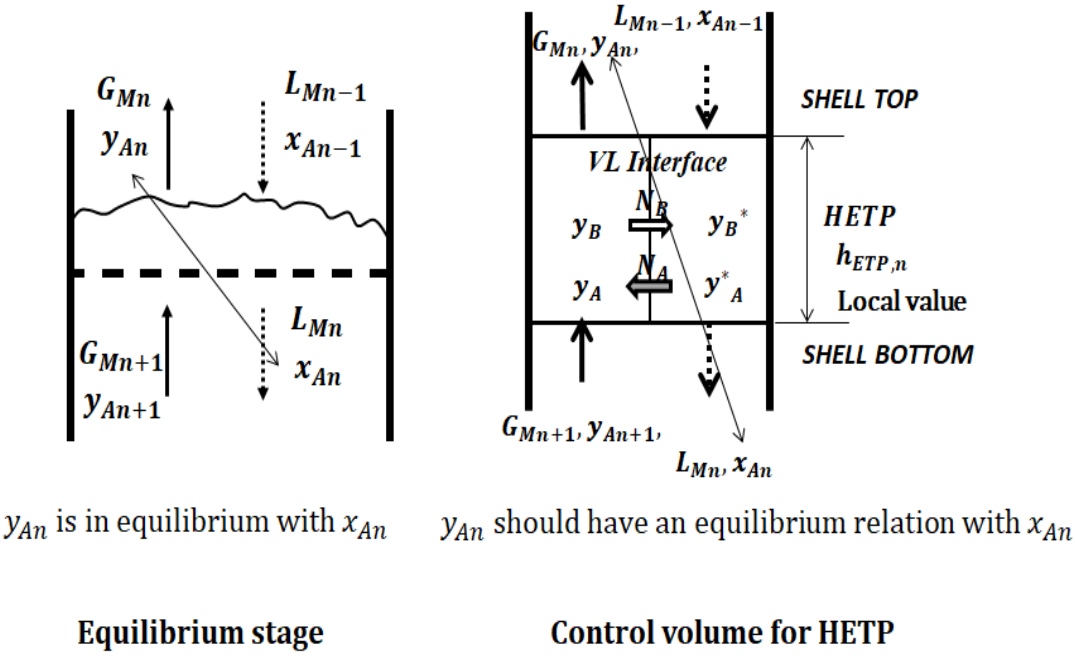

Fig. 12.2-3. Interrelation of HETP for a real packed column with equilibrium stage in an ideal column

If the required number of theoretical stages (i.e., control volumes) is *N*, the total height of the packed column Z_T for the given separation specification can be calculated as

$$Z_T = \sum_{n=1}^{N} h_{ETP,n} = \sum_{n=1}^{N} \frac{G_{Mn} y_{An} - G_{Mn+1} y_{An+1}}{K_{yA,n} a \left(y^*_{An} - y_{An}\right)_{l.m.}} \tag{12.2-13}$$

Usually $H_{OG} = G_M / K_{yA} a$ varies with vertical height of the packing section. For ideal solutions, G_{Mn} is kept almost constant. In addition, if we use an averaged value of H_{OG}, the above equation can be simplified as

$$Z_T = \sum_{n=1}^{N} h_{ETP,n} = \left(\frac{G_M}{K_{yA} a}\right)_{av} \sum_{n=1}^{N} \frac{y_{An} - y_{An+1}}{\left(y^*_{An} - y_{An}\right)_{l.m.}} \tag{12.2-14}$$

This equation coincides with Eq.(12.2-7).

[PROBLEM 12.2-P1] Fig.12.2-P1 shows the relation of HETP with H_{OG}. Derive the following relation between HETP and HTU_{OG}:

$$HETP = \frac{\ln \lambda}{\lambda - 1} H_{OG} \tag{12.2-P1}$$

where λ is the stripping factor defined by the slope ratio of equilibrium curve and operating line.

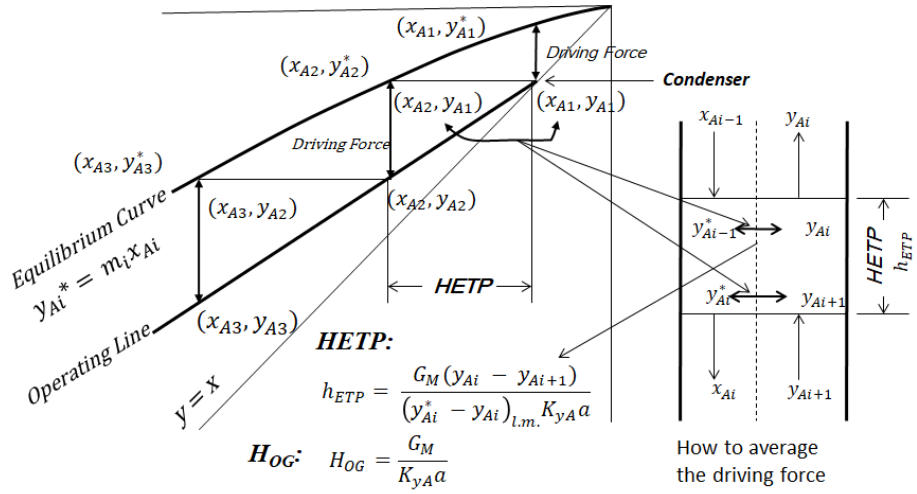

Fig. 12.2-P1. Relation of HETP with HTU.

12.3 Analogy between Mass and Enthalpy Transfer in a Packed Column Distillation Process[1,2)]

A packed column distillation process takes place with non-isothermal and counter-diffusional interphase mass transfer accompanied with phase transformation. Essentially the distillation efficiency such as HETP should vary streamwise upward in the vertical direction. There is an experimental work observing such a complicated transport phenomenon inside the packed distillation column. This work[1)] deals with a semi-empirical model by making up the mutual defects between the experiment in a real packed column and the computer-aided process simulation based on the equilibrium model. It is instructive to introduce here the experimental results obtained in a commercial-scale column equipped with wire-mesh corrugated structured packing.

Let us consider the mass transfer of more-volatile component A from the liquid- to the vapor-phase through the interface. The total-reflux distillation experiment was performed with methanol-ethanol binary system. Similarly to Eq.12.2-12, the interphase transfer of mass and enthalpy can be expressed by the following equations defining a cylindrical control volume shown in Fig. 12.3-1:

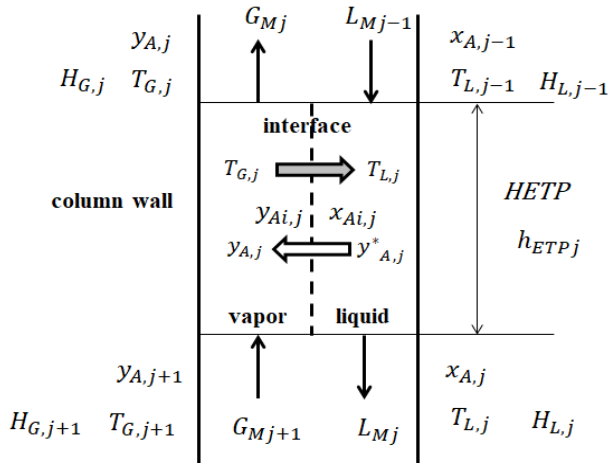

Fig. 12.3-1. Control volume of *j* th ideal stage defined in a real column

The shell balances of mass and enthalpy are set up over the j-stage control volume:
(Mass transfer)

$$G_{Mj}y_{Aj} - G_{Mj+1}y_{Aj+1} = (k_{yA}a)_j(y_{Aj,i} - y_{Aj})h_{ETPj} \quad (12.3\text{-}1)$$
$$= (k_{xA}a)_j(x_{Aj} - x_{Aj,i})h_{ETPj}$$
$$= (K_{yA}a)_j\left(y^*_{Aj} - y_{Aj}\right)_{l.m.} h_{ETPj}$$

(Enthalpy transfer)

$$G_{Mj+1}H_{Gj+1} - G_{Mj}H_{Gj} = (h_Ga)_j(T_{Gj} - T_{ij})h_{ETPj} \quad (12.3\text{-}2)$$
$$= (h_La)_j(T_{ij} - T_{Lj})h_{ETPj}$$
$$= (Ua)_j(T_G - T_L)_{l.m.}h_{ETPj}$$

It is a key point of modeling to give the height h_{ETPj} for defining the control volume.
Here G_{Mj}, L_{Mj} denote vapor and liquid molar velocity (kmol/m^{2}s), $k_{yA}a$, $k_{xA}a$, $K_{yA}a$ the volumetric mass transfer coefficients (kmol/m^{3}s), h_Ga, h_La, Ua the volumetric heat transfer coefficients (W/m^{3}K), y_A, x_A the vapor- and liquid-phase mole fractions of component A, and T_G, T_L the vapor- and liquid-phase temperatures (K). The subscript *j* indicates *j*th ideal stage and *i* implies the vapor-liquid interface. The asterisk y^*_{Aj} is the bulk concentration of the liquid phase expressed with the units of the vapor-phase concentration.
In this work, local variations of not only the mass and enthalpy transfer coefficients but also the HETPs are determined by the distillation experiment conducted in a real packed column with the aid of computer process simulation. An understanding of analogy between mass and enthalpy transfer is possible because the enthalpy transfer is fulfilled primarily by the transferring volatile components themselves.

It can be considered that the superficial vapor velocity is kept almost constant in the vertical direction in the packing section, similarly to the free stream of the boundary layer flow over a flat plate.

In order to consider the interrelation between mass and enthalpy transfer in the vapor-phase, the local j-factors for mass and enthalpy transfer are defined respectively as

$$j_{DG} = \frac{k_{yA}a}{a_pG_M}Sc_G^{2/3} \quad (12.3\text{-}3)$$

$$j_{HG} = \frac{h_Ga}{a_pCp_GG}Pr_G^{2/3} \quad (12.3\text{-}4)$$

In a manner similar to the local analysis of boundary layer flow over a flat plate, the following local length Reynolds number is defined on the basis of superficial relative velocity $u_s = u_{Gs} - u_{Ls}$:

$$Re_{zG} = \frac{u_s\rho_G(Z/d_{eq})}{a_p\mu_G} \quad (12.3\text{-}5)$$

where Z is the vertically upward distance from the bottom of the packing section, d_{eq} the equivalent diameter of the structured packing, and a_p the specific surface area per unit volume of the packing.

Fig.12.3-2 show one of the experimental results of the boundary-layer-like plot of j-factors against local Reynolds number. Here F is the F-factor defined at the top of the packing section for the experimental condition.

The F-factor defined by using the superficial vapor velocity u_{Gs} measured at the top and its vapor density ρ_G is

$$F = u_{Gs}\sqrt{\rho_G} \tag{12.3-6}$$

The position of the left-side ordinate shown in Fig.12.3-2 corresponds to the bottom of the packing section. It has been found that the local coefficients of mass and enthalpy transfer decrease downstream in the vertical direction like the boundary layer over a hot flat plate. If this control volume approach based on the superficial vapor velocity is approved, as shown in Fig.12.3-3, local variation of the j-factors in a packed distillation column resembles that of the single-phase boundary layer flow over a flat plate. Only the difference between the two cases is that the vapor stream with constant superficial velocity has streamwise variation of vapor composition in the packed column whereas the free stream has uniform constant concentration in the boundary layer flow. It can be conjectured that the same boundary-layer-like tendency can also be observed in the wetted-wall distillation column.

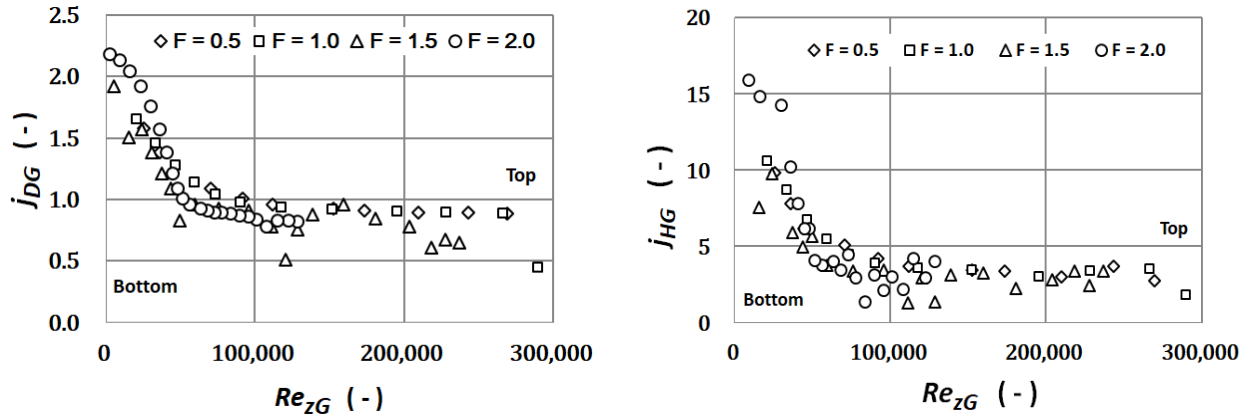

Fig.12.3-2. Similarity plot of j-factors against length Reynolds number

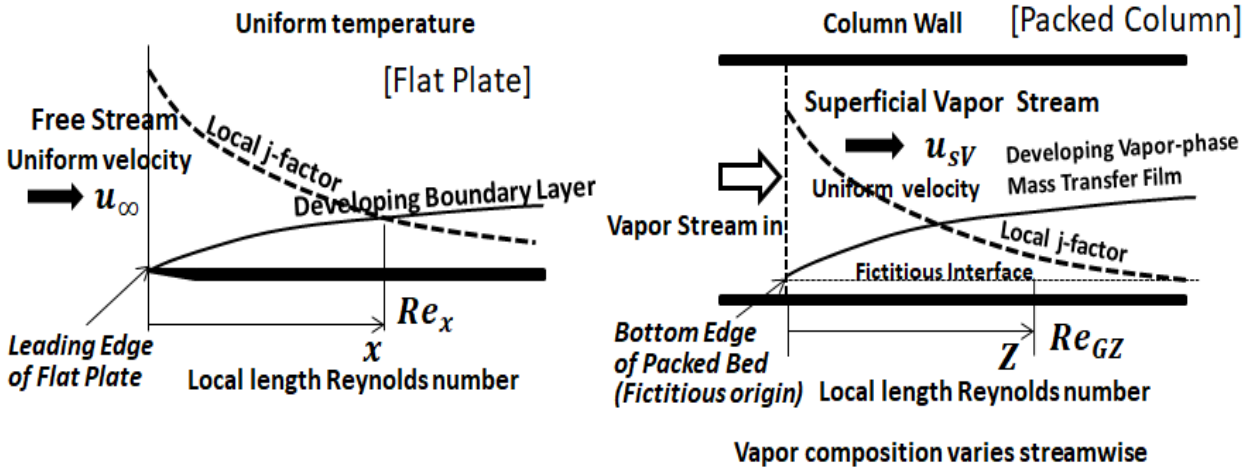

Fig.12.3-3. Comparison of packed column distillation with boundary layer flow over a flat plate

It is very interesting that the j-factors j_{DG}, j_{HG} indicate the same dependency of local length Reynolds numbers. This suggests that local similarity exists between simultaneous mass and enthalpy transfer in the vapor-phase film. Therefore $j_{HG}/j_{DG} =$ C (constant) leads to :

$$\frac{j_{HG}}{j_{DG}} = \frac{(h_G/Cp_G)}{k_{yA}} \left(\frac{Pr_G}{Sc_G}\right)^{2/3} \tag{12.3-7}$$

This implies that the distillation process takes place with the similar transfer processes expressed by

$$\frac{h_G/Cp_G}{k_{yA}} = C\ Le^{-2/3} \tag{12.3-8}$$

The liquid-phase j-factors also indicate similar dependency but the results are omitted owing to the complicated mechanism beyond the scope of the book.

Although the bottom edge of the packing section should correspond to the sharp leading edge of the flat plate, it can be taken into account that the fictitious origin $z = 0$ slightly shifts depending on the top F-factor.

1. Nishimura, G., Kataoka, K., Noda, H., and Ohmura, N., Proc. 30th European Symposium on Computer Aided Process Engineering (ESCAPE30), 1-6, May 24-27, Milano, Italy (2020)
2. Nishimura, G., Kataoka, K., Noda, H., and Ohmura, N., Journal of Advanced Chemical Engineering, Vol.11, Issue 2, (2021)

Nomenclature

a	effective interfacial area per unit packed volume, [m^2/m^3]
a_p	specific surface area per unit packed volume, [m^2/m^3]
Cp	heat capacity, [J/kmol K]
D_{ABG}, D_{ABL}	diffusivity in gas- and liquid-phase, [m^2/s]
d_{eq}	equivalent diameter, [m]
F	F-factor [(m/s)(kg/m^3)$^{0.5}$]
G	superficial vapor mass velocity, [kg/m^2s]
G_M	superficial molar vapor velocity, [kmol/m^2s]
$H_A,\ H_B$	latent heat (enthalpy) of component A, B, [J/kmol]
H_{OG}, H_G, H_L	height of transfer unit, OG:overall, G:vapor phase, L:liquid phase, [-]
$H_V,\ H_L$	enthalpy of vapor and liquid, [J/kmol]
h_{ETP}	HETP (Height Equivalent to a Theoretical Plate), [m]
h_G, h_L	vapor-phase and liquid-phase heat transfer coefficient, [W/m^2K]
$j_{DG},\ j_{HG}$	j-factor for mass and enthalpy transfer in vapor phase, [-]
K_x, K_y	overall mass transfer coefficients defined by vapor-phase and liquid-phase concentrations [kmol/m^2s]
k_x, k_y	mass transfer coefficients of vapor-phase and liquid-phase film [kmol/m^2s]
L_M	superficial molar liquid velocity, [kmol/m^2s]
m	slope of equilibrium curve, dy/dx,
N_A, N_B	molar mass flux of component A, B, [kmol/m^2s]
n	control volume/stage number, [-]
Q	enthalpy flux, [J/m^2s]
$Re_x,\ Re_z$	length Reynolds number, [-]
S	cross-sectional area of packed columns, [m^2]
Sc	Schmidt number, [-]
T_G, T_L	temperature of vapor- and liquid-phase, [K]
U	overall enthalpy transfer coefficient, [W/m^2K]
x_A, y_A	mole fraction of component A in liquid- and vapor-phase, [-]
z	vertical distance from the bottom of packing section, [m]
Z_T	total height of packing section, [m]
δ_G, δ_L	thickness of gas-phase and liquid-phase film, [m]
κ_G, κ_L	thermal conductivity of vapor- and liquid-phase, [J/m s K]
ϱ_G, ρ_L	molar density of vapor and liquid, [kmol/m^3]

Subscripts

A, B	component A, B
G, L	gas-phase, liquid-phase
i	interface
T	temperature

CHAPTER 13

SIMULTANEOUS HEAT AND MASS TRANSFER - II

13.1 Theory of Simultaneous Heat and Mass Transfer II (Humidification and Dehumidification)

When a condensable vapor A is condensed from a gas mixture, enthalpy transfer occurs by two effects: one is the conductive heat transfer due to the temperature gradient; the other is the enthalpy transfer due to the mass transfer.

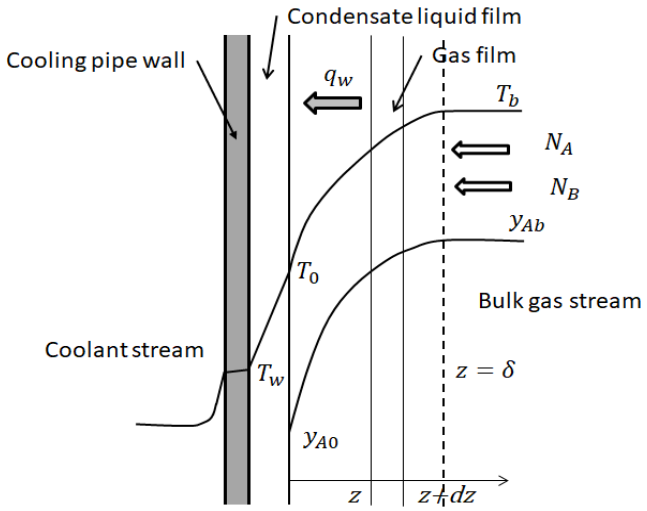

Fig.13.1-1. Schematic temperature and concentration profiles in the neighborhood of a cooling pipe wall

Fig-13.1 shows schematic picture of temperature and concentration profiles in the neighborhood of a cooling pipe wall, on which condensate liquid is falling filmwise.

Let us consider the enthalpy transfer through a gas-phase film of thickness δ on the gas-liquid interface. The total flux of enthalpy into the gas-phase film is made up of the conductive heat flux $-\kappa(\partial T/\partial z)$ and the enthalpy flux due to diffusion $N_A C_{pA}(T - T_0) + N_B C_{pB}(T - T_0)$.

Here T_0 is a standard-state temperature to be selected later, and C_{pA}, C_{pB} are the molar heat capacities of components A and B. The vertical variation in the thickness and composition of the gas-phase film is assumed to be small compared to the variation in the transverse z-direction.

From the mass balance over a differential control volume of thickness $dz \times 1 \times 1$

$$N_A|_{z+dz} - N_A|_z = 0 \quad \rightarrow \quad \frac{\partial N_A}{\partial z} = 0$$
$$N_B|_{z+dz} - N_B|_z = 0 \quad \rightarrow \quad \frac{\partial N_B}{\partial z} = 0 \qquad (13.1\text{-}1)$$

Therefore

$$N_A = N_{A0} = const$$
$$N_B = N_{B0} = const \qquad (13.1\text{-}2)$$

According to the Fick's law

$$N_A - y_A(N_A + N_B) = -c\,D_{AB}\,\frac{\partial y_A}{\partial z} \tag{13.1-3}$$

where y_A is mole fraction of component A and c the molar density of the gas-phase film.
Since $N_A = N_{A0}$ and $N_B = N_{B0}$, the equation becomes

$$N_{A0} - y_A(N_{A0} + N_{B0}) = -c\,D_{AB}\,\frac{\partial y_A}{\partial z}$$

Then the equation to be solved for the concentration distribution is

$$\frac{dy_A}{dz} - \frac{N_{A0}+N_{B0}}{cD_{AB}}\,y_A = -\frac{N_{A0}}{cD_{AB}} \tag{13.1-4}$$

Integration gives

$$y_A = \frac{N_{A0}}{N_{A0}+N_{B0}} + C_1\,exp\left(\frac{N_{A0}+N_{B0}}{cD_{AB}}\,z\right) \tag{13.1-5}$$

The integration constant C_1 can be evaluated using the boundary condition $y_A = y_{A0}$ at $z = 0$:

$$C_1 = y_{A0} - \frac{N_{A0}}{N_{A0} + N_{B0}}$$

Then the solution for concentration distribution in the gas film is

$$y_A = \frac{N_{A0}}{N_{A0}+N_{B0}} + \left(y_{A0} - \frac{N_{A0}}{N_{A0}+N_{B0}}\right) exp\left(\frac{N_{A0}+N_{B0}}{cD_{AB}}\,z\right) \tag{13.1-6}$$

That is

$$\frac{y_A - \frac{N_{A0}}{N_{A0}+N_{B0}}}{y_{A0} - \frac{N_{A0}}{N_{A0}+N_{B0}}} = exp\left(\frac{N_{A0}+N_{B0}}{cD_{AB}}\,z\right) \tag{13.1-7}$$

On the other hand, setting up the enthalpy balance over the same control volume,

$$-\kappa\left(\frac{\partial T}{\partial z} + \frac{\partial^2 T}{\partial z^2}\,dz\right) + \kappa\,\frac{\partial T}{\partial z} + N_A Cp_A(T - T_0)|_{z+dz} + N_B Cp_B(T - T_0)|_{z+dz} - N_A Cp_A(T - T_0)|_z - N_B Cp_B(T - T_0)|_z = 0$$

Then

$$-\frac{d^2 T}{dz^2} + \frac{N_A Cp_A + N_B Cp_B}{\kappa}\,\frac{dT}{dz} = 0 \tag{13.1-8}$$

The equation to be solved for the temperature distribution is

$$\frac{d^2 T}{dz^2} - K\,\frac{dT}{dz} = 0 \tag{13.1-9}$$

where $K = \frac{N_A Cp_A + N_B Cp_B}{\kappa}$

The boundary conditions are

$$T = T_b \quad \text{at} \quad z = \delta$$
$$T = T_0 \quad \text{at} \quad z = 0 \tag{13.1-10}$$

The solution is

$$T = T_0 + (T_b - T_0)\,\frac{1-\exp(C_0 z/\delta)}{1-\exp(C_0)} \tag{13.1-11}$$

where

$$C_0 = \frac{N_A Cp_A + N_B Cp_B}{\kappa/\delta}$$

The temperature gradient can be calculated as

$$\frac{\partial T}{\partial z} = (T_b - T_0)\,\frac{-(C_0/\delta)\exp(C_0 z/\delta)}{1-\exp(C_0)} \tag{13.1-12}$$

Using the heat transfer coefficient of the gas-phase film defined by the film theory, the heat flux at the interface is

$$q_w = \kappa\,\frac{\partial T}{\partial z}\Big|_{z=0} = -(\kappa/\delta)(T_b - T_0)\frac{C_0}{1-\exp(C_0)} = h\,(T_b - T_0)\,\frac{C_0}{\exp(C_0)-1} \tag{13.1-13}$$

$$\psi = \frac{C_0}{\exp(C_0)-1} \tag{13.1-14}$$

If we take the interface temperature T_0 as the standard-state temperature, q_w becomes equal to the total enthalpy flux at the interface. The function ψ is called the Ackermann correction factor for the mass transfer. If the Ackermann correction factor is plotted against the mass transfer rate factor C_0, we get Figure 13.1-2 .

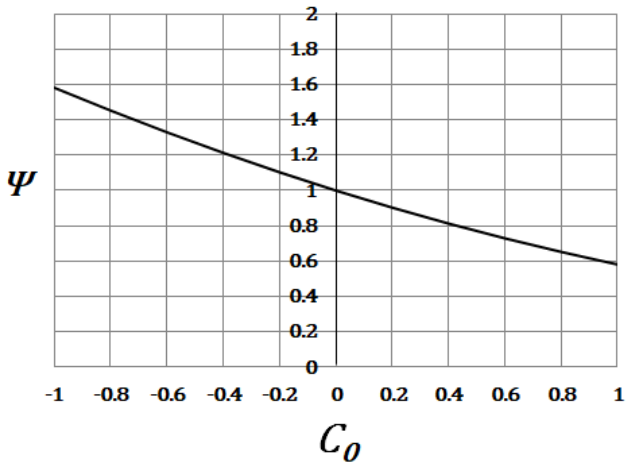

Fig. 13.1-2. Variation of the Ackermann correction factor with the mass transfer rate factor

In the case when the mass transfer of A and B is toward the interface, as in condensation, C_0 is negative. Then $\psi > 1$. This suggests that the apparent heat transfer coefficient $h\,\psi$ is increased by the mass transfer. In the case when the mass transfer of A and B is in opposite directions, as in evaporation, C_0 is positive. Then $\psi < 1$. This suggests that the apparent heat transfer coefficient $h\,\psi$ is decreased by the mass transfer.

For processes in which a phase change occurs at the interface, as in evaporation or condensation, an additional latent enthalpy effect should be taken into account. The total flux of enthalpy into the surface of condensate film which receives mass fluxes N_{A0} and N_{B0} is the sum of q_w and the latent enthalpy change

$$Q = q_w - (N_A \Delta H_A + N_B \Delta H_B) \tag{13.1-15}$$

Note that N_A and N_B are negative for condensation, but that Q and q_w are positive.
If only one component A condenses, $N_B = 0$. Then

$$N_A = -c\,D_{AB}\,\frac{1}{1-y_A}\,\frac{\partial y_A}{\partial z}$$

Since $N_A = N_{A0} = const$

$$\int_0^{\delta} N_{A0}\,dz = c\,D_{AB}\int_{y_{A0}}^{y_{Ab}} -\frac{dy_A}{1-y_A}$$

That is

$$N_{A0} = \frac{c\,D_{AB}}{\delta}\ln\frac{1-y_{Ab}}{1-y_{A0}} = k_y \ln\frac{1-y_{Ab}}{1-y_{A0}} \tag{13.1-16}$$

Here k_y is the mass transfer coefficient in the gas-phase film in kmol A/m^2 s.
The total enthalpy flux at the interface where only one component A condenses is

$$Q = h\,(T_b - T_0)\,\frac{C_0}{\exp(C_0)-1} - \Delta H_A\,k_y\,ln\frac{1-y_{Ab}}{1-y_{A0}} \tag{13.1-17}$$

Here $C_0 = N_A\,Cp_A/h$. Note that $ln\frac{1-y_{Ab}}{1-y_{A0}}$ is negative for condensation.

13.2 Simultaneous Heat and Mass Transfer for Humidification and Evaporative Cooling

13.2-1 Theory of wet-bulb temperature

Let us consider a wet- and dry-bulb thermos meter shown in Fig.13.2-1.

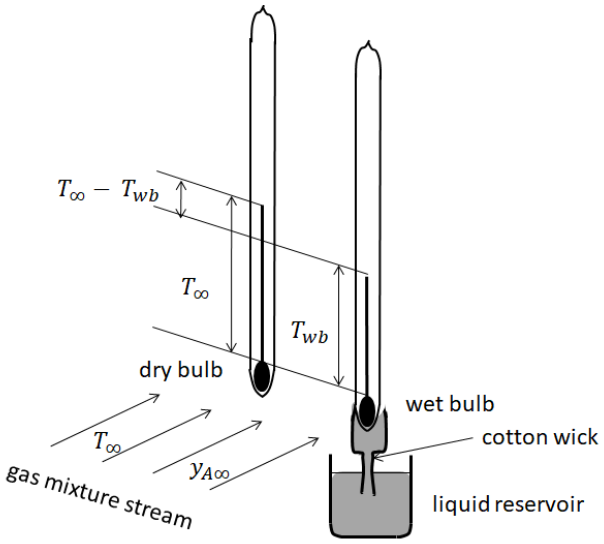

Fig. 13.2-1. Wet- and dry-bulb thermometers

One thermometer bulb (dry bulb) is left bare, and the other (wet bulb) is wrapped with cotton wick that is kept wet with a pure liquid A (Usually water). A gas mixture of condensable gas A (Usually water vapor) and non-condensable gas B (Usually air) flows over the thermometer bulbs.

The dry-bulb temperature is the same as the temperature of the approaching gas mixture T_∞. The wet-bulb temperature T_{wb}, which is approximately equal to the surface temperature of the wet wick, is kept lower than T_∞ owing to the steady evaporation of liquid A; heat is transferred to the gas-liquid interface of the wet wick and fresh liquid A is continuously supplied to the interface from the reservoir by capillary effect. At steady state the heat flux to the interface becomes equal to the enthalpy requirement for the evaporation of liquid A.

The mass flux due to evaporation at the interface is given by Eq. (13.1-16)

$$N_{A0} = k_y \ln \frac{1-y_{A\infty}}{1-y_{Awb}}$$

where k_y is the mass transfer coefficient in the gas-phase film and y_{Awb} is the gas concentration at the interface. The heat flux to the interface for evaporation is given by (13.1-13):

$$q_w = h_G\,(T_\infty - T_{wb})\,\frac{C_0}{\exp(C_0) - 1}$$

where T_{wb} is the temperature at the interface. Thus

$$h_G\,(T_\infty - T_{wb})\,\frac{C_0}{\exp(C_0)-1} = \Delta H_{ev}\,k_y \ln \frac{1-y_{A\infty}}{1-y_{Awb}} \qquad (13.2\text{-}1)$$

where ΔH_{ev} is the molar heat of evaporation. In this case $N_B = 0$ and $C_0 = N_A\,Cp_A/h_G$ is positive. According to the Colburn's analogy between heat and mass transfer

$$j_H = j_D \quad \text{or} \quad \frac{h_G}{Cp\,G}\,Pr^{2/3} = \frac{k_y}{G_M}\,Sc^{2/3} \qquad (13.2\text{-}2)$$

Here G_M is the molar velocity having units of kmol/m^{2}s.

Substituting the analogy into the above equation

$$(T_\infty - T_{wb})\,\frac{C_0}{\exp(C_0)-1} = \frac{\Delta H_{ev}}{Cp_m}\left(\frac{Pr}{Sc}\right)^{2/3} \ln \frac{1-y_{A\infty}}{1-y_{Awb}} \qquad (13.2\text{-}3)$$

where $Cp_m = M_{av}\,Cp$ is the molar specific heat of the approaching gas mixture. The ratio Pr/Sc is known as Lewis number Le. The mole fraction y_{Awb} at the interface is the equilibrium concentration, which can be determined by the vapor pressure p_{Avap} of liquid a at T_{wb} and the total pressure P:

$$y_{Awb} = p_{Avap}/P \qquad (13.2\text{-}4)$$

The approaching gas concentration $y_{A\infty}$ can be calculated using the above equation with the temperatures T_∞ and T_{wb} measured by the dry- and wet-bulb thermometer.

As a simpler example, consider the same wet- and dry-bulb thermometer for the air-water system. Since the Ackermann correction factor ψ is very close to unity in usual mass transfer situations, the heat input to the interface is

$$q_G = h_G\,(T_G - T_{wb}) \qquad (\mathrm{J/m^2 s}) \tag{13.2-5}$$

Introducing the humidity instead of the mole fraction of water vapor y_A,

$$H = \frac{M_A\,y_A}{M_B\,(1-y_A)} \qquad \left(\frac{\text{kg–water vapor}}{\text{kg–dry air}}\right) \tag{13.2-6}$$

where M_A and M_B are the molecular weights of water and air, respectively.

The mass transfer of water vapor from the interface is

$$N_A = k_H\,(H_{wb} - H_G) \tag{13.2-7}$$

where H_{wb} is the equilibrium humidity at the wet bulb temperature and k_H the mass transfer coefficient in kg-dry air/m^{2}s. At steady state all of the heat input is consumed for the evaporation of water and the interface temperature is kept at T_{wb}. Then the steady-state enthalpy balance is

$$h_G\,(T_G - T_{wb}) = \Delta H_{ev} k_H\,(H_{wb} - H_G) \tag{13.2-8}$$

where ΔH_{ev} is the heat of evaporation of water at T_{wb} (J/kg-water).

Introducing the mass humid heat capacity

$$C_H = Cp_a + H\,Cp_w \qquad \left(\frac{\text{J}}{\text{(kg–dry air)K}}\right) \tag{13.2-9}$$

The Colburn's analogy $(j_H = j_D)$ can be written as

$$\frac{h_G}{C_H G}\,Pr^{2/3} = \frac{k_H}{G}\,Sc^{2/3} \qquad \text{or}$$

$$\frac{h_G}{k_H C_H} = Le^{-2/3} \tag{13.2-10}$$

Here G is the mass velocity of the approaching gas on dry basis.

For the air-water system, the Lewis number is very close to unity. Then

$$\frac{h_G}{k_H C_H} \cong 1 \qquad \text{(air-water system)} \tag{13.2-11}$$

This is known as the Lewis relation.

Using the Lewis relation,

$$T_G - T_{wb} = \frac{\Delta H_{ev}}{C_H}\,(H_{wb} - H_G) \qquad \text{or}$$

$$C_H\,T_G + \Delta H_{ev}\,H_G = C_H\,T_{wb} + \Delta H_{ev}\,H_{wb} \tag{13.2-12}$$

This is an important equation for calculating the humidity H_G of the approaching air at T_G from the wet-bulb temperature T_{wb}.

The total enthalpy of humid air is defined as

$$i_H = C_H\,(T - T_0) + \Delta H_{ev}\,H \tag{13.2-13}$$

where T_0 is the standard-state temperature. Then the above equation becomes

$$i_{HG} = i_{Hwb} \tag{13.2-14}$$

The equation indicates that the enthalpy of the bulk humid air is equal to that of air saturated with water. The equation can be rewritten as

$$H_G = -\frac{C_H}{\Delta H_{ev}}\,(T_G - T_{wb}) + H_{wb} \tag{13.2-15}$$

If unsaturated air is brought into contact with the surface covered with liquid water, the air-water interface will be kept at the constant wet-bulb temperature T_{wb} while T_G and H_G change.

Next consider a spray chamber shown in Fig.13.2-2.

Unsaturated air entering at H and T is cooled and humidified by sprayed water. Water is circulated by a pump and small amount of water is continuously supplied to make up the evaporated water. At steady state the water temperature is kept at a definite saturation temperature T_{as}, and the air leaving the chamber is in equilibrium with the water. This is called "adiabatic-saturation temperature."

For the air-water system, the adiabatic-saturation temperature becomes essentially equal to the wet-bulb temperature.

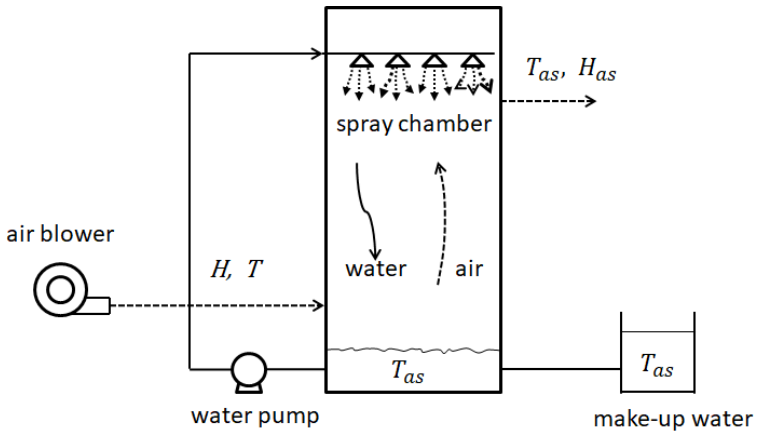

Fig.13.2-2. Spray chamber for air humidification

13.2-2 Humidity chart

A humidity chart for the air-water system at 1 atm is shown in Fig.13.2-3.

The line marked 100% gives the humidity of saturated air as a function of air temperature. Any point (H, T) below the saturation line represents an undersaturated mixture of air and water vapor. The slanting lines are called adiabatic-cooling lines, each of which is drawn with the slope of $-C_H/\Delta H_{ev}$ for a given constant adiabatic-saturation temperature. The relative humidity H_R is defined as the ratio of the partial pressure of the water vapor to the vapor pressure of water at the gas temperature.

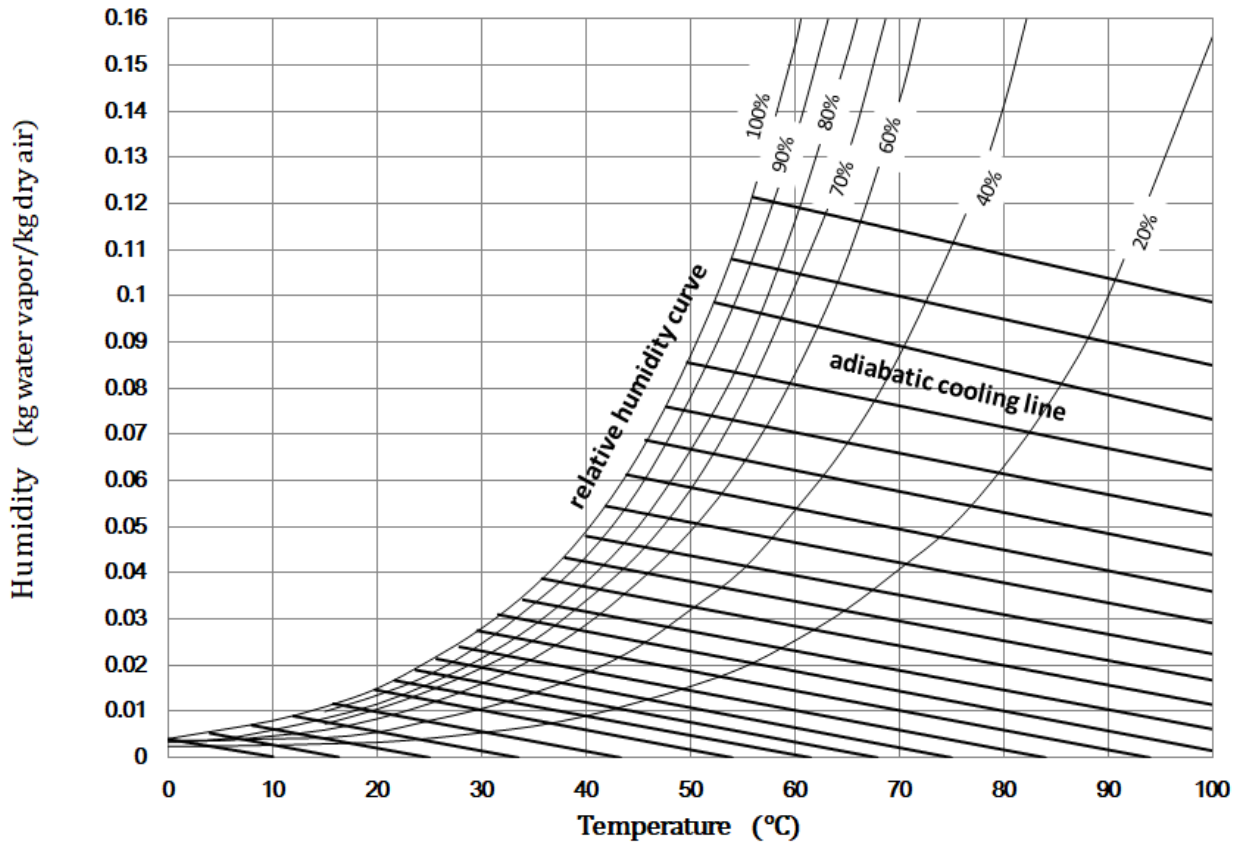

Fig.13.2-3. Humidity Chart (Air-water system at 1 atm)

[EXAMPLE 13.2-1] A water droplet initially having a diameter $Dp = 3$ mm is suspended in the humid hot air stream (temperature $T_b = 98\,C = 371\,K$, humidity $H_b = 0.03$ kg-water/kg-dry air, pressure $p = 1$ atm $= 1.0133 \times 10^5$ Pa, average velocity $v_\infty = 0.3$ m/s). What are the temperature and humidity of the droplet surface? How long does it take for the droplet to be completely evaporated? The average mass transfer coefficient around a sphere is given by the Ranz and Marshall equation:

$$\frac{v_f k_H Dp}{D_{AB}} = 2 + 0.6\left(\frac{\rho_f v_\infty Dp}{\mu_f}\right)^{1/2} Sc^{1/3}$$

The physical properties for the humid air are given by

$$\mu = 10.53 \times 10^{-6}\sqrt{T}$$

$$D_{AB}\,v = 5.01 \times 10^{-9}\sqrt{T^3}$$

$$Sc = 0.60$$

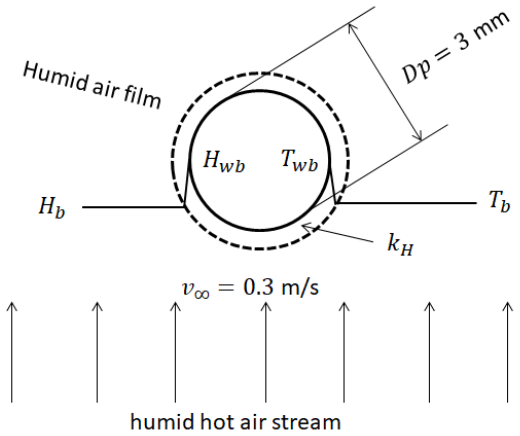

Fig.13.2-E1. Water droplet surrounded by hot humid air stream

Solution:

The interface temperature should be the wet-bulb temperature T_{wb} and the interface humidity is the equilibrium humidity H_{wb} corresponding to T_{wb}. From the humidity chart, $T_{wb} = 42$ C = 315 K, and $H_{wb} = 0.054$ kg-water/kg-dry air. The film temperature and humidity are $T_f = (T_{wb} + T_b)/2 = 70$ C = 343 K, $H_f = (H_{wb} + H_b)/2 = 0.041$ kg-water/kg-dry air. At this film condition, the specific volume $v_f = 1.03$ m^3/kg-dry air. The density is

$\rho_f = (1$ kg-dry air/kg-dry air $+ 0.041$ kg-water/kg-dry air $)/(1.03$ m^3 humid air/kg-dry air$) = 1.01$ kg/m^3.

The viscosity is

$$\mu_f = 10.53 \times 10^{-6}\sqrt{343} = 1.95 \times 10^{-5} \text{ kg/m s}$$

$$D_{AB} = 5.01 \times 10^{-9}(343)^{3/2} = 0.318 \times 10^{-4} \text{ m}^2\text{/s}$$

From the Ranz and Marshall equation

$$k_H = \frac{D_{AB}}{v_f Dp}\left(2 + 0.6\left(\frac{v_\infty Dp\,\rho_f}{\mu_f}\right)^{\frac{1}{2}} Sc^{\frac{1}{3}}\right)$$

$$= \frac{0.318 \times 10^{-4}}{1.03\,Dp}\left(2 + 0.6\left(\frac{0.3 \times Dp \times 1.01}{1.95 \times 10^{-5}}\right)^{\frac{1}{2}}(0.6)^{\frac{1}{3}}\right) = \frac{1}{Dp}\left(0.6175 \times 10^{-4} + 0.003245\sqrt{Dp}\right) \quad (1)$$

The mass transfer of water vapor can be expressed for the droplet:

$$\frac{d}{dt}\left(\frac{\pi}{6}\,Dp^3\,\rho_L\right) = k_H(\pi\,Dp^2)(H_{wb} - H_b) \quad (2)$$

where ρ_L is the water density. From the equation,

$\frac{d\,Dp}{dt} = \frac{2(H_{wb} - H_b)}{\rho_L}\, k_H = \frac{2(0.054-0.03)}{1000}\, k_H = 4.8 \times 10^{-5}\, k_H$ (3)

Substituting Eq. (1) into Eq. (3)

$\frac{d\,Dp}{dt} = \frac{1}{Dp}\,(2.964 \times 10^{-9} + 1.5576 \times 10^{-7}\sqrt{Dp}\,)$ (4)

This equation can be numerically integrated to get the required time. The result is given in the following table.

Table 13.2-E1 Numerical calculation of time required for evaporation of a water droplet

t (min)	T (s)	Δ t (s)	Dp (m)	Δ Dp (m)
0	0	60	0.003	
1	60	60	0.00277	0.000230
2	120	60	0.00253	0.000242
3	180	60	0.00227	0.000256
4	240	60	0.00200	0.000274
5	300	60	0.00170	0.000298
6	360	60	0.00137	0.000331
7	420	60	0.000988	0.000382
8	480	60	0.000511	0.000477
8.66	519.4	39.4	0	0.000511

The time required for the evaporation of the droplet is 8.66 min.

13.3 Evaporative Cooling ----- Water Cooling Tower -----

Water can be cooled by exposing its surface to air. Packed towers are widely used in order to get cool water to be recirculated for heat exchangers and other process equipment.

Fig. 13.3-1 shows a water cooling tower. Water to be cooled is brought into contact with air whose adiabatic-saturation temperature is lower than the water temperature. The air entering at the side of the tower flows up across the water stream as it falls through the packing.

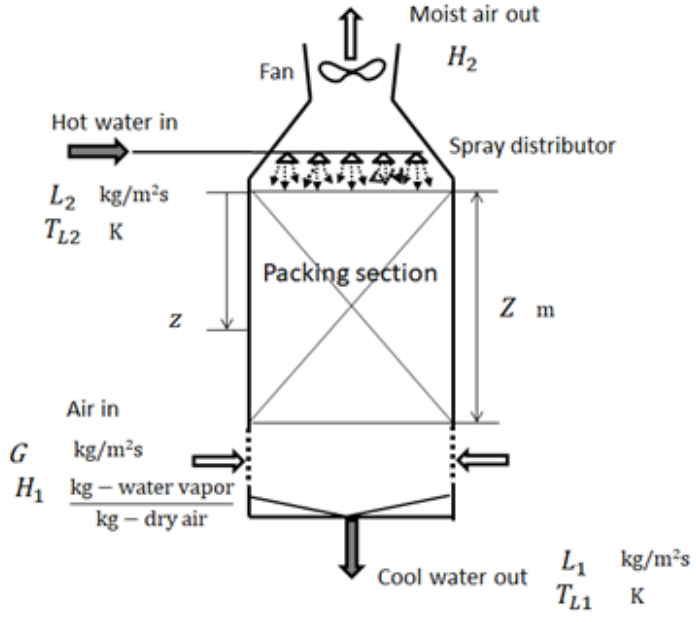

Fig. 13.3-1. Water cooling tower

The material balances of water are

$$L_2 - L_1 = G\,(H_2 - H_1) \quad (13.3\text{-}1)$$

$$L_2 - L = G\,(H_2 - H) \quad (13.3\text{-}2)$$

where G is the mass velocity of the air on dry basis.

Similarly the enthalpy balances are

$$G\,(i_{G2} - i_{G1}) = L_2 Cp_L T_{L2} - L_1 Cp_L T_{L1} \quad (13.3\text{-}3)$$

$$G\,(i_{G2} - i_G) = L_2 Cp_L T_{L2} - L Cp_L T_L \quad (13.3\text{-}4)$$

The rate of water evaporation $(L_2 - L_1)$ is small compared with the liquid flow rate L_2:

$$L_2 \cong L_1 \cong L \quad (13.3\text{-}5)$$

Then the above enthalpy balance equation can be approximated as

$$G(i_{G2} - i_{G1}) \cong L_2 Cp_L (T_{L2} - T_{L1}) \quad (13.3\text{-}6)$$

and

$$G(i_{G2} - i_G) \cong L_2 Cp_L (T_{L2} - T_L) \quad (13.3\text{-}7)$$

The last equation can be rewritten as

$$i_G = \frac{L_2 Cp_L}{G}(T_L - T_{L2}) + i_{G2} \quad (13.3\text{-}8)$$

This is called the operating line equation.

The mass balance taken around a differential section of height dz is

$$dL = G\,dH = k_H a\,(H^* - H)\,dz \quad (13.3\text{-}9)$$

The transfer rate of sensible heat in the gas-phase film is

$$dq_G = h_G a\,(T^* - T_G)\,dz = G\,C_H dT_G \quad (13.3\text{-}10)$$

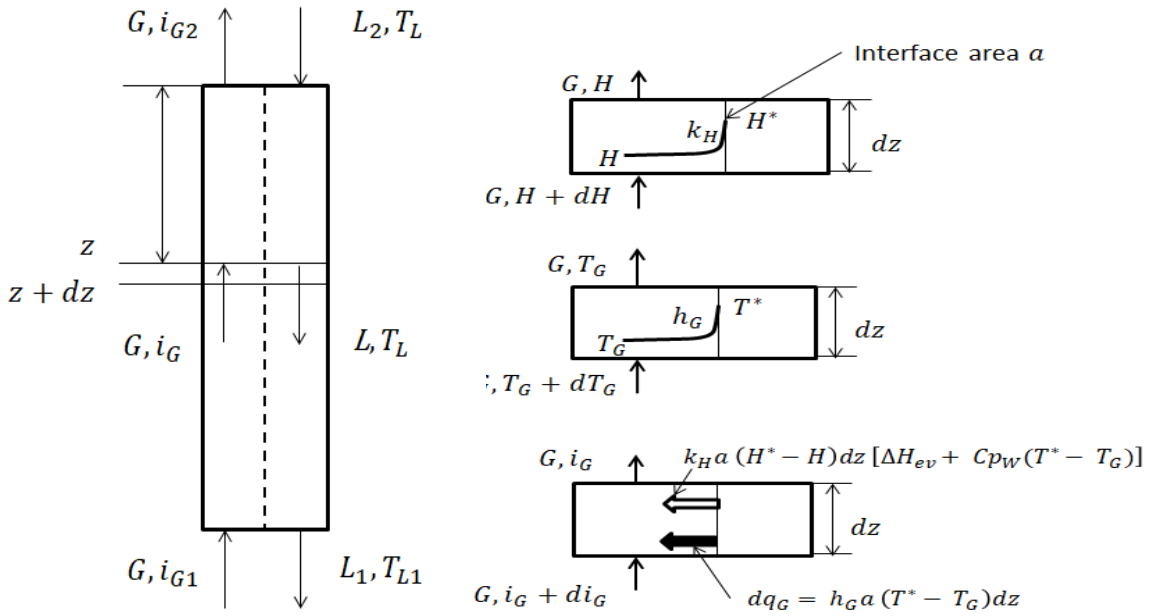

Fig. 13.3-2. Shell balance of mass and enthalpy

The rate of heat transfer in the liquid-phase film is

$$dq_L = h_L a\,(T_L - T^*)dz = L\,Cp_L\,dT_L \quad (13.3\text{-}11)$$

Introducing the total enthalpy of humid air

$$i_G = C_H\,(T_G - T_0) + \Delta H_{ev} H \quad (13.3\text{-}12)$$

The enthalpy transfer due to the evaporated water is

$$G\,dH\,[\Delta H_{ev} + Cp_W\,(T^* - T_G)] \quad (13.3\text{-}13)$$

Here T^* is the interface temperature, which is kept at the wet-bulb temperature. The Cp_W is the

heat capacity of water vapor. The enthalpy balance around the same differential section of height dz is

$$G\,di_G = h_G a(T^* - T_G)dz + k_H a\,(H^* - H)dz\,[\Delta H_{ev} + Cp_W(T^* - T_G)]$$
$$= k_H a\,dz\left[(i_G^* - i_G) + \left(\frac{h_G}{k_H C_H}C_H - Cp_a\right)(T^* - T_G)\right] \quad (13.3\text{-}14)$$

For the air-water system

$$\frac{h_G}{k_H C_H}C_H - Cp_a \cong Cp_a\left(\frac{h_G}{k_H C0_H} - 1\right) \cong 0 \quad (13.3\text{-}15)$$

Then we get

$$G\,di_G = k_H a(i_G^* - i_G)\,dz \quad (13.3\text{-}16)$$

The required height of packing is

$$Z_T = \int_0^{Z_T} dz = \frac{G}{k_H a}\int_{i_{G1}}^{i_{G2}} \frac{di_G}{i_G^* - i_G} = H_{TG}N_G \quad (13.3\text{-}17)$$

where

$$N_G = \int_{i_{G1}}^{i_{G2}} \frac{di_G}{i_G^* - i_G} \quad \text{and} \quad H_{TG} = \frac{G}{k_H a}$$

The above equation can be approximated as

$$Z_T = \frac{G}{k_H a}\frac{i_{G2} - i_{G1}}{(i_G^* - i_G)_{l.m.}} \quad (13.3\text{-}18)$$

Fig. 13.3-3 shows the relation between the equilibrium line and operating line.

$$G\,di_G = k_H a(i_G^* - i_G)\,dz$$
$$G\,C_H\,dT_G = h_G a\,(T^* - T_G)dz \quad (13.3\text{-}19)$$

Dividing the former equation by the latter equation

$$\frac{di_G}{dT_G} = \left(\frac{k_H C_H}{h_G}\right)\frac{i_G^* - i_G}{T^* - T_G} \cong \frac{i_G^* - i_G}{T^* - T_G} \quad (13\text{-}.3\text{-}20)$$

Similarly

$$G\,di_G = k_H a(i_G^* - i_G)\,dz$$
$$L\,C_L\,dT_L = h_L a\,(T_L - T^*)\,dz \quad (13.3\text{-}21)$$

Dividing the former equation by the latter equation

$$\frac{di_G}{dT_L} = \frac{L\,C_L}{G}\left(\frac{k_H}{h_L}\right)\frac{i_G^* - i_G}{T_L - T^*} \quad (13.3\text{-}22)$$

This is called the tie line equation which gives the relation between (i_G, T_L) and (i_G^*, T^*).

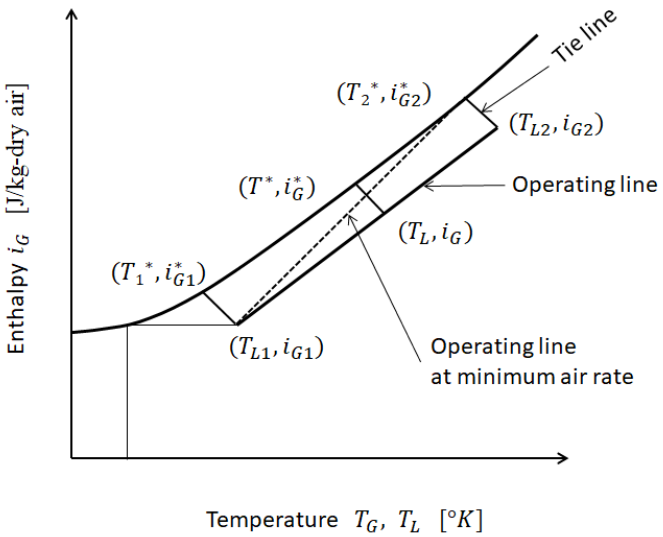

Fig.13.3-3. Relation of operating line with equilibrium line

Nomenclature

a	effective interfacial area, [m^2/m^3 packed volume]
C_H	mass humid heat capacity, [J/(kg-dry air)K]
Cp	heat capacity, [J/kg K]
D_{AB}	diffusivity, [m^2/s]
Dp	diameter of droplet, [m]
G	flow rate of dry air, [kg/s]
H	humidity, [kg-water vapor/kg-dry air]
H_{TG}	HTU (Height of Transfer Unit) of packed bed, [m]
h	heat transfer coefficient, [W/m^2K]
h_G	gas-film heat transfer coefficient, [W/m^2K]
i_G, i_H	total enthalpy of humid air, [J/kg-dry air]
k_H	mass transfer coefficient, [kg-dry air/m^2s]
k_y	gas-film mass transfer coefficient, [kg/m^2s/mass fraction]
Le	Lewis number, [-]
L	liquid (water) flow rate, [kg/s]
N_G	NTU (Number of Transfer Unit) of packed bed, [-]
N_A, N_B	mass flux of component A, B, [kg/m^2s]
p_{Avap}	vapor pressure of water
Pr	Prandtl number. [-]
q_G	enthalpy flux, [J/m^2s]
q_w	heat flux at wall, [J/m^2s]
Sc	Schmidt number, [-]
T_G, T_L	gas and liquid temperature, [K]
T_∞, T_w	temperature at gas bulk and wall, [K]
t	time, [s]
v	velocity
y	mass fraction, [-]
z	distance from condensate film surface, [m]
ΔH_{ev}	heat of evaporation of water, [J/kg]
δ	thickness of gas-phase film, [m]
κ	thermal conductivity of gas phase, [J/m s K]
ψ	Ackermann correction factor, [-]

Subcripts

f	film
H	humid
L	liquid
W	water
wb	wet-bulb
0	surface of condensate film
1, 2	inlet, outlet

CHAPTER 14

IONIC MASS TRANSPORT

14.1 Electrolytic Cell

It should be kept in mind that the transport phenomena occurring during electrolysis are so complicated that we had better study a very simple case of ionic mass transfer in an aqueous electrolytic cell.

Let us consider an electrolytic cell in which two electrodes are separated by an ionically conducting liquid such as an aqueous solution of electrolyte. If an electric current generated by an external emf (electromotive force such as potential difference or voltage) flows through the electrolytic cell, an electrode reaction takes place by the following three steps:

(1) Transfer of ions from the bulk of the solution to the surface of either of the two electrodes
(2) Electrochemical reactions at both electrodes
(3) Formation of reaction products and their deposition on the surface of the electrodes or their removal from that surface

This phenomenon can be considered as a special case of a heterogeneous chemical reaction.

Generally the diffusivity D_{AB} m^2/s for a single electrolyte at infinite dilution is given by the Nernst-Haskell equation:

$$D_{AB} = \frac{RT}{Fa^2} \frac{(1/n_+ + 1/n_-)}{(1/\lambda_+^0 + 1/\lambda_-^0)}$$

where T is temperature (K), R is gas constant (J/K kmol), λ_+^0, λ_-^0 are the limiting ionic conductances of cation and anion, respectively $(A/m^2)(V/m)(kg\text{-}equiv/m^3)$, n_+, n_- are the valences of cation and anion, respectively (-), and Fa is Faraday constant (A s/kg-equiv.).

In a system of mixed electrolytes, the unidirectional diffusion of each ion species results from a combination of electrical potential and concentration gradients.

As shown in Fig. 14.1-1, an anode of metal M undergoes the dissolution by the anode reaction to generate M^+ ions. The M^+ ions arriving at the cathode receive electrons due to the cathode reaction (discharge of metal ions) and the deposition of the reduced M occurs on the cathode surface.
The molar flux of M^+ ions transferring in the electrolytic solution at rest is given by

$$N_A = -c\, D_{AB} \left[\nabla x_A + \frac{M_A x_A}{R\,T} \frac{\epsilon_A}{m_A} \nabla\Phi\right] \qquad (14.1\text{-}1)$$

where x_A is mole fraction of M^+ ions, M_A the molecular weight, ϵ_A the ionic charge, and m_A the ionic mass.

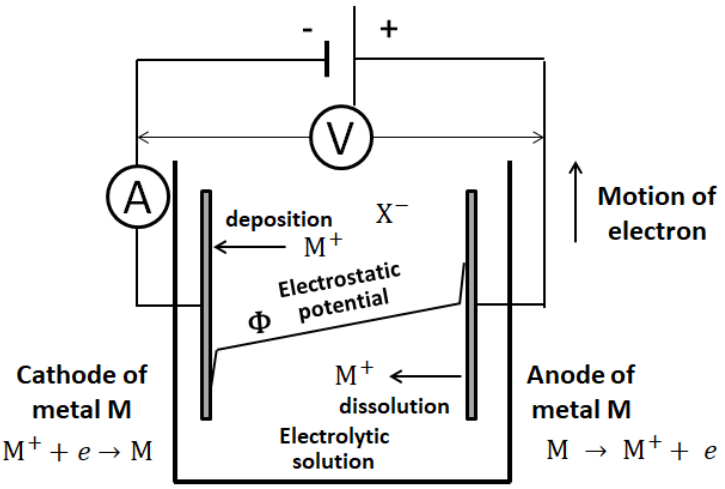

Fig. 14.1-1. Electrolytic cell (aqueous solution of electrolytic ions M^+ and X^-)

The first term implies the ordinary diffusion due to the concentration gradient ∇x_A of ions and the second term the electric diffusion due to the electrostatic potential $\nabla\Phi$. The ions are moved by the Coulomb force generated due to the gradient of the electrostatic potential.
The rate of the electrochemical reaction, i.e., the electric current flowing through the cell increases rapidly with the applied emf.

14.2 Ionic Mass Transport in an Electrochemical Reaction System

Let us consider an aqueous solution of salts in an electrolytic cell. In general, the individual species diffuse irreversibly when they are subjected to several unequal external forces. For simplicity, we neglect the effects of pressure, gravity, and thermal diffusions. Then we shall consider the ordinary diffusion due to the concentration gradients and the forced diffusion due to the electrostatic force. We shall furthermore confine our attention to a dilute solution of copper sulfate with sulfuric acid serving as the unreactive supporting electrolyte.

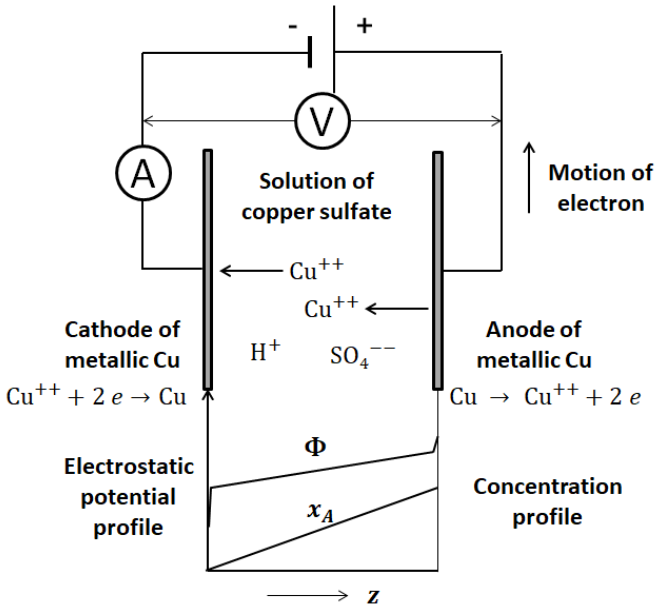

Fig. 14.2-1. Electrolytic cell filled with aqueous solution of electrolytes: Cu^{++}, H^+, SO_4^{--}

Let us consider a simple cell (Fig. 14.2-1) filled with a ternary electrolytic solution of three ionic species: Cu^{++}, H^{+}, SO_4^{--}. A voltage is imposed upon the cell that is sufficient to cause the copper ion concentration at the cathode to drop essentially to zero. The only electrode reactions are dissolution of the anode (copper plate) and deposition of Cu^{++} on the cathode. The molar flux of the Cu^{++}, that is, the electrode reaction rate is proportional to the current density in the cell. When the voltage imposed between the anode and cathode is increased, the reaction rate is increased. The distribution of electrostatic potential shown in Fig.14.2-1 is formed in the condition when the electrical conductivity is not very high owing to the dilute solution. However the concentration of the unreactive supporting electrolyte becomes so high that the gradient of electrostatic potential reduces to almost zero owing to very high electrical conductivity of the solution. In this condition, the copper ions diffuse only due to the concentration gradient of the reactive ions Cu^{++}.

14.3 Mass Transfer Measurements by an Electrochemical Technique[1,2,3,4)]

If the concentration of sulfuric acid is sufficiently high, the electric conductivity becomes so high that the gradient of the electrostatic potential becomes negligibly small over the entire electric field in the cell. In this state the copper ions diffuse only due to the ordinary diffusion. Most of the voltage drop between the anode and cathode occurs in the electric double layers formed on the surfaces of these electrodes. The thickness of the electric double layers is negligibly small as compared to the diffusion layer. When the electrode voltage E is increased, the current density I shows the variation shown in Fig.14.3-1. When the electrode potential E exceeds the characteristic discharge potential V_0, the deposition of Cu starts at the cathode. When E becomes sufficiently large (larger than E_d), the current density no longer increases owing to the insufficient supply of Cu^{++} by mass transfer. This is called the diffusion-controlling condition or the limiting current condition. That is, the electrode reaction is controlled by the mass transfer of Cu^{++} ions.

In this condition, the concentration of Cu^{++} becomes essentially zero on the cathode surface.

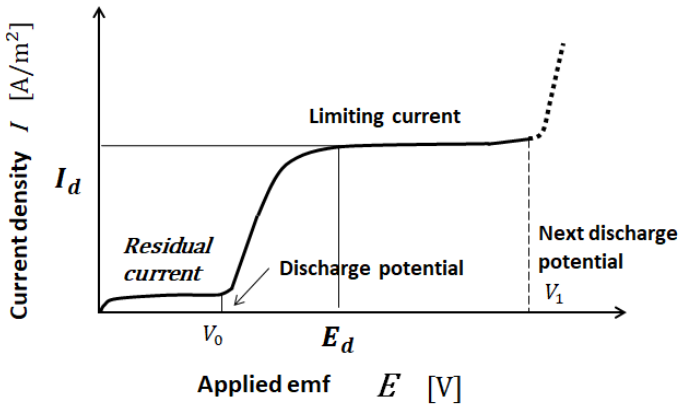

Fig. 14.3-1. Variation of current density with electrode voltage

If the applied emf becomes further greater than the next discharge potential V_1, the next electrode reaction will occur, as shown by the dotted line in Fig.14.3-1. For example, in this case, hydrogen bubbles due to the discharge of hydrogen ions may be released from the cathode surface.

It is possible to observe time-dependent, local coefficients of convective mass transfer if we utilize the electrochemical technique above mentioned.[1,4)]

For example, the working fluid is an aqueous solution having equimolar concentrations (0.01 M)

of potassium ferri- and ferro-cyanide and a 1 M concentration of potassium hydroxide KOH as an unreactive supporting electrolyte.[2,3)]

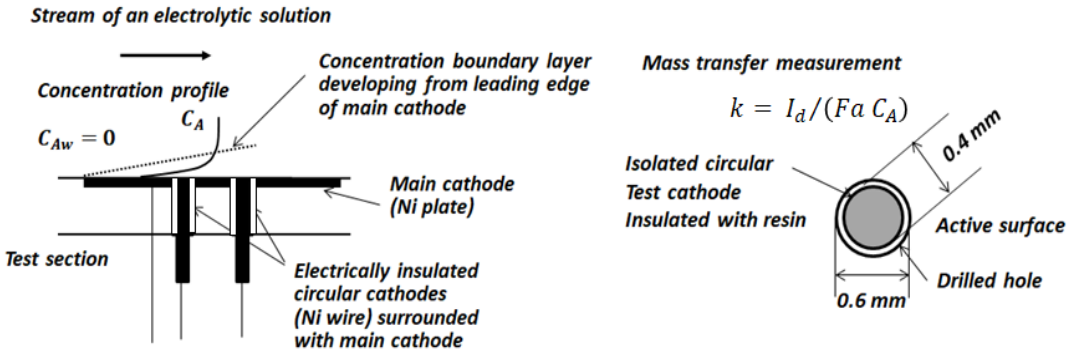

Fig. 14.3-2. Position of main and isolated test cathodes. Dimensions given are in mm.

Its Schmidt number is kept at $Sc = 1{,}800$ by controlling the fluid temperature.

As shown in Fig. 14.3-2, a nickel plate is stuck on the surface of the test section serving as the main cathode. Another large plate is placed as the anode, usually somewhere on the downstream side.

The following electrode reaction takes place under the diffusion-controlling condition:

[cathode] $Fe(CN)_6^{3-} + e^- \rightarrow Fe(CN)_6^{4-}$ [anode] $Fe(CN)_6^{4-} \rightarrow Fe(CN)_6^{3-} + e^-$

In this case, an electrode reaction does not involve deposition of material, but merely a change in the valence of an ion.

A small circular cathode made from nickel wire is embedded into a circular drilled hole drilled on the wall of the main cathode. The surface area of the main cathode is much smaller than that of the anode. Therefore the current density I A/m^2 at the anode becomes so small that the convective ionic mass transfer on the cathode only can be observed. In addition, if the small circular cathode (test cathode) is held at the same potential as the main cathode, local time-dependent mass transfer can be observed at the position of the test cathode.

The ionic mass flux N_A is given by

$$N_A = I_d/Fa = k(C_A - C_{Aw}) \qquad (14.3\text{-}1)$$

Under the diffusion-controlling condition, the concentration of $Fe(CN)_6^{3-}$ on the cathode surface C_{Aw} becomes zero. Then the local mass transfer coefficient k m/s is calculated by the equation:

$$k = I_d/Fa\ C_A \qquad (14.3\text{-}2)$$

where I_d (A/m^2) is the limiting current density on the test cathode, Fa the Faraday constant (= 96,500 C/kg-equiv.) and C_A the bulk concentration of $Fe(CN)_6^{3-}$ in kg-equiv./m^3. Since the concentration becomes zero on the cathode surfaces in the limiting current condition, the term C_A in Eq. (14.3-1) implies the concentration difference as the driving force.

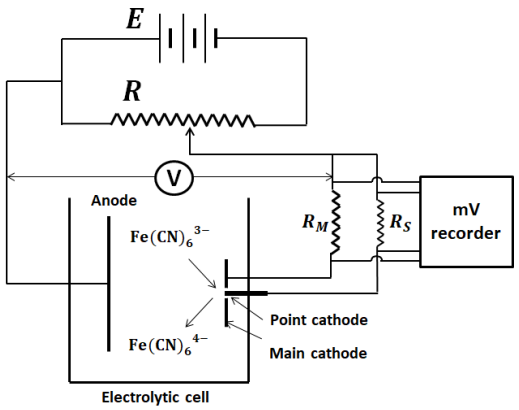

Fig. 14.3-3 Simple circuit for observing time-dependent ionic mass transfer

The fluctuating electric current which the $Fe(CN)_6^{3-}$ ions discharge on the test cathode (surface area S) can be observed as the time-dependent local mass flux of $Fe(CN)_6^{3-}$ions. A simple circuit is shown in Fig. 14.3-3. The time-dependent current density $i_d = (V_s/R_s)/S$ at the point cathode can be observed from the voltage drop V_S at the standard resistance R_S.

1. Kataoka, K., H. Doi and T. Komai: *Int. J. Heat Mass Transfer,* vol.20, pp.57-63 (1977).
2. Kataoka, K., Y. Kamiyama, S. Hashimoto and T. Komai: *J. Fluid Mech.*, vol.119, pp.91-105 (1982).
3. Hanratty, T. J.: *Phys. Fluids Suppl.*, vol.10, S126 (1967).
4. Mizushina, T.: Advances in Heat Transfer (1971), Vol.7, p.87. Academic.

14.4 Measurements of Velocity Gradient on a Wall[2,3,4)]

In addition, this electrochemical method can also measure local, time-dependent values of the velocity gradient on a solid surface for liquid flow observation. As shown in Fig.14.4-1, rectangular test cathodes are fabricated by inserting L mm thick nickel sheets into L_B mm long slits. The velocity-gradient measurement is carried out by measuring the limiting current between the test cathode and the anode.

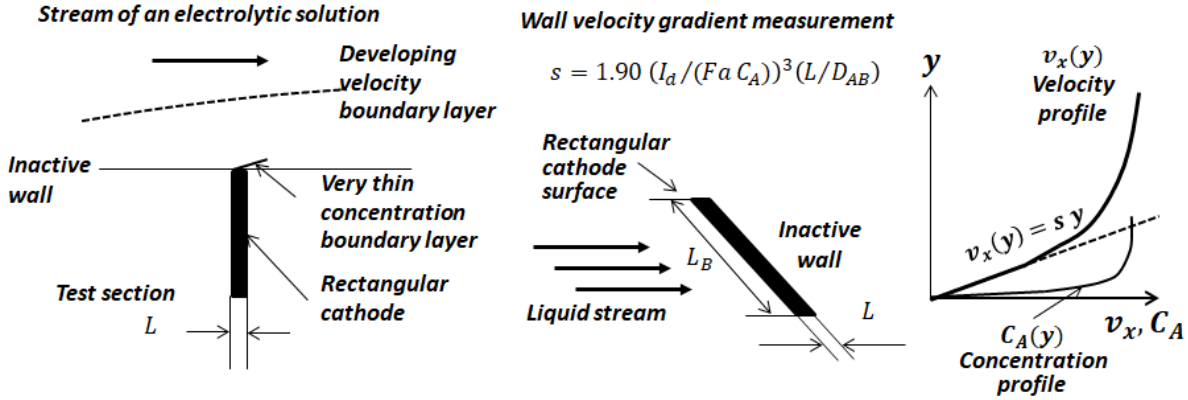

Fig.14.4-1 Isolated cathode for measuring velocity gradient on the wall

Owing to the high Schmidt number ($Sc = 1{,}800$ for an electrolytic solution of $Fe(CN)_6^{3-}$ and $Fe(CN)_6^{4-}$), the concentration boundary layer developing from the leading edge of a test cathode is much smaller in the thickness than the velocity boundary layer. Therefore the velocity can be assumed to be linear near the wall.

By measuring the current density I_d on each test cathode under the limiting current condition, local time-dependent velocity gradient on the wall s can be determined as

$$s = 1.90\,(I_d/Fa\,C_A)^3\left(L/{D_{AB}}^2\right) \qquad (14.4\text{-}1)$$

where D_{AB} is the diffusivity of $Fe(CN)_6^{3-}$ion.

The above equation can be obtained by the boundary layer analysis, which will be described in Chapter 18.

This electrochemical method can observe fluctuating velocity-gradients within the viscous sublayer of turbulent flows. It should be kept in mind that there usually appear definite velocity fluctuations even in the viscous sublayer due to the influence of the turbulence generated in the buffer zone. For an example,[1)] by using this velocity-gradient measurement, local variation of the near-wall velocity gradient is observed in the impingement region struck by a free jet of an electrolytic solution of $Fe(CN)_6^{3-}$ and $Fe(CN)_6^{4-}$. If you refer to the journal shown below, you will find the lateral distribution of velocity-gradient on the wall of the impingement region and its turbulence intensity.

1. Kataoka, K., Y. Kamiyama, S. Hashimoto and T. Komai: *J. Fluid Mech.*, vol.119, pp.91-105 (1982).

[PROBLEM 14-1] An aqueous solution of electrolytes consisting of 0.02 kg-equiv./m^3 $Fe(CN)_6^{3-}$ and $Fe(CN)_6^{4-}$ with the supporting electrolyte of 1 kmol/m^3 KOH is flowing at a flow rate of 0.001 m^3/s in a rectangular channel shown in Fig.14-P.1. The density, viscosity, and diffusivity of the solution are 1,010 kg/m^3, 0.0015 Pa s, and 8.3×10^{-10} m^2/s, respectively. Owing to the supporting electrolyte the ionic diffusion of $Fe(CN)_6^{3-}$ due to the electrical potential can be neglected. The bulk concentration of the reactant ion $Fe(CN)_6^{3-}$ can be assumed to be 0.02 kg-equiv./m^3. The active surface area of each test cathode is 0.5 mm x 3 mm = 1.5 mm^2.

(a) Examine whether this flow is turbulent or not.

(b) When the main cathode is made active at the same as the EMF (V) of the test cathodes, the two test cathodes indicate the (time-averaged) limiting currents of 8×10^{-2} and 5.3×10^{-2} μA, respectively.
Calculate the local mass transfer coefficient k $(\mathrm{m/s})$ at the position of each test cathode.

(c) When the main cathode is made inactive, those two test cathodes indicate the (time-averaged) limiting currents of 5.2 and 4.7 μA, respectively.
Calculate the local velocity-gradient s $(1/\mathrm{s})$ at the position of each test cathode on the inside wall of the channel.

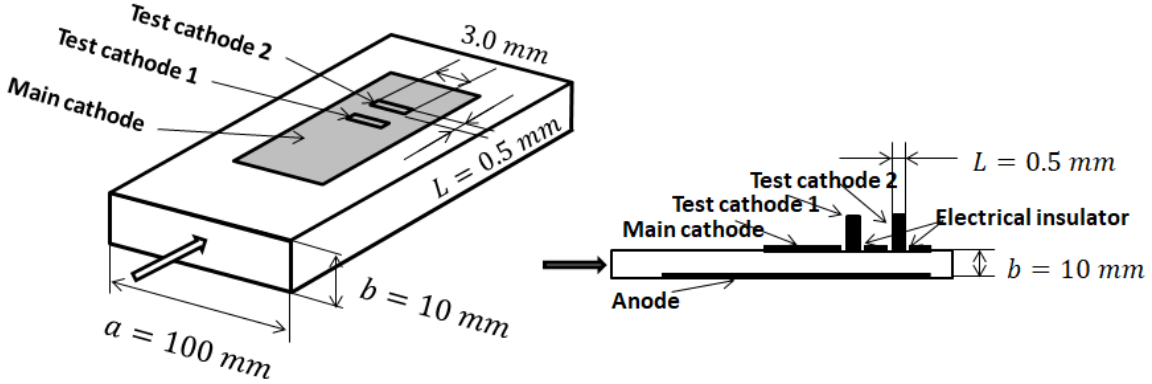

Fig.14-P1. Measurement of mass transfer and velocity-gradient at wall by an electrochemical method

Nomenclature

c	total molar density, [kmol/m^3]
C_A	concentration of reactant ion, [kmol/m^3]
D_{AB}	diffusivity of ion A, [m^2/s]
E	electrode potential, [V]
Fa	Faraday constant = 96,500 A s/kg-equiv.
I	current density, [A/m^2]
I_d	limiting current density, [A/m^2]
k	ionic mass transfer coefficient, [kmol/m^{2}s]
L	length of test cathode in stream direction, [m]
M_A	molecular weight, [kg/kmol]
N_A	molar flux of reactant ion A, [kmol ion/m^{2}s]
R	gas constant, [J/kmol K]
S	electrode surface area, [m^2]
s	velocity gradient at electrode surface, [1/s]
T	temperature, [K]
x_A	molar concentration (fraction) of reactant ion, [kmol/kmol]
ϵ	ionic charge
Φ	electrostatic potential, [EMF]

Subcripts

D	limiting current
w	electrode surface

CHAPTER 15

HEAT TRANSFER WITH PHASE TRANSFORMATION

15.1 Condensation

15.1-1 Heat transfer for condensation

Let us study the condensation of pure vapor.

When a pure vapor saturated at a given pressure comes in contact with a cooled surface, the change from vapor to liquid occurs isothermally at the saturation or equilibrium temperature.

The pressure in the bulk of the vapor phase is very slightly greater than the saturation pressure of the condensate surface. As shown in Fig. 15.1-1, the mass transfer toward the vapor-liquid interface occurs due to the self-diffusion. The latent heat released must flow through the condensate to the cooled surface. The main resistance to heat transfer lies in the condensate film and the vapor phase is assumed at the uniform equilibrium temperature.

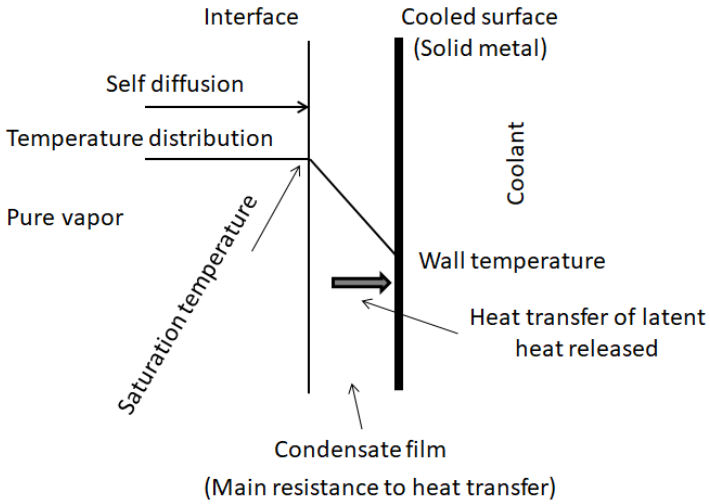

Fig.15.1-1. Pure vapor condensation

If the condensate does not wet the cooled surface, individual droplets grow by coalescence and run down the surface under the influence of gravity. This is called “dropwise condensation.” If the condensate wets the cooled surface, a continuous liquid film is formed over the cooled surface. This is called “filmwise condensation.” Dropwise condensation gives much higher rate of condensation than filmwise condensation because bare cooled surface of the condenser is directly exposed to the vapor stream. Steam is the only one pure vapor known to condense in a dropwise manner in the particular condition of the cooled surface. The dropwise condensation is very difficult to achieve or maintain in commercial equipment; it is customary in condenser design to assume filmwise condensation.

15.1-2 Film condensation of pure vapor on a vertical wall

Let us consider the problem of filmwise condensation of a pure saturated vapor on a vertical wall shown in Fig.15.1-2.

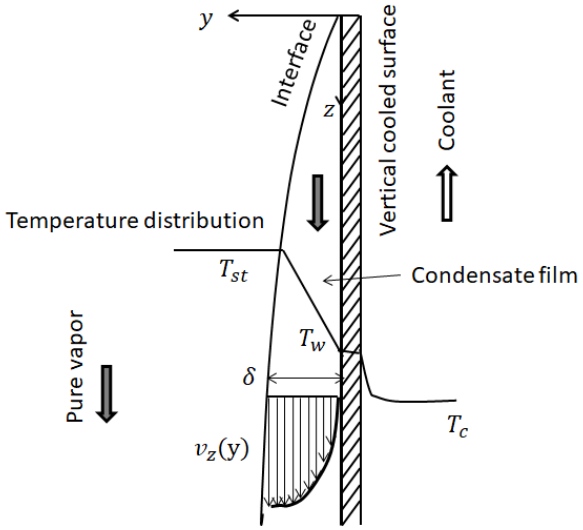

Fig. 15.1-2. Laminar falling film of condensate in filmwise condensation

To illustrate the classical Nusselt approach the following assumptions are made:

(1) The pure vapor is at the saturation temperature T_{st}
(2) The heat delivered by the condensing vapor is latent heat only and the latent heat released at the interface is transported solely by the heat conduction through the condensate film.
(3) The condensate film drains in non-rippling laminar flow.
(4) The condensate film is so thin that the temperature distribution in it is linear.
(5) The cooled surface of the solid is at a constant temperature T_w.
(6) The shear at the liquid-vapor interface is negligible.
(7) The curvature of the condensate film is negligible, so that the heat flux is very nearly normal to the wall.

The film thickness increases from top to bottom cumulatively, so the condensing coefficient (heat transfer coefficient) for a vapor condensing on a vertical surface decreases from top to bottom.

The equation of motion to be applied is

$$\rho_L\left(\frac{\partial v_z}{\partial t}+ v_x\frac{\partial v_z}{\partial x}+ v_y\frac{\partial v_z}{\partial y}+ v_z\frac{\partial v_z}{\partial z}\right)= -\frac{\partial p}{\partial z}+ \mu_L\left(\frac{\partial^2 v_z}{\partial x^2}+\frac{\partial^2 v_z}{\partial y^2}+\frac{\partial^2 v_z}{\partial z^2}\right)+(\rho_L - \rho_V)\,g_z$$

(1) The z- component velocity v_z does not change in the transverse direction x,
(2) The static pressure does not change greatly in the flow direction; $\frac{\partial p}{\partial z} \cong 0$, and
(3) The velocity distribution does not change in the streamwise direction; $\frac{\partial v_z}{\partial z} \cong 0$,

Under steady-state conditions the equation of motion on the laminar falling film of the condensate is, neglecting inertia (convective) terms

$$\mu_L\frac{\partial^2 v_z}{\partial y^2}= (\rho_L - \rho_V)\,g_z \qquad (15.1\text{-}1)$$

At high operating pressures, buoyancy forces occur in the liquid layer and the right side term has the density difference $(\rho_L - \rho_V)$ in place of ρ_L. The equation of motion reduces to

$$\frac{d^2 v_z}{dy^2}= -\left(\frac{\rho_L - \rho_V}{\mu_L}\right)g \qquad (15.1\text{-}2)$$

Assuming the film thickness δ at z, the boundary conditions are

$v_z = 0$ at $y = 0$

$\frac{d\,v_z}{dy} = 0$ at $y = \delta$ (15.1-3)

Integration gives the velocity distribution in the condensate film:

$$v_z = \left(\frac{\rho_L - \rho_V}{\mu_L}\right) g \left(\delta y - \frac{1}{2} y^2\right) \quad (15.1\text{-}4)$$

Using the velocity profile, the mass flow rate per unit width perpendicular to yz plane is

$$\Gamma = \int_0^\delta \rho_L v_z \, dy = \frac{\rho_L(\rho_L - \rho_V) g\, \delta^3}{3\,\mu_L} \quad (15.1\text{-}5)$$

Differentiating with respect to δ

$$\frac{d\,\Gamma}{d\delta} = \frac{\rho_L(\rho_L - \rho_V) g\, \delta^2}{\mu_L} \quad (15.1\text{-}6)$$

The following boundary conditions for applying the equation of energy to the condensate film are used:

$T = T_w$ at $y = 0$

$T = T_{st}$ at $y = \delta$ (15.1-7)

As a result, the following linear temperature distribution can be obtained:

$$T - T_w = (T_{st} - T_w)\,\frac{y}{\delta} \quad (15.1\text{-}8)$$

To consider the temperature drop within the condensate film, the average enthalpy change (modified latent heat) $\Delta H'_{fg}$ of the vapor in condensing to liquid and subcooling to the average liquid temperature of the condensate film can be calculated as

$$\Delta H'_{fg} = \Delta H_{fg} + Cp_L(T_{st} - T_m) = \Delta H_{fg} + \frac{\int_0^\delta \rho_L v_z\, Cp_L(T_{st} - T) dy}{\int_0^\delta \rho_L v_z\, dy}$$

$$= \Delta H_{fg} + \frac{1}{\Gamma}\int_0^\delta \rho_L v_z\, Cp_L(T_{st} - T) dy$$

$$= \Delta H_{fg} + \frac{3}{8}\, Cp_L(T_{st} - T_w) \quad (15.1\text{-}9)$$

where ΔH_{fg} is the latent heat at the saturation temperature.

15.1-3 Condensation heat transfer coefficient

In a segment of the falling film the vapor condenses at a rate of $\mathrm{d}\Gamma$ and the heat liberated $\Delta H'_{fg}\,\mathrm{d}\Gamma$ must flow through the film δ from T_{st} to T_w by conduction.

$$q_y(dz \times 1) = \kappa_L\,\frac{T_{st} - T_w}{\delta}\,(dz \times 1) = \Delta H'_{fg}\,\mathrm{d}\Gamma \times 1$$

Substituting Eq.(15.1-6) into the above equation

$$\delta^3\, d\delta = \frac{\kappa_L \mu_L (T_{st} - T_w)}{\rho_L(\rho_L - \rho_V) g\, \Delta H'_{fg}}\, dz \quad (15.1\text{-}10)$$

Integration from $\delta = 0$ (at $z = 0$) to $\delta = \delta$ (at $z = z$) gives

$$\delta = \left[\frac{4\kappa_L \mu_L (T_{st} - T_w)}{\rho_L(\rho_L - \rho_V) g\, \Delta H'_{fg}}\, z\right]^{1/4} \quad (15.1\text{-}11)$$

The local condensing coefficient can be defined as $h_c = \kappa_L/\delta$. Then

$$h_c = \left[\frac{\rho_L(\rho_L - \rho_V) g\, \Delta H'_{fg} {\kappa_L}^3}{4\mu_L (T_{st} - T_w) z}\right]^{1/4} \quad (15.1\text{-}12)$$

The average condensing coefficient $\overline{h_c}$ for a vapor condensing on a vertical plate of height L is obtained integrating the local value h_c over the height L:

$$\overline{h_c} = \frac{1}{L}\int_0^L h_c\, dz = \frac{2\sqrt{2}}{3}\left[\frac{\rho_L(\rho_L - \rho_V) g\, \Delta H'_{fg} {\kappa_L}^3}{\mu_L (T_{st} - T_w) L}\right]^{1/4} \quad (15.1\text{-}13)$$

All the physical properties are evaluated at the arithmetic mean temperature

$$T_f = (T_{st} + T_w)/2$$

This is the analytical result Nusselt[1)] first achieved.

Although the foregoing analysis was made for a vertical flat plate, the development is also valid for the inside and outside surfaces of vertical tubes if the tubes are large in diameter, compared with the film thickness.

1. Nusselt, W.; *Z. Ver. Dtsch. Ing.*, **60**, 541-546, 569-575 (1916)

15.1-4 Engineering design of an overhead condenser

By using a vertical 1-1 condenser shown below, 3,000 kg/h of a saturated vapor mixture of 98 mol% of n-pentane which comes from the top of a distillation column at 55℃ (= 327 K) and 1.7 atm (= 0.172 MPa) is to be condensed completely at 51.7 ℃ (= 324.7 K).

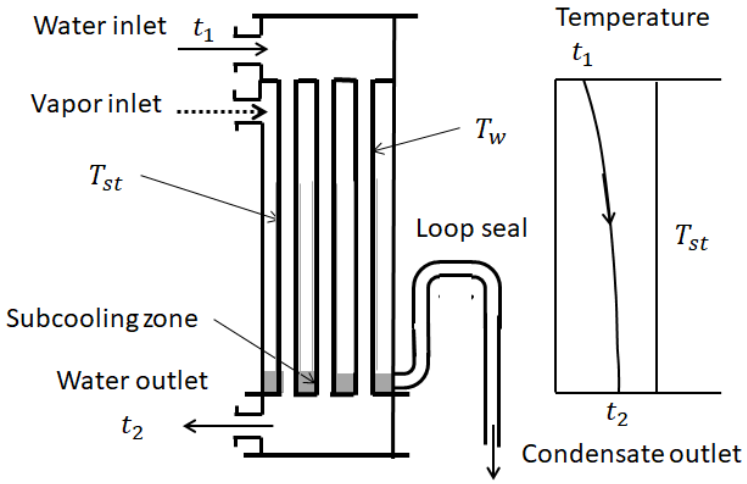

Fig. 15.1-3. Vertical 1-1 condenser

As the cooling medium, 70,000 kg/h of water at 32℃ (= 305 K) will be used. Only for simplicity of calculation, shell baffles are omitted in the equipment. There will exist a short zone of subcooling at the bottom, but we neglect the contribution of heat transfer from this zone to heat balance. Determine the number of heat transfer tubes if 3 m long steel tubes of 25 mm OD and 22 mm ID are used.

From enthalpy chart, the enthalpy difference between n-pentane vapor at 55 ℃ and liquid at 51.7 ℃ is given by

$\Delta H_{fg} = 3.37 \times 10^5$ J/kg

This is a little higher than the latent heat of propane vapor at the saturation temperature owing to the effect of subcooling.

Solution:

The heat to be absorbed by cooling water is

$$Q = (3000 \text{ kg/h})(\text{h}/3{,}600 \text{ s})(3.37 \times 10^5 \text{ J/kg}) = 2.81 \times 10^5 \text{ W}$$

The outlet water temperature is

$$t_2 = (Q/W\,Cp_w) + t_1$$

$$= \frac{2.81 \times 10^5}{(70{,}000 \text{ kg/h})(\text{h}/3{,}600 \text{ s})(1 \text{ kcal/kg K})(4.184 \times 10^3 \text{ J/kcal})} + 32 = 35.5℃$$

The average temperature of condensing vapor is

$$T_{st} = (55 + 51.7)/2 = 53.4 ℃$$

The average temperature of water is

$$t_c = (35.5 + 32)/2 = 33.8 ℃$$

Assume the overall heat transfer coefficient

$$U_o = 525 \text{ J/m}^2\text{s K}$$

The logarithmic mean of temperature differences is

$$(\Delta T)_{l.m.} = \frac{(T_{st} - t_1) - (T_{st} - t_2)}{\ln \frac{T_{st} - t_1}{T_{st} - t_2}}$$

$$= \frac{(53.4 - 32) - (53.4 - 35.5)}{\ln \frac{53.4 - 32}{53.4 - 35.5}} = 19.6\ K$$

The heat transfer surface for condensation is

$$A_o = \frac{Q}{U_o(\Delta T)_{l.m.}} = \frac{2.81 \times 10^5 \text{ J/s}}{(525 \text{ J/m}^2\text{s K})(19.6 \text{ K})} = 27.3 \text{ m}^2$$

The outside surface of a tube for heat transfer is

$$a_o = \pi d_o L = \pi(0.025\text{m})(3 \text{ m}) = 0.236 \text{ m}^2$$

The total number of tubes is

$$N = A_o/a_o = (27.3 \text{ m}^2)/(0.236 \text{ m}^2) = 115.6 < 116$$

The following empirical equation is used to calculate the inside heat transfer coefficient:

$$\frac{h_i d_i}{\kappa_w} = 0.023 \left(\frac{G_i d_i}{\mu_w}\right)^{0.8} Pr^{1/3}$$

The mass velocity is

$$G_i = \frac{W}{(\pi/4){d_i}^2 N} = \frac{(70{,}000 \text{ kg/h})(\text{h}/3{,}600 \text{ s})}{(\pi/4)(0.022 \text{ m})^2(116)} = 441 \text{ kg/m}^2\text{s}$$

The physical properties of water at $t_c = 33.8$ ℃ are

$\mu_w = 8 \times 10^{-4}$ kg/m s, $\kappa_w = 0.622$ J/m s K, Pr = 4.5

$Re_i = G_i d_i/\mu_w = \frac{(441 \text{ kg/m}^2\text{s})(0.022 \text{ m})}{8 \times 10^{-4} \text{ kg/m s}} = 1.21 \times 10^4$ (turbulent flow)

The inside heat transfer coefficient is

$$h_i = (0.023)\left(\frac{0.622 \text{ J/m s K}}{0.022 \text{ m}}\right)(12{,}100)^{0.8}(4.5)^{1/3} = 1{,}980 \text{ J/m}^2\text{s K}$$

Assume the condensing coefficient

$$\overline{h_c} = 737 \text{ J/m}^2\text{s K}$$

The tube wall temperature can be calculated with omission of the resistance of the tube metal as

$$q = \frac{T_{st} - t_c}{\frac{1}{\overline{h_c}} + \frac{1}{h_i}\frac{d_o}{d_i}} = \frac{T_w - t_c}{\frac{1}{h_i}\frac{d_o}{d_i}}$$

From the equation

$$T_w = 33.8 + \frac{\frac{1}{1980}\frac{0.025}{0.022}}{\frac{1}{737} + \frac{1}{1980}\frac{0.025}{0.022}}(53.4 - 33.8) = 39.6℃$$

The physical properties of liquid n-pentane at $T_f = (53.4 + 39.6)/2 = 46.6$ ℃ are

$\kappa_L = 0.133$ J/m s K , $\mu_L = 1.9 \times 10^{-4}$ kg/m s , $\rho_L = 600$ J/m^3 ,

$Cp_L = 2.39 \times 10^3$ J/kg K

At the operating pressure

$$\rho_L \cong \rho_L - \rho_V$$

The average enthalpy change $\Delta H"_{fg}$ is

$$\Delta H'_{fg} = \Delta H_{fg} + \frac{3}{8} Cp_L(T_{st} - T_w)$$

$$= 3.37 \times 10^5 + (3/8)(2.39 \times 10^3)(53.4 - 39.6) = 3.49 \times 10^5 \text{ J/kg}$$

Using Eq. (15.1-13)

$$\overline{h_c} = \frac{2\sqrt{2}}{3}\left[\frac{\rho_L(\rho_L - \rho_V)g\,\Delta H'_{fg}\kappa_L{}^3}{\mu_L(T_{st} - T_w)L}\right]^{1/4}$$

$$= (0.943)\left[\frac{(600\ \text{kg/m}^3)^2\,(9.8\ \text{m/s}^2)(3.49\times 10^5\ \text{J/kg})}{(1.9\times 10^{-4}\ \text{kg/m s})(3\ \text{m})(53.4-39.6)}\times(0.133\ \text{J/m s K})^3\right]^{1/4}$$

$$= 734.6\ J/m^2 s\ K$$

The calculated value is almost equal to the assumed value 737 $\text{J/m}^2\text{s K}$.
Then the overall heat transfer coefficient can be obtained with the calculated h_i and h_c:

$$U_o = \frac{1}{\frac{1}{734.6} + \frac{1}{1980}\frac{0.025}{0.022}} = 519\ \text{J/m}^2\text{s K}$$

The assumed value 525 $\text{J/m}^2\text{s K}$ is within 2% of the calculated value.
The total number of heat transfer tubes is

$$N = \frac{Q}{U_o(\Delta T)_{l.m.}a_o} = 117$$

For simplicity we neglected the heat transfer resistance due to the fouling and tube metal effects, but the omission of these resistances should sometimes be checked in design calculation.

15.2 Evaporation

15.2-1 Heat transfer for boiling

Boiling is another example of heat transfer processes with phase change.
There are two general boiling operations: pool boiling and forced boiling. Boiling water in a kettle, which is at or near saturation temperature without forced convective flow or agitation, is the first example, where many water vapor bubbles generating are agitating the liquid pool very strongly. Water, which flows in heat exchangers with vapor formation, is the second example. The heat flux is much larger than that obtainable without phase change.

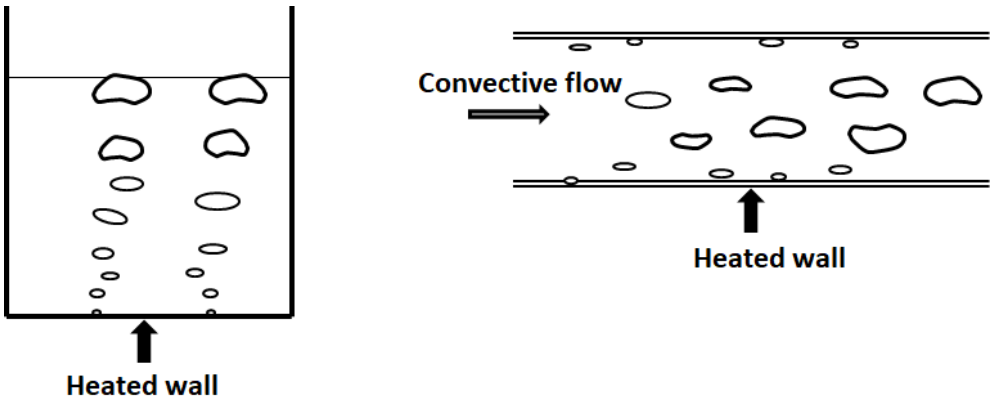

Fig. 15.2-1. Pool boiling and forced boiling

15.2-2 Pool boiling

The pool-boiling heat transfer can be understood in the form of the so-called boiling curve, i.e., the curve of heat flux versus the temperature difference ΔT_{ex} between the heated wall and the surrounding saturated fluid (simply called the excess temperature).

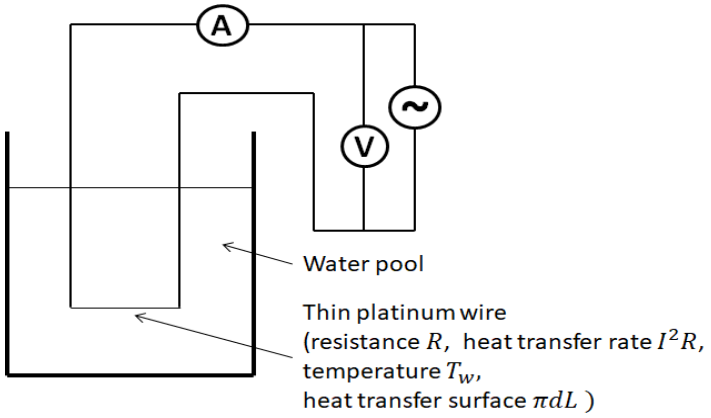

Fig. 15.2-2. Nukiyama's experimental system for observing various boiling regimes

To acquire a physical understanding of pool boiling, we shall consider the famous Nikiyama's experiment[1)].

His experimental setup is shown in Fig. 15.2-2. A thin platinum wire is immersed in a pool of distilled water controlled to be kept at a given temperature $T_f < T_{st}$ at atmospheric pressure, which is not much lower than the saturation temperature. Let us consider the electrically heated platinum resistance wire. We can easily obtain the boiling curve by measuring the surface area of the wire, the electric power input, and the temperature of the wire with the aid of the temperature-resistance relationship.

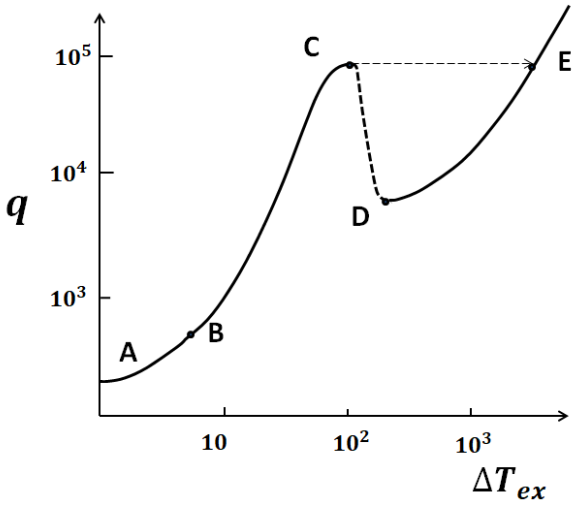

Fig. 15.2-3. A typical boiling curve for a wire immersed in a pool of water

1. Nukiyama, S., *J. Soc. Mech. Eng., Japan*, **37**(206), 367 (1934)

Fig. 15.2-3 is a schematically drawn typical boiling curve for a wire, where the heat flux is plotted as a function of the excess temperature. As long as the temperature of the wire does not exceed the boiling point by more than a few degrees (AB range), heat is transferred to the water bulk by free convection without phase change. As the temperature of the wire is increased, a point B is reached where the energy level of water adjacent to the wire surface becomes so high that water vapor bubbles are generated at a small number of discrete sites. This is the beginning of the nucleate boiling regime (BC Range). As vapor bubbles form and grow on the heating surface, they push hot water from the vicinity of the wire into the colder water bulk. As the heat flux is raised and the number of bubbles is increased, the bubbles begin to coalesce and the heat transfer by evaporation

becomes predominant. As the excess temperature further increases, the number of sites at which bubbles form increases rapidly, and then the bubbles coalesce to form continuous vapor columns which causes a reduction of effectiveness of each site. The heat flux no longer increases, i.e., when the heat flux reaches a maximum at point C, a further increase of the temperature causes a decrease in the rate of heat flow (dotted line). This maximum heat flux occurs at the critical excess temperature (referred to as the burnout point). When the excess temperature goes beyond Point C, provided that the melting point of the wire is sufficiently high, a transition from nucleate to film boiling will take place. This case corresponds to a transition from point C to E in Fig. 15.2-3. Provided that the wire heater has a low melting point, the heater will melt, i.e., burnout occurs. The remaining regime of the curve (beyond D) is the fully developed film boiling. The heat transport through the vapor film is by conduction and radiation to the vapor-liquid interface where vaporization takes place.

The forced convective boiling curve is similar to that for pool boiling. But the regimes are made complicated by the effects of velocity, subcooling, and different vapor-liquid flow patterns.

15.2-3 Heat transfer correlation for pool boiling

In boiling heat transfer, except for the physical properties of the vapor and liquid, the latent heat of vaporization, the surface tension, the surface characteristics, and the pressure should be considered. Owing to the great number of variables involved, there is no single correlation equation applicable to the entire range of pool boiling. Owing to the complicatedness, only the following widely accepted semiempirical equation proposed by Rohsenow[1)] is introduced:

$$q = \mu_L \Delta H_{fg} \sqrt{\frac{(\rho_L - \rho_V)g}{\sigma}} \left[\frac{Cp_L(T_w - T_{st})}{\Delta H_{fg} Pr_L{}^s C_{sf}}\right]^3 \qquad (15.2\text{-}1)$$

where Cp_L: specific heat of saturated liquid in J/kg K
C_{sf}: experimental constant, dimensionless
g : gravitational acceleration in m/s^2
ΔH_{fg}: enthalpy of vaporization in J/kg
Pr_L : Prandtl number of saturated liquid, dimensionless
q : heat flux per unit area of heated surface in J/m^{2}s
$T_w - T_{st}$: excess temperature in K
μ_L : liquid viscosity in kg/m s
σ : surface tension in N/m
ρ_L, ρ_V : densities of saturated liquid and vapor in kg/m^3

1. Rohsenow, W. M., *Trans. ASME*, **74**, 969 (1952)

Table 15.2-1 Experimental constants for nucleate boiling[1)]

Fluid- Heated Surface Combination	Constant C_{sf}	Exponent s
Water on Ground and Polished Stainless Steel	0.0080	1.0
Water on Mechanically Polished Stainless Steel	0.0132	1.0
Water – brass, Water – nickel	0.0060	1.0
Water – platinum	0.0130	1.0
Water – copper	0.0130	1.0
Ethanol – chromium	0.0027	1.7
Isopropanol – copper	0.00225	1.7
35% K_2CO_3 – copper	0.0054	1.7
Benzene – chromium	0.0100	1.7
n-Pentane – chromium	0.015	1.7

These constants are picked up from the table of Kreith's book.

1. Kreith, F.; "Principles of Heat Transfer," 3trd ed., Intext Press, Inc., 1973

Eq.(15.2-1) indicates that the heat flux in nucleate boiling is proportional to the cube of the excess temperature. The experimental constant C_{sf} depends on the particular fluid- heated surface combination and is affected by the surface roughness of the heater.

Table 15.2-1 gives the experimental values. The exponent s of the Prandtl number is 1.0 for water but 1.7 for all other fluids.

15.2-4 Critical Heat Flux[1,2,3)]

The critical heat flux is a very important characteristic giving the heat flux at which a transition occurs from nucleate to film boiling. The prediction of the critical heat flux is very important from two engineering viewpoints because this value indicates the maximum performance for many systems and the great drop in heat flux beyond this point sometimes results in the destruction (burnout) of the heating surface owing to the accompanied rise in surface temperature.

One of many proposed models is Zuber's one[1)]:

$$q_{max} = \frac{\pi}{24}\rho_V \Delta H_{fg}\left[\frac{\sigma(\rho_L - \rho_V)g}{{\rho_V}^2}\right]^{1/4}\left(\frac{\rho_L}{\rho_L + \rho_V}\right)^{-1/2} \quad (15.2\text{-}2)$$

This equation was obtained based on hydrodynamic instability theory postulating that the volume flow rate of vapor from the heated surface should be equal to that of liquid flow toward the surface. Any other correlations do not differ greatly in the form from Zuber's equation.

1. Zuber, N. and M. Tribus; "Further Remarks on the Stability of Boiling Heat Transfer," Rep.58-5, Dept of Eng., Univ. of Calif., Los Angeles (1958)
2. Rohsenow, W. M.; "A Method of Correlating Heat-Transfer Data for Surface Boiling Liquids," *Trans. ASME*, **74**, pp. 969 (1952)
3. Rohsenow, W. M.; "Boiling Heat Transfer," Dev. In Heat Transfer, W. M. Rohsenow, ed. (Cambridge, Massachusetts: MIT Press, 1964), pp.169-260

[EXAMPLE 15.3-1] Estimate the heat flux for water boiling on a mechanically polished clean stainless steel at 1 atm and 110℃ (= 383 K) surface temperature and compare it with the critical heat flux to confirm the nucleate boiling.

Solution:

From Table 15.3-1, $C_{sf} = 0.0132$ for the fluid-surface combination.

The appropriate physical properties at 100℃ and 1 atm are

$\Delta H_{fg} = 539$ kcal/kg $= 2.26 \times 10^6$ J/kg, $\rho_L = 961.8$ kg/m^3, $\rho_V = 0.598$ kg/m^3 (from steam table)

$Pr_L = 1.78$, $\mu_L = 0.130 \times 10^{-3}$ kg/m s, $Cp_L = 4.18 \times 10^3$ J/kg K, $\sigma = 0.0588$

The excess temperature $\Delta T_{ex} = 110 - 100 = 10\,K$.

From Eq. (15.2-1)

$$q = (0.130 \times 10^{-3})(2.26 \times 10^6)\left[\frac{(961.8 - 0.598)(9.8)}{0.0588}\right]^{\frac{1}{2}}\left[\frac{(4.18 \times 10^3)(10)}{(2.26 \times 10^6)(1.78)(0.0132)}\right]^3$$

$$= 5.736 \times 10^4 \text{ J/m}^2\text{s}$$

From Zuber's equation

$$q_{max} = \frac{\pi}{24}(0.598)(2.26 \times 10^6) \times \left[\frac{(0.0588)(961.8 - 0.598)(9.8)}{0.598^2}\right]^{\frac{1}{4}}\left(\frac{961.8}{961.8 + 0.6}\right)^{\frac{1}{2}} = 1.11 \times 10^6$$

It has been confirmed that the assumption of nucleate boiling is valid because $q < q_{max}$.

Nomenclature

A_o	total heat transfer surface area, [m^2]
a_o	outside surface area of a heat transfer tube, [m^2]
Cp	heat capacity, [J/kg K]
d_i	inside diameter of heat transfer tube, [m]

g	gravitational acceleration, [m/s^2]
h_c	condensing coefficient, [J/m^{2}sK]
h_i	inside heat transfer coefficient, [J/m^{2}sK]
L	height of vertical plate, [m] or tube length, [m]
N	number of tubes, [-]
Pr	Prandtl number, [-]
p	pressure, [Pa]
q	heat flux, [J/m^{2}s]
t	time, [s] or temperature, [K]
v_x, v_y, v_z	velocity components in rectangular coordinates, [m/s]
U_o	overall heat transfer coefficient on outside surface basis, [W/m^{2}K]
W	mass flow rate, [kg/s]
x, y, z	rectangular coordinates, [m]
Γ	mass flow rate per unit width of falling condensate film, [kg/s m]
δ	thickness of condensate film, [m]
ΔH_{fg}	latent heat of evaporation, [J/kg]
ΔT	temperature difference, [K]
κ	thermal conductivity of condensate liquid, [J/m s K]
G	mass velocity, [kg/m^{2}s]
μ	viscosity, [kg/m s]
ρ	density, [kg/m^3]
σ	surface tension, [N/m]

Subcripts

f	film
L	liquid
l.m.	logarithmic mean
st	saturated
V	vapor
W	wall

CHAPTER 16

MASS TRANSFER WITH CHEMICAL REACTION

16.1 Diffusion with Homogeneous Chemical Reaction

16.1-1 Diffusion with a homogeneous reaction in a stagnant fluid
------- Penetration theory -------

In gas absorption process, chemical reaction can be used to provide greater capacity of solvent for solute gas and greater rate of absorption than could be obtained by pure physical absorption only.

Much industrial gas-liquid contacting equipment usually operates with repeated short contacts of the two phases. Therefore let us consider the unsteady diffusion of dissolved gas from interface into a semi-infinite stagnant liquid mixture by use of the Higbie's penetration theory. The irreversible first-order chemical reaction occurs between the dissolved gas A and one component B in the liquid phase with the reaction - rate constant k_1.

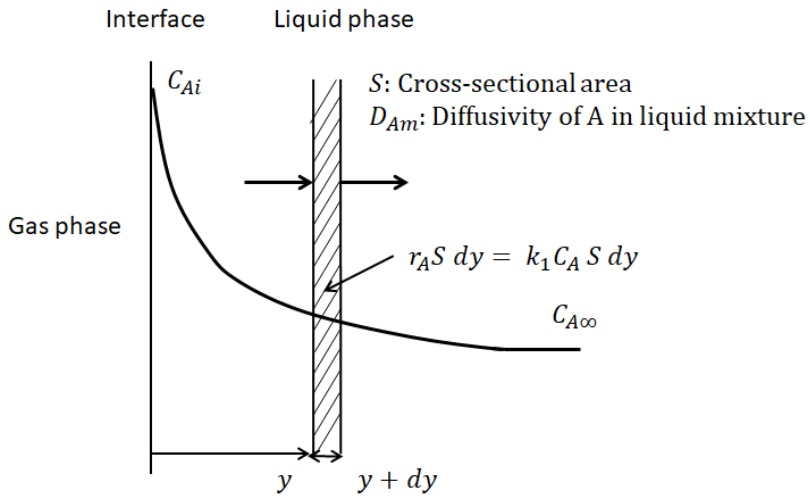

Fig. 16.1-1. Gas absorption accompanied with a first-order chemical reaction in liquid phase

Setting up mass balance over a differential control volume $S\,dy$ apart y from the interface

$$\left(-D_{Am}\left.\frac{\partial C_A}{\partial y}\right|_{y} + D_{Am}\left.\frac{\partial C_A}{\partial y}\right|_{y+dy}\right)S = \frac{\partial C_A}{\partial t}\,S\,dy + k_1 C_A S\,dy$$

or

$$D_{Am}\frac{\partial^2 C_A}{\partial y^2} = \frac{\partial C_A}{\partial t} + k_1 C_A \qquad (16.1\text{-}1)$$

Introducing a new variable $C_A' = C_A - C_{A\infty}$

$$D_{Am}\frac{\partial^2 C_{A'}}{\partial y^2} = \frac{\partial C_{A'}}{\partial t} + k_1 C_A{}' \qquad (16.1\text{-}2)$$

The boundary conditions are

$C_A' = C_{Ai} - C_{A\infty}$ at $y = 0$
$C_A' = 0$ at $y = \infty$ (16.1-3)

Taking the *s*-multiplied Laplace transform of Eq. (16.1-2)

$$D_{Am}\,\overline{\frac{d^2C_A'}{dy^2}} = s\,\overline{C_A'} + k_1\,\overline{C_A'} \quad \text{or} \quad \overline{\frac{d^2C_A'}{dy^2}} - \left(\frac{k_1+s}{D_{Am}}\right)\overline{C_A'} = 0 \tag{16.1-4}$$

The boundary conditions are

$\overline{C_A'} = C_{Ai} - C_{A\infty}$ at $y = 0$
$\overline{C_A'} = 0$ at $y = \infty$ (16.1-5)

The general solution to Eq. (16.1-4) is

$$\overline{C_A'} = a\,exp\left(\sqrt{\frac{k_1+s}{D_{Am}}}\,y\right) + b\,exp\left(-\sqrt{\frac{k_1+s}{D_{Am}}}\,y\right) \tag{16.1-6}$$

Using the boundary conditions

$$\overline{C_A'} = (C_{Ai} - C_{A\infty})\;exp\left(-\sqrt{\frac{k_1+s}{D_{Am}}}\,y\right) \tag{16.1-7}$$

The mass flux at the interface is expressible as

$$\overline{N_A} = -D_{Am}\frac{d\,\overline{C_A'}}{dy}\bigg|_{y=0} = (C_{Ai} - C_{A\infty})\sqrt{(k_1+s)D_{Am}} \tag{16.1-8}$$

Taking the inverse Laplace transform, the mass flux becomes

$$N_A = (C_{Ai} - C_{A\infty})\sqrt{k_1 D_{Am}}\left[\text{erf}(k_1t)^{1/2} + \frac{\exp(-k_1t)}{\sqrt{\pi\,k_1t}}\right] \tag{16.1-9}$$

For pure physical diffusion, i.e., $k_1 = 0$

$$\overline{N_{A0}} = (C_{Ai} - C_{A\infty})\sqrt{s\,D_{Am}}$$

or

$$N_{A0} = (C_{Ai} - C_{A\infty})\sqrt{\frac{D_{Am}}{\pi\,t}} \tag{16.1-10}$$

Note that Eq. (16.1-10) is equivalent with Eq. (6.7-10) if the exposure time t is replaced by z/V.

The average rate of absorption over the total exposure time t can be calculated as

$$W_A = \int_0^t N_A\,dt \Big/ \int_0^t dt = (C_{Ai} - C_{A\infty})\sqrt{D_{Am}k_1}\left[\left(1 + \frac{1}{2\,k_1t}\right)\text{erf}\,(k_1t)^{1/2} + \frac{\exp(-k_1t)}{\sqrt{\pi\,k_1t}}\right] \tag{16.1-11}$$

The corresponding time-average mass transfer coefficient k_L is

$$k_L = \sqrt{D_{Am}k_1}\left[\left(1 + \frac{1}{2\,k_1t}\right)\text{erf}\,(k_1t)^{1/2} + \frac{\exp(-k_1t)}{\sqrt{\pi\,k_1t}}\right] \tag{16.1-12}$$

Taking the time-average of Eq. (16.1-10)

$$k_{L0} = \sqrt{\frac{4\,D_{Am}}{\pi\,t}} \tag{16.1-13}$$

Here k_{L0} is the mass transfer coefficient without chemical reaction.

Introducing a ratio β of the mass transfer rate with and without reaction

$$\beta = \sqrt{\frac{\pi\,k_1t}{4}}\left[\left(1 + \frac{1}{2\,k_1t}\right)\text{erf}\,(k_1t)^{1/2} + \frac{\exp(-k_1t)}{\sqrt{\pi\,k_1t}}\right] \tag{16.1-14}$$

For small values of k_1t

$$\beta = 1 + \frac{k_1t}{3} - \frac{(k_1t)^2}{30} + --- \tag{16.1-15}$$

This reaction factor indicates the deviation from the purely physical mass transfer ($\beta = 1$).

For large values of k_1t

$$\beta = \sqrt{\frac{\pi}{4}}\left[\sqrt{k_1t} + \frac{1}{2\sqrt{k_1t}} - - - -\right] \tag{16.1-16}$$

If the exposure time and reaction-rate constant are given, the reaction factor can be calculated. The reaction factor calculated by the penetration theory is in good agreement with that calculated by other theories (Film theory and surface renewal theory).

16.1-2 Gas absorption with first-order chemical reaction

Let us consider a packed column gas absorber shown in Fig. 16.1-2, in which the first-order chemical reaction of a dissolved gas A is carried out with a continuous stream of liquid mixture.

Setting up mass balance over a differential control volume $S\,dz$ in the packing section

$$k_L a\,(C_{Ai} - C_{AL})S\,dz + (C_{AL}|_z - C_{AL}|_{z+dz})L_M\,S/\rho_M - k_1 C_{AL}\,S\,dz\,\varepsilon = 0 \qquad (16.1\text{-}17)$$

or

$$k_L a\,(C_{Ai} - C_{AL}) = \frac{L_M}{\rho_M}\frac{d\,C_{AL}}{dz} + \varepsilon\,k_1 C_{AL} \qquad (16.1\text{-}18)$$

where k_L is the liquid-phase mass transfer coefficient with reaction, ρ_M the total molar density, and ε the volume fraction of liquid in the packing section.

The total number of transfer units $N_L = Z_T \rho_M k_L^{\circ} a/L_M$ and the number of transfer units $n_L = z\ \rho_M k_L^{\circ} a/L_M$ are introduced using the liquid-phase mass transfer coefficient k_L° for purely physical absorption.

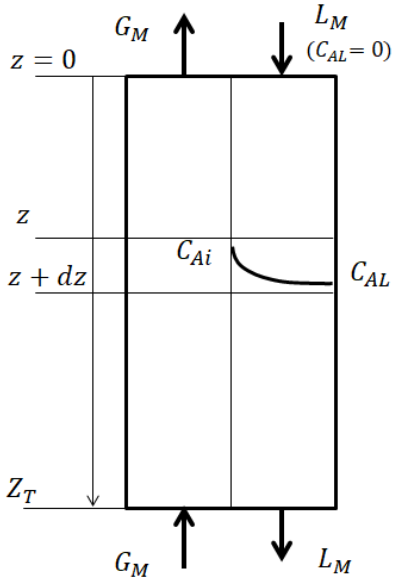

Fig. 16.1-2. Packed column gas absorber accompanied by a first-order homogeneous chemical reaction

The total holdup time (i.e., the so-called residence time) is calculated as

$$\theta = \varepsilon\,S\,Z_T\rho_M/L_M S = \varepsilon\,Z_T\rho_M/L_M \qquad (16.1\text{-}19)$$

The above equation becomes

$$\frac{d\,C_{AL}}{dz} + \frac{k_L\rho_M}{L_M}\left(a + \frac{k_1}{k_L}\varepsilon\right)C_{AL} = k_L a\,C_{Ai}\,\frac{\rho_M}{L_M} \qquad (16.1\text{-}20)$$

Using the number of transfer units n_L and the time of exposure θ

$$\frac{d\,C_{AL}}{dn_L} + \left(\beta + \frac{k_1}{N_L}\theta\right)C_{AL} = \beta\,C_{Ai} \qquad (16.1\text{-}21)$$

The boundary condition is

$$C_{AL} = 0 \quad \text{at} \quad z = 0$$

The following solution indicates the vertical variation in the bulk concentration of component A:

$$C_{AL} = C_{Ai}\left(\frac{\beta\,N_L}{k_1\theta + \beta\,N_L}\right)\{1 - \exp[-(k_1\theta + \beta\,N_L)(n_L/N_L)]\} \qquad (16.1\text{-}22)$$

Then the total rate of absorption per unit cross-sectional area can be calculated as

$$N_{AT} = \int_0^{Z_T} k_L a(C_{Ai} - C_{AL})\,dz = \beta\,\frac{L_M}{\rho_M}\int_0^{N_L}(C_{Ai} - C_{AL})\,dn_L$$

$$= C_{Ai}\,\frac{L_M}{\rho_M}\left(\frac{\beta\,N_L}{\beta\,N_L + k_1\theta}\right)\left\{k_1\theta + \frac{\beta\,N_L}{\beta\,N_L + k_1\theta}\,[1 - \exp(-(\beta\,N_L + k_1\theta))]\right\} \qquad (16.1\text{-}23)$$

If the reaction factor β and the total holdup time θ are given, the total rate of absorption can be

calculated using the physical absorption data. However the exposure time is generally difficult to estimate as for the film thickness in the film theory.

For practical design problem, the following equations can be used:

$$N_A = K_G\left(p_A - p_A^{*`}\right) = k_G(p_A - p_{Ai}) = \beta\, k_L^{\circ}(C_{Ai} - C_{AL}) \qquad (16.1\text{-}24)$$

and

$$\frac{1}{K_G} = \frac{1}{k_G} + \frac{H}{\beta\, k_L^{\circ}} \qquad (16.1\text{-}25)$$

Here H is the Henry's constant for purely physical equilibrium and $p_A^{*`}$ is the concentration of unreacted gas A expressed in units of gas-phase concentration, i.e., $p_A^{*`} = H\, C_{AL}$.

16.2 Gas Absorption with Instantaneous Bimolecular Reaction

Many industrially important absorption processes are accompanied by bimolecular reaction

$$\mathrm{A} + \nu\,\mathrm{B} \rightarrow \text{products}$$

The irreversible chemical reaction such as $SO_2 + 2\,NaOH \rightarrow Na_2SO_3 + H_2O$ occurs in the liquid phase between a dissolved gas reactant A and a nonvolatile reactant B which is initially present in the liquid phase.

The problem of liquid-phase diffusion with bimolecular reactions has not yet been solved analytically, except for some simple cases. One of the extreme cases occurs when the reaction rate is so large that A and B react immediately and completely on a plane (or a very thin zone) which moves with time. The reaction plane which was initially located at the interface is now at a distance $z_r(t)$ from the interface.

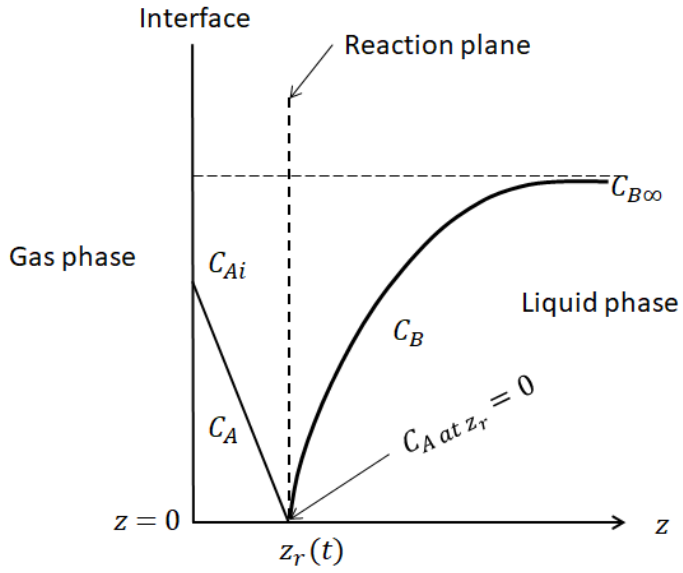

Fig. 16.2-1. Schematic composition profile of gas absorption with bimolecular reaction

As shown in Fig.16.2-1, the reaction rate $r = k_2 C_A C_B$ is zero everywhere, except at the reaction plane. In the region between the interface and the moving reaction plane, the concentration of A is obtained by solving the transient diffusion equation for A without reaction; the same is true for B in the semi-infinite liquid body on the right side of the moving reaction plane. Therefore the penetration theory will also be used.

The set of differential equations to be solved are

$$\frac{\partial C_A}{\partial t} = D_{Aw}\frac{\partial^2 C_A}{\partial z^2} \qquad C_B = 0 \qquad 0 \le z \le z_r(t) \qquad (16.2\text{-}1)$$

$$\frac{\partial C_B}{\partial t} = D_{Bw}\frac{\partial^2 C_B}{\partial z^2} \qquad C_A = 0 \qquad z_r(t) \le z \le \infty \qquad (16.2\text{-}2)$$

where D_{Aw} and D_{Bw} are diffusivities of A and B in the solution, respectively. Note that any reaction does not appear in the above equations.

The general solutions to the above two equations are of the form

$$\frac{C_A}{C_{Ai}} = K_1 + K_2 \operatorname{erf} \frac{z}{2\sqrt{D_{Aw} t}} \qquad 0 \le z \le z_r(t) \tag{16.2-3}$$

$$\frac{C_B}{C_{B\infty}} = K_3 + K_4 \operatorname{erf} \frac{z}{2\sqrt{D_{Bw} t}} \qquad z_r(t) \le z \le \infty \tag{16.2-4}$$

At the reaction plane, A and B react immediately.

$$C_A = C_B = 0 \qquad \text{at} \quad z = z_r(t) \tag{16.2-5}$$

Therefore from perfect differentia

$$dC_A = \left(\frac{\partial C_A}{\partial z_r}\right)_t dz_r + \left(\frac{\partial C_A}{\partial t}\right)_{z_r} dt = 0 \tag{16.2-6}$$

From this equation

$$\frac{dz_r}{dt} = -\left(\frac{\partial C_A}{\partial t}\right)_{z_r} \Big/ \left(\frac{\partial C_A}{\partial z_r}\right)_t \tag{16.2-7}$$

From Eq. (16.2-3)

$$\left(\frac{\partial C_A}{\partial t}\right)_{z_r} = K_2 C_{Ai} \frac{2}{\sqrt{\pi}} \left(-\frac{1}{2\,t}\right) \exp\left(-\frac{{z_r}^2}{4\,D_{Aw}\,t}\right) \frac{z_r}{2\sqrt{D_{Aw}\,t}}$$

$$\left(\frac{\partial C_A}{\partial z_r}\right)_t = K_2 C_{Ai} \frac{2}{\sqrt{\pi}} \left(\frac{1}{z_r}\right) \exp\left(-\frac{{z_r}^2}{4\,D_{Aw}\,t}\right) \frac{z_r}{2\sqrt{D_{Aw}\,t}}$$

Substitute these relations into Eq. (16.2-7)

$$\frac{dz_r}{dt} = \frac{z_r}{2\,t} \tag{16.2-8}$$

Integration gives

$$z_r(t) = \sqrt{4\,\alpha\,t} \tag{16.2-9}$$

where $\sqrt{4\,\alpha}$ is an arbitrarily chosen integration constant. These five integration constants K_1, K_2, K_3, K_4, and α can be evaluated by the following five initial and boundary conditions:

I.C. or B.C.1	at $t = 0$	$C_B = C_{B\infty}$	$0 \le z \le \infty$
or	at $z = \infty$	$C_B = C_{B\infty}$	$t > 0$
B.C.2	at $z = 0$	$C_A = C_{Ai}$	
B.C.3	at $z = z_r$	$C_A = 0$	(16.2-10)
B.C.4	at $z = z_r$	$C_B = 0$	
B.C.5	at $z = z_r$	$-\nu\, D_{Aw} \frac{\partial C_A}{\partial z} = D_{Bw} \frac{\partial C_B}{\partial z}$	

The last boundary condition comes from the stoichiometric requirement that one mole of A reacts with ν moles of B.

From B.C.2 $\quad K_1 = 1$

From B.C.3 $\quad K_2 = -\frac{1}{\operatorname{erf} \frac{z_r}{2\sqrt{D_{Aw} t}}} = -\frac{1}{\operatorname{erf} \sqrt{\frac{\alpha}{D_{Aw}}}}$

From B.C.1 $\quad K_3 = 1 - K_4$

From B.C.4 $\quad 0 = (1 - K_4) + K_4 \operatorname{erf} \sqrt{\frac{\alpha}{D_{Bw}}}$

Therefore $\quad K_4 = \frac{1}{1 - \operatorname{erf} \sqrt{\frac{\alpha}{D_{Bw}}}}$

Then $\quad K_3 = 1 - \frac{1}{1 - \operatorname{erf} \sqrt{\frac{\alpha}{D_{Bw}}}}$

$$\left.\frac{\partial C_A}{\partial z}\right|_{z_r} = -\frac{1}{\operatorname{erf} \sqrt{\frac{\alpha}{D_{Aw}}}} C_{Ai} \frac{2}{\sqrt{\pi}} \exp\left(-\frac{{z_r}^2}{4\,D_{Aw}\,t}\right) \frac{1}{2\sqrt{D_{Aw}\,t}} \tag{16.2-11}$$

$$\left.\frac{\partial C_B}{\partial z}\right|_{z_r} = \frac{1}{1-\text{erf}\sqrt{\frac{\alpha}{D_{Bw}}}} C_{B\infty}\frac{2}{\sqrt{\pi}}\exp\left(-\frac{{z_r}^2}{4\,D_{Bw}\,t}\right)\frac{1}{2\sqrt{D_{Bw}\,t}} \tag{16.2-12}$$

Substitute these relations with Eq. (16.2-9) into B.C.5

$$\exp\left(\frac{\alpha}{D_{Bw}}\right)\left[1-\text{erf}\sqrt{\frac{\alpha}{D_{Bw}}}\right] = \exp\left(\frac{\alpha}{D_{Aw}}\right)\text{erf}\sqrt{\frac{\alpha}{D_{Aw}}}\sqrt{\frac{D_{Bw}}{D_{Aw}}}\frac{C_B}{\nu\,C_{Ai}} \tag{16.2-13}$$

This equation should be solved by trial and error method to determine α.

The concentration profiles of A and B are given by

$$\frac{C_A}{C_{Ai}} = 1 - \frac{1}{\text{erf}\sqrt{\frac{\alpha}{D_{Aw}}}}\text{erf}\frac{z}{2\sqrt{D_{Aw}\,t}} \qquad 0 \le z \le z_r(t) \tag{16.2-14}$$

$$\frac{C_B}{C_{B\infty}} = 1 - \frac{1}{1-\text{erf}\sqrt{\frac{\alpha}{D_{Bw}}}} + \frac{\text{erf}\frac{z}{2\sqrt{D_{Bw}\,t}}}{1-\text{erf}\sqrt{\frac{\alpha}{D_{Bw}}}} \qquad z_r(t) \le z \le \infty \tag{16.2-15}$$

Then the rate of absorption can be calculated as

$$N_A|_{z=0} = -D_{Aw}\left.\frac{\partial C_A}{\partial z}\right|_{z=0} = \frac{1}{\text{erf}\sqrt{\frac{\alpha}{D_{Aw}}}}\sqrt{\frac{D_{Aw}}{\pi t}}C_{Ai} \tag{16.2-16}$$

The average rate of absorption over the total exposure time t is

$$W_A = \int_0^t N_A|_{z=0}dt \Big/ \int_0^t dt = \frac{1}{\text{erf}\sqrt{\frac{\alpha}{D_{Aw}}}}\sqrt{\frac{4\,D_{Aw}}{\pi t}}C_{Ai} \tag{16.2-17}$$

The coefficient in front of C_{Ai} is the mass transfer coefficient with bimolecular chemical reaction:

$$k_L = \sqrt{\frac{4\,D_{Aw}}{\pi t}} \Big/ \text{erf}\sqrt{\frac{\alpha}{D_{Aw}}} \tag{16.2-18}$$

Comparing with the result of purely physical diffusion, Eq. (16.1-13), the reaction factor is given by

$$\beta = \frac{1}{\text{erf}\sqrt{\frac{\alpha}{D_{Aw}}}} \tag{16.2-19}$$

From here, the case when α is sufficiently small in comparison with D_{Aw} and D_{Bw} will be considered to obtain the reaction factor as a function of known variables. It will be shown later that this situation can be obtained when $C_{B\infty}$ is sufficiently large with respect to C_{Ai}.

For small α

$$\exp\left(\frac{\alpha}{D_{Aw}}\right) = 1 + \frac{\alpha}{D_{Aw}} + \frac{1}{2}\left(\frac{\alpha}{D_{Aw}}\right)^2 + - - - - -$$

$$\text{erf}\sqrt{\frac{\alpha}{D_{Aw}}} = \frac{2}{\sqrt{\pi}}\left[\left(\frac{\alpha}{D_{Aw}}\right)^{1/2} - \frac{1}{3}\left(\frac{\alpha}{D_{Aw}}\right)^{3/2} + \frac{1}{10}\left(\frac{\alpha}{D_{Aw}}\right)^{5/2} - - - -\right]$$

$$1 - \text{erf}\sqrt{\frac{\alpha}{D_{Bw}}} = 1 - \frac{2}{\sqrt{\pi}}\left[\left(\frac{\alpha}{D_{Bw}}\right)^{1/2} - \frac{1}{3}\left(\frac{\alpha}{D_{Bw}}\right)^{3/2} + \frac{1}{10}\left(\frac{\alpha}{D_{Bw}}\right)^{5/2} - - - -\right]$$

Substitute these relations into Eq. (16.2-13)

$$\left[1 - \frac{2}{\sqrt{\pi}}\left[\left(\frac{\alpha}{D_{Bw}}\right)^{1/2} - \frac{1}{3}\left(\frac{\alpha}{D_{Bw}}\right)^{3/2} + \frac{1}{10}\left(\frac{\alpha}{D_{Bw}}\right)^{5/2} - - - -\right]\right]$$
$$= \left[1 + \frac{\alpha}{D_{Aw}} + \frac{1}{2}\left(\frac{\alpha}{D_{Aw}}\right)^2 + - - -\right]\frac{2}{\sqrt{\pi}}\left[\left(\frac{\alpha}{D_{Aw}}\right)^{1/2} - \frac{1}{3}\left(\frac{\alpha}{D_{Aw}}\right)^{3/2} + \frac{1}{10}\left(\frac{\alpha}{D_{Aw}}\right)^{5/2} - -\right.$$
$$\left. - -\right]\sqrt{\frac{D_{Bw}}{D_{Aw}}}\frac{C_{B\infty}}{\nu\,C_{Ai}}\left[1 + \frac{\alpha}{D_{Bw}} + \frac{1}{2}\left(\frac{\alpha}{D_{Bw}}\right)^2 + - - -\right]$$

For $\alpha \ll D_{Aw}$ and D_{Bw}, the above equation can be approximated and rearranged as

$$1 - \frac{2}{\sqrt{\pi}}\sqrt{\frac{\alpha}{D_{Bw}}} \cong \frac{2}{\sqrt{\pi}}\sqrt{\frac{\alpha}{D_{Aw}}}\sqrt{\frac{D_{Bw}}{D_{Aw}}}\frac{C_{B\infty}}{\nu\,C_{Ai}}$$

The equation can be solved

$$\alpha = \frac{\pi}{4}\left[\frac{1}{\sqrt{D_{Bw}}} + \frac{1}{\sqrt{D_{Aw}}}\sqrt{\frac{D_{Bw}}{D_{Aw}}}\frac{C_{B\infty}}{\nu\, C_{Ai}}\right]^{-2} \qquad \text{for small } \alpha \tag{16.2-20}$$

This equation suggests that α becomes small when $C_{B\infty}$ is sufficiently large compared with C_{Ai}. The larger $C_{B\infty}$ is, the closer the reaction plane remains to the interface.

The reaction factor can also be approximated for small α:

$$\beta = \frac{1}{\operatorname{erf}\sqrt{\frac{\alpha}{D_{Aw}}}} \cong \frac{1}{\frac{2}{\sqrt{\pi}}\sqrt{\frac{\alpha}{D_{Aw}}}} \tag{16.2-21}$$

Substitute Eq. (16.2-20) into the above equation

$$\beta = \sqrt{\frac{D_{Aw}}{D_{Bw}}} + \sqrt{\frac{D_{Bw}}{D_{Aw}}}\frac{C_{B\infty}}{\nu\, C_{Ai}} \qquad \text{for large } C_{B\infty} \tag{16.2-22}$$

In the case when $D_{Aw} \cong D_{Bw}$

$$\beta = 1 + \frac{C_{B\infty}}{\nu\, C_{Ai}} \qquad \text{for the case of large } C_{B\infty} \text{ and } D_{Aw} \cong D_{Bw} \tag{16.2-23}$$

Unlike the results obtained for purely physical absorption or absorption with first-order reaction, the rate of absorption with second-order reaction is not proportional to the concentration of the substance being absorbed. It should be noticed that even when the interfacial concentration C_{Ai} is very small owing to small concentration of A in the gas phase, the absorption rate may become large owing to the effect of C_B. According to Eq. (16.2-22),

The reaction factor is a function of diffusivities D_{Aw}, D_{Bw}, bulk concentration C_B, and interfacial concentration C_{Ai} only. This result can be applied to any type of absorption equipment since α is not a function of equipment geometry and flow conditions.

Regarding the global climate change by CO_2 emission due to fossil fuel use, many chemical and electric power companies were challenging the technical development of reactive gas absorption using aqueous amine solvents for CO_2 capture. One possible reaction between CO_2 and monoethanol amine in the aqueous solution can be considered as

$$2\,\mathrm{RNH_2} + \mathrm{CO_2} \leftrightarrow \mathrm{RNHCOO^-} + \mathrm{RNH_3^+}$$

This is an endothermic bimolecular reaction. This topic is not dealt with here owing to its difficult mechanism.

16.3 Design of Packed Absorption Towers

Let us study a practical design of gas absorbers by using the following example.

[EXAMPLE 16.2-1] A packed absorption tower is to be designed for the removal of SO_2 from air by chemical absorption in an aqueous solution of sodium hydroxide. The tower has an inside diameter of 0.5 m and is packed with 1-in. ceramic Raschig rings. An absorption may be assumed isothermal at 25℃(= 298 K) and 1 atm (= 1.013×10^5 Pa). The air stream containing 10 mol% of SO_2 enters the tower from the bottom at a rate of 40 kmol/m^{2}h. The aqueous solution containing 2 M-NaOH (=7.4 wt% = 3.47 mol%) enters the tower from the top at a rate of 400 kmol/m^{2}h. Estimate the height of packing required to remove 95% of SO_2 from the airstream.

Solution:

(1) First step: Calculation of mass transfer coefficient k_G, k_L° for physical absorption

(a) Gas-phase mass transfer coefficient k_G:

Due to the low concentration of SO_2 in air, the viscosity and density of air can be used for the airstream:

$\mu_G = 1.85 \times 10^{-5}$ kg/m s, $\rho_G = 1.19$ kg/m^3. The diffusivity of SO_2 in air can be calculated by Hirschfelder *et al.* equation: $D_{Ag} = 1.27 \times 10^{-5}$ m^2/s.

The Schmidt number is

$$Sc_G = \frac{\mu_G}{\rho_G D_{Ag}} = 1.22$$

The mass velocities are

$$G = (40\ \text{kmol/m}^2\text{h})[(0.90)(29) + (1 - 0.90)(64)]\ \text{kg/kmol} = 1{,}300\ \text{kg/m}^2\text{h}$$

$$\text{L} = (400\ \text{kmol/m}^2\text{h})[(0.965)(18) + (0.0347)(40)]\ \text{kg/kmol} = 7{,}500\ \text{kg/m}^2\text{h}$$

Gas-phase mass transfer coefficient

For these values of mass velocities, Eq. (10.4-6) can be used to estimate k_G:

$$H_G = c\, G^p\, L^q \left(\frac{\mu_G}{\rho_G D_G}\right)^{2/3} \tag{16.3-1}$$

For 1-in. Raschig ring, $p = 0.32,\ q = -0.51,\ c = 3.07$. Then

$$H_G = (3.07)(1300)^{0.32}(7500)^{-0.51}(1.22)^{2/3} = 0.365\ \text{m}$$

From Table 10.4-2, $D_p = 0.0254$ m, $a_t = 190\ \text{m}^2/\text{m}^3$.

The surface tension of water at 25℃ is

$$\sigma = 72.0\ \text{dyne/cm} = 0.072\ \text{N/m}.$$

The interfacial area a is calculated by using Eq. (10.4-5) as follows:

$$a = 0.0406\ (7500)^{0.455}(72.0)^{-0.83}(2.54)^{-0.48} = 46.2\ \text{m}^2/\text{m}^3 \tag{16.3-2}$$

From the definition of H_G: $H_G = \overline{G_M}/k_y a$

Assuming $\overline{G_M} = G_{M1}$

$$k_y = \frac{\overline{G_M}}{H_G a} = \frac{(40\ \text{kmol/m}^2\text{h})}{(0.365\ \text{m})(46.2\ \text{m}^2/\text{m}^3)} = 2.37\ \text{kmol/m}^2\text{h}$$

Therefore

$$k_G = k_y^*/p_B = y_B k_y/p_B = k_y/P = 2.37\ \text{kmol/m}^2\text{h atm} \tag{16.3-3}$$

(b) Liquid-phase mass transfer coefficient k_L°:

The viscosity and density of water at 25℃ can be used:

$$\mu_L = 0.895\ \text{cP} = 0.895 \times 10^{-3}\ \text{kg/m s},\ \rho_L = 997\ \text{kg/m}^3.$$

The diffusivity of SO_2 in water $D_{Aw} = 1.85 \times 10^{-9}\ \text{m}^2/\text{s}$.

The Schmidt number is

$$Sc_L = \frac{0.895 \times 10^{-3}}{(997)(1.85 \times 10^{-9})} = 485$$

Liquid-phase mass transfer coefficient

$L = 7500/3600 = 2.083\ \text{kg/m}^2\text{s}$. Eq. (10.4-1) can be used to estimate k_L° for 1-in. Raschig rings ($\alpha = 430,\ n = 0.22$):

$$H_L = \frac{1}{430}\left(\frac{2.083}{0.895 \times 10^{-3}}\right)^{0.22}(485)^{0.5} = 0.282\ \text{m}$$

From the definition of H_L: $H_L = \overline{L_M}/k_x a$. Assume $\overline{L_M} = L_{M2}$

$$k_x = \frac{\overline{L_M}}{H_L a} = \frac{400\ \text{kmol/m}^2\text{h}}{(0.282\ m)(46.2\ \text{m}^2/\text{m}^3)} = 30.7\ \text{kmol/m}^2\text{h}$$

Therefore

$$k_L = k_x^*/C_B = x_B k_x/C_B = k_x/c = (18\ \text{m}^3/1000\ \text{kmol})(30.7\ \text{kmol/m}^2\text{h}) = 0.553\ \text{m/h} \tag{16.3-4}$$

(2) Second step: Equilibrium relationship of SO_2 – electrolytic solution system:

Strictly speaking, the SO_2 – water system does not follow Henry's law. For simplicity, over a range of very low partial pressure ($0 \le p_A \le 0.1$) the equilibrium curve can be roughly approximated by a linear relationship, i.e., Henry's law:

$$p_A = 0.54\ C_A \tag{16.3-5}$$

Here the Henry's constant $H_w = 0.54\ \text{atm m}^3/\text{kmol}$.

(a) Effect of ions in an electrolytic solution

In general, the solubility of gas is decreased by the presence of ions in an electrolytic solution. According to van Krevelen and Hoftijzer[1,2], the Henry's constant for the solution can be related by the following empirical equation:

Table 16.3-1 Equilibrium relation of SO_2 – water system

p_A atm	C_A kmol/m^3
0.793	1.17
0.519	0.783
0.248	0.391
0.143	0.243
0.0908	0.156
0.0599	0.109
0.0408	0.0779
0.0223	0.0469
0.0134	0.0312
0.00917	0.0235
0.00520	0.0156
0.00191	0.00783
0.000724	0.00312

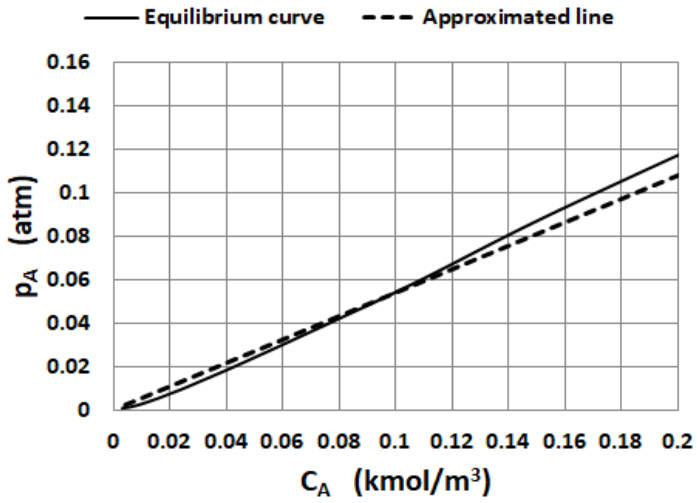

Fig. 16.3-1. Approximation of equilibrium curve

$$\log \frac{H_w}{H} = -\sum_j h_j I_j \qquad (16.3\text{-}6)$$

Here I_j is the ionic strength and $h_j = h_+ + h_- + h_G$ is the empirical constant.
The ionic strength can be calculated by

$$I = \frac{1}{2}\sum_i z_i{}^2 C_i \qquad (16.3\text{-}6)$$

where z_i is the number of positive or negative charges on an ion having molarity C_i .

1. Van Krevelen, D. W. and P.J. Hoftijzer: *Rec. Trav. Chim.*, vol.67, 563 (1943)
2. Van Krevelen, D. W. and P.J. Hoftijzer: Chim. Ind. XXI Congr. Int., Chim. Ind., p.168 (1948)
3. Sherwood, T. K., R. L. Pigford, and C.R. Wilke: "Mass Transfer," p. McGraw-Hill, New York (1975)

The h values are listed in Table 16.3-2.

Table 16.3-2 Constants in Eq. (16.3-6)

cations	h_+ m^3/kg – ion	anions	h_- m^3/kg – ion	gas	h_G m^3/kmol
H^+	0.0	OH^-	0.066	H_2	-0.002
Na^+	0.091	Cl^-	0.021	O_2	0.022
K^+	0.074	$SO_4{}^{--}$	0.022	CO_2	-0.019
$NH_4{}^+$	0.028	$CO_3{}^{--}$	0.021	NH_3	-0.054
Mg^{++}	0.051	Br^-	0.012	SO_2	-0.103
Ca^{++}	0.053	$SO_3{}^{--}$	0.001	H_2S	-0.033

The above h_G values were picked up from the data taken at 25℃.

1. Danckwerts, P.V.: "Gas–Liquid Reaction," p.19, McGraw–Hill, Nerw York (1970)

(b) At the top of the tower

For NaOH $C_1 = 2\ \text{kg} - \text{ion Na}^+/\text{m}^3 \qquad z_1 = 1$

$C_2 = 2\ \text{kg} - \text{ion OH}^-/\text{m}^3 \qquad z_2 = 1$

$$I = \frac{1}{2}\left((2)(1)^2 + (2)(1)^2\right) = 2$$

From Table 16.2-2,

$$h = h_G + h_+ + h_- = -0.103 + 0.091 + 0.066 = 0.054$$

$$\log \frac{H_w}{H} = -\sum_j h_j I_j = -(0.054)(2) = -0.108 \qquad (16.3\text{-}7)$$

Then the Henry's constant for the electrolytic solution is calculated as

$\frac{H_w}{H} = 0.78 \rightarrow H = H_W/0.78$ = 0.54/0.78 = 0.69 atm m^3/kmol

Molar velocity of NaOH at the top = (400)(0.0347) = 13.88 kmol/m^{2}h

Rate of SO_2 removed from air = (40)(0.10)(0.95) = 3.8 kmol/m^{2}h

Molar velocity of SO_2 at the top = (40)(0.10)(1 – 0.95) = 0.2 kmol/m^{2}h

Rate of NaOH consumed for the reaction = (2)(3.8) = 7.6 kmol/m^{2}h

(c) At the bottom of the tower

Molar velocity of NaOH = 13.88 – 7.6 = 6.28 kmol/m^{2}h

Concentration of NaOH $\cong 6.28/400 = 0.0157$ (mole fraction)

$$C_{NaOH} \cong \frac{1000}{18}\frac{0.0157}{1-0.0157} = 0.89\ \text{kmol/m}^3$$

Molar velocity of Na_2SO_3 = 3.8 kmol/m^{2}h

Concentration of $Na_2SO_3 \cong 3.8/400 = 0.0095$ (mole fraction)

$$C_{Na_2SO_3} \cong \frac{1000}{18}\frac{0.0095}{1-0.0095} = 0.53\ \text{kmol/m}^3$$

For NaOH $h = -0.103 + 0.091 + 0.066 = 0.054$

$$I = (1/2)\left((0.89)(1)^2 + (0.89)(1)^2\right) = 0.89$$

For Na_2SO_3 $h = -0.103 + 0.091 + 0.001 = -0.011$

$$I = (1/2)\left((0.53)(2)^2 + (0.53 \times 2)(1)^2\right) = 1.59$$

Then

$$\log \frac{H_w}{H} = -\left((0.054)(0.89) + (-0.011)(1.59)\right) = -0.0306 \qquad (16.3\text{-}8)$$

Averaging between the top and bottom

$$\log \frac{H_w}{H} = -\frac{0.108 + 0.0306}{2} = -0.0693$$

The Henry's constant averaged over the tower is calculated as

$\frac{H_w}{H} = 0.852 \rightarrow H = H_W/0.78$ = 0.54/0.852 = 0.634 atm m^3/kmol (16.3-9)

(3) Third step: Absorption rate

$$N_A = k_G(p_A - p_{Ai}) = \beta\, k_L^\circ\, C_{Ai} = \left[\sqrt{\frac{D_{Aw}}{D_{Bw}}} + \sqrt{\frac{D_{Bw}}{D_{Aw}}}\frac{C_{B\infty}}{\nu\, C_{Ai}}\right] k_L^\circ\, C_{Ai} = k_L^\circ\left[\sqrt{\frac{D_{Aw}}{D_{Bw}}}\, C_{Ai} + \sqrt{\frac{D_{Bw}}{D_{Aw}}}\frac{C_{B\infty}}{\nu}\right] \qquad (16.3\text{-}10)$$

Diffusivity of NaOH in water is given from literature: $D_{Bw} = 1.25\ 10^{-9}$ m^2/s (at 25℃). The effect of Na_2SO_3 on the liquid-phase diffusivities D_{Aw}, D_{Bw} is assumed negligibly small due to the low concentration.

For the present case $D_{Aw} \cong D_{Bw}$.

Therefore

$$N_A = k_G(p_A - p_{Ai}) = k_L^\circ \left(C_{Ai} + \frac{C_{B\infty}}{\nu}\right)$$
$$= \frac{p_A - p_{Ai}}{\frac{1}{k_G}} = \frac{H\,C_{Ai} + H\,C_{B\infty}/\nu}{\frac{H}{k_L^\circ}} = \frac{p_A + H\,C_{B\infty}/\nu}{\frac{1}{k_G} + \frac{H}{k_L^\circ}} \quad (16.3\text{-}11)$$

(4) Fourth step: Overall mass transfer coefficient K_G

$$\frac{1}{K_G} = \frac{1}{k_G} + \frac{H}{k_L^\circ} = \frac{1}{2.37} + \frac{0.66}{0.553} = 1.62$$
$$K_G = 0.62 \text{ kmol/m}^2\text{h atm}$$

(5) Fifth step: Mass balance

Mass balance can be set up over the packing section between $z = 0$ and z to get the operating-line equation:

$$2 \times (\text{molar rate of } SO_2 \text{ absorbed}) = (\text{molar rate of NaOH consumed})$$
$$\nu\, G_M' \left(\frac{p_A}{1-p_A} - \frac{p_{A2}}{1-p_{A2}}\right) = L_{M2}x_{B2} - L_M(C_{B\infty}/c) \quad (16.3\text{-}12)$$

where c is the molar density of the solution in kg/m^3.

Due to the very low concentration of ions, the molar velocity L_M and molar density c can be considered constant over the whole height of the packing section.

$$c \cong \frac{1000}{18} + 2 = 57.6 \text{ kmol/m}^3 \quad \text{at the top}$$
$$c \cong \frac{1000}{18} + 0.89 + 0.53 + 0.53 = 57.5 \text{ kmol/m}^3 \quad \text{at the bottom}$$
$$L_M \cong L_{M2} = 400 \text{ kmol/m}^2\text{h}$$

Mass balance over the differential volume element dz is

$$\nu\, G_M'\, d\left(\frac{p_A}{1-p_A}\right) = \nu\, G_M' \frac{dp_A}{(1-p_A)^2} = K_G a\, dz \left(p_A + \frac{H\,C_{B\infty}}{\nu}\right) \quad (16.3\text{-}13)$$

The height of the packing section is given by

$$Z_T = \frac{\nu\, G_M'}{K_G a} \int_{p_{A2}}^{p_{A1}} \frac{dp_A}{\left(p_A + \frac{H\,C_{B\infty}}{\nu}\right)(1-p_A)^2} \quad (16.3\text{-}14)$$

Using the HTU = $\frac{\nu\,\overline{G_M'}}{K_G a}$ averaged over the packing section from the top through the bottom

$$Z_T = \frac{\nu\,\overline{G_M'}}{K_G a} \int_{p_{A2}}^{p_{A1}} \frac{dp_A}{\left(p_A + \frac{H\,C_{B\infty}}{\nu}\right)(1-p_A)} \quad (16.3\text{-}15)$$

The reaction has the following form of irreversible bimolecular reaction

$$SO_2 + 2\,NaOH \rightarrow Na_2SO_3 + H_2O$$

Therefore $\nu = 2$

The modified Henry's constant $H = 0.66$ atm m^3/kmol

and the overall coefficient $K_G = 0.62$ kmol/m^{2}h atm

$$\overline{G_M} = (G_{M1} + G_{M2})/2 = (40 + 36.2)/2 = 38.1 \text{ kmol/m}^2\text{h}$$

First the bulk concentration of NaOH corresponding to the partial pressure of SO_2 is calculated at each section by using the operating-line equation:

$$C_{B\infty} = \frac{c}{L_M}\left\{L_{M2}x_{B2} - \nu\, G_M'\left[\frac{p_A}{1-p_A} - \frac{p_{A2}}{1-p_{A2}}\right]\right\} = 2.06 - 10.4\frac{p_A}{1-p_A} \quad (16.3\text{-}16)$$

Next the equation shown below can be integrated numerically or graphically to get the height of packing:

$$Z_T = \frac{(2)(38.1 \text{ kmol/m}^2\text{h})}{(0.62 \text{ kmol/m}^2\text{h atm})(46.2 \text{ m}^2/\text{m}^3)} \int_{0.00552}^{0.10} \frac{dp_A}{\left(p_A + \frac{0.66\,C_{B\infty}}{2}\right)(1 - p_A)}$$

Here $p_{A2} = 0.2/(G_M' + 0.2) = 0.2/(36 + 0.20) = 0.00552$ atm

p_A	$C_{B\infty}$	$1/(p_A + 0.33\ C_{B\infty})(1 - p_A)$
0.00552	2.00	1.511
0.010	1.955	1.542
0.015	1.902	1.580
0.020	1.848	1.620
0.025	1.793	1.663
0.030	1.738	1.708
0.035	1.683	1.755
0.040	1.627	1.806
0.045	1.570	1.860
0.050	1.513	1.916
0.055	1.455	1.977
0.060	1.396	2.043
0.065	1.337	2.113
0.070	1.277	2.188
0.075	1.217	2.268
0.080	1.156	2.355
0.,085	1.094	2.450
0.090	1.031	2.554
0.095	0.968	2.666
0.100	0.904	2.789

$$\sum \frac{\Delta p_A}{(p_A + 0.33\ C_{B\infty})(1 - p_A)}$$
$$= \left(\frac{1}{2}\right)(1.511 + 1.542)(0.01 - 0.00552) + \left(\frac{1}{2}\right)(1.542 + 1.580)(0.015 - 0.01)$$
$$+ \cdots\cdots\cdots + \left(\frac{1}{2}\right)(2.666 + 2.789)(0.1 - 0.095) = 0.190\ \text{atm}^{-1}$$

Finally the required height of the packing section is

$$Z_T = (2.66\ \text{m atm})(0.190\ \text{atm}^{-1}) = 0.505\ \text{m}$$

From a viewpoint of practical engineering design, this result seems to be smaller than expected. It is usually necessary to take into account the safety factor.

Nomenclature

a	effective interfacial area in packing section, [m^2/m^3]
C_A	molar concentration of component A, [kmol/m3]
H	Henry's constant, [-]
D_{Am}, D_{Aw}	diffusivity of component A, [m^2/s]
D_{Bw}	diffusivity of component B, [m^2/s]
G	mass velocity of gas, [kg/m^2s]
H_G	HTU (Height of Transfer Unit) of gas phase, [m]
I_j	ionic strength,
k_1	reaction-rate constant of first-order reaction, [1/s]
k_L	liquid-phase mass transfer coefficient, [m/s]
K_G, k_G	overall and gas-phase mass transfer coefficient, [m/s] or [$kmol/m^2s$ Pa]
L	mass velocity of liquid, [kg/m^2s]
L_M	superficial molar velocity of liquid, [$kmol/m^2s$]
N_A	mass flux, [$kmol/m^2s$]
N_L	liquid-phase number of transfer units, [-]
p	partial pressure, [Pa]
r_A	rate of first-order reaction, [$kmol/m^3s$]
S	area of surface perpendicular to mass transfer, [m^2]
Sc	Schmidt number, [-]
W	mass flow rate, [kg/s]
t	time, [s]
y	liquid-side coordinate perpendicular to interface, [m]

z	vertical coordinate of packed column, [m]
Z_T	height of packed column, [m]
z_i	number of positive or negative charges, [-]
z_r	position of reaction plane, [m]
α	integration constant, [m^2/s]
β	reaction factor, [-]
ε	volume fraction of liquid in packing section, [-]
θ	total holdup time, [s]
∞	bulk

Subcripts

A	component A
B	component B
f	film
G	gas phase
i	interface
L	liquid phase
M	molar

CHAPTER 17

TURBULENT TRANSPORT PHENOMENA

17.1 Fundamental Equations of Turbulent Transport

17.1-1 Fundamental properties of turbulent flows

Most flows occurring in practical engineering processes are turbulent. Turbulent flow always occurs at high Reynolds number. We know that laminar motion in a circular tube tends to become unstable at Reynolds numbers above about 2,100 in the presence of small disturbances, and a transition to turbulent flow will occur.

One characteristic of turbulent flows is the irregularity: the velocity at any point varies with time in both magnitude and direction. Turbulence is rotational and three dimensional. Fig.17.1-1 is a fluctuating curve imitating the real oscillogram of one component of the fluctuating velocities taken by a hot-wire anemometer placed at a point in the turbulent flowfield. Regarding the principle of hot-wire anemometry, you can refer to Section 9.7-2 of Chapter 9. The static pressure has also similar fluctuations, which can be observed by using a piezo-electric pressure transducer.

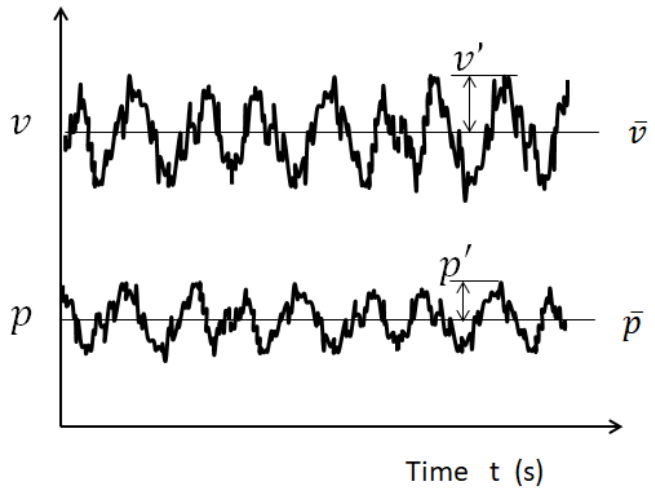

Fig.17.1-1. Oscillogram of velocity and pressure of turbulent flow

We can notice from these fluctuating oscillograms that they are not without a certain degree of regularity from a statistical point of view. The instantaneous velocity v can be decomposed into a time-averaged velocity $\bar{v}$ and velocity fluctuations v', such that

$$v(x,y,z,t) = \bar{v}\,(x,y,z) + v'(x,y,z,t) \qquad (17.1\text{-}1)$$

The time average is defined by

$$\bar{v} = \lim_{T\to\infty} \frac{1}{T} \int_{t_0}^{t_0+T} v\, dt \qquad (17.1\text{-}2)$$

At steady state $\frac{\partial \bar{v}}{\partial t} = 0$

The velocity measured by a pitot tube is approximately equal to the time-averaged velocity, except for turbulent flows which have extremely high turbulence intensity. Turbulence consists of the

superposition of various, small periodic motions on large-scale intermittent motions. It is like the orchestral sound consisting of the superposition of various, high-frequency sounds on low-frequency sounds.

The instantaneous velocity fluctuations can become negative very often.

Therefore the time-averaged value of a fluctuating quantity is zero by definition, for example,

$$\bar{v'} = \lim_{T\to\infty} \frac{1}{T} \int_{t_0}^{t_0+T} (v - \bar{v}) dt = \lim_{T\to\infty} \frac{1}{T} \int_{t_0}^{t_0+T} v\, dt - \bar{v} = 0 \qquad (17.1\text{-}3)$$

However the squared values cannot be negative. As a measure of the magnitude of the turbulence, the intensity of turbulence is defined as

$$Tu = \frac{\sqrt{\overline{v'^2}}}{\bar{v}} \qquad (17.1\text{-}4)$$

, which may have values 0.01 to 0.10 in typical turbulent pipe flows.

Of many methods for the measurement of turbulent velocity, the hot-wire anemometer is the most useful. As described in Section 9.7-2, the principle of hot-wire anemometry is based on the convective heat transfer from a very fine heated wire to the approaching stream. The detecting element consists of a very fine short metal wire (e.g. 5 μm dia. And 5 mm long platinum wire for air stream), which is heated by an electric current to a constant temperature above the stream temperature. The wire is placed perpendicular to the velo0city component to be measured. The rate of heat loss to the ambient stream from the wire is proportional to the square root of the stream velocity $\sqrt{v}$ in the usual stream condition. The wire is of such low heat capacity that the temperature of the wire can follow the rapid velocity fluctuations. The rate of heat loss is equal to the rate of heat generated by the electric current through the wire, I^2R, where I is the electric current and R the electric resistance of the wire. In the usual measuring method, the electric resistance is controlled to be kept constant as far as possible by using an electronic feedback system. Instead, the feedback system changes the current through the wire as soon as a variation in electric resistance occurs. The response time to the change in approach velocity is of the order shorter than 0.1 ms.

Then we have the relation between I^2 and v:

$$I^2R = \alpha + \beta\sqrt{v} \qquad (17.1\text{-}5)$$

where α and β are usually determined by experiment.

If we substitute $I = \bar{I} + I'$ and $v = \bar{v} + v'$ into the Eq.(17.1-5), we get the approximate relation between I' and v':

$$\bar{I}^2R = \alpha + \beta\sqrt{\bar{v}} \quad \text{(mean velocity)}$$

$$I' = \frac{\beta}{4\bar{I}R} \frac{\sqrt{\bar{v}}}{\bar{v}} v' \quad \text{(velocity fluctuation)} \qquad (17.1\text{-}6)$$

The last equation is obtained as the first approximation when $v' \ll \bar{v}$, i.e. $I' \ll \bar{I}$.

The usual block diagram of hot-wire anemometry is shown in Fig.17.1-2.

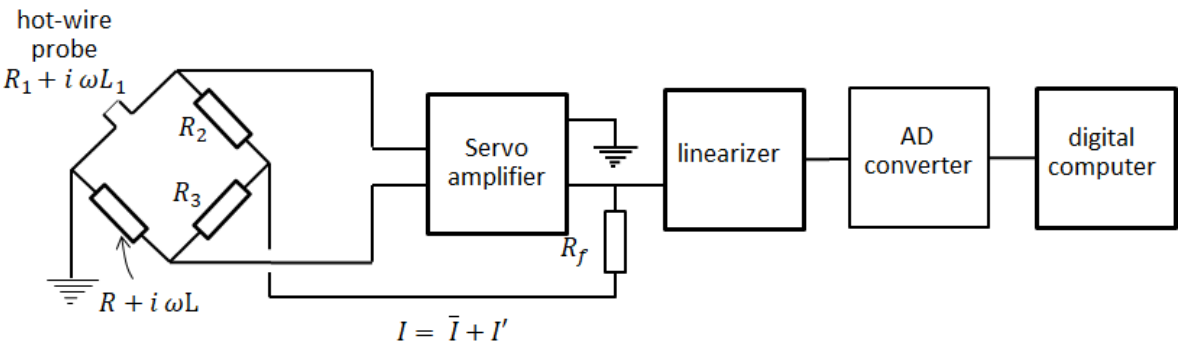

Fig. 17.1-2. Block diagram of hot-wire anemometer for constant temperature method

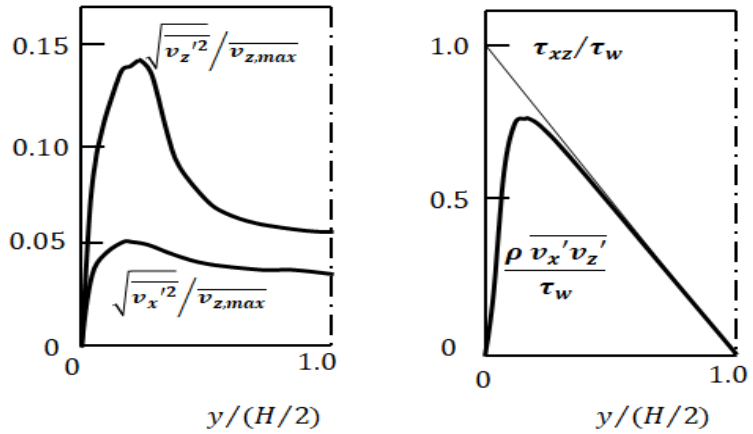

Fig. 17.1-3. Distribution of velocity fluctuations and Reynolds stress in a rectangular channel

As shown in Fig.17.1-3, the turbulence intensity in a rectangular channel becomes maximum near the wall.

The fluctuations $\sqrt{\overline{v_z'^2}}$ in the streamwise direction, or in the z direction, are greater than the fluctuations $\sqrt{\overline{v_x'^2}}$ in the transverse direction, or in the x direction. In the vicinity of the wall, molecular momentum transport becomes important but the fluctuations become very small. Turbulent flow in a pipe also has similar tendency.

Such properties and structure of turbulent flows are described in detail in Sec. 17.2~ 17.5.

17.1-2 Equation of motion for turbulent flows

Turbulence is a continuum phenomenon taking place in a continuum fluid. It is true that the equation of motion applies to turbulent flow, for example,

$$\frac{\partial(\rho v_x)}{\partial t}+\frac{\partial(\rho v_x v_x)}{\partial x}+\frac{\partial(\rho v_x v_y)}{\partial y}+\frac{\partial(\rho v_x v_z)}{\partial z}=-\frac{\partial p}{\partial x}+\mu\left(\frac{\partial^2 v_x}{\partial x^2}+\frac{\partial^2 v_x}{\partial y^2}+\frac{\partial^2 v_x}{\partial z^2}\right) \tag{17.1-7}$$

The instantaneous velocity and pressure can be decomposed into a time-averaged value and its fluctuations, such that

$$\begin{aligned} v_x &= \overline{v_x}+v_x' \\ v_y &= \overline{v_y}+v_y' \\ v_z &= \overline{v_z}+v_z' \\ p &= \bar{p}+p' \end{aligned} \tag{17.1-8}$$

Substituting these instantaneous quantities into Eq.(17.1-7) and averaging the resultant equation with respect to time, we get the equation of motion governing the mean (time-averaged) flow:

$$\frac{\partial(\rho\overline{v_x})}{\partial t}+\frac{\partial(\rho\overline{v_x}\,\overline{v_x})}{\partial x}+\frac{\partial(\rho\overline{v_x}\,\overline{v_y})}{\partial y}+\frac{\partial(\rho\overline{v_x}\,\overline{v_z})}{\partial z}=-\frac{\partial\bar{p}}{\partial x}+\mu\left(\frac{\partial^2\overline{v_x}}{\partial x^2}+\frac{\partial^2\overline{v_x}}{\partial y^2}+\frac{\partial^2\overline{v_x}}{\partial z^2}\right)$$
$$-\left(\frac{\partial(\rho\overline{v_x'v_x'})}{\partial x}+\frac{\partial(\rho\overline{v_x'v_y'})}{\partial y}+\frac{\partial(\rho\overline{v_x'v_z'})}{\partial z}\right) \tag{17.1-9}$$

In steady turbulent flow field, $\frac{\partial(\rho\overline{v_x})}{\partial t}$

In the averaging process, the terms consisting of a product of a mean value and a fluctuation vanish in the following way:

$$\overline{v_x v_y}=\overline{(\overline{v_x}+v_x')(\overline{v_y}+v_y')}=\overline{\overline{v_x}\,\overline{v_y}+\overline{v_x}\,v_y'+v_x'\overline{v_y}+v_x'\,v_y'}=\overline{v_x}\,\overline{v_y}+\overline{v_x'\,v_y'}$$

Here the mean value is regarded as a mere constant coefficient as far as the averaging is concerned.

17.1-3 Equations of energy and mass transport for turbulent flows

The equation of energy can also be used for turbulent heat transport with constant properties:

$$\frac{\partial(\rho CpT)}{\partial t}+\frac{\partial(\rho Cpv_xT)}{\partial x}+\frac{\partial(\rho Cpv_yT)}{\partial y}+\frac{\partial(\rho Cpv_zT)}{\partial z}=\kappa\left(\frac{\partial^2 T}{\partial x^2}+\frac{\partial^2 T}{\partial y^2}+\frac{\partial^2 T}{\partial z^2}\right) \quad (17.1\text{-}10)$$

The instantaneous temperature can be decomposed as

$$T=\overline{T}+\mathrm{T}' \quad (17.1\text{-}11)$$

In similar manner of averaging, we get

$$\frac{\partial(\rho Cp\overline{T})}{\partial t}+\frac{\partial(\rho Cp\overline{v_x}\,\overline{T})}{\partial x}+\frac{\partial(\rho Cp\overline{v_y}\,\overline{T})}{\partial y}+\frac{\partial(\rho Cp\overline{v_z}\,\overline{T})}{\partial z}=\kappa\left(\frac{\partial^2\overline{T}}{\partial x^2}+\frac{\partial^2\overline{T}}{\partial y^2}+\frac{\partial^2\overline{T}}{\partial z^2}\right)$$
$$\underline{-\left(\frac{\partial(\rho Cp\overline{v_x{}'T'})}{\partial x}+\frac{\partial(\rho Cp\overline{v_y{}'T'})}{\partial y}+\frac{\partial(\rho Cp\overline{v_z{}'T'})}{\partial z}\right)} \quad (17.1\text{-}12)$$

In steady turbulent temperature field, $\frac{\partial(\rho Cp\overline{T})}{\partial t}=0$

Similarly for turbulent mass transport without chemical reaction

$$\frac{\partial\,\overline{C_A}}{\partial t}+\frac{\partial(\overline{v_x}\,\overline{C_A})}{\partial x}+\frac{\partial(\overline{v_y}\,\overline{C_A})}{\partial y}+\frac{\partial(\overline{v_z}\,\overline{C_A})}{\partial z}=D\left(\frac{\partial^2\,\overline{C_A}}{\partial x^2}+\frac{\partial^2\,\overline{C_A}}{\partial y^2}+\frac{\partial^2\,\overline{C_A}}{\partial z^2}\right)$$
$$\underline{-\left(\frac{\partial(\overline{v_x{}'C_A{}'})}{\partial x}+\frac{\partial(\overline{v_y{}'C_A{}'})}{\partial y}+\frac{\partial(\overline{v_z{}'C_A{}'})}{\partial z}\right)} \quad (17.1\text{-}13)$$

In steady turbulent concentration field, $\frac{\partial\,\overline{C_A}}{\partial t}=0$

17.2 Phenomenological Understanding of Turbulent Transport

17.2-1 Effect of Nonlinear interaction of turbulence

In those three equations Eqs.(17.1-6), (17.1-9), and (17.1-10), new terms indicated by underlines arise.

They are concerned with the turbulent transport by eddy motion coming from nonlinear interaction of fluctuations. If these nonlinear effects of turbulence were not existent, the time-averaged distributions of velocity, temperature, and concentration would become the same as those for laminar transport.

The following group forms nine components of the turbulent momentum-flux tensor:

$$\tau_{xx}^{(t)}=-\rho\overline{v_x{}'v_x{}'} \qquad \tau_{xy}^{(t)}=\tau_{yx}^{(t)}=-\rho\overline{v_y{}'v_x{}'} \qquad \tau_{xz}^{(t)}=\tau_{zx}^{(t)}=-\rho\overline{v_z{}'v_x{}'}$$

$$\tau_{yy}^{(t)}=-\rho\overline{v_y{}'v_y{}'} \qquad \tau_{yz}^{(t)}=\tau_{zy}^{(t)}=-\rho\overline{v_y{}'v_z{}'} \qquad \tau_{zz}^{(t)}=-\rho\overline{v_z{}'v_z{}'}$$

These are usually referred to as the Reynolds stresses. The diagonal components $\tau_{xx}^{(t)}$, $\tau_{yy}^{(t)}$, $\tau_{zz}^{(t)}$ are turbulent normal stresses. In many turbulent flows they contribute little to the momentum transfer. The off-diagonal components $\tau_{xy}^{(t)}=\tau_{yx}^{(t)}$, $\tau_{yz}^{(t)}=\tau_{zy}^{(t)}$, $\tau_{xz}^{(t)}=\tau_{zx}^{(t)}$ are turbulent shear stresses. They play a dominant role in momentum transfer, except in the viscous sublayer near the wall where molecular transport is predominant.

We know that the distribution of time-averaged velocity for turbulent flow in a circular pipe is much flatter in the main flow region than for laminar flow. That fact is due to the Reynolds stresses.

We can interpret the effect of mixing due to eddy motion large in the transverse direction in main flow region.

The following group forms three components of turbulent heat-flux vector:

$$q_x^{(t)}=-\rho Cp\overline{v_x{}'T'} \qquad q_y^{(t)}=-\rho Cp\overline{v_y{}'T'} \qquad q_z^{(t)}=-\rho Cp\overline{v_z{}'T'}$$

They play an important role in heat transfer.

Similarly the following group forms three components of turbulent mass-flux vector:

$$j_x^{(t)}=-\overline{v_x{}'C_A{}'} \qquad j_y^{(t)}=-\overline{v_y{}'C_A{}'} \qquad j_z^{(t)}=-\overline{v_z{}'C_A{}'}$$

17.2-2 Mixing length theory and eddy diffusivity

A complete understanding of turbulent transport phenomena needs a quantitative description of turbulence, including the turbulence intensity and the size of eddies. Many direct numerical analyses based on physical models have been developed. Unfortunately, however, these approaches are beyond the level of this course.

Historically speaking, the Prandtl's mixing length model continues to serve as a background useful for the understanding of turbulent transport. One approach to the solution of turbulent momentum transport problems is to postulate a relation between the turbulent momentum-flux $\tau_{xy}^{(t)}$ and the mean rate of strain (velocity gradient) $\partial\overline{v_x}/\partial y$. It is clear that the greater the velocity gradient, the larger will be the v_x' induced by a v_y', and hence the larger will be $\tau_{yx}^{(t)} = -\rho\overline{v_y' v_x'}$.

The random motion of fluid lumps (eddies) in turbulent flow results in turbulent transfer of momentum, energy, and mass. In analogy with the mean free path in the gas kinetic theory, the so-called Prandtl mixing length l is a measure of the distance a large scale eddy travels before it breaks up and loses its identity.

Fig. 17.2-1 indicates a model of eddy interchange between two parallel layers set apart by a mixing length.

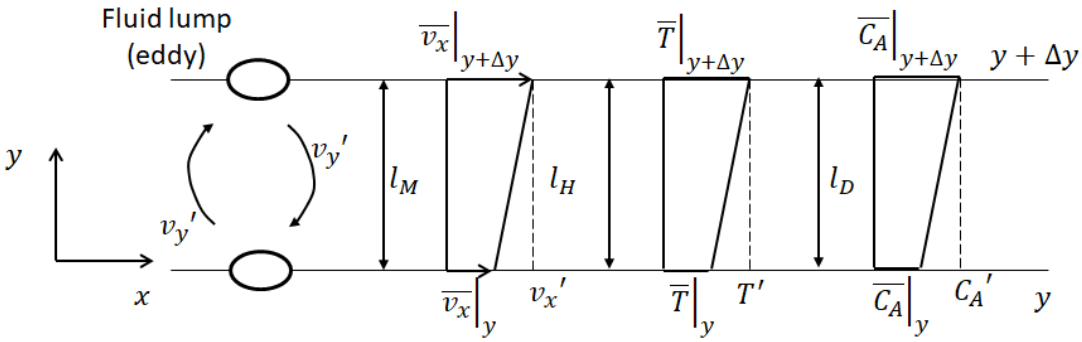

Fig.17.2-1 Mixing length theory

The transverse transport of momentum, energy, and mass is caused as a result of eddy interchange between two parallel layers as follows:

$$\tau_{yx}^{(t)} = \rho\overline{v_x}|_y\, v_y' - \rho\overline{v_x}|_{y+\Delta y}\, v_y' = -\rho v_y' l_M \frac{d\,\overline{v_x}}{dy} \tag{17.2-1}$$

$$q_y^{(t)} = \rho C_p \overline{T}\big|_y\, v_y' - \rho C_p \overline{T}\big|_{y+\Delta y}\, v_y' = -\rho C_p v_y' l_H \frac{d\,\overline{T}}{dy} \tag{17.2-2}$$

$$j_y^{(t)} = \overline{C_A}\big|_y\, v_y' - \overline{C_A}\big|_{y+\Delta y}\, v_y' = -v_y' l_D \frac{d\,\overline{C_A}}{dy} \tag{17.2-3}$$

in which the mixing length l is defined as the differential distance between the two layers Δy.

If we assume that $\overline{v_x}|_{y+\Delta y} - \overline{v_x}|_y \cong v_x'$, $\overline{T}\big|_{y+\Delta y} - \overline{T}\big|_y \cong T'$, and $\overline{C_A}\big|_{y+\Delta y} - \overline{C_A}\big|_y \cong C_A'$,

the turbulent transport fluxes can be obtained as

$$\tau_{yx}^{(t)} = -\rho v_y' v_x' \tag{17.2-4}$$

$$q_y^{(t)} = -\rho C_p v_y' T' \tag{17.2-5}$$

$$j_y^{(t)} = -v_y' C_A' \tag{17.2-6}$$

In Eqs. (17.2-1), (17.2-2), and (17.2-3), the products of velocity fluctuation and mixing length $v_y' l_M$, $v_y' l_H$, $v_y' l_D$ have the unit of diffusivity m^2/s. Therefore the eddy diffusivities are defined as

$$\tau_{yx}^{(t)} = -\rho\varepsilon_M \frac{d\,\overline{v_x}}{dy} \tag{17.2-7}$$

$$q_y^{(t)} = -\rho C_p \varepsilon_H \frac{d\,\overline{T}}{dy} \tag{17.2-8}$$

$$j_y^{(t)} = -\varepsilon_D \frac{d\,\overline{C_A}}{dy} \tag{17.2-9}$$

They are not a property of the fluid but vary with the flow conditions. They are much greater than molecular diffusivities ν, α, D_{AB} in the turbulent flow region. These eddy diffusivities ε_M, ε_H, ε_D are not only a property of fluids but a flow parameter as well. When molecular motion still prevails,

the total momentum-flux can be expressed as

$$\tau_{yx} = \tau_{yx}^{(l)} + \tau_{yx}^{(t)} = -\rho(\nu + \varepsilon_M)\frac{d\overline{v_x}}{dy} \quad (17.2\text{-}10)$$

Similarly

$$q_y = q_y^{(l)} + q_y^{(t)} = -\rho Cp(\alpha + \varepsilon_H)\frac{d\overline{T}}{dy} \quad (17.2\text{-}11)$$

$$j_y = j_y^{(l)} + j_y^{(t)} = -(D_{AB} + \varepsilon_D)\frac{d\overline{C_A}}{dy} \quad (17.2\text{-}12)$$

In a fully-developed pipe flow, the shear stress distribution is linear whether the flow is laminar or turbulent:

$$\tau_{rz} = \frac{r}{R}\tau_w \quad (17.2\text{-}13)$$

Therefore the eddy diffusivity ε_M can be evaluated from the measured velocity distribution by using the following equation:

$$\frac{\varepsilon_M}{\nu} = \frac{\tau_w\frac{r}{R}}{-\mu\frac{d\overline{v_z}}{dr}} - 1 \quad (17.2\text{-}14)$$

Fig. 17.2-2 shows the radial distribution of eddy diffusivity in the fully developed flow region in a circular pipe. These curves are schematically drawn taking into consideration many empirical data. The maximum of ε_M/ν occurs at the intermediate position between the axis and wall. This may be due to the fact that the turbulent eddy motion is produced there. As the axis is approached, ε_M/ν decreases from the maximum value. In the neighborhood of the pipe axis, it is too difficult to determine the eddy diffusivity owing to the fact that both the denominator and numerator of Eq. (17.2-14) become almost zero. Still ε_M/ν is much larger than unity, except very near the pipe wall. We should notice that these ε_M/ν distribution curves resemble the turbulence intensity curves in Fig. 7.1-3. However it should be kept in mind that the turbulent kinetic energy is generated much closer to the pipe wall.

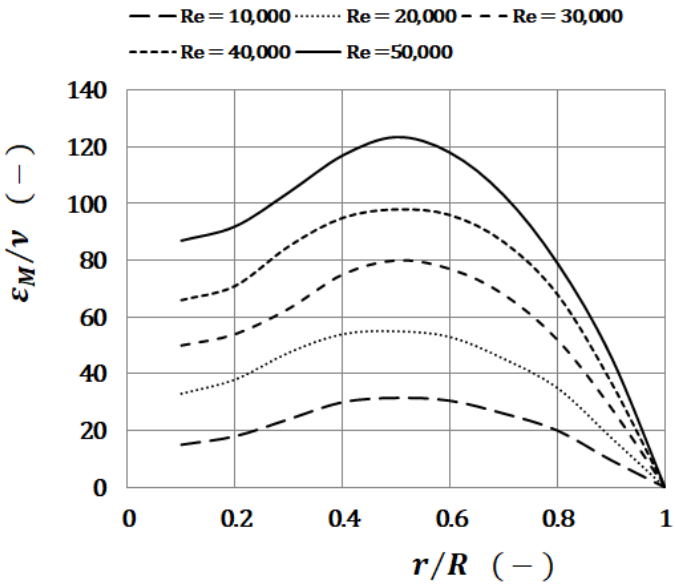

Fig. 17.2-2. Radial distribution of eddy diffusivity for momentum in a circular tube flow

17.2-3 Mixing length model based on turbulence correlation

We have already understood a qualitative explanation of the generation of turbulent motion in Chapter 3. At this section, let us consider the concept of "mixing length" again by using the more rigorous theory of turbulence.

Consider a traveling fluid element which starts from a level $y = 0$ at time $t = 0$ and passes an arbitrary level y at time t. Figure 18.2-3 is the turbulent velocity field for explanation of the mixing length theory.

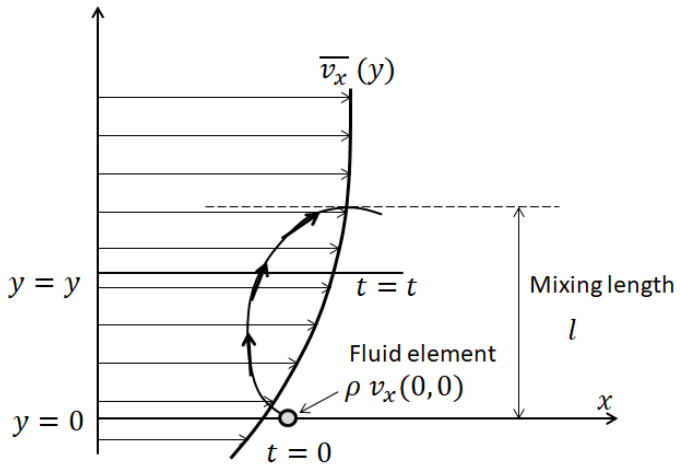

Fig. 17.2-3. Mixing length model based on turbulence correlation

If the fluid element does not lose its original momentum $\rho\, v_x(0,0)$ as it moves in the transverse direction, a momentum deficit at y and t is

$$\Delta M = \rho\, v_x(y,t) - \rho\, v_x(0,0) = \varrho\big(\overline{v_x}(y) - \overline{v_x}(0)\big) + \varrho(v_x'(y,t) - v_x'(0,0)) \qquad (17.2\text{-}15)$$

Since the intensity of turbulence in many turbulent flows has values in the neighborhood of 1 to 10%, the second term is small compared to the first one:

$$\Delta M \cong \varrho\big(\overline{v_x}(y) - \overline{v_x}(0)\big)$$

For small values of y, the velocity difference can be approximated by the first term of the Taylor series:

$$\Delta M \cong \varrho[\overline{v_x}(y) - \overline{v_x}(0)] = \rho \left.\frac{d\,\overline{v_x}}{dy}\right|_{y=0} y \qquad (17.2\text{-}16)$$

The volume of the fluid transported per unit area and unit time is the transverse component v_y' of the instantaneous velocity of the traveling fluid element.

From Lagrangian viewpoint

$$v_y' = \frac{d\,y}{dt} \qquad (17.2\text{-}17)$$

where y is the position of the fluid element. Since the momentum flux has dimensions of (momentum/volume)(volume/area/time), the average turbulent momentum-flux at $y = 0$ can be expressed as

$$\tau_{yx}^{(t)}\Big|_{y=0} = \Delta M\, \overline{v_y'} = \rho \left.\frac{d\,\overline{v_x}}{dy}\right|_{y=0} \overline{v_y' y} = \rho \left.\frac{d\,\overline{v_x}}{dy}\right|_{y=0} \overline{y \left.\frac{d\,y}{dt}\right|_{y=0}} = \frac{1}{2}\,\rho \left.\frac{d\,\overline{v_x}}{dy}\right|_{y=0} \left.\overline{\frac{d\,y^2}{dt}}\right|_{y=0} \qquad (17.2\text{-}18)$$

The overbar denotes an average taken over a large number of moving fluid elements starting from $y = 0$.

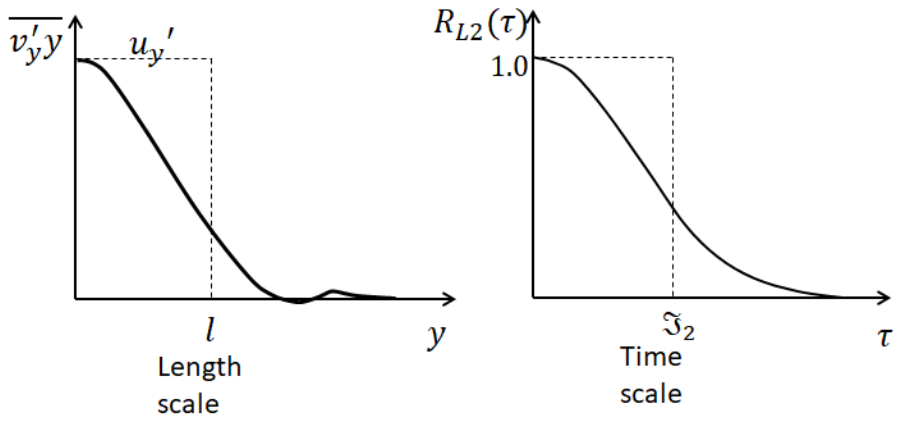

Fig. 17.2-4 Significance of length scale and time scale

Therefore we can assume that the correlation $\overline{v_y{}'y}$ becomes essentially zero at a distance y comparable to a transverse length scale l. If the RMS velocity $\sqrt{\overline{v_y{}'^2}}$ is denoted by $u_y{}'$, the correlation $\overline{v_y{}'y}$ is of order $u_y{}'l$:

$$\overline{v_y{}'y} = K_1 u_y{}' l \tag{17.2-19}$$

This transverse length scale is called "mixing length." Therefore the turbulent momentum-flux can be written as

$$\tau_{yx}^{(t)} = K_1 \rho u_y' l \frac{d\,\overline{v_x}}{dy} \tag{17.2-20}$$

Usually the mixing length l absorbs the unknown numerical coefficient because it is of order one: $K_1 l = l_M$.

If the mixing length l and the RMS velocity turbulence $u_y{}'$ were known over the entire flow field, the equation of motion could be solved. The mixing length can be considered to be proportional to the size of the larger eddies which play a predominant role in the turbulent momentum transport.

The distance y traveled for time t by the fluid element is

$$y = \int_0^t v_y'(t')dt' \tag{17.2-21}$$

The correlation $\overline{v_y{}'y}$ becomes

$$\overline{v_y{}'(t)y} = \overline{v_y'(t)\int_0^t v_y'(t')dt'} = \overline{\int_0^t v_y'(t)v_y'(t')dt'} \tag{17.2-22}$$

The averaging is performed with respect to the number of the moving fluid elements starting from $y = 0$.

The correlation $\overline{v_y'(t)v_y'(t')}$ does not depend on the reference time but on the time difference $t - t' = \tau$.

Then the correlation becomes a Lagrangian correlation coefficient:

$$R_{L2}(\tau) = \frac{\overline{v_y'(t)v_y'(t-\tau)}}{u_y{}'^2} \tag{17.2-23}$$

The Lagrangian integral time scale $\Im_2$ can be regarded as a measure of the time interval which is long enough for fluid elements to travel the length scale (mixing length) l:

$$\Im_2 = \int_0^\infty R_{L2}(\tau)\,d\tau \tag{17.2-24}$$

The Lagrangian correlation implies that as the time interval τ becomes large, the velocity fluctuation $v_y{}'(t)$ does not resemble $v_y{}'(t-\tau)$ in wave form, that is, the degree of correlation between $v_y{}'(t)$ and $v_y{}'(t-\tau)$ falls.

Then the turbulent momentum-flux is expressed as

$$\tau_{yx}^{(t)} = \rho \frac{d\,\overline{v_x}}{dy}\int_0^\infty v_y'(t)v_y'(t-\tau)d\tau = \rho \frac{d\,\overline{v_x}}{dy}\int_0^\infty u_y{}'^2 R_{L2}(\tau)d\tau = \rho \frac{d\,\overline{v_x}}{dy} u_y{}'^2 \Im_2 \tag{17.2-25}$$

A Lagrangian integral length scale l_L is used as

$$l_L = u_y' \Im_2 \tag{17.2-26}$$

On the other hand, the Eulerian integral scale l is defined by

$$u_y{}'^2 l = \int_0^\infty \overline{v_y{}'(y)v_y{}'(0)}\,dy \tag{17.2-27}$$

The overbar denotes an average taken over a long time interval with zero time delay between the two velocity fluctuations. If the l_L and l are assumed of the same order of magnitude,

$$\tau_{yx}^{(t)} = K_M \rho\, u_y'\, l \frac{d\,\overline{v_x}}{dy} \tag{17.2-28}$$

This suggests that the turbulent momentum-flux can be estimated using the Eulerian integral scale l.

From the definition of Reynolds stresses

$$\tau_{yx}^{(t)} = \rho\,\overline{v_y{}'v_x{}'} \tag{17.2-29}$$

Comparing these equations, it is found that

$$u_x' = K\, l \frac{d\,\overline{v_x}}{dy} \tag{17.2-30}$$

We can obtain similar expressions of turbulent heat- and mass-fluxes:

$$q_y^{(t)} = K_H \rho Cp\, u_y' \, l \, \frac{d\overline{T}}{dy} \quad (17.2\text{-}31)$$

$$j_y^{(t)} = K_D u_y' \, l \, \frac{d\overline{C}}{dy} \quad (17.2\text{-}32)$$

The numerical coefficients $K_M,\ K_H,\ K_D$ are of order one.

Finally it has been found that the eddy diffusivities are of order $u_y' \, l$:

$$\varepsilon_M = u_y' l_M \quad (17.2\text{-}33)$$

$$\varepsilon_H = u_y' l_H \quad (17.2\text{-}34)$$

$$\varepsilon_D = u_y' l_D \quad (17.2\text{-}35)$$

The ratio of the Reynolds stress to the laminar viscous stress is usually very large in most part of the flow field except near the wall.

$$\frac{\tau_{yx}^{(t)}}{\tau_{yx}^{(l)}} = \frac{\rho \varepsilon_M \frac{d\overline{v_x}}{dy}}{\rho \nu \frac{d\overline{v_x}}{dy}} = \frac{\varepsilon_M}{\nu} = K_1 \, \frac{u_y' \, l}{\nu} \quad (17.2\text{-}36)$$

The term $u_y{}' l/\nu$ is sometimes called "eddy Reynolds number."

17.3 Structure of Turbulence

17.3-1 Energy spectrum of kinetic energy

It will be instructive to find the regularity in seemingly-chaotic turbulent flows by a statistical approach. If the statistical properties such as $\overline{v_x{}'^2}$, $\overline{v_x{}' v_y{}'}$, etc. are time-independent, the turbulent flow is characterized as being stationary. If the statistical properties do not vary in space, it is said that the turbulent flow is homogeneous. If the statistical properties are invariant with direction, it is said that the turbulent flow is isotropic: $\overline{v_x{}'^2} = \overline{v_y{}'^2} = \overline{v_z{}'^2}$.

It is well known that the turbulent flow behind a uniform grid has a turbulent structure close to locally homogeneous isotropic turbulence. Turbulent flow in a circular pipe, especially that near to the wall, is neither homogeneous nor isotropic.

A constant average value of $\overline{v'^2}$ exists in the flowfield statistically homogeneous with respect to time.

The kinetic energy of turbulence is expressible as

$$\frac{1}{2} \rho \left(\overline{v_x{}'^2} + \overline{v_y{}'^2} + \overline{v_y{}'^2} \right)$$

To describe turbulent motion quantitatively, it is necessary to introduce a concept of the intensity and scale of turbulence. The intensity of the turbulent velocity fluctuations is defined as the root-mean-square value divided by the mean flow velocity:

$$Tu_v = \frac{\sqrt{\overline{v_x{}'^2}}}{\overline{v_x}} \quad (17.3\text{-}1)$$

We usually use the velocity fluctuation component in the same direction as the main flow. Turbulence consists of the superposition of various, small periodic motions on large-scale motions. The small periodic motions come from a certain vortex motion, the extent of which is called "eddy." In other words, turbulence consists of the superposition of eddies of various sizes. The eddy size corresponds to the frequency of the periodic motion. The smaller an eddy, the higher the frequency.

As shown in Fig. 17.3-1, a large scale eddy consists of a large number of small eddies. All eddies are moving approximately at the average velocity $\overline{v_x}$. They can be considered to be transported by the mean flow. When a hot-wire is placed perpendicular to the velocity $\overline{v_x}$, the time required for a small eddy to pass by the wire is shorter than that for a large eddy. Each amplitude of the oscillations corresponds to the turbulent kinetic energy each eddy has.

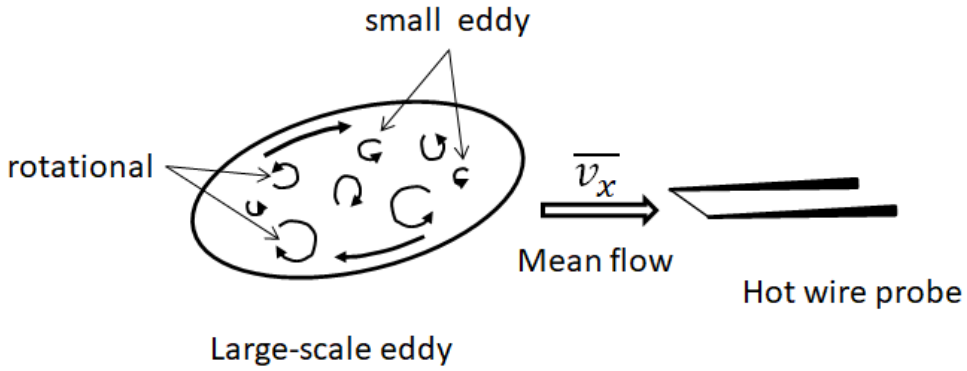

Fig. 17.3-1. Structure of a large-scale eddy containing various-sized small eddy motions

Fig. 17.3-2 explains the relation between eddy size and fluctuation frequency. An energy spectrum describes the distribution of the kinetic energy $\overline{{v_x}'^2}$ of the turbulence in the frequency domain. This analysis of turbulence is similar to the frequency analysis applied to light waves and sound waves.

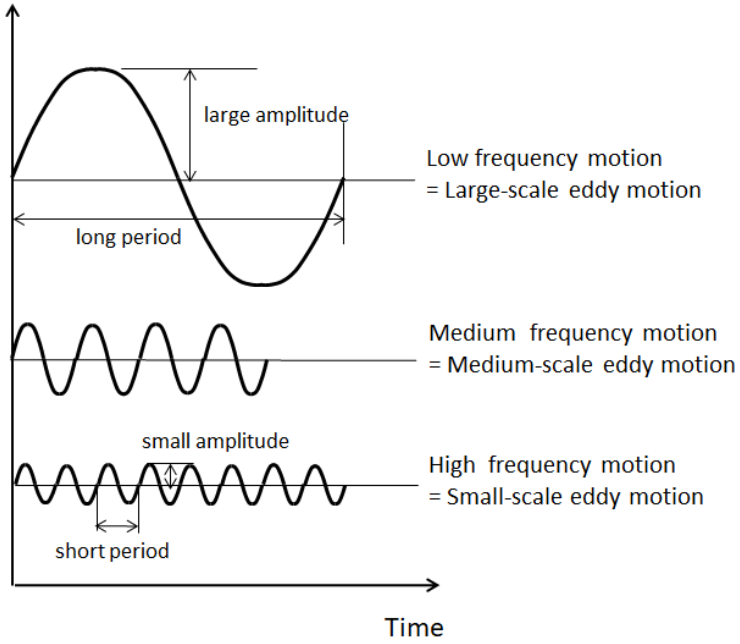

Fig. 17.3-2. Relation between eddy size and fluctuation frequency

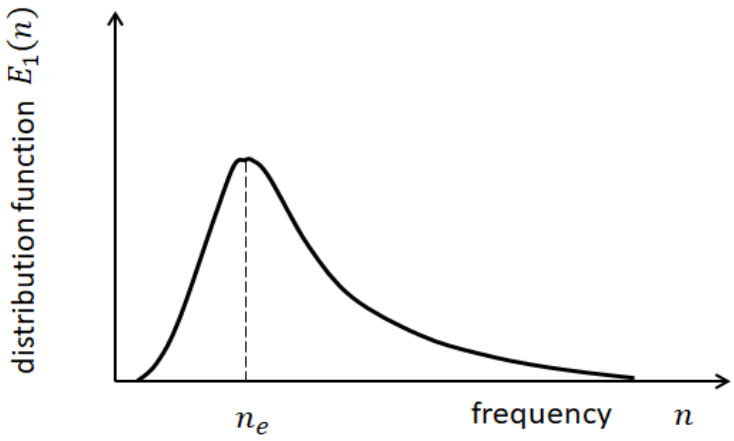

Fig. 17.3-3. Schematic curve of energy spectrum

Fig. 17.3-3 is a one-dimensional energy spectrum, where the distribution function $E_1(n)$ is similar to a probability density function.

The contribution to $\overline{v_x{}'^2}$ of the frequencies between n and $n+dn$ is given by $\overline{v_x{}'^2}E_1(n)dn$.
By definition, $\int_0^\infty E_1(n)dn = 1$
The one-dimensional energy spectrum can be measured by a hot-wire anemometer. Signals from the wire are time-averaged to get $\overline{v_x}$ and the original signals v_x are subtracted $\overline{v_x}$ to get $v_x{}'$. Then the fluctuations $v_x{}'$ are passed through a filter circuit which can filtrate the oscillations between n and $n+dn$. The filtrated oscillations are squared and time-averaged to get $\overline{v_x{}'^2}E_1(n)$.
At the present time, a digital computer is often used for the statistical analyses of this kind. Signals of fluctuating velocities are first digitalized by an AD converter and stored as a time history into the memory of the computer. The energy spectrum can be obtained from the Fourier transforms of the fluctuating velocity vs. time record.

Turbulence is dissipative. The smaller an eddy, the greater the velocity gradient within the eddy. Therefore the viscous shear stress counteracts the very high frequency eddying motion. There is a statistical lower limit to the size of the smallest eddy. The highest frequency range in the energy spectra corresponds to the smallest eddies. Even the smallest eddies are far larger than the mean free path of the molecules of the fluid. That is, turbulence is a continuum phenomenon. The kinetic energy of turbulence is always converted into the internal energy (heat) of the fluid owing to the deformation work by viscous shear stresses in the smallest eddies.

Therefore turbulence needs a continuous supply of energy to make up for the kinetic energy loss. The kinetic energy is extracted from the mean flow by large eddies which correspond to low frequency range in energy spectra. The generation of small-scale fluctuations is due to the nonlinear interaction of large-scale fluctuations.

Suppose two components of velocity fluctuations to be of the form:

$$v_x' = \sum_m A_m \cos 2\pi mt \tag{17.3-2}$$

$$v_y' = \sum_n B_n \cos 2\pi nt \tag{17.3-3}$$

The product of these two functions implies the nonlinear interaction as follows:

$$\begin{aligned} v_x' v_y{}' &= \sum_m \sum_n A_m B_n \cos 2\pi mt \cos 2\pi nt \\ &= \sum_m \sum_n \tfrac{1}{2} A_m B_n \left(\cos 2\pi(m+n)t + \cos 2\pi(m-n)t\right) \end{aligned} \tag{17.3-4}$$

Here the higher frequency fluctuations $\cos 2\pi(m+n)t$ and the lower frequency fluctuations $\cos 2\pi(m-n)t$ are produced due to the nonlinear interactions $\cos 2\pi mt$ and $\cos 2\pi nt$. In the case when $m=n$, the time-average lower frequency component $\cos 2\pi(m-n)t$ implies the effect of velocity fluctuations on the mean motion:

$$\begin{aligned} \overline{v_x' v_y{}'} &= 0 \qquad (m \neq n) \\ &= \sum_n \tfrac{1}{2} A_n B_n \qquad (m = n) \end{aligned} \tag{17.3-5}$$

This suggests that the mean velocity distribution is distorted owing to the nonlinear interaction. As shown in Fig. 17.3-4, in this manner, a spectral energy transfer from the energy-containing eddies (large eddies) to smaller eddies occurs. Finally the viscous dissipation occurs by the smallest eddies approximately at the same rate as the production of the kinetic energy. This also suggests that the structure of turbulence is in dynamical equilibrium in which local inputs (production) of kinetic energy balance local losses of kinetic energy.
Therefore we need a measure of eddy size and often determine the extent of the flowfield where the fluid motion (e.g. velocities) have a certain correlation with each other.

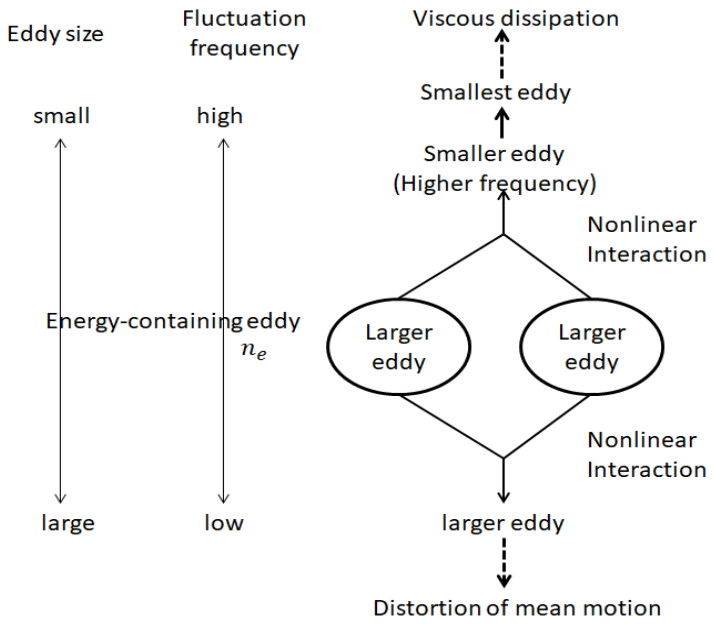

Fig. 17.3-4. Spectral energy transfer by nonlinear interaction of velocity fluctuations

17.3-2 Spatial and temporal correlations ----- Definition of eddy sizes

The size and orientation of eddies can be defined with the aid of the spatial correlation between fluctuations measured simultaneously at two positions.

From the Eulerian point of view, a longitudinal velocity correlation coefficient $f(r)$ is defined between the longitudinal velocity fluctuation components measured at two points, the distance of which is r:

$$f(r) = \frac{\overline{v_x'(x)v_x'(x+r)}}{\sqrt{\overline{v_x'(x)^2}}\sqrt{\overline{v_x'(x+r)^2}}} \tag{17.3-6}$$

In homogeneous turbulent flowfield

$$\sqrt{\overline{v_x'(x)^2}} = \sqrt{\overline{v_x'(x+r)^2}}$$

Then

$$f(r) = \frac{\overline{v_x'(x)v_x'(x+r)}}{\overline{v_x'^2}} \tag{17.3-7}$$

Fig.17.3-5 is a qualitative sketch of longitudinal velocity correlation.

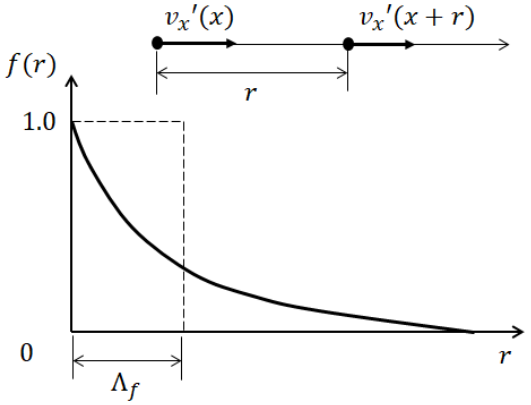

Fig. 17.3-5. Longitudinal velocity correlation

Similarly a lateral velocity correlation coefficient $g(r)$ is defined between the lateral velocity fluctuation components measured at two points, the distance of which is r:

$$g(r) = \frac{\overline{v_y'(x)v_y'(x+r)}}{\overline{v_y'^2}} \tag{17.3-8}$$

Fig.17.3-6 is a sketch of lateral velocity correlation.

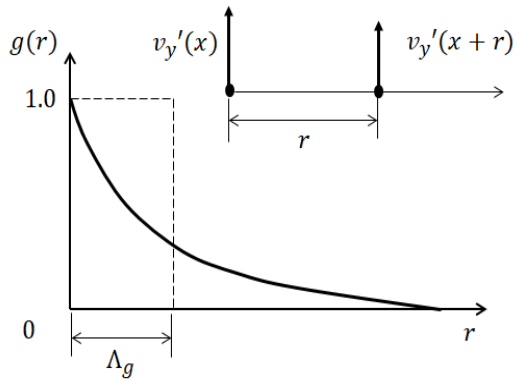

Fig.17.3-6. Lateral velocity correlation

These space correlations can be measured by using two sets of hot-wire anemometers. One hot-wire is fixed at a position x and the other is placed at any arbitrary position $x+r$. Signals $v_x(x)$ and $v_x(x+r)$ from the two hot-wires are subtracted their time-averaged values $\overline{v_x(x)}$ and $\overline{v_x(x+r)}$ to get their fluctuations $v_x'(x)$ and $v_x'(x+r)$. Their fluctuations are multiplied each other with zero time delay and averaged with respect to time to get the correlation $\overline{v_x'(x)v_x'(x+r)}$. If the two fluid elements are very close together, they must be moving at nearly the same velocities. That is, there is a high degree of correlation between the two fluid elements.
From definition, $f(0) = 1$ and $g(0) = 1$

As the distance r increases, the correlation becomes low. We often need a measure of the size of larger eddies which contribute very much to convective transfer of momentum, heat, and mass. In particular, the surface renewal motion due to those large-scale eddies in the neighborhood of the interface is very effective in interphase heat and mass transport.

As the Eulerian macroscale of turbulence, two integral length scales are defined:

$$\Lambda_f = \int_0^\infty f(r)dr \tag{17.3-9}$$

$$\Lambda_g = \int_0^\infty g(r)dr \tag{17.3-10}$$

They are considered to be a measure of the largest space interval in which two velocity fluctuations are correlated with each other, i.e., the fluid elements at two points move substantially in the same direction.

From Lagrangian point of view, another correlation coefficient can be defined between velocity fluctuations of the same fluid particle at different times:

$$R_L(\tau) = \frac{\overline{v_{x'}(x,y,z,t)v_{x'}(x,y,z,t+\tau)}}{\overline{v_{x'}(x,y,z)^2}} \tag{17.3-11}$$

This is known as the Lagrangian autocorrelation coefficient.

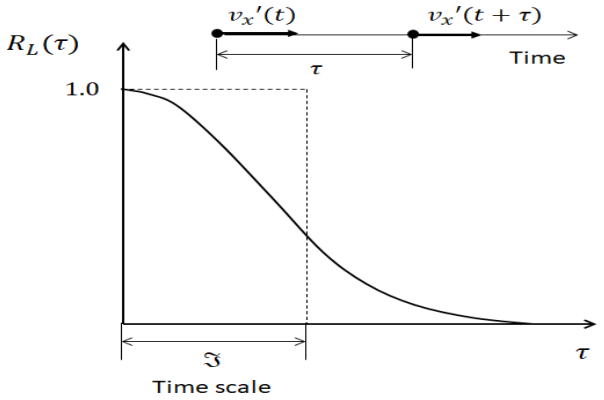

Fig. 17.3-7. Lagrangian autocorrelation

Fig. 17.3-7 is a sketch of Lagrangian autocorrelation. This autocorrelation can be calculated with the aid of time-delay circuit from the fluctuations measured by a hot-wire anemometer.

A Lagrangian integral time scale is defined by

$$\Im = \int_0^\infty R_L(\tau)\, d\tau \qquad (17.3\text{-}12)$$

This can be considered to be a measure of the longest time interval during which $v_x'(t)$ is correlated with itself, i.e., a fluid element persists in a motion in a given direction.

If a homogeneous turbulent flowfield has a constant mean velocity $\overline{v_x}$,

$$\Lambda_f = \Im\, \overline{v_x} \qquad (17.3\text{-}13)$$

These macroscales of turbulence are of great importance in connection with turbulent transport of momentum, heat, and mass.

17.4 Velocity Distribution of Turbulent Flow inside a Circular Pipe

Let us derive the turbulent velocity distribution in the fully-developed region.
The total shear stress has a linear distribution whether the flow is laminar or turbulent:

$$\tau_{rz} = \frac{r}{R}\tau_w \qquad (17.4\text{-}1)$$

We may use three layer concept although the velocity change in the radial direction is continuous: the viscous sublayer, where viscous effect is predominant; the buffer layer, where the viscous and turbulent effects are of comparable importance; and the turbulent core, where purely viscous effect is of negligible importance. It can be considered that the time-smoothed velocity at a point is a function of local conditions from the wall of the pipe. Therefore the distance from the wall $y = R - r$ is used instead of r as the transverse coordinate.

[EXAMPLE 17.4-1] Dimensional Analysis

Show that the time-smoothed velocity distribution in turbulent shear layer should be a function of two dimensionless groups by application of dimensional analysis:

$$\frac{\overline{v_x}}{\sqrt{\tau_w/\rho}} = f\left(\frac{y\sqrt{\tau_w/\rho}}{\nu}\right) \qquad (17.4\text{-E1})$$

Solution: If we denote characteristic velocity and length by U and Y, respectively, we can formally express the velocity distribution as

$$\frac{\overline{v_x}}{U} = f\left(\frac{y}{Y}\right) \qquad (17.4\text{-E2})$$

The time-smoothed velocity is a function of local conditions from the nearest wall. Thus

$$\frac{y}{Y} = y\,{\tau_w}^a\,\varrho^b\mu^c = L\left(\frac{M}{L\,T^2}\right)^a\left(\frac{M}{L^3}\right)^b\left(\frac{M}{L\,T}\right)^c = L^{1-a-3b-c}\,M^{a+b+c}\,T^{-2a-c} \qquad (17.4\text{-E3})$$

In order that the right side of Eq.(17.3-E3) should be dimensionless, $a = 1/2$, $b = 1/2$, and $c = -1$.
This implies

$$\frac{y}{Y} = \frac{y\sqrt{\tau_w/\varrho}}{\nu} = y^+ \quad (17.4\text{-E4})$$

Similarly

$$\frac{\overline{v_x}}{U} = \overline{v_x}\,\tau_w{}^A\,\varrho^B\mu^C = L^{1-A-3B-C}\,M^{A+B+C}\,T^{-1-2A-C} \quad (17.4\text{-E5})$$

The right side should be dimensionless. Then $A = -1/2$, $B = 1/2$, and $C = 0$.
This implies

$$\frac{\overline{v_x}}{U} = \frac{\overline{v_x}}{\sqrt{\tau_w/\varrho}} = u^+ \quad (17.4\text{-E6})$$

As a result

$$u^+ = f(y^+) \quad (17.4\text{-E7})$$

We have found that the velocity distribution should be expressed using the above functional form.

Viscous sublayer

In the region very close to the pipe wall, the shear stress will vary only slightly from τ_w and the turbulent effect is negligibly small. Thus

$$\tau_w = \varrho\,\nu\,\frac{d\,\overline{v_z}}{dy} \quad (17.4\text{-2})$$

Rearranging the terms $d\overline{v_z} = \frac{\tau_w}{\varrho\,\nu}\,dy$ and integrating in dimensionless form,

$$\frac{\overline{v_z}}{\sqrt{\tau_w/\varrho}} = \frac{y\sqrt{\tau_w/\varrho}}{\nu} + C_1$$

Using the boundary condition that $\overline{v_z} = 0$ at $y = 0$, C_1 must be zero.
We get the velocity distribution in the viscous sublayer:

$$u^+ = y^+ \quad (17.4\text{-3})$$

The term $\sqrt{\tau_w/\varrho}$, which has the dimension of velocity, is called the friction velocity.
The friction velocity is denoted by u^*.

Buffer layer

In this layer, the laminar and turbulent effects are both important. We cannot derive analytically the velocity distribution. One of empirical equations is

$$u^+ = -3.05 + 5.00\ln y^+ \quad (17.4\text{-4})$$

Turbulent core

In this region, the turbulent effect is predominant. The total shear stress can be written as

$$\tau_{rz} = \tau_{rz}^{(t)} = \varrho\,u_y'\,l_M\,\frac{d\,\overline{v_z}}{dy} \quad (17.4\text{-5})$$

Assuming that the RMS velocity u_y' in the transverse direction is proportional to the RMS velocity u_z' in the axial direction:

$$u_y' = C_2\,u_z' \quad (17.4\text{-6})$$

For small y,

$$u_z' \cong K\,l_M\,\frac{d\,\overline{v_z}}{dy} \quad (17.4\text{-7})$$

Then we obtain

$$\tau_{rz} = \tau_{rz}^{(t)} = \varrho\,l_M{}^2\left(\frac{d\,\overline{v_z}}{dy}\right)^2 \quad (17.4\text{-8})$$

The numerical coefficients C_2 and K are absorbed in the unknown mixing length l_M.
From the shear stress distribution

$$\tau_{rz} = \tau_w\left(\frac{R-y}{R}\right) = \varrho\,l_M{}^2\left(\frac{d\,\overline{v_z}}{dy}\right)^2 \quad (17.4\text{-9})$$

The equation of motion for turbulent pipe flows can also be written as

$$0 = \frac{P_0 - P_L}{L} - \frac{1}{r}\frac{d}{dr}(r\,\tau_{rz}) \qquad (17.4\text{-}10)$$

where $\tau_{rz} = \tau_{rz}^{(l)} + \tau_{rz}^{(t)}$

Integrating with the boundary condition $\tau_{rz} = 0$ at $r = 0$,

$$\tau_{rz} = \frac{(P_0 - P_L)R}{2L}\frac{r}{R} = \tau_w \frac{r}{R}$$

That is

$$\tau_w = \frac{(P_0 - P_L)R}{2L} \qquad (17.4\text{-}11)$$

This implies that the frictional force at the wall balances the pressure force acting on the flow cross-section whether the flow is laminar or turbulent. It is known that the turbulent velocity profile is almost flat in most part of the flow cross-section and that the steep velocity change takes place near the wall.

Then Prandtl assumed that τ_{rz} do not vary markedly from its wall value τ_w

$$\tau_{rz} \cong \tau_w = \varrho\, l_M{}^2 \left(\frac{d\,\overline{v_z}}{dy}\right)^2 \qquad (17.4\text{-}12)$$

This assumption made in the turbulent core should be considered as a very rough estimation.

Further, he assumed that the mixing length l_M is simply proportional to the distance from the wall, that is

$$l_M = \kappa\, y \qquad (17.4\text{-}13)$$

Thus the equation to be solved becomes

$$\frac{\tau_w}{\rho} = \kappa^2 y^2 \left(\frac{d\,\overline{v_z}}{dy}\right)^2 \qquad (17.4\text{-}14)$$

Taking the square root

$$\frac{d\,\overline{v_z}}{dy} = \frac{u^*}{\kappa\, y} \qquad (17.4\text{-}15)$$

Integrating from the outer edge of the buffer layer y_b,

$$\overline{v_z} - \overline{v_{z,b}} = \frac{1}{\kappa}\, u^* \ln\frac{y}{y_b} \qquad (17.4\text{-}16)$$

In dimensionless form

$$u^+ - u_b^+ = \frac{1}{\kappa}\ln\frac{y^+}{y_b^+} \qquad (17.4\text{-}17)$$

We may expect that experimental turbulent velocity profiles will give a universal curve in u^+, y^+ coordinates that is logarithmic over the turbulent core and linear immediately adjacent to the pipe wall.

The universal velocity profile empirically obtained is expressed by

Viscous sublayer	$y^+ \le 5$	$u^+ = y^+$	(17.4-18)
Buffer layer	$5 \le y^+ \le 30$	$u^+ = -3.05 + 5.0 \ln y^+$	(17.4-19)
Turbulent core	$y^+ \ge 30$	$u^+ = 5.5 + 2.5 \ln y^+$	(17.4-20)

From many experimental data, it is known that the universal constant κ is given by 0.4. The above semi-empirical universal velocity distribution law is valid over a wide range $Re > 20{,}000$ in the magnitude of time-smoothed velocity. However the three-layer model involves discontinuities in eddy diffusivity ε_M and non-zero velocity gradient at the pipe axis because the model does not take into consideration the continuity in velocity gradients at the boundaries of these three layers. In particular, Eq.(17.4-20) cannot meet the real boundary condition $\partial\overline{v_z}/\partial r = 0$ at $r = 0$.

[PROBLEM 17.4-P1] As a set of universal velocity distribution for a circular tube flow, Eqs. (17.4-18~20) were obtained. Plot the dimensionless velocity against the dimensionless distance from the wall u^+ vs. $\log y^+$ in a semi-logarithmic coordinates. A Newtonian fluid ($\rho = 1{,}000$ kg/m^3, $\mu = 0.0012$ Pa s) is flowing in at an average velocity $\langle\overline{v_z}\rangle = 1.5$ m/s in a circular tube (inside diameter $D_i = 1.0$ m). What is the friction factor? What is the wall shear stress τ_w? In this fully-developed turbulent flow region, obtain a radial distribution of the time-averaged axial velocity $\overline{v_z}/\langle\overline{v_z}\rangle$ vs. r/R.

17.5 Turbulent Structure and Role of Eddies

17.5-1 Turbulent structure in a circular pipe flow

Let us study again a turbulent flow in a circular pipe from a viewpoint of chemical engineering processes. Fig. 17.5-1 shows the radial distributions of the turbulence intensity and the Reynolds stress.

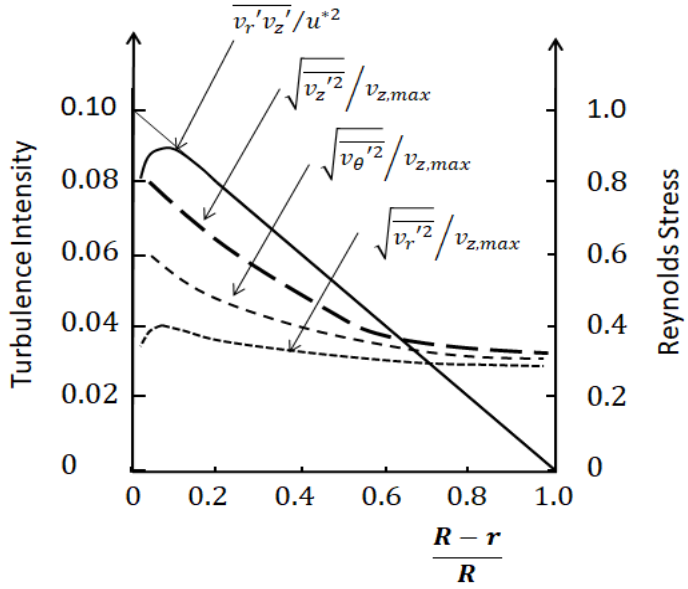

Fig. 17.5-1. Schematic picture of radial distributions of turbulence intensity and Reynolds stress

The turbulence intensity of the axial component velocity fluctuations $\overline{v_z'^2}$ is much larger than those of other components $\overline{v_\theta'^2}$ and $\overline{v_r'^2}$ in the main part of the flowfield and becomes a maximum in the vicinity of the pipe wall. However, as the pipe axis is approached, the flow becomes nearly isotropic: $\overline{v_z'^2} = \overline{v_\theta'^2} = \overline{v_r'^2}$.

The Reynolds stress also shows a maximum in the vicinity of the wall. The buffer layer can be considered as a constant source for the turbulent kinetic energy. The turbulent kinetic energy $\overline{v_z'^2}$ is produced from the gradient of the mean velocity $\partial\overline{v_z}/\partial r$ through the Reynolds stress $-\overline{v_r'v_z'}$ mainly in the buffer layer ($y^+ \cong 15$), where both $\partial\overline{v_z}/\partial r$ and $-\overline{v_r'v_z'}$ are very large. Large eddies generated in this region are called "the energy-containing eddies" since they have the largest energy density $E_1(n)_{max}$ in the energy spectrum.

The integral scale Λ_f is determined mainly by the size of the larger energy-containing eddies. Even in the fully-developed flow, there exist more permanent largest eddies, which contain much less energy than the energy-containing eddies. In the vicinity of the wall the spectral energy-transfer occurs from the energy-containing eddies (low frequency) to smaller and smaller eddies (higher and higher frequencies).

The rate of energy production is nearly in dynamical equilibrium with the rate of energy dissipation. We should know that this kinetic energy balance is utilized for the principle of scale-up design of an agitated vessel. (see Section 20.3)

Still there is a turbulent diffusion flux of the residual kinetic energy from the energy-producing zone toward the pipe axis. This is the only supply of kinetic energy in the central part where there is no source of turbulence energy. Thus the energy transferred by turbulent diffusion is consumed by dissipation. This implies that the energy-containing eddies in the energy-producing zone are much larger than those in the central part and that the dissipating eddies in the energy-producing zone are

much smaller than those in the central part. In the turbulent core large eddies are elongated in the z-direction: the integral scale Λ_f in the z-direction is larger than the integral scales Λ_g in the r- and θ-direction. It is known that at high Reynolds numbers, for example, Λ_f becomes of the order of $0.5\,R$ whereas Λ_g is of the order of $0.2\,R$.

17.5-2 Roles of turbulent eddies in transport processes

When we study various processes involving heat and mass transports, it is necessary to distinguish fluid particles (small eddies) from fluid lumps (large eddies).

Fluid particle is a very small volume of the fluid (of the order of microscale), but far larger than the mean free path of the fluid molecules. Within such a fluid particle, the velocity, temperature, and concentration can be assumed uniform. Fluid lump is a much larger volume of the fluid which consists of a large number of fluid particles. The size of such a fluid lump is of the order of the integral scale and as big as the width of turbulent flowfield (e.g. the radius for pipe flows, the half-radius for free jet flows, and the thickness for boundary layer flows).

In usual turbulent flows, the turbulent transport of momentum, heat, and mass is controlled mainly by fluid lumps. However the size of the eddies which play a predominant role in heat and mass transfer may be slightly different from that of the eddies controlling momentum transfer.

Turbulent diffusion is one of the most important factors in chemical engineering. Chemical engineers make use of turbulence to mix and homogenize fluid mixtures as well as to accelerate the rates of heat and mass transfer. Chemical reaction rates are often accelerated by turbulent mixing. For heterogeneous chemical reactions such as the liquid-liquid reaction in an agitated vessel, the relative size between the discrete liquid particles and the surrounding eddies is an important factor in relation with the rate of reaction. If the Reynolds number is raised in an apparatus, the integral scale remains almost constant but the microscale tends to become small: a turbulent flow at a relatively high Reynolds number has a relatively “fine” small-scale structure. Combustion processes also involve turbulence and often depend on the turbulent mixing and diffusion of fuel gases and oxidizer. For mist flow in pipes of boiler, the relative size between small water droplets and turbulent eddies of steam stream may be an important factor in consideration of the turbulent diffusion of water droplets toward the heat transfer wall.

In this text, the film theory was mainly adopted for the study of heat and mass transfer across the interfaces separating phases.

However it should be kept in mind that the recent hydrodynamic studies pay attention to the turbulent eddying motion near the interface. There are many attempts to relate the turbulent energy spectrum to mass transport behavior near the gas-liquid interface from a viewpoint of large energy-containing eddies which control the mass transport rate.

Very recently various sophisticated statistical studies have demonstrated with the aid of visualization techniques the existence of “coherent” (or well-ordered) structure in the wall layer of wall-bounded turbulent flows: there are intermittent large-scale interactions between wall layer and outer layer. The low-speed streaks of fluid are lifted up (ejected) from the wall by the stretched vortex-like structure, and then the high-speed outer layer appears by the sweep motion called “bursting.” It plays an important role in the production of turbulence and the turbulent transport processes. There are some attempts to relate the interphase transport rates to the intermittent renewal of fluid lumps near the interface by bursting motion.

Nomenclature

C_A	molar concentration of component A, [kmol/m3]
Cp	heat capacity, [J/kg K]
$E_1(n)$	one-dimensional energy spectrum, [-]
$f(r)$	longitudinal velocity correlation coefficient, [-]
$g(r)$	lateral velocity correlation coefficient, [-]
I	electric current, [A]

j	mass flux, [kmol/m^{2}s]
l_M, l_H, l_D	mixing length of momentum, heat, and mass, [m]
l_L	Lagrangian integral length scale, [m]
p	pressure, [Pa]
q	heat flux, [J/m^{2}s]
R	electric resistance, [Ω] or pipe radius, [m]
Re	Reynolds number, [-]
R_{L2}	Lagrangian correlation, [-]
r	radial coordinate, [m], or distance between two points of lateral correlation, [m]
T	temperature, [K]
Tu	turbulence intensity, [-]
t	time, [s]
u^*	friction velocity, [m/s]
u^+	dimensionless velocity = $\frac{\overline{v_z}}{\sqrt{\tau_w/\varrho}}$
v_x, v_y, v_z	velocity component in rectangular coordinates, [m/s]
x, y, z	rectangular coordinates, [m]
y^+	dimensionless distance from wall = $\frac{y\sqrt{\tau_w/\varrho}}{\nu}$
ΔM	momentum deficit, [kg/m^{2}s]
$\varepsilon_M, \varepsilon_H, \varepsilon_D$	eddy diffusivity of momentum, heat, and mass, [m^2/s]
κ	thermal conductivity, [W/m K]
Λ_f	Eulerian integral longitudinal length scale, [m]
Λ_g	Eulerian integral lateral length scale, [m]
μ	viscosity, [kg/m s]
ν	kinematic viscosity or diffusivity of momentum, [m^2/s]:
ρ	density, [kg/m^3]
τ	momentum flux or shear stress, [kg/s^{2}m] or [N/m^2] or time difference, [s]
$\mathfrak{I}_2$	time scale, [s]

Superscripts

‘	fluctuation
$\overline{}$	time-averaged
(l)	laminar
(t)	turbulent

Subcripts

A	component A
w	wall

CHAPTER 18

BOUNDARY LAYER THEORY

18.1 Stream Function[1)]

For a two-dimensional, incompressible flow, i.e., $\rho = \text{const}$, and $\partial/\partial z = 0$, the equations of continuity and motion are given by

$$\frac{\partial v_x}{\partial x} + \frac{\partial v_y}{\partial y} = 0 \qquad (18.1\text{-}1)$$

$$v_x \frac{\partial v_x}{\partial x} + v_y \frac{\partial v_x}{\partial y} = -\frac{1}{\rho}\frac{\partial p}{\partial x} + \nu\left(\frac{\partial^2 v_x}{\partial x^2} + \frac{\partial^2 v_x}{\partial y^2}\right) \qquad (18.1\text{-}2)$$

$$v_x \frac{\partial v_y}{\partial x} + v_y \frac{\partial v_y}{\partial y} = -\frac{1}{\rho}\frac{\partial p}{\partial y} + \nu\left(\frac{\partial^2 v_y}{\partial x^2} + \frac{\partial^2 v_y}{\partial y^2}\right) \qquad (18.1\text{-}3)$$

The set of equations can be simplified into one equation with one unknown variable by introducing a new function $\psi(x, y)$ called "stream function."

The function is defined so that the equation of continuity is satisfied automatically:

$$v_x = \frac{\partial \psi}{\partial y} \quad \text{and} \quad v_y = -\frac{\partial \psi}{\partial x} \qquad (18.1\text{-}4)$$

Since ψ is a function of x and y, the total derivative is

$$d\psi = \frac{\partial \psi}{\partial x}\,\mathrm{dx} + \frac{\partial \psi}{\partial y}\,\mathrm{dy} = -v_y\,\mathrm{dx} + v_x\,\mathrm{dy}$$

If ψ = const (i.e., $d\psi = 0$)

$$\left.\frac{dy}{dx}\right|_{\psi = const} = \frac{v_y}{v_x} \qquad (18.1\text{-}5)$$

The path $\psi = const$ is seen to represent a streamline since the streamline is tangent to the velocity vector

$$\vec{v} = v_x\,\vec{i} + v_y\,\vec{j} \qquad (18.1\text{-}6)$$

Fig. 18.1-1 indicates definition of stream function.

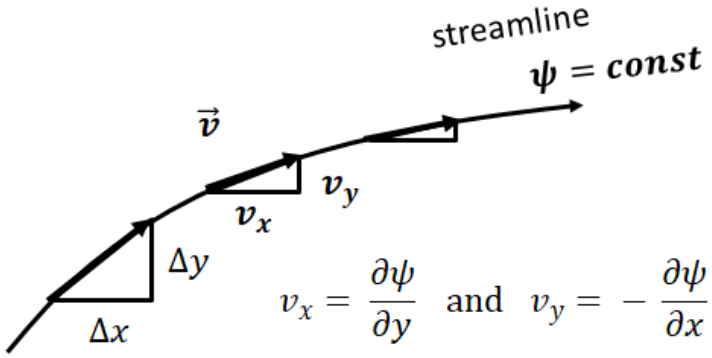

Fig. 18.1-1. Definition of stream function ψ

Differentiating Eq. (18.1-2) with respect to y and Eq. (18.1-3) with respect to x and combining these two equations to eliminate the pressure terms, we get

$$\left(\frac{\partial v_x}{\partial x}+\frac{\partial v_y}{\partial y}\right)\left(\frac{\partial v_x}{\partial y}-\frac{\partial v_y}{\partial x}\right)+\left(v_x\frac{\partial}{\partial x}+v_y\frac{\partial}{\partial y}\right)\left(\frac{\partial v_x}{\partial y}-\frac{\partial v_y}{\partial x}\right)$$
$$=\nu\left(\frac{\partial^2}{\partial x^2}+\frac{\partial^2}{\partial y^2}\right)\left(\frac{\partial v_x}{\partial y}-\frac{\partial v_y}{\partial x}\right) \qquad (18.1\text{-}7)$$

Substituting ψ into Eq. (18.1-6)

$$\left(\frac{\partial\psi}{\partial y}\frac{\partial}{\partial x}-\frac{\partial\psi}{\partial x}\frac{\partial}{\partial y}\right)\left(\frac{\partial^2\psi}{\partial x^2}+\frac{\partial^2\psi}{\partial y^2}\right)=\nu\left(\frac{\partial^2}{\partial x^2}+\frac{\partial^2}{\partial y^2}\right)\left(\frac{\partial^2\psi}{\partial x^2}+\frac{\partial^2\psi}{\partial y^2}\right)$$

Then we get a fourth-order differential equation with one unknown, ψ:

$$-\frac{\partial(\psi,\nabla^2\psi)}{\partial(x,y)}=\nu\,\nabla^4\psi \qquad (18.1\text{-}8)$$

Still its general solution is very difficult owing to its nonlinearity.

Here

$$\nabla^2=\frac{\partial^2}{\partial x^2}+\frac{\partial^2}{\partial y^2}\quad\text{and}\quad\nabla^4=\left(\frac{\partial^2}{\partial x^2}+\frac{\partial^2}{\partial y^2}\right)\left(\frac{\partial^2}{\partial x^2}+\frac{\partial^2}{\partial y^2}\right) \qquad (18.1\text{-}9)$$

$$\frac{\partial(f,g)}{\partial(x,y)}=\begin{vmatrix}\partial f/\partial x & \partial f/\partial y\\ \partial g/\partial x & \partial g/\partial y\end{vmatrix}=\frac{\partial f}{\partial x}\frac{\partial g}{\partial y}-\frac{\partial f}{\partial y}\frac{\partial g}{\partial x}$$

The equation for two-dimensional flow (i.e., $v_z=0$ and $\partial v_r/\partial z=\partial v_\theta/\partial z=0$) can be expressed in cylindrical coordinates:

$$-\frac{1}{r}\frac{\partial(\psi,\nabla^2\psi)}{\partial(r,\theta)}=\nu\,\nabla^4\psi \qquad (18.1\text{-}10)$$

$$\nabla^2=\frac{\partial^2}{\partial r^2}+\frac{1}{r}\frac{\partial}{\partial r}+\frac{1}{r^2}\frac{\partial^2}{\partial\theta^2}$$

Here the stream function ψ is defined as

$$v_r=\frac{1}{r}\frac{\partial\psi}{\partial\theta}\quad\text{and}\quad v_\theta=-\frac{\partial\psi}{\partial r}$$

[PROBLEM 18.1-1]

For an inviscid uniform fluid flow over a stationary cylinder (radius R), the stream function can

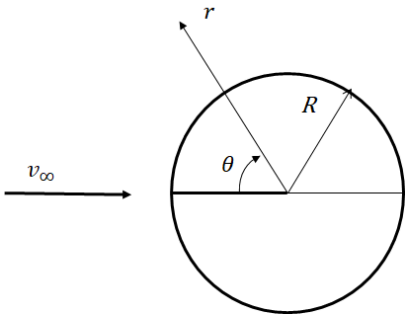

be expressed as

$$\psi=v_\infty\left(r-\frac{R^2}{r}\right)\sin\theta$$

The circle $r=R$ itself must be a streamline.

Draw the streamlines around the cylinder and obtain the velocity components v_r and v_θ.

18.2 Boundary Layer Solution of Laminar Flow along a Flat Plate[2)]

This example is instructive for the understanding of local variations of friction factor and Nusselt number in developing flows.

As shown in Fig. 18.1-2, the flat plate is heated at constant wall temperature T_w.

The approaching fluid has uniform velocity v_∞ and uniform temperature T_∞.

The thickness of the velocity boundary layer is defined as follows.

Usually the thickness δ is taken as the distance away from the surface of the flat plate where the velocity reaches 99% of the free-stream velocity. Similarly the thickness of the temperature boundary layer δ_T is defined as the distance away from the surface (the outer edge of the boundary layer) where the fluid temperature reaches 99% of the free-stream temperature.

Obtain the expressions of local friction factor and local Nusselt number in terms of local Reynolds number.

1. Bird, R. B., Stewart, W. E., and Lightfoot, E. N., "Transport Phenomena," Wiley, New York (1960)
2. Schlichting, H., "Boundary Layer Theory," 4th ed., McGraw-Hill, New York (1960)

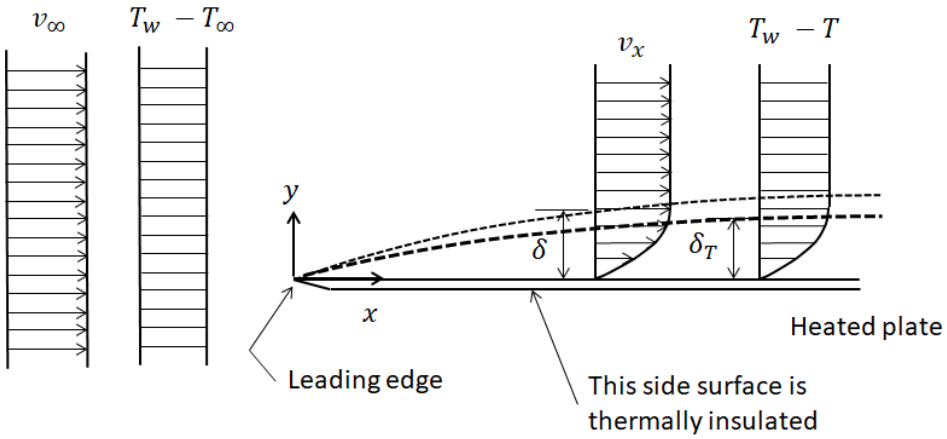

Fig. 18.2-1. Boundary layer flow along a heated flat plate

The local Reynolds number called "length Reynolds number" is defined using the distance x from the leading edge:

$$Re_x = \frac{v_\infty x}{\nu} \tag{18.2-1}$$

The following two-dimensional flow equations can be applied:

$$v_x \frac{\partial v_x}{\partial x} + v_y \frac{\partial v_x}{\partial y} = -\frac{1}{\rho}\frac{\partial p}{\partial x} + \nu \left(\frac{\partial^2 v_x}{\partial x^2} + \frac{\partial^2 v_x}{\partial y^2}\right) \tag{18.2-2}$$

$$v_x \frac{\partial T}{\partial x} + v_y \frac{\partial T}{\partial y} = \alpha \left(\frac{\partial^2 T}{\partial x^2} + \frac{\partial^2 T}{\partial y^2}\right) \tag{18.2-3}$$

where $\nu = \mu/\rho \quad and \quad \alpha = \kappa/\rho\, Cp.$

The free stream velocity outside the boundary layer and pressure are kept at

$v_\infty = const$ and $\frac{d\,P}{dx} = 0$

For convenience, the temperature T is replaced by the temperature difference $T_w - T$.

When the Reynolds number is sufficiently large, the thickness of the boundary layer is very small as compared to the x-directed (streamwise) distance. Therefore the variation of the x-velocity and temperature is very small in the x direction than in the y direction.

$\frac{\partial v_x}{\partial x} \ll \frac{\partial v_x}{\partial y}$ and $\frac{\partial T}{\partial x} \ll \frac{\partial T}{\partial y}$

The boundary layer equations to be solved become

$$\frac{\partial v_x}{\partial x} + \frac{\partial v_x}{\partial y} = 0 \tag{18.2-4}$$

$$v_x \frac{\partial v_x}{\partial x} + v_y \frac{\partial v_x}{\partial y} = \nu \frac{\partial^2 v_x}{\partial y^2} \tag{18.2-5}$$

$$v_x \frac{\partial (T_w - T)}{\partial x} + v_y \frac{\partial (T_w - T)}{\partial y} = \alpha \frac{\partial^2 (T_w - T)}{\partial y^2} \quad (18.2\text{-}6)$$

If the Prandtl number is unity, i.e., $\Pr = 1$, Eqs. (18.2-5) and (18.2-6) are the same in form. This suggests that the dimensionless velocity profiles are coincident with the dimensionless temperature profiles.

From the equation of continuity Eq. (18.2-4),

$$v_y = -\int_0^y \frac{\partial v_x}{\partial x}\, dy \quad (18.2\text{-}7)$$

Substituting this equation into Eqs. (18.2-5) and (18.2-6),

$$v_x \frac{\partial v_x}{\partial x} - \frac{\partial v_x}{\partial y} \int_0^y \frac{\partial v_x}{\partial x}\, dy = \nu \frac{\partial^2 v_x}{\partial y^2} \quad (18.2\text{-}8)$$

$$v_x \frac{\partial (T_w - T)}{\partial x} - \frac{\partial (T_w - T)}{\partial y} \int_0^y \frac{\partial v_x}{\partial x}\, dy = \alpha \frac{\partial^2 (T_w - T)}{\partial y^2} \quad (18.2\text{-}9)$$

The boundary conditions are

B.C.1 $y = 0$: $v_x = 0$

B.C.2 $y = \delta$: $v_x = v_\infty$ (18.2-10)

B.C.3 $y = 0$: $T_w - T = 0$

B.C.4 $y = \delta_T$: $T_w - T = T_w - T_\infty$ (18.2-11)

It is reasonable to assume that the velocity profiles and the temperature profiles are respectively similar at various distances from the leading edge. This implies that the velocity distribution curves and the temperature distribution curves for various distances can be made coincident with one another by selecting the free-stream quantities v_∞ and $T_w - T_\infty$, and the boundary layer thickness δ and δ_T, respectively. The principle of similarity in the velocity and temperature profiles can be analytically expressed as

$$\phi(\eta) = \frac{v_x}{v_\infty} \qquad \eta = \frac{y}{\delta(x)} \quad (18.2\text{-}12)$$

$$\Theta(\eta_T) = \frac{T_w - T}{T_w - T_\infty} \qquad \eta_T = \frac{y}{\delta_T(x)} \quad (18.2\text{-}13)$$

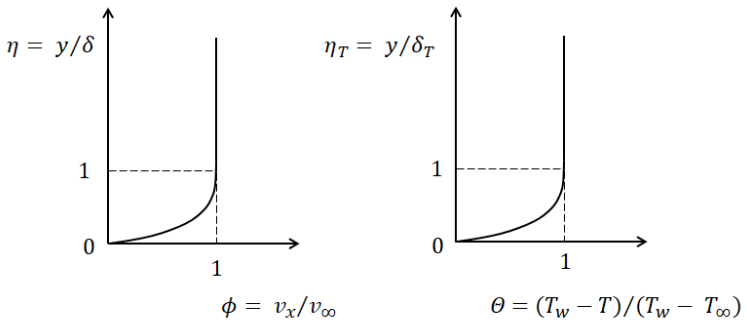

Fig. 18.2-2 Velocity and temperature profiles based on similarity transformation

The boundary layer thickness δ and δ_T are a function of x. Eqs. (18.2-12) and (18.2-13) constitute a very important set of variables for a variable transformation, known as the similarity transformation. It is further assumed that the ratio of δ_T to δ is a constant independent of the developing distance x:

$$\Delta = \delta_T / \delta = const \quad (18.2\text{-}14)$$

Using the new variables, the boundary layer equations can be transformed as follows.

$$v_x \frac{\partial v_x}{\partial x} = -\eta\, \phi' \phi\, \frac{{v_\infty}^2}{\delta} \frac{d\,\delta}{dx}$$

$$-\frac{\partial v_x}{\partial y} \int_0^y \frac{\partial v_x}{\partial x}\, dy = \left(\phi' \int_0^\eta \eta\, \phi' d\eta \right) \frac{{v_\infty}^2}{\delta} \frac{d\,\delta}{dx}$$

$$\nu \frac{\partial^2 v_x}{\partial y^2} = \nu \frac{v_\infty}{\delta^2} \phi''$$

Then Eq. (18.2-8) becomes

$$\left(\phi' \int_0^\eta \eta\, \phi' d\eta - \eta\, \phi' \phi\right) \delta \frac{d\,\delta}{dx} = \frac{\nu}{v_\infty} \phi'' \qquad (18.2\text{-}15)$$

where $\phi' = d\phi / d\,\eta$.

Using $\delta_T = \delta\, \Delta$,

$$v_x \frac{\partial (T_w - T)}{\partial x} = -\eta_T \Theta' \phi \frac{v_\infty (T_w - T_\infty)}{\delta} \frac{d\,\delta}{dx}$$

$$-\frac{\partial (T_w - T)}{\partial y} \int_0^y \frac{\partial v_x}{\partial x} dy = \Theta' \int_0^\eta \eta\, \phi' d\eta \frac{v_\infty (T_w - T_\infty)}{\Delta \delta} \frac{d\,\delta}{dx}$$

$$\alpha \frac{\partial^2 (T_w - T)}{\partial y^2} = \frac{\alpha (T_w - T_\infty)}{\Delta^2 \delta^2} \Theta''$$

Then Eq. (18.2-9) becomes

$$\Delta^2 \left[\frac{\Theta'}{\Delta} \int_0^\eta \eta\, \phi' \phi\, d\eta - \eta_T \Theta' \phi\right] \delta \frac{d\,\delta}{dx} = \frac{\alpha}{v_\infty} \Theta'' \qquad (18.2\text{-}16)$$

where $\Theta' = d\Theta / d\eta_T$.

If Eq. (18.2-15) is integrated over the boundary layer thickness (from $\eta = 0$ to 1), a first-order ordinary differential equation for δ can be obtained:

$$\int_0^1 \left(\phi' \int_0^\eta \eta\, \phi' d\eta - \eta\, \phi' \phi\right) d\eta\, \delta \frac{d\,\delta}{dx} = -\frac{\nu}{v_\infty} \phi'(0) \qquad (18.2\text{-}17)$$

in which the boundary condition $\partial v_x / y = 0$ at $y = \delta$ has been applied. If the velocity distribution function $\phi(\eta)$ is known, the above equation can be solved. Therefore a polynomial of the fourth degree is assumed:

$$\phi(\eta) = a + b\ \eta + c\ \eta^2 + d\ \eta^3 + e\ \eta^4 \qquad (18.2\text{-}18)$$

Five boundary conditions necessary to evaluate the five unknown constants, a, b, c, d, e are considered for an approximate distribution function, shown in Fig. 18.2-3.

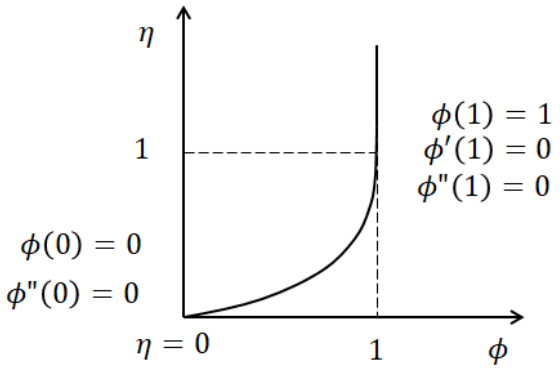

B.C.1	$\eta = 0$	:	$\phi = 0$
B.C.2	$\eta = 0$	:	$\phi'' = 0$
B.C.3	$\eta = 1$	:	$\phi = 1$
B.C.4	$\eta = 1$	:	$\phi' = 0$
B.C.5	$\eta = 1$	:	$\phi'' = 0$

Fig. 18.2-3. Approximate velocity distribution function

The second boundary condition can be obtained by taking the limit of the boundary layer equation as y goes to zero. The condition states that the second derivative of the velocity v_x at the wall is equal to the pressure gradient. The fifth condition implies that the velocity curve has a point of inflexion at the outer edge of the boundary layer.

Thus the approximate velocity distribution is obtained:

$$\phi(\eta) = 2\,\eta - 2\ \eta^3 + \eta^4 \qquad (18.2\text{-}19)$$

Substituting the above function into Eq. (18.2-17)

$$\delta \frac{d\,\delta}{dx} = \frac{630}{37} \frac{\nu}{v_\infty} \qquad (18.2\text{-}20)$$

Integrating with respect to x

$$\delta = \sqrt{\frac{1260}{37} \frac{\nu}{v_\infty} x} \qquad (18.2\text{-}21)$$

in which the initial condition (at $x = 0,\ \delta = 0$) has been used. The local friction factor f_x can be defined as

$$f_x = \frac{\tau_w(x)}{\frac{1}{2}\rho\, {v_\infty}^2} \tag{18.2-22}$$

Applying the polynomial velocity function to the Newton's law of viscosity,

$$\tau_w(x) = \mu \left.\frac{\partial v_x}{\partial y}\right|_{y=0} = \frac{\mu\, v_\infty}{\delta(x)}\, \phi'(0) = \sqrt{\frac{37}{315}\,\frac{\rho \mu\, {v_\infty}^3}{x}} \tag{18.2-23}$$

Substituting into Eq. (18.2-22), the local friction factor can be obtained in a function of length Reynolds number:

$$f_x = \frac{\sqrt{148/315}}{\sqrt{v_\infty x/\nu}} \cong \frac{0.685}{{Re_x}^{1/2}} \tag{18.2-24}$$

Regarding the temperature boundary layer, in the same manner as in the approximation of velocity function, we get the following polynomial function for the temperature distribution:

$$\Theta(\eta_T) = 2\,\eta_T - 2\,{\eta_T}^3 + {\eta_T}^4 \tag{18.2-25}$$

The boundary layer thickness ratio Δ has two possibilities : $\Delta \le 1$ and $\Delta \ge 1$. If Pr = 1, Δ becomes unity. We consider the case when the temperature boundary layer is thinner than the velocity boundary layer: $\Delta \le 1$.

The relation between η and η_T is

$$\eta = \eta_T \Delta \tag{18.2-26}$$

Integrating Eq.(18.2-16) over the temperature boundary layer thickness (from $\eta_T = 0$ to 1),

$$\Delta^2 \int_0^1 \left[\frac{\Theta'}{\Delta}\int_0^{\eta_T\Delta} \eta\,\phi'\phi\, d\eta - \eta_T \Theta'\phi(\eta_T\Delta)\right] d\eta_T\; \delta\frac{d\,\delta}{dx} = -\frac{\alpha}{v_\infty}\Theta'(0) \tag{18.2-27}$$

in which the boundary condition ($\partial T/\partial y = 0$ at $y = \delta_T$) has been applied.

Dividing Eq.(18.2-27) by Eq.(18.2-17)

$$\frac{\Delta^2 \int_0^1 \left[\frac{\Theta'}{\Delta}\int_0^{\eta_T\Delta} \eta\,\phi'\phi\, d\eta - \eta_T\Theta'\phi(\eta_T\Delta)\right] d\eta_T}{\int_0^1 \left(\phi' \int_0^\eta \eta\,\phi' d\eta - \eta\,\phi'\phi\right) d\eta} = \frac{1}{Pr}\,\frac{\Theta'(0)}{\phi'(0)} \tag{18.2-28}$$

Substituting Eqs.(18.2-19) and (18.2-25) into Eq.(18.2-28) and calculating the integrations, we get

$$\frac{1}{15}\Delta^3 - \frac{3}{280}\Delta^5 + \frac{1}{360}\Delta^6 = \frac{37}{630}\,\frac{1}{Pr} \qquad (\Delta \le 1) \tag{18.2-29}$$

The six-order algebraic equation can be approximated within 5% error by

$$\Delta = Pr^{-1/3} \tag{18.2-30}$$

According to Fourier's law

$$q_x(x) = \kappa \left.\frac{\partial T}{\partial y}\right|_{y=0} = \frac{2\,\kappa}{\Delta\,\delta}\,(T_w - T_\infty) \tag{18.2-31}$$

The local heat transfer coefficient and the local Nusselt number are defined as

$$q_w = h_x(T_w - T_\infty) \tag{18.2-32}$$

$$Nu_x = \frac{h_x x}{\kappa} = \frac{q_w\, x}{\kappa\,(T_w - T_\infty)} \tag{18.2-33}$$

By using Eqs. (18.2-21), Eq.(18.2-30), and (18.2-31), Eq.18.2-33) becomes

$$Nu_x = \frac{2}{\Delta\,\delta} = 2\sqrt{\frac{37}{1260}}\,{Re_x}^{1/2}\,Pr^{1/3} = 0.343\,{Re_x}^{1/2}\,Pr^{1/3} \tag{18.2-34}$$

It has been found that the local friction factor is inversely proportional to the square root of the local Reynolds number (length Reynolds number) and that the local Nusselt number is proportional to the square root of the local Reynolds number and the 1/3 power of the Prandtl number.

The j-factor for heat transfer is defined as

$$j_{Hx} = \frac{Nu_x}{Re_x\, Pr^{1/3}} \tag{18.2-35}$$

If the j-factor is calculated from Eq.(18.2-34)

$$j_{Hx} = \frac{0.343}{{Re_x}^{1/2}} \tag{18.2-36}$$

From Eq.(17-2-24)

$$\frac{f_x}{2} = \frac{0.343}{{Re_x}^{1/2}} \tag{18.2-37}$$

It has been demonstrated that the analogy $j_H = f_x/2$ between momentum and heat transfer holds

exactly between momentum and heat transfer for laminar boundary layer flow over a flat plate.
If we continue this approach of the boundary layer over a flat plate similarly for mass transfer, the following result can be obtained for laminar flow:

$$Sh_x = 0.343\, {Re_x}^{1/2}\, Sc^{1/3} \tag{18.2-38}$$

where the Sherwood number is defined as

$$Sh_x = \frac{c\, k_x x}{D_{AB}} \tag{18.2-39}$$

It has been confirmed that the Chilton-Colburn analogy relation exists between heat and mass transfer

$$j_D = j_H \tag{18.2-40}$$

where the j-factor for mass transfer is defined as

$$j_{Dx} = \frac{Sh_x}{Re_x\, Sc^{1/3}} \tag{18.2-41}$$

Similar method is available for turbulent boundary layer flow.
This boundary layer theory gives a valuable concept for the analogy between momentum and heat transfer. The section of convective heat transfer in a circular pipe flow in Chapter 8 also gives the same analogy relation Eq.(8.2-14).

18.3 Integral Equation of Boundary Layer Flow

18.3-1 Momentum integral equation of boundary layer flow over a flat plate

It is usually difficult to obtain an exact solution of the boundary layer equations.
An approximate method is available to overcome this difficulty.
The boundary layer equation for steady two-dimensional flow in the x-direction is

$$\rho\left(v_x \frac{\partial v_x}{\partial x} + v_y \frac{\partial v_x}{\partial y}\right) = -\frac{dp}{dx} + \mu \frac{\partial^2 v_x}{\partial y^2} \tag{18.3-1}$$

The equation of motion for external flow (potential flow) is

$$\rho\, v_\infty \frac{dv_\infty}{dx} = -\frac{d\,p}{dx} \tag{18.3-2}$$

Substituting Eq. (18.3-2) into Eq. (18.3-1)

$$v_x \frac{\partial v_x}{\partial x} + v_y \frac{\partial v_x}{\partial y} = v_\infty \frac{dv_\infty}{dx} + \nu \frac{\partial^2 v_x}{\partial y^2} \tag{18.3-3}$$

Integrating this equation with respect to y from $y = 0$ (wall) to $y = \delta$ (the outer edge of the boundary layer)

$$\int_0^\delta \left(v_x \frac{\partial v_x}{\partial x} + v_y \frac{\partial v_x}{\partial y} - v_\infty \frac{dv_\infty}{dx}\right) dy = \mu \frac{\partial v_x}{\partial y}\bigg|_0^\delta = -\frac{\tau_w}{\rho} \tag{18.3-4}$$

Substituting the equation of continuity: $v_y = -\int_0^y \frac{\partial v_x}{\partial x}\, dy$

$$\int_0^\delta \left(v_x \frac{\partial v_x}{\partial x} - \frac{\partial v_x}{\partial y}\int_0^y \frac{\partial v_x}{\partial x}\, dy - v_\infty \frac{dv_\infty}{dx}\right) dy = -\frac{\tau_w}{\rho} \tag{18.3-5}$$

The second term is integrated by parts

$$\int_0^\delta \left(\frac{\partial v_x}{\partial y}\int_0^y \frac{\partial v_x}{\partial x}\, dy\right) dy = v_\infty \int_0^\delta \frac{\partial v_x}{\partial x}\, dy - \int_0^\delta v_x \frac{\partial v_x}{\partial x}\, dy$$

Then Eq. (18.3-5) becomes

$$\int_0^\delta \left(2v_x \frac{\partial v_x}{\partial x} - v_\infty \frac{\partial v_x}{\partial x} - v_\infty \frac{dv_\infty}{dx}\right) dy = -\frac{\tau_w}{\rho}$$

This equation can be contracted to

$$\int_0^\delta \frac{\partial}{\partial x}\left(v_x(v_\infty - v_x)\right) dy + \frac{dv_\infty}{dx}\int_0^\delta (v_\infty - v_x) dy = \frac{\tau_w}{\rho} \tag{18.3-6}$$

The following two meaningful thicknesses can be introduced

$$v_\infty \delta_D = \int_0^\delta (v_\infty - v_x) dy$$

$$\rho v_\infty v_\infty \delta_m = \rho \int_0^\delta v_x (v_\infty - v_x) dy$$

where δ_D and δ_m are the displacement thickness and momentum thickness.
The integral equation becomes

$$\frac{\tau_w}{\rho} = \frac{d}{dx} v_\infty{}^2 \delta_m + v_\infty \delta_D \frac{dv_\infty}{dx} \quad (18.3\text{-}7)$$

This is the boundary-layer equation in integral form, which is valid both for laminar and turbulent flows.
Therefore this equation is useful for a macroscopic analysis of turbulent flows.

18.3-2 Energy integral equation of boundary layer flow

The thermal boundary layer equation is given by

$$v_x \frac{\partial T}{\partial x} + v_y \frac{\partial T}{\partial y} = \alpha \frac{\partial^2 T}{\partial y^2} \quad (18.3\text{-}8)$$

Substituting the equation of continuity

$$v_x \frac{\partial T}{\partial x} - \frac{\partial T}{\partial y} \int_0^y \frac{\partial v_x}{\partial x} dy = \alpha \frac{\partial^2 T}{\partial y^2} \quad (18.3\text{-}9)$$

Integrating from $y = 0$ to $y = \delta_T$ (the outer edge of the thermal boundary layer)

$$\int_0^{\delta_T} \left(v_x \frac{\partial T}{\partial x} - \frac{\partial T}{\partial y} \int_0^y \frac{\partial v_x}{\partial x} dy \right) dy = \alpha \left. \frac{\partial T}{\partial y} \right|_0^{\delta_T} = - \frac{q_w}{\rho Cp}$$

Using a temperature difference $\Theta = T_\infty - T$ in place of T

$$\int_0^{\delta_T} \left(v_x \frac{\partial \Theta}{\partial x} - \frac{\partial \Theta}{\partial y} \int_0^y \frac{\partial v_x}{\partial x} dy \right) dy = - \frac{q_w}{\rho Cp} \quad (18.3\text{-}10)$$

The second term is integrated by parts

$$\int_0^{\delta_T} \left(\frac{\partial \Theta}{\partial y} \int_0^y \frac{\partial v_x}{\partial x} dy \right) dy = \Theta_\infty \int_0^{\delta_T} \frac{\partial v_x}{\partial x} dy - \int_0^{\delta_T} \Theta \frac{\partial v_x}{\partial x} dy$$

Since the first term becomes zero, the equation reduces to

$$\int_0^{\delta_T} \left(v_x \frac{\partial \Theta}{\partial x} + \Theta \frac{\partial v_x}{\partial x} \right) dy = - \frac{q_w}{\rho Cp}$$

That is

$$\frac{d}{dx} \int_0^{\delta_T} \Theta v_x dy = - \frac{q_w}{\rho Cp} \quad (18.3\text{-}11)$$

This is the boundary-layer energy equation in integral form, which is also valid both for laminar and turbulent flows.

18.3-3 Turbulent boundary layer flow[1)]

As shown in Fig. 18.3-1, in the initial section of laminar boundary layer, the boundary layer thickness increases with the length Reynolds number Re_x. Eventually its instabilities cause the boundary layer to become turbulent. For the level of free-stream turbulence 0.5%, the critical length Reynolds number for transition on a smooth flat plate with a sharp leading edge can be assumed as

$$3 \times 10^5 \leq Re_x \leq 5 \times 10^5$$

1. Schlichting, H., "Boundary Layer Theory," 4th ed., McGraw-Hill, New York (1960)

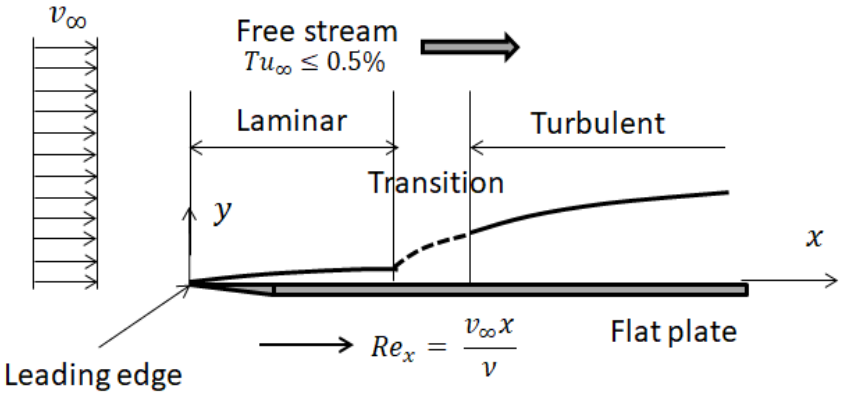

Fig. 18.3-1. Transition to turbulent boundary layer on a flat plate

The transition region, which is unstable and oscillatory in nature, has a finite length. Owing to the transverse exchange of fluid elements, the velocity distribution in the turbulent boundary layer is much flatter than that in the laminar boundary layer.

If a thin wire (called "tripping wire") is mounted near the leading edge of the flat plate, a turbulent boundary layer starts to grow from the beginning.

The integral form of the boundary layer equation can be used as a simple tool for analyzing difficult turbulent boundary layer flows. In addition, a simple solution can be obtained if a one-seventh power law is assumed for the velocity profile in the turbulent boundary layer.

For moderately high Reynolds numbers, the one-seventh power law is of the form:

$$u^+ = 8.74\, y^{+1/7}$$

From the definition of u^+ and y^+

$$v_x = 8.74\, v^* \left(\frac{y\, v^*}{\nu}\right)^{1/7} \tag{18.3-12}$$

where $v^* = \sqrt{\tau_w/\rho}$ is called "friction velocity."

At the outer edge of the boundary layer

$$u^+ = {v_\infty}^+ \text{ at } y = \delta$$

Applying Eq. (18.3-12) at the outer edge ($y = \delta$), the wall shear stress is calculated as

$$\tau_w = 0.0225\, \rho\, {v_\infty}^2 \left(\frac{\delta\, v_\infty}{\nu}\right)^{-1/4} \tag{18.3-13}$$

Substituting the power law into the defining equations of displacement and momentum thicknesses,

$$v_\infty\, \delta_d = \int_0^\delta (v_\infty - v_x)\, dy = \frac{1}{8}\, v_\infty \delta$$

$$\rho\, {v_\infty}^2\, \delta_m = \rho \int_0^\delta v_x (v_\infty - v_x) dy = 0.0972\, \rho\, {v_\infty}^2\, \delta$$

For this case (uniform constant velocity free stream)

$$\frac{d\, v_\infty}{dx} = 0 \tag{18.3-14}$$

Therefore the integral momentum equation becomes

$$\frac{\tau_w}{\rho} = \frac{d}{dx}\, {v_\infty}^2\, \delta_m \tag{18.3-15}$$

Substituting Eq.(18.3-13) into Eq.(18.3-15)

$$\delta^{1/4}\, \frac{d\, \delta}{dx} = 0.231 \left(\frac{\nu}{v_\infty}\right)^{1/4} \tag{18.3-16}$$

Integrating this with the boundary condition $\delta = 0$ at $x = 0$,

$$\frac{4}{5}\, \delta^{5/4} = 0.231 \left(\frac{\nu}{v_\infty}\right)^{1/4} x$$

From this equation, the following equation is obtained as a result:

$$\frac{\delta}{x} = 0.37\ {Re_x}^{-1/5} \tag{18.3-17}$$

It has been found that the dimensionless thickness of the turbulent boundary layer δ/x decreases with ${Re_x}^{-1/5}$.

Combining the defining equation of local friction factor with Eq.(18.3-13),

$$f_x = \frac{\tau_w}{\frac{1}{2}\rho\, {v_\infty}^2} = 2 \times 0.0225 \left(\frac{\delta}{x}\frac{x\, v_\infty}{\nu}\right)^{-1/4} = 0.058\ {Re_x}^{-1/5} \tag{18.3-18}$$

This is a very important result. As distinct from the laminar boundary layer, the local friction factor is correlated well with ${Re_x}^{-1/5}$.

This equation is in good agreement with experiments for Re_x up to several millions.

For the case of turbulent heat transfer from a heated flat plate,

$$j_H = \frac{Nu_x}{Re_x Pr^{1/3}} \sim C\ {Re_x}^{-1/5}$$

It should be kept in mind that the analogy between momentum and heat transfers still holds for turbulent boundary layer flow. The empirical coefficient C is difficult to determine because of the uncertainty in the location of the transition region.

18.4 Application of Stream Function (Impinging Flow)

Plane stagnation flow shown in Fig.18.4-1 can be solved using the stream function. Fluid approaching from the positive y direction is turned aside by the plane $y = 0$. The free stream outside the boundary layer has the following velocity parallel to the plane:

$$v_{xp} \to c\, x \quad \text{as} \quad y \to \infty \tag{18.4-1}$$

This velocity can be obtained by the potential flow theory assuming non-viscous flow.

However the no-slip" condition should be satisfied at the surface of the plane.

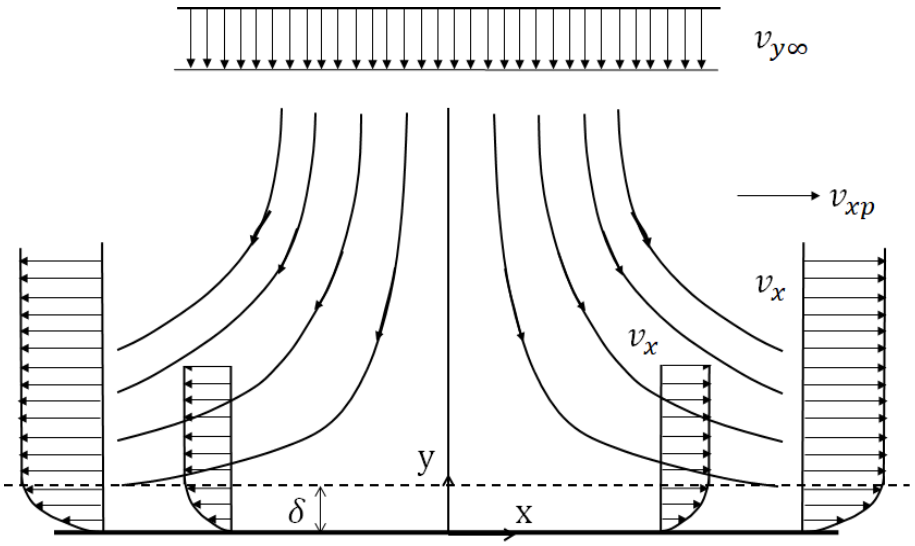

Fig.18.4-1 Stagnation flow impinging on a flat plane

The stream function is defined by Eq. (18.1-4):

$$v_x = \frac{\partial \psi}{\partial y} \quad \text{and} \quad v_y = -\frac{\partial \psi}{\partial x}$$

The equation to be solved is

$$-\frac{\partial\,(\psi, \nabla^2\psi)}{\partial\,(x,y)} = \nu\, \nabla^4 \psi \tag{18.4-2}$$

The boundary conditions are

$$\frac{\partial \psi}{\partial y} \to c\,x \quad \text{as} \quad y \to \infty \tag{18.4-3}$$

$$\frac{\partial \psi}{\partial x} = \frac{\partial \psi}{\partial x} = 0 \quad \text{at} \quad y = 0 \tag{18.4-4}$$

The first boundary condition suggests that the solution should be of the form

$$\psi = x\, f(y) \tag{18.4-5}$$

With this assumption, the main differential equation reduces to

$$-f\, f''' + f' f'' = \nu\, f^{iv} \tag{18.4-6}$$

where the primes denote differentiation with respect to y. This can be integrated once with respect to y

$$(f')^2 - f\, f'' - \nu\, f''' = K^2 \tag{18.4-7}$$

where K^2 is an integration constant. This equation can be simplified by a variable transformation. Let us define

$$\varphi = \frac{f}{\sqrt{K\nu}} \quad \text{and} \quad \eta = \sqrt{\frac{K}{\nu}}\, y \tag{18.4-8}$$

Then Eq.(18.3-7) becomes

$$\varphi''' + \varphi\, \varphi'' - (\varphi')^2 + 1 = 0 \tag{18.4-9}$$

Here the primes denote differentiation with respect to η.

The corresponding boundary conditions are

$$\varphi' \to 1 \quad \text{as} \quad \eta \to \infty \tag{18.4-10}$$

$$\varphi = \varphi' = 0 \quad \text{at} \quad \eta = 0 \tag{18.4-11}$$

The solution numerically calculated from Eq. (18.4-9) is shown in Fig.18.4-2.

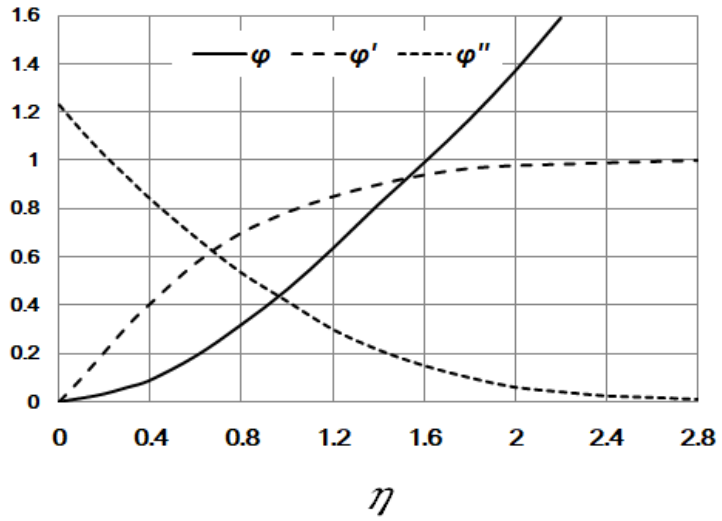

Fig.18.4-2. Numerically calculated solution of Eq.(18.4-9)

The x-component velocity $\varphi' = v_x/v_{xp}$ becomes 0.99 when $\eta = 2.4$. This indicates that the thickness of the boundary layer is given by

$$\delta = \eta_\delta \sqrt{\nu/K} = 2.4\,\sqrt{\nu/K} \tag{18.4-12}$$

It should be noted that the boundary layer thickness remains constant in the impingement region. This velocity boundary layer thickness δ also has a relation with the thermal boundary layer thickness δ_T. The integration constant K depends on the flow condition such as the approach velocity $v_{y\infty}$.

18.5 Impinging Jet Heat Transfer[1,2)]

This kind of impinging flows are very often practically applied for heating/cooling and drying technologies such as the drying of paper or film. For example, a free air jet issuing from a convergent nozzle is made striking normally onto a large flat plate, as shown in Fig.18.5-1.

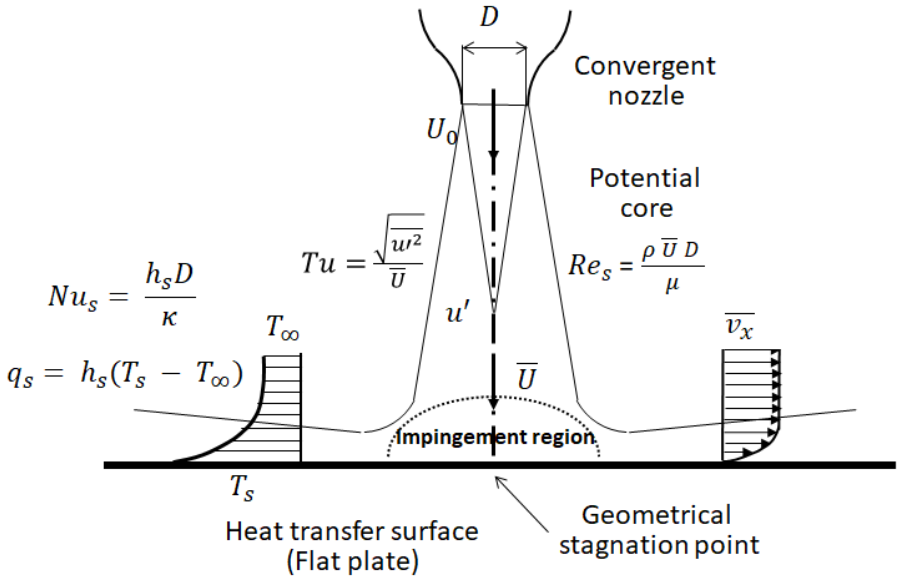

Fig.18.5-1. Schematic picture of jet impingement on a flat plate with heat transfer

When the nozzle-to-plate spacing is small, the free jet impinges on the flat plate without loss of its initial velocity before it becomes developed. The central jet impingement region around the stagnation point resembles the central region of impinging flow above-mentioned. An important question arises as to where the flat plane as a heat transfer surface should be placed to maximize the stagnation-point heat flux. When the spacing is large, the free jet becomes fully developed before it impinges. In the fully developed free jet region, the jet velocity decays in inverse proportional to the axial distance from the nozzle exit. The following impingement jet heat transfer correlation at the stagnation point is available as an example[1,2)]:

$$\frac{Nu_s}{{Re_s}^{1/2} Pr^{1/2}} = C\,(1 + \epsilon)\left(\frac{Nu}{{Re_s}^{1/2} Pr^{1/2}}\right)_{TF} \tag{18.4-13}$$

where the constant C was empirically obtained to be 0.88 for gas flow Pr $\leq$ 1 in our research.

The Reynolds number $Re_s = \rho D\,\overline{U}/\mu$ and the turbulence intensity $Tu = \sqrt{\overline{u'^2}}/\overline{U}$ are defined as the quantities of free jet at the position of the heat transfer plate.

The coefficient ϵ gives a factor of heat transfer enhancement due to the turbulence effect, which can be considered as a function of $Tu\sqrt{Re_s}$ defined on the centerline of the approaching jet. The subscript TF implies the turbulence-free condition (laminar flow solution).

We should know that it is one of the appropriate methods effective for the augmentation of convective heat transfer to strike a turbulent stream on a heat transfer surface like the above example.

For example, a shell-and-tube heat exchanger usually has the shell-side structure striking the shell-side stream on the tube bundles perpendicularly by the installed baffle plates.

1. Kataoka, K., Sahara, R., Ase, H. and Harada, T., *J. Chem. Eng. Japan*, **20**(1), 71 (1987)f
2. Kataoka, K., Suguro, M., Degawa, H., Maruo, K. and Mihata, I., *Int. J. Heat Mass Transfer*, **30**(3), 559 (1987)

18.6 Boundary-layer Analysis for Velocity-gradient Measurement

In Chapter 14.4 it was introduced that an electrochemical method can measure local velocity-gradient on the wall of liquid flow. A rectangular test cathode has ionic mass transfer on its surface under the diffusion-controlling condition, where the bulk concentration of reacting ion is C_A but the concentration at the wall (cathode surface) C_{Aw} becomes zero. Therefore the ionic mass flux on the cathode is given by

$N_A = I_d/Fa = kC_A$

The velocity gradient s on the wall is given by

$$s = 1.90\,(I_d/Fa\,C_A)^3\left(L/{D_{AB}}^2\right) = 1.90\,k^3\left(L/{D_{AB}}^2\right) \qquad (14.4\text{-}1)$$

Let us study again how this equation can be obtained by using the boundary layer theory in this section.

The two-dimensional boundary equation of laminar mass transfer can be written as

$$v_x\frac{\partial C_A}{\partial x} + v_y\frac{\partial C_A}{\partial y} = D_{AB}\frac{\partial^2 C_A}{\partial y^2}$$

Using the equation of continuity

$$v_x\frac{\partial C_A}{\partial x} - \frac{\partial C_A}{\partial y}\int_0^y \frac{\partial v_x}{\partial x}dy = D_{AB}\frac{\partial^2 C_A}{\partial y^2} \qquad (18.6\text{-}1)$$

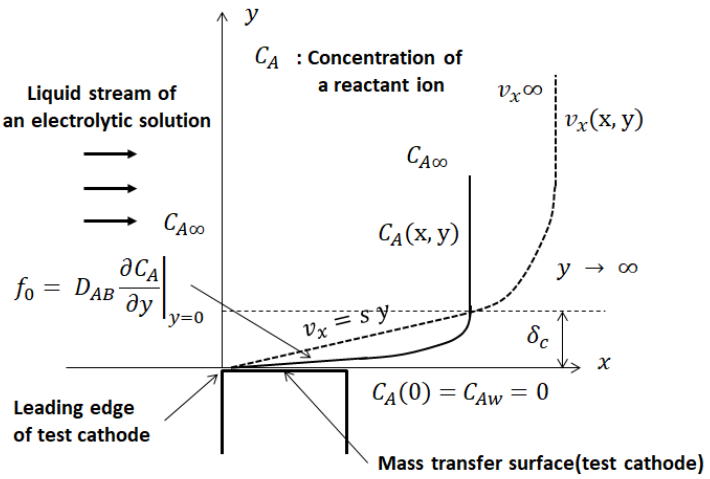

Fig.18.6-1 Velocity profile and concentration profile on an isolated cathode

As shown in Fig.18.6-1, the concentration boundary layer begins from the leading edge of the cathode while the velocity boundary layer has been developing from far ahead. Therefore within the concentration boundary layer on the test cathode the velocity profile can be assumed linear: $v_x = s\,y$, where s is the velocity gradient on the wall. In addition, the velocity change over the streamwise length of the test cathode is very small: $\partial v_x/\partial x \cong 0$.

The boundary layer equation reduces to

$$sy\frac{\partial C_A}{\partial x} = D_{AB}\frac{\partial^2 C_A}{\partial y^2} \qquad (18.6\text{-}2)$$

Dividing the equation by y to define a new (mass flux) function $f = D_{AB}(\partial C_A/\partial y)$ and then differentiating with respect to y:

$$s\frac{\partial f}{\partial x} = D_{AB}\frac{\partial}{\partial y}\left(\frac{1}{y}\frac{\partial f}{\partial y}\right) \qquad (18.6\text{-}3)$$

By the following variable transformation

$\psi = f/f_0,\ \eta = y/\delta_c,\ \ \lambda = D_{AB}x/s\,{\delta_c}^3$ (18.6-4)

where δ_C is the concentration boundary layer thickness

The above equation is made dimensionless:

$\frac{\partial\psi}{\partial\lambda} = \frac{\partial}{\partial\eta}\left(\frac{1}{\eta}\frac{\partial\psi}{\partial\eta}\right)$ (18.6-5)

With boundary conditions

B.C. 1: at $\lambda = 0,\quad \psi = 0$ (18.6-6)

B.C. 2: at $\eta = 0,\quad \psi = 1$

B.C. 3: at $\eta = \infty,\ \psi = 0$

This equation can be solved analytically by the combination of variables by using then following independent variable:

$\chi = \frac{\eta}{\sqrt[3]{9\,\lambda}}$ (18.6-7)

Finally the mass flux equation becomes

$\chi\,\psi'' + (3\,\chi^3 - 1)\,\psi' = 0$ (18.6-8)

The boundary conditions become:

B.C. 1: at $\chi = 0,\quad \psi = 1$ (18.6-9)

B.C. 2: at $\chi = \infty,\quad \psi = 0$

The primes mean differentiation with respect to : $\psi' = d\psi/d\chi$

The solution is

$\psi = \frac{\int_\chi^\infty \chi\,e^{-\chi^3}\,d\chi}{\int_0^\infty \chi\,e^{-\chi^3}\,d\chi} = \frac{3}{\Gamma(2/3)}\int_\chi^\infty \chi\,e^{-\chi^3}\,d\chi$ (18.6-10)

Here the calculation procedure for solving Eq.(18.6-8) by the method of combination of variables is omitted owing to the limitation of page allocation.

The concentration profile can be obtained by integration:

$\int_{C_A}^{C_{A\infty}} dC_A = -\frac{1}{D_{AB}}\int_y^\infty f\,dy = (C_{A\infty} - C_A(y))$ (18.6-11)

The dimensionless concentration is given by

$\Lambda = \frac{C_A - C_{A\infty}}{\delta_c f_0/D_{AB}} = \sqrt[3]{9\lambda}\int_\chi^\infty \psi\,d\chi$ (18.6-12)

where

$f_0 = D_{AB}\left.\frac{\partial C_A}{\partial y}\right|_{y=0}$ (18.6-13)

Substituting Eq.(18.6-10) into the integration of Eq.(18.6-12), the following equation is obtained:

$\Lambda = \sqrt[3]{9\lambda}\left[\frac{e^{-\chi^3}}{\Gamma(2/3)} - \chi\left\{1 - \frac{\Gamma(\frac{2}{3},\chi^3)}{\Gamma\left(\frac{2}{3}\right)}\right\}\right]$ (18.6-14)

where $\Gamma(p,x)$ is called "incomplete gamma function," which is defined as

$\Gamma(p,x) = \int_x^\infty t^{p-1}\,e^{-t}\,dt$ (18.6-15)

Since the mass transfer wall lies at $\chi = 0$, $\Gamma(\frac{2}{3},\chi^3)$ becomes $\Gamma(2/3)$ and the second term disappears.

The gamma function is also defined as

$\Gamma(p) = \int_0^\infty x^{p-1}\,e^{-x}\,dx$ (18.6-16)

, which gives $\Gamma(2/3) \cong 1.35411$.

Then Eq.(18.6-13) can be written at the wall $\chi = 0$ as

$\Lambda_{\chi=0} = \frac{C_{A\infty} - C_{Aw}}{\delta_c f_0/D_{AB}} = \frac{\sqrt[3]{9\lambda}}{\Gamma(2/3)} = \frac{\sqrt[3]{9}\left(\frac{D_{AB}x}{s\,{\delta_c}^3}\right)^{1/3}}{\Gamma(2/3)} = 1$ (18.6-17)

because according to the film theory the following relation is valid at any position x

$$f_0 = D_{AB}\left.\frac{\partial C_A}{\partial y}\right|_{y=0} = D_{AB}\frac{C_{A\infty} - C_{Aw}}{\delta_c}$$

Then from Eq.(18.6-14)

$$s = \left[\frac{\sqrt[3]{9}}{\Gamma(2/3)}\right]^3 \left(\frac{D_{AB}}{{\delta_c}^3}\right) x = \left[\frac{\sqrt[3]{9}}{\Gamma(2/3)}\right]^3 \left(\frac{D_{AB}}{\delta_c}\right)^3 \frac{x}{{D_{AB}}^2} = \left[\frac{\sqrt[3]{9}}{\Gamma(2/3)}\right]^3 k^3 \frac{x}{{D_{AB}}^2} \qquad (18.6\text{-}18)$$

The velocity-gradient at the wall of the test cathode averaged over the electrode length from $x = 0$ to $x = L$ is,

$$s = \left[\frac{\sqrt[3]{9}}{\Gamma(2/3)}\right]^3 k^3 \frac{1}{{D_{AB}}^2} \frac{1}{L} \int_0^L x\, dx = \frac{1}{2}\left[\frac{\sqrt[3]{9}}{\Gamma(2/3)}\right]^3 k^3 \frac{L}{{D_{AB}}^2} \cong 1.8124\, k^3 \frac{L}{{D_{AB}}^2} \qquad (18.4\text{-}19)$$

This result coincides to Eq. (14.4-1) but the coefficient 1.8124 is slightly different from the coefficient 1.90 of Eq. (14.4-1).

It is interesting that this electrochemical method can observe fluctuating velocity gradients in the viscous sublayer of various turbulent flows.

Nomenclature

C_A	molar concentration of reactant ion A, [kmol/m^3]
Cp	heat capacity, [J/kg K]
D_{AB}	diffusivity of component A, [m^2/s]
Fa	Faraday constant (96,500 C/kg-equiv.),
f	mass-flux function, [kmol/m^{2}s]
f_x	local friction factor, [-]
I_d	limiting current density, [A/m^2]
j_{Dx}	local j-factor for mass transfer, [-]
j_{Hx}	local j-factor for heat transfer, [-]
L	length of rectangular electrode in flow direction, [m]
Nu_x	local Nusselt number, [-]
Pr	Prandtl number, [-]
p	pressure, [Pa]
q_x	local heat flux, [J/m^{2}s]
Re_x	local length Reynolds number, [-]
r, θ, z	cylindrical coordinates, [m, - , m]
Sc	Schmidt number, [-]
Sh_x	local Sherwood number, [-]
s	velocity gradient at wall, [1/s]
T	temperature, [K]
u^+	dimensionless velocity = $\frac{\overline{v_z}}{\sqrt{\tau_w/\varrho}}$
u^*	friction velocity, [m/s]
v_x, v_y, v_z	velocity component in rectangular coordinates, [m/s]
v_∞	free-stream velocity, [m/s]
x, y, z	rectangular coordinates, [m]
y^+	dimensionless distance from wall = $\frac{y\sqrt{\tau_w/\varrho}}{\nu}$
α	thermal diffusivity, [m^2/s]
Δ	thickness ratio of thermal to velocity boundary layer, [-]
$\delta,\ \delta_T$	thickness of velocity and temperature boundary layer, [m]
δ_c	concentration boundary layer thickness, [m]
δ_D	displacement thickness of boundary layer, [m]
δ_m	momentum thickness of boundary layer, [m]
ϵ	heat transfer enhancement factor, [-]
Θ	temperature difference, [K]
Λ	dimensionless concentration difference, [-]
ν	kinematic viscosity or diffusivity of momentum, [m^2/s]:
ρ	density, [kg/m^3]
ψ	stream function, [m^2/s]

Subcripts

p	potential flow
s	stagnation point of impinging jet
w	wall
∞	free stream

CHAPTER 19

FREE COVECTION

19.1 Boundary Layer Approach

Fluid motion caused by the gradients of the fluid density is called “natural or free convection.”

As a simple example we shall consider a natural laminar flow along a vertical flat plate which is heated at a constant temperature T_w and surrounded by a large volume of the gas fluid at a constant temperature T_∞. When $T_w > T_\infty$, in the neighborhood of the plate the fluid flows upward due to the buoyancy force and has a boundary layer structure as shown in Fig.19.1-1. For simplicity the physical properties are assumed constant except for the fluid density in the buoyancy term.

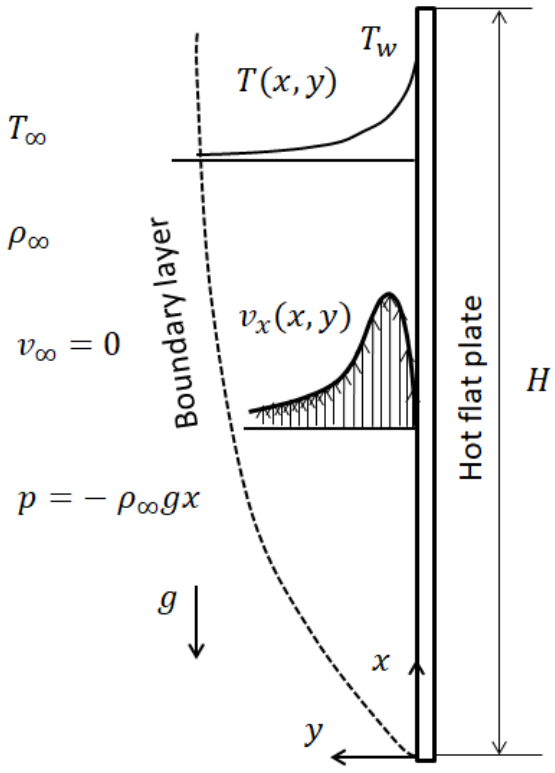

Fig. 19.1-1. Natural flow along a vertical hot plate

(The following theoretical approach is not so easy to follow for this course. This section can be skipped, except for the heat transfer correlations given in the latter part, which are useful for engineering calculations.)

The following two-dimensional flow equations can be applied[1,2]:

$$\rho_\infty \left(v_x \frac{\partial v_x}{\partial x} + v_y \frac{\partial v_x}{\partial y} \right) = -\frac{\partial p}{\partial x} + \mu \left(\frac{\partial^2 v_x}{\partial x^2} + \frac{\partial^2 v_x}{\partial y^2} \right) - \rho g \qquad (19.1\text{-}1)$$

The pressure in each horizontal plane is equal to the gravitational pressure

$$p = -\rho_\infty g\, x$$

where ρ_∞ is the density at T_∞. The density ρ at T can be expanded in a Taylor series about the reference temperature T_∞:

$$\rho = \rho_\infty + \left.\frac{\partial\rho}{\partial T}\right|_{T_\infty}(T - T_\infty) + --- \cong \rho_\infty - \rho_\infty\beta(T - T_\infty) \tag{19.1-2}$$

where $\beta = -\frac{1}{\rho_\infty}\left.\frac{\partial\rho}{\partial T}\right|_{T_\infty}$ is the coefficient of volume expansion. For gases $\beta = \frac{1}{T_\infty}$

Therefore the buoyancy force is given by

$$-\frac{\partial p}{\partial x} - \rho g = \rho_\infty\beta(T - T_\infty)g = \rho_\infty g\,\frac{T - T_\infty}{T_\infty} \tag{19.1-3}$$

Thus we get the following set of equations:

$$\frac{\partial v_x}{\partial x} + \frac{\partial v_y}{\partial y} = 0$$

$$v_x\frac{\partial v_x}{\partial x} + v_y\frac{\partial v_x}{\partial y} = \nu\left(\frac{\partial^2 v_x}{\partial x^2} + \frac{\partial^2 v_x}{\partial y^2}\right) + g\,\frac{T - T_\infty}{T_\infty}$$

$$v_x\frac{\partial T}{\partial x} + v_y\frac{\partial T}{\partial y} = \alpha\left(\frac{\partial^2 T}{\partial x^2} + \frac{\partial^2 T}{\partial y^2}\right) \tag{19.1-4}$$

where $\nu = \mu/\rho \quad and \quad \alpha = \kappa/\rho\,Cp.$

By the boundary layer approximation

$$\frac{\partial^2 v_x}{\partial x^2} \cong 0 \quad \text{and} \quad \frac{\partial^2 T}{\partial x^2} \cong 0$$

Here in place of T, the dimensionless local temperature $\Theta = (T - T_\infty)/(T_w - T_\infty)$ is introduced.

Thus the equations to be solved are

$$\frac{\partial v_x}{\partial x} + \frac{\partial v_y}{\partial y} = 0 \tag{19.1-5}$$

$$v_x\frac{\partial v_x}{\partial x} + v_y\frac{\partial v_x}{\partial y} = \nu\,\frac{\partial^2 v_x}{\partial y^2} + g\,\frac{(T_w - T_\infty)}{T_\infty}\,\Theta \tag{19.1-6}$$

$$v_x\frac{\partial\Theta}{\partial x} + v_y\frac{\partial\Theta}{\partial y} = \alpha\,\frac{\partial^2\Theta}{\partial y^2} \tag{19.1-7}$$

The boundary conditions are

$$v_x = v_y = 0, \qquad \Theta = 1 \qquad \text{at } y = 0$$

$$v_x = 0 \quad \Theta = 0 \quad \text{at } y = \infty \tag{19.1-8}$$

Firstly we should consider what similarity transformation is appropriate for this problem.

The stream function is introduced

$$\frac{\psi(x,y)}{f(x)} = \zeta(\eta) \qquad \eta = \frac{y}{L(x)} \tag{19.1-9}$$

This is a kind of the similarity transformation. Here $\zeta(\eta)$ is a dimensionless stream function which is a function of η alone, η the dimensionless y-coordinate, L an unknown characteristic length relating to the boundary layer thickness, and $f(x)$ the unknown function to be determined.

The velocity components are

$$v_x = \frac{\partial\psi}{\partial y} = f(x)\zeta'\,\frac{1}{L} \tag{19.1-10}$$

$$v_y = -\frac{\partial\psi}{\partial x} = -f'(x)\,\zeta(\eta) + \eta\zeta'\,\frac{f(x)}{L}\,\frac{dL}{dx} \tag{19.1-11}$$

where $\zeta' = d\zeta/d\eta$ and $f'(x) = df/dx.$

Substituting into the equation of motion,

$$\frac{f\,f'}{L^2}\,[(\zeta')^2 - \zeta''\zeta] - \frac{f^2}{L^3}\,\frac{dL}{dx}(\zeta')^2 = \frac{\nu\,f}{L^3}\,\zeta''' + g\,\frac{T_w - T_\infty}{T_\infty}\,\Theta \tag{19.1-12}$$

Dividing through by $f\,f'/L^2$

$$[(\zeta')^2 - \zeta''\zeta] - \frac{f}{f'L}\,\frac{dL}{dx}\,(\zeta')^2 = \frac{\nu}{L\,f'}\,\zeta''' + g\,\frac{T_w - T_\infty}{T_\infty}\frac{L^2}{f\,f'}\,\Theta \tag{19.1-13}$$

Each term should be dimensionless. Thus

$$\frac{f}{f'L}\,\frac{dL}{dx} = K_1, \quad \frac{\nu}{L\,f'} = K_2, \quad g\,\frac{T_w - T_\infty}{T_\infty}\frac{L^2}{f\,f'} = K_3 \tag{19.1-14}$$

From the three equations of Eq. (19.1-14)

$$L^3 \frac{dL}{dx} = \frac{K_1 K_3}{{K_2}^2} \frac{\nu^2}{g \frac{T_w - T_\infty}{T_\infty}} \quad (19.1\text{-}15)$$

The arbitrary constant $K_1 K_3 / {K_2}^2$ can be taken as unity without loss of generality. Integration with the initial condition $L = 0$ at $x = 0$ gives

$$L = \sqrt[4]{\frac{4\,\nu^2\,T_\infty}{g\,(T_w - T_\infty)}}\ \sqrt[4]{x} = \frac{1}{\gamma}\ \sqrt[4]{x} \quad (19.1\text{-}16)$$

This suggests that the velocity and temperature boundary layer thicknesses are proportional to $x^{1/4}$. For convenience K_2 is taken as 1/3 in the second equation of Eq.(19.1-14). Then

$$f(x) = 4\,\nu\,\gamma\,x^{3/4} \quad (19.1\text{-}17)$$

It has been found that the similarity transformation is of the form:

$$\eta = \gamma\ \frac{y}{\sqrt[4]{x}} \quad (19.1\text{-}18)$$

$$\psi(x,y) = 4\,\nu\,\gamma\,x^{3/4}\ \zeta(\eta) \quad (19.1\text{-}19)$$

The velocity components become

$$v_x = 4\,\nu\,\gamma^2\,x^{1/2}\,\zeta' \quad (19.1\text{-}20)$$

$$v_y = \nu\,\gamma\,x^{-1/4}(\eta\zeta' - 3\,\zeta) \quad (19.1\text{-}21)$$

The boundary layer equations to be solved become a set of ordinary differential equation:

$$\zeta''' + 3\,\zeta'\,\zeta - 2\,(\zeta')^2 + \Theta = 0 \quad (19.1\text{-}22)$$

$$\Theta'' + 3\,Pr\,\zeta\,\Theta' = 0 \quad (19.1\text{-}23)$$

where primes denote differentiation with respect to η.

The boundary conditions are

$$\zeta = \zeta' = 0 \quad \Theta = 1 \quad \text{at } \eta = 0 \quad (19.1\text{-}24)$$

$$\zeta' = 0 \quad \Theta = 0 \quad \text{at } \eta = \infty \quad (19.1\text{-}25)$$

This set of equations is very difficult to solve analytically. Owing to the limitation of this course, the numerical solutions are not shown here. It is known that the numerical solutions are in good agreement with the experimental distributions obtained by Schmidt and Beckmann[1)].

1. Schmidt, E. and Beckmann, W., *Tech. Mech. U. Thermodynamik*, **1**, 341 and 391 (1930)
2. Schuh, H., Boundary Layers of Temperature, in W. Tollmien (ed.), "Boundary Layers," British Ministry of Supply, German Document Center, Ref. 3220T (1948)

19.2 Free Convection Heat Transfer

By using the numerical solutions, the wall heat-flux can be calculated as

$$q_w = -\kappa \left.\frac{\partial T}{\partial y}\right|_{y=0} = -\kappa \left.\frac{\partial T}{\partial \Theta}\frac{d\Theta}{d\eta}\frac{\partial \eta}{\partial y}\right|_{y=0} = -\kappa(T_w - T_\infty)\ \frac{\gamma}{\sqrt[4]{x}} \left.\frac{d\Theta}{d\eta}\right|_{\eta=0} \quad (19.2\text{-}1)$$

For $\mathrm{Pr} = 0.73$ (air) the dimensionless temperature gradient at the wall is given by the numerical solution:

$$\left.\frac{d\Theta}{d\eta}\right|_{\eta=0} = -0.508 \quad (19.2\text{-}2)$$

The heat transfer coefficient can be defined as

$$h_x = \frac{q_w}{T_w - T_\infty} \quad (19.2\text{-}3)$$

Then the local Nusselt number becomes

$$Nu_x = \frac{h_x\,x}{\kappa} = 0.508\gamma\,x^{3/4} = \frac{0.508}{4^{1/4}}\left[\frac{g\,x^3(T_w - T_\infty)}{\nu^2 T_\infty}\right]^{1/4} = 0.359\ {Gr_x}^{1/4} \quad (19.2\text{-}4)$$

where Gr_x is the local Grashof number.

The average Nusselt number can be determined by the following integration:

$$Nu_{,m} = \frac{h_m\,H}{\kappa} = 0.508\,\gamma\ \int_0^H x^{-1/4}\,dx = 0.677\ {Gr_H}^{1/4} \quad (19.2\text{-}5)$$

Here the Grashof number is the ratio of the buoyant to the viscous force:

$$Gr_H = \frac{g\,H^3(T_w - T_\infty)}{\nu^2 T_\infty} \qquad (19.2\text{-}6)$$

This result, Eq.(19.2-5) is very important to understand the empirical heat transfer correlations for the laminar free convection. This suggests that the average Nusselt number is proportional to one-fourth power of the Grashof number for laminar free convection.

The transition from laminar to turbulent flow occurs in the range $10^8 < Gr_H \Pr < 10^{10}$.

The following empirical equations are recommended by Eckert and Jackson[1]:

$$Nu_m = 0.555\,(Gr_H Pr)^{1/4} \qquad Gr_H \Pr < 10^9 \qquad \text{(Laminar flow)} \qquad (19.2\text{-}7)$$

$$Nu_m = 0.021\,(Gr_H Pr)^{2/5} \qquad Gr_H \Pr > 10^9 \qquad \text{(Turbulent flow)} \qquad (19.2\text{-}8)$$

1. Eckert, E. R. G., and Jackson, T. W., NACA RFM 50 D25, July (1950)

These correlation equations Eqs.(19.2-7) and (19.2-8) are also applicable to a vertical hot cylinder.

For a long horizontal hot cylinder, experimental data have been correlated by McAdams[1]:

$$Nu_m = \frac{h_m D}{\kappa} = 0.525\,(Gr_D Pr)^{1/4} \qquad Gr_D \Pr > 10^4 \qquad (19.2\text{-}9)$$

where $Gr_D = \frac{g\,D^3(T_w - T_\infty)}{\nu^2 T_\infty}$

1. McAdams, W. A., Heat Transmission, Second ed., McGraw-Hill, New York (1942)

[EXAMPLE 19.2-1]

Calculate the heat loss from the outside surface of a big cylindrical furnace, which consists of the composite wall of three materials: fire-clay brick, insulating brick, and iron. As shown in Fig. 19.2-E1, the melted iron well mixed at a constant temperature T_i keeps the inside surface of the fire-clay brick at T_i. The surrounding air is assumed to be stationary at a constant temperature T_∞. In the neighborhood of the furnace, the air rises owing to the buoyancy force. The furnace is H in height and D_o in outside diameter. The heat loss from the top of the furnace is neglected only for simplicity. For this case there exist four heat-transfer resistances in series.

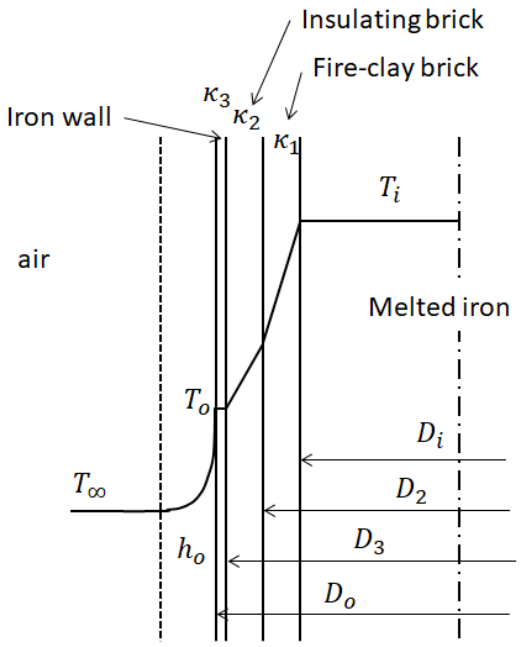

Fig.19.2-E1. Heat loss from the outside vertical wall of a furnace

The overall heat-transfer resistance is expressed as

$$\frac{1}{U_o} = \frac{1}{h_o} + \frac{(D_o - D_3)/2}{\kappa_3}\frac{D_o}{D_{3av}} + \frac{(D_3 - D_2)/2}{\kappa_2}\frac{D_o}{D_{2av}} + \frac{(D_2 - D_i)/2}{\kappa_1}\frac{D_o}{D_{1av}} \quad (19.2\text{-E1})$$

where

$$D_{3av} = \frac{D_o - D_3}{\ln(D_o/D_3)}, \quad D_{2av} = \frac{D_3 - D_2}{\ln(D_3/D_2)}, \quad D_{1av} = \frac{D_2 - D_i}{\ln(D_2/D_i)}$$

Here the outside heat-transfer coefficient h_o can be obtained by calculating from Eq. (19.2-7) or Eq.(19.2-8).

The temperature T_o at the outside surface of the furnace is necessary to determine the Grashof number.

The following heat-balance equation can be used:

$$U_o\,\pi D_o H\,(T_i - T_\infty) = \frac{\pi D_o H (T_i - T_\infty)}{\frac{(D_o - D_3)/2}{\kappa_3}\frac{D_o}{D_{3av}} + \frac{(D_3 - D_2)/2}{\kappa_2}\frac{D_o}{D_{2av}} + \frac{(D_2 - D_i)/2}{\kappa_1}\frac{D_o}{D_{1av}}} \quad (19.2\text{-E2})$$

The outside surface temperature T_o can be calculated by the use of trial and error method in the above equation.

Then the total heat-loss is given by

$$Q = U_o\,\pi D_o H\,(T_i - T_\infty) \quad (19.2\text{-E3})$$

[PROBLEM]

An LD converter is a furnace used for reduction of the carbon concentration in melted iron. A supersonic oxygen gas jet impinges on the melted iron to remove carbon as CO from it. The wall consists of three layers: refractory brick layer (κ_1= 6.1 W/m K), insulating brick layer (κ_2= 3.1 W/m K), and a steel plate (κ_3= 44 W/m K). Their thicknesses are 450 mm, 200 mm, and 50 mm, respectively. The melted iron is kept at uniform temperature 1,800 K owing to the strong jet agitation. The surrounding air is at $T_\infty = 313\ K$.

Calculate the heat loss from the vertical wall of this LD converter. What is the surface temperature of the steel plate?

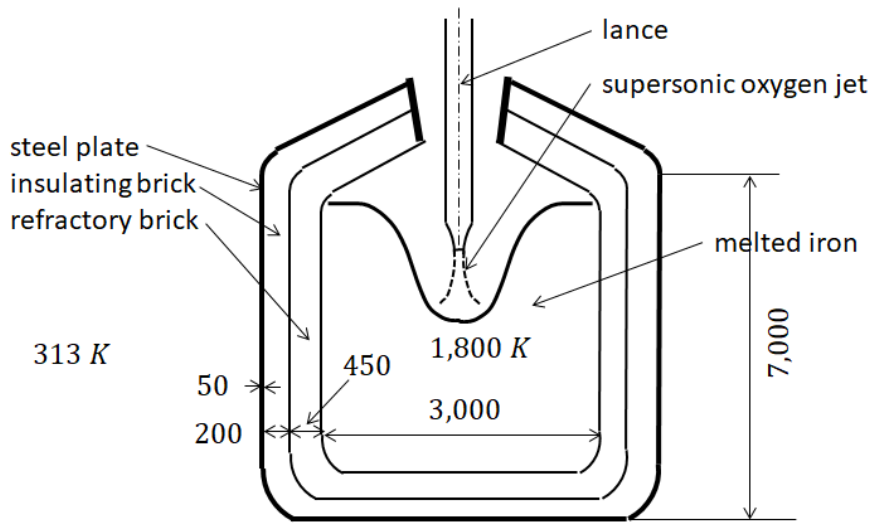

Fig. 19.2-P1. Heat Loss from an LD converter. Dimensions given are in mm

Nomenclature

D	cylinder diameter, [m]
g	gravitational acceleration, [m/s^2]
Gr_H	Grashof number, [-]
Gr_x	local Grashof number, [-]
h_x	local heat transfer coefficient, [W/m^{2}K]
L	unknown characteristic length, [m]
Nu_x	local Nusselt number, [-]
Pr	Prandtl number, [-]
p	pressure, [Pa]
Q	heat loss, [J/s]
q_w	wall heat flux, [J/m^{2}s]
Re_x	length Reynolds number, [-]
T	temperature, [K]
U	overall heat transfer coefficient, [W/m^{2}K]
v_x, v_y, v_z	velocity component in rectangular coordinates, [m/s]
x, y, z	rectangular coordinates, [m]
α	thermal diffusivity, [m^2/s]
β	coefficient of volume expansion, [1/K]
Θ	dimensionless local temperature, [-]
κ	thermal conductivity, [W/m K]
μ	viscosity, [kg/m s]
ν	kinematic viscosity, [m^2/s]:
ρ	density, [kg/m^3]
ψ	stream function, [m^2/s]

Subcripts

D	cylinder
h	hot plate
m	averaged
w	wall
∞	bulk fluid

CHAPTER 20

AGITATION

20.1 Agitation and Mixing of Liquids

Agitation technology is very often utilized for the following purposes:
(1) Suspending solid particles or dissolving solid into liquid, (2) blending miscible liquids, (3) dispersing a second liquid, immiscible with the first one to form an emulsion, (4) dispersing a gas as the bubbles through the liquid, and (5) promoting heat transfer or chemical reaction.

20.1-1 General structure of agitation equipment

A typical agitation vessel is shown in Fig.20.1-1. An impeller is mounted on an overhung shaft, which is driven by a motor. The proportions of the tank vary widely, depending on various purposes. For the case of a standardized practical design, accessories such as inlet and outlet nozzles, coils, jackets, measuring-device wells are necessary.

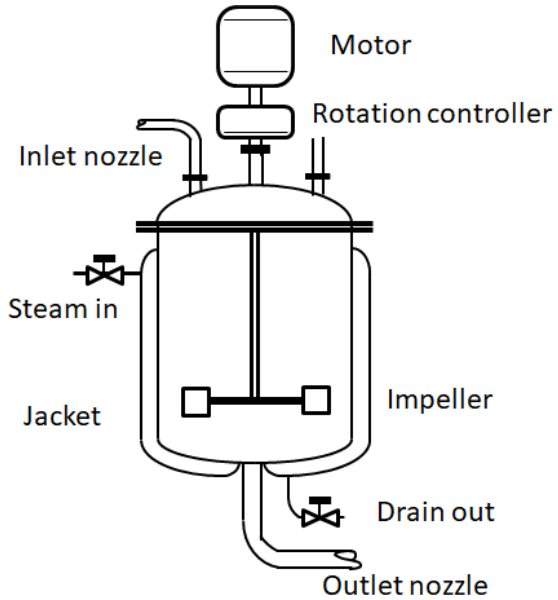

Fig.20.1-1. Standard structure of agitation vessel

The impeller agitators are classified into two types: the axial-flow impeller generates currents parallel with the impeller shaft axis and the radial-flow impeller generates currents in a tangential or radial direction.

Several propeller designs efficient in liquids of low viscosity are illustrated in Fig.20.1-2: (a) standard screw-type, three blades, (b) open straight blade-type, four blades, (c) turbine bladed disk-type, eight blades, (d) vertical curved blade-type, eight blades.

Two agitators employed for high viscosity or non-Newtonian liquids are shown in Fig.20.1-3: (a) anchor-type, (b) helical ribbon-type.

Flows in these kinds of agitating vessels are three-dimensional and very complicated. Therefore to obtain theoretical solutions by using the equation of motion is very difficult, especially for turbulent flows. In addition, the structure of agitated vessels is so complicated that it is also very difficult to specify the boundary conditions. The commercial simulator packages based on the CFD models (computational fluid dynamics) are available for very viscous or laminar Newtonian fluid flows. Although the main flow caused by the rotation of an impeller is tangential, the tangential velocity component is not so effective for mixing. The radial and longitudinal components are important for the mixing action. In addition, the rotational fluid flow following a circular path around the shaft creates an undesirable vortex at the surface of the liquid.

In addition, a ring doughnut-shaped isolated mixing region having independent circular motion is formed in each central region above and below the impellers for unbaffled tanks. The effect of mixing is not so good in the isolated mixing region. Generally the preferable method of suppressing the vortex formation is to install baffles.

Usually several vertical baffle plates are fixed to the inner wall of the tank.

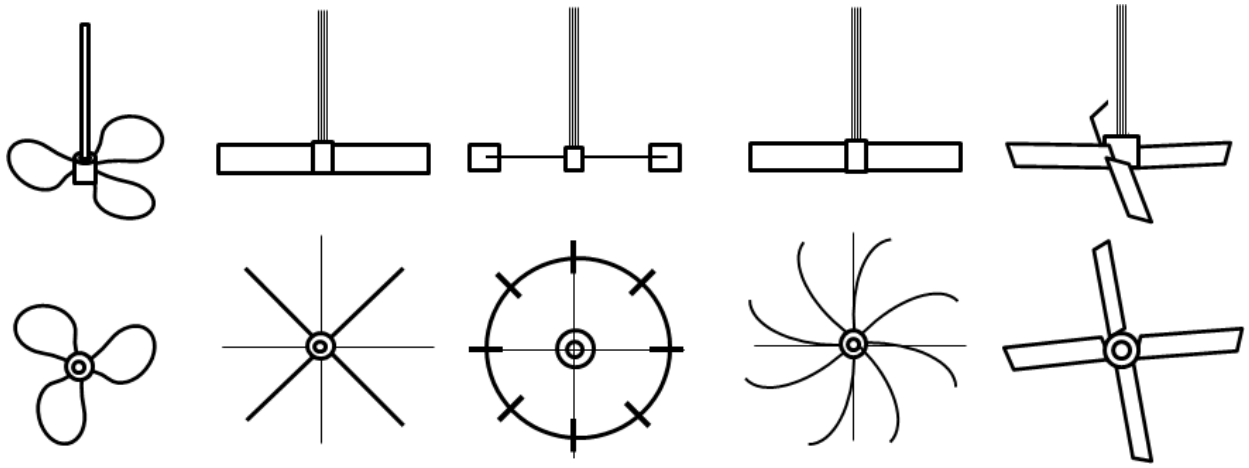

Fig.20.1-2. Impellers for low viscosity fluids: (a) marine-type propeller, three blades, (b) open straight blade turbine, four blades, (c) bladed disk turbine, eight blades, (d) vertical curved blade turbine, eight blades, (e) pitched-blade turbine, four blades

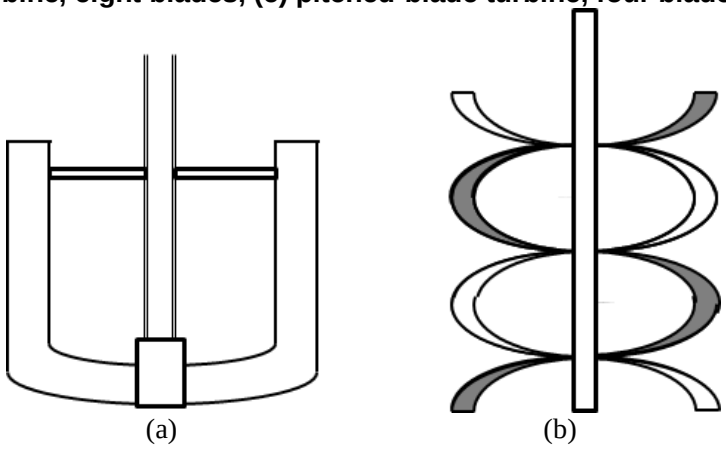

Fig.20.1-3. Impellors for high viscosity or non-Newtonian fluids: (a) anchor, (b) helical ribbon

20.1-2 Flow patterns in agitated vessels

Let us consider the flow pattern of a turbine-type agitated vessel as an example. It is necessary to

observe the radial and longitudinal velocity components. Figure 20.1-4 shows the flow currents formed in a cylindrical, baffled agitated vessel equipped with a turbine agitator. The plane of observation passes through the impeller shaft and in front of baffle plates. Fluid leaves the impeller outward in a radial direction, separates into longitudinal streams flowing upward or downward over the baffle, flows inward toward the rotation axis, and ultimately returns to the impeller intake. In the bottom region below the agitator, similar circulating flow is formed.

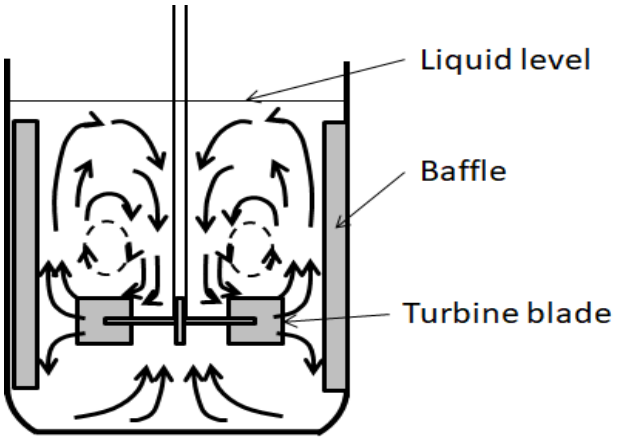

Fig.20.1-4. Schematic picture of circulation flow pattern in a turbine agitator tank

20.2 Power Consumption in Agitated Vessels

20.2-1 Dimensional analysis

In the design of an agitated vessel, it is very important to consider the power required to drive the impeller.

The power consumption P in agitation for a certain type of impeller can be obtained by the following dimensional analysis. When the impeller of the lever length R is rotated at an angular velocity ω, the form drag acting on the blade is proportional to the kinetic energy per unit volume $(1/2)\rho {v_\theta}^2$ (i.e., a kind of pressure) and the acting surface area A, where $v_\theta = R\omega$ and A are the characteristic (peripheral) velocity and area, respectively. The torque acting on the impeller can be considered as (torque) = (force)·(lever length), i.e., $(1/2)\rho {v_\theta}^2 A \times R$. Therefore the power input (work/time) should be a function of torque times angular velocity, i.e., $(1/2)\rho {v_\theta}^2 A \times R\omega$.

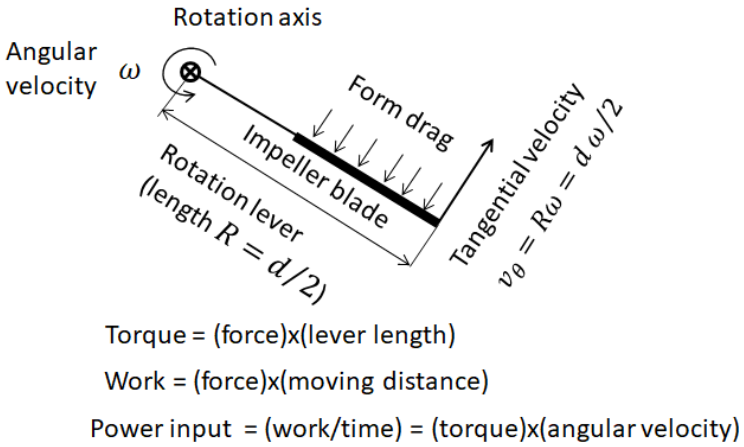

Fig.20.2-1. Relation of torque with rotating impeller

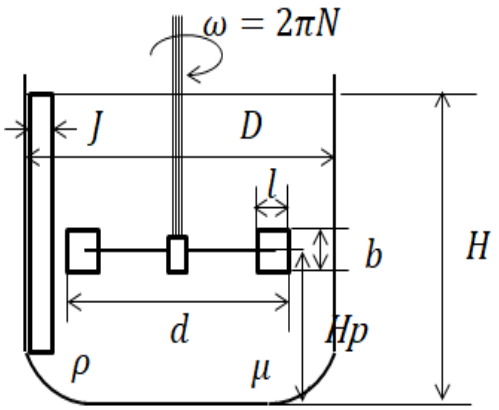

Fig.20.2-2. Dimensions of rotating turbine impeller in a tank

Since the peripheral speed of the tip of the impeller is given by $2\pi\,(d/2)N$, the Reynolds number of agitators is defined as

$$Re = \frac{d^2 N\,\rho}{\mu} \qquad (20.2\text{-}1)$$

where d is the impeller diameter and N the rotation number. Thus the power consumption should have the following functional form:

$$P = C\;(1/2)\rho\;{v_\theta}^3\;A$$

In the dimensional analysis, the common variables are: the length (blade diameter), d; the velocity (peripheral velocity), $d\,N$; the fluid viscosity, μ; the density, ρ; the acceleration of gravity, g; the area, $A \sim d^2$;

Here the power consumption is made dimensionless as

$$Np = \frac{P}{\rho N^3 d^5} \qquad (20.2\text{-}2)$$

This is called “the power number,” which can be considered to be analogous in physical meaning to the friction factor in a circular pipe flow.

(Dimensional analysis)

Many chemical engineering problems cannot be solved theoretically unless enough is known about the physical situations. The physics of mixing in an agitated tank is also so difficult that we cannot help relying on the following dimensional analysis. It may be expected that the power consumption depends on the following variables:

$$Np = a'\,d^{b'}N^{c'}\rho^{d'}\mu^{e'}g^{f'}$$
$$= a'L^{b'}t^{-c'}(M/L^3)^{d'}(M/Lt)^{e'}(L/t^2)^{f'} \qquad (20.2\text{-}3)$$

where M, L, t are the dimensions of mass, length, and time, respectively.

Buckingham’s theorem states: if an equation is dimensionally homogeneous, it can be reduced to a relationship among a complete set of dimensionless products.

In order for the above equation to be dimensionally homogeneous, the following conditions should hold:

M: $0 = d' + e'$

L: $0 = b' - 3d' - e' + f'$

t: $0 = -c' - e' - 2f'$

From these equations, the three of the five unknowns can be expressed in terms of the remaining two unknowns:

$c' = 2b' - 3d'$

$e' = -d'$

$f' = -b' + 2d'$

Finally it has been found that the power number equation should have the following functional form:

$$Np = a' d^{b'} N^{2b'-3d'} \rho^{d'} \mu^{-d'} g^{-b'+2d'}$$
$$= a' \left(\frac{\rho d^2 N}{\mu}\right)^{d'} \left(\frac{d\,N^2}{g}\right)^{(b'-2d')} \quad (20.2\text{-}4)$$

The first term is the Reynolds number and the second term is called "Froude number." These dimensionless groups have the physical meanings: the Reynolds number $Re = \frac{\text{inertial force}}{\text{viscous force}} = \frac{d^2 N \rho}{\mu}$ and the Froude number $Fr = \frac{\text{inertial force}}{\text{gravity force}} = \frac{V^2}{Lg} = \frac{d\,N^2}{g}$. (20.2-5)

The effect of the Froude number is usually very small if baffles are installed.

The unknowns a', d', $b' - 2d'$ should be determined by experiment.

Except for the Reynolds number and the power number, the pumping number sometimes called the flow number used as one more dimensionless key variable is defined as

$$Nq = \frac{q}{N\,d^3} \quad (20.2\text{-}6)$$

The volumetric flow rate q through the impeller can be assumed proportional to the peripheral velocity $\pi d\,N$ times the area $\pi d\,b$ swept out by the tips of the impeller blades: $q \sim N\,d^3$ because of $b \sim d$. As the pumping number is increased, the time required for one round of the circulating stream is decreased. Therefore the pumping number is also very important for promoting the mixing effect.

The pumping number tends to increase with the Reynolds number, and becomes almost constant in the turbulent flow, where it depends on the ratio of impeller diameter to tank diameter d/D.

20.2-2 Power correlations

In the last section (20.2-1), we have learnt that the power number is a function of the Reynolds number and the Froude number. However if baffle plates are installed in a tank, almost flat horizontal liquid level is kept. In this condition, the power number does not depend on the Froude number. Only for simplicity, Fig.20.2-3 shows the empirical correlations of the power number for some different impellers given for the case of baffled tanks.

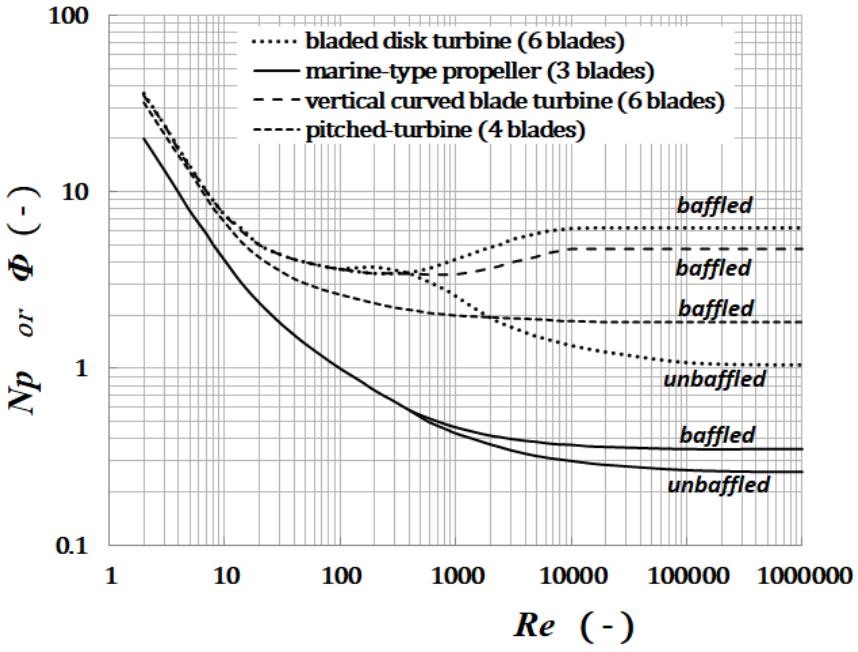

Fig. 20.2-3. Correlations of Impeller power number with Reynolds number for agitator tanks. (*Np* for baffled, *Φ* for unbaffled.)

In the range of high Reynolds numbers $Re \geq 10{,}000$, the power number becomes almost constant and independent of the Reynolds number. This effect due to baffles may be similar to the constant friction factor in the range of high Reynolds numbers for circular rough pipes. For the radial-flow type impellers, at low Reynolds numbers $Re \leq 500$, the lines of Np vs. Re for both baffled and unbaffled tanks coincide, and the slope of the line on logarithmic coordinates is – 1. This implies the laminar flow range. When the power requirement is calculated, we should consider the effect of system geometry in the terms of shape factors such as $S_1 = D/d,\ S_2 = Hp/d,\ S_3 = l/d,\ S_4 = b/d,\ S_5 = H/d$. These dimensions are given in Fig.20.2-2.

Usually typical proportions of agitated tanks are given to dimensions of the agitated tank and location and dimensions of the impeller for standardization.

For vigorous agitation in a baffled tank, the liquid surface is slightly disturbed but usually kept flat, so that the effect of the Froude number on the power number is not necessary to consider.

For the case of low-viscosity liquid in an unbaffled agitated tank, there is vortex formation on the liquid surface owing to centrifugal force. The effect of radially-varying liquid depth is related with the Froude number. Therefore the effect of the Froude number on the power number should be taken into account by the following modified power number:

$$\Phi = Np\, Fr^m \tag{20.2-7}$$

Here m is a function of the Reynolds number.

$$m = \frac{a - \log Re}{b} \tag{20.2-8}$$

For example, for propellers $(d/D = 1/3)$, $a = 2.1$ and $b = 18.0$ and for disk turbine $(d/D = 1/3)$, $a = 1.0$ and $b = 40.0$.

20.3 Heat Transfer in an Agitated Tank

Generally a chemical tank reactor has complicated structures of not only the heating jacket but also the tube coils shown in Fig.20.3-1. The tube coils are often used for the heat input into or removal from the central region of reacting fluids. In the engineering book specialized for agitation and mixing, various heat transfer correlations are available. Owing to the limitation of this book scope, many heat transfer correlations cannot be treated.

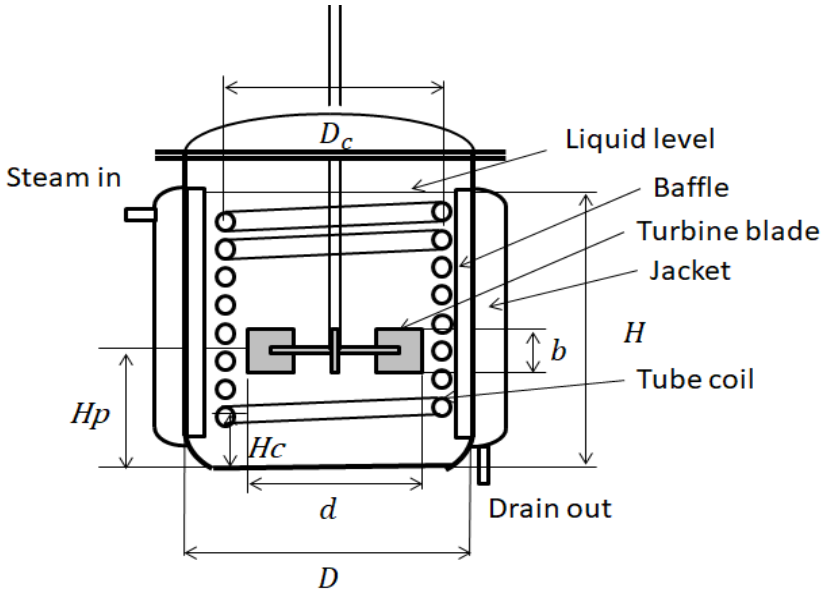

Fig.20.3-1 Ordinary chemical batch reactor

In this section, let us consider a simple flow reactor of jacketed agitated vessel without coils and baffle plates shown in Fig.20.3-2. No chemical reaction is assumed to take place in the vessel only for simplicity and convenience. There is neither endothermic nor exothermic reaction within the vessel.

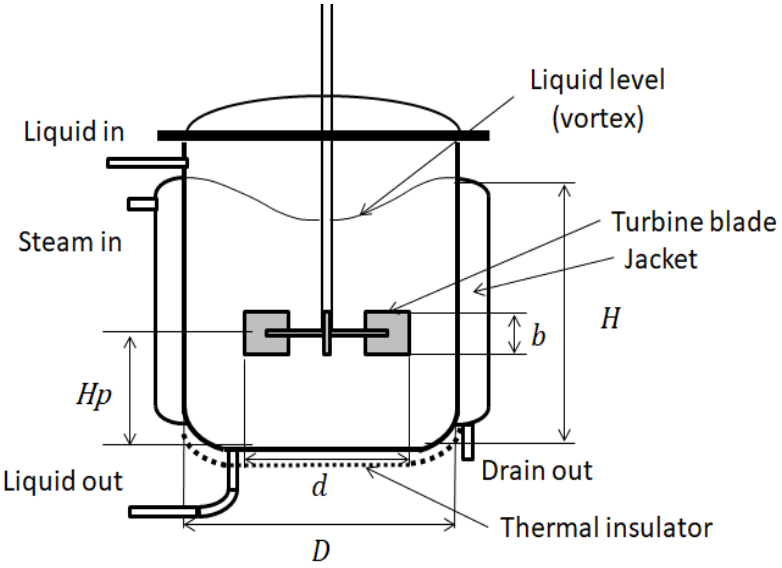

Fig.20.3-2 Heat transfer in a continuous flow reactor of jacketed tank unbaffled

A liquid is being continuously heated by the steam jacket of an agitated tank. Heat is supplied by condensation of steam from the outside jacket (i.e. from the inside wall of the vessel.). Usually the thermal resistance of the condensate film and tank wall can be assumed small compared to that of the liquid in the tank. Therefore the main resistance lies in the convective heat transfer on the inside wall of the reactor. The unjacketed portion of the tank is also assumed to be well insulated.

One example of heat correlation for constant physical properties is given by the following equation[1, 2]:

$$Nu = \frac{h_i D}{\kappa} = \alpha\, Re^{2/3} Pr^{1/3} \left(\frac{\mu}{\mu_w}\right)^{0.14} \qquad (20.3\text{-}1)$$

Depending on various agitators and arrangements of the vessels, the coefficient α varies considerably. For the case of pitched-blade turbine agitator tank unbaffled , $\alpha = 0.44$ can be used in the above equation.

1. Uhl, V. W., and Gray, J. B., "Mixing," vol.1, p.284, Academic, New York (1966)
2. Chilton, T. H., Drew, T. B., and Jebens, R.H., Ind. Eng. Chem., 36, 510 (1944)

20.4 Scale-up of Agitated Tank Design

The performance characteristics are generally determined empirically by correlating measured data as a function of dimensionless numbers. Those correlation equations consisting of dimensionless groups are employed for scale-up design. Under the condition of geometric similarity, appropriate correlations or rules should be selected depending on the physical purpose of the chemical equipment to be scaled-up. We know that the power given by an impeller is continuously dissipated in the form of irreversible degradation of mechanical energy to thermal energy of the liquid in a tank. Therefore the amount of power consumed by the specified impeller per unit volume of liquid can be considered as a measure of mixing effectiveness. Usually many power correlations are available for scale-up of various agitators and vessels.

Let us consider the scale-up design of low-viscosity liquid mixing. The subscript of variables 1 denotes the smaller-scale system such as laboratory and/or pilot-plant tanks and 2 denotes the larger-scale system to be scaled-up.

The following three conditions should be considered as the fundamental rule of scale-up from the smaller-scale to the larger-scale system, i.e. (1) to (2):

The power numbers and flow numbers of the system 1 and 2 should be equal to each other

$$Np_1 = Np_2 \quad (20.4\text{-}1)$$

$$Nq_1 = Nq_2 \quad (20.4\text{-}2)$$

(1) Low-viscosity homogeneous liquid solution:

The power consumption per unit volume P_v $(\mathrm{W/m^3})$ should be equal to each other:

$$P_{v1} = P_{v2} \quad (20.4\text{-}3)$$

This scale-up condition implies that the rate of the mechanical energy dissipated per unit volume of liquid should be equal to each other between the smaller-scale and larger-scale systems. In other words, the flow condition in a unit volume should be the same in the both systems. However strictly speaking, even in this condition, it is too difficult to make the flow structure same between the two systems because the rotation number obtained by the scale-up rules is usually much smaller in the larger-scale system than in the smaller-scale system.

The liquid level is assumed equal to the tank diameter: $H/D = 1$. If the ratio of the impeller diameter to the tank diameter is given by $k = d/D$, the power consumption per unit volume can be expressed as

$$P_v = P/[(\pi/4)D^2H] = \rho N^3 d^5 Np/[(\pi/4)(d/k)^2(d/k)] \sim N^3 d^2 Np \quad (20.4\text{-}4)$$

Therefore the rotation number of the larger-scale system is given by

$$N_2 = (d_1/d_2)^{2/3}(Np_2/Np_1)^{1/3}N_1 \quad (20.4\text{-}5)$$

As can be seen in Fig.20.2-3, the power number becomes almost constant in the wide range of the Reynolds number in the turbulent flow condition. Therefore even if the Reynolds numbers of the two systems are different, the power numbers can be assumed to be equal to each other: $Np_2 = Np_1$

By using this relation, the Reynolds number and power consumption become

$$Re_2 = {d_2}^2 N_2 \rho/\mu = (d_2/d_1)^2(N_2/N_1)\, Re_1 = (d_2/d_1)^{4/3} Re_1 \quad (20.4\text{-}6)$$

$$P_2 = Np_2 \rho {N_2}^3 {d_2}^5 = (N_2/N_1)^3(d_2/d_1)^5 P_1 = (d_2/d_1)^3 P_1 \quad (20.4\text{-}7)$$

According to these results, when the impeller diameter is scale-upped by eight times, i.e., $d_2 = 8 \times d_1$with the tank diameter $D_2 = 8 \times D_1$, the rotation number reduces to $N_2 = (1/4) \times N_1$. However the Reynolds number and power consumption should become very large as $Re_2 = 16 \times Re_1$ *and* $P_2 = 512 \times P_1$.

In scale-up of tanks assuming equal power consumption per unit volume (sometimes called agitation intensity), there is a possibility of forming the weak mixing regions here and there in the larger-scale system owing to small rotation number of the agitator of the larger-scale system.

(2) Mixing of liquid-liquid dispersion:

The gradient of the peripheral velocity near the tips of the impeller is important to break liquid lumps into small droplets. Therefore the scale-up rule for this purpose is given by

$$N_2 = (d_1/d_2)N_1 \quad (20.4\text{-}8)$$

In the turbulent flow region, we can assume $Np_2 = Np_1$

Therefore the power consumption is given by

$$P_2 = (N_2/N_1)^3(d_2/d_1)^5 P_1 = (d_2/d_1)^2 P_1 \quad (20.4\text{-}9)$$

The Reynolds number also becomes

$$Re_2 = (d_2/d_1)^2(N_2/N_1)\, Re_1 = (d_2/d_1) Re_1 \quad (20.4\text{-}10)$$

Emulsified polymerization reactors belong to this case. However the reactor tank should be unbaffled because a baffled reactor has a problem of undesirable polymer deposition in the concave

stagnant region between the baffle plates.

(3) Heat transfer of jacketed vessels

Firstly we should consider the power consumption per unit volume to be equal between the systems 1 and 2.

The flow condition will be fully turbulent. Therefore $Np_2 = Np_1$.

The rotation number for the larger-scale system is given by using Eq. (20.4-5):

$$N_2/N_1 = (d_1/d_2)^{2/3} \tag{20.4-5}$$

In usual scale-up of jacketed vessels with heating or cooling jackets, the heat exchange rate requirement can be expressed as

$$Q_2/Q_1 = h_2\, D_2H_2(T_w - T_L)_2/h_1\, D_1H_1(T_w - T_L)_1 \tag{20.4-11}$$

where h_1, h_2 are the heat transfer coefficients of the two systems, respectively.

From the purpose of scale-up, the temperature difference $\Delta T = T_w - T_L$ should be equal to each other between the smaller-scale and the larger-scale systems.

The geometric similarity is adopted for standardization of system design: $d \sim D$ and $H \sim d$.

The new length ratio of scale-up is given by

$$\lambda = D_2/D_1 = d_2/d_1 \tag{20.4-12}$$

Therefore

$$Q_2/Q_1 = h_2{D_2}^2/h_1{D_1}^2 \tag{20.4-13}$$

According to the heat transfer correlation equation Eq. (20.3-1),

$$Nu = \frac{h_i D}{\kappa} = \alpha\, Re^{2/3} Pr^{1/3} \left(\frac{\mu}{\mu_w}\right)^{0.14}$$

In these two systems, $Pr_2 = Pr_1$ and $(\mu/\mu_w)_2 = (\mu/\mu_w)_1$. Then from the above equation, the heat transfer coefficient is

$$\frac{h_2}{h_1} = \left(\frac{D_1}{D_2}\right)\left(\frac{Re_2}{Re_1}\right)^{2/3} \tag{20.4-14}$$

From Eq. (20.4-5), $N_2/N_1 = (d_1/d_2)^{2/3}$ under the condition of $Np_2 = Np_1$. Then Eq.(20.4-6) becomes

$$\frac{Re_2}{Re_1} = \left(\frac{d_2}{d_1}\right)^2 \left(\frac{N_2}{N_1}\right) = \left(\frac{d_2}{d_1}\right)^{4/3} = \lambda^{4/3} \tag{20.4-15}$$

The Reynolds number becomes large but the rotation number of the agitator is made small.

Finally

$$\frac{Q_2}{Q_1} = \frac{h_2}{h_1}\left(\frac{D_2}{D_1}\right)^2 = \left[\left(\frac{D_1}{D_2}\right)\left(\frac{Re_2}{Re_1}\right)^{2/3}\right]\left(\frac{D_2}{D_1}\right)^2 = \left(\frac{d_2}{d_1}\right)^{8/9}\left(\frac{D_2}{D_1}\right) = \lambda^{17/9} \sim \lambda^{1.89} \tag{20.4-16}$$

From Eq.(20.4-14), the heat transfer coefficient is given by

$$\frac{h_2}{h_1} = \left(\frac{D_1}{D_2}\right)\left(\frac{Re_2}{Re_1}\right)^{2/3} = \left(\frac{D_1}{D_2}\right)\left[\left(\frac{d_2}{d_1}\right)^{4/3}\right]^{2/3} = \lambda^{-1/9} \tag{20.4-17}$$

It has been found that the heat transfer coefficient for the larger-scale system becomes a little bit smaller than that for the smaller-scale system.

Nomenclature

D	agitated tank/vessel diameter, [m]
Fr	Froude number, [-]
g	gravitational acceleration, [m/s^2]
b	impeller width, [m]
d	diameter of impeller, [m]
H	depth of liquid in vessel, [m]
H_p	height of impeller above vessel floor, [m]
h_i	heat transfer coefficient on the inside surface of vessel, [W/m^{2}K]
J	width of baffles, [m]

l	length of impeller blades, [m]
N	rotation number of agitator, [1/s]
Np	power number, [-]
Nq	flow number, [-]
Nu	Nusselt number, [-]
P	power consumption, [W]
Pr	Prandtl number, [-]
P_v	power consumption per unit volume, [W/m^3]
Q	heat exchange rate, [W]
R	length of rotating lever (= d/2), [m]
Re	Reynolds number, [-]
T	temperature, [K]
v_θ	peripheral velocity, [m/s]
κ	thermal conductivity, [W/m K]
λ	scale-up length ratio, [-]
μ	viscosity, [kg/m s]
ρ	density, [kg/m^3]
Φ	modified power number, [-]
ω	angular velocity, [1/s]

Subscripts

w	wall
1	small-scale system
2	large-scale system scaled up

INDEX